

**Proceedings of the Second Workshop
on
General Relativity and Gravitation**

— WASEDA UNIVERSITY CONFERENCE CENTER —

January 18-20, 1993

Editors : K. MAEDA
Y. ERIGUCHI
T. FUTAMASE
H. ISHIHARA
Y. KOJIMA

PREFACE

The Second Workshop on General Relativity and Gravitation was held at Waseda University Conference Center from January 18 to 20, 1993. The workshop was supported by a Grant-in Aid for Scientific Research on Priority Areas (No.04234211) from the Japanese Ministry of Education, Science and Culture. This proceedings volume was also partially supported by a Grant-in Aid for Scientific Research on Priority Areas "Gravitational Wave Astronomy"(No.04234105).

The main purpose of this series of workshops is to review the latest observational and theoretical work in gravitational physics and relativistic astrophysics. A further purpose is to promote lively and stimulating interactions between researchers working in fields related to relativity and gravity – including particle physics, astrophysics, cosmology.

142 researchers participated from the above many fields, and 57 speakers gave 10 invited talks and 48 short contributions.

K. Maeda	(<i>Waseda University</i>)
Y. Eriguchi	(<i>University of Tokyo</i>)
T. Futamase	(<i>Hirosaki University</i>)
H. Ishihara	(<i>Kyoto University</i>)
Y. Kojima	(<i>Tokyo Metropolitan University</i>)

1. Introduction

The purpose of this study is to investigate the effects of various factors on the growth of a certain type of bacteria. The study was conducted over a period of six weeks, during which time the bacteria were grown under different conditions. The results of the study are presented in the following sections.

The first section of the study is a review of the literature on the growth of bacteria. This section discusses the various factors that can affect bacterial growth, such as temperature, pH, and nutrient availability. It also discusses the different methods used to measure bacterial growth.

The second section of the study is a description of the experimental methods used. This section details the procedures for growing the bacteria, the conditions used, and the methods used to measure growth.

The results of the study are presented in the following sections. The first section discusses the effects of temperature on bacterial growth. The second section discusses the effects of pH on bacterial growth. The third section discusses the effects of nutrient availability on bacterial growth. The fourth section discusses the effects of the different growth methods on bacterial growth.

CONTENTS

<i>PREFACE</i>	iii
----------------------	-----

Monday, January 18

Afternoon Session

Chairman: H. ISHIHARA

Singularities in the Classical Spacetimes

H. KODAMA	1
-----------------	---

Compactification of 3D Homogeneous Spaces

Y. FUJIWARA	22
-------------------	----

Compact Homogeneous Universes

T. KOIKE, M. TANIMOTO and A. HOSOYA	35
---	----

(Coffee Break)

Chairman: K. MAEDA

Unified Models and Possible Time-Nonvariability of the "Constants"

Y. FUJII and M. OMOTE	46
-----------------------------	----

Application of the Wormhole Mechanism to the Decaying Cosmological Constant Model

T. NISHIOKA	*
-------------------	---

Wave Function of the Universe in Topological and in Einstein 2-form Gravity

A. NAKAMICHI	49
--------------------	----

Quantum Fluctuation of Black Hole Horizons

K. NAKAMURA, S. KONNO, Y. OSHIRO and A. TOMIMATU	59
--	----

Pathological Divergence in Perturbative Quantum Field Theory in Spacetime with Accelerated Expansion

K. YAMAMOTO	69
-------------------	----

Unification of Gravity, Gauge and Higgs Fields by Confined Quantum Fields

T. ISSE	75
---------------	----

Quantum Gravity from 4- ϵ Dimension

K. GOUROKU	87
------------------	----

A Teleparallel Theory of (2+1)-Dimensional Gravity	
T. KAWAI	92
Some Models for the Description of the Scale-Dependent Topology	
M. SERIU	100
<i>(Coffee Break)</i>	
<u>Chairman:</u> A. HOSOYA	
Integrable Cosmology	
M. YOSHIMURA	107
Cosmological Application of CGHS Model	
A. HOSOYA, T. MISHIMA and A. NAKAMICHI	135
On the Mass of Two Dimensional Quantum Black Hole	
T. TADA and S. UEHARA	145
Quantum Gravity and Black Hole	
K. HAMADA and A. TSUCHIYA	148
One-loop Counterterms in 2d Dilaton-Maxwell Quantum Gravity	
E. ELIZALDE, S. NAFTULIN and S.D. ODINTSOV	156
Role of the 5th Coordinate in Wessen's 5D STM Theory of Gravity	
T. FUKUI	166
 Tuesday, January 19	
<i>Morning Session</i>	
<u>Chairman:</u> A. Tomimatsu	
Turns of General Relativity (Contents)	
H. SATO	171
Energy, Momentum and Angular-Momentum Currents in General Relativity	
K. NOMURA, K. HAYASHI and T. SHIRAFUJI	172
Black Holes with Non-Abelian Hair and their Thermodynamic Properties	
T. TORII and K. MAEDA	176
Exact Solution for a Black Hole with a Thin Disk	
T. AZUMA	186
Exact Solutions to the Einstein Equation with Scalar Fields	
T. KOIKAWA	191
<i>(Coffee Break)</i>	

Chairman: T. FUTAMASE

Inhomogeneities in the de Sitter Space-Time

K. NAKAO 201

The Properties of Black Holes in the Asymptotically de Sitter Space-Time

T. SHIROMIZU, K. NAKAO, H. KODAMA and K. MAEDA 222

Shock Wave Geometry with Cosmological Constant

M. HOTTA *

Pattern Formation in the Expanding Universe

J. SODA 229

Afternoon Session

Chairman: K. TOMITA

Time Variations of X-rays from Black Hole Candidates and Low Mass Binary Neutron Stars

S. MIYAMOTO 238

Gravitational Waves and γ -ray Bursts

T. NAKAMURA *

Naked Singularity Dries up?

T. NAKAMURA, M. SHIBATA and K. NAKAO 250

Scattering of Maximally-Charged Dilaton Black Holes

K. SHIRAISHI 270

Non-Equilibrium Thermodynamic Fluctuations of Black Holes

O. KABURAKI 277

Thermodynamics of Kerr Black Hole and its Applications to Two Hole Coalescence Problem and Inner Horizon Dynamics

S. HORIUCHI and I. OKAMOTO 283

Evaporation of a Collapsing Shell with Scalar Field Production

Y. OSHIRO, S. KONNO, K. NAKAMURA and A. TOMIMATSU 293

(Coffee Break)

Chairman: T. NAKAMURA

Stability of Magnetohydrodynamical Accretion onto a Black Hole

M. YOKOSAWA 301

Slow Evolution of Black Hole Magnetospheres

T. UCHIDA 310

Plasma Accretion in the Vicinity of a Black Hole

K. HIROTANI, A. TOMIMATSU and M. TAKAHASHI 316

Accretion of a Hot Plasma onto the Central Black Hole : Fokker-Planck Formulation F. YABUKI and F. TAKAHARA.....	326
Particle Acceleration around Neutron Stars with Comets, Planets and Black Hole H. HANAMI	334

Wednesday, January 20

Morning Session

Chairman: Y. ERIGUCHI

Experiment for Gravitational-Wave Detection and the LIGO Project S. KAWAMURA	339
Direct Imaging Interferometer – 2D to 5D Signal Processing – T. DAISHIDO, K. ASUMA, K. NISHIBORI, J. NAKAJIMA, E. OTOBE, N. WATANABE, Y. ARAMAKI, H. KOBAYASHI, T. SAITO, N. TANAKA, T. HOSHIKAWA, S. KOMATSU, H. OHARA and S. IWASE	351
Survey of the Galactic Transient Radio Sources with the Spatial FFT Interferometer E. OTOBE, J. NAKAJIMA, T. SAITO, N. TANAKA, H. KOBAYASHI, N. WATANABE, Y. ARAMAKI and T. DAISHIDO	352

(Coffee Break)

Chairman: Y. KOJIMA

Coalescence of Spinning Binary Neutron Stars M. SHIBATA, T. NAKAMURA and K. OOHARA.....	355
Gravitational Wave Induced by a Particle Orbiting around a Schwarzschild Black Hole T. TANAKA, M. SHIBATA, M. SASAKI, H. TAGOSHI and T. NAKAMURA.....	375
Gravitational Wave Burst Produced by Merging of Central Black Holes of Galaxies T. EBISUZAKI, T. FUKUSHIGE and J. MAKINO	382

Afternoon Session

Chairman: J. YOKOYAMA

Implication of the COBE-DMR and South-Pole Experiments on CMB Anisotropies to Inflationary Cosmology M. SASAKI	387
The Anisotropy of Cosmic Microwave Background Radiation Produced by Gravitational Wave S. NAKAMURA, N. YOSHINO, S. KOBAYASHI and A. HOSOYA	401
Smoothing of the Anisotropy of the Cosmic Background Radiation by Gravitational Scattering T. FUKUSHIGE, J. MAKINO and T. EBISUZAKI	410

Image Deformation due to Gravitational Lensing in a Universe with High-Redshift Quasar Clustering

K. TOMITA 420

Towards a More Realistic Inhomogeneous Cosmology

M. KASAI *

Expanding Surface of a Void and Universe Model

N. SAKAI, K. MAEDA and H. SATO 427

(Coffee Break)

Chairman: M. SASAKI

Chaotic Inflation Driven by a Sneutrino Field

H. MURAYAMA, H. SUZUKI, T. YANAGIDA and J. YOKOYAMA 437

Density Fluctuations of Hyperextended Inflation

M. MARUNO *

Generation of Gravitational Wave in the First Order Phase Transition

Y. SUZUKI 445

Annihilation of Domain Walls

M. NAGASAWA 450

False Vacuum Decay in Generalized Einstein Gravity

T. MAKI 460

Fate of Inhomogeneity in Schwarzschild-de Sitter Space-Time

S. KONNO and Y. NAMBU 464

Turns of General Relativity (in Japanese)

H. SATO 469

*** manuscript not available**

Singularities in the Classical Spacetimes

Hideo Kodama

*Department of Fundamental Sciences, FIHS
Kyoto University, Kyoto 606*

Singularities of spacetimes have been one of the main subjects in the study of general relativity throughout since its early stage. The culmination was the proof of the singularity theorems by Penrose and Hawking during the years 1965-1970. Though these theorems established the generic nature of the occurrence of singularities in physical spacetimes, they tell almost nothing about the structures and the physical influences of singularities. Though these remaining problems are not fully resolved yet, lots of important results have been accumulated so far through the investigation by many people. In this article, with the recent increasing interest in these problems in mind, which was provoked by the progresses in numerical relativity and the gravitational wave astrophysics, I briefly overview the development mainly after 1970 in the study of singularities in the classical spacetimes. For more comprehensive and detained treatments of the topic as well as its early history, the reader is referred to the books [HE73], [BE81], [Wal84], the reviews [Pen68], [Ger71], [ES77], [TCE80], [Sei83], [Cla87] and the articles in the proceedings of the singularity symposium in GRG8[Eil79].

1 What are the spacetime singularities?

Singularities appear in various aspects of physics. The spacetime singularities, however, constitutes a quite peculiar class among them. For example, singularities in field theories are usually the break down of continuity or smoothness of field configurations at some points in spacetime. There the values of fields may be ill-defined at singularities, but their spacetime locations are well-defined, which lets the term singular points make sense. In contrast the singularities of a spacetime cannot be any portion of a physical spacetime itself because the physical laws cannot be written down at points where the spacetime structure loses meaning, at least in general relativity. This feature makes it a very subtle problem to define the spacetime singularities precisely. Of course there may be theories in which the spacetime structure in the usual sense need not be defined everywhere, but we are not concerned with such theories in this article.

Historically spacetime singularities were first recognized as the divergence of curvature toward the boundaries of spacetimes described by simple exact solutions such as the Friedmann solution and the Schwarzschild solution. However, as more exact solutions were found and their

global structures were investigated, it was realized that spacetime singularities are not always associated with the divergence of curvature.

The most peculiar example is the Taub-NUT spacetime[Mis63,MT69], which is the only vacuum solution of Bianchi type IX found so far. Its metric is given by

$$l^{-2}ds^2 = -\frac{dt^2}{U} + 4U(d\psi + \cos\theta d\phi)^2 + (t^2 + 1)(d\theta^2 + \sin^2\theta d\phi^2), \quad (1)$$

where U is the function of time t given by

$$U = \frac{2mt + 1 - t^2}{t^2 + 1}, \quad (2)$$

θ , ϕ and ψ are the Euler angle of the 3-sphere, and $l(\neq 0)$ and m are constants. Though the metric component g_{tt} diverges and the determinant of the spatial metric vanishes as t tends to $t_{\pm} = m \pm \sqrt{m^2 + 1}$, the components of the curvature tensor with respect to a natural orthonormal tetrad are all finite in this limit. This is explicitly seen from the expression for the chiral combinations of the curvature form ${}^+\mathcal{R}_{ab} := (\mathcal{R}_{ab} + i * \mathcal{R}_{ab})/2$ with respect to the natural orthonormal dual basis θ^a ,

$${}^+\mathcal{R}_{0I} = \lambda_I(g - if)(\theta^0 \wedge \theta^I + i * (\theta \wedge \theta)^{0I}), \quad (I = 1, 2, 3) \quad (3)$$

where $\lambda_1 = 1$, $\lambda_2 = \lambda_3 = -1/2$ and

$$f = \frac{m(1 - 3t^2) + t(t^2 - 3)}{(t^2 + 1)^3}, \quad g = \frac{mt(3 - t^2) + 1 - 3t^2}{(t^2 + 1)^3}. \quad (4)$$

Thus the surfaces $t = t_{\pm}$ are expected to be similar to the horizon in black hole spacetimes. This expectation is true. Actually it can be easily shown that they are null and the spacetime can be extended across them to yield a maximally extension with topology $S^3 \times \mathbb{R}$ [HE73].

This maximally extended Taub-NUT spacetime appears to be completely regular because the orthonormal-tetrad components of the curvature tensor are all uniformly bounded as is seen from the above expressions. However, when one examines the behavior of geodesics, one encounters a peculiar phenomenon: there exist a family of timelike and null geodesics which are inextensible but have finite affine lengths and converge to the null surfaces $t = t_{\pm}$ [MT69,RS75]. This implies that some geodesic observers can exist only for a finite proper time. Thus, though the curvature tensor is well-behaved everywhere, this spacetime should be regarded to be physically singular. Since the badly-behaved geodesics in the present case are contained in the compact region $t_- \leq t \leq t_+$, this type of singular behavior is called an *imprisonment*.

From the lessons from this example and others, most people now define the singular spacetimes as those that contain incomplete inextensible curves[TCE80]. To make this definition

exact, one must specify the category of curves to be considered. As we will see in the next section, only non-spacelike geodesics are considered in the most singularity theorems. However, as was pointed out by Geroch[Ger68], there exist spacetimes which are geodesically complete, yet contain incomplete timelike curves with bounded acceleration. Clearly such spacetimes are physically badly-behaved. Hence people usually extend the category to general non-spacelike curves.

One technical problem arises in this extension. It is to define the incompleteness of a general non-spacelike curve for which the affine parameter may not be defined. This problem was first discussed by Schmidt and solved by introducing the *generalized affine parameter* for a general non-spacelike curve defined as follows[Sch71,Sch72]. Let γ be a non-spacelike curve with a parameter t and $\{(e_a)_p\}$ be an orthonormal basis of the tangent space T_p at a point $p \in \gamma$. The parallel transport of $\{(e_a)_p\}$ defines a orthonormal tetrad $\{e_a\}$ along γ . Then the generalized affine parameter u of γ is defined in terms of the tetrad components V^a of the tangent vector $V = \gamma_* \partial_t$ as

$$u := \int_p \left(\sum_a V^a V^a \right)^{1/2} dt. \quad (5)$$

The value of this parameter depends on the choice of $(e_a)_p$ as well as p . However, one can easily show that the finiteness of the generalized affine parameter is preserved even if one changes the choice. In particular the completeness of a curve is defined in terms of it without ambiguity, and coincides with the ordinary definition for geodesics.

The completeness with respect to this generalized affine parameter is called the *b-completeness*. It is because the spacetime is b-complete if and only if the principal orthogonal bundle $\pi : O(M) \rightarrow M$ associated with the spacetime metric is complete as a metric space with respect to the natural positive definite Riemannian metric of $O(M)$ [HE73]. For Riemannian manifolds the b-completeness and the geodesical completeness (g-completeness for brevity) are equivalent. However, the former is strictly stronger than the latter for Lorentzian spacetime as stated above.

One should note that, though the b-completeness is a quite elegant concept mathematically, it is too strong for the arguments of spacetime singularities because it requires the completeness for space-like curves as well as non-spacelike curves. Hence the b-completeness is applied to only non-spacelike curves in this article unless otherwise stated. The structure of singularities in b-incomplete spacetimes and its classification will be discussed in detail in §3.

2 When do singularities occur?

As established by the singularity theorems by Hawking and Penrose, physical spacetimes are singular quite generally. The most essential reason for it is the universal attractive nature of gravity. Though this nature has a physical origin, it can be given a quite simple mathematical expression.

Let $x^\mu(\lambda, \sigma)$ be a family of geodesics with affine parameter λ . Then from the commutativity of $V^\mu = \partial x^\mu / \partial \lambda$ and $Z^\mu = \partial x^\mu / \partial \sigma$, we obtain the geodesic deviation equation

$$\nabla_V^2 Z = \mathcal{R}(V, Z)V, \quad (6)$$

where \mathcal{R} is the Riemannian curvature tensor.

In the case where the geodesics are timelike, by expanding the vectors in terms of the orthonormal Fermi basis $E_0 = V, E_I (I = 1, 2, 3)$, the change of Z along the geodesic is expressed as

$$\frac{dZ^I}{d\lambda} = Z^J \nabla_J V_I, \quad (7)$$

$$\nabla_J V_I = \frac{1}{3} \delta_{IJ} \theta + \sigma_{IJ} + \omega_{IJ}, \quad (8)$$

where σ_{IJ} is the symmetric traceless part and ω_{IJ} the anti-symmetric part. From this expression one sees that θ, σ_{IJ} and ω_{IJ} represent the *expansion*, the *shear* and the *rotation* of a spatial volume comoving with the family of geodesics, respectively. In terms of these quantities the geodesic deviation equation (6) can be written as the evolution equations for these quantities. In particular the expansion θ satisfies the well-known *Raychaudhuri equation* [Ray55, HE73]

$$\frac{d\theta}{d\tau} = -R_{ab} V^a V^b + \omega_{IJ} \omega^{IJ} - \sigma_{IJ} \sigma^{IJ} - \frac{1}{3} \theta^2. \quad (9)$$

From this equation it follows that, if $R_{ab} V^a V^b \geq 0$ and ω_{IJ} vanishes, the relative expansion of the neighboring geodesics is always decelerated. Here the term containing ω_{IJ} represents the effect of the centrifugal force by rotation. Hence the Raychaudhuri equation shows that the gravity acts attractively if and only if $R_{ab} V^a V^b \geq 0$ for any time-like vector V . This condition is called the *timelike convergence condition*.

If the spacetime metric satisfies the Einstein equations, the timelike convergence condition can be rewritten as the condition on the energy-momentum tensor:

$$T_{ab} V^a V^b \geq \left(\frac{1}{2} T - \frac{\Lambda}{\kappa^2} \right) V^a V_a. \quad (10)$$

Roughly speaking, this condition represents the local positivity of the energy, although, to be exact, it is slightly weaker than that. For example, if T_{ab} is diagonalizable with g_{ab} , it is written

as[HE73]

$$\rho + P_I \geq 0 (I = 1, 2, 3), \quad \rho + \sum_I P_I \geq \frac{2\Lambda}{\kappa^2}. \quad (11)$$

For the case $\Lambda = 0$ the condition (10) is called the *strong energy condition*.

If the timelike convergence condition is satisfied, it can be easily shown that a hypersurface-orthogonal geodesics focuses locally within a finite affine time once they begin to contract. In fact, since the rotation of a hypersurface-orthogonal geodesics vanishes, it follows from the Raychaudhuri equation that θ satisfies the inequality

$$\theta(\lambda) \leq \frac{1}{1/\theta(0) + \lambda/3} \quad (12)$$

if $\theta(0) < 0$, hence $\theta \rightarrow -\infty$ at some $\lambda \leq 3/|\theta(0)|$.

This result implies that the spacetimes which contain only irrotational dust clouds are singular since dust particles move along geodesics and the material density diverges if the geodesics converge[Ray57]. However, we cannot conclude from this argument that singularities generally occur even for dust systems because the rotation which acts repulsively may prevent the focusing. For example, Anderson, Morgan and Thorne[AMT72] showed that a collapsing counter-rotating dust cylinder with vanishing total angular momentum bounces without producing singularities. Moreover, if the pressure of matter does not vanish, the focusing of geodesics has nothing to do with the behavior of matter.

Thus from the physical standpoint the geodesic focusing property has no direct relation to the occurrence of singularities. However, from the geometrical standpoint, it has a deep consequence. What plays an important role there is the concept of the *conjugate points*.

Two points p and q on a geodesic γ are said to be conjugate along γ if there exists a nontrivial field Z along γ which satisfies the geodesic deviation equation (6) and vanished at p and q simultaneously. This intuitively means that there exists a geodesic which is infinitesimally close to γ and intersects with it at p and q . Similarly a point p is said to be conjugate to a three surface \mathcal{H} along a geodesic γ which passes through p and intersects with \mathcal{H} orthogonally if there exists a vector field Z satisfying Eq.(6) which is orthogonal to γ and vanished at p . An important property of the conjugate points is that if a non-spacelike geodesic γ contains a pair of conjugate points it can be deformed to a longer timelike curve[HE73, Prop. 4.5.8, Prop.4.5.10]. Similarly a geodesic γ orthogonal to a three surface \mathcal{H} can be deformed to a longer curve orthogonal to \mathcal{H} if there is a point conjugate to \mathcal{H} on γ [HE73, Prop. 4.5.9].

This property of the conjugate points is to be contrasted with the fact that, in a globally hyperbolic spacetime, for any causally separated pair of points there exists a unique geodesic connecting them of the maximum length, and for any point p in the future(past) Cauchy

4) *There exists at least one of the following:*

- i) *a compact achronal set without edge,*
- ii) *a closed trapped surface,*
- iii) *a past (or future) trapped point.*

In this theorem the condition 2) implies that for any non-spacelike geodesic there exists a point on it at which $V_{[a}R_{b]cd[e}V_{f]}V^cV^d \neq 0$ where V is the tangent vector to the geodesic.

Although the statements of these four famous singularity theorems are slightly different from one another, they all have the same structure in that the occurrence of singularities are deduced from the convergence condition, the causality condition, and the existence of a trapped set. Among these three types of conditions, the imposition of the last one is quite natural since the singularities are expected to occur only under the circumstances where the gravitational field is sufficiently strong as in gravitational collapse and in the early universe. In fact, for example, the third condition in the second Hawking's theorem cannot be made weaker because an exact geodesically complete solution is found by Senovilla[Sen90,CFS92] in which the other two conditions are satisfied but the trapping condition is violated only along a single null geodesic through a point.

In contrast the requirement on the causality appears to be just technical and inessential to the occurrence of singularities. Nevertheless, no general singularity theorem with this requirement eliminated has been established yet, although some arguments suggesting that the violation of causality does not lead to the avoidance of singularities have been given by Tipler[Tip76,Tip77].

Finally requiring the convergence condition is also natural since it represents the attractive nature of gravity as we have seen at the beginning of this section. In contrast to the trapping condition, however, this condition can be replaced by a weaker requirement. It is because it is mainly used to deduce the existence of conjugate points in the proof. For example it was shown by Tipler[Tip78] that in Hawking-Penrose's theorem the strong energy condition can be replaced by the weak energy condition, that is, $T_{ab}V^aV^b \geq 0$ for any timelike vector V , together with the strong energy condition on the average along every complete timelike geodesic. Recently Borde[Bor87] and Kánnár[Kan91] further pursued this line of refinement, and proved the following focusing theorem:

Theorem 5 (Borde1987) *Let γ be a complete non-spacelike geodesic with affine parameter λ and let $V = \partial_\lambda$ be its tangent vector. Then, if the following two conditions are satisfied, γ contains a pair of conjugate points:*

- 1) *The generic condition is satisfied on γ .*

- 2) For any $\epsilon > 0$ there exists a number $B > 0$ such that for any pair of affine parameters $\lambda_1 < \lambda_2$ there exist two intervals of the real number, $I_1(< \lambda_1)$ and $I_2(> \lambda_2)$, both of which have lengths larger than B , and the following inequality is satisfied:

$$\int_{t''}^{t'''} R_{ab} V^a V^b d\lambda \geq -\epsilon, \quad \forall t' \in I_1, \forall t'' \in I_2.$$

In this theorem the local convergence condition is replaced by a nonlocal one. In particular it implies that the singularity theorem may be extended to the semi-classical theory of general relativity for which the local positivity of the energy-momentum tensor is not satisfied.

3 What types of singularities occur?

Although the singularity theorems make clear the conditions for the occurrence of singularities in a quite generic form, they give no information on the structure of singularities expected. They just tell that there exists an incomplete geodesic. This is a quite unsatisfactory feature of the theorems because we cannot discuss the physical influences of the singularities. In this section we overview the progress in the investigation of this advanced problem after the establishment of the singularity theorems.

3.1 Classification of singularities

In the discussion of the structure of singularities there is one important technical point to be noticed first of all. It is the differentiability class and the extension of the spacetime structure.

In general relativity there is a large freedom in the choice of the base spacetime manifold. For example, if a metric g satisfies the Einstein equations on a manifold M , its restriction to a four-dimensional submanifold M' of M is also a solution to the Einstein equations. This restriction makes the spacetime singular even if the original one is complete. However, the singularities arising from such restriction seem to be unphysical. Hence it is suggested that, if one wants to investigate the structure of physical singularities, one must find a maximal extension of the spacetime. This procedure, however, provokes some subtle problems.

First one must specify the smoothness of the metric and the manifold structure because weakening the smoothness requirement in general yields a larger extension. One natural criterion for the smoothness is expected to be given by the wellposedness of the Einstein equations. This, however, does not give a definite answer. For, the Einstein equations is meaningful in the distributional sense if the metric is at least of class C^1 - while the weakest smoothness condition so far proved for the existence and the uniqueness of a solution to the Cauchy problem of the Einstein equations is $W^{2.5+\epsilon}$ ($\epsilon > 0$) on the metric [HKM77]. Here the metric is of

class C^k - if it has $(k - 1)$ -th continuous derivatives and the k -th derivatives are bounded almost everywhere, and of class W^α if the generalized derivatives up to the α -th order are square integrable (if α is not integer, the precise definition of the Sobolev space W^α requires the pseudo-differential operator). Though the necessary condition for the metric to be $W^{2.5+\epsilon}$ is that it is of $C^{0.5+\epsilon}$ (Hölder continuity), the best sufficient condition in the category of class C^k is $C^{2.5+\epsilon}$. Thus the wellposedness of the Einstein equations cannot be expressed by a simple smoothness condition.

Another possible criterion for the smoothness is given by the singularity theorems. Since the existence and uniqueness of geodesics is guaranteed only for the metric of class C^2 -, the singularity theorems hold under the same condition [HE73]. However, just for the b-completeness to be defined, the metric is required to be of class C^1 -.

Thus there is no natural smoothness condition at present. In the discussion of singularities it is common to consider in the class C^0 - for the curvature tensor, which corresponds to the class C^2 - for the metric, because it is the widest class in which the singularity theorems holds. In the following the differentiability is specified by the smoothness of the curvature tensor unless otherwise stated.

The second problem is the nonuniqueness of the extension. Here the nonuniqueness arises from two origins. First in the class C^2 - the solution to the Cauchy problem may not be unique as stated above. Though this nonuniqueness disappears if one requires a sufficiently stronger smoothness, it tends to make the spacetimes appear more singular. Second the maximal extensions may not be globally hyperbolic as in the black hole solutions. In such cases there appears the Cauchy horizon and the extension across it is obviously not unique. This nonuniqueness cannot be eliminated by weakening the smoothness, and is a quite cumbersome one. Some people may argue that the very occurrence of the Cauchy horizon implies that the spacetime is singular. However, we should be more open-minded on this point because the real spacetime may not be globally hyperbolic. In the following we shall not be worried about this nonuniqueness problem.

As explained in the first section, singularities are not points of the physical spacetime, but just implies that there exist some incomplete non-spacelike curve. When the differentiability class of the spacetime is specified, singularities are usually classified in terms of the behavior of the curvature tensor along the incomplete curve as follows [HE73, ES77]. Let γ be an inextendible incomplete non-spacelike curve. First if the curve can be extended to be a complete curve by some extension of the spacetime in the class C^k for the curvature tensor, γ is said to approach a C^k -regular singularity. Otherwise, it is said to approach a C^k -singularity. In the following it is assumed that all the C^k -regular singularities are eliminated by a maximal extension.

Let R_{abcd} be the components of the Riemannian curvature tensor with respect to the parallelly transported orthonormal frame along γ . If R_{abcd} is of class C^k along γ , γ is said to approach a C^k *quasi-regular singularity*, and otherwise a C^k *p.p. (parallelly-propagated) curvature singularity*. For the latter, if all the polynomial combinations of R_{abcd} stay in the class C^k along γ , it is said to be a C^k *n.s.p. (non-scalar-polynomial) curvature singularity*, and otherwise a C^k *s.p. (scalar-polynomial) curvature singularity*.

3.2 Quasi-regular singularities

One typical example of the quasi-regular singularity is the conic singularity obtained, for example, by cutting a wedge from the Minkowski spacetime and identifying the surfaces, which appears in the spacetime containing a cosmic string. Another is the Misner singularity obtained by identifying the Minkowski spacetime by some discrete group generated by a boost [Mis67, ES77]. The singularity of the Taub-NUT space is also of this type.

The most important characterization of the quasi-regular singularities is the local extendibility theorem proved by Clarke [Cla73] which states:

Theorem 6 (Clarke1973) *For any curve γ which approaches a quasi-regular singularity, there exists an extension of a neighborhood of γ in which γ can be extended to a longer curve.*

This theorem implies that the quasi-regular singularity has a global nature, and suggests that it occurs only in special spacetimes. Clarke has shown that it is the case at least in the globally hyperbolic region [Cla75, Cla76]:

Theorem 7 (Clarke1975,1976) *Let γ be an inextensible incomplete non-spacelike curve in a C^{0-} maximally extended spacetime which is globally hyperbolic. If R_{abcd} is not asymptotically algebraically special along γ , γ approaches a C^{0-} p.p. curvature singularity.*

This theorem implies that if quasi-regular singularities occur, the spacetime has the Cauchy horizon in general, and they are on or outside it, since the algebraic special nature of the curvature tensor is not stable against perturbations. Further, if the Cauchy horizon is unstable against perturbations, which implies that the strong cosmic censorship holds in generic spacetimes, all the singularities are p.p. curvature ones in general. Thus the quasi-regular singularities are not expected to occur in the physical spacetime.

In §1 we saw that the incomplete curves in the Taub-NUT spacetime are imprisoned. For the quasi-regular singularity it can be shown that this imprisonment occurs also only in specialized spacetimes [HE73]:

Theorem 8 *If p is a limit point of a curve γ which approaches a quasi-regular singularity, there exists a non-spacelike vector $K \in T_p$ such that $R_{ab}K^aK^b = 0$, and the Weyl tensor is algebraically special at p . Further the Weyl tensor and the Ricci tensor are asymptotically specialized along γ .*

Finally Clarke showed that the quasi-regular singularity has a primordial nature (for the precise definition of the primordialness of a singularity and the proof of the statement, see [Cla76]).

3.3 Non-scalar polynomial curvature singularities

In a Riemannian space with a positive definite metric the tetrad components are all regular if all the scalar polynomials constructed from them are regular. However, it does not hold in the Lorentzian spacetimes. To see this, note that there exists only two independent complex scalar polynomials of the Weyl tensor which are expressed in terms of the complex null-tetrad components of the Weyl tensor in the Newman-Penrose formalism, Ψ_1, \dots, Ψ_4 , as

$$I = \Psi_0\Psi_4 - 4\Psi_1\Psi_3 + 3\Psi_2^2, \quad (13)$$

$$J = \begin{vmatrix} \Psi_0 & \Psi_1 & \Psi_2 \\ \Psi_1 & \Psi_2 & \Psi_3 \\ \Psi_2 & \Psi_3 & \Psi_4 \end{vmatrix}. \quad (14)$$

In particular for the Petrov type III and N, since $I = J = 0$, all the singularities are of n.s.p. type if vacuum. For the other algebraically special types (II and D) for which $I^3 = 27J^2$, even if some of Ψ_j 's are singular, all the scalar polynomials may be regular if the combinations $\Psi_0\Psi_4$ and $\Psi_1\Psi_3$, and Ψ_2 are regular. A similar cancellation of divergence can occur also for the type I. For example an appropriate conformal transformation of spacetimes with the Misner singularity yields spacetimes with n.s.p. curvature singularities from Theorem 8 because the transformation will make $R_{ab}K^aK^b$ nonvanishing at the limit points while it preserves the Weyl tensor.

Another example is the singular plane wave solution explained below. It is shown that quasi-regular singularities occur also in some tilted cosmological models.

The important characterization of the quasi-regular singularity is given by the following theorem by Siklos and Clarke [Cla79]:

Theorem 9 *Let γ be a non-spacelike curve approaching a p.p. curvature singularity, and have a neighborhood which is space- and time-orientable and has a spin structure. Then the singularity is of n.s.p. type if and only if there exists a tetrad field in a neighborhood of γ with respect to which every component R_{abcd} is bounded.*

This theorem implies that the n.s.p. singularity occurs due to a bad behavior of the parallelly propagated frame field. I will illustrate this point by the example of the singular plane wave[ES77].

The p.p wave solution is given by the metric

$$ds^2 = dx^2 + dy^2 + 2dudv + 2H(x, y, u)du^2, \quad (15)$$

where H is the function given by

$$H = \frac{1}{2}A(u)[(x^2 - y^2)\cos\Phi(u) - 2xy\sin\Phi(u)] \quad (16)$$

with arbitrary functions $A(u)$ and $\Phi(u)$. With respect to the orthonormal frame

$$\begin{aligned} e_0 &= \frac{1}{\sqrt{2}}[\partial_u - (1 + H)\partial_v], & \frac{1}{\sqrt{2}}[\partial_u + (1 - H)\partial_v], \\ e_2 &= \partial_x, & e_3 = \partial_y, \end{aligned} \quad (17)$$

and its dual basis

$$\begin{aligned} \theta^0 &= \frac{1}{\sqrt{2}}[(1 - H)du - dv], & \theta^1 &= \frac{1}{\sqrt{2}}[(1 + H)du + dv], \\ \theta^2 &= dx, & \theta^3 &= dy, \end{aligned} \quad (18)$$

the connection forms are given by

$$\omega_{I2} + i\omega_{I3} = (x - iy)Ae^{-i\Phi}(\theta^0 + \theta^1) \quad (I = 0, 1), \quad (19)$$

and the chiral combination of the curvature forms by

$${}^+\mathcal{R}_{01} = 0, \quad (20)$$

$${}^+\mathcal{R}_{0J} = \frac{i^{J-2}}{2}Ae^{-i\Phi}(\theta^0 + \theta^1) \wedge (\theta^2 + i\theta^3) \quad (J = 2, 3). \quad (21)$$

This shows that the spacetime is of Petrov type III.

From these equations it is easily seen that the curve γ defined by $x = y = 0$ and $u = -v = s/\sqrt{2}$ is a geodesic with affine parameter s , and e_a defined above is parallel along it. Thus the spacetime is p.p. curvature singular if $A(u)e^{-i\Phi(u)}$ is a singular function of u . Since it is of Petrov type III, the singularity must be of n.s.p. type.

Now let us rotate and boost the frame e_a to define the new frame \bar{e}_a ,

$$\bar{e}_0 \pm \bar{e}_1 = e^{\pm\ell(u)}(e_0 \pm e_1), \quad (22)$$

$$\bar{e}_2 + i\bar{e}_3 = e^{-\Phi(u)/2}(e_2 + ie_3), \quad (23)$$

and its dual basis

$$\bar{\theta}^0 \pm \bar{\theta}^1 = e^{\mp \xi(u)}(\theta^0 \pm \theta^1), \quad (24)$$

$$\bar{\theta}^2 + i\bar{\theta}^3 = e^{-\Phi(u)/2}(\theta^2 + i\theta^3), \quad (25)$$

where $\xi(u)$ is an arbitrary function of u . Then the curvature forms are expressed as

$${}^+\bar{\mathcal{R}}_{01} = 0, \quad (26)$$

$${}^+\bar{\mathcal{R}}_{0J} = \frac{i^{J-2}}{2} A e^{2\xi} (\bar{\theta}^0 + \bar{\theta}^1) \wedge (\bar{\theta}^2 + i\bar{\theta}^3) \quad (J = 2, 3). \quad (27)$$

Thus if ξ is chosen so that it cancels the singularity of A , the components of the Riemannian curvature tensor become regular in the new frame. For example, if ξ is take as $\xi = -\frac{1}{2} \log(1 + A^2)$, the nonvanishing component of the curvature tensor is expressed as

$$A e^{2\xi} = \frac{A(u)}{1 + A(u)^2}, \quad (28)$$

which is of class C^{0-} regardless of the smoothness of $A(u)$.

4 Cosmic Censorship

4.1 Cosmic censorship hypothesis

The discussion on the structure of singularities in the previous section shows that the singularities predicted by the singularity theorems are in general associated with the divergence of the spacetime curvature. Thus the classical laws will not be applied around the singularities any longer, and the behavior of the spacetime and matter there should be determined by a new theory, such as quantum gravity. However, such modification of the structure around singularities may not have a physical importance. For example, though the cosmic initial singularity is *naked* in the sense that some of the past-inextendible non-spacelike curves are incomplete, we do not have to worry about its structure or influence in investigating the recent evolution of the universe, provided that the initial singularity is causally separated from the present by some Cauchy surface on which the initial condition for the later evolution is specified. Similarly if the singularities produced by gravitational collapses are always confined within the horizons, they cannot have any physical influence on the observers staying outside the horizons.

From these observations and the very fact that no violent phenomena which appear to be produced by spacetime singularities have been observed so far, Penrose proposed the hypothesis that all the singularities other than the initial singularities are hidden by the horizons in the asymptotically flat physical spacetimes [Pen69]. This hypothesis is called *the weak cosmic*

censorship hypothesis. In the mathematical language it is expressed by the condition $\mathcal{I}^+ \subset \overline{D^+(S, \bar{M})}$. Here S is a partial Cauchy surface, \bar{M} is the unphysical spacetime constructed as the union of the physical spacetime M and its causal infinity ∂M (see §4.2), and $\mathcal{I}^+ \subset M$ is the future causal infinity of the asymptotically flat region. An asymptotically flat spacetime satisfying this condition is said to be *future asymptotically predictable* from a partial Cauchy surface S .

Though the singularities become harmless for observers staying outside the horizons under the weak cosmic censorship hypothesis, they may still be disastrous for observers falling into the black holes. This distinction of observers seems to be quite artificial from the physical point of view because the physical evolution of the spacetime structure has the local nature. From this viewpoint Penrose later introduced *the strong cosmic censorship hypothesis* which states that the maximally extended physical spacetime is globally hyperbolic [Pen79]. This implies that the spacetime singularities would be harmless even locally apart from the initial singularities.

These cosmic censorship hypotheses do not hold in their most generic forms because there exist some counterexamples. The simplest one is given by the gravitational collapse of spherical dust shells. In this system, if a sufficiently large inward velocity is given to an outer shell initially, its trajectory crosses with that of an inner shell before they enter the horizon to produce a naked singularity [YSM73, MYS74]. This type of singularity is called a *shell-crossing singularity*. It is shown that the shell-crossing singularity occurs also for spheroidal dust-shell collapse [Sze75]. Another example is *the shell-focusing singularity* which is, for example, produced at the center in the spherical dust collapse under appropriate initial conditions [Chr84, New86]. Null dust is also shown to produce a shell-focusing naked singularity [Kur84, Pap85, Hol86]. Since all these examples are concerned with dust systems, one may suspect that these singularities would be avoided in the physical spacetime because the pressure does not vanishes for realistic matter. This suspicion has not been clearly rejected or proved yet, although Ori and Piran showed that the shell-focusing singularity occurs in self-similar spherical collapse of matter with a bounded pressure [OP87, Lak88].

Recent numerical study of gravitational collapse also provides some counterexamples or examples which suggest the breakdown of the hypothesis. For example, Nakamura et al [NST88] constructed a sequence of time-symmetric initial data for the poloidal dust ellipsoid collapse in which there appear no apparent horizon but the curvature increases without bound at some points on the symmetry axis. Later it was numerically shown that the curvature grows without bound but no apparent horizon appears in the time-symmetric poloidal collapse if the ellipsoid has a sufficient long poloidal form initially [ST91]. It was also shown that the inclusion of

rotation does not change the result[ST92].

The breakdown of the weak cosmic censorship which these examples are concerned with is closely related with *the hoop conjecture* proposed by Thorne[Tho72] and the related conjecture called *the isoperimetric conjecture* by Gibbons[Gib84]. These conjectures assert that a trapped surface is formed only if the circumference or the area of the surface of a region is smaller than some constant multiple of the mass contained in the region. They have been so far exactly formulated and proved only for some special systems such as the spherically symmetric system[Mal91a,BMO88], the null dust-shell collapse[BIL91,BIL92,Bo92,Tod92], and the momentarily static and conformally flat initial data[Mal91b,Fla92](see also [SY83,Omu86]). If these conjectures are true, naked singularities would be formed by gravitational collapse of matter with a sufficiently elongated shape under the assumption that a trapped surface is formed if the horizon exists. However, the latter assumption, though quite likely to hold, has not been proved yet.

These examples and the related work show that the cosmic censorship hypothesis would be valid only under some strong additional assumptions. In the following we briefly describe a couple of theorems proved by Krolak which state that the cosmic censorship hypotheses hold under some geometrical assumptions.

4.2 Krolak's theorems

We must give some definitions to state the theorems by Krolak. An open past set W ($I^-(W) = W$) of a spacetime M is said to be a *IP*(*indecomposable past*) if it cannot be written as a union of two nonempty open past sets. Further a IP W is called a *PIP*(*proper IP*) if $W = I^-(p)$ for some point $p \in M$, and a *TIP*(*terminal IP*) otherwise. It was shown by Geroch and others[GKP72] that W is a TIP if and only if there exists a future inextensible curve γ such that $W = I^-(\gamma)$.

If a TIP is written as $I^-(\gamma)$ in terms of a future complete curve γ , it represents a future infinity point and called a ∞ -TIP. The other TIPs are called *singular TIPs* and represent the singularities of the spacetime. Similarly by replacing I^- by I^+ , IFs, PIFs, TIFs and others are defined. The set of all ∞ -TIPs and ∞ -TIFs is called *the causal boundary* of M and denoted by ∂M . In the weakly asymptotically simple and empty spacetime ∂M has two disconnected components \mathcal{I}^+ and \mathcal{I}^- , which are a future and a past set, respectively, and both are diffeomorphic to $S^2 \times \mathbb{R}$. The union of M and ∂M is denoted by \bar{M} .

A singular TIP X in a weakly asymptotically simple and empty spacetime M is said to be *nakedly singular* if $X \subset J^-(\mathcal{I}^+, \bar{M}) \cap M$ and $X \subset I^-(p)$ for some point $p \in \overline{J^-(\mathcal{I}^+, \bar{M})} \cap M$. A nakedly singular TIP X is further said to be of *strong curvature type* if for any null geodesic

generator γ of $\dot{X} \neq \emptyset$ and for any null geodesic congruence around γ and for any point p on γ , there exists a point $q \in \gamma \cap I^+(p)$ such that $\theta(q) < 0$ where θ is the expansion rate of the congruence. A spacetime is said to satisfy *the strong curvature condition* if all the naked singular TIPs are of strong curvature type, to satisfy *the simplicity condition* if for any naked singular TIP X there exists a null geodesic generator γ of \dot{X} such that there exist a sequence γ_i of achronal null geodesics to I^+ which converge to γ , and to satisfy *the trapped surface condition* if for any naked singular TIP X there exists a trapped surface T such that $T \cap \bar{X} \cap I^+(S) \neq \emptyset$.

A spacetime M is said to be *regular partially future asymptotically predictable* from a partial Cauchy surface S if $I^+ \subset J^+(S, \bar{M})$, $\overline{D^+(S, \bar{M})} \cap \lambda \neq \emptyset$ for any null geodesic generator λ of I^+ , and for any past inextendible non-spacelike curve γ in $J^+(S)$ there exists a point $s \in S$ such that $\gamma \subset I^+(s)$. These conditions say that the partial Cauchy surface S is visible from the future infinity and the singularities are located in the future of S .

In terms of these definitions Krolak's theorem on the weak cosmic censorship is expressed as follows[Kro86]:

Theorem 10 (Krolak1986) *Let M be a regular partially future asymptotically predictable from a asymptotically regular partial Cauchy surface S . Then M is future asymptotically predictable from S if the following three conditions are satisfied:*

- 1) *The null-convergence condition holds.*
- 2) *The strong causality condition holds.*
- 3) *Either a) the simplicity condition and the strong curvature condition or b) the trapped surface condition is satisfied.*

A partial Cauchy surface S is said to be *properly separated* from $H^+(S)$ if the causal simplicity fails on a null geodesic generator γ of $H^+(S)$ in the past of some point $p \in \gamma$, and $J^-(p)$ has a future inextendible generator λ such that $\lambda \cap I^+(S) \neq \emptyset$. Further a spacetime is said to be *future nakedly singular relative to S* if λ is future incomplete and γ is past incomplete.

Krolak recently proved that the strong cosmic censorship holds for strong curvature singularities if the partial Cauchy surface is properly separated from its Cauchy horizon[Kro92]:

Theorem 11 (Krolak1992) *A spacetime cannot be future naked relative to a partial Cauchy surface S if S is properly separated from $H^+(S)$ and the following three conditions are satisfied:*

- 1) *the null-convergence condition,*
- 2) *the strong causality condition,*
- 3) *the strong curvature condition.*

References

- [AMT72] Anderson, T.L. , Morgan, T.A. , and Thorne, K.S. Gravitational collapse of counter-rotating dust cylinders. *Bull. Am. Phys. Soc.*, 2-17:516, 1972.
- [BE81] Beem, J.K. and Ehrlich, P.E. *Global Lorentzian Geometry*. Marcel Dekker, New York, 1981.
- [BIL91] Barrabès, C. , Israel, W. , and Letelier, P.S. *Phys. Lett. A*, 160:41, 1991.
- [BIL92] Barrabès, C. , Israel, W. , and Letelier, P.S. *Phys. Lett. A*, 161:562(E), 1992.
- [BMO88] Bizon, P. , Malec, E. , and O'Murchadha, N. *Phys. Rev. Lett.*, 61:1147, 1988.
- [Bo92] Barrabès, C. and others. Geometric inequalities and the hoop conjecture. *Class. Quantum Grav.*, 9:L105–L110, 1992.
- [Bor87] Borde, A. *Class. Quantum Grav.*, 4:343, 1987.
- [CFS92] Chinea, F.J. , Fernández-Jambrina, L. , and Senovilla, J.M.M. Singularity-free space-time. *Phys. Rev. D*, 45:481–486, 1992.
- [Chr84] Christodoulou, D. Violation of cosmic censorship in the gravitational collapse of a dust cloud. *Comm. Math. Phys.*, 93:171–195, 1984.
- [Cla73] Clarke, C.J.S. Local extensions in singular space-times. *Comm. Math. Phys.*, 32:205–214, 1973.
- [Cla75] Clarke, C.J.S. Singularities in globally hyperbolic space-time. *Comm. Math. Phys.*, 41:65–78, 1975.
- [Cla76] Clarke, C.J.S. Space-time singularities. *Comm. Math. Phys.*, 49:17–23, 1976.
- [Cla79] Clarke, C. The nature of singularities. *Gen. Rel. Grav.*, 10:999–1002, 1979.
- [Cla87] Clarke, C.J.S. Report on the symposium on asymptotia, singularities and global structure. In MacCallum, M.A.H., editor, *Proc. 11th GRG*, pages 291–297, Cambridge Univ. Press, 1987.
- [Ell79] Ellis, G.F.R., editor. *Gen. Rel. Grav. 10, Proc. GRG8 symposium on Singularities in General Relativity*, Plenum, 1979.
- [ES77] Ellis, G.F.R. and Schmidt, B.G. Singular space-times. *Gen. Rel. Grav.*, 8:915–954, 1977.
- [Fla92] Flanagan, E. Trapped surfaces in nonspherical initial data sets and the hoop conjecture. *Phys. Rev. D*, 46:1429–1439, 1992.
- [Ger68] Geroch, R. What is a singularity in general relativity? *Ann. Phys.*, 48:526–540, 1968.

- [Ger71] Geroch, R. Space-time structure from a global viewpoint. In Sachs, R., editor, *General Relativity and Cosmology, Proc. Int. School in Physics, Enrico Fermi Course XLVII*, pages 71–99, Academic Press, 1971.
- [Gib84] Gibbons, G.W. In Willmore, T.J. and Hitchin, N.J., editors, *Global Riemannian Geometry*, page , Ellis Horwood, Chichester, 1984.
- [GKP72] Geroch, R. , Kronheimer, E.H. , and Penrose, R. Ideal points in space-time. *Proc. R. Soc. London A*, 327:545–567, 1972.
- [Haw67] Hawking, S. The occurrence of singularities in cosmology iii. *Proc. R. Soc. London A*, 300:187–201, 1967.
- [HE68] Hawking, S.W. and Ellis, G.F.R. The cosmic black-body radiation and the existence of singularities in our universe. *Astrophys. J.*, 152:25–36, 1968.
- [HE73] Hawking, S.W. and Ellis, G.F.R. *The Large Scale Structure of Space-time*. Cambridge Univ. Press, Cambridge, 1973.
- [HKM77] Hughes, T.J.R. , Kato, T. , and Marsden, J.E. Well posed quasi-linear second-order hyperbolic systems with application to nonlinear elastodynamics and general relativity. *Arch. Rat. Mech. Anal.*, 63:273–294, 1977.
- [Hol86] Hollier, G.P. Papapetrou’s naked singularity is a strong curvature singularity. *Class. Quantum Grav.*, 3:L111–L114, 1986.
- [HP70] Hawking, S.W. and Penrose, R. The singularities of gravitational collapse and cosmology. *Proc. R. Soc. London A*, 314:529–548, 1970.
- [Kan91] Kannar, J. *Class. Quantum Grav.*, 8:L179, 1991.
- [Kro86] Krolak, A. Towards the proof of the cosmic censorship hypothesis. *Class. Quantum Grav.*, 3:267–280, 1986.
- [Kro92] Krolak, A. Strong curvature singularities and causal simplicity. *J. Math. Phys.*, 33:701–704, 1992.
- [Kur84] Kuroda, Y. *Prog. Theor. Phys.*, 72:63–72, 1984.
- [Lak88] Lake, K. Comments on “naked singularities in self-similar spherical gravitational collapse”. *Phys. Rev. Lett.*, 60:241, 1988.
- [Mal91a] Malec, E. *Acta Phys. Pol. B*, 22:829, 1991.
- [Mal91b] Malec, E. Hoop conjecture and trapped surfaces in nonspherical massive systems. *Phys. Rev. Lett.*, 67:949–952, 1991.
- [Mis63] Misner, C. The flatter regions of newmann, unti and tambrino’s generalized schwarzschild space. *J. Math. Phys.*, 4:924–937, 1963.

- [Mis67] Misner, C.W. Taub-nut space as a counterexample to almost anything. In Ehlers, J., editor, *Relativity Theory and Astrophysics: I. Relativity and Cosmology*, Amer. Math. Soc. Lec. in Appl. Math., vol.8, page , American Mathematical Society, 1967.
- [MT69] Misner, C.W. and Taub, A.H. A singularity free empty universe. *Sov. Phys.—JETP*, 28:122–133, 1969.
- [MYS74] Müller zum Hagen, H. , Yodzis, P. , and Seifert, H.J. On the occurrence of naked singularities in general relativity. ii. *Comm. Math. Phys.*, 37:29–40, 1974.
- [New86] Newman, R.P.A.C. Strengths of naked singularities in tolmán-bondi spacetimes. *Class. Quantum Grav.*, 3:527–539, 1986.
- [NST88] Nakamura, T. , Shapiro, S.L. , and Teukolsky, S.A. Naked singularities and the hoop conjecture: an analytic exploration. *Phys. Rev. D*, 38:2972–2978, 1988.
- [Omu86] O'murchadha, N. *Phys. Rev. Lett.*, 57:2466, 1986.
- [OP87] Ori, A. and Piran, T. Naked singularities in self-similar spherical gravitational collapse. *Phys. Rev. Lett.*, 59:2137–2140, 1987.
- [Pap85] Papapetrou, A. In Krishna-Rao, J., editor, *A random walk in general relativity*, page , Wiley Eastern, New Delhi, 1985.
- [Pen65] Penrose, R. Gravitational collapse and space-time singularities. *Phys. Rev. Lett.*, 14:57–59, 1965.
- [Pen68] Penrose, R. Structure of space-time. In DeWitt, C.M. and Wheeler, J.A., editors, *Battelle Rencontres 1967*, Lectures in Mathematics and Physics, pages 121–235, W.A. Benjamin, New York, 1968.
- [Pen69] Penrose, R. Gravitational collapse: the role of general relativity. *Riv. Nuovo Cimento*, 1:252–276, 1969.
- [Pen79] Penrose, R. Singularities and time asymmetry. In Hawking, S.W. and Israel, W., editors, *General Relativity: An Einstein Centenary Survey*, pages 531–638, Cambridge Univ. Press, Cambridge, 1979.
- [Ray55] Raychaudhuri, A.K. Relativistic cosmology. *Phys. Rev.*, 98:1123–1126, 1955.
- [Ray57] Raychaudhuri, A.K. Singular states in relativistic cosmology. *Phys. Rev.*, 106:172–173, 1957.
- [RS75] Ryan, M.P. and Shapley, L.C. *Homogeneous Relativistic Cosmologies*. Princeton Univ. Press, Princeton, 1975.
- [Sch71] Schmidt, B.G. A new definition of singular points in general relativity. *Gen. Rel. Grav.*, 1:269–280, 1971.
- [Sch72] Schmidt, B.G. Local completeness of the b-boundary. *Comm. Math. Phys.*, 29:49–54, 1972.

- [Sei83] Seifert, H.-J. Black holes, singularities, and topology. In Schmutzer, E., editor, *Proc. 9th GRG*, pages 133–147, Cambridge Univ. Press, 1983.
- [Sen90] Senovilla, J.M.M. New class of inhomogeneous cosmological perfect-fluid solutions without big-bang singularity. *Phys. Rev. Lett.*, 64:2219–2221, 1990.
- [ST91] Shapiro, S.L. and Teukolsky, S.A. Formation of naked singularities: the violation of cosmic censorship. *Phys. Rev. Lett.*, 66:994–997, 1991.
- [ST92] Shapiro, S.L. and Teukolsky, S.A. Gravitational collapse of rotating spheroids and the formation of naked singularities. *Phys. Rev. D*, 45:2006–2012, 1992.
- [SY83] Schoen, R. and Yau, S.-T. *Comm. Math. Phys.*, 90:575, 1983.
- [Sze75] Szekeres, P. Quasispherical gravitational collapse. *Phys. Rev. D*, 12:2941–2948, 1975.
- [TCE80] Tipler, F.J. , Clarke, C.J.S. , and Ellis, G.F.R. Singularities and horizons — a review article. In Held, A., editor, *General Relativity and Gravitation, vol.2*, pages 97–206, Plenum Press, 1980.
- [Tho72] Thorne, K.S. In Klauder, J., editor, *Magic without Magic*, page , Freeman, San Francisco, 1972.
- [Tip76] Tipler, F.J. Causality violation in asymptotically flat space-times. *Phys. Rev. Lett.*, 37:879–882, 1976.
- [Tip77] Tipler, F.J. Singularities and causal violation. *Ann. Phys.*, 108:1–36, 1977.
- [Tip78] Tipler, F.J. Energy conditions and spacetime singularities. *Phys. Rev. D*, 17:2521–2528, 1978.
- [Tod92] Tod, K.P. The hoop conjecture and the gibbons-penrose construction of trapped surfaces. *Class. Quantum Grav.*, 9:1581–1591, 1992.
- [Wal84] Wald, R.M. *General Relativity*. Univ. Chicago Press, Chicago, 1984.
- [YSM73] Yodzis, P. , Seifert, H.J. , and Müller zum Hagen, H. On the occurrence of naked singularities in general relativity. *Comm. Math. Phys.*, 34:135–148, 1973.

Compactification of 3D Homogeneous Spaces*

Yoshihisa FUJIWARA†

Department of Fundamental Sciences, FIHS, Kyoto University, Kyoto, Japan

1. Introduction and Summary

It has been many times mentioned and studied from different viewpoints that topology of space or space-time may cause some significant role in classical and quantum gravity. (An earlier view is lucidly described in [2]. And the reader can find related topics, also in this conference; see *e.g.*, M. Seriu, T. Koike, M. Tanimoto in this volume.) In order to understand such aspects of gravity it is important to investigate global dynamics of gravity which is closely related with topology and global geometry of space or space-time.

The standard canonical formalism of general relativity treats a space-time as a dynamical deformation of a spacelike hypersurface and its three-dimensional geometry under an appropriate gauge condition. One needs to know what are the dynamical degrees of freedom of three-dimensional geometry and how they evolve in time, in order to study such global aspects of classical and quantum gravity. Though it is not an easy problem, one can consider several toy models, one of which is (2+1)-dimensional gravity [3][4][5]. The basic reason why it serves as an interesting model is that, in (2+1)-dimensional space-time, there are no local gravitational-wave modes that is of little interest for study of global dynamics. Instead one has global dynamical modes that are related to the so-called “moduli” of a 2-manifold representing spacelike hypersurface. By global dynamics in gravity, we mean such dynamical degrees of freedom whose presence essentially depends on topology of spatial manifold. One can explicitly examine classical and quantum gravity in this (2+1)-dimensional gravity in the case that spatial 2-manifold is a torus, for example.

When one proceeds to consider the real life of (3+1)-dimensional gravity, it should be

* This is based on the work [1] by Y. F., Hideki Ishihara and Hideo Kodama.

† Supported in part by JSPS Fellowships for Japanese Junior Scientists.

first made clear what is global dynamics in $(3+1)$ -dimension. It seems not so easy, as in the $(2+1)$ -dimensional case, to define global deformation of three-dimensional spatial manifold in the full dynamics of $(3+1)$ -dimensional gravity. Especially we have no idea whether one is able to extract global dynamics in arbitrary inhomogeneous geometries and how the nonlinear coupling between such global dynamical degrees of freedom and local gravitational-wave modes or some matter fields can be disentangled and solved. As a first step towards the understanding of such problems, we restrict our attention to a locally homogeneous manifold, or the spatially homogeneous cosmology. That is, the so-called Bianchi model, well known in general relativity, which has been widely studied by many people (see [6][7] for example). In the model, a space-time is assumed to have symmetry, namely spatially homogeneity. Since the gravitational degrees of freedom are reduced to be finite in this model, it gives an appropriate system for us to understand the full complexity of the Einstein equations and physical cosmology described by it.

In this talk, we study Bianchi model whose homogeneous spatial hypersurfaces are compact without boundary, i.e. closed. Space-time will be therefore assumed to be a product of a closed 3-manifold and a (portion of) real line. First of our purposes is to make clear the relation between the Bianchi type symmetry of space-time and spatial compactness from geometrical viewpoint. By doing it we would like to show some interesting kinematical properties intrinsic to such closed Bianchi models. Some of them were mentioned in some works by other people, but under somewhat restrictive conditions. We do not assume such restrictions in our geometrical argument and shall make clear some points unnoticed in the literature. And, in order to show them, we utilize a recent mathematical result on three-dimensional manifold by Thurston and others. This is the second purpose of this talk, because this mathematical stuff seems to be significant for future investigation in the line described above. It might also serves as a useful tool in other fields in general relativity. Finally we comment on how one can define global dynamics in such spatially homogeneous models.

2. Locally Homogeneous Spaces and Bianchi Cosmology

Let us begin with a general description of homogeneity in geometry. A Riemannian manifold (M, g) is defined to be *locally homogeneous*, if for every pair of points $x, y \in M$ there are neighborhoods U and V of x and y , for which there exists a local isometry mapping (U, x) to (V, y) . Such local isometries do not, in general, extend to isometries of the whole (M, g) .

Let us denote the *full* group of isometries of (M, g) by $\text{Isom}(M, g)$. Then if for every pair of points $x, y \in M$ there is an isometry $\Phi \in \text{Isom}(M, g)$ such that $\Phi(x) = y$, that is, $\text{Isom}(M, g)$ acts transitively on M , one says that (M, g) is (*globally*) *homogeneous*. Since it is a standard fact that a simply-connected and locally homogeneous manifold is globally homogeneous, the universal covering space $(\widetilde{M}, \widetilde{g})$ of a locally homogeneous manifold (M, g) must be homogeneous. For our convenience, we shall say that a homogeneous manifold (M, g) is *simply homogeneous* if $\text{Isom}(M, g)$ has a three-dimensional subgroup G_3 that acts *simply-transitively* on M . In that case, we call the G_3 a *homogeneity group*. If the universal covering space of a locally homogeneous manifold is simply homogeneous with a homogeneity group G_3 , then we shall call it a locally homogeneous manifold with a homogeneity group G_3 .

The usual Bianchi model starts with the following assumptions for spatial homogeneity. A three-dimensional Lie group G_3 acts on a space-time as a group of isometries of the space-time, such that each orbit is a spacelike hypersurface Σ on which G_3 acts *simply-transitively*. The space-time considered is topologically a product space $\Sigma \times \mathbb{R}$. We have a family of 3-manifolds $(\Sigma, g(t))$ for each $t \in \mathbb{R}$, where g is the spatial metric intrinsic to Σ . Then it follows that G_3 acts simply-transitively on each $(\Sigma, g(t))$ as a group of isometries of $(\Sigma, g(t))$. In the above terms, $(\Sigma, g(t))$ is simply homogeneous.

Such a Riemannian manifold is well understood in the context of Bianchi cosmology. (See [6][7] for references and complete information on the definitions and the notations below.) Denote by C_{IJ}^K ($I, J, K = 1 \sim 3$) the structure constant of the Lie algebra of G_3 with respect to a certain basis $\{\xi_I\}$: $[\xi_I, \xi_J] = C_{IJ}^K \xi_K$. Then there *globally* exists on M an invariant basis $\{X_I\}$ which one can choose so that

$$[X_I, X_J] = -C_{IJ}^K X_K, \quad (1)$$

and its invariant dual basis $\{\chi^I\}$ which satisfies the Maurer-Cartan equation

$$d\chi^I = \frac{1}{2} C_{JK}^I \chi^J \wedge \chi^K. \quad (2)$$

The metric g on M can be expressed in terms of χ^I as

$$ds^2 = g_{IJ} \chi^I \chi^J, \quad (3)$$

where g_{IJ} is a nonsingular constant matrix. Thus the Riemannian metric of a simply homogeneous manifold can be completely specified by the Lie algebra of G_3 and a constant matrix

g_{IJ} .

The three-dimensional real Lie algebras are completely classified into the well-known Bianchi types. They are denoted as I, II, III, IV, V, VI(A), VII(A), VIII and IX. Here VI(A) and VII(A) are one-parameter families of algebras and III is isomorphic to VI(A = 1). They are subdivided into class A and B according to whether the trace of the structure constant $a_I \equiv \frac{1}{2} C_{IJ}^I$ has a vanishing norm $(\delta^{IJ} a_I a_J)^{1/2}$ or not. Class A consists of I, II, VI(0), VII(0), VIII and IX, while the other types, IV, V, III=VI(1), VI(A \neq 0), VII(A \neq 0) belong to class B.

For a given Bianchi Lie algebras I~IX, there exists a unique (up to a constant matrix g_{IJ}) *simply-connected* Riemannian manifold M diffeomorphic to a simply-connected Lie group G which is uniquely determined by the given algebra. G is then a group of isometries acting simply-transitively on M . Therefore, for a simply-connected and simply homogeneous manifold with a homogeneity group G_3 , its topology is determined by the Bianchi type of the Lie algebra of G_3 while its metric is given by (3). Especially, M is diffeomorphic to either \mathbf{R}^3 or S^3 depending on whether G_3 is of the type I~VIII or IX respectively.

However, it is not adequate for a general study of spatially homogeneous space-times to restrict only on those simply homogeneous manifolds as spatial homogeneous sections. In fact, when one can construct a compact manifold by identifying certain points in a simply homogeneous manifold, it usually lowers the dimension of the group of isometries so that the resulting manifold is not simply homogeneous any longer. For example, it can be shown that a homogeneous spatial section in every class B Bianchi model cannot be simply homogeneous if it is compact (see [13][1] for it). More simple example which is easily understood and appealing to one's vision is given in the following drawing. They are a 3-torus (Fig. 1) and a "twisted" 3-torus (Fig. 2). With a standard flat metric on each 3-manifold, the former is simply homogeneous while the latter is not. Note that one can cut the twisted torus and glue two such cutted pieces to obtain a torus (in other words, a torus is a double covering space of a twisted torus). 3-torus is simply homogeneous, but the twisted 3-torus is not.

Therefore we should also include in our consideration a locally homogeneous manifold whose universal covering space is simply homogeneous. More explicitly, we shall consider a wider class of spatially homogeneous space-times as follows. A three-dimensional Lie group G_3 is now assumed to act on the *universal covering space* of a space-time as a group of isometries, such that each orbit is a spacelike hypersurface $\tilde{\Sigma}$ on which G_3 acts simply-transitively. Then

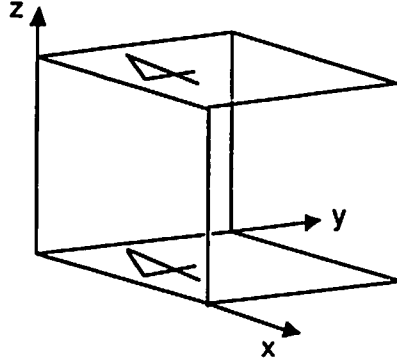


Figure 1. A torus constructed by identifying three pairs of opposite faces of a cube which is embedded in Euclidean space. Each pair is identified by one of three translations in the direction x , y or z . (For example, see a letter “4” on the top and bottom faces identified by z -translation.) Since it is clear that the three independent periodic translations are global (continuous) isometries of the torus, it is a simply homogeneous space. In fact, $\text{Isom}(M, g)$ is isomorphic to $S^1 \times S^1 \times S^1 \times (\text{discrete group})$ as a group.

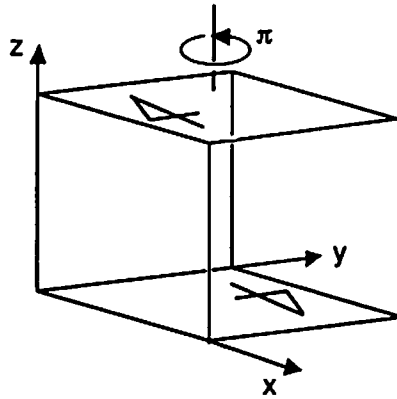


Figure 2. A “twisted” torus constructed by identifying three pairs of opposite faces of a cube in Euclidean space. The identification is the same as above except that one pair of opposite faces is identified by a translation with a twist involved. In the figure, it is z -translation with a half of full turn along z axis (see a letter “4” on the top and bottom faces identified by it). It can be observed that only z -translation survives as a global (continuous) isometry of this twisted torus. Therefore it is not a simply homogeneous space. In fact, $\text{Isom}(M, g)$ is isomorphic to $S^1 \times (\text{discrete group})$ as a group.

G_3 acts simply-transitively on each $\tilde{\Sigma}$ as a group of isometries of $\tilde{\Sigma}$, so the underlying manifold Σ is a locally homogeneous manifold with a homogeneity group G_3 . We will concentrate on the study of Σ in the following, which is denoted by (M, g) . Henceforth we assume that M is closed.

Let us now study in general a locally homogeneous 3-manifold (M, g) with a homogeneity group G_3 . Consider its universal covering space (\tilde{M}, \tilde{g}) with a covering map p . A covering transformation is a homeomorphism $\gamma: \tilde{M} \rightarrow \tilde{M}$ such that $p \circ \gamma = p$. The set of covering transformations is a group under composition, which is called a covering transformation group Γ . Because in this case Γ is a discrete subgroup of $\text{Isom}(\tilde{M}, \tilde{g})$, acting freely and properly discontinuously on \tilde{M} , M is isometric to the quotient space \tilde{M}/Γ . Thus in order to study M one has to examine Γ and \tilde{M} . \tilde{M} is, as shown above, simply homogeneous so that its structure is determined by the homogeneity group G_3 . Note that G_3 is in general a subgroup of $\text{Isom}(\tilde{M}, \tilde{g})$. In what follows, we will classify all the possible geometries of (\tilde{M}, \tilde{g}) by employing a modern viewpoint of “geometry” and show some relations between those geometries and the Bianchi types. How one can choose Γ to obtain a compact locally homogeneous manifold $M \cong \tilde{M}/\Gamma$ depends on each class of geometry.

3. Thurston's Eight Geometries

In a modern approach, “geometry” can be viewed in the following way (see [8][9][10], for example). Suppose that X is a manifold and G is a group acting on X . G is assumed to act transitively on X with compact point stabilizer (the isotropy subgroup of G at any point of X is compact). Then a “geometry” is the pair (X, G) and the properties of X invariant under the action of G . One can recover the ordinary viewpoint of differential geometry by finding a G -invariant metric on X . (Its existence is guaranteed since G 's stabilizer is compact at every point. And as G acts transitively on X , the metric is complete.) In general, there would be many different G -invariant metrics on X so that X can have a variety of properties. For instance, as is easily seen from above, the universal covering (\tilde{M}, \tilde{g}) of a locally homogeneous (M, g) and its isometry group $\text{Isom}(\tilde{M}, \tilde{g})$ are an example of (X, G) .

Thurston [9] classified all the three-dimensional geometries under the following restrictions. In this classification, two geometries (X, G) and (X', G') are defined to be equivalent if there is a diffeomorphism of X with X' which casts the action of G on X onto that of G' on X' .

First of all, X is assumed simply-connected for one can always study universal covering spaces if necessary. Secondly, we restrict ourselves to the case that G is maximal. It means that when two groups G_1 and G_2 such that $G_1 \subset G_2$ can both act on X , one should take G_2 as G . In our consideration above, $G = \text{Isom}(\widetilde{M}, \widetilde{g})$ is maximal when one chooses \widetilde{g} appropriately by changing g_{IJ} in the metric (3) so that the full isometry group $\text{Isom}(\widetilde{M}, \widetilde{g})$ becomes maximum. So, for example, (E^3, \mathbf{R}^3) is out of consideration, where E^3 is the Euclidean space and \mathbf{R}^3 acts on it as translations. Rather, one should take the full isometry group of E^3 , namely the three-dimensional Euclidean group $E(3)$, as G . Finally, it is assumed that G has a subgroup Γ which acts on X as a covering group so that X/Γ becomes compact. Then the geometry is said to admit a compact quotient. Now the Thurston's theorem can be stated as follows:

Theorem. *Any maximal and simply-connected three-dimensional geometry which admits a compact quotient is equivalent to one of the eight geometries $(X, \text{Isom}X)$ described below.*

- (i) $X = S^3$, the spherical geometry. $\text{Isom}X = SO(4)$.
- (ii) $X = E^3$, the Euclidean geometry. $\text{Isom}X = E(3)^+$.
- (iii) $X = H^3$, the hyperbolic geometry. $\text{Isom}X = PSL(2, \mathbf{C})$.
- (iv) $X = S^2 \times E^1$. $\text{Isom}X = (\text{Isom}S^2 \times \text{Isom}E^1)^+$.
- (v) $X = H^2 \times E^1$. $\text{Isom}X = (\text{Isom}H^2 \times \text{Isom}E^1)^+$.
- (vi) $X = \widetilde{T_1(H^2)}$, the universal covering space of unit tangent space of H^2 . $\text{Isom}X = \text{Isom}H^2 \times \mathbf{R}$.
- (vii) $X = Nil$, the Heisenberg group.
- (viii) $X = Sol$, a solvable three-dimensional Lie group.

Some remarks follow. Here $\text{Isom}X$ means only orientation preserving isometries. Γ should be a discrete subgroup of this $\text{Isom}X$ in order that X/Γ be orientable. The isometries corresponding to (vii) and (viii) are omitted. The dimension of $\text{Isom}X$ is 6 for (i)~(iii), 4 for (iv)~(vii), and 3 for (viii). Nil and Sol spaces are three-dimensional Lie groups whose Lie algebra is of Bianchi type II and VI(0) respectively. $\widetilde{T_1(H^2)}$ is equivalent to $\widetilde{SL_2}\mathbf{R}$ which can be also regarded as the universal covering of the Lie group of Bianchi type VIII. Final remark is that all the possibilities of a compact quotients are known for all the classes except the hyperbolic geometry (iii). For complete information, the reader should refer to [9][10].

We would like to comment on how such a classification has a great significance in studying topology of 3-manifold. Let us consider a three-dimensional manifold M which is assumed to be orientable and compact without boundary for simplicity. M has no Riemannian metric a priori. In order to examine the topology of M ,

1. first decompose it into prime manifolds. Denoting the connected sum of two manifolds M_1 and M_2 by $M_1 \# M_2$, then a 3-manifold is called *prime* if any expression M as $M_1 \# M_2$ implies M_1 or M_2 being homeomorphic to S^3 . (For example, S^3 and T^3 are prime manifolds.) It is shown that M can be expressed as a finite connected sum of prime manifolds and that the pieces of prime manifolds are unique.
2. Let us then consider prime manifolds M .
 - a. The fundamental group $\pi_1(M)$ is a finite group. (e.g. $\pi_1(S^3)$ is trivial.) It is a conjecture that such M admits a geometry modelled on S^3 . It should be mentioned that this conjecture contains the famous Poincaré conjecture as a corollary.
 - b. $\pi_1(M)$ is an infinite group. (e.g. $\pi_1(T^3)$ is isometric to $\mathbb{Z} \times \mathbb{Z} \times \mathbb{Z}$ as a group.)
 - b1. One class of such M admits a non-separating embedded 2-sphere in it. Since M is prime, any separating 2-sphere (i.e. which separates M into two disconnected pieces) bounds a 3-ball. Observe that $S^2 \times S^1$ admits a non-separating 2-sphere. M is said *irreducible* if it is prime and does not possess any non-separating sphere. In fact, $S^2 \times S^1$ is the only example which is not irreducible. Clearly $S^2 \times S^1$ admits a geometric structure modelled on $S^2 \times E^1$.
 - b2. Now remains the other class, namely, irreducible manifolds with infinite $\pi_1(M)$. Decompose it further into a finite number of smaller pieces by cutting M along 2-tori which are disjoint, two-sided incompressible[†]. (In the special case that M is a torus bundle of S^1 of a certain type, M itself admits *Sol* geometry without doing this torus decomposition.) This decomposition is unique in a sense. The resulting each piece is either a *Seifert fiber space* or a manifold with no embedded incompressible torus within it (or sometimes both). A Seifert fiber space is a 3-manifold which is a union of disjoint circles S^1 in a particular way. All the Seifert fiber spaces are divided into six classes of the eight geometries stated

† A two-sided 2-surface N is said *incompressible* if every simple curve on N which bounds a 2-disk in M with interior disjoint from N also bounds a 2-disk on N itself.

above, i.e. except H^3 and *Sol*, according to which geometries they admit. Thus one has to consider an irreducible 3-manifold with no embedded incompressible torus. If it belongs to a class called Haken manifolds* and is not a Sifert fiber space, then it is a theorem that it possesses hyperbolic geometry H^3 . If it is not a Haken manifold, it is a conjecture that such a manifold is a Sifert fiber space or admits hyperbolic structure.

In summary, the Geometrization Conjecture asserts that any closed 3-manifold can be decomposed into a finite number of pieces in a canonical way, each of which admits one of the eight geometries. Since it can be shown that each of these geometric pieces admits one and only one geometry and every topology of them is known except for H^3 . In order to study global dynamics in gravity and to make clear the interplay between it and the topology of space or space-time, one has to know *what is the possible topology of 3-manifolds*. The answer to this question is given by this Geometrization Conjecture if its assertion is really the case.

4. Some Kinematical Properties of Closed Bianchi Models

Returning to our study of locally homogeneous manifolds, we recall that the homogeneity group G_3 is assumed to be a subgroup of $\text{Isom}(\widetilde{M}, \widetilde{g})$ for any metric of the form (3). Since in the Thurston's classification $G = \text{Isom}(\widetilde{M}, \widetilde{g})$ must be maximal, G_3 is a subgroup of G which belongs to one of the eight classes. From this we can deduce two interesting consequences.

(A) No anisotropic expansion is allowed for Bianchi model V with a closed spatial section.

Consider the universal covering space $(\widetilde{M}, \widetilde{g})$ of a closed spatial section that is a locally homogeneous spacelike hypersurface in Bianchi V space-time. Since $(\widetilde{M}, \widetilde{g})$ is simply homogeneous, the metric \widetilde{g} is of the form (3). According to Milnor [11](Special Example 1.7), for the Lie algebra of Bianchi type V, $(\widetilde{M}, \widetilde{g})$ is necessarily isometric to a maximally symmetric space with a negative constant curvature of a certain magnitude, whatever one chooses as g_{IJ} in (3). Equivalently, $(\widetilde{M}, \widetilde{g})$ is always the hyperbolic geometry (iii) in the above classification. This fact means that each locally homogeneous spacelike hypersurface in Bianchi V space-time is locally isometric to a negative constant curvature space. But it does not immediately imply that anisotropic expansion is impossible (e.g. it does not for Bianchi I model whose homogeneous spatial section

* A 3-manifold is called a *Haken manifold* if it is prime and contains a two-sided incompressible 2-surface which is not a S^2 .

is flat). For there possibly remains a continuous choice of the covering transformation group Γ for constructing $M \cong \widetilde{M}/\Gamma$. In other words, we may have the freedom of “moduli” of a closed manifold. However, no such freedom arises in this hyperbolic geometry due to the Mostow rigidity theorem (see [8][9]). The theorem asserts that if two closed manifolds with hyperbolic geometry are homeomorphic to each other, they are actually isometric to each other. So a Bianchi V homogeneous universe is rigid allowing only a change of overall scale factor. Thus the proposition was proved.

(B) Bianchi IV and VI ($A \neq 0, 1$) with a closed spatial section does not exist.

The proof is easy. The homogeneity group must be a subgroup of one of the eight isometry groups in the classification. However, it cannot be for the homogeneity group of Bianchi type IV or VI ($A \neq 0, 1$), as is explicitly shown by examining the Lie algebras of them and the above eight classes. Therefore, no closed Bianchi IV and VI ($A \neq 0, 1$) exists.

We can proceed further and study the correspondence between the Bianchi models and the Thurston’s eight geometries. The result is summarized in Table 1 and Table 2. This can be obtained from the consideration of the proof of the Thurston’s classification theorem [10]. From the table it can be seen that a closed locally homogeneous manifold with the homogeneity group VII ($A \neq 0$) admits the hyperbolic geometry as the case of V so that no anisotropic expansion is admitted also for this type VII ($A \neq 0$). Also note that the geometry of (iv) $S^2 \times E^1$ corresponds to the Kantowski-Sachs model, rather than the Bianchi models considered here.

Essentially the same correspondence between the Thurston’s classification and the Bianchi types was presented by Fagundes [12]. The fact (B) was also mentioned in it. However, it was assumed that the covering transformation group Γ is always a discrete subgroup of the homogeneity group G_3 . (This is not true in general in our assumptions, and causes a substantial difference for class B models as is explained below.) And our approach here is a group theoretical one which clarifies the relation among G_3 , Γ and the eight maximal groups in the Thurston’s classification. Such an approach is also useful in studying under what conditions class B Bianchi models can be compactified. (An interested reader can find it in [1].) Related is a more general study of Bianchi cosmology with compact spatial sections, by Ashtekar and Samuel [13]. The compactification problem is connected to the absence of general scheme of variational principle [14] where one imposes the spatial homogeneity before taking variation of an action.

Bianchi Type	Geometry	Isotropy	Bianchi Type	Geometry	Isotropy
Class A			Class B		
I	R^3	e	III=VI(1)	$H^2 \times E^1$	$SO(2)$
	$E^2 \times R$	$SO(2)$		$\widetilde{SL_2}R$	$SO(2)$
	E^3	$SO(3)$	IV	—	
II	Heisenberg G	e	V	H^3	$SO(3)$
	Nil	$SO(2)$	VI(A \neq 0,1)	—	
VI(0)	Sol=E(1,1)	e	VII(A \neq 0)	H^3	$SO(3)$
VII(0)	$E(2)$	e			
	E^3	$SO(3)$			
VIII	$\widetilde{SL_2}R$	e			
	$\widetilde{SL_2}R$	$SO(2)$			
IX	$SU(2) \approx S^3$	e			
	$SU(2) \approx S^3$	$SO(2)$			
	S^3	$SO(3)$			

Table 1: Geometry of the compactified Bianchi type

Thurston Type	Bianchi Type	
	Class A	Class B
E^3	I, VII(0)	
H^3		V, VII(A \neq 0)
S^3	IX	
$S^2 \times E^1$	—	—
$H^2 \times E^1$		III=VI(1)
$\widetilde{SL_2}R$	VIII	III=VI(1)
Nil	II	
Sol	VI(0)	

Table 2: The correspondence between the Thurston type and the Bianchi type

5. Concluding Remark

Finally we would like to briefly comment on how such study of closed Bianchi models can be used to investigate global dynamics in $(3+1)$ -dimensional gravity.

As explained in the first section, it should be first made clear what is global dynamics in $(3+1)$ -dimension. Since, in contrast such a $(2+1)$ -dimensional gravity model, one has to treat both the local gravitational-wave modes and global modes which are nonlinearly coupled with each other, one has no apparent way to extract the global dynamics out of the full $(3+1)$ -dimensional gravity. As a first step to understand it, we restricted our attention to spatially homogeneous space-times. As we have observed, each spatially homogeneous space is a locally homogeneous manifold which can be recovered from its universal covering space as a quotient space. This is in the same situation as one could define “moduli” of a closed 2-manifold. Especially one can describe how global modes can be incorporated and expressed into the dynamical variable, i.e. spatial 3-metric by examining the construction of a closed 3-manifold out of the universal covering space in a concrete way. But since the universal covering space is not always a maximally symmetric space as we saw in Thurston’s theorem, it is necessary to distinguish anisotropy from the freedom of moduli now. Then, one can define moduli of a locally homogeneous 3-manifold by examining the possible quotient spaces of each type of universal covering spaces (this was recently studied by another group [15]). It is noted that this viewpoint concentrates only on the geometry of spatial sections so that it may need a certain modification in the space-time construction.

As the next step, one can take into account a deviation from the locally homogeneity presented here. One thing is to include a small fluctuation of local gravitational-wave modes in an appropriate perturbation scheme, or to examine the coupling of the global modes with some matter fields. Another is to consider “topological inhomogeneity”. The Geometrization Conjecture described earlier tells us that any compact 3-manifold has a geometric decomposition into pieces, each element of which admits one geometry of the eight classes. Then it is an interesting problem what is a possible geometry on a manifold that is a connected-sum of such prime manifolds and how one can glue two locally homogeneous geometries of different types along a junction surface in between.

REFERENCES

1. Y. Fujiwara, H. Ishihara and H. Kodama, "Comments on Closed Bianchi Models", preprint KUCP-55.
2. J. A. Wheeler, in *Battelle Rencontres*, ed. C. DeWitt and J. A. Wheeler, (W. A. Benjamin, New York, 1968).
3. V. Moncrief, *J. Math. Phys.* **30** (1989) 2907.
4. A. Hosoya and K. Nakao, *Class. Quantum Grav.* **7** (1990) 163;
Prog. Theor. Phys. **84** (1990) 739,
 Y. Fujiwara and J. Soda, *Prog. Theor. Phys.* **83** (1990) 733.
5. T. Okamura and H. Ishihara, *Phys. Rev.* **D46** (1992) 572; to appear in *Phys. Rev.*
6. M. P. Jr. Ryan and L. C. Shepley, *Homogeneous Relativistic Cosmologies*, (Princeton University Press, Princeton, 1975).
7. D. Kramer, H. Stephani, M. MacCallum and E. Herlt, *Exact Solutions of Einstein's Field Equations*, (Cambridge University Press, Cambridge, 1980).
8. W. P. Thurston, *The Geometry and Topology of 3-manifolds*, to be published by Princeton University Press, 1978/79.
9. W. P. Thurston, *Bull. Amer. Math. Soc.* **6** (1982) 357.
10. P. Scott, *Bull. London Math. Soc.* **15** (1983) 401.
11. J. Milnor, *Adv. in Math.* **21** (1976) 293.
12. H. V. Fagundes, *Phys. Rev. Lett.* **54** (1985) 1200;
Gen. Rel. Grav. **24** (1992) 199.
13. A. Ashtekar and J. Samuel, *Class. Quantum Grav.* **8** (1991) 2191.
14. M. A. H. MacCallum and A. H. Taub, *Commun. Math. Phys.* **25** (1972) 173.
15. A. Hosoya, T. Koike and M. Tanimoto, "Compact Homogeneous Universes", preprint TIT/HEP-208/COSMO-26.

Compact Homogeneous Universes¹

TATSUHIKO KOIKE², MASAYUKI TANIMOTO³ AND AKIO HOSOYA⁴

*Department of Physics, Tokyo Institute of
Technology, Oh-Okayama Meguroku, Tokyo 152, Japan*

ABSTRACT

A thorough classification of the topologies of compact homogeneous universes is given except for the hyperbolic spaces and their global degrees of freedom are completely worked out. To obtain compact universes spatial points are identified by discrete subgroups of the isometry group of the generalized Thurston geometries, which are related to the Bianchi and the Kantowski-Sachs-Nariai universes. The degrees of freedom are explicitly presented, which consist of the ones of the universal covering space and the Teichmüller parameters.

¹This talk is base on Totyo Institute of Technology preprint TIT/HEP-208/COSMO-26.

²E-mail address: bartok@phys.titech.ac.jp

³E-mail address: prince@phys.titech.ac.jp

⁴E-mail address: ahosoya@phys.titech.ac.jp

1 Introduction

In the standard cosmology we normally assume homogeneity and isotropy of the Universe. On the basis of this cosmological principle the Friedmann-Robertson-Walker metric is constructed and Big-Bang Cosmology has been successfully developed in the theory of Einstein gravity [1].

The homogeneous but *anisotropic* universe models, the Bianchi [2, 3] and the Kantowski-Sachs-Nariai universes [4, 5], have been studied from various motivations [6]. For example, people have attempted to clarify the properties of the initial singularity and also attacked the basic problem why the present Universe looks so isotropic by studying the time evolution of the homogeneous anisotropic models [7].

In the present paper we shall study *compact* (locally) homogeneous universes. The investigation of compact universes may be important when we are interested in the possibility of our Universe to have a non-trivial topology or its topology change. The former aspect was studied by Fang and Sato [8] and by Ellis [9] in a special model of torus universe. For the latter we note that the famous theorem by Geroch [10] on topology change assumes the compactness of spatial manifold.

It will be more intriguing to study the geometries of compact locally homogeneous universes when we investigate minisuperspace models in quantum gravity. There it is necessary to make explicit the global degrees of freedom corresponding to deformation of the compact universes.

Our strategy to attack compact locally homogeneous space M is the following. First we consider the universal covering space \tilde{M} of M and specify a group G which transitively acts on \tilde{M} . The metric is constructed so that it is invariant under the group G . So the universal covering space \tilde{M} is endowed with a homogeneous metric. Second we compactify the geometry $(\tilde{M}, \text{Isom}\tilde{M})$ by identifying the points in \tilde{M} by a discrete subgroup Γ of the isometry group $\text{Isom}\tilde{M}$ which acts on \tilde{M} freely. This gives us a compact locally homogeneous space $M = \tilde{M}/\Gamma$ [11].

The degrees of freedom consist of the ones for the universal cover and the Teichmüller deformations variables which parametrize the discrete subgroup Γ . For example, Bianchi

IX universe has two degrees of freedom with no Teichmüller parameters. As we shall see in the subsequent sections, Bianchi VI(0) universe has one universal cover degree of freedom and one Teichmüller parameter.

Ashtekar and Samuel [12] have also investigated global degrees of freedom of compact locally homogeneous universes. However, they restricted their definition of locally homogeneous space so that the discrete group Γ is a subgroup of a *3-dimensional group*, the Bianchi group. Our definition of locally homogeneous space seems more natural and general and coincides with the one adopted by mathematicians. For example, they have excluded compact hyperbolic spaces by restricting Γ to a subgroup of the Bianchi V group in the Bianchi V model with the Poincaré metric. In fact the Bianchi V model can be compactified by using the largest isometry group $\text{PSL}(2, \mathbb{C}) \supset \text{Bianchi V group}$.

We shall appeal to Thurston's theorem [11] and its slight generalization to enumerate all possible geometries $(\tilde{M}, \text{Isom}\tilde{M})$ which admit compact quotients.

Fagundes [13] also realized the relationship between the Thurston and the Bianchi type geometries but did not classify topologies nor considered the global degrees of freedom.

Here we present a complete classification of the topologies of compact locally homogeneous universes and study the global degrees of freedom by looking for possible deformations of the universal covering spaces and explicitly constructing the representations of the fundamental group $\pi_1(M)$ in the isometry group $\text{Isom}\tilde{M}$ except for the compact hyperbolic 3-manifolds.

2 Compact locally homogeneous models

A spacetime is represented by a pair $(^{(4)}M, g_{ab})$, where $^{(4)}M$ is a 4-manifold and g_{ab} is a Lorentzian 4-metric. We 3+1 decompose the spacetime, i.e. we think of a spacetime $(^{(4)}M, g_{ab})$ as the time evolution of a Riemannian 3-metric $h_{ab}(t)$ on a 3-manifold M . We require that this decomposition is synchronous; the lapse function is unity and the shift vector vanishes. Then the 4-metric can be written as

$$g_{ab} = -(dt)_a(dt)_b + h_{ab}. \quad (1)$$

We say a spacetime $(M, h_{ab}(t))$ to be *spatially locally homogeneous* if $h_{ab}(t)$ for every t is locally homogeneous. We say $(M, h_{ab}(t))$ to be *spatially compact* if M is compact.

Let $(M, h_{ab}(t))$ be a spatially compact locally homogeneous spacetime. Let us separate the conformal factor $a(t)$ from $h_{ab}(t)$ as

$$h_{ab}(t) = a^2(t)\bar{h}_{ab}(t) \quad (2)$$

and think of \bar{h}_{ab} as the dynamical variables. Therefore, the physical degrees of freedom are the numbers needed to parametrize \bar{h}_{ab} . Hereafter we omit the bar of \bar{h}_{ab} and simply denote it by h_{ab} .

As mentioned in the previous section, M has a unique universal cover \tilde{M} up to diffeomorphisms, and $(M, h_{ab}(t))$ is metrically diffeomorphic to $(\tilde{M}, \tilde{h}_{ab}(t))/\Gamma(t)$ where \tilde{h}_{ab} is homogeneous and Γ is a discrete subgroup of $\text{Isom}(\tilde{M}, \tilde{h}_{ab})$. All $\Gamma(t)$ must be isomorphic for all $\tilde{M}/\Gamma(t)$ to have the same topology.

The degrees of freedom can be separated into two categories, those of the universal cover and the Teichmüller parameters. Thinking of a manifold M as a quotient \tilde{M}/Γ of a simply connected homogeneous manifold \tilde{M} naturally leads us to separating the degrees of freedom of h_{ab} into those of \tilde{h}_{ab} and those of Γ , i.e. those of the universal cover $(\tilde{M}, \tilde{h}_{ab})$ and the Teichmüller parameters. Here we should recall that there is freedom of diffeomorphisms in giving a universal cover \tilde{M} of M . If ϕ is an orientation preserving diffeomorphism from \tilde{M} onto itself, $(\tilde{M}, \tilde{h}_{ab})/\Gamma$ and $(\tilde{M}, \phi_*\tilde{h}_{ab})/\phi_*\Gamma\phi^{-1}$ are diffeomorphic metrically and have the same orientation. This means that different pairs of \tilde{h}_{ab} and Γ may give the same manifold (M, h_{ab}) . To avoid this uninteresting freedom emerged from diffeomorphisms, and recalling that we have already put aside the conformal factor, we define the degrees of freedom of the universal covering manifold as those of

$$\frac{\{\text{homogeneous metrics on a simply connected manifold which admit compact quotients}\}}{\{\text{orientation preserving diffeomorphisms}\} \{\text{global conformal transformations}\}}. \quad (3)$$

We say that there are degrees of freedom of the universal cover if these equivalence classes can be smoothly deformed.

Once a metric on the universal cover \tilde{M} is fixed, the isometry group of \tilde{M} is determined. Remaining deformations of the manifold M are the Teichmüller deformations.

3 Locally homogeneous spaces

A metric on a manifold M is said to be (*globally*) *homogeneous* if the isometry group acts transitively on M , i.e. for any points $p, q \in M$ there exists an isometry which takes p into q . A metric on a manifold M is said to be *locally homogeneous* if for any points $p, q \in M$ there exist neighborhoods U, V and an isometry $(U, p) \rightarrow (V, q)$. The difference between global and local homogeneity is that in the latter case the isometry may not be globally defined.

Any locally homogeneous manifold is diffeomorphic to the quotient of a simply connected homogeneous manifold by a discrete subgroup of the isometry group. Conversely, a quotient space of a homogeneous Riemannian manifold by an appropriate subgroup of the isometry group is locally homogeneous. X/Γ is a locally homogeneous Riemannian manifold if Γ is a discrete subgroup of $\text{Isom}X$ and acts freely on X . So our task is to find out all possible discrete subgroups Γ of $\text{Isom}X$ which acts freely on X and makes X/Γ compact.

4 Geometries and Thurston's theorem

In order to state precisely and take advantage of the result obtained in the recent study in 3-manifolds, we use the term 'geometry' in a specific sense. A *geometry* is a pair (X, G) where X is a manifold and G is a group acting transitively on X with compact point stabilizers. Geometries (X, G) and (X', G') are *equivalent* if there is a diffeomorphism $\phi : X \rightarrow X'$ with $\bar{\phi} : g \mapsto \phi \circ g \circ \phi^{-1}$ being an isomorphism from G onto G' . Let us call ϕ an *equivalence map*. A geometry (X, G') is a *subgeometry* of (X, G) if G' is a subgroup of G . A geometry is *maximal* if it is not a proper subgeometry of any geometries.

Although a geometry (X, G) is merely a pair of a manifold X and a group G and has nothing to do with Riemannian metrics on X itself, one can discuss homogeneous Riemannian metrics from the viewpoint of geometries. This is because one can construct a complete homogeneous metric from a geometry (X, G) as follows.

We quote the theorem of Thurston which is of great use in classifying all compact, locally homogeneous spaces.

THEOREM 1 (Thurston) *Any maximal, simply connected 3-dimensional geometry which admits a compact quotient is equivalent to the geometry $(X, \text{Isom}X)$ where X is one of E^3 , H^3 , S^3 , $S^2 \times \mathbf{R}$, $H^2 \times \mathbf{R}$, $\widetilde{\text{SL}}(2, \mathbf{R})$, Nil, or Sol.*

A brief proof can be found in Scott [11]. Each X in the theorem is a manifold with a certain ‘standard’ Riemannian metric on it. E^n , H^n , and S^n denotes the 3-dimensional Euclidean, Hyperbolic, and spherical manifolds, respectively, and $\widetilde{\text{SL}}(2, \mathbf{R})$, Nil, and Sol are 3-dimensional Lie groups with an invariant Riemannian metrics and correspond to Bianchi VIII, II, and VI(0) spaces, respectively.

Note that this Riemannian metric on X is not of essential importance in the theorem but is simply useful to express a group G in a geometry (X, G) as $\text{Isom}X$ and the action of G on X . For example, $(E^3, \text{Isom}E^3)$ means the same as $(\mathbf{R}^3, \text{IO}(3))$.

5 The Teichmüller space

Let \tilde{M} be a simply connected homogeneous Riemannian manifold with its metric \tilde{h}_{ab} fixed. Let M be a quotient of \tilde{M} by a discrete subgroup Γ of $\text{Isom}\tilde{M}$. The Teichmüller space of M is the space of all smooth deformations of M irrespective of its size, keeping the condition that M is a quotient of $(\tilde{M}, \tilde{h}_{ab})$.

Let us put it more precisely. Let $\text{Rep}(M)$ denote the space of all discrete and faithful representations $\rho : \pi_1(M) \rightarrow \text{Isom}^+ \tilde{M}$. Let us call a diffeomorphism $\phi : \tilde{M} \rightarrow \tilde{M}$ a global conformal isometry if $\phi_* \tilde{h}_{ab} = \text{const.} \cdot \tilde{h}_{ab}$. Let us define a relation \sim in $\text{Rep}(M)$ such that $\rho \sim \rho'$ holds if there exists a global conformal isometry ϕ of \tilde{M} connected to the identity which gives $\rho'(a) = \phi \circ \rho(a) \circ \phi^{-1}$ for any $a \in \pi_1(M)$. It defines an equivalence relation in $\text{Rep}(M)$. We define the *Teichmüller space* as

$$\text{Teich}(M) = \text{Rep}(M) / \sim . \quad (4)$$

The Teichmüller space is a manifold. The numbers used to parametrize the Teichmüller space are called the *Teichmüller parameters*.

If two representations ρ and ρ' correspond to the same point in $\text{Teich}(M)$, the above global conformal isometry ϕ on \tilde{M} induces a well-defined global conformal isometry from \tilde{M}/Γ onto \tilde{M}/Γ' , where $\Gamma = \rho(\pi_1(M))$ and $\Gamma' = \rho'(\pi_1(M))$. This is because for any $\gamma \in \Gamma$ there exists unique $\gamma' \in \Gamma'$ such that $\phi \circ \gamma = \gamma' \circ \phi$, which guarantees that $\phi(\tilde{M}/\Gamma) = \tilde{M}/\Gamma'$.

The Teichmüller parameters constitute a subset of dynamical variables of locally homogeneous universes.

6 Results

In this section we explain the procedure to get all universal covers and the one to get compact quotients. The whole results are shown in the tables in [14].

Theorem 1 tells us all simply connected *maximal* geometries which admits compact quotients. But we want to consider a general locally homogeneous metric on a compact manifold, so the requirement that the geometry be maximal is too strong for our purpose. For example, Bianchi IX space does not satisfy this requirement; the geometry $(S^3(\text{topologically}), \text{SU}(2))$ is a subgeometry of the isotropic 3-sphere $(S^3, \text{SO}(4))$. In general, if (X, G') is a subgeometry of (X, G) then G' is a subgroup of G and acts transitively on X . It follows that the stabilizer of G' is a subgroup of that of G . In other words, a metric on a maximal geometry is more isotropic than those on any of its subgeometries.

Theorem 1 says nothing about nonmaximal geometries which have compact quotients. Nevertheless we can show that we have only to consider subgeometries of the above eight geometries. Let (X, G') be a simply connected 3-geometry which admits a compact quotient. Then there is a discrete freely acting subgroup Γ' of G' which makes X/Γ' compact. Let (X, G) be a maximal geometry which has (X, G') as its subgeometry. Then Γ' is a subgroup of G which makes X/Γ' compact, so our maximal, simply connected geometry (X, G) admits compact quotients. By Theorem 1 our maximal geometry (X, G) is one of the eight Thurston geometries, which proves that (X, G') is a subgeometry of one of the eight Thurston geometries.

If a Riemannian manifold $(\tilde{M}, \tilde{h}_{ab})$ admits compact quotients then the geometry $(\tilde{M}, \text{Isom}^+ \tilde{M})$ is a subgeometry of the eight Thurston maximal geometries. Our strategy is to consider all subgeometries (\tilde{M}, G) of the Thurston geometries and G -invariant metrics on \tilde{M} . Here we must recall that G may not be the isometry group itself, i.e. it may be the case that the G -invariant metric on \tilde{M} admits a larger isometry group than G . So it is necessary to find the whole $\text{Isom}^+ \tilde{M}$ in each case. Of course, if (M, \tilde{h}_{ab}) and (M, \tilde{h}'_{ab}) are in the same equivalence class then $\text{Isom}^+(\tilde{M}, \tilde{h}_{ab})$ and $\text{Isom}^+(\tilde{M}, \tilde{h}'_{ab})$ are isomorphic.

We adopt the following procedure to find all equivalence classes of homogeneous metrics on a simply connected manifold which admit compact quotients and their isometry groups:

- 1) List up all subgeometries (\tilde{M}, G) of each of the Thurston geometries.
- 2) For each subgeometry (\tilde{M}, G) , form a general G -invariant Riemannian metric \tilde{h}'_{ab} on \tilde{M} .
- 3) Transform the metric into a certain simple 'representative metric' \tilde{h}_{ab} by diffeomorphisms together with global conformal transformations and find the equivalence classes.
- 4) Find the isometry group of $(\tilde{M}, \tilde{h}_{ab})$.

We thus get all possible universal covers of locally homogeneous Riemannian manifolds. Logically speaking, equivalence classes thus found do not necessarily have to admit compact quotients. So we have another task.

- 5) Make sure whether the equivalence class really admits compact quotients. The Bianchi classification [2, 3] is of great use in carrying out the procedure given above, for it is the classification of all simply connected 3-dimensional Lie groups up to isomorphisms.

We emphasize that the Thurston geometries are the maximal 3-dimensional geometries which give compact quotients while the BKS_N geometries are the minimal 3-dimensional geometries.

We found that the number U of degrees of freedom of the universal cover is

$$U = 5 - \dim(\text{Aut}(\text{Alg}G)) \quad (5)$$

for the Bianchi geometries with $\dim(\text{Aut}(\text{Alg}G)) \geq 5$, and $U = 0$ for those with $\dim(\text{Aut}(\text{Alg}G)) < 5$.

The equivalence classes (3) which give the universal covers of all orientable compact locally homogeneous Riemannian manifolds is given as below.

THEOREM 2 *Any simply connected 3-dimensional Riemannian manifold which admits a compact quotient is one of the types in Table 2 up to orientation preserving diffeomorphism and global conformal transformation.*

The number of the degrees of freedom is the number of parameters in the representative metric. The degrees of freedom are also characterized by free parameters appearing in the relative ratios of the nonvanishing principal sectional curvatures. These ratios can be chosen to be dynamical variables.

All compact locally homogeneous Riemannian manifold and their Teichmüller spaces are obtained by the following procedure.

1) Pick up a Thurston geometry X (say, E^3) and list up all compact locally homogeneous manifolds $M \cong X/\Gamma$ modeled on $(X, \text{Isom}^+ X)$.

2) List up all types (say, Type a1 and Type a2) of universal covers \tilde{M} which is subgeometries of $(X, \text{Isom}^+ X)$.

3) For each universal cover type, check whether X/Γ can be modeled on $(\tilde{M}, \text{Isom} \tilde{M})$ or not by checking whether Γ is a subgroup of $\text{Isom} \tilde{M}$.

4) Find their Teichmüller spaces.

Note that a representation $\rho : \pi_1(M) \rightarrow \text{Isom}^+ \tilde{M}$ is determined by the images of the fixed generators of $\pi_1(M)$.

For the universal covers which have L and R types, we show the results of L type; the representations in R type can be obtained in the same way.

The compact quotients and their dynamical degrees of freedom are in [14]. The total degrees of freedom F is the sum of the degrees of freedom U of the universal cover and the dimension T of the Teichmüller space.

7 Conclusion and discussions

We have worked out the classification of topologies of compact locally homogeneous universes except for hyperbolic 3-manifolds studying possible fundamental groups for each

Thurston geometry.

We have extracted the global degrees of freedom which consist of two parts. One is the degrees of freedom of the universal covers, while the other is the Teichmüller deformations which parametrize the discrete subgroup Γ of the isometry group. The Teichmüller parameters are obtained by constructing the representation of the fundamental group in the isometry group.

Intuitively the difference of the two degrees of freedom is the following. Assuming the homogeneity of the Universe one can *locally* determine the universal cover degrees of freedom by measuring all ratios of the sectional curvatures. In a sense these are interpreted as local anisotropies. In order to know the Teichmüller parameters, on the other hand, we probably have to send many space explorers, who are supposed to measure the times taken by all possible round trips around non-trivial loops, etc.. In short, the Teichmüller parameters are global quantities.

We have not discussed the dynamics of our compact universes in the present work. In a separate paper we will study the Einstein gravity for a compact locally homogeneous universes and give a list of supermetrics in terms of the global variables discussed in this paper.

Thurston conjectured that all possible topologies of compact 3-manifolds can be classified considering connected sums and torus sums of the prime manifolds which are given by the compact quotients of the eight geometries [15]. This may lead us to a speculation that at least some aspects of general inhomogeneous universe are understood by studying combinations of the compact locally homogeneous spaces.

It will be also interesting to investigate quantum field theory in the compact locally homogeneous spaces which have non-trivial topologies. We naturally expect the Cashmir effects, etc..

We hope our present work furnishes a mathematical base on which a new field of cosmology develops.

References

- [1] S. Weinberg. *Gravitation and cosmology*. Wiley, New York, 1972.
- [2] L. D. Landau and E. M. Lifshitz. *Classical theory of Fields*. MIT, Reading, 1971.
- [3] R. M. Wald. *General Relativity*. University of Chicago Press, Chicago, 1984.
- [4] H. Nariai. On a new cosmological solution of einstein's field equations of gravitation. *Sci. Rep. Tohoku Univ., I*, 35:62, 1951.
- [5] R. Kantowski and R. K Sachs. Some spatially homogeneous anisotropic relativistic cosmological models. *J. Math. Phys.*, 7:443, 1967.
- [6] V. A. Belinski, I. M. Khalatnikov, and E. M. Lifshitz. Oscillatory approach to a singular point in the relativistic cosmology. *Adv. in Phys.*, 19:525, 1970.
- [7] M. P. Ryan and L. C. Shepley. *Homogeneous Relativistic Cosmologies*. Princeton Series in Physics. Princeton University Press, Princeton, 1975.
- [8] L. Z. Fang and Sato H. Is the periodicity in the distribution of quasar red shifts an evidence of multiply connected universe? *Gen. Rel. Grav.*, 17:1117, 1985.
- [9] G. F. R. Ellis. Topology and cosmology. *Gen. Rel. Grav.*, 2:7, 1971.
- [10] R. P. Geroch. Topology in general relativity. *J. Math. Phys.*, 8:782, 1967.
- [11] P. Scott. The geometries of 3-manifolds. *Bull. London Math. Soc.*, 15:401, 1983.
- [12] A. Ashtekar and J. Samuel. Bianchi cosmologies: the role of spatial topology. *Class. Quantum Grav.*, 8:2191, 1991.
- [13] Helio. V. Fag. Closed spaces in cosmology. *Gen. Rel. Grav.*, 24:199, 1992.
- [14] T. Koike, M. Tanimoto, and A. Hosoya. Compact homogeneous universes. dec 1992. Tokyo Institute of Technology preprint, TIT/HEP-208/COSMO-26.
- [15] W. P. Thurston. Three dimensional manifolds, kleinian groups and hyperbolic geometry. *Bull. Amer. Math. Soc.*, 6:357, 1982.

Unified Models and Possible Time-Nonvariability of the “Constants”

Yasunori Fujii

Nihon Fukushi University

Okuda, Chita-gun, Aichi, 470-32 Japan

and

Minoru Omote

Department of Physics, Hiyoshi, Keio University

Hiyoshi, Yokohama, 223 Japan

Scalar fields are indispensable constituents in most of the theoretical models of unification. Among them a dilaton-like (or JBD-like) field and those corresponding to the radii of compactified spaces are of special interest, because they have the “nonminimal gravitational couplings,” and couple also to the fields of other elementary particles, particularly through their kinetic terms.

It is also noticed that the scalar fields can be spatially uniform depending only on the cosmic time t , as solutions of the cosmological equations for the Robertson-Walker universe. As a consequence, the gravitational constant as well as other coupling constants should vary with t , resulting eventually in the time-variability of particle masses.

The gravitational constant is unique in that it can be made truly constant by applying a conformal transformation which diagonalizes the mixing between the scalar fields and the metric field [1]. But other “constants” (coupling constants and masses) are still left time-dependent in general. This can be seen most easily in a gauge field A_μ^I with the kinetic term which is usually multiplied by a function $Z(\phi)$ of the scalar field $\phi(t)$. To make the kinetic term canonical one applies a “wave-function renormalization” $A_\mu^I \rightarrow Z^{-1/2} A_\mu^I$, resulting in redefining the gauge coupling constant $e \rightarrow Z^{-1/2} e$, which now depends on the cosmic time t . Notice that the combination $\sqrt{-g} g^{\mu\rho} g^{\nu\sigma}$ which appears in the kinetic term is conformally invariant by itself in 4 dimensions.

Of course one may expect that the scalar field had settled in one of the potential minima in a sufficiently early epoch leaving no observable trace of time-variation in late times. In this scenario, however, the value of the potential minimum plays a role of a cosmological constant, hence creating another source of the problem. It was pointed out that at least one scalar field should keep

growing to infinity to avoid the cosmological constant problem [2]. In fact most of the models of "a decaying cosmological constant" the scalar field behaves generically like t^α , as the cosmological constant itself decreases like t^{-2} [1,3]. If, as in many models, the factor Z is a power function of the scalar field, the coupling constants would vary like powers of t , predicting $\dot{e}/e \sim t^{-1}$, which would give values of the order of 10^{-10}y^{-1} at the present epoch.

On the experimental side, however, the reported analyses give upper bounds which are already below the level of 10^{-10}y^{-1} by several orders of magnitude [4,5]. The most stringent is the one for the strong coupling constant squared: $\dot{\alpha}_s/\alpha_s \lesssim 10^{-19}\text{y}^{-1}$ as obtained from the depletion of Sm isotope in Oklo [5]. It should be admitted that none of the analyses are entirely free from uncertainties; one might suspect some coincidence or conspiracy. It is nevertheless remarkable that no evidence has ever emerged for time-dependences. It seems that we face a serious conflict between the observation and the theoretical models if we add a requirement that the cosmological constant pose no problem.

We suggest a promising remedy based on our finding that the cosmological equations allow an interesting solution of the scalar field; it may stay nearly constant for some time [1,6]. If one can adjust the parameters such that this time interval extends to the present epoch, no observable time-variability would ensue though the scalar field would have varied considerably in the remote past (probably earlier than the time of nucleosynthesis) and should vary in the future.

This behavior is a consequence of a delicate competition between the force due to the potential and the frictional force provided by the cosmological expansion [6]. This is essentially the same as "relaxation oscillation," a typical nonlinear effect, known by many examples in our daily experience.

The effect seems to be a rather common feature of an exponential potential of the scalar field, as will appear naturally in the model of a decaying cosmological constant [1]. Details will be reported in a separate paper.

References

1. Y. Fujii and T. Nishioka, *Phys. Rev.* **D42** (1990), 361.
2. S. Weinberg, *Rev. Mod. Phys.* **61** (1989), 1.
3. A.D. Dolgov, in *The Very Early Universe*, Proc. Nuffield Workshop, Cambridge, England, 1982, eds. G.W. Gibbons and S.T. Siklos (Cambridge University Press, Cambridge, 1982); L.H. Ford, *Phys. Rev.* **D35** (1987), 2339.
4. F.J. Dyson, *Phys. Rev. Lett.* **19** (1967), 1291; P.C.W. Davies, *J. Phys.* **A5** (1972), 1296; A.M. Wolf, R.L. Brown and M.S. Roberts, *Phys. Rev. Lett.* **37** (1976), 179.
5. A.I. Shlyakhter, *Nature* **264** (1976), 340.
6. Y. Fujii and T. Nishioka, *Phys. Lett.* **B254** (1991), 347.

Wave Function of the Universe in Topological and in Einstein 2-form Gravity[†]

AKIKA NAKAMICHI^{*}

*Department of Physics, Tokyo Institute of Technology
Oh-okayama, Meguro-ku, Tokyo 152, Japan*

ABSTRACT

We clarify the relation between 2-form Einstein gravity and its topological version. The physical space of the topological version is contained in that of the Einstein gravity. Moreover a new vector field is introduced into 2-form Einstein gravity to restore the large symmetry of its topological version. The wave function of the universe is obtained for each model.

[†] Talk given at the Workshop on General Relativity and Gravitation held at Waseda University, January 18-20, 1993.

^{*} e-mail address: akika@phys.titech.ac.jp

1. Introduction

Topological gravity is expected to elucidate the global (topological) aspects of gravity. In Ref.[1], a topological version of four dimensional Einstein gravity is proposed. This topological version is obtained by modifying an alternative formulation of gravity enlightened by Capovilla et al.[2], in which anti-self-dual 2-forms are used as fundamental variables. This formulation, which we call 2-form Einstein gravity, leads to the canonical formalism discovered by Ashtekar [3]. Investigating the relation between 2-form Einstein gravity and its topological version, we found that, a unique quantum state in the latter turns out to be one of the physical states in the former. This physical state is interpreted as the wave function of the universe.

Moreover in Ref.[4], a new vector field is introduced into 2-form Einstein gravity to restore the large symmetry of its topological version. We also obtain the wave function of the universe in the new system.

2. Symmetries

Einstein Gravity

The action of (Euclidean) 2-form Einstein gravity is given in terms of 2-form Σ^k and SU(2) spin connection 1-form ω^k in the presence of a cosmological constant Λ ,

$$S = \int \Sigma^k \wedge R_k - \frac{\Lambda}{24} \Sigma^k \wedge \Sigma_k + \frac{\alpha}{2} \psi_{kl} \Sigma^k \wedge \Sigma^l, \quad (1)$$

where $R_k \equiv d\omega_k + (\omega \times \omega)_k$, ψ_{kl} is a symmetric trace-free Lagrange multiplier field, and α is a constant parameter. The SU(2) indices $i, j, k, \dots = 1, 2, 3$, in the fields imply that they transform under the *chiral* local-Lorentz representation

(1,0) of $SU(2) \times SU(2)$ [5]. In this formulation, the metric $g_{\mu\nu}$ is defined as¹¹

$$g^{\frac{1}{2}} g_{\mu\nu} = -\frac{1}{12} \epsilon^{\alpha\beta\gamma\delta} \Sigma_{\mu\alpha} \cdot (\Sigma_{\beta\gamma} \times \Sigma_{\delta\nu}) , \quad g \equiv \det(g_{\mu\nu}) . \quad (2)$$

Using this definition, we find that the action (1) is equivalent to the usual Einstein-Hilbert action [2,6].

Since the action (1) describes general relativity, it is invariant under the local-Lorentz transformation and diffeomorphism,

$$\delta\omega^k = D\theta_0^k + \mathcal{L}_\xi \omega^k , \quad \delta\Sigma^k = [\Sigma, \theta_0]^k + \mathcal{L}_\xi \Sigma^k , \quad (3)$$

where \mathcal{L}_ξ is the Lie derivative with respect to a vector field ξ^μ , and the local-Lorentz transformation corresponds to the $SU(2)$ gauge transformation with a parameter θ_0^k .

Topological Gravity

From the equations of motion, the multiplier field ψ_{kl} is determined to be proportional to the anti-self-dual part of the Weyl tensor, which governs the modes of the gravitational wave. Therefore the topological version of the theory is obtained by simply dropping the last term in the action (1), that is, by setting $\alpha = 0$ [1]:

$$S_{\alpha=0} = \int \Sigma^k \wedge R_k - \frac{\Lambda}{24} \Sigma^k \wedge \Sigma_k . \quad (4)$$

In this case, a new symmetry generated by a parameter 1-form θ_1^k emerges in addition to diffeomorphism and the local-Lorentz (with θ_0^k) symmetries,

$$\delta\omega^k = D\theta_0^k + \frac{\Lambda}{12} \theta_1^k , \quad \delta\Sigma^k = 2(\Sigma \times \theta_0)^k + D\theta_1^k . \quad (5)$$

Here diffeomorphism with a vector field ξ^μ is implicitly included in the above local-Lorentz and θ_1^k -transformations as we can see by setting $\theta_0^k = \xi^\nu \omega_\nu^k$ and

¹¹ We use the notation for the $SU(2)$ indices, $F \cdot G \equiv F^i G^i$ and $(F \times G)^i \equiv \epsilon_{ijk} F^j G^k$, where ϵ_{ijk} is the structure constant of $SU(2)$.

$\theta_{1\mu}^k = 2\xi^\nu \Sigma_{\nu\mu}^k$. The theory turns out to be on-shell reducible in the sense that the transformation laws (5) are invariant, modulo the equations of motion, under

$$\delta\theta_0^k = -\frac{\Lambda}{12}\epsilon_0^k, \quad \delta\theta_1^k = D\epsilon_0^k. \quad (6)$$

This means that not all of the parameters in (5) are independent.

New System

From the view point of the topological gravity, one can see that the large θ_1^k -symmetry is partially broken in Einstein gravity leaving only diffeomorphism and local-Lorentz symmetries intact and, as a result, the modes of the gravitational wave are induced. The obstruction for the θ_1^k -symmetry is the last term in the action (1). We can restore the symmetry by introducing a vector field (1-form) η^k in the last term as follows,

$$\frac{\alpha}{2} \int \psi_{kl} \Sigma^k \wedge \Sigma^l \Rightarrow \frac{\alpha}{2} \int \psi_{kl} \hat{\Sigma}^k \wedge \hat{\Sigma}^l, \quad \hat{\Sigma}^k \equiv \Sigma^k - D\eta^k + \frac{\Lambda}{12}(\eta \times \eta)^k. \quad (7)$$

This makes our new system invariant under the θ_1^k -transformation in (5) with $\delta\eta^k = \theta_1^k$, together with diffeomorphism and the local-Lorentz transformation:

$$\begin{aligned} \delta\omega^k &= D\theta_0^k + \mathcal{L}_\xi \omega^k + \frac{\Lambda}{12}\theta_1^k, & \delta\Sigma^k &= [\Sigma, \theta_0]^k + \mathcal{L}_\xi \Sigma^k + D\theta_1^k. \\ \delta\eta^k &= [\eta, \theta_0]^k + \mathcal{L}_\xi \eta^k + \theta_1^k. \end{aligned} \quad (8)$$

They are all independent and hence there is no reducibility in the system. It is easily shown that the new system is equivalent to Einstein gravity, by choosing the gauge condition, $\eta^k = 0$, for the θ_1^k -symmetry. Indeed physical degrees of freedom of the new system is 2: the modes of the gravitational wave.

3. Physical states

Topological Gravity

In the topological case ($\alpha = 0$), the action (4) becomes in canonical form:

$$S = \int dt \int d^3x [\dot{\omega}_a \cdot B^a - \omega_0 \cdot \varphi - \Sigma_{a0} \cdot \phi^a] . \quad (9)$$

The canonical variables are ω_a^k and their conjugate momenta $B_k^a \equiv \varepsilon^{abc} \Sigma_{bc}^k$, which are the spatial components of the spin connection ω^k and the 2-form Σ^k . Varying (9) with respect to their time components ω_0^k and Σ_{a0}^k , we get two sets of constraints,

$$\varphi_k \equiv -D_a B_k^a \approx 0 , \quad \phi_k^a \equiv 2 (\varepsilon^{abc} R_{bc}^k - \frac{\Lambda}{12} B_k^a) \approx 0 . \quad (10)$$

The Poisson brackets among them are given by

$$\begin{aligned} \{\varphi_i(\mathbf{x}), \varphi_j(\mathbf{y})\} &= -2 \varepsilon_{ijk} \varphi_k(\mathbf{x}) \delta^3(\mathbf{x} - \mathbf{y}) , & \{\phi_i^a(\mathbf{x}), \phi_j^b(\mathbf{y})\} &= 0 , \\ \{\varphi_i(\mathbf{x}), \phi_j^a(\mathbf{y})\} &= -2 \varepsilon_{ijk} \phi_k^a(\mathbf{x}) \delta^3(\mathbf{x} - \mathbf{y}) . \end{aligned} \quad (11)$$

All the constraints are of first class and the algebra is closed. The constraints φ_k and ϕ_k^a generate the local-Lorentz and θ_1^k -transformations in (5) respectively. In this canonical formulation, the on-shell reducibility (6) appears as a linear dependence of the constraints,

$$D_a \phi_k^a - \frac{\Lambda}{6} \varphi_k = 0 . \quad (12)$$

In the Dirac approach for quantization, one has to impose quantum conditions to choose physical wave functional Ψ . In the topological case with $\Lambda \neq 0$, these

conditions can be expressed using the constraints (10) in ω_a^k representation,

$$\begin{aligned}\varphi_k(\omega, \delta/\delta\omega)\Psi(\omega) &= iD_a(\delta/\delta\omega_a^k)\Psi(\omega) = 0, \\ \phi_k^a(\omega, \delta/\delta\omega)\Psi(\omega) &= 2(\epsilon^{abc}R_{bc}^k + i\frac{\Lambda}{12}\delta/\delta\omega_a^k)\Psi(\omega) = 0.\end{aligned}\quad (13)$$

Since these equations are linear differential equations, we can easily solve them to obtain the unique functional of ω_a^k ,

$$\Psi(\omega) = \exp\left(\frac{6i}{\Lambda}I_{C-S}\right), \quad I_{C-S} \equiv \int d^3x \epsilon^{abc}\omega_a \cdot (\partial_b\omega_c + \frac{2}{3}(\omega_b \times \omega_c)), \quad (14)$$

where I_{C-S} is the Chern-Simons term on the three-dimensional boundary. This type of solution is also found in a different version of topological gravity [7]. The functional $\Psi(\omega)$ is the wave function of the universe in four dimensional (Euclidean) topological gravity. It can also be considered as the BRST invariant vacuum, because it is the unique representative annihilated by the BRST operator [1].

Einstein Gravity

On the other hand in the Einstein gravity ($\alpha \neq 0$), we have to solve the constraint equations, which can be considered as five linear equations for nine Lagrange multipliers Σ_{a0}^k [2]. The solution is expressed with four arbitrary variables N^a (shift vector) and \underline{N} (lapse density of weight -1),

$$\Sigma_{a0}^k = -\frac{1}{4}\epsilon_{abc}[N^b B_c^e + \underline{N}(B^b \times B^e)^k]. \quad (15)$$

Substituting this result for the canonical action (9), we now have four constraints, together with φ_k in (10), which are associated with the Lagrange multipliers N^a and \underline{N} ,

$$\begin{aligned}C_a &\equiv \frac{1}{4}\epsilon_{abc}B^b \cdot \phi^c = B^b \cdot R_{ab} \approx 0, \\ C &\equiv \frac{1}{4}\epsilon_{abc}(B^a \times B^b) \cdot \phi^c = (B^a \times B^b) \cdot (R_{ab} - \frac{\Lambda}{24}\epsilon_{abc}B^c) \approx 0.\end{aligned}\quad (16)$$

We can identify φ_k , C_a and C with the independent first class constraints cor-

responding to the generators of the local-Lorentz transformation, spatial diffeomorphism and temporal diffeomorphism respectively.

An important observation is that all the constraints in the Einstein Gravity are linear combinations of those in the topological version. Especially four diffeomorphism generators C_a and C in (16) are linearly dependent on nine ‘new-type’ generators ϕ_k^a in (10). We see that $\Psi(\omega)$ in (14) becomes a special solution of all quantum constraints in the Einstein gravity if the operator ordering is arranged as in (16). This ordering is consistent with the commutation relations among the constraint operators [8]. This $\Psi(\omega)$ is nothing but the Euclidean version of the wave functional discovered by Kodama [9,10]. Therefore the physical space of the topological gravity is contained in that of the Einstein gravity.

New System

With the vector field η^k , the action becomes in canonical form,

$$S = \int dt \int d^3x [\dot{\omega}_a \cdot B^a - \omega_0 \cdot \varphi - \Sigma_{a0} \cdot \phi^a - 2\alpha\psi_{kl}\hat{\Sigma}_{a0}^k\hat{B}_l^a], \quad (17)$$

where $\hat{B}_k^a \equiv \epsilon^{abc}\hat{\Sigma}_{bc}^k$ is the spatial components of the 2-form $\hat{\Sigma}^k$. Again we have to solve the constraint equation derived by varying (17) with respect to ψ_{kl} . The solution is expressed by using four arbitrary variables N^a and \underline{N} ,

$$\Sigma_{a0}^k = -\frac{1}{4}\epsilon_{abc}[N^b\hat{B}_k^c + \underline{N}(\hat{B}^b \times \hat{B}^c)^k] - \frac{1}{2}\dot{\eta}_a^k - (\omega_0 \times \eta_a)^k + \frac{1}{2}\hat{D}_a\eta_0^k. \quad (18)$$

Substituting this result for the canonical action (17), we get four sets of constraints:

$$\begin{aligned} \hat{\varphi}_k &\equiv -D_a B_k^a - 2(\eta_a \times \eta \pi^a)^k \approx 0, \\ \hat{\phi}_k^a &\equiv 2(\epsilon^{abc}R_{bc}^k - \frac{\Lambda}{12}B_k^a) - 2\eta \pi_k^a \approx 0, \\ H_a &\equiv \frac{1}{4}\epsilon_{abc}\hat{B}^b \cdot (\hat{\phi}^c + 2\eta \pi^c) \approx 0, \\ \mathcal{H} &\equiv \frac{1}{4}\epsilon_{abc}(\hat{B}^a \times \hat{B}^b) \cdot (\hat{\phi}^c + 2\eta \pi^c) \approx 0. \end{aligned} \quad (19)$$

The fields $\eta \pi_k^a$ are the conjugate momenta of the spatial components of η_a^k . Next

we redefine the constraint H_a as

$$\mathcal{H}_a \equiv 2H_a + \omega_a \cdot \hat{\varphi} - \frac{1}{2}\epsilon_{abc}(\hat{B}^b - B^b) \cdot \hat{\varphi}^c. \quad (20)$$

The new constraint \mathcal{H}_a generates the spatial diffeomorphism. The non-zero Poisson brackets among the constraints are given by

$$\begin{aligned} \{\hat{\varphi}[g_1], \hat{\varphi}[g_2]\} &= -2\hat{\varphi}[(g_1 \times g_2)], & \{\hat{\varphi}[g], \hat{\varphi}^a[h_a]\} &= -2\hat{\varphi}^a[(g \times h_a)], \\ \{\mathcal{H}[\underline{N}], \mathcal{H}[\underline{M}]\} &= \mathcal{H}_a[L^a] - \hat{\varphi}[L^a \omega_a] + \frac{1}{2}\hat{\varphi}^a[\epsilon_{abc}L^b(\hat{B}^c - B^c)], \end{aligned} \quad (21)$$

where $\hat{\varphi}[g_1] \equiv \int d^3x g_1^k \hat{\varphi}_k$, $\hat{\varphi}^a[h_a] \equiv \int d^3x h_a^k \hat{\varphi}_k^a$, $L^a \equiv \hat{B}^a \cdot \hat{B}^b (M \partial_b \underline{N} - \underline{N} \partial_b M)$.

All the constraints in the system are of first class. Among them, $\hat{\varphi}_k$ and $\hat{\varphi}_k^a$ are identified with the generators of the local-Lorentz and θ_1^k -transformations in (8) respectively. The constraint \mathcal{H} generates temporal diffeomorphism while \mathcal{H}_a the spatial one.

As in the previous cases, quantum conditions are

$$\begin{aligned} \hat{\varphi}_k(\omega, \delta/\delta\omega, \eta, \delta/\delta\eta)\Psi(\omega, \eta) &= 0, & \hat{\varphi}_k^a(\omega, \delta/\delta\omega, \eta, \delta/\delta\eta)\Psi(\omega, \eta) &= 0, \\ \mathcal{H}_a(\omega, \delta/\delta\omega, \eta, \delta/\delta\eta)\Psi(\omega, \eta) &= 0, & \mathcal{H}(\omega, \delta/\delta\omega, \eta, \delta/\delta\eta)\Psi(\omega, \eta) &= 0. \end{aligned} \quad (22)$$

These linear differential equations are solved as the following:

$$\begin{aligned} \Psi(\omega, \eta) &= \exp\left[\frac{6i}{\Lambda}I_{C-S} + \beta(I_{C-S} - \frac{\Lambda}{6}I_{New})\right], \\ I_{New} &\equiv \int d^3x \epsilon^{abc} \eta_a \cdot R_{bc} - \frac{\Lambda}{24} \int d^3x \epsilon^{abc} \eta_a \cdot D_b \eta_c \\ &\quad + \frac{4}{3} \left(\frac{\Lambda}{24}\right)^2 \int d^3x \epsilon^{abc} \eta_a \cdot (\eta_b \times \eta_c), \end{aligned} \quad (23)$$

where β is a constant parameter. If we choose it as $-\frac{6}{\Lambda}i$, the wave function of the Universe becomes

$$\Psi(\omega, \eta) = \exp(iI_{New}). \quad (24)$$

This solution is suitable for both $\Lambda = 0$ and $\Lambda \neq 0$ cases. The detailed behavior of this functional will be reported in Ref.[11].

4. Summary

We have clarified the relation between the 2-form Einstein gravity and its topological version. The physical space of the topological version is contained in that of the Einstein gravity.

Moreover the vector field η^k is introduced into 2-form Einstein gravity to restore the large symmetry of its topological version. Since this new model has the modes of the gravitational wave, it is equivalent to the Einstein gravity. It may be a good strategy in quantum gravity to study models with large symmetry, in addition to local Lorentz and diffeomorphisms.

We have obtained the wave function of the universe for each model.

Acknowledgements

I am grateful to Prof. H.Y. Lee and Dr. T. Ueno for the collaboration.

REFERENCES

1. H.Y. Lee, A. Nakamichi, and T. Ueno, '*Topological 2-form Gravity in Four Dimensions*', to be published in Phys. Rev. D47 (1993).
2. R. Capovilla, J. Dell, T. Jacobson and L. Mason, Class. Quantum Grav. 8 (1991) 41.
3. A. Ashtekar, Phys. Rev. D36 (1987) 1587; '*New Perspectives in Canonical Gravity*', (Bibliopolous, Naples, Italy, 1988).
4. A. Nakamichi and T. Ueno, '*New Vector Field and BRST Charges in 2-form Einstein Gravity*', TIT/HEP-206/COSMO-24, February 1993.
5. R. Penrose and W. Rindler, '*Spinors and Space-time*' Vols. I, II (Cambridge University Press, Cambridge, 1984).
6. T. Jacobson and L. Smolin, Class. Quantum Grav. 5 (1988) 583.
7. G.T. Horowitz, Commun. Math. Phys. 125 (1989) 417.
8. A. Ashtekar, Phys. Rev. Lett. 57 (1986) 2244.
9. H. Kodama, Phys. Rev. D42 (1990) 2548.
10. H. Ikemori, in '*Proceeding of the Workshop on Quantum Gravity and Topology*', edited by I. Oda (Institute for Nuclear Study, University of Tokyo, 1991).
11. A. Nakamichi and T. Ueno, in preparation.

Quantum Fluctuation of Black Hole Horizons

Kouji Nakamura, Shigelu Konno, Yoshimi Oshiro,
and Akira Tomimatsu

*Department of Physics, Nagoya University
Chikusa-ku, Nagoya 464-01, Japan*

Abstract

In a classical Schwarzschild spacetime, two horizons, which are the apparent horizon and the event horizon, are degenerate. We also discussed the separation of black hole horizons using the canonical quantization of gravity. We introduce local mass and expansion of null geodesics as quantum operators. Hence, we can obtain the wave function of black hole interior as a mass eigenstate by using minisuperspace model. From this wave function, one can consider the quantum trajectory which represents a black hole geometry where the apparent horizon is located inside a event horizon by the uncertainty principle of geometry.

1 Introduction

Since the discovery of Hawking radiation, many works have been devoted to the analysis of the quantum evaporation of black holes. In particular, the problem of final fates of evaporating black holes has been much debated. In Hawking's semiclassical calculation, the emitted radiation was found to be exactly thermal. Then, if a black hole evaporates completely, an initially pure quantum state must evolve to a mixed state. This is known as the information loss paradox. As was emphasized by Preskill[1], it is very difficult to resolve the serious puzzle in quantum mechanics and general relativity. Before reaching the final resolution, we must develop quantum theories of the black hole geometry.

A possible way of treating the horizon as a quantum system is to apply the Wheeler-DeWitt equation[2] to spherically symmetric spacetime. The Wheeler-DeWitt approach will be viable as a quantum theory of a horizon[3]. To advance this prospect, in this paper, we want to clarify the quantum feature of the horizon from the Wheeler-DeWitt equation.

We will consider static states of a spherically symmetric black hole instead of its evolutionary states. In classical relativity the apparent horizon is always located just on the event horizon. The degeneracy of the two horizons can be removed owing to quantum fluctuation of the metric. This was first pointed out by York[4] under the semiclassical approximation. The purpose of our work is to give a Wheeler-DeWitt description for the interesting quantum phenomenon.

For a vacuum, spherically symmetric spacetime we can choose the metric dependent on a radial coordinate r only. Note that if we are concerned with the interior geometry of black holes, the coordinate r plays the role of a time coordinate, and we have a time slicing on the homogeneous spatial hypersurface $r = \text{const}$. Because of this homogeneity, one can use the minisuperspace model which is used in quantum cosmology.

In Sec.2 we construct the canonical variables from the metric for the interior geometry and write down the Hamiltonian. The spherically symmetric metric permits us to introduce the locally-defined gravitational mass[5] and the expansion of null geodesics, which are represented by the canonical variables. The mass is required to be conserved for the spherically symmetric Ricci flat system, and the expansion of null geodesics is used to determine the position of the apparent horizon. Our key idea is to treat these geometrical quantities as quantum-mechanical operators. Nambu and Sasaki[6] discussed the WKB solutions of the Wheeler-DeWitt equation by using classical trajectories in the minisuperspace. We specify the exact solution representing the interior of the static hole as an eigenstate of the mass operator. In Sec.3 we discussed the WKB approximation for our wave function, then one can obtain the classical trajectory and classify the minisuperspace into classically allowed region and forbidden region. From the wave function, in Sec.4, we discuss the quantum separation of the apparent and event horizons. In the minisuperspace of the metric we find the classically forbidden region between the two horizons, where the amplitude of the wave function is exponentially suppressed. We arrive at the conclusion that the Wheeler-DeWitt equation can give a plausible wave function to model quantum fluctuations of the

horizon geometry.

2 Canonical properties and Wave Function for Black Hole

We follow the standard canonical formulation of general relativity. Let us consider the extended Schwarzschild spacetime with the metric written in the form

$$ds^2 = -\frac{\alpha^2}{u}dT^2 + u dX^2 + v(d\theta^2 + \sin^2\theta d\phi^2), \quad (2.1)$$

where α is the lapse function. T can be identical with the Schwarzschild spherical coordinate r which works as a time-coordinate inside the black hole, and under the gauge condition $\alpha = 1$ the metric given by

$$u = \frac{2Gm}{T} - 1, \quad v = T^2 \quad (2.2)$$

becomes independent of the coordinate X . In this paper we will treat the metric fluctuations of black hole interior by assuming the Kantowski-Sachs minisuperspace model such that $\alpha = \alpha(T)$, $u = u(T)$, $v = v(T)$.

From the Einstein Lagrangian of this system, one can obtain the canonical momenta conjugate to the variables u and v

$$\Pi_u = -\frac{V}{4G\alpha} \dot{v}, \quad \Pi_v = -\frac{V}{4G} \left(\frac{\dot{u}}{\alpha} + \frac{u\dot{v}}{\alpha v} \right). \quad (2.3)$$

where the dots denote derivatives with respect to the coordinate T , and the length $V = \int dX$ is assumed to be a finite constant for our convention, and the Hamiltonian written in the form

$$\begin{aligned} H &= \Pi_u \dot{u} + \Pi_v \dot{v} - L \\ &= \frac{4G\alpha}{V} \left[-\Pi_u \Pi_v + \frac{u\Pi_u^2}{2v} - \frac{V^2}{8G^2} \right]. \end{aligned} \quad (2.4)$$

gives the dynamical constraint $H = 0$.

To quantize the system, we make the usual substitutions for the momenta

$$\Pi_u \rightarrow \frac{\hbar}{i} \frac{\partial}{\partial u}, \quad \Pi_v \rightarrow \frac{\hbar}{i} \frac{\partial}{\partial v}, \quad (2.5)$$

Then the quantum state of the black hole interior is represented by the wave function $\Psi(u, v)$ on the minisuperspace, which satisfies the Wheeler-DeWitt equation

$$H\Psi = \frac{4G\alpha}{V} \left(-\Pi_u \Pi_v + \frac{u^p \Pi_u u^{1-p} \Pi_u}{2v} - \frac{V^2}{8G^2} \right) \Psi = 0. \quad (2.6)$$

For the spherically symmetric metric satisfying the vacuum Einstein equations, we have a locally defined gravitational mass M as a dynamical constant. If we use the canonical momenta (2.3), M has the form

$$M = \frac{2Gu^p \Pi_u u^{1-p} \Pi_u}{V^2 v^{1/2}} + \frac{v^{1/2}}{2G}. \quad (2.7)$$

which is weakly commutable with the Hamiltonian as follows,

$$[H, M]\Psi = \frac{2iG\hbar \Pi_u}{V^2 v^{1/2}} H\Psi = 0. \quad (2.8)$$

This commutation relation means physical state Ψ can be obtained as a mass eigenstate;

$$M\Psi = m\Psi, \quad (2.9)$$

where m is the mass eigenvalue. The Wheeler-DeWitt equation $H\Psi = 0$ supplemented by the condition (2.9) of the mass eigenstate gives the unique exact solution

$$\Psi = N \frac{z^p}{(v - 2Gmv^{1/2})^p} H_p^{(1)}(z), \quad (2.10)$$

where N is an arbitrary constant, and

$$z = \frac{V}{G\hbar} \sqrt{-u(v - 2Gmv^{1/2})} \quad (2.11)$$

The choice of the Hankel function of the first class $H_p^{(1)}$ is due to the requirement of the black hole state[6].

Inside the black hole there exists a trapped region bounded by the apparent horizon, which is defined in terms of the expansion of null geodesics. Following Carter[7], we consider a null-vector decomposition of the metric (2.1),

$$g_{ab} = -\beta_a l_b - \beta_b l_a + \gamma_{ab}, \quad (2.12)$$

with

$$\begin{aligned} l^a l_a &= \beta^a \beta_a = 0, & l^a \beta_a &= -1, \\ l^a \gamma_{ab} &= \beta^a \gamma_{ab} = 0, \end{aligned} \quad (2.13)$$

where l^a and β^a are the vector fields tangent to outgoing and incoming null rays respectively. In spherical symmetric system, these two null-vectors are necessarily tangent to null geodesics. Then, from the expansions for outgoing and ingoing null rays given by

$$\theta_+ = l^a_{;a} + \beta^a l^b l_{a;b}, \quad \theta_- = \beta^a_{;a} + l^a \beta^b \beta_{a;b}. \quad (2.14)$$

and we obtain the expansion operator

$$\theta_- \theta_+ = \frac{8G^2 u^p \Pi_u u^{1-p} \Pi_u}{V^2 v^2}. \quad (2.15)$$

The substituting of Eq.(2.3) leads to the relation of expansion operator and mass operator.

$$\theta_- \theta_+ = -\frac{2}{v} \left(1 - \frac{2GM}{v^{1/2}} \right) \quad (2.16)$$

In classical geometry, both θ_+ and θ_- become negative in the trapped region, and $\theta_+ = 0$ on the apparent horizon. The event horizon will be the null surface $u = 0$, where in the Schwarzschild spacetime the expansion θ_+ also vanishes. In the quantum versions, we must treat $\theta_- \theta_+$ as an operator. Then the trapped region will mean that $\Psi^* \theta_- \theta_+ \Psi > 0$, and the apparent horizon will be located at the surface $\Psi^* \theta_- \theta_+ \Psi = 0$ where Ψ corresponds to mass eigenstate (2.10). In the minisuperspace with the coordinates u and v , we require the positions of the apparent and event horizons to be $v^{1/2} = 2Gm$ and $u = 0$ respectively. The wave function (2.10) will describe the quantum separation of the two horizons.

3 WKB approximation and minisuperspace

WKB approximation for wave function is given by

$$\Psi \sim e^{i\mathcal{I}} \quad (3.1)$$

So, $\hbar z$ corresponds to the classical action of this system.

$$\hbar z = S \quad (3.2)$$

This wave function is same as the one given by Nambu and Sasaki up to its coefficient. One can obtain the trajectories of classical solutions on the $(u, v^{1/2})$ -plane.

From the Hamilton-Jacobi's theory, we can obtain the classical trajectory

$$u = -c \left(1 - \frac{2Gm}{v^{1/2}} \right), \quad (3.3)$$

where c is the constant of integration. This solution is independent of the choice of the laps function α . One can easily see that the constant of integration c must be positive from the other classical equations. The classical trajectories with different value of c represent only one physical trajectory, since the constant of integration c represents the degree of freedom of the scale transformation of the coordinate X .

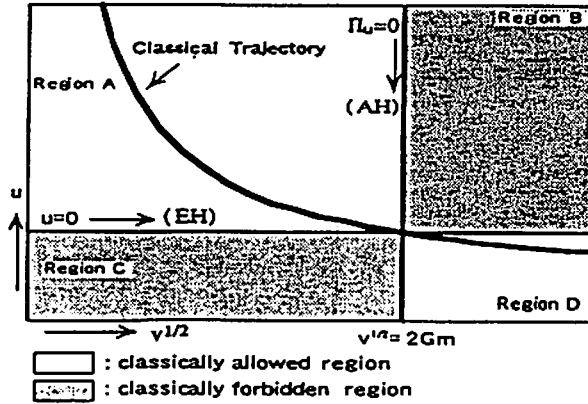


Fig1.
The classification of (u, v) -plane. Classical action is real in the region A and C, and imaginary in B and D. The interior of hole is represented by $u > 0$.

Using whether the classical action S (3.2) is real or imaginary, one can classify the (u, v) -plane into 4-regions as follows (Fig.1):

- region A : $u > 0$ and $v^{1/2} < r_g$,
- region B : $u > 0$ and $v^{1/2} > r_g$,
- region C : $u < 0$ and $v^{1/2} < r_g$,
- region D : $u < 0$ and $v^{1/2} > r_g$,

where $r_g = 2Gm$. Wave function has oscillating behavior in the region A and D, and has exponential dumping in B and C. However in the region C and D, $3 + 1$ formalism becomes broken down, i.e. the T -direction changes to spacelike from timelike, and the X -direction changes to timelike from spacelike. So, we restrict our consideration to the region A and B.

The region A where the classical action S is real (and then $\Pi_u^2 > 0$) is classically allowed region and the region B where the classical action S is imaginary (and then is $\Pi_u^2 < 0$) is classically forbidden region. We note that $u > 0$ in both of the region A and B. It is reasonable to interpret that the existence of the region B suggests that a quantum geometrical region is constructed outside the apparent horizon $v^{1/2} = r_g$ of a black hole due to the uncertainty principle. So, we consider the quantum fluctuation of black hole geometry in the next section.

4 Separation of Apparent Horizon and Event Horizons

In the Sec.3, it is shown that classical trajectories (3.3) are only in the region A. We must note that each trajectory (line) in (u, v) -plane represents a geometry of black hole. In the region A, the expansion of null geodesics $\theta_- \theta_+$ is positive, so the part of a trajectory in region A represents a trapped region of its geometry (since incoming expansion θ_- has a negative value in the black hole case). In the region B, $\theta_+ \theta_-$ become negative since the canonical momentum Π_u become imaginary. Then, the part of a trajectory in the region B represents an untrapped region of its geometry nevertheless $u > 0$. So, the point $v^{1/2} = r_g$ on a trajectory is the apparent horizon of a hole as mentioned in Sec.2.

Event horizon is null surface which is the locus of outgoing future-directed null geodesics rays that never manage to reach arbitrarily large distances from the hole. So, the location of the event horizon of a trajectory in (u, v) -plane (which represents a black hole geometry) can be easily obtained as a null surface. The point $u(T) = 0$ on a trajectory (this coincide a $T = \text{const.}$ surface) is a null surface of its geometry. Then, this point on a trajectory represents the event horizon of its geometry.

But this point $u = 0$ cannot be the apparent horizon if $v^{1/2} \neq r_g$ as mentioned in Sec.2 since expansion of null geodesics $\Psi^* \theta_- \theta_+ \Psi$ does not vanish. At classical level, these two points ($u = 0$ and $v^{1/2} = r_g$) coincide, which can be regarded as a degeneracy. However, quantum behavior of the expansion

(2.15) become different from classical one due to the uncertainty principle

$$\Delta u \cdot \Delta \Pi_u \sim \hbar. \quad (4.1)$$

By this uncertainty principle, $\Psi^* \theta_+ \theta_- \Psi$ cannot become exactly zero due to the factor $u \Pi_u^2$. So, one cannot define the position of apparent horizon by $u = 0$ at quantum level.

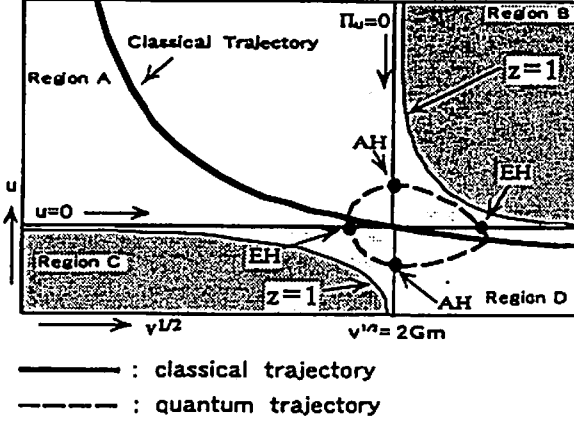


Fig2. The classical trajectory and a quantum trajectory in (u,v) -plane. A quantum trajectory represents a geometry in which the apparent horizon and the event horizon are separated.

If the quantum trajectory passing through the region B (Fig.2) exist, it represents the geometry in which the area of the apparent horizon and the area of the event horizon is different. The existence of such a trajectory is possible since the amplitude of wave function is not exact zero in classically forbidden region. Furthermore, from the spacetime metric (2.1), one can easily see that the apparent horizon $v^{1/2} = r_g$ in the quantum trajectory passing through the region B is spacelike, since a $v(T)^{1/2} = \text{const.}$ surface coincide a $T = \text{const.}$ surface by our minisuperspace model and $u > 0$ in the regions A and B. Thus one can see the violation of the horizons' degeneracy from our wave function. It is reasonable to consider that this quantum separation of the apparent and the event horizon has something to do with York's one.

Unfortunately, the precise quantum mechanical amplitude of this separation (the amplitude of a quantum trajectory passing through the region B) cannot be given by our wave function due to the ambiguity of our model, for example, it is about divergence factor V , or about the normalization of our

wave function and so on. We cannot obtain more interpretation of our wave function. So, the analysis of a different model are necessary to make sure that our interpretations of the wave function of a black hole are correct.

5 Conclusion and Discussion

We remark our conclusion in this paper. We consider the state of the geometry of a Schwarzschild black hole interior as a preliminary work toward the understanding of the quantum state of evaporating black hole and then consider the quantum behavior of static black hole geometry. Then we can obtain the exact solution of Wheeler-DeWitt equation describe the interior of black hole as the mass eigenstate by minisuperspace model. The WKB approximation of this wave function corresponds to one which was obtained by Nambu and Sasaki up to its coefficient. And we discussed the possibility of the spontaneous separation of the apparent and the event horizon of a hole. Then, we can conclude from our wave function that the apparent and event horizon can be separate spontaneously due to the uncertainty principle of gravity. Unfortunately, precise quantum mechanical amplitude cannot be obtained due to our ambiguity of our model. To make sure whether our interpretations of our wave function are physically correct or not, the analysis by the other models are necessary.

In our model, $3 + 1$ formalism is broken in the regions where $u < 0$ (i.e. the region C and D in Fig.2) since the $T = \text{const.}$ surface change from spacelike hypersurface to timelike. However, these regions seem also describe the exterior of the event horizon, since the classical action is real in the region D and the classical trajectory (3.3) which can be obtained from our wave function represents Schwarzschild metric. If one stands at the opposite point of view, one can interpret that our wave function predicts the fact that there are compact region and its outside region with boundary $u = 0$ in a space and these two regions are expressed by single coordinate whose time coordinate T in the compact region change to space coordinate in its outside region. Furthermore, if our wave function describes the exterior of black hole, one can consider the quantum trajectory passing through C, and then one can easily see that the apparent horizon in this trajectory is $v^{1/2} = r_g$ and this apparent horizon become timelike since $v(T) = \text{const.}$ surface coincide and $u < 0$ in the regions C and D (Fig2). This quantum trajectory represents the quantum geometry analogous to York's argument rather than the trajectory

passing through the region B.

However, as we mentioned above, $3 + 1$ formalism becomes broken down in these regions, and T -direction changes to spacelike from timelike in them, and we have no answer for the problem that what influences appear by this breaking down of canonical formalism. So, we have no answer for the question that our wave function really describes the exterior of black hole or not. To answer this problem, one must consider the other model and this work remains as a future one.

References

- [1] J.Preskill, "Do Black Holes Destroy Information?", Preprint CALT-68-1819 (1992).
- [2] B.S. DeWitt, *Phys. Rev.* **160**, 1113,(1967).
- [3] L.M.C.S. Rodrigues, I.D. Soares, J. Zanelli, *Phys. Rev. Lett.* **62**, 9, (1989).
C.O. Lousto, F.D. Mazzitelli, *Int. J. Mod. Phys. A* **6**, 1017, (1991).
A. Tomimatsu, *Phys. Let. B* **289**, 283, (1992).
- [4] J. W. York, Jr. *Phys. Rev. D* **28**, 12, 2929,(1983).
- [5] W. Fischler, D. Morgan, and J. Polchinski, *Phys.Rev. D***42**, 12, 4042, (1990).
- [6] Y. Nambu and M. Sasaki, *Prog. Theor. Phys.* **79**, 96, (1988).
- [7] B. Carter, in *General Relativity*, edited by S.W. Hawking and W. Israel (Cambridge University Press, Cambridge,1979).

Pathological divergence in perturbative quantum field theory in spacetime with accelerated expansion

KAZUHIRO YAMAMOTO

*Uji Research Center, Yukawa Institute for Theoretical Physics
Kyoto University, Uji 611, Japan*

Abstract : We show that perturbative quantum field theory may break down in curved spacetime with accelerated expansion[1]. We consider $\lambda\phi^p$ -theory ($p = 3, 4, 5, \dots$) with curvature coupling $\xi R\phi^2$ in de Sitter space and perturbatively evaluate the n -point function. We find the vertex-integral over all spacetime points diverges for a certain range of the mass and curvature coupling. In particular, for $\lambda\phi^4$ -theory with $\xi = 0$, the divergence arises for $m^2/H^2 \leq 27/16$ where H^{-1} is the de Sitter radius. Then we show that the same type of divergence arises quite generally in a spacetime with accelerated expansion. Since it is caused by unboundedly accelerated expansion of spacetime, we call it the superexpansionary divergence.

In spite of its importance, it is generally very difficult to formulate a quantum field theory in curved spacetime in a rigorous and tractable manner. An exception is that in de Sitter spacetime. Thanks to the maximal symmetry characterized by the de Sitter group, $O(1, 4)$, various exact formulas can be used to quantize a field[2,3,4]. Furthermore it is cosmologically realistic in the sense that our universe is believed to have undergone an inflationary expanding phase at the early stage which can be well approximated by the de Sitter spacetime. In the present paper we consider a self-interacting scalar field in the de Sitter background. Calculating the connected part of an n -point spatial correlation function, we show that a new type of pathological divergence may appear in the theory, which is of purely geometrical origin. We also note that this is a common phenomenon in spacetime with accelerated expansion and discuss its implications to the inflationary cosmology. Plank units with $c = \hbar = G = 1$ are used throughout.

Let us start with a free scalar field with the following Lagrangian,

$$\mathcal{L} = -\frac{1}{2} (g^{\mu\nu} \phi_{;\mu} \phi_{;\nu} + m^2 \phi^2 + \xi R \phi^2), \quad (1)$$

where R is the scalar curvature and ξ is a constant. For the moment we focus on the de Sitter spacetime with the metric

$$ds^2 = -dt^2 + e^{2Ht} dx^2 = \frac{1}{(-H\eta)^2} (-d\eta^2 + dx^2). \quad (2)$$

where H is a constant and η is the conformal time defined by $e^{Ht} = 1/(-H\eta)$ for $-\infty < \eta < 0$. The above coordinate represents only the upper-half region of the maximally extended de Sitter spacetime. The entire spacetime including the lower-half region may also be expressed in terms of the above coordinates by simply extending the domain of η to $-\infty < 1/(-\eta) < \infty$ (i.e., $0 < \eta < \infty$ and $-\infty < \eta < 0$; see Fig. 1).

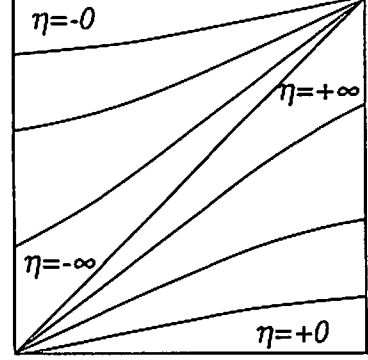


Fig.1

In the coordinates given by Eq.(2), the scalar field $\phi(x)$ can easily be quantized as

$$\phi(x) = \int \frac{d^3k}{(2\pi)^{3/2}} \left[\varphi_k(\eta) a_k e^{ikx} + \varphi_k^*(\eta) a_k^\dagger e^{-ikx} \right]. \quad (3)$$

Here a_k and a_k^\dagger are the annihilation and creation operators, respectively, and $\varphi_k(\eta)$ is the corresponding positive frequency mode function for an appropriately chosen vacuum state. For the Euclidean vacuum state, which respects the full de Sitter invariance, the mode function $\varphi_k(\eta)$ is given by

$$\begin{aligned} \varphi_k(\eta) &= e^{i\theta} \frac{\sqrt{\pi}}{2} H(-\eta)^{3/2} e^{i\nu\pi/2} H_\nu^{(1)}(-k\eta); \quad (-\infty < 1/(-\eta) < \infty), \\ \nu &:= \sqrt{\frac{9}{4} - \left(\frac{m^2}{H^2} + 12\xi\right)}, \end{aligned} \quad (4)$$

where $H_\nu^{(1)}$ is a Hankel function of the first kind. We choose the arbitrary phase factor

$e^{i\theta}$ as $\theta = -i\pi/4$ for which the equality $\varphi_k(-\eta) = \varphi_k(\eta)^*$ is satisfied [4]. The Feynman propagator has been explicitly calculated in the literature [2,3,5,6],

Now we introduce the following self-interaction:

$$\mathcal{L}_I = -\frac{1}{4!}\lambda\phi^4. \quad (5)$$

Following the general prescription for perturbative quantum field theory, we can calculate n -point Green functions. Here let us focus on the equal-time limit of the n -point expectation value with respect to an in-vacuum, $|0, in\rangle^*$ [7]. This limit gives the n -point spatial correlation function which is physically observable in principle. We first consider the 4-point function, then the connected part is given by the following expression in the first-order perturbation:

$$G_{(4)}^c(x_1, x_2, x_3, x_4; \eta) = 2\lambda \text{Im} \left[\int d^4y \sqrt{-g(y)} \Delta(y, x_1) \Delta(y, x_2) \Delta(y, x_3) \Delta(y, x_4) \right], \quad (6)$$

where $x_i = (\eta, \mathbf{x}_i)$, $y = (\eta', \mathbf{y})$, $\Delta(y, x_i) = \langle 0|T\phi(y)\phi(x_i)|0\rangle$, which is the free Feynman propagator, and the integration with respect to vertex y ranges the whole region in the past of η . Using Eqs. (3), we obtain the formal expression for the connected 4-point function as

$$\begin{aligned} G_{(4)}^c(x_1, x_2, x_3, x_4; \eta) &= 2\lambda \text{Im} \left[\prod_{i=1}^4 \left[\int \frac{d^3k_i}{(2\pi)^3} \right] (2\pi)^3 \delta\left(\sum_{i=1}^4 \mathbf{k}_i\right) \exp\left(i \sum_{i=1}^4 \mathbf{k}_i \cdot \mathbf{x}_i\right) \right. \\ &\quad \times \prod_{i=1}^4 [\varphi_{k_i}(\eta)] \left(\int_{-\infty}^{\eta} d\eta' + \int_0^{\infty} d\eta' \right) \frac{1}{(H\eta')^4} \prod_{i=1}^4 [\varphi_{k_i}^*(\eta')] \Big], \end{aligned} \quad (7)$$

where we have assumed that η is in the upper-half region, or $-\infty < \eta < 0$. In the above expression, the η' -integration may diverge depending on the values of mass and/or the

* In the de Sitter spacetime with a de Sitter invariant vacuum state, the in-vacuum is equal to the out-vacuum. Hence the common formalism for transition amplitudes gives the same result.

nonminimal coupling constant ξ . Namely, in the limit $\eta' \rightarrow 0$, $\varphi_k(\eta')$ has power-law dependence of η , $\varphi_k(\eta') \propto |\eta'|^c$, where $c := \frac{3}{2} - \nu$, while the volume element $\sqrt{-g(\eta')}$ expands in proportion to $|\eta'|^{-4}$. Therefore the integration with respect to η' diverges in the limit $\eta' \rightarrow 0$, if $-4 + 4c \leq -1$, i.e., $c \leq 3/4$.

In the above we have considered the 4-point function in the first order of perturbation. This type of divergence, however, occurs in all orders of perturbation. As is clear from the above arguments, this divergence is caused by the expansion of the spatial volume at past infinity. Hence we call it the *superexpansionary* divergence[6]. Thus we conclude that the conventional perturbative expansion is not well-defined in de Sitter spacetime for a scalar field with $c \leq 3/4$, or

$$\frac{m^2}{H^2} + 12\xi \leq \frac{27}{16}. \quad (8)$$

Note that this feature is not limited to $\lambda\phi^4$ -theory. For $\lambda\phi^p$ -theory ($p = 3, 4, 5, \dots$), the above constraint is generalized to $m^2/H^2 + 12\xi \leq 9(p-1)/p^2$.

Since the superexpansionary divergence is of spacetime origin, one expects that it also arises in other spacetimes with unboundedly accelerated expansion. To see this, let us consider a spacetime filled with a matter with the equation of state : $P = -(n + \frac{1}{3})/(n+1)\rho$, where $n(>0)$ is a constant, ρ and P denote density and pressure of the matter, respectively. Assuming the spatially closed Friedmann-Robertson-Walker metric, one can solve the Einstein equation to find

$$ds^2 = \frac{1}{H_*^2} \frac{1}{\cos(\alpha\tau)^{2/\alpha}} (-d\tau^2 + d\sigma_3^2), \quad (9)$$

where $\alpha := n/(n+1)$, H_* is a constant and $d\sigma_3^2$ is the metric on three-dimensional unit sphere. In the limit $\alpha\tau \rightarrow \pm\pi/2$, the scale factor a is related to the proper cosmic time, which is defined by $dt = d\tau/a$, as $a \propto t^{1+n}$. In this sense one may regard this spacetime as power-law background. In the limit $n \rightarrow \infty$, this reduce to the de Sitter spacetime.

We consider a nonminimally coupled scalar field with the Lagrangian (1), in this spacetime. Then the field can be quantized using the harmonics on S_3 [2,6]. In the

massless case, mode functions can be solved analytically. In terms of their asymptotic behavior at $\alpha\tau \rightarrow \pm\pi/2$ we find that the superexpansionary divergence appears if

$$\sqrt{\frac{1}{4} - \frac{(6\xi - 1)(\alpha + 1)}{\alpha^2}} \leq \frac{2 + \alpha}{2\alpha} - \frac{1}{p} \left(\frac{4 - \alpha}{\alpha} \right). \quad (10)$$

For a massive scalar field, it is difficult to analytically solve the equation of motion for any mode. However, the existence of superexpansionary divergence depends only on the asymptotic behavior of the mode function at $\alpha\tau \rightarrow \pm\pi/2$, where we can find analytic expression. The superexpansionary divergence is absent as long as $p \geq 3$ for a massive field in this spacetime. This is interpreted as follows. In the power law background, the Hubble parameter becomes smaller and smaller as spacetime expands, and consequently the scalar field becomes relatively more and more massive.

Let us now briefly discuss cosmological implications of the superexpansionary divergence. As long as only in-vacuum expectation values are concerned, this divergence apparently comes from the unbounded expansion of spatial volume at past infinity. Hence, if we take an expanding phase of the spacetime only, *e.g.*, the upper half region of de Sitter space in Fig.1, the divergence does not appear in Eq. (7), because η' -integration runs only $-\infty < \eta' \leq \eta$. Since this is usually the case of inflationary cosmology, the superexpansionary divergence should not cause any difficulty in evaluating various expectation values of quantum fluctuations. However, since the de Sitter invariance of the expectation values is explicitly broken in this case even for a massive scalar field, it becomes quite unclear whether expectation values thus calculated at, say, time η are really independent of the portion of spacetime considered, as $\eta \rightarrow -0$. For example, for a certain class of inflationary models, the relevant part of de Sitter space is that covered by $0 < \tau < \pi/2$ of the spatially closed metric, Eq. (9) with $\alpha = 1$, and the resulting expectation values for this case may differ from those calculated for the part covered by $-\infty < \eta < 0$ of the spatially flat metric. Although this issue remains to be solved, in connection with it we note that for a field massive enough to avoid the superexpansionary divergence, the vacuum expectation values for the maximally extended de Sitter space and those for the upper half of it have qualitatively very different asymptotic forms.

In any case, it is very interesting if the global spacetime structure should qualitatively affect the behavior of quantities such as spatial correlation functions. Observational implications surely deserve further study.

We do not claim that interacting quantum field theory does not exist in spacetime with accelerated expansion. In conclusion, It is the conventional interaction picture with *free* asymptotic states at future and past infinity that fails.

REFERENCES

1. M. Sasaki, H. Suzuki, K. Yamamoto and J. Yokoyama, preprint YITP/U-92-23; KUNS-1154; TU-413.
 2. N. A. Chernikov and E. A. Tagirov, *Ann. Inst. Henri Poincaré* **9A** (1968) 109.
 3. T. S. Bunch and P. C. W. Davies, *Proc. R. Soc. London* **A360** (1978) 117.
 4. B. Allen, *Phys. Rev.* **D32** (1985) 3136.
 5. N. D. Birrell and P. C. W. Davies, *Quantum fields in curved space* (Cambridge University Press, 1982).
 6. E. A. Tagirov, *Ann. Phys.* **76** (1973) 561.
 7. M. Sasaki, H. Suzuki, K. Yamamoto and J. Yokoyama, preprint YITP/U-92-24; KUNS-1155; TU-414.
- R. D. Jordan, *Phys. Rev.* **D33** (1986) 444.

Unification of Gravity, Gauge and Higgs Fields by Confined Quantum Fields

Toshiki Isse

Department of Physics Osaka University

1 Effective action for scalar field

We first discuss classical dynamics of free fields that are contained in a subspace V_* of an $N+4$ dimensional flat space V . A metric of V is $\eta_{\alpha\beta} = \text{diag}(-1, 1, \dots, 1)$ ($\alpha, \beta = 0, 1, \dots, N+3$). We regard V_* as a neighborhood of a four dimensional submanifold M arbitrarily embedded into V . In other words, we assume an existence of some physical object \emptyset (we call it template of spacetime) which confines quantized free fields inside the neighborhood of M . In the case of spin 1/2 fields, the system is shown to be described by an infinite number of fields in M , interacting with gravity ($g_{\mu\nu}$), $SO(N)$ gauge fields (A_μ) and an N -plet of scalar fields (ϕ^a). The fields $g_{\mu\nu}$, A_μ and ϕ^a are determined from embedding functions of M and correspond respectively to the induced metric, the normal connection and the extrinsic curvature of M . In this talk, we study low energy effective theory of the system. Investigating quantum effects caused by the massive modes of the fields we will show that Einstein- $SO(N)$ -Yang-Mills-Higgs theory is induced as a low energy effective theory of the system. The fields ϕ^a will be shown to behave as Higgs fields.

We first study classical dynamics of a free massless scalar field that is contained in the neighborhood V_* of M . The Neumann boundary condition is imposed on a boundary of V_* . The action of the system is described by

$$S_{\text{scalar}}[D, X] = \int_{V_*} dZ^{N+4} \left(-\eta^{\alpha\beta} \frac{\partial D^*(Z)}{\partial Z^\alpha} \frac{\partial D(Z)}{\partial Z^\beta} + \text{constant} \right), \quad (1.1)$$

The exact definition of V_* will be given shortly. We find that the appropriate coordinates to describe V_* are given by the curvilinear coordinates (x_μ, ζ^a) , where

$x_\mu (\mu = 0, 1, 2, 3)$ are the coordinates tangent to M and ς^a ($a = 1, \dots, N$) are the ones normal to M . The line element of V is written in the new coordinates,

$$ds^2 = \sum_{\mu, \nu=0}^3 g_{\mu\nu}(x, \varsigma) dx^\mu dx^\nu + \sum_{a=1}^N d\varsigma^a d\varsigma^a. \quad (1.2)$$

We can choose $\varsigma^a = 0$ on the manifold M , so that $x_\mu (\mu = 0, 1, 2, 3)$ can be regarded as the coordinates of M . Using the new coordinates, we define the neighborhood V_* as a region that satisfies $|\varsigma^a| \leq l/2$, ($a = 1, \dots, N$). We can always find the above coordinates if all focal points lie outside the neighborhood of M . In order to satisfy the above condition, M has to be embedded so that the smallest focal length $d(X)$ is larger than $\ell/2$. In the new coordinates, the Lagrangian of the system is written by

$$\begin{aligned} S_{\text{scalar}}[D, X] = & \int_{V_*} \sqrt{-g(X(x))} dx^4 d\varsigma^N [g^{\mu\nu}(X(x))(1 + \Delta) \frac{\partial D^*(x, \varsigma)}{\partial x^\mu} \frac{\partial D(x, \varsigma)}{\partial x^\nu} \\ & + (1 + \Delta') \frac{\partial D^*(x, \varsigma)}{\partial \varsigma^b} \frac{\partial D(x, \varsigma)}{\partial \varsigma^b} + \text{constant}], \end{aligned} \quad (1.3a)$$

where $g_{\mu\nu}(X(x))$ is the induced metric of M and the correction terms Δ and Δ' are order of magnitude [1]

$$\Delta \cong \Delta' \cong O\left(\frac{\ell}{d(X)}\right). \quad (1.3b)$$

We neglect the correction terms Δ and Δ' as we are interested only in the limit $\ell/d(X) \rightarrow 0$. We will discuss the physical meaning of the limit later. Then we decompose the scalar field into a Fourier series with respect to ς^a ,

$$D(x^\mu, \varsigma^a) = l^{-N/2} \sum_n D(x^\mu, n) \exp(i2\pi n^a \cdot \varsigma^a / l). \quad (1.4)$$

We substitute the above expression into the action (1.3a) and integrate over the

ς^a variables, neglecting Δ and Δ' . We find

$$\begin{aligned}
& S_{scalar}[D, X] \\
&= \int_M dx^4 \sqrt{g(x)} \left[\sum_n (-g^{\mu\nu}(x)) \frac{\partial D^*(x, n)}{\partial x^\mu} \frac{\partial D(x, n)}{\partial x^\nu} + M_n^2 |D(x, n)|^2 \right. \\
&\quad \left. + \text{constant} \right],
\end{aligned} \tag{1.5}$$

where

$$M_n^2 = \left(\frac{2\pi n}{\ell} \right)^2. \tag{1.6}$$

The mass of $n(\neq 0)$ modes are very large, when l is very small. The massive modes cannot be excited classically in low energy physics. We find, however, that quantum effects caused by the massive modes are not negligible. The massive modes of the fields are influenced by the configuration of the submanifold, which itself provides the gravity. It is therefore natural to expect that the quantum effects caused by the massive modes generate dynamics of the gravity. Such an idea was first introduced by Sakharov and Zeldovich [2][3]. The effective Lagrangian of the system is obtained by path integrating all massive modes. We write the effective Lagrangian of the system as

$$L_{total\ eff}^{(0)} = L_{zero-mode}^{(0)} + L_{eff}^{(0)} + \sqrt{-g(x)} \text{constant}, \tag{1.7}$$

where $L_{eff}^{(0)}(g)$ is given as follows,

$$\begin{aligned}
L_{eff}^{(0)} &= \sum_{n \neq 0} i \text{Tr} \ln [-\nabla_\mu \nabla^\mu + M_n] \\
&= \sum_{n \neq 0} L_{eff}^{(0)}(n).
\end{aligned} \tag{1.8}$$

As the gravitational fields are background fields and D is a bilinear field, it is sufficient to compute one-loop effective action of mode n ; $L_{eff}^{(0)}(n)$. We

evaluate $L_{eff}^{(0)}(n)$ by using a heat kernel technique developed by De-Witt and Schwinger[4][5],

$$L_{eff}^{(0)}(n) = i \int_0^\infty \frac{g^{1/2} e^{-iM_n^2 s}}{(4\pi i s)^{2+\epsilon/2}} \sum_{r=0}^\infty a_r (is)^r \frac{ds}{is}. \quad (1.9)$$

Here we used a dimensional regularization $n=4+\epsilon$, where n is taken to be the dimension of the submanifold M . a_r are the De-Witt Schwinger coefficients. Carrying out the s integration we obtain

$$L_{eff}^{(0)}(n) = \frac{g^{1/2}}{(4\pi)^2} \sum_{r=0}^\infty \Gamma(r-2-\epsilon/2) \left(\frac{2\pi}{\ell}\right)^2 n^{2-r+2+\epsilon/2} a_r. \quad (1.10)$$

The mode sum of the effective action can be calculated by using Epstein zeta functions;

$$\zeta_N(a_1, \dots, a_N; s) = \sum_{n_1=-\infty}^\infty \cdots \sum_{n_N=-\infty}^\infty [(a_1 n_1)^2 + \cdots + (a_N n_N)^2]^{-s/2}, \quad (1.11)$$

$$\zeta_N(s) \equiv \zeta_N(1, \dots, 1; s) \quad (1.12),$$

where the prime indicates that we should omit the term for which all $n_i = 0$. The final expression for $L_{eff}^{(0)}$ is

$$L_{eff}^{(0)} = \sqrt{g(X(x))} \left(\frac{\Gamma(N/2+2) \zeta_N(N+4)}{\pi^{N/2+2} \ell^4} + \frac{\Gamma(N/2+1) \zeta_N(N+2)}{24\pi^{N/2+2} \ell^2} R \right. \\ \left. + \frac{1}{8\pi^2 \epsilon} \left[\frac{R^2}{72} + \frac{R^{\mu\nu\lambda\rho} R_{\mu\nu\lambda\rho}}{180} - \frac{R^{\mu\nu} R_{\mu\nu}}{180} \right] + \left(\frac{\ell}{2\pi}\right)^2 \frac{1}{\epsilon} [\text{higher order terms}] \right) \quad (1.13)$$

where higher order terms are given by the following finite terms,

$$\frac{1}{(4\pi)^2} \sum_{r=1}^\infty \Gamma(r) \epsilon \zeta_N(2r-\epsilon) \left(\frac{\ell}{2\pi}\right)^{2r-2} a_{r+2}. \quad (1.14)$$

It is known that $\zeta_N(s)$ is convergent when $s > N$ and that it has simple poles at $s = N, N-1, \dots, 1[7]$. Therefore the coefficients a_0 and a_1 are finite while a_r ($[(N+5)/2] \geq r \geq 2$) are divergent as $\epsilon \rightarrow 0$.

2 Effective action for spinor fields

In this section we discuss the spinor case. The action of free spinor fields contained in the neighborhood V_* of M is,

$$S_{spinor}[\Phi, X] = \frac{1}{2} \int_{V_*} dZ^{N+4} [i\bar{\Phi}(Z)\Gamma^\alpha \left(\frac{\partial}{\partial Z^\alpha} - \frac{\bar{\partial}}{\partial Z^\alpha} \right) \Phi(Z) + constant]. \quad (2.1)$$

As in the case of the scalar fields we write the action in the coordinates x_μ, ς^a . Then we decompose the spinor fields into a Fourier series with respect to ς^a and integrate over ς^a in the limit $\ell/d(X) \rightarrow 0$. We find the action in the limit;

$$\begin{aligned} S_{spinor}[\Phi, X] &= \int_M \sqrt{-g(x)} dx^4 \left(\frac{i}{2} \bar{\Phi}(x, n) \Gamma^\mu(x) \frac{\partial \Phi(x, n)}{\partial x^\mu} - \frac{i}{2} \frac{\partial \bar{\Phi}(x, n)}{\partial x^\mu} \Gamma^\mu(x) \Phi(x, n) \right. \\ &\quad \left. + \frac{i2\pi n^a}{\ell} \bar{\Phi}(x, n) \Gamma^a \frac{\partial \Phi(x, n)}{\partial \varsigma^a} \right)_{\varsigma=0} + constant, \end{aligned} \quad (2.2)$$

where $\Phi(x^\mu, n)$ are Fourier components of the spinor fields and

$$\Gamma^\mu(x) \equiv \sum_{\alpha=0}^{N+3} \frac{\partial x^\mu}{\partial Z^\alpha} \Big|_{\varsigma=0} \Gamma^\alpha. \quad (2.3)$$

We have to perform a local transformation on the fields $\Phi(x, n)$ to make fields transforming as spinors on M . The transformation is given as follows

$$\Phi(x, n) \rightarrow \Psi(x, n) = \rho^{-1}(e(x)) \Phi(x, n), \quad (2.4)$$

where $e(x)$ is an $SO(1, N+3)$ matrix field on M and ρ is a spinor representation of $e(x)$. The field $e(x)$ is defined by putting $N+4$ column vectors $e_i(x)$ ($i=0, \dots, N+3$) on M successively

$$e(x) = [e_0(x) \dots e_3(x) e_4(x) \dots e_{N+3}(x)]. \quad (2.5)$$

Here $e_0(x), \dots, e_3(x)$ are orthonormal vectors (in V) tangent to M and $e_4(x), \dots, e_{N+3}(x)$ are orthonormal vectors normal to M [8]. The action (2.2) is written in

terms of $\Psi(x, n)$

$$S_{spinor}[\Phi, X] = \int_M \sqrt{-g(x)} dx^4 \left(i \sum_n \bar{\Psi}(x, n) [\gamma^\mu(x) \bar{\nabla}_\mu + im_n] \Psi(x, n) + constant \right), \quad (2.6)$$

where

$$\bar{\nabla}_\mu \equiv \frac{\bar{\partial}}{\partial x^\mu} + \omega_\mu^{lm}(e(x)) \frac{[\gamma_l, \gamma_m]}{8} + A_\mu^{ab}(e(x)) \frac{[\hat{\Gamma}_a, \hat{\Gamma}_b]}{8}, \quad (2.7a)$$

$$\omega_\mu^{lm}(e(x)) = \sum_{\alpha=0}^{N+3} [e^{-1}(x)]_\alpha^l \frac{\partial [e(x)]_m^\alpha}{\partial x^\mu}, \quad (2.7b)$$

$$A_\mu^{ab}(e(x)) = \sum_{\alpha=0}^{N+3} [e^{-1}(x)]_\alpha^{a+3} \frac{\partial [e(x)]_{b+3}^\alpha}{\partial x^\mu}, \quad (2.7c)$$

$$m_n = \frac{2\pi n^a \Gamma^{3+a}}{\ell}. \quad (2.7c)$$

We showed in Ref.[1] that ω_μ and A_μ are identified as a spin connection and an $SO(N)$ gauge field respectively and that $\Psi(x, n)$ transforms as a $2^{[N/2]}$ -plet of Dirac spinors on M . A local Lorentz (a gauge) transformation corresponds to a transformation of the orthonormal vectors $e_0(x), \dots, e_3(x)$ ($e_4(x), \dots, e_{3+N}(x)$). The fields ω_μ and A_μ are determined by the embedding functions of M modulo the Local Lorentz and the gauge transformations. Note that ω_μ and A_μ are not independent and that they are both nontrivial connections. In addition to the action (2.1) we consider the following surface term ,

$$S_{surface} = \int_{V_+} dZ^{N+4} h \bar{\Phi} \Gamma^\alpha \left(\frac{\bar{\partial}}{\partial Z^\alpha} + \frac{\bar{\partial}}{\partial Z^\alpha} \right), \quad (2.8)$$

where h is an arbitrary constant. Following the same procedure as discussed above, we find that the surface term (2.8) induces a simple Yukawa interaction

and an N-plet of scalar fields,

$$S_{surface} = \int_M dx^4 \sqrt{-g(x)} h \bar{\Psi}(x, n) \not{\beta} \Psi(x, n). \quad (2.9)$$

where

$$\not{\beta} = \phi^a \Gamma^{3+a}, \quad (2.10)$$

$$\phi^a \equiv \sum_{l=0}^3 \phi_l^{l \ 3+a}. \quad (2.11)$$

The field $\phi_\mu^{l \ 3+a}$ is called extrinsic curvature of M and is given by $e(x)$ as

$$\phi_\mu^{l \ 3+a} = \sum_{\alpha=0}^{N+3} [e^{-1}(x)]_\alpha^l \frac{\partial [e(x)]^{\alpha 3+a}}{\partial x^\mu}. \quad (2.12)$$

We find that the final expression for the action in the limit $\ell/d(X) \rightarrow 0$ is

$$\begin{aligned} S_{spinor}[\Phi, X] \\ = \int_M \sqrt{-g(x)} dx^4 \left[\sum_n \bar{\Psi}(x, n) (i\gamma^\mu(x) \vec{\nabla}_\mu + h \not{\beta} - m_n) \Psi(x, n) + \text{constant} \right]. \end{aligned} \quad (2.13)$$

As in the case of the scalar, an effective Lagrangian of the system is obtained by path integrating all massive modes,

$$L_{total \ eff}^{(1/2)} = L_{zero-mode}^{(1/2)} + L_{eff}^{(1/2)} + \sqrt{-g(x)} \text{constant}, \quad (2.14)$$

where

$$\begin{aligned} L_{eff}^{(1/2)} &= - \sum_{n \neq 0} i \text{Tr} \ln [i\gamma^\mu \nabla_\mu + (h \not{\beta} - m_n)] \\ &= \sum_{n \neq 0} L_{eff}^{(1/2)}(n). \end{aligned} \quad (2.15)$$

The effective action is written as

$$\begin{aligned}
L_{eff}^{(1/2)} = & \sqrt{-g} (\ell^{-4} c_1 + \ell^{-2} [c_2 R + c_3 \phi^2] \\
& - \frac{N_F}{(4\pi)^2 \varepsilon} \left[\frac{R^2}{72} - \frac{R_{\mu\nu} R^{\mu\nu}}{45} - \frac{7 R_{\mu\nu\lambda\rho} R^{\mu\nu\lambda\rho}}{360} \right. \\
& - \frac{2}{3N_F} \text{tr} F_{\mu\nu} F^{\mu\nu} + 2h^2 (\nabla_\mu \phi)^a (\nabla_\mu \phi)_a + 2h^4 (\phi^2)^2 \\
& \left. + \frac{1}{3} h^2 \phi^2 R \right] + \frac{\ell^2}{\varepsilon} [\text{higer order terms}]).
\end{aligned} \tag{2.16}$$

Here

$$c_1 = -\frac{2N_F \Gamma(N/2 + 2) \zeta_N(N + 4)}{\pi^{N/2+2}} \tag{2.17a}$$

$$c_2 = \frac{N_F \Gamma(N/2 + 1) \zeta_N(N + 2)}{24\pi^{N/2+2}} \tag{2.17b}$$

$$c_3 = \frac{(1 + 2/N) N_F \Gamma(N/2 + 1) \zeta_N(N + 2) h^2}{2\pi^{N/2+2}}, \tag{2.17c}$$

and $[\text{higer order terms}]$ represent finite contributions from $a_r^{(1/2)} (r \geq 3)$

3 Interpretation of effective action

In quantum field theory divergent terms are renormalized by redefining coupling constants and fields. We cannot, however, remove the divergent terms in eq.(1.17) and eq.(2.16) by usual renormalization prescription; coupling constants to be renormalized do not exist in our original Lagrangians (1.1),(2.1). Is it a difficulty in our theory? The answer is no. The theory we developed here is nothing but a free field theory restricted in a finite region V_* of the embedding space V . Therefore we must obtain some reasonable physical results from eq.(1.17) and eq.(2.16). We will propose a possible effective Lagrangian which describe quantum fluctuation of the system. We would like to search for a physically reasonable effective Lagrangian by the following method. We assume that

there exist finite physical fields denoted by $\tilde{X}^\alpha(x)$, $\tilde{\Psi}(x, 0)$ and $\tilde{D}(x, 0)$, which are defined respectively by rescaling the original fields

$$X^\alpha(x) = \epsilon^{-\lambda/2} \tilde{X}^\alpha(x) \quad (3.1a)$$

$$\Psi(x, 0) = (N_F/6\pi^2)^{1/2} \kappa_\varphi \epsilon^{-\lambda_\varphi} \tilde{\Psi}(x, 0) \quad (3.1b)$$

$$D(x, 0) = (N_F/6\pi^2)^{1/2} \kappa_D \epsilon^{-\lambda_D} \tilde{D}(x, 0). \quad (3.1c)$$

where κ_φ and κ_D are arbitrary constants. The parameters λ , λ_φ , and λ_D are introduced as powers of ϵ multiplying the original fields. In other words, we regard $X^\alpha(x)$, $\Psi(x, 0)$ and $D(x, 0)$ as divergent fields. Eq. (3.1a) implies

$$g_{\mu\nu}(X(x)) = \epsilon^{-\lambda} \tilde{g}_{\mu\nu}(\tilde{X}(x)) \quad (3.2)$$

$$e_\mu^I = \epsilon^{-\lambda/2} \tilde{e}_\mu^I. \quad (3.3)$$

Consider a corresponding system that consists of both spinor fields and N_B scalar fields. Taking into account the fact that the fields $\tilde{X}^\alpha(x)$, $\tilde{\Psi}(x, 0)$ and $\tilde{D}(x, 0)$ are finite, we factorize a leading divergent coefficient as an overall factor of the effective Lagrangian of this system. For example, when $\lambda = 2$ ($\lambda_D = (1 - \lambda)/2, \lambda_\varphi = (1 - 3\lambda/2)/2$), the effective action is written as

$$L_{eff} = \frac{\kappa_\varphi^2 N_F}{6\pi^2 \epsilon} L_{eff}^{phys} \quad (3.4)$$

Here L_{eff}^{phys} is a finite Lagrangian of the physical fields,

$$\begin{aligned}
L_{eff}^{phys} &= \sqrt{-\tilde{g}} \left[- \sum_{A=1}^{N_B} \partial_\mu \tilde{D}^{*(A)}(x, 0) \partial^\mu \tilde{D}^{*(A)}(x, 0) \right. \\
&\quad - \tilde{\Psi}(x, 0) (i \tilde{\gamma}^\mu \nabla_\mu + \kappa_\varphi \hat{\phi}^a \Gamma^{a+3}) \tilde{\Psi}(x, 0) + \text{constant} + \frac{1}{16\pi G} \tilde{R} \\
&\quad - \sum_{c=1}^{\dim SO(N)} \frac{F_{\mu\nu}^{(c)} F^{(c)\mu\nu}}{4\kappa_\varphi^2} - \frac{1}{2} (\nabla_\mu \hat{\phi})^2 + \frac{m^2}{2} \hat{\phi}^2 - \frac{\kappa_\varphi^2}{3} (\hat{\phi}^2)^2 - \frac{\hat{\phi}^2 \tilde{R}}{8\kappa_\varphi^2} \\
&\quad \left. + \frac{3}{4\kappa_\varphi^2} \left[\left(\frac{N_B}{N_F} - \frac{1}{2} \right) \frac{\tilde{R}^2}{72} + \left(-\frac{N_B}{N_F} + 2 \right) \frac{\tilde{R}_{\mu\nu} \tilde{R}^{\mu\nu}}{180} + \left(\frac{4N_B}{N_F} + 7 \right) \frac{\tilde{R}_{\mu\nu\lambda\rho} \tilde{R}^{\mu\nu\lambda\rho}}{720} \right] \right]
\end{aligned} \tag{3.5}$$

where

$$\frac{1}{16\pi G} = \frac{\Gamma(N/2 + 2) \varsigma_N(N + 4)}{4\kappa_\varphi^2 \pi^{N/2} \ell^2} \left(\frac{N_B}{N_F} + 1 \right) \tag{3.6}$$

$$m^2 = \frac{(1 + 2/N) \Gamma(N/2 + 1) \varsigma_N(N + 2)}{\kappa_\varphi^2 \pi^{N/2} \ell^2} \tag{3.7}$$

$$\hat{\phi}^a \equiv \frac{\hbar}{\kappa_\varphi} \sqrt{3/2} \tilde{\phi}^a. \tag{3.8}$$

As the overall factor of the Lagrangian does not effect equation of motion, we can regard L_{eff}^{phys} as a possible effective Lagrangian which describes the effective theory of the system. Of course the classical Lagrangian obtained here depends on the choice of the definition of the physical fields $\tilde{X}^a(x)$, $\tilde{\Psi}(x, 0)$ and $\tilde{D}(x, 0)$, namely the choice of the values λ , λ_φ , and λ_D . All possible effective Lagrangians are classified by λ , λ_φ , and λ_D . We find a classification with respect to λ is physicaly the most relevant. A table [1] provides the classification with respect to λ . Remember the condition of the embedding; $d(X) > \ell/2$ and the correction terms Δ and Δ' discussed in section two. They are written in terms of the finite

fields \tilde{X}^α as

$$d(\tilde{X}) > \varepsilon^{\lambda/2} \ell/2 \quad (3.9)$$

$$\Delta \cong \Delta' \cong O(\varepsilon^{\lambda/2} \ell/d(\tilde{X})). \quad (3.10)$$

If $\lambda > 0$, the condition of the embedding is automatically satisfied and the correction terms approach zero in the limit $\varepsilon \rightarrow 0$.

The table [1] shows that energy scale of the system increases as the value λ decreases. A plausible effective Lagrangian which describes the system in the lowest energy scale is in a case $\lambda > 1$. However in this case the system is unstable. When $\lambda = 1$ (in the second lowest energy scale) the effective Lagrangian L_{eff}^{phys} includes Einstein-Yang-Mills-Higgs action. In this case gauge symmetry is broken spontaneously and the fermions and the gauge fields obtain mass. If $0 < \lambda < 1$, the symmetry breakdown does not happen nor the effective action L_{eff}^{phys} includes Einstein action. If $\lambda < 0$, the calculation of the effective action of the system becomes meaningless. In this case $\ell/d(X)$, which we neglected, becomes infinitely large. The system is described not as a four dimensional effective theory in M but as an $N+4$ dimensional free field theory in V_* .

4 Discussions and Conclusion

The effective Lagrangian which describes the lowest energy scale of the system includes Einstein-Yang-Mills-Higgs action. Gravity, $SO(N)$ gauge fields and Higgs fields are induced themselves by embedding functions of M . However these three kind of fields are not independent. We hope that the difficulty might be overcome by introducing other type of surface terms to the original action ; for example $k_2 \partial_\alpha (\partial_\beta \tilde{\Phi} \Gamma^\alpha \Gamma^\beta \Gamma^\gamma \partial_\gamma \Phi)$ or $k_3 \partial_\alpha (\partial_\beta \partial_\delta \tilde{\Phi} \Gamma^\alpha \Gamma^\beta \Gamma^\gamma \Gamma^\delta \Gamma^\epsilon \partial_\gamma \partial_\epsilon \Phi) \dots$ The above surface terms are dimensionally reduced to Yukawa interaction terms in M . You can easily find that they include various representation of Higgs fields, ϕ^{abc} or ϕ^{abcde} . They are obtained also by contracting the spacetime indicies of the extrinsic curvature of M . As the constants k_2 and k_3 are dimensionfull, it is expected that

the fields ϕ^{abc} and ϕ^{abcde} might make a various energy scales of the symmetry break down. If it is the case, we can consider the gravity, the $SO(N)$ gauge fields and Higgs fields as independent fields in sufficiently low energy. It is a future task to build a model that can reproduce the standard GUT theories of $SU(5)$, $SO(10)$, or E_6 .

ACKNOWLEDGMENTS

I am very grateful to K. Kikkawa, H. Itoyama, H. Kunitomo, H. Suzuki and T. Kurimoto for useful discussions and comments.

REFERENCES

- [1] T. Isse, (hep-th/9211002, OU-HET 170)
- [2] A. D. Saharov, Sov. Phys. Doklady 12 (1968), 1040 Ya. B Zeldovich, Zh. Eksp. Teor. Fiz. Pisma Red 6 (1967), 883
- [3] for review see, S.L. Adler, Rev. Mod. Phys., 54 (1982), 729
- [4] B.S. DeWitt, in Gravity, groups and topology II, ed. B.S. De Witt and R. Stora (North-Holland, Amsterdam, 1984) p. 393
- [5] P.B. Gilkey, J. Diff. Geom. 10 (1975) 601
- [6] J. Ambjorn and S. Wolfram, Ann. Phys. 147 (1983), 1
- [7] K. Kirsten, J. Math. Phys. 32 (1990) 3008,
- [8] S.Kobayashi. and K.Nomizu, Foundation of Differential Geometry vol I, II (Interscience Publishers , New York, 1969)

Quantum gravity from 4- ϵ dimension

Kazuo GHOROKU

Department of Physics, Fukuoka Institute of Technology,

Wajiro, Higashi-ku, Fukuoka 811-02, Japan

It is one of the most important problem to find a theory which could provide us a reliable calculation of quantum gravitational-effects on some physical quantities. Although superstring theory could be considered as such a theory, it is hard to get a meaningful result in terms of this theory at four dimension ($d = 4$). Since any kind of successful field theory in the four dimension is renormalizable, one would expect a renormalizable theory also in the gravity. We can really make a renormalizable, gravitational theory [1] by adding quadratic terms of the curvature to the Einstein gravity, but it is not unitary since massive ghost appears in this theory.

In order to evade the this problem, Tomboulis [2] has previously proposed $1/N$ -expansion formalism, where the effective lagrangian ($L_{eff}^{1/2}$) is obtained by integrating out N -fermion fields,

$$L_{eff}^{1/2} = N \sqrt{-g} \left(\kappa^2 R + \lambda + \text{Tr} \ln_R(O_{1/2}) \right), \quad (1)$$

This is used for the perturbative calculation of the quantum metric-fluctuations. In eq.(1), $\kappa = \kappa_R \mu^{1-\epsilon}/N^{1/2}$, $\lambda = \lambda_R \mu^{4-\epsilon}/N$ and $O_{1/2} = \gamma^\mu D_\mu$. κ_R and λ_R are the renormalized gravitational constant and the renormalized cosmological constant respectively,

and $Tr \ln_R(O_{1/2})$ denotes the regularized fermion-loop correction. Due to the terms induced by the fermion loop-corrections, a complex conjugate pole appears instead of the massive ghost in the graviton propagator derived from $L_{eff}^{1/2}$. As a result, the perturbative unitarity can be realized in terms of the Lee-Wick mechanism. However the original theory should include higher derivative terms in order to renormalize the divergences of the fermion loop-corrections, so the theory is essentially the higher derivative theory which includes a massive ghost.

Our proposal is to apply the $1/N$ -expansion scheme to the theory of $d = 4 - \epsilon$ in order to resolve the dilemma of the renormalizability and the unitarity. In $d = 4 - \epsilon$, the logarithmic divergences do not appear, so the higher derivative terms are not necessary. Then, the ghost can be eliminated in the theory defined in $d = 4 - \epsilon$, and it would be unitary in this sense. Therefore, it is possible to perform a consistent calculations of the quantum gravity in $d = 4 - \epsilon$ in terms of $1/N$ -expansion. There is an interesting idea [3] that the fractal dimension, $d = 4 - \epsilon$, would be realized effectively due to the non-perturbative effect of black-holes. But we do not investigate on this point here, and we consider that the world of $d = 4$ is realistic. Our idea is that we use $L_{eff}^{1/2}$ to calculate the physical quantity in $d = 4 - \epsilon$ leaving ϵ finite in order to keep the unitarity and the renormalizability. After finishing the calculation, we examine the limit of $\epsilon = 0$ for the calculated quantity in order to see the physical aspects in the realistic four dimension.

However, $L_{eff}^{1/2}$ is not available in executing the perturbative calculation in $d = 4 - \epsilon$, because the graviton propagator obtained from $L_{eff}^{1/2}$ has a tachyonic-pole. This undesirable situation can be improved if we consider the spin-3/2 fields as N matter-fields. The gravitational term induced by the loop of the spin-3/2 fields has the opposite sign to that of $L_{eff}^{1/2}$. As a result, the tachyonic pole does not appear in the graviton propagator

obtained from $L_{eff}^{3/2}$,

$$L_{eff}^{3/2} = N\sqrt{-g}\left(\kappa^2 R + \lambda + Tr \ln_R(O_{3/2}) - 3Tr \ln_R(O_{1/2})\right), \quad (2)$$

and we instead find a complex conjugate poles other than the usual massless pole. In eq.(2), the gauge condition and the constraint for the spin-3/2 field are taken according to ref.[4]. Then we can perform the perturbative calculation satisfying the unitarity if the Lee-Wick mechanism works.

Several authors [5] have studied the problem of whether the radiative correction of gravitational modes could give rise to a spontaneous symmetry breaking as in the gauge theories [6]. But all those approaches are performed just in four dimension, where no reliable theory of quantum gravity exists. We here investigate the same problem in terms of $L_{eff}^{3/2}$ given above, and the result is continued to $d = 4$. Here we consider the case of that the cosmological constant λ is fine tuned to zero.

We add to $L_{eff}^{3/2}$ the following scalar(ϕ)-part

$$L_\phi = \sqrt{-g}\left(\frac{1}{2}g^{\mu\nu}\partial_\mu\phi\partial_\nu\phi + \zeta\phi^2 R + N^{-1}\gamma\phi^4\right). \quad (3)$$

Then the following one loop potential is obtained,

$$V^{(1)} = -P(d)\frac{1}{\alpha(d)}\sum_{n=0}^{\infty}\frac{(-G)^n}{n!}\alpha^{-\frac{2}{d}n}(d)\Gamma(1+\frac{2}{d}n)I(n;\phi), \quad (4)$$

where $P(d) = \frac{\pi^{d/2}}{d(2\pi)^d\Gamma(d/2)}$ and

$$I(n; \phi) = \lim_{\eta \rightarrow 0} \int_{\eta}^{\infty} \frac{ds}{s} s^{(1-2/d)n} e^{-\gamma \phi^4 s}. \quad (5)$$

Since $\alpha(d) \propto \Gamma(2-d/2)$, α is very large near $d = 4$. So we expanded the effective potential in the series of $1/\alpha$. In the integration of eq.(5), the ultraviolet cutoff η is introduced because the integral diverges for $n = 0, 1$ and 2 . For large $\alpha(d)$, the most dominant term is that of $n = 0$, so we can approximate $V^{(1)}$ as follows.

$$V^{(1)} \sim -\frac{2}{d} P(d) \frac{\gamma}{\alpha(d)} \phi^4 \lim_{\eta \rightarrow 0} \int_{\eta \gamma \phi^4}^{\infty} \frac{dx}{x} x^{-1} e^{-x} \quad (6)$$

$$= -\frac{2}{d} P(d) \frac{\gamma}{\alpha(d)} \left[\phi^4 (\ln \phi^4 - b) + \lim_{\eta \rightarrow 0} \left(\frac{\eta^{-1}}{\gamma} + \phi^4 \ln \eta \right) \right]. \quad (7)$$

The terms which diverge at $\eta = 0$ can be absorbed into the cosmological constant by a suitable renormalization. The remaining finite term in Eq.(7) has a similar form to that of the Coleman-Weinberg potential induced by the radiative correction, but its sign is opposite. Then the minimum of the potential, $V = V^0 + V^{(1)}$, is the trivial one, $\langle \phi \rangle = 0$. This implies that the gravitational effect can not bring on a spontaneous breaking of a symmetry as in a gauge theory.

Nextly, we consider the limit of $\epsilon = 0$ in our calculation. In this limit, $\alpha(d) \propto 1/\epsilon$ near $\epsilon = 0$. Then we do not need any subtraction in the four dimensional limit, and there is no problem in taking the limit, $\epsilon = 0$, of $V^{(1)}$. And we obtain the following null result,

$$\lim_{\epsilon \rightarrow 0} V^{(1)} = 0. \quad (8)$$

So it can be said that the quantum effect of gravitation does not contribute to the four-dimensional effective potential of a scalar within our calculational scheme. Then the other effect like a radiative correction of a gauge field would be necessary to provide the vacuum expectation value of a scalar.

References

- [1] K.S. Stelle, Phys. Rev., D16(1977)953; J. Julve and M. Tonin, Nuovo Cimento, 46B(1978)137.
- [2] E. Tomboulis, Phys. Lett., 70B(1977)361.
- [3] L. Crane and L. Smolin, Nucl. Phys., B267(1986)714.
- [4] M.J. Perry, Nucl. Phys., B143(1978)114.
- [5] L. Smolin, Nucl. Phys., B160(1979)253; A. Zee, Phys. Rev., D23(1981)858; S. Ichinose, Nucl. phys., B231(1984)335; K. Ghoroku, Phys. Lett., 159B(1985)275.
- [6] S. Coleman and E. Weinberg, Phys. Rev., D7(1973)1888.

A Teleparallel Theory of (2+1)-Dimensional Gravity

Toshiharu Kawai

Department of Physics, Osaka City University

Osaka 558

A theory of (2+1)-dimensional gravity is developed on the basis of the Weitzenböck space-time characterized by the metricity condition and by the vanishing curvature tensor. The fundamental gravitational field variables are dreibein fields and the gravity is attributed to the torsion. The most general gravitational Lagrangian quadratic in the torsion tensor is given by $L_G = \alpha t^{klm} t_{klm} + \beta v^k v_k + \gamma a^{klm} a_{klm}$. Here, t_{klm} , v_k and a_{klm} are irreducible components of the torsion tensor, and α , β and γ are real parameters. A condition is imposed on α and β by the requirement that the theory has a correct Newtonian limit. Static circularly symmetric exact solutions of the gravitational field equation in the vacuum are given. They are classified into two types by the signature of $\alpha\beta$. The space-times given by the solutions have event horizons, if and only if $\alpha(3\alpha+4\beta) < 0$. Singularity structures of these space-times are also examined.

§1. Introduction

Recently, the Einstein theory of (2+1)-dimensional gravity has attracted considerable attentions,^{1)~6)} but it does not have a Newtonian limit.^{1), 2)} For the (1+1)-dimensional case, there is a theory⁷⁾ having a correct Newtonian limit. Thus, it is natural to raise a question: Is'nt there a relativistic theory of (2+1)-

dimensional gravity having a Newtonian limit? For the (3+1)-dimensional case, a teleparallel theory of gravity, named new general relativity,⁸⁾ is known to describe well all the observed gravitational phenomena in the same level as the Einstein theory.

In the present note, we give a teleparallel theory of (2+1)-dimensional gravity having a Newtonian limit.

§2. dreibeins, covariant derivative and teleparallelism

The three-dimensional space-time M is assumed to be a differentiable manifold endowed with the Lorentzian metric $g = g_{\mu\nu} dx^\mu \otimes dx^\nu$ ($\mu, \nu = 0, 1, 2$) related to the fields $e^k = e^k_\mu dx^\mu$ ($k = 0, 1, 2$) through the relation $g_{\mu\nu} = e^k_\mu \eta_{kl} e^l_\nu$. Here, (η_{kl}) is the Minkowskian metric, $(\eta_{kl}) \stackrel{\text{def}}{=} \text{diag}(-1, 1, 1)$, and $\{x^\mu; \mu = 0, 1, 2\}$ is a local coordinate of the space-time. The fields $e_k = e^\mu_k \partial / \partial x^\mu$, which are dual to e^k , are the dreibein fields. Field strength of e^k_μ is given by

$$T^k_{\mu\nu} = e^k_{\nu, \mu} - e^k_{\mu, \nu}. \quad (2.1)$$

We define the covariant derivative of the Lorentzian vector field V^k by

$$\nabla_l V^k = e^\mu_l \partial_\mu V^k. \quad (2.2)$$

For the world vector fields $W = W^\mu \partial / \partial x^\mu$, the covariant derivative with respect to the affine connection $\Gamma^\mu_{\lambda\nu}$ is given by

$$\nabla_\nu W^\mu = \partial_\nu W^\mu + \Gamma^\mu_{\lambda\nu} W^\lambda. \quad (2.3)$$

The requirement

$$\nabla_l V^k = e^\nu_l e^k_\mu \nabla_\nu V^\mu \quad (2.4)$$

for $V^\mu \stackrel{\text{def}}{=} e^\mu_k V^k$ leads to

$$\Gamma^\mu_{\lambda\nu} = e^\nu_k e^k_{\nu, \lambda}. \quad (2.5)$$

and hence we have

$$T_{\mu\nu}^k = e_{\lambda}^k T_{\mu\nu}^{\lambda} \stackrel{\text{def}}{=} e_{\lambda}^k (\Gamma_{\nu\mu}^{\lambda} - \Gamma_{\mu\nu}^{\lambda}), \quad (2.6)$$

$$R_{\nu\lambda\rho}^{\mu} \stackrel{\text{def}}{=} \Gamma_{\nu\rho,\lambda}^{\mu} - \Gamma_{\nu\lambda,\rho}^{\mu} + \Gamma_{\tau\lambda}^{\mu} \Gamma_{\nu\rho}^{\tau} - \Gamma_{\tau\rho}^{\mu} \Gamma_{\nu\lambda}^{\tau} \equiv 0, \quad (2.7)$$

$$\nabla_{\lambda} g_{\mu\nu} \stackrel{\text{def}}{=} \partial_{\lambda} g_{\mu\nu} - \Gamma_{\mu\lambda}^{\rho} g_{\rho\nu} - \Gamma_{\nu\lambda}^{\rho} g_{\mu\rho} \equiv 0. \quad (2.8)$$

The components $T_{\mu\nu}^{\lambda}$ and $R_{\nu\lambda\rho}^{\mu}$ are those of the torsion tensor and of the curvature tensor, respectively. Equation (2.7) implies the teleparallelism, and it together with Eq.(2.8) means that M is the Weitzenböck space-time.

§3. Lagrangian and gravitational field equation

For the matter field φ belonging to a representation of the three-dimensional Lorentz group, $L_M(\varphi, \nabla_k \varphi)$ with $\nabla_k \varphi \stackrel{\text{def}}{=} e_k^{\mu} \partial_{\mu} \varphi$ is a Lagrangian invariant under global Lorentz transformation and under general coordinate transformation, if $L_M(\varphi, \partial_k \varphi)$ is an invariant Lagrangian on the three-dimensional Minkowskian space-time.

For the dreibein fields e_k , the most general Lagrangian, which is invariant under the transformations stated above and is quadratic in the torsion tensor, is given by

$$L_G = \alpha t^{klm} t_{klm} + \beta v^k v_k + \gamma a^{klm} a_{klm}. \quad (3.1)$$

Here, t_{klm} , v_k and a_{klm} are the irreducible components of T_{klm} , which are defined by

$$t_{klm} \stackrel{\text{def}}{=} \frac{1}{2} (T_{klm} + T_{lkm}) + \frac{1}{4} (\eta_{mk} v_l + \eta_{ml} v_k) - \frac{1}{2} \eta_{kl} v_m, \quad (3.2)$$

$$v_k \stackrel{\text{def}}{=} T_{lk}^l, \quad (3.3)$$

$$a_{klm} \stackrel{\text{def}}{=} \frac{1}{3} (T_{klm} + T_{mkl} + T_{lmk}), \quad (3.4)$$

respectively, and α, β and γ are real constant parameters.

Then,

$$I \stackrel{\text{def}}{=} \frac{1}{c} \int L d^3x \quad (3.5)$$

gives the total action of the system, where c is the light velocity in the vacuum and L is defined by

$$L \stackrel{\text{def}}{=} \sqrt{-g} \left(L_G + L_H(\varphi, \nabla_k \varphi) \right) \quad (3.6)$$

with $g \stackrel{\text{def}}{=} \det(g_{\mu\nu})$.

The gravitational field equation following from the action I is

$$-2\nabla^k F_{ijk} + 2v^k F_{ijk} + 2H_{ij} - \eta_{ij} L_G = T_{ij} \quad (3.7)$$

with

$$F_{ijk} \stackrel{\text{def}}{=} \alpha(t_{ijk} - t_{ikj}) + \beta(\eta_{ij} v_k - \eta_{ik} v_j) + 2\gamma a_{ijk} = -F_{ikj}, \quad (3.8)$$

$$H_{ij} \stackrel{\text{def}}{=} T_{mn} F^{mn}_{ij} - \frac{1}{2} T_{jmn} F^{mn}_i = H_{ji}, \quad (3.9)$$

$$\nabla^k F_{ijk} \stackrel{\text{def}}{=} e^{\mu k} \partial_\mu F_{ijk}. \quad (3.10)$$

$$T_{ij} \stackrel{\text{def}}{=} \frac{1}{\sqrt{-g}} e^\mu_j \frac{\delta(\sqrt{-g} L_H)}{\delta e^\mu_i} \quad (3.11)$$

§4. Classical test particle and light ray

The world line of a freely falling classical test body is the geodesics of the metric $g = g_{\mu\nu} dx^\mu \otimes dx^\nu$, if the effects due to the^{*} "spin" of the fundamental constituent particles can be ignored.

Light rays propagate along the null geodesics of the metric g , which can be shown on the basis of the electromagnetic Lagrangian $L_{em} \stackrel{\text{def}}{=} -g^{\mu\rho} g^{\nu\sigma} F_{\mu\nu} F_{\rho\sigma} / 4$ with $F_{\mu\nu} = \partial_\mu A_\nu - \partial_\nu A_\mu$, as in the case of the Einstein theory in the (3+1)-dimensional space-time.

^{*}) By "spin", we mean here the quantum number associated with the three-dimensional Lorentz group.

§5. Static circularly symmetric gravitational field

We consider a static, circularly symmetric gravitational field produced by a static circularly symmetric body. We can assume, without loss of generality, that (e^k_μ) has a diagonal form,

$$(e^k_\mu) = \begin{pmatrix} A(r) & 0 & 0 \\ 0 & B(r) & 0 \\ 0 & 0 & B(r) \end{pmatrix} \quad (5.1)$$

with $r \stackrel{\text{def}}{=} \sqrt{(x^1)^2 + (x^2)^2}$, which leads to $a_{klm} = 0$.

(A) Newtonian limit

First, we consider the case for which the conditions^{*)}

$$T_{00} \simeq \rho c^2 \gg |T_{ab}| \simeq 0, \quad a, b = 1, 2, \quad (5.2)$$

$$A \simeq 1 \simeq B, \quad \frac{dA}{dr} \simeq 0 \simeq \frac{dB}{dr} \quad (5.3)$$

are satisfied, where ρ is the mass density of a gravitating body.

For this case, the field equation (3.7) takes the following form:

$$(3\alpha + 4\beta)\Delta A - (3\alpha - 4\beta)\Delta B \simeq -2\rho c^2, \quad (5.4a)$$

$$(3\alpha - 4\beta)\frac{dA}{dr} - (3\alpha + 4\beta)\frac{dB}{dr} \simeq 0, \quad (5.4b)$$

where T_{ab} and terms quadratic in dA/dr and dB/dr have been neglected.

Here, Δ stands for the Laplacian of the two-dimensional Euclidean space. From Eqs. (5.4a) and (5.4b), we can show that the potential U defined by

$$g_{00} = -A^2 = -1 - \frac{2U}{c^2} \quad (5.5)$$

gives the Newtonian potential and that the equation of motion of a slowly moving classical test particle agrees with that in the Newton theory, if and only if

^{*)} Circularly symmetric solutions are possible, only if

$$T_{0a} = 0 = T_{a0}, \quad a = 1, 2.$$

$$3\alpha+4\beta=-\frac{96\alpha\beta\pi G}{c^2}, \quad \alpha\beta\neq 0, \quad (5.6)$$

which we shall assume hereafter. Here, $G(\neq 0)$ is the Newton gravitational constant for the case of two-dimensional space.

(B) Exact vacuum solutions

The exact solutions of Eq.(3.7) with $T_{ij}=0$ are obtained for e^k_μ having the expression (5.1). They are classified into two types by the signature of $\alpha\beta$.

(B.1) The case with $\alpha\beta < 0$

For this case, the solution, which is normalized as $A(r_0)=1=B(r_0)$ for some positive constant r_0 , is given by

$$A(r)=X(r)Y(r), \quad B(r)=\left(X(r)\right)^{\frac{1-\Lambda}{1+\Lambda}}\left(Y(r)\right)^{\frac{1+\Lambda}{1-\Lambda}}. \quad (5.7)$$

Here, we have defined $\Lambda \stackrel{\text{def}}{=} \sqrt{-4\beta/3\alpha}$ and

$$X(r) \stackrel{\text{def}}{=} \left(1 + \frac{1+\Lambda}{4\Lambda} K_1 \ln \frac{r}{r_0}\right), \quad Y(r) \stackrel{\text{def}}{=} \left(1 - \frac{1-\Lambda}{4\Lambda} K_2 \ln \frac{r}{r_0}\right) \quad (5.8)$$

with real constants K_1 and K_2 satisfying the relation

$$K_1 K_2 - (1+\Lambda)K_1 - (1-\Lambda)K_2 = 0. \quad (5.9)$$

The potential U defined by Eq.(5.5) agrees, around $r=r_0$, with the Newton potential produced by a central gravitating body having a mass H , if and only if

$$\frac{c^2}{4\Lambda} \{(1+\Lambda)K_1 - (1-\Lambda)K_2\} = 2GH. \quad (5.10)$$

(B.2) The case with $\alpha\beta > 0$

For this case, the solution normalized as $A(r_0)=1=B(r_0)$ is

$$A(r)=|Z(r)|^2, \quad B(r)=\left(Z(r)\right)^{\frac{i-\Omega}{i+\Omega}}\left(\{Z(r)^*\}\right)^{\frac{i+\Omega}{i-\Omega}}, \quad (5.11)$$

where $\Omega \stackrel{\text{def}}{=} \sqrt{4\beta/3\alpha}$ and

$$Z(r) \stackrel{\text{def}}{=} 1 + \frac{i+\Omega}{4i\Omega} K \ln \frac{r}{r_0} \quad (5.12)$$

with K being a complex constant satisfying the relation

$$|K|^2 + (i + \Omega)K - (i - \Omega)K^* = 0. \quad (5.13)$$

The potential U agrees, around $r=r_0$, with the Newton potential produced by a central gravitating body having a mass M , if and only if

$$\frac{c^2}{4i\Omega} \{ (i + \Omega)K + (i - \Omega)K^* \} = 2GM, \quad (5.14)$$

which can be satisfied, if $\Omega^2 + 1 \geq |4\Omega GM|/c^2$.

§6. Event horizons and singularities of the space-times

given by the solutions (5.7) and (5.11)

By singularity, we mean here the point(s) at which $t^{klm}t_{klm}$ and/or $v^k v_k$ do not have derivatives. By effective singularity,*) we mean the point(s) at which the Riemann-Christoffel scalar curvature does not have derivative(s).

(A) The space-time given by the solution (5.7)

Let a_1 and a_2 be the solutions of $X(r)=0$ and $Y(r)=0$, respectively; $X(a_1)=0$ and $Y(a_2)=0$. Then, we have the following:

<1> For the case with $\Lambda > 3$, the circles $r=a_1$ and $r=a_2$ are both event horizons.

<2> For the case with $3 \geq \Lambda > 1$, the circle $r=a_1$ is an event horizon.

To reach the circle $r=a_2$, classical particle needs infinitely long time, even when it is measured by its own proper time. Thus, the circle $r=a_2$ is an "ultra" event

*) Note the following: The Riemann-Christoffel curvature tensor is not the curvature tensor of the Weitzenböck space-time, but in our theory, classical test particles and light rays "feel" this curvature.

horizon in this sense.

<3> When $\Lambda < 1$, there is no event horizon at all.

<4> There are singularities and also effective singularities both at the origin $r=0$ and at $r=a_1$.

<5> For the case with $\Lambda > 5$, the circle $r=a_2$ is a singularity.

<6> For the case with $\Lambda < 1$, the circle $r=a_2$ is a singularity and also an effective singularity.

(B) The space-time given by the solution (5.11)

There is no event horizon in this space-time, but it has a singularity and an effective singularity at $r=0$.

From (A) and (B), we know that these space-times have event horizons, if and only if $\alpha(3\alpha+4\beta) < 0$.

References

- 1) S. Giddings, J. Abbott and K. Kuchar, Gen. Rel. Grav. 16 (1984), 751.
- 2) S. Deser, R. Jackiw and G. 't Hooft, Ann. Phys. 152 (1984), 220.
- 3) J. B. Brown, *Lower Dimensional Gravity* (World Scientific, 1988).
- 4) Y. Fujiwara, S. Higuchi, A. Hosoya, T. Mishima and M. Sino, Phys. Rev. D44 (1991), 1763.
- 5) H. H. Soleng, Gen. Rel. Grav. 24 (1992), 1131.
- 6) B. Reznik, Phys. Rev. D45(1992), 2151.
- 7) A. E. Sikkema and R. B. Mann, Class. Quantum Grav. 8 (1991), 219.
- 8) K. Hayashi and T. Shirafuji, Phys. Rev. D19 (1979), 3524.

Some Models for the description of the Scale-Dependent Topology

Masafumi Seriu

Department of Physics, Faculty of Science,

Kyoto University, Kyoto 606, Japan

* * *

The foam-like structure is one possible picture for the space-time near the Planck scale, which is supposed to occur due to the quantum fluctuation. Using a simple two-dimensional space with one topological handle as our model of this structure, we investigate the scattering problem of a massless scalar field on this space. With this model, we focus on the following effects, (a) How the scattering cross-section changes depending on the variety of topologies. and (b) How the twist of the handle affects the cross-section. We found out that there are the systematic topology-dependence and the twist effect in the cross-section. Our models can also be regarded, to some extent, as a quantitative description of the "scale-dependent topology", the approximate topology coming from the limitation of the energy scale of a probe.

* * *

The "space-time foam" is one of the most exciting pictures for space-time which is naturally deduced from the quantum theory of gravity.^[1] This is the speculation that the space-time structure may be topologically complicated at very small scale because of the drastic metric fluctuation which dominates near at the Planck scale.

This structure leads us to the concept of the scale-dependent topology of space-time. Topology of a certain space can be characterized as a collection of non-trivial loops allowed on the space. In physical situations, the role of these allowed loops are played by the possible paths of a probe injected to a region in question. In order to detect some topological handle, the wave length of the probe should be as short as the size of the handle. Thus, the finer structures, characterized by shorter loops than the wavelength of the probe, are smoothed

out. In other words, the higher the energy scale of a probe is, the finer topological structure appears.

We will be benefitted well if we successfully obtain a precise, quantitative description of how effective topology of space-time changes according to the change of the observational scale on our side, for there are many scale-dependent phenomena accompanying this effective topology, e.g. 1) "charge without charge" due to Wheeler.^{[2],[3]} 2) the effective topology change ^[4]. 3) some theories for explanation of the smallness of the cosmological constant.

We here present one possible approach for the quantitative investigation of the scale-dependence in the microscopic space-time structure. We are here interested in how an observer "feels" the space-time structure where he lives in through his experiments with energy-scale in hand, for all of the above and the other phenomena results from this type of effective, approximated topological structure in the observer's neighborhood. Our approach, being local in nature, may be considered as supplementing many other discussions related to global topology and topology change of the universe^[5]; The former concerns only local, effective topology and emphasize the observational effects, while the latter concerns the global, mathematical structure of the universe at the expense of the clear connection with observations.

As the scattering experiment is the most basic experiment for the investigation of a certain structure, let us set up the scattering problem regarding various topological handles as a scatter. In order to define the scattering cross-section clearly, the asymptotic region is needed as usual. Although this necessity may be undesirable for the full description of the foamlike structure, we set up models with asymptotic region because such a scattering process can be regarded as an elementary process, just like in particle physics. To make calculations as simple as possible, we reduce the space dimension from 3 to 2, believing that the essence of the phenomena is grasped well even by this simplification. With this model, we focus on the following effects,

(a) How the scattering cross-section changes depending on the variety of topologies.

(b) How the twist of the handle affects the cross-section.

We prepare a two-dimensional flat space, remove a disk with radius a from it. By the variety of the ways to identify the edge of the hole, we obtain a size a region with various topologies. We consider a massless scalar field Φ on this space. We can express Φ as a superposition of solutions for

$$(\Delta + k^2)\Phi = 0 \quad , \quad \Phi \xrightarrow{kr \rightarrow \infty} e^{ikx} + f(\theta) \frac{e^{i(kr - \pi/4)}}{\sqrt{kr}} \quad .$$

Thus

$$\Phi = e^{ikx} + \sum_{m=-\infty}^{\infty} i^m \frac{a_m}{2} H_m^{(1)}(kr) e^{im\theta} = \sum_{m=-\infty}^{\infty} i^m (J_m(kr) + \frac{a_m}{2} H_m^{(1)}(kr)) e^{im\theta} \quad .$$

In this form of expansion, the cross-section can be expressed as

$$\sigma(\theta) = \frac{1}{2\pi k} \left| \sum_{m=-\infty}^{\infty} a_m e^{im\theta} \right|^2 \quad .$$

For example, consider a $(\mathbf{R}P^2 \# \mathbf{R}P^2 \# \mathbf{R}P^2)$ -handle. As $(\mathbf{R}P^2 \# \mathbf{R}P^2 \# \mathbf{R}P^2) \sim aabbcc \sim abcab^{-1}c^{-1}$, we set the boundary condition for Φ on $r = a$ region

$$\Phi(r = a, \theta = \bar{\theta}) = \Phi(r = a, \theta = \pi + \bar{\theta}) \quad ,$$

$$\Phi(r = a, \theta = \frac{\pi}{3} + \bar{\theta}) = \Phi(r = a, \theta = -\frac{\pi}{3} - \bar{\theta}) \quad , \quad \text{for } 0 \leq \bar{\theta} \leq \frac{\pi}{3}$$

$$\Phi(r = a, \theta = \frac{2}{3}\pi + \bar{\theta}) = \Phi(r = a, \theta = -\bar{\theta}) \quad ,$$

and with the same identification ,

$$\frac{d\Phi}{dr}(p) = -\frac{d\Phi}{dr}(p') \quad \text{at } p \equiv p' \quad .$$

Note that the signs in front of $\bar{\theta}$ in (4) correspond to the identification directions of edges and they reflect topological informations of the handle. Then, we easily obtain

$$a_m = \begin{cases} -2 \Gamma_m & \text{for } m=0 \bmod 6 = 0, \pm 6, \pm 12, \dots \\ 0 & \text{others} \end{cases}$$

where

$$\Gamma_m(x) := \frac{J_m'(x)}{H_m^{(1)'}(x)} \xrightarrow{x \rightarrow 0} \begin{cases} i \frac{\pi}{4} x^2 & (m \neq 0) \\ -i \pi \frac{1}{|m|!(|m|-1)!} \left(\frac{x}{2}\right)^{2|m|} & (m = 0) \end{cases}$$

Note that the selection of m 's is mainly controlled by (4) while (5) only determines the precise values of a_m 's. In the same way, we can determine a_m 's for the other variety of topologies of the handle. See the *Table*.

We should also note the following points.

- 1°) The form of $\sigma(\theta)$ is $2\pi k\sigma(\theta) = A + B(\theta)$. The θ -independent part A is of order $(ka)^4$, coming from $a_0 = -2\Gamma_0 = -2i\pi\left(\frac{ka}{2}\right)^2$. It is not the topological effect but the curvature scattering at the handle and it is common to all topologies.
- 2°) The topological effects appear in the θ -dependent part $B(\theta)$ in a prominent fashion. We can read from *Table* the general feature: The more the topology of the handle become complicated, the longer the period of allowed m 's becomes, and so the smaller the $B(\theta)$ term becomes.
- 3°) There are different ways to construct a certain handle. For example, $T^2 \# T^2 \sim abcd a^{-1} b^{-1} c^{-1} d^{-1} \sim (aba^{-1} b^{-1})(cdc^{-1} d^{-1}) \sim \dots$. It is easy to show that, however, the resulting a_m 's are independent of those choices. Thus, a_m 's certainly carry topological informations of a handle.
- 4°) Fix one topology for the handle (e.g. $T^2 \# T^2$). Then, one can show that the more the handle is distorted, the smaller $B(\theta)$ becomes.
- 5°) When the genus g is fixed, the order of magnitude of $B(\theta)$ does not depend on the orientability of the handle.

Let us now study the effect of a twist of a handle on the propagation of a field. Although the size of a handle maybe microscopic, the angle ϕ of a twist can be macroscopic, so that it is worth studying its effect.

As a model, we consider a two-dimensional flat space and remove from it two identical disks of radius a with a relative separation D . ($D > 2a$ is the only restriction for D . D maybe $D \gg a$ or $D = O(a)$.) By the identification

$$(r = a, \theta = \bar{\theta}) \equiv (r' = a, \theta' = \bar{\theta} + \phi),$$

we obtain a space with topology $(\mathbf{R}P^2 \# \mathbf{R}P^2) \# \mathbf{R}^2$, which contains one handle (the Klein's bottle) twisted by ϕ .

On this space, we again consider a massless scalar field Φ . Using the addition theorem for $H_m^{(1)}$ [6],[7], Φ , expressed in terms of (r, θ) , can be re-expressed in terms of (r', θ') :

$$\Phi = \sum_{n=-\infty}^{\infty} i^n \{ e^{ikD} J_n(kr') + \sum_{m=-\infty}^{\infty} i^m \frac{a_m}{2} J_{m-n}(kr') H_n^{(1)}(kD) \} e^{in\theta'}.$$

Setting the boundary condition for Φ , $\Phi(r = a, \theta = \bar{\theta}) \equiv \Phi(r' = a, \theta' = \bar{\theta} + \phi)$, we obtain the recurrent relation for a_m 's,

$$a_n = 2(e^{ikD} e^{in\phi} - 1) \gamma_n + e^{in\phi} \beta_n \sum_{m=-\infty}^{\infty} i^m J_{m-n}(ka) a_m,$$

where

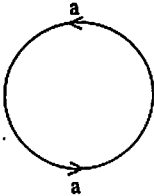
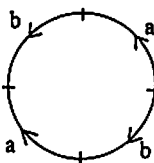
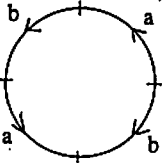
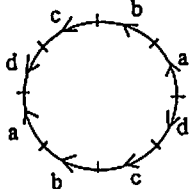
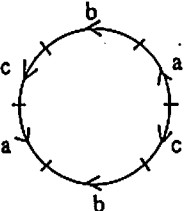
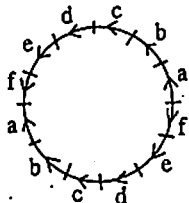
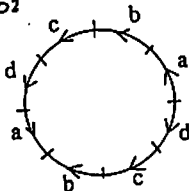
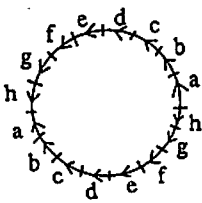
$$\beta_n := \frac{H_n^{(1)}(kD)}{H_n^{(1)}(ka)} \xrightarrow{ka \ll 1} \begin{cases} \frac{\ln(\frac{kD}{2} + \gamma)}{\ln(\frac{ka}{2} + \gamma)} & n = 0 \\ (\frac{a}{D})^{|n|} & n \neq 0 \end{cases}$$

The twist effect in the cross-section emerges in $O((ka)^2 \sin^2 \frac{kD}{2})$. The deflection occurs in the components of waves that went through the handle, so that the order of magnitude of the twist-terms becomes the same as that of the other terms.

We have above investigated some “observational” effects due to the topological handle by setting the scattering problem of a scalar field. In spite of their simplicity, our models provide some quantitative descriptions of the scale-dependent topology . For example, the difference and the similarity between two cross-sections for $T^2 \# T^2$ and for $T^2 \# T^2 \# T^2$ (see Table) show, in terms of ka , how various handles will be detected as the energy scale of a probe changes. For fixed ka , handles with complicated topology are “polished out” and only handles with simpler topology remains. We should finally note that the above approach is far from the complete description of the effective space-time structure and that the scale-dependent description of geometry in addition to that of topology will be more significant and complicated. For more details, see ref.[8].

REFERENCES

1. J.A. Wheeler, *Ann. Phys.* **2** (1957), 604
2. See, e.g., C.W. Misner and J.A. Wheeler, *Ann. Phys.* **2** (1957), 525;
J.A. Wheeler, *Geometrodynamics* (Academic Press, New York, 1962)
3. R. Sorkin, *J. Phys.* **A10** (1977), 717
4. M. Visser, *Phys. Rev.* **D41** (1990), 1116
5. e.g. G.W. Gibbons and J.B. Hartle, *Phys. Rev.* **D42** (1990), 2458 ;
G.W. Gibbons and S.W. Hawking, *Commun. Math. Phys.* **142** (1990), 1
6. J.L. Friedman, N. Papastamatiou, L. Parker and H. Zhang, *Nucl. Phys.* **B309** (1988), 533
7. J.A. Stratton, *Electromagnetic Theory* (McGraw Hill, 1941) §6.11
8. M. Seriu, preprint KUNS 1172

genus	Non-Orientable	Orientable
1	RP^2  $a_m = \mp 2\Gamma_m \begin{pmatrix} \text{even} \\ \text{odd} \end{pmatrix}$	T^2  $a_m = \begin{cases} \mp 2\Gamma_m & \begin{pmatrix} 0, & 4, & 8, & \dots \\ & 2, & 6, & 10, & \dots \end{pmatrix} \\ 0 & \text{(odd)} \end{cases}$
2	$RP^2 \# RP^2$  $a_m = \begin{cases} -2\Gamma_m & (0, 4, 8 \dots) \\ 0 & \text{(others)} \end{cases}$	$T^2 \# T^2$  $a_m = \begin{cases} \mp 2\Gamma_m & \begin{pmatrix} 0, & 8, & 16, & \dots \\ & 4, & 12, & 20, & \dots \end{pmatrix} \\ 0 & \text{(others)} \end{cases}$
3	$RP^2 \# RP^2 \# RP^2$  $a_m = \begin{cases} -2\Gamma_m & (0, 6, 12, 18 \dots) \\ 0 & \text{(others)} \end{cases}$	$T^2 \# T^2 \# T^2$  $a_m = \begin{cases} \mp 2\Gamma_m & \begin{pmatrix} 0, & 12, & 24, & \dots \\ & 6, & 18, & 30 & \dots \end{pmatrix} \\ 0 & \text{(others)} \end{cases}$
4	$RP^2 \# RP^2 \# RP^2 \# RP^2$  $a_m = \begin{cases} \mp 2\Gamma_m & \begin{pmatrix} 0, & 16, & \dots \\ & 8, & 24, & \dots \end{pmatrix} \\ 0 & \text{(other)} \end{cases}$	$T^2 \# T^2 \# T^2 \# T^2$  $a_m = \begin{cases} \mp 2\Gamma_m & \begin{pmatrix} 0, & 16, & \dots \\ & 8, & 24, & \dots \end{pmatrix} \\ 0 & \text{(others)} \end{cases}$

Table

Integrable Cosmology

M.Yoshimura

Department of Physics, Tohoku University

Sendai 980 Japan

Abstract

A proper incorporation of quantum back reaction is crucial to resolving some important issues discussed at the interface of gravity and quantum mechanics. Two dimensional dilaton gravity theories provide a class of toy models in which the semiclassical quantum correction is under analytic control. Some recent works on a quantum decay of de Sitter spacetime are reviewed, with a special emphasis on integrable models, integrable including the semiclassical quantum effect. Arguments are also put forward to indicate that even the nonintegrable model shares the same universality class as integrable models with regard to the end point of cosmological evolution.

I. Introduction: Importance of semiclassical analysis

Relevance of gravity in the quest of the fundamental law at microscopic distance scales is always dubious from a practical viewpoint. But the success of the unified theories has led to a daring venture of the ultimate unification with gravity, culminating in the superstring theory. Although the idea of the superstring theory is far reaching and promising in the long run, progress has slowed down, and one perhaps needs a big quantum jump to go a step forward.

In considering gravity in the quantum context, one should not forget the plain fact that there are a few unsolved, important problems at the very root of the foundation of quantum gravity. Quantum mechanics is based on the premise that the time axis is defined in a global sense and is endowed with a special universal meaning in contrast to other spatial coordinates. Yet the Einstein gravity tells that the time is a relative notion.

The situation becomes acute with the presence of event horizon in the black hole geometry, because the timelike direction locally defined on the horizon loses its meaning to an observer sitting far away from the horizon. This has led to the discovery of Hawking radiation [1]. Closer examination of the Hawking radiation however reveals a number of puzzles [2]; Hawking radiation has a thermal spectrum, which seems to imply that gravitational collapse of a quantum mechanical state leads to a mixed state, clearly violating the fundamental principle of quantum mechanics. What might be happening here is either that quantum mechanical correlation is hidden in emitted particles [3], or that there is a huge, effectively infinite degeneracy of states at the Planck mass scale black hole [4], storing information of the initial collapsing state until the very end of black hole evaporation. Personally, I believe that yet another possibility should be pursued; back reaction due to particle emission should be incorporated to examine evolution of the spacetime structure, and it might be just so that the concept of event horizon is only approximate and there is no fundamental difficulty of quantum mechanical development, although in practice there is a rich spectrum of physics yet to be explored.

There are many problems to each of these proposed resolutions [2]. Only detailed and careful examination may solve all this problem, revealing subtleties so far ignored. As a minimum requirement one has to set up a scheme to incorporate quantum back reaction into a semiclassical framework so that one can follow time evolution of black

hole evaporation until the very end.

Until very recently there has been no tractable model to study the back reaction problem at a quantitative level. Callan, Giddings, Harvey, and Strominger [5] (CGHS) recently proposed an interesting toy model in two spacetime dimensions to discuss black hole evaporation. They considered two dimensional dilaton gravity. A nice feature of this model is that in the large N limit quantum correction to the classical system is governed by one loop matter field integration which yields an unambiguous trace of the energy-momentum tensor known as the trace anomaly. Combined with the energy-momentum conservation, the stress tensor component is almost uniquely determined by the background metric, up to two arbitrary functions of one variable. These functions must be fixed by boundary condition in a problem at hand. For instance, in the case of black hole formation the boundary condition is given by the fact that there has not been any outgoing flux of radiation from the collapsing body prior to the black hole formation. This condition turns out restrictive enough to yield Hawking radiation and recession of the event horizon due to the back reaction.

Unfortunately, one cannot pursue black hole evaporation until the end point, because in this model a curvature singularity develops and it approaches the receding event horizon from inside the hole, and at the end the semiclassical approximation breaks down [6]–[10]. It is not clear that this is due to a bad choice of the model, or due to a more fundamental problem.

I have explored another important realm of the quantum back reaction related to gravity [11], [12], [13]. This is the process of quantum decay of de Sitter spacetime. My initial motivation was a possibility of realizing a self-terminating inflationary universe model. The inflationary scenario is an interesting idea to solve two outstanding problems in cosmology; the horizon and the flatness problem. The whole idea however rests with the temporary presence of a cosmological constant to be eliminated in the end, which has no deep reason to be so, from the point of fundamental microphysics. It would be nice if there is an intrinsic mechanism of quantum decay of exponentially expanding universe. Again two dimensional dilaton gravity provides an interesting toy model to study this problem, and fortunately in this case one can pursue the quantum decay to the end. I will review the present status of two dimensional dilaton cosmology, substantially supplementing the background material.

II. Two dimensional dilaton gravity

It is well known that the two dimensional Einstein gravity is trivial and has a null content. For instance, the Einstein-Hilbert action $\int \sqrt{-g} R$ is a topological quantity and the Lagrangian density is a total divergence. Nontrivial gravity is either induced by quantum effect of matter fields or is introduced by another degree of freedom such as the dilaton field. We choose to introduce a dilaton degree of freedom denoted by φ in the present context. The classical action we mainly consider is then

$$S_r = \frac{1}{2\pi} \int d^2x \sqrt{-g} [e^{-2\varphi} (-R - 4 \partial_\mu \varphi \partial^\mu \varphi + 4\lambda^2) + L^{(m)}]. \quad (1)$$

We call this model the reversed CGHS model, because it differs from the original CGHS [5] model in two signs of the curvature and the dilaton kinetic terms. The cosmological constant λ sets a length scale in the theory. A novel feature of dilaton gravity is that the coupling factor $e^{2\varphi}$ acts as a varying gravitational constant, as in the Brans-Dicke theory in four dimensions. We often consider as a matter Lagrangian $L^{(m)}$ a set of N massless fields;

$$L^{(f)} = -\frac{1}{2} \sum_{i=1}^N \partial_\mu f_i \partial^\mu f_i. \quad (2)$$

We digress to discuss the most frequently used coordinate system called the conformal gauge. By a coordinate transformation we may take the metric in the form of

$$ds^2 = 2g_{+-} dx^+ dx^- = -e^{2\rho} dx^+ dx^-, \quad x^\pm = x^0 \pm x^1. \quad (3)$$

Our convention of the affine connection and the curvature is

$$\Gamma_{\beta\gamma}^\alpha = \frac{1}{2} g^{\alpha\sigma} (g_{\beta\sigma,\gamma} + g_{\gamma\sigma,\beta} - g_{\beta\gamma,\sigma}), \quad (4)$$

$$R_{\mu\nu} = R_{\mu\alpha\nu}^\alpha, \quad R_{\mu\beta\nu}^\alpha = \partial_\beta \Gamma_{\mu\nu}^\alpha - \partial_\nu \Gamma_{\mu\beta}^\alpha + \Gamma_{\mu\nu}^\sigma \Gamma_{\beta\sigma}^\alpha - \Gamma_{\nu\sigma}^\alpha \Gamma_{\mu\beta}^\sigma. \quad (5)$$

Nonvanishing components in the conformal gauge are given by

$$g_{+-} = -\frac{1}{2} e^{2\rho}, \quad (6)$$

$$\Gamma_{++}^+ = 2\partial_+ \rho, \quad \Gamma_{--}^- = 2\partial_- \rho, \quad (7)$$

$$R_{+-} = -2\partial_+ \partial_- \rho, \quad R = 8e^{-2\rho} \partial_+ \partial_- \rho. \quad (8)$$

Covariant derivative is expressed by

$$\varphi_{;+;-} = \partial_+ \partial_- \varphi, \quad \varphi_{;\pm;\pm} = \partial_\pm^2 \varphi - 2\partial_\pm \rho \partial_\pm \varphi, \quad (9)$$

$$\square \varphi = \frac{1}{\sqrt{-g}} \partial_\mu (\sqrt{-g} g^{\mu\nu} \partial_\nu \varphi) = -4e^{-2\rho} \partial_+ \partial_- \varphi. \quad (10)$$

Armed with these formulas, one may derive the well known peculiar identity in two dimensions:

$$R_{\mu\nu} = \frac{g_{\mu\nu}}{\det g_{\mu\nu}} R_{0101}. \quad (11)$$

This means among other things that a vanishing Ricci scalar gives a vanishing Riemann tensor, hence a locally flat spacetime.

Although the above action may look strange to some reader, it is recast into a perhaps more familiar form with a Weyl rescaling,

$$g_{\mu\nu} = e^{2\varphi} \hat{g}_{\mu\nu}. \quad (12)$$

In the rescaled system

$$S_r = \frac{1}{2\pi} \int d^2x \sqrt{-\hat{g}} [-e^{-2\varphi} \hat{R} + 4\lambda^2 + e^{2\varphi} L^{(m)}], \quad (13)$$

modulo a total divergence. Hence the matter is directly coupled to the dilaton field in this form. We shall exclusively use the original form of the action, but it is useful to keep in mind this alternative expression.

Derivation of field equations is a nontrivial exercise. One has to use the following important identity for the metric variation; for an arbitrary function f ,

$$\sqrt{-g} f g^{\mu\nu} \delta R_{\mu\nu} = f \partial_\mu (\sqrt{-g} w^\mu) = -\sqrt{-g} (f_{;\mu;\nu} - g_{\mu\nu} f_{;\alpha}^{\alpha}) \delta g^{\mu\nu}, \quad (14)$$

modulo a total divergence, where w^μ is a 4-vector given by

$$w^\mu = g^{\alpha\beta} \delta \Gamma_{\alpha\beta}^\mu - g^{\mu\alpha} \delta \Gamma_{\alpha\beta}^\beta. \quad (15)$$

Furthermore in two dimensions alone

$$R_{\mu\nu} - \frac{1}{2} g_{\mu\nu} R = 0. \quad (16)$$

This remark leads to the classical field equations in the reversed model,

$$\varphi_{;\mu;\nu} - g_{\mu\nu} \square \varphi + g_{\mu\nu} \varphi_{,\rho} \varphi^{,\rho} + \lambda^2 g_{\mu\nu} = \frac{1}{4} e^{2\varphi} T_{\mu\nu}^{(m)}, \quad (17)$$

$$\square \varphi - \lambda^2 + \frac{1}{4} R - \varphi_{,\rho} \varphi^{,\rho} = 0, \quad (18)$$

$$T_{\mu\nu}^{(m); \nu} = 0. \quad (19)$$

The energy-momentum tensor $T_{\mu\nu}^{(m)}$ is written in the case of massless fields as

$$T_{\mu\nu}^{(f)} = -\partial_\mu f_i \partial_\nu f_i + \frac{1}{2} g_{\mu\nu} \partial_\sigma f_i \partial^\sigma f_i. \quad (20)$$

Hence

$$T_\rho^{(f)\rho} = 0, \quad T_0^{(f)0} = -T_1^{(f)1}. \quad (21)$$

As to the classical matter one may equally well take the one dimensional ideal gas obeying the same traceless condition Eq.21.

We now discuss integrability of the classical model. Field equation in the conformal gauge takes the following form for a set of massless fields,

$$-\partial_+ \partial_- \varphi + 2 \partial_+ \varphi \partial_- \varphi - \frac{\lambda^2}{2} e^{2\rho} = 0, \quad (22)$$

$$\partial_\pm^2 \varphi - 2 \partial_\pm \rho \partial_\pm \varphi = -\frac{1}{4} e^{2\varphi} (\partial_\pm f_i)^2, \quad (23)$$

$$-4 e^{-2\rho} \partial_+ \partial_- \varphi - \lambda^2 + 2 e^{-2\rho} \partial_+ \partial_- \rho + 4 e^{-2\rho} \partial_+ \varphi \partial_- \varphi = 0, \quad (24)$$

$$\partial_+ \partial_- f_i = 0. \quad (25)$$

The first $+-$ metric equation combined with the third dilaton equation yields

$$\partial_+ \partial_- (\rho - \varphi) = 0, \quad (26)$$

$$\partial_+ \partial_- e^{-2\varphi} = \lambda^2 e^{2(\rho - \varphi)}. \quad (27)$$

Thus $\rho - \varphi$ and f_i are both free fields, and may be written as

$$\rho - \varphi = G_+(x^+) + G_-(x^-), \quad f = f_+(x^+) + f_-(x^-). \quad (28)$$

The constraint equation corresponding to the metric $\pm\pm$ variation is

$$\partial_\pm^2 e^{-2\varphi} - 2 \partial_\pm (\rho - \varphi) \partial_\pm e^{-2\varphi} = \frac{1}{2} (\partial_\pm f_i)^2. \quad (29)$$

We may understand the role of constraint equation as relating three free fields, f_\pm and G_\pm , already introduced, and a new one from the homogeneous solution of Eq.27.

Integrability of the classical system is better understood by introduction of new field variables,

$$\psi_+ = -\frac{2}{\sqrt{\kappa}} e^{-2\varphi}, \quad \psi_- = \sqrt{\kappa} (\rho - \varphi). \quad (30)$$

Here κ is an arbitrary parameter and is fixed later when quantum correction is included. Field equations and the constraint equation in terms of ψ_{\pm} are given by

$$\partial_+ \partial_- \psi_- = 0, \quad (31)$$

$$\partial_+ \partial_- \psi_+ = -\frac{2\lambda^2}{\sqrt{\kappa}} e^{(2/\sqrt{\kappa})\psi_-}, \quad (32)$$

$$-\frac{\sqrt{\kappa}}{2} \partial_{\pm}^2 \psi_+ + \partial_{\pm} \psi_+ \partial_{\pm} \psi_- - \frac{1}{2} (\partial_{\pm} f_i)^2 = 0. \quad (33)$$

The classical action in terms of ψ_{\pm} is given by

$$S_r = \frac{1}{\pi} \int d^2 x \left[-\partial_+ \psi_+ \partial_- \psi_- + \lambda^2 e^{(2/\sqrt{\kappa})\psi_-} + \frac{1}{2} \sum_{i=1}^N \partial_+ f_i \partial_- f_i \right]. \quad (34)$$

An important fact related to the integrability is a symmetry under the following variation of fields [14]:

$$\delta \psi_+ = \epsilon, \quad \delta \psi_- = 0. \quad (35)$$

At the end of this section we remark on the original CGHS model. The classical action of the original CGHS model is given by

$$S_o = \frac{1}{2\pi} \int d^2 x \sqrt{-g} \left[e^{-2\varphi} (R + 4 \partial_{\mu} \varphi \partial^{\mu} \varphi + 4\lambda^2) + L^{(m)} \right]. \quad (36)$$

Field equations of the original model are obtained from the reversed model by the following replacement,

$$\lambda^2 \rightarrow -\lambda^2, \quad T_{\mu\nu}^{(m)} \rightarrow -T_{\mu\nu}^{(m)}. \quad (37)$$

Nature of gravity in these two models are quite different. We shall make some comment on cosmology in the original model later on.

III. Dilaton cosmology and inflationary universe model

The reversed CGHS model has interesting cosmological applications [11] in contrast to the original CGHS model. The original model is an interesting laboratory to investigate in great depth black hole formation and the end point of Hawking radiation, while the reversed model gives an interesting toy model to study an evolving inflationary universe and the quantum decay of de Sitter spacetime. It is regrettable,

but it is true that in two dimensions there is no single theory among models so far known, describing both acceptable black hole and acceptable cosmological solutions at the same time.

Among general solutions of the reversed CGHS model, we discuss in this section cosmological solutions assuming homogeneity, namely, suppressing x^1 dependence. The basic set of equations are then

$$\partial_0^2 \psi_- = 0, \quad (38)$$

$$\partial_0^2 \psi_+ = -\frac{8\lambda^2}{\sqrt{\kappa}} e^{\frac{2}{\sqrt{\kappa}} \psi_-}, \quad (39)$$

$$\partial_0^2 f_i = 0, \quad (40)$$

$$-\frac{\sqrt{\kappa}}{2} \partial_0^2 \psi_+ + \partial_0 \psi_+ \partial_0 \psi_- - \frac{1}{2} (\partial_0 f_i)^2 = 0. \quad (41)$$

where ∂_0 denotes x^0 derivative. General solution to these is given by

$$\psi_- = \frac{\sqrt{\kappa}}{2} B x^0, \quad (42)$$

$$\psi_+ = \frac{2}{\sqrt{\kappa}} \left[-\frac{4\lambda^2}{B^2} e^{Bx^0} + D x^0 + C \right], \quad (43)$$

$$f_i = f_{1,i} x^0, \quad (44)$$

$$BD - \frac{1}{2} f_{1,i}^2 = 0. \quad (45)$$

In terms of ρ and φ ,

$$e^{2\varphi} = \frac{B^2}{4\lambda^2} \frac{1}{e^{Bx^0} - \frac{f_{1,i}^2}{8\lambda^2} Bx^0 - \frac{B^2}{4\lambda^2} C}, \quad (46)$$

$$e^{2\rho} = \frac{B^2}{4\lambda^2} \frac{e^{Bx^0}}{e^{Bx^0} - \frac{f_{1,i}^2}{8\lambda^2} Bx^0 - \frac{B^2}{4\lambda^2} C}, \quad (47)$$

$$R = 4\lambda^2 \left[-1 + e^{-Bx^0} \frac{(e^{Bx^0} - \frac{f_{1,i}^2}{8\lambda^2})^2}{e^{Bx^0} - \frac{f_{1,i}^2}{8\lambda^2} Bx^0 - \frac{B^2}{4\lambda^2} C} \right]. \quad (48)$$

We take without loss of generality $B > 0$ throughout this paper, because the other case is readily obtained by time reversal. Existence of a curvature singularity besides the initial or the final singularity is unavoidable, if the right hand side of Eq.43 has a positive maximum, namely, if

$$\frac{f_{1,i}^2}{8\lambda^2} \left(1 - \ln \frac{f_{1,i}^2}{8\lambda^2} \right) - \frac{B^2 C}{4\lambda^2} < 0. \quad (49)$$

The curvature singularity occurs at the zero of the denominator factors in the above equations, namely at a finite x^0 obeying

$$e^{Bx^0} - \frac{f_{1,i}^2}{8\lambda^2} Bx^0 - \frac{B^2}{4\lambda^2} C = 0. \quad (50)$$

At this singularity the coupling $e^{2\varphi}$ also diverges.

An important special case however exists if a fine tuning of the parameters is made to eliminate the curvature singularity;

$$\frac{f_{1,i}^2}{8\lambda^2} (1 - \ln \frac{f_{1,i}^2}{8\lambda^2}) - \frac{B^2 C}{4\lambda^2} = 0. \quad (51)$$

This special case describes an evolving de Sitter spacetime, as is made clear shortly. With this parameter choice, or equivalently by taking in the previous general solution

$$\frac{B^2}{4\lambda^2} C = \frac{f_{1,i}^2}{8\lambda^2}, \quad Bx^0 \rightarrow Bx^0 + \ln \frac{f_{1,i}^2}{8\lambda^2}, \quad (52)$$

one has

$$e^{2\rho} = \frac{B^2}{4\lambda^2} \frac{e^{Bx^0}}{e^{Bx^0} - Bx^0 - 1}, \quad (53)$$

$$R = 4\lambda^2 \left[-1 + e^{-Bx^0} \frac{(e^{Bx^0} - 1)^2}{e^{Bx^0} - Bx^0 - 1} \right], \quad (54)$$

$$e^{2\varphi} = \frac{2B^2}{f_{1,i}^2} \frac{1}{e^{Bx^0} - Bx^0 - 1}. \quad (55)$$

The range of coordinate time is $-\infty < x^0 < 0$, as is explained shortly.

It is often useful to introduce the comoving coordinate defined by

$$ds^2 = -d\tau^2 + a(\tau)^2 (dx^1)^2, \quad (56)$$

$$a(\tau) = e^\rho, \quad \tau = \int_{-\infty}^{x^0} dx^0 e^\rho, \quad (57)$$

with the range $\tau > 0$.

One may deduce limiting behavior at $x^0 = \pm\infty$. Initial time behavior at $x^0 = -\infty$, or $\tau = 0$, is given by

$$\lambda\tau \sim (-Bx^0)^{-\frac{1}{2}} e^{\frac{1}{2} Bx^0}, \quad (58)$$

$$a(\tau) \sim \frac{1}{2} B\tau, \quad R \sim \frac{1}{(\tau \ln \lambda\tau)^2}, \quad (59)$$

$$e^\varphi \sim \frac{B}{\sqrt{f_{1,i}^2}} (-\ln \lambda\tau)^{-\frac{1}{2}}. \quad (60)$$

One sees that matter effect is crucial in this cosmological model; the limit $f_i \rightarrow 0$ is not allowed. The time dependence of the scale factor $a(\tau)$ is an expected behavior for the hot big bang model with massless radiation in two dimensions. This is ascertained by noting the classical energy-momentum tensor due to f -matter,

$$a^2(\tau) T_0^{(f)0} = -a^2(\tau) T_1^{(f)1} = \frac{1}{2} f_{1,i}^2. \quad (61)$$

The same behavior is expected for the one dimensional ideal gas with $\rho = p \propto a^{-2}$.

Late time behavior at $x^0 = 0^-$, or $\tau = \infty$, is given by

$$\tau \sim -(\sqrt{2}\lambda)^{-1} \ln(-\sqrt{2}\lambda x^0), \quad (62)$$

$$a(\tau) = e^\rho \sim \frac{1}{\sqrt{2}\lambda(-x^0)} \sim e^{\sqrt{2}\lambda\tau}, \quad R \sim 4\lambda^2, \quad (63)$$

$$e^\varphi \sim \frac{2}{\sqrt{f_{1,i}^2(-x^0)}}. \quad (64)$$

$$(65)$$

This is the behavior expected for a de Sitter spacetime with $H = \frac{1}{a} \frac{da}{d\tau} \sim \sqrt{2}\lambda$. Indeed one can show that a stationary de Sitter spacetime given by

$$e^\rho = \frac{1}{\sqrt{2}\lambda(-x^0)}, \quad (66)$$

$$e^\varphi = \frac{2}{\sqrt{f_{1,i}^2(-x^0)}}, \quad (67)$$

is an exact solution of field equations.

The behavior of coupling strength in this inflationary model is as follows. Initially it is in the weak coupling region; $\kappa e^{2\varphi} \ll 1$, behaving like $e^{2\varphi} \propto (-Bx^0)^{-1}$ with $x^0 \sim -\infty$. In the de Sitter phase it is in the strong coupling region like $e^{2\varphi} \propto (-x^0)^{-2}$ with $x^0 = 0^-$.

Actually, there is another class of solution in which the parameter B above is replaced by $-B$ with $B > 0$: the time reversed solution. This class of solution describes an evolving spacetime that begins with a flat spacetime at $x^0 = -\infty$ and ends with the de Sitter spacetime at $x^0 = 0$. We shall call this model the cold universe model (CUM), while the previous one the hot universe model (HUM). In this paper we shall focus on HUM simply because this model mimics a realistic hot big bang.

IV. Semiclassical quantum back reaction: Decay of de Sitter spacetime

Both in the black hole evaporation and the de Sitter space decay a proper treatment of quantum back reaction is important. In two dimensional dilaton gravity we are considering, this correction is incorporated in a set of semiclassical equations.

In the large N limit the leading quantum effect is given by one loop matter field integration in the path integral approach. The net effect of N massless fields is the trace anomaly,

$$\langle T \rangle = -\frac{\kappa}{2\pi} R, \quad (68)$$

or the effective Polyakov action [15];

$$S_q = -\frac{\kappa}{8\pi} \int d^2x \sqrt{-g} R \frac{1}{\square} R, \quad (69)$$

with $\kappa = \frac{N}{12}$. A proper treatment of ghosts [16] leads to a modification of κ ;

$$\kappa = \hbar \frac{N - 24}{12}. \quad (70)$$

Since we take the large N limit, we will ignore this difference. In the conformal gauge the Polyakov action takes the form of

$$S_q = -\frac{\kappa}{\pi} \int d^2x \partial_+ \rho \partial_- \rho, \quad (71)$$

modulo a total divergence.

The trace anomaly supplemented by the energy-momentum conservation leads to a more specific form of the stress tensor components [5], [17]. In the conformal gauge with nonvanishing g_{+-} , $\Gamma_{\pm\pm}^\pm$ alone, the conservation equation $T_{\mu\nu}^\nu = 0$ leads to

$$\partial_- T_{++} + \partial_+ T_{+-} - \Gamma_{++}^+ T_{+-} = 0, \quad (72)$$

$$\partial_+ T_{--} + \partial_- T_{+-} - \Gamma_{--}^- T_{+-} = 0. \quad (73)$$

Since the trace of the stress tensor is given by

$$T = 2g^{+-} T_{+-} = -4e^{-2\rho} T_{+-}, \quad (74)$$

the conservation implies integrability with a known trace anomaly;

$$\langle T_{+-} \rangle = \frac{\kappa}{\pi} \partial_+ \partial_- \rho. \quad (75)$$

Combined together, an explicit computation yields

$$\partial_- \langle T_{++} \rangle = -\frac{\kappa}{\pi} (\partial_- \partial_+^2 \rho - 2 \partial_+ \rho \partial_- \partial_+ \rho), \quad (76)$$

$$= -\frac{\kappa}{\pi} \partial_- (\partial_+^2 \rho - \partial_+ \rho \partial_+ \rho). \quad (77)$$

$$(78)$$

Hence

$$\langle T_{++} \rangle = -\frac{\kappa}{\pi} [\partial_+^2 \rho - \partial_+ \rho \partial_+ \rho + t_+(x^+)]. \quad (79)$$

Similarly, working with $--$ component we obtain both of

$$\langle T_{\pm\pm} \rangle = -\frac{\kappa}{\pi} [\partial_{\pm}^2 \rho - \partial_{\pm} \rho \partial_{\pm} \rho + t_{\pm}(x^{\pm})]. \quad (80)$$

Two arbitrary functions $t_{\pm}(x^{\pm})$ are to be determined by boundary condition depending on a problem one wishes to address.

Written in terms of the mixed tensor component, one has in the case of homogeneous cosmology,

$$\langle T_0^0 \rangle = -a^{-2} \frac{\kappa}{\pi} \left[\frac{1}{2} \rho'^2 - t_+ - t_- \right], \quad (81)$$

$$\langle T_1^1 \rangle = -a^{-2} \frac{\kappa}{\pi} \left[\rho'' - \frac{1}{2} \rho'^2 + t_+ + t_- \right], \quad (82)$$

$$\langle T_1^0 \rangle = -\langle T_0^1 \rangle = a^{-2} \frac{\kappa}{\pi} [t_+ - t_-], \quad (83)$$

where the prime $' = \frac{\partial}{\partial x^0}$.

An important point to note is that the quantum stress tensor is determined by a combination of the background geometry and the boundary condition. In the semi-classical approximation we adopt here, quantum back reaction is thus incorporated as an effective stress tensor term and one has to solve the entire system with back reaction included.

We now propose how to choose the boundary condition in our cosmological situations: there should be no incoming flux besides the classically specified one. A similar proposal of no incoming flux was made in the case of black hole formation in the original CGHS model, leading to Hawking radiation. The cosmological boundary condition implies that at the initial null infinity of $x^{\pm} = -\infty$ there should be no quantum flux computed from Eqs.80. The limiting formula for ρ at $x^0 = -\infty$ is

$$e^{\rho} \sim \frac{B}{2\lambda} (-Bx^0)^{-\frac{1}{2}} e^{\frac{1}{2} Bx^0}. \quad (84)$$

Using this general asymptotic form, one derives the asymptotic quantum flux; at infinite null past of $x^\pm = -\infty$

$$\langle T_0^0 \rangle = -\langle T_1^1 \rangle = a^{-2} \frac{\kappa}{\pi} \left[-\frac{B^2}{8} + t_+ + t_- \right], \quad (85)$$

$$\langle T_1^0 \rangle = -\langle T_0^1 \rangle = a^{-2} \frac{\kappa}{\pi} [t_+ - t_-]. \quad (86)$$

Thus from the no quantum flux boundary condition, one finds that

$$t_\pm(x^\pm) = \frac{B^2}{16}. \quad (87)$$

We thus conclude that no quantum flux condition gives the unique boundary term, and this is true even in the case with arbitrary inhomogeneities.

In considering application to the evolving de Sitter model it is instructive to first fix the background metric and work out the Polyakov stress tensor. This approach based on the fixed background without considering back reaction is not our ultimate goal, but it is the way how Hawking radiation was first derived in the black hole geometry [1]. The behavior of the quantum stress tensor in the de Sitter phase is readily computed with the boundary function already fixed. At $x^0 = 0^-$

$$\langle T_0^0 \rangle = \langle T_1^1 \rangle = -\frac{\kappa}{\pi} \lambda^2, \quad \langle T_1^0 \rangle = \langle T_0^1 \rangle = 0, \quad (88)$$

from Eq.66. The result is insensitive to the boundary function t_\pm just determined. This is an important result: it clearly implies [11] that the dominant back reaction effect in the de Sitter background is not a thermal emission of massless particles, but it is more like a negative cosmological constant. On the other hand, Gibbons and Hawking [18] argued that Hawking radiation should occur in the de Sitter spacetime owing to the presence of future event horizon. However, in this explicit evolving model the Gibbons-Hawking picture is not realized.

One has to go beyond the fixed background approach, in order to properly assess the back reaction problem. The idea is to incorporate one loop quantum stress tensor into a set of semiclassical equations. For instance, one may use the effective Polyakov action as a starting basis of analysis;

$$S_{eff} = \frac{1}{\pi} \int d^2x \left[e^{-2\varphi} (-2 \partial_+ \rho \partial_- \varphi - 2 \partial_+ \varphi \partial_- \rho \right. \quad (89)$$

$$\left. + 4 \partial_+ \varphi \partial_- \varphi + \lambda^2 e^{2\rho} \right) + \frac{1}{4} \sum_{i=1}^N \partial_+ f_i \partial_- f_i - \frac{N}{12} \partial_+ \rho \partial_- \rho \left. \right]. \quad (90)$$

In practice this is a difficult task, because the quantum system is not analytically solvable unlike the classical system.

As a matter of principle, however, the quantum system presents no essential difficulty. A very nice feature of the reversed CGHS model is that no singular behavior is expected, unlike in the original CGHS model. The singularity appears in zeros of kinetic coefficients. Denoting the kinetic functional coefficients by $\frac{1}{\pi} \partial_+ \Phi M \partial_- \Phi$, with Φ a $(N+2)$ -vector and M a $(N+2) \times (N+2)$ matrix, one finds that

$$\det M = -4 e^{-4\varphi} \left(1 + \frac{N}{12} e^{2\varphi}\right) \left(\frac{1}{4}\right)^N \neq 0. \quad (91)$$

Note however that in the original CGHS model

$$\det M = -4 e^{-4\varphi} \left(1 - \frac{N}{12} e^{2\varphi}\right) \left(\frac{1}{4}\right)^N. \quad (92)$$

Hence a curvature singularity is expected at $\frac{N}{12} e^{2\varphi} = 1$, in the original model.

A set of semiclassical equations may be written in terms of the comoving coordinates. With the dot implying τ (comoving time) derivative,

$$\left(1 + \frac{N}{12} e^{2\varphi}\right) (\dot{H} + H^2) = 2(\dot{\varphi}^2 - \lambda^2), \quad (93)$$

$$\left(1 + \frac{N}{12} e^{2\varphi}\right) (\ddot{\varphi} + H\dot{\varphi}) = 2\left(1 + \frac{N}{24} e^{2\varphi}\right) (\dot{\varphi}^2 - \lambda^2), \quad (94)$$

$$\ddot{\varphi} - H\dot{\varphi} = -\frac{1}{4} f_{1,i}^2 e^{2\varphi-2\rho} - \frac{N}{24} e^{2\varphi} \left(\dot{H} + \frac{B^2}{4} e^{-2\rho}\right), \quad (95)$$

where $H = \dot{\rho}$. Elimination of the second derivative terms leads to

$$\dot{\varphi}^2 - \lambda^2 - H\dot{\varphi} + \frac{1}{8} e^{2\varphi-2\rho} (f_{1,i}^2 + \frac{NB^2}{24}) - \frac{N}{48} e^{2\varphi} H^2 = 0. \quad (96)$$

Taking the large N limit formally yields

$$\dot{H} + H^2 = 0, \quad (97)$$

$$\ddot{\varphi} + H\dot{\varphi} = \dot{\varphi}^2 - \lambda^2, \quad (98)$$

$$\dot{H} + \frac{B^2}{4} e^{-2\rho} = 0. \quad (99)$$

Analysis of these equations, including perturbation around the classical solution, was made in [11]. Roughly, what happens is as follows: The classical phase matches to the large N solution, which in the end goes back to the classical solution again. Result thus suggests a quantum decay of de Sitter spacetime in such a way that the

quantum back reaction makes it possible to bypass either the strict de Sitter phase or the classical singularity. Instead of repeating this analysis we shall describe in more detail integrable models in which some of these features are more quantitatively understood.

At the end of this section we make a brief comment on the original CGHS model, in particular, why we do not consider this model. The original CGHS model does not have interesting cosmological solutions analogous to the big bang model in four dimensions, as pointed out in [11], [19]. It is however true that with the cosmological constant reversed, $\lambda^2 \rightarrow -\lambda^2$, there exists a big bang type solution starting with an initial singularity, in a limited parameter region [20]. A closer examination of this solution shows that the initial behavior is governed by the strong coupling limit, $N e^{2\varphi} \gg 1$. Thus effect of full quantum gravity neglected in the present approach is important at initial times. Moreover, due to the singular behavior of this strong coupling region, one cannot determine the boundary function t_{\pm} which is crucial in our discussion. Hence even if one restricts application of the model to late time behavior in which the semiclassical approximation is justified, there is uncontrollable ambiguity. From these reasons we do not consider the original CGHS model.

V. Integrable models

At the moment there are two types of integrable models known [14], [21], [12], integrable in a strong sense including the semiclassical quantum correction. Both models are constructed so that they satisfy the symmetry already encountered at the classical level. Thus we maintain the symmetry under the following variation of fields:

$$\delta\psi_+ = \epsilon, \quad \delta\psi_- = 0. \quad (100)$$

We also demand the total action S in terms of ψ_{\pm} to have the same form as the classical one S_r ,

$$S = \frac{1}{\pi} \int d^2x \left[-\partial_+ \psi_+ \partial_- \psi_- + \lambda^2 e^{(2/\sqrt{\kappa})\psi_-} + \frac{1}{2} \sum_{i=1}^N \partial_+ f_i \partial_- f_i \right]. \quad (101)$$

Phrased this way, we seek a new relation of ψ_{\pm} in terms of ρ and φ . Of two known examples, we mainly present the RST model [14] due to the simplicity of presentation.

The modified action of the reversed RST model is $S = S_r + S_q$, with S_q given by

$$S_q = -\frac{\kappa}{8\pi} \int d^2x \sqrt{-g} \left[R \frac{1}{\square} R + 2\varphi R \right]. \quad (102)$$

In the conformal gauge the crucial new definition of ψ_{\pm} that leads to the integrability is

$$\psi_+ = -\frac{2}{\sqrt{\kappa}} e^{-2\varphi} + \sqrt{\kappa} \rho, \quad \psi_- = \sqrt{\kappa} (\rho - \varphi). \quad (103)$$

We may explain this result by the following heuristic argument. The sum of the classical and the Polyakov terms is written as

$$-2\partial_+ e^{-2\varphi} \partial_- (\rho - \varphi) + \kappa \partial_+ \rho \partial_- \rho = \partial_+ \psi_+ \partial_- \psi_- + \kappa \partial_+ \rho \partial_- \varphi, \quad (104)$$

where the last term in this equation is, modulo a total divergence, equal to

$$\frac{\kappa}{4} \sqrt{-g} \varphi R, \quad (105)$$

in the conformal gauge. Elimination of this term yields S_q of Eq.102, resulting in S of Eq.101.

The constraint equation of the reversed RST model is written as

$$\kappa t_{\pm}(x^{\pm}) = -\frac{\sqrt{\kappa}}{2} \partial_{\pm}^2 (\psi_+ + \psi_-) + \partial_{\pm} \psi_+ \partial_{\pm} \psi_- - \frac{1}{2} (\partial_{\pm} f_i)^2. \quad (106)$$

We get the same set of dynamical equations as in the classical theory,

$$\partial_+ \partial_- \psi_- = 0, \quad (107)$$

$$\partial_+ \partial_- \psi_+ = -\frac{2\lambda^2}{\sqrt{\kappa}} e^{(2/\sqrt{\kappa})\psi_-}. \quad (108)$$

We thus have a number of constrained free fields ψ_- , f_i , and ψ_+ that exponentially couples to ψ_- .

Before we give a detailed discussion on this reversed RST model with quantum correction incorporated, we state our main conclusion on our analysis of this model: (1) we either have regular solutions or solutions in which the weak coupling semi-classical approximation breaks down; (2) a set of solutions exist, realizing a decaying de Sitter spacetime with accompanying radiation, however radiation being different from that expected in the Gibbons-Hawking picture.

We now present cosmological solutions assuming homogeneity. The dynamical equation, Eqs.107, 108, is trivially integrated to yield

$$\psi_- = \frac{\sqrt{\kappa}}{2} B x^0, \quad (109)$$

$$\psi_+ = -\frac{8\lambda^2}{\sqrt{\kappa}B^2} e^{Bx^0} + \left(\frac{2}{\sqrt{\kappa}}D + \frac{\sqrt{\kappa}}{2}B\right)x^0 + \frac{2}{\sqrt{\kappa}}C, \quad (110)$$

with B, C , and D integration constants. The constraint equation, with these inserted, is

$$\kappa t_{\pm}(x^{\pm}) = \frac{1}{8}(2BD + \frac{\kappa}{2}B^2 - f_{1,i}^2), \quad (111)$$

with $f_{1,i}$ a constant of motion for f - fields; $f_i(x^0) = f_{0,i} + f_{1,i}x^0$. We shall further discuss the boundary condition later on. Exactly the same solution follows for one dimensional ideal gas obeying

$$T_0^0 = -T_1^1 \propto e^{-2\rho}. \quad (112)$$

Using the definition of ψ_{\pm} and eliminating ρ , we derive

$$e^{-2\varphi} - \frac{\kappa}{2}\varphi = \frac{4\lambda^2}{B^2}e^{Bx^0} - Dx^0 - C. \quad (113)$$

With φ known, the other field is given by

$$\rho = \varphi + \frac{B}{2}x^0. \quad (114)$$

The most important feature of this solution is that the determinantal equation Eq.113 has a monotonic behavior ranging from ∞ to $-\infty$ as a function of φ on the left hand side. This means that for any choice of x^0 and x^1 reality of φ is guaranteed. This is not true in the classical limit with $\kappa = 0$. Of course, a large positive φ , hence an even larger $e^{2\varphi}$, implies a breakdown of the semiclassical approximation. Thus one must be careful not to rely on the large φ region in order to derive some definite conclusion within the semiclassical approximation. The region in which the semiclassical approximation breaks down occurs in a portion of spacetime where the right hand side of Eq.113 becomes strongly negative.

Important quantity for the classification of solutions is the sign of D , assuming as always $B > 0$. If $D < 0$, the right hand side of the determinantal equation Eq.113 is monotonically increasing from $-\infty$ to ∞ as x^0 increases. Combined with the

monotonic behavior of the left hand side as a function of φ , one finds that at initial times the solution is in the strong coupling region; $\kappa e^{2\varphi} \gg 1$. A further detailed analysis shows that

$$e^\varphi \sim e^{(2\xi/\kappa)|Bx^0|}, \quad R \sim e^{(1-\frac{2\xi}{\kappa})|Bx^0|}, \quad (115)$$

in the asymptotically quantum region, where $\xi = |\frac{D}{B}|$. The semiclassical approximation breaks down in the asymptotic region and we shall not discuss this case any further.

On the other hand, if $D > 0$, the right hand side of Eq.113 has a minimum at some finite x^0 . In this case the solution has a classical behavior with $\varphi = -\infty$, in the asymptotic region of infinite past and infinite future. At intermediate x^0 near the minimum quantum effects may become significant.

The comoving time defined as before behaves in the asymptotic region like

$$\frac{B}{2} \tau \sim \frac{1}{\sqrt{-Dx^0}} e^{(Bx^0/2)} \quad (116)$$

at $x^0 \sim -\infty$ and

$$\lambda \tau \sim \frac{B}{2} x^0 \quad (117)$$

at $x^0 \sim \infty$, with the range of τ extending to ∞ .

The asymptotic behavior at infinite past of $\tau = 0$ is given by

$$e^\varphi \sim \frac{1}{\sqrt{-Dx^0}} \sim \frac{1}{\sqrt{-2\xi \ln(B\tau/2)}}, \quad (118)$$

$$a \sim \frac{1}{\sqrt{-Dx^0}} e^{(Bx^0/2)} \sim \frac{B}{2} \tau, \quad (119)$$

$$R \sim D \frac{e^{-Bx^0}}{-x^0} \sim \frac{1}{(\tau \ln \tau)^2}. \quad (120)$$

We shall adopt the same boundary condition as before; no incoming quantum flux besides the classically specified one. With the conformal coupling term φR added in the reversed RST model, the quantum stress tensor is modified to

$$\langle T_{+-} \rangle = \frac{\kappa}{2\pi} \partial_+ \partial_- (2\rho - \varphi), \quad (121)$$

$$\langle T_{\pm\pm} \rangle = -\frac{\kappa}{\pi} \left[\partial_\pm^2 \rho - (\partial_\pm \rho)^2 + t_\pm(x^\pm) + \partial_\pm \rho \partial_\pm \varphi - \frac{1}{2} \partial_\pm^2 \varphi \right]. \quad (122)$$

Using this quantum flux and the limiting behavior of fields at $x^0 = -\infty$, one determines the boundary function from the no incoming flux condition;

$$t_{\pm}(x^{\pm}) = \frac{B^2}{16}. \quad (123)$$

Thus the constraint equation Eq.111 simply reduces to

$$D = \frac{f_{1,i}^2}{2B}, \quad (124)$$

as in the classical case.

At infinite future of $\tau = \infty$

$$e^{\varphi} \sim \frac{B}{2\lambda} e^{-(Bx^0/2)} \sim \frac{B}{2\lambda} e^{-\lambda\tau}, \quad (125)$$

$$a \sim \frac{B}{2\lambda} \left[1 + \frac{B^2}{8\lambda^2} \left(\xi + \frac{\kappa}{4} \right) Bx^0 e^{-Bx^0} \right] \sim \frac{B}{2\lambda} + O(\lambda\tau e^{-2\lambda\tau}), \quad (126)$$

$$R \sim B^2 \left(\xi + \frac{\kappa}{4} \right) Bx^0 e^{-Bx^0} \sim O(\lambda\tau e^{-2\lambda\tau}). \quad (127)$$

We arrive at an important conclusion on the final state of the universe: the universe approaches a flat spacetime of dimensionless size $\frac{B}{2\lambda}$. Measured by the comoving time scale, the rate of this approach to the final state is given by the time $\frac{1}{2\lambda}$. Furthermore the approach is via contraction. This suggests existence of a maximum size at an earlier epoch.

Indeed, the maximal size is computed by the condition; $a' = 0$. By a straightforward computation we derive an exact equation [12] for the maximal size a_m ;

$$\left(\frac{a_m}{a_f} \right)^{2\zeta} = \xi^{\zeta-1} \zeta e^{-\zeta\eta+1} \left(\frac{a_m^2}{a_f^2} - 1 \right), \quad (128)$$

with $\zeta = \frac{4\xi}{4\xi+\kappa}$, and

$$\xi = \frac{D}{B}, \quad \eta = \frac{C}{\xi} + \ln \frac{BD}{4\lambda^2}. \quad (129)$$

The scale factor a_f is the final one;

$$a_f = \frac{B}{2\lambda}. \quad (130)$$

This can be simplified in a number of cases. For $a_m \gg a_f$,

$$a_m^2 \sim \xi e^{\frac{\zeta\eta-1}{1-\zeta}} \zeta^{-\frac{1}{1-\zeta}} a_f^2. \quad (131)$$

In the limit of $\kappa \rightarrow 0$

$$a_m \sim e^{2\xi(\eta-1)/\kappa} \sqrt{\xi} a_f. \quad (132)$$

In the large κ limit

$$a_m \sim \frac{1}{2} \sqrt{\frac{\kappa}{e}} a_f. \quad (133)$$

In principle an arbitrarily large universe is possible.

Energy balance between the classical and the quantum contribution is presumably a clue to understand the nature of quantum correction. It would be useful to follow evolution of the quantum stress tensor, Eqs.121, 122, although there is no unique way to separate this contribution from other terms, due to the presence of conformal coupling term φR . Useful combinations of the mixed stress tensor components are

$$\rho_{eff} = \frac{1}{2} (\langle T_0^0 \rangle - \langle T_1^1 \rangle), \quad (134)$$

$$\Lambda_{eff} = \frac{1}{2} (\langle T_0^0 \rangle + \langle T_1^1 \rangle), \quad (135)$$

which may be regarded as an effective quantum energy density and an effective quantum cosmological constant, respectively. There is a simple relation: $\Lambda_{eff} = -\frac{\kappa}{8\pi} R$. The limiting behavior is given by

$$\rho_{eff} = \frac{1}{a^2} O\left(\frac{\kappa}{x^0}\right), \quad \Lambda_{eff} = \frac{1}{a^2} O\left(\frac{\kappa}{(x^0)^2}\right), \quad (136)$$

at $x_0 \sim -\infty$, indicating that quantum effects are initially subdominant, and

$$\rho_{eff} = \frac{1}{a^2} \frac{\kappa B^2}{8\pi}, \quad \Lambda_{eff} = \frac{1}{a^2} O(\kappa x^0 e^{-Bx^0}), \quad (137)$$

at $x_0 \sim \infty$. It then yields a global amount of created energy at the final epoch,

$$\langle T_0^0 \rangle = -\langle T_1^1 \rangle = \frac{1}{a_f^2} \frac{\kappa B^2}{8\pi} = \frac{\kappa \lambda^2}{2\pi}, \quad (138)$$

in the form of massless particles. In the extreme large N limit this reduces to $\frac{N}{24\pi} \lambda^2$. Note that this result is insensitive to the parameters in the solution, or the initial condition. We shall further show in the next section that this result is universal even in the presence of inhomogeneities.

It is useful to make a comparison to the Gibbons-Hawking conjecture [18] in the case of de Sitter spacetime. They argue that the presence of future event horizon gives rise to a thermal emission of massless particles with a temperature of

$$T_{GH} = \frac{H}{2\pi} = \frac{\sqrt{2}\lambda}{2\pi}, \quad (139)$$

where the Hubble parameter H is replaced by that in the de Sitter phase of our evolving cosmological solution. This leads to an energy density,

$$\rho_{GH} = \frac{N}{12\pi} \lambda^2. \quad (140)$$

This differs from our final increment of energy, by a factor of 2, this one larger than the created energy in our final universe. It is not clear, however, that we are making a fair comparison. The usual procedure to derive the Hawking radiation would be to insert the classical background in the formula of quantum correction $\langle T_{\mu\nu} \rangle$ without considering the back reaction. Then one would get

$$\langle T_0^0 \rangle = \langle T_1^1 \rangle = -\frac{\kappa \lambda^2}{\pi}, \quad (141)$$

as already noted previously. Namely, what comes out from our study of the integrable model with quantum back reaction taken into account is that the Gibbons-Hawking radiation does not occur in the classical de Sitter phase, and furthermore the final energy output after all transient phenomena end is the half of the Gibbons-Hawking radiation.

Another evidence against the Gibbons-Hawking picture is given by time dependence of the energy output. As verified quantitatively in [12], most of the energy creation occurs in the late contracting phase of evolution. It is thus difficult to identify this radiation as associated with the expanding epoch of de Sitter spacetime.

VI. No hair theorem in integrable cosmology

We extend our semiclassical analysis to cosmology with an arbitrary degree of inhomogeneities [13]. We shall first present result in the integrable model of the reversed CGHS model. Later we shall mention how the general result is further extended to other integrable and nonintegrable models.

The most interesting result of general inhomogeneous solution is validity of a form of cosmic no hair theorem. The cosmic no hair theorem may be viewed in broad terms as an approach to a smooth universe despite initial irregularities [22], [23]. In the literature it is often discussed in connection with a final state of de Sitter spacetime [24], [25], [23]. But we shall consider the theorem in a somewhat more general context.

In our problem the final universe turns out to be a flat spacetime in two dimensions with a universally created matter, irrespective of arbitrarily large initial inhomogeneities. We shall prove this result for matter distribution arbitrarily localized in null coordinates.

We start with general inhomogeneous solution in the reversed RST model;

$$e^{-2\varphi} - \frac{\kappa}{2}\varphi = \frac{4\lambda^2}{B^2} e^{Bx^0} g_+(x^+) g_-(x^-) - Dx^0 - C - h_+(x^+) - h_-(x^-) \quad (142)$$

$$\rho = \varphi + \frac{1}{2}Bx^0 + \frac{1}{2} \left[\ln(g_+ + \frac{2}{B}g'_+) + \ln(g_- + \frac{2}{B}g'_-) \right], \quad (143)$$

with $g_{\pm} > 0$. This is the most general solution written in a form convenient to facilitate its comparison to the homogeneous case. The homogeneous cosmological solution is given by setting both g_{\pm} equal to 1 and both h_{\pm} vanishing. We now make a coordinate gauge choice within the conformal gauge such that new $Bx^{\pm'} = Bx^{\pm} + 2\ln g_{\pm}$. In this new coordinate $g'_{\pm} = 1$, and

$$e^{-2\varphi} - \frac{\kappa}{2}\varphi = \frac{4\lambda^2}{B^2} e^{Bx^0} - Dx^0 - C - h_+(x^+) - h_-(x^-), \quad (144)$$

$$\rho = \varphi + \frac{1}{2}Bx^0. \quad (145)$$

The constraint equation in this new gauge is

$$h''_{\pm} - \frac{B}{2}h'_{\pm} = -\frac{1}{2}(\partial_{\pm}f_i)^2 + \frac{1}{4}BD + \frac{1}{16}\kappa B^2 - \kappa t_{\pm}(x^{\pm}). \quad (146)$$

We can put forward the no incoming boundary condition as in the previous argument for the homogeneous case. Despite the presence of the inhomogeneity we get the same boundary function. First, note that at $x^{\pm} = -\infty$ the asymptotic behavior of the dilaton field is given by

$$\varphi \sim -\frac{1}{2} \ln \left[-\frac{D}{2}x^{\pm} - h_{\pm} \right], \quad (147)$$

barring a cancellation between D and h_{\pm} terms, and one can show, using Eqs.121, 122, that

$$\langle T_{\pm\pm} \rangle \sim 0, \quad (148)$$

$$\langle T_{\pm\pm} \rangle \sim -\frac{\kappa}{\pi} \left(t_{\pm} - \frac{B^2}{16} \right). \quad (149)$$

This yields that both

$$t_{\pm} = \frac{B^2}{16}. \quad (150)$$

We thus conclude that no quantum flux condition gives the unique boundary term, even in the case with arbitrary inhomogeneities.

Superficially this result is equivalent to demanding both the κ dependent and the κ independent terms in the constraint equation Eq.146 vanish, hence the terminology of the classical boundary condition was used in Ref.[12]. But we use the full quantum solution even for the contribution identified as a classical one, hence the κ dependent term in Eq.146 does not correspond to the quantum stress tensor Eq.122. Because of this the quantum stress tensor has a nontrivial functional behavior at finite spacetime points.

The general solution in the homogeneous gauge having no incoming quantum flux at null infinite past is summarized by the three equations: Eqs.144, 145 and the constraint equation giving h_{\pm} :

$$h''_{\pm} - \frac{B}{2}h'_{\pm} = -\frac{1}{2}(\partial_{\pm}f_i)^2 + \frac{1}{4}BD. \quad (151)$$

The homogeneous universe model has

$$h_{\pm} = 0, \quad \frac{1}{2}(\partial_{\pm}f_i)^2 = \frac{1}{4}BD. \quad (152)$$

Hence the right hand side of Eq.151 measures deviation from the homogeneous matter distribution.

When we consider inhomogeneous matter distribution, we shall restrict to inhomogeneity localized in null coordinates. Thus we assume that the right hand side of Eq.151 has a finite support. This means that for a large enough x^{\pm} the function h_{\pm} obeys the homogeneous differential equation, and the limiting behavior at large x^0 is given by

$$h_{\pm} \sim e^{\frac{B}{2}x^{\pm}}. \quad (153)$$

This is important in later discussion of the cosmic no hair theorem.

The scalar curvature is computed from the general solution as

$$R = -\frac{4\lambda^2}{1 + \frac{\kappa}{4}e^{2\varphi}} + 4e^{2\varphi - Bx^0} \frac{[\frac{2\lambda^2}{B}e^{Bx^0} - \frac{D}{2} - h'_+][\frac{2\lambda^2}{B}e^{Bx^0} - \frac{D}{2} - h'_-]}{[1 + \frac{\kappa}{4}e^{2\varphi}]^3}. \quad (154)$$

This equation is not written in a closed form as a function of x^0 , because the coupling strength $e^{2\varphi}$ must be computed from the transcendental equation Eq.144. Nevertheless this expression is useful in many occasions. Let us first work out the classical

limit, $\kappa = 0$, of this formula. In this case

$$R = -4\lambda^2 + 4e^{-Bx^0} \frac{[\frac{2\lambda^2}{B}e^{Bx^0} - \frac{D}{2} - h'_+][\frac{2\lambda^2}{B}e^{Bx^0} - \frac{D}{2} - h'_-]}{[\frac{4\lambda^2}{B^2}e^{Bx^0} - Dx^0 - C - h_+ - h_-]}. \quad (155)$$

Classical singularity thus appears whenever

$$\frac{4\lambda^2}{B^2}e^{Bx^0} - Dx^0 - C - h_+ - h_- = 0. \quad (156)$$

Note that classical singularities may show up in several places at different times, even when the homogeneous part defined without h_{\pm} term is regular at all finite x^0 . The situation may be regarded as a model of evolving universe with an arbitrary degree of inhomogeneities which is usually considered to develop into black holes.

The general trend of effect of inhomogeneous matter is as follows: as the matter content $\frac{1}{2}(\partial_{\pm}f_i)^2$ increases, h_{\pm} becomes more negative, reducing singular behavior. On the other hand, as the matter content $\frac{1}{2}(\partial_{\pm}f_i)^2$ decreases, h_{\pm} becomes more positive, enhancing singular behavior. Thus the void, and not the lump, tends to increase more curvature. This is a peculiarity of the reversed model and is hoped to be discussed more fully elsewhere.

The universal nature of the final state is valid in a more extended class of two dimensional dilaton gravity theories, beyond the reversed RST model so far discussed. Let us assume first that the theory is integrable in the form of

$$e^{-2\varphi} - f(\varphi) = \frac{4\lambda^2}{B^2}e^{Bx^0} - Dx^0 - C - h_+ - h_-, \quad (157)$$

$$\rho - \varphi + g(\varphi) = \frac{1}{2}Bx^0. \quad (158)$$

For instance, in the BCDA model [21] based on the conformal field theory the two functions are given by

$$f(\varphi) = e^{-2\varphi} - F(\varphi), \quad g(\varphi) = \varphi - \frac{1}{\kappa}f(\varphi), \quad (159)$$

$$F(\varphi) = e^{-\varphi}\sqrt{e^{-2\varphi} + \kappa} + \kappa \ln[e^{-\varphi} + \sqrt{\kappa + e^{-2\varphi}}] - \frac{\kappa}{2} \ln 4e. \quad (160)$$

As φ varies from $-\infty$ to ∞ , $F(\varphi)$ changes according to

$$e^{-2\varphi} - \kappa\varphi + O[\kappa^2 e^{2\varphi}] \rightarrow \frac{\kappa}{2} \ln \frac{\kappa}{4e} + 2\sqrt{\kappa}e^{-\varphi}. \quad (161)$$

All integrable models of this class have the classical limit of the same form,

$$e^{-2\varphi} = \frac{4\lambda^2}{B^2}e^{Bx^0} - Dx^0 - C, \quad (162)$$

$$2(\rho - \varphi) = Bx^0. \quad (163)$$

This must be so, because all these models have the same classical limit of the reversed CGHS model. But the point here is that the classical $\kappa = 0$ limit and the weak coupling $e^{2\varphi} = 0$ limit coincide. This is understandable in the large N limit we consider, since $\kappa e^{2\varphi}$ is the expansion parameter of quantum loop correction.

The next leading corrections to the classical equations, Eqs.162, 163, are different in various models. In the reversed BCDA model the classical term is modified to the order of κ according to

$$e^{-2\varphi} \Rightarrow e^{-2\varphi} - \kappa \varphi, \quad 2(\rho - \varphi) \Rightarrow 2(\rho - \varphi) + \frac{\kappa}{4} e^{2\varphi}, \quad (164)$$

while in the reversed RST model it is

$$e^{-2\varphi} \Rightarrow e^{-2\varphi} - \frac{\kappa}{2} \varphi, \quad 2(\rho - \varphi) \Rightarrow 2(\rho - \varphi). \quad (165)$$

One then derives a universal classical behavior; at $x^0 = -\infty$

$$\varphi \sim -\frac{1}{2} \ln(-Dx^0) + O\left(\kappa \frac{\ln(-Dx^0)}{x^0}\right), \quad (166)$$

$$\rho \sim \frac{B}{2} x^0 - \frac{1}{2} \ln(-Dx^0), \quad (167)$$

and at $x^0 = \infty$

$$\varphi \sim -\frac{B}{2} x^0 + \ln \frac{B}{2\lambda}, \quad (168)$$

$$\rho \sim \ln \frac{B}{2\lambda} + O[x^0 e^{-Bx^0}]. \quad (169)$$

Of course, at intermediate x^0 occurrence of model dependence is unavoidable, but existence of semiclassical solution linking two limiting classical behaviors is guaranteed if one assumes validity of the asymptotic weak coupling scheme. The classical behavior at $x^0 = \infty$ immediately yields the final flat universe of the cosmological scale factor $\frac{B}{2\lambda}$, and of the vanishing curvature of the form,

$$R \sim O[x^0 e^{-Bx^0}]. \quad (170)$$

Both in the reversed RST and BCDA models the approach to the final flat universe is made by passing through a contracting phase, but contraction rate is different in the two models.

For an asymptotic quantum stress tensor one may take the original Polyakov form,

$$\langle T_{\pm\pm} \rangle = -\frac{\kappa}{\pi} \left[\partial_{\pm}^2 \rho - (\partial_{\pm} \rho)^2 + t_{\pm}(x^{\pm}) \right]. \quad (171)$$

Although the reversed RST model has an additional contribution to this stress tensor due to the conformal coupling term φR as seen from Eq.122, the additional piece turns out subdominant at both the initial and final stages of cosmological evolution. We hence regard the above choice of quantum stress tensor quite adequate for our purposes.

At $x^0 = -\infty$ the dominant stress component is computed from Eqs.166, 167

$$\langle T_{\pm\pm} \rangle \sim -\frac{\kappa}{\pi} \left(t_{\pm} - \frac{B^2}{16} \right). \quad (172)$$

Thus no incoming flux condition gives the same unique boundary term as before, $t_{\pm} = \frac{B^2}{16}$. With this given, one derives from Eqs.168, 169 the asymptotic flux at future infinity, $x^0 = \infty$,

$$\langle T_{\pm\pm} \rangle \sim -\frac{\kappa B^2}{16\pi}. \quad (173)$$

It then gives the universal flux of created radiation in the final flat universe,

$$\langle T_0^0 \rangle \sim -\langle T_1^1 \rangle \sim \frac{\kappa \lambda^2}{2\pi}. \quad (174)$$

Note that this flux is insensitive to the initial condition and is determined by the fundamental constants in the theory. This derivation makes clear importance of the initial boundary condition and the limiting classical behavior, to get the universal quantum flux.

The status of the original nonintegrable model [11] is as follows. Assuming the Polyakov form of quantum stress tensor, one immediately finds that to the leading \hbar order the universality of the final state with the definite amount of created radiation holds. In the next leading order of \hbar^2 there is a deviation from the integrable model, if one strictly takes the original Polyakov form [13]. In terms of κ expansion the leading κ behavior is however not adequate to the discussion of order \hbar^2 , and one needs the next two loop quantum correction not considered here, in order to establish the next leading \hbar^2 correction.

In summary, I have discussed tractable models of quantum back reaction in two dimensional cosmology. In the context of inflationary universe scenario these models provide a concrete mechanism of quantum decay of de Sitter spacetime, without relying on the fine tuning of microphysics parameters.

References

- [1] S.W.Hawking, Commun.Math.Phys. **43**, 199(1975).
- [2] For a review, J.Preskill, *Do Black Holes Destroy Information?*, Caltech preprint, CALT-68-1819, 1992.
- [3] G.'t Hooft, Nucl.Phys.**B335**, 138(1990), and references therein.
- [4] Y.Aharonov, A.Casher, and S.Nussinov, Phys.Lett.**191B**, 51(1987).
- [5] C.G.Callan, S.B.Giddings, J.A.Harvey and A.Strominger, Phys.Rev. **D45**, 1005(1992).
- [6] J.G.Russo, L.Susskind and L.Thorlacius, Phys.Lett.**292B**,13(1992).
- [7] T.Banks, A.Dabholkar, M.R.Douglas and M.O'Loughlin, Phys.Rev.**D45**, 3607(1992).
- [8] S.W.Hawking, Phys.Rev.Lett. **69**, 406(1992).
- [9] B.Birner, S.B.Giddings, J.A.Harvey, and A.Strominger, Phys.Rev.**D46**, 638(1992).
- [10] L.Susskind and L.Thorlacius, Nucl.Phys. **B382**, 123(1992).
- [11] M.Yoshimura, *Quantum Decay of de Sitter Universe and Inflation without Fine Tuning in 1+1 Dimensions*, Tohoku University preprint, TU/92/416, September 1992; Phys. Rev.D, in press.
- [12] M.Hotta, Y.Suzuki, Y.Tamiya, and M.Yoshimura, *Quantum Back Reaction in Integrable Cosmology*, Tohoku University preprint, TU/93/426, January 1993; Phys.Rev.D, in press.
- [13] M.Hotta, Y.Suzuki, Y.Tamiya, and M.Yoshimura, *Universality of Final State in Two Dimensional Dilaton Cosmology*, Tohoku University preprint, TU/93/431, April 1993.
- [14] J.G.Russo, L.Susskind and L.Thorlacius, Phys.Rev.**D46**, 3444(1992).
- [15] A.M.Polyakov, Phys.Lett. **103B**, 207(1981).

- [16] A.Strominger, Phys.Rev. **D46**, 4396(1992).
- [17] S.M.Christensen and S.A.Fulling, Phys.Rev.**D15**, 2088(1977).
- [18] G.W.Gibbons and S.W.Hawking, Phys.Rev.**D15**, 2738(1977).
- [19] F.D.Mazzitelli and J.G.Russo, *Dilaton Quantum Cosmology in Two Dimensions*, University of Texas preprint, UTTG-28-92, November 1992.
- [20] In a somewhat different context this model was also considered by T.Mishima and A.Nakamichi, *Chronology Protection in Two-Dimensional Dilaton Gravity*, Tokyo Institute of Technology preprint, TIT/HEP-218/COSMO-29, April 1993.
- [21] A.Bilal and C.G.Callan, *Liouville Models of Black Hole Evaporation*, Princeton University preprint, PUPT-1320, May 1992;
S.P.de Alwis, Phys.Lett.**289B**, 278(1992).
- [22] F.Hoyle and J.V.Narlikar, Proc.R.Soc. **A273**, 1(1963);
G.W.Gibbons and S.W.Hawking, Phys.Rev.**D15**, 2738(1977).
- [23] For a review, D.S.Goldwirth and T.Piran, Phys.Rept. **214**, 223(1992).
- [24] R.M.Wald, Phys.Rev. **D28**, 2118(1983).
- [25] J.D.Barrow, Phys.Lett. **180B**, 335(1986).

Cosmological Application of CGHS Model

Akio Hosoya ^{*}, Takashi Mishima [†] and Akika Nakamichi [◊]

^{*}, [◊] *Department of Physics, Tokyo Institute of Technology*

Oh-okayama, Meguro-ku, Tokyo 152, Japan

[†] *Institute for Nuclear Study, University of Tokyo*

Midori-cho, Tanashi-shi, Tokyo 188, Japan

1

Recently Callan, Giddings, Harvey and Strominger[1] (abbreviated as CGHS) provided the useful toy model of (1+1)-dimensional gravity. They attempted to analyze the back reaction of the Hawking radiation[2] on the two-dimensional analogue of black hole geometry in a consistent way by the use of this model. In their first paper, CGHS developed their original scenario as follows: First introducing 1+1 dimensional dilaton gravity, CGHS found the solutions corresponding to black hole formation, and showed occurrence of the Hawking radiation on the spacetime background they obtained. Next including quantum effect from quantized conformal matters as Polyakov term[3], they gave the possibility to analyze the back reaction of Hawking effect in a leading semi-classical approximation consistently, even though their first scenario on the quantum black hole was too simple. Up to the present, many works have studied the behavior of quantum black hole in this model[4].

On the other hand in general relativity, there are other interesting problems which must be resolved taking account of quantum effect besides the problem of Hawking radiation. For example, since Morris, Thorne and Yurtsever[5] pointed out the possibility of making a time-machine, quantum effect on the spacetime in which closed time-like curves appear (abbreviated as CTC-spacetime) has been discussed by several authors [6,7,8,9,10]. One of the most important problems in

[◊] e-mail address: akika@phys.titech.ac.jp

this subject is whether CTC-spacetime still continues to be or not due to quantum effect. On this problem, Hawking suggested that the laws of physics prevent the appearance of closed time-like curves(so called 'Chronology Protection Conjecture'). In four dimensions the analyses on this problem so far have been done only on the fixed background spacetimes. So it must be interesting to treat such spacetimes including back-reaction in closed form even in lower dimensions.

In this paper we will investigate the quantum back reaction problem on the stability of the CTC-spacetime in two dimensional model of dilaton gravity. Following the CGHS scenario, we apply this model to compact one dimensional universe. In the first half we give a classical solution corresponding to CTC-spacetime: an analogue of Misner universe. Then we show the disappearance of this spacetime due to inhomogeneity even any fine-tuning introduced. In the second half we introduce quantum effect and observe the re-appearance of such a CTC-spacetime if some fine-tuning of parameter is introduced.

2

We consider the 1 + 1 dimensional renormalizable theory of gravity coupled to a dilaton scalar field ϕ and N massless conformal fields f_i . The classical action is

$$S = \frac{1}{2\pi} \int d^2x \sqrt{-g} [e^{-2\phi} (R + 4(\nabla\phi)^2 - 4\lambda^2) - \frac{1}{2} \sum_{i=1}^N (\nabla f_i)^2] , \quad (01)$$

where R is the scalar curvature, λ^2 is a cosmological constant. This model differs from the original C.G.H.S. model in the sign of the cosmological term.

The equations of motion derived from (01) are

$$\begin{aligned} 0 &= -4\partial_+\partial_-\phi + 2\partial_+\partial_-\rho + 4\partial_+\phi\partial_-\phi - \lambda^2 e^{2\rho} , \\ 0 &= \partial_+\partial_-\phi - \partial_+\partial_-\rho , \\ 0 &= \partial_+\partial_-\phi , \end{aligned} \quad (02)$$

in the conformal gauge:

$$g_{\mu\nu} dx^\mu dx^\nu = -e^{2\rho} dx^+ dx^- , \quad (03)$$

where $x^\pm = t \pm x$. In addition the following constraints have to be imposed:

$$4e^{-2\phi}(\partial_\pm^2\phi - 2\partial_\pm\rho\partial_\pm\phi) = \sum_{i=1}^N \partial_\pm f_i \partial_\pm f_i. \quad (04)$$

In the following we adopt the periodic boundary condition that (t, x) identifies with $(t, x + L)$ and the initial condition that the Universe start from static cylinder with usual Minkowski metric at the past infinity. Then the general form of the solutions is given as follows:

$$\begin{aligned} e^{-2\phi} &= u_+ + u_- + \frac{4\lambda^2}{a^2} e^{at}, \\ e^{2\rho} &= e^{-2\lambda t} e^{2\phi}, \end{aligned} \quad (05)$$

where u_+ and u_- are chiral periodic functions which satisfy the following equations from the constraints (04):

$$0 = \partial_\pm^2 u_\pm + \lambda \partial_\pm u_\pm + \frac{1}{2} \partial_\pm f \partial_\pm f. \quad (06)$$

3

When there is no matter field, general solutions that satisfying the periodic boundary conditions depend only on time:

$$\begin{aligned} e^{2\phi} &= (M + e^{-2\lambda t})^{-1}, \\ e^{2\rho} &= e^{-2\lambda t} e^{2\phi}, \end{aligned} \quad (07)$$

where M is the arbitrary constant. We classify the behavior of the solutions into three types with respect to the sign of M .

When M equals to 0, the solution becomes an analogue of the Linear Dilaton Vacuum solution in C.G.H.S. model. The world is a static cylinder spacetime.

When M is negative, we see from (07) that the observer meet some singularity in the finite proper time. From the expression of scalar curvature R :

$$R = -\frac{4\lambda^2 M}{M + e^{-2\lambda t}}, \quad (08)$$

this singularity prove to be the essential singularity. In fact this singularity is the same as the one in the 1 + 1 dimensional black-hole treated in CGHS.

On the other hand when M is positive, the space collapses into zero volume in finite proper time(as coordinate time t goes to $+\infty$). But from (08) the scalar curvature still remains finite value $-4\lambda^2$ at the point. Hence we expect that the spacetime can be extended. In fact, if one define the coordinates:

$$\begin{cases} \eta = -e^{-2\lambda t}, \\ \psi = t \pm x, \end{cases} \quad (09)$$

the metric g on the manifold \mathcal{M} which is defined by (t, x) then takes the form g' given by

$$ds^2 = \frac{-1}{M - \eta} (\eta d\psi^2 + \frac{1}{\lambda} d\psi d\eta). \quad (010)$$

This is analytic on the manifold \mathcal{M}' defined by ψ and by $-\infty < \eta < M$. The region $\eta < 0$ of (\mathcal{M}', g') is isometric with (\mathcal{M}, g) . The behavior of (\mathcal{M}', g') is shown in Fig.1. In the region $\eta > 0$ of \mathcal{M}' the closed timelike curves appear, because the roles of t and x are replaced. The surface $\eta = 0$ is the boundary of the Cauchy Development; that is the Cauchy Horizon. This extension is the same way as in the case of Misner space (we have two dimensional version when $\lambda = 0$) and Taub-NUT space [11]. Hawking uses Misner space to discuss the chronology protection conjecture [9].

In the rest of the paper we investigate the conjecture in this model both from the viewpoint at classical and the quantum level.

In this section we consider the Universe with classical massless scalar fields. The solutions of (04) satisfying the periodic boundary condition always exist with arbitrary configurations of the scalar fields. If we expand the scalar fields in Fourier series:

$$f(x^+, x^-) = f_+(x^+) + f_-(x^-),$$

$$f_{\pm} = \alpha_{\pm} + \sqrt{\frac{\epsilon}{2}} x^{\pm} + \sum_{n=1}^{\infty} (a_n^{\pm} \sin \frac{2\pi n}{L} x^{\pm} + b_n^{\pm} \cos \frac{2\pi n}{L} x^{\pm}), \quad (011)$$

here α_{\pm}, a_n^{\pm} and b_n^{\pm} are the expansion coefficients. we obtain the solution as follows

$$e^{-2\phi} = M - \left\{ \frac{\epsilon}{2\lambda} + \frac{1}{2\lambda} \Sigma \right\} t + e^{-2\lambda t} + (\text{oscillation part}),$$

$$\Sigma = \sum_{n=1}^{\infty} \left(\frac{2\pi n}{L} \right)^2 [(a_n^{\pm})^2 + (b_n^{\pm})^2], \quad (012)$$

where the fourth term in the right hand side of the first equation in (012) is the oscillation part, that is the sum of the trigonometric functions. From (012) it should be noted that any classical configuration of matter fields makes a finite contribution to the term proportional to time, which cause divergence of the scalar curvature. Therefore the Universe inevitably meets singularity at $t = \infty$ and cannot extend to the region with closed time-like curves.

From now on we study how the classical solution change by including back reaction.

In two dimensions, the quantum effect of massless matter fields is completely determined by conformal anomaly. [3] The quantum effective action is sum of the classical action (01) and the Polyakov term induced by N matter fields:

$$S_{\text{quantum}} = -\frac{\kappa}{8\pi} \int d^2x \sqrt{-g(x)} \int d^2x' \sqrt{-g(x')} R(x) G(x, x') R(x'), \quad (013)$$

here κ is $\frac{N}{12}$ and $G(x, x')$ is a Green function of the scalar fields. κ is assumed to

be a large number for introducing $1/N$ -expansion. Further we add the following term introduced by Russo et al.[12] to the above action:

$$S'_{quantum} = -\frac{\kappa}{8\pi} \int d^2x \sqrt{-g} 2\phi R. \quad (014)$$

Introducing the following field redefinition

$$\begin{aligned} \chi &= \sqrt{\kappa} \left(\rho - \frac{1}{2}\phi + \frac{1}{\kappa}e^{-2\phi} \right), \\ \Omega &= \sqrt{\kappa} \left(\frac{1}{2}\phi + \frac{1}{\kappa}e^{-2\phi} \right), \end{aligned} \quad (015)$$

then the semi-classical equations of motion becomes in very simple form:

$$\begin{aligned} \partial_+ \partial_- \chi &= -\frac{\lambda^2}{\sqrt{\kappa}} e^{\frac{2}{\sqrt{\kappa}}(\chi-\omega)}, \\ \partial_+ \partial_- (\chi - \omega) &= 0, \end{aligned} \quad (016)$$

and

$$\partial_{\pm} f \cdot \partial_{\pm} f - 2\kappa t_{\pm}(x_{\pm}) = -\partial_{\pm}\chi\partial_{\pm}\chi + \partial_{\pm}\Omega\partial_{\pm}\Omega + \sqrt{\kappa}\partial_{\pm}^2\chi, \quad (017)$$

where \cdot denotes the sum of i and t_{\pm} are arbitrary chiral functions to be determined by the boundary conditions and f_i is interpreted as macroscopic behavior of quantized fields. With the zero-mode contribution included(i.e. the homogeneous configuration of matter: $\langle f \rangle = \sqrt{2\epsilon} t$), the solution of the equations (016) and (017) is as follows

$$\begin{aligned} \sqrt{\kappa}\chi &= M - \frac{2\kappa}{\lambda} \left(\frac{\lambda^2}{4} - t_{vev} + \frac{\epsilon}{4\kappa} \right) t + e^{-2\lambda t}, \\ \sqrt{\kappa}\Omega &= M + \frac{2\kappa}{\lambda} \left(\frac{\lambda^2}{4} + t_{vev} - \frac{\epsilon}{4\kappa} \right) t + e^{-2\lambda t}, \end{aligned} \quad (018)$$

where $t_{vev} = t_{\pm} = \frac{\pi^2}{L^2}$ due to the Casimir effect.

From the equations (015) and (018), we know the qualitative behavior of ϕ as a function of time t (Fig.2).

We examine whether quantum version of CTC-spacetime realizes or not. First from (015) and (018), we obtain

$$2\rho = 2\phi - 2\lambda t. \quad (019)$$

To get CTC-spacetime, 2ϕ must become linear in t as $t \rightarrow \infty$ in the conformal flat gauge. By comparing $\Omega - \phi$ and $\Omega - t$ relations, we know the corresponding solutions exist in the following region of parameters:

$$\begin{aligned} M &> \sqrt{\kappa} \Omega_{cr}, \\ \varepsilon &= \kappa \lambda^2 + 4\kappa t_{ev}. \end{aligned} \quad (020)$$

where Ω_{cr} is the local minimum of Ω in $\Omega - \phi$ relation (Fig.2(a)). It should be noted that the value of dilaton at $\eta = 0$ can be adjusted so small one that the semi-classical approximation is valid.

6

The spacetime structure of $1 + 1$ dimensional compact Universe have been studied in two dimensional model of dilaton gravity. First we gave a classical solution corresponding to the spacetime in which closed time-like curves appear and show the instability of this spacetime due to the existence of matters. Next we observed the appearance of quantum analogue of such a CTC-spacetime needed some fine tuning of parameters. Thus it can be said that the chronology protection holds in a weak sense in this model.

As further investigations, it is more interesting to understand the classical and semi-classical behaviours of the compact universe treated in this paper with full quantization of two dimensional dilaton gravity[13, 14]. Especially, the construction of the physical states having such classical and semi-classical behaviours is required.

One of the authors(T. M.) would like to acknowledge Y. Onozawa, M. Siino and K. Watanabe for enjoyable discussions.

REFERENCES

1. C. G. Callan, S. B. Giddings, J. A. Harvey and A. Strominger, *Phys. Rev. D* **45** (1992) R1005.
2. S. W. Hawking, *Comm. Math. Phys.* **43** (1975) 199.
3. A. M. Polyakov, *Phys. Lett.* **B103** (1981) 207.
4. J. A. Harvey, A. Strominger *Quantum Aspects of Black Hole*, EFI-92-41, September 1992 and references therein.
5. M. S. Morris, K. S. Thorne and U. Yurtsever, *Phys. Rev. Lett.* **61** (1988) 1446.
6. J. Friedman, M. S. Morris, I. D. Novikov, F. Echeverria, G. Klinkhammer, K. S. Thorne, U. Yurtsever, *Phys. Rev. D* **42** (1990) 1915.
7. V. P. Frolov, *Phys. Rev. D* **43** (1991) 3878.
8. W. Kim, K. S. Thorne, *Phys. Rev. D* **43** (1991) 3929.
9. S. W. Hawking, *Phys. Rev. D* **46** (1992) 603.
10. B. S. Kay, *The Principle of Locality and Quantum Field Theory on (Non Globally Hyperbolic) Curved Spacetimes*, DAMTP/R-92/22, July 92.
11. S. W. Hawking, G. F. R. Ellis, *The Large Scale Structure of Space-Time*, Cambridge Univ. Press, (1982).
12. J. G. Russo, L. Susskind, L. Thorlacius, *The Endpoint of Hawking Radiation*, Stanford University preprint, SU-ITP-92-17, June 1992, to appear in Physical Review D.
13. N. Sakai, *c=1 Two Dimensional Quantum Gravity*, TIT/HEP-205, hep-th@xxx/920, August 1992.
14. Y. Matsumura, N. Sakai, Y. Tanii, T. Uchino, *Correlation Functions in Two Dimensional Dilaton Gravity*, TIT/HEP-204, STUPP-92-131, August 1992.

Figure Captions

Fig.1 Misner-lyp universe;
 $t = +\infty (\eta = 0)$ is a closed null geodesics. The region: $(\eta < 0)$ is Globally
 hyperbolic Spacetime, and the region: $(\eta > 0)$ have Closed Time-like Curves.

Fig.2 $\Omega - \phi$ and $\Omega - t$ relations;

(a) $\Omega - \phi$ relation, (b) $\Omega - t$ relation

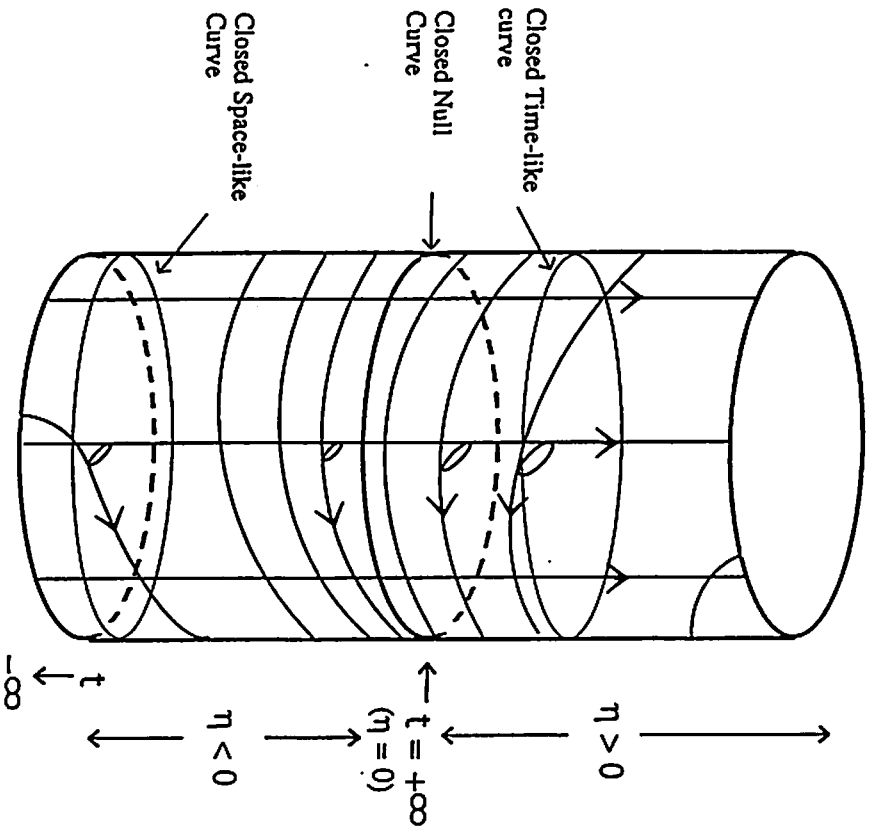


Fig.1

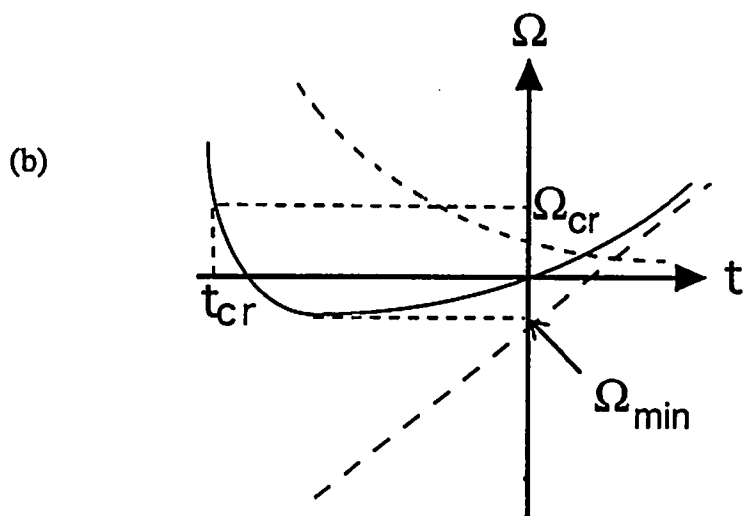
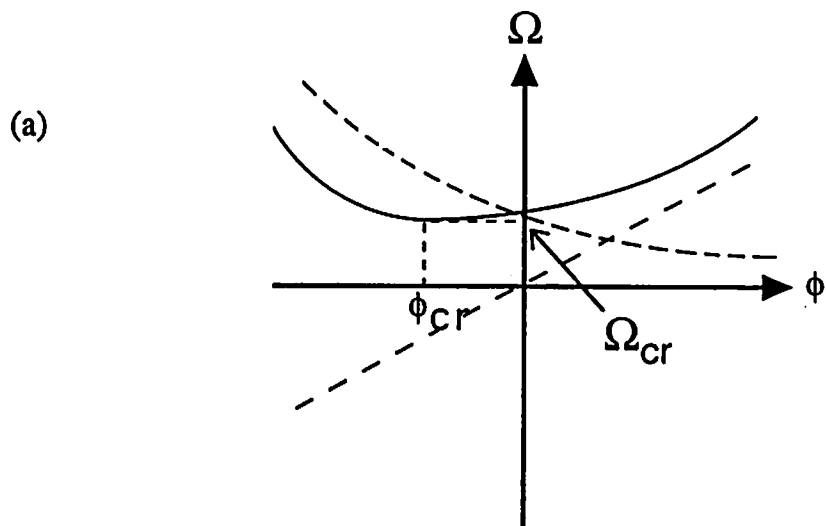


Fig.2

ON THE MASS OF TWO DIMENSIONAL QUANTUM BLACK HOLE

Tsukasa TADA¹

Shozo UEHARA²

*Uji Research Center
Yukawa Institute for Theoretical Physics
Kyoto University, Uji 611, Japan*

In this talk we shall consider the mass of 2dimensional quantum black hole especially. Recently two dimensional toy model of quantum black hole has been attracting much interest. Many features of CGHS model[2] and its modified version [3-8] have been discussed. But we shall here concentrate on the problem of the mass among many other problems.

Here we shall first introduce a kind of mass function, that is the mass that observed at each point of space-time and next calculate its value for CGHS model. Up to now our study is limited to semiclassical analysis.

To begin with, let me show the action, which we are going to study.

$$S = \frac{1}{2\pi} \int d^2x \sqrt{-g} e^{-2\phi} (R + 4(\nabla\phi)^2 + 4\lambda^2),$$

where ϕ is dilaton and λ is a constant. Here ϕ is for dilaton, which couples to scalar curvature R and its kinetic term. And this λ is a some constant, here we take it positive. It corresponds to a cosmological constant of gravitational system in *higher dimension* when we think this action as a spherically reduced model from higher dimension.

In particular we would like to point out that the above action resembles the action of spherically symmetric model of four dimensional grav-

ity. So keeping in mind its resemblance will be helpful in the following study. In fact it is pointed out that the above mentioned action is obtained by taking large D limit for D -dimensional spherically symmetric gravitational system [9].

Now we are going to analyze this model through the canonical formalism. As usual we decompose the metric in the following form;

$$g_{ab} = \begin{pmatrix} -N_0^2 + \frac{N_1^2}{\gamma} & N_1 \\ N_1 & \gamma \end{pmatrix}.$$

Here N_0 is known as lapse and N_1 is shift. γ stands for a dynamical degree of freedom of gravitational sector and these γ and ϕ , dilaton are two dynamical degrees of freedom in the present model.

Thus in terms of canonical variable, that is γ, ϕ and their conjugate momenta, π_γ, π_ϕ , the above action is written as ;

$$S = \int \pi_\phi \dot{\phi} + \pi_\gamma \dot{\gamma} - N_0 \mathcal{H}_0 - N_1 \mathcal{H}_1.$$

Here $\dot{}$ is for time derivative and \mathcal{H}_0 and \mathcal{H}_1 are the generators of time and space re-parametrization.

Therefore we obtain these two constraint:

$$\begin{cases} \mathcal{H}_0(\pi_\phi, \phi, \pi_\gamma, \gamma) = 0 \\ \mathcal{H}_1(\pi_\phi, \phi, \pi_\gamma, \gamma) = 0 \end{cases}.$$

They are rather complicated equation in terms of γ, ϕ, π_ϕ and π_γ . Next we shall combine these two equations to get a new quantity.

We find that these combination of two generators is nothing but a total derivative of \mathcal{M} as

¹ Soryuushi Shougakukai Fellow

² Work partially supported by Grant-in-Aid for Scientific Research of the Ministry of Education, Science and Culture No.02302020

follows;

$$0 = \mathcal{H}_0 \times \frac{2\phi'}{\lambda\sqrt{\gamma}} + \mathcal{H}_1 \times \frac{(-4)\gamma\pi_\gamma e^{2\phi}}{\lambda} = \mathcal{M}'.$$

Here ' denotes the spatial derivative and

$$\mathcal{M} \equiv \frac{4\gamma\pi_\gamma^2}{\lambda} e^{2\phi} - \frac{(\phi')^2}{\lambda\gamma} e^{-2\phi} + \lambda e^{-2\phi}.$$

It can be written in covariant form;

$$\mathcal{M} = \frac{e^{-2\phi}}{2} \left[\lambda^2 - g^{ab} \nabla_a \phi \nabla_b \phi \right].$$

The above quantity is nothing but two dimensional version of local mass which is first introduced in the study of spherically symmetric model of four dimensional gravitational system by Fischler Morgan and Polchinski [10]. The present system is very similar to spherically symmetric four dimensional gravity, hence we could imitate their construction in four dimensional. And very recently this quantity has applied to the evaporating Black Hole by Tomimatsu[11]. Our initial motivation is to apply this method to the CGHS model.

Rewriting with more usual form of metric;

$$g_{+-} = -\frac{1}{2}e^{2\rho}, \quad g_{++} = g_{--} = 0,$$

in conformal gauge and with light-cone coordinate x^+ and x^- , we find :

$$\mathcal{M} = \frac{1}{\lambda} \left[4e^{-2\rho} e^{-2\phi} \partial_+ \phi \partial_- \phi + \lambda^2 e^{-2\phi} \right].$$

Here ρ is for Liouville field as usual.

In CGHS model conformal matter couples to the two-dimensional dilatonic gravity. And we consider the situation that a matter shock-wave is coming to the origin. The most eminent feature of this model is that it can be exactly solved in classical case. So we can follow the whole process of matter collapsing though it is classical. One can expect that this model resolves the secret of gravitational collapse and formation of black hole because of its similarity to four dimensional spherically symmetric model.

Let us show the exact solution of this model when this matter shock-wave comes in. Here we

denote matter field by f and there you can see the shock-wave on the line of $x^+ = x_0^+$.

$$\frac{1}{2} \partial_+ f \partial_+ f = \frac{M}{\lambda x_0^+} \delta(x^+ - x_0^+)$$

Where M is a free parameter that represent the magnitude of the shock-wave and this is proved to be a mass of black hole later.

Then the classical solution of this model becomes as follows.

$$ds^2 = e^{2\rho} dx^+ dx^- \\ = \frac{dx^+ dx^-}{-\frac{M}{\lambda x_0^+} (x^+ - x_0^+) \theta(x^+ - x_0^+) - \lambda^2 x^+ x^-}$$

For this geometry we find the local mass expression as follows;

$$\mathcal{M}(x^+, x^-) = M \theta(x^+ - x_0^+)$$

So far the classical theory, now we would like to proceed to the quantum theory. We incorporate quantum effect through including trace anomaly term;

$$\kappa \partial_+ \partial_- \rho$$

into the action. Here κ depends on the number of matter fields and we assume it is rather positively large. This gives us an one-loop effective action and make us possible to large-N analysis.

One finds that the model is no longer exactly solvable once we incorporate the quantum effect through the anomaly. Many features in classical theory become different. For example ϕ does not coincide with ρ , and the analysis breaks down at some large value of ϕ , etc. So our analytical study is limited to the region near the classical region. That is, we can only analyze on the matter shock-wave line and past null infinity where space-time is asymptotically flat and the quantum fluctuation is very small (Fig. 1).

First at past null infinity, where x^- goes to minus infinity;

$$\mathcal{M}|_{x^- \rightarrow -\infty} = M \theta(x^+ - x_0^+)$$

There the result coincide completely with one of classical theory, as one may expect. That is after matter shock wave passes, one finds the value M stays constant in past null infinity.

Fig.1. Plot of local mass function on Penrose diagram.

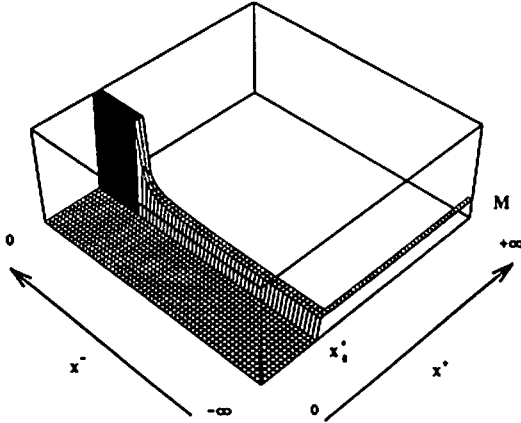
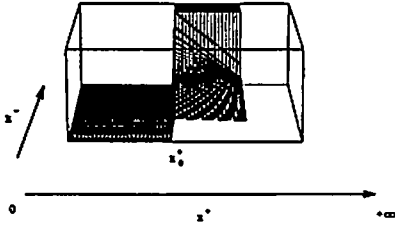


Fig.2. Decreasing of the mass towards x^+ direction is shown.



Secondly, we proceed to the result on the matter shock-wave line. On this line the value of local mass expression take like this.

$$\mathcal{M}(x_0^+, x^-) = M \sqrt{\frac{-\lambda^2 x_0^+ x^-}{-\lambda^2 x_0^+ x^- - \kappa}}$$

It increases along the matter shock-wave line to the horizon and actually diverges at the critical point, where semi-classical equation breaks down, sometimes it referred as a quantum singularity. Of course its value at past null infinity is M as one can easily see.

Also we have calculated its derivative along x^+ and find it decreases towards x^+ direction outside the apparent horizon. It slowly reaches zero at past null infinity (Fig.2).

The area painted white in Fig. 1. is left for further study with numerical calculation, which

is now in progress. Therefore it is difficult and may be dangerous to drag some conclusion from these result because most crucial region is not yet analyzed.

So let us close this talk with the comment that the situation on mass seems to be rather different for 2d CGHS model comparing 4d case. There is some evidence already in the classical physics. For example, applying the inverse Kruskal-Szekeres transformation to the static solution of 2d dilatonic system we find

$$ds^2 = \frac{1}{\left(1 - \frac{r_s}{r}(1 - e^{-r/r_s})\right)} \times \left[-\left(1 - \frac{r_s}{r}\right)(dt)^2 + \frac{(dr)^2}{1 - \frac{r_s}{r}} \right],$$

where $r_s = \frac{1}{2\lambda}$. This form is in usual t, r coordinate and what to be compared with Schwarzschild solution. There is no parameter M in the above form so the difference is obvious.

Note added: Recently we have noticed that the same local mass is also considered in [12].

References

- [1] T. Tada and S. Uehara, preprint YITP/U-92-37, hep-th/9301020
- [2] C.G. Callan, S.B. Giddings, J.A. Harvey and A. Strominger, Phys. Rev. D45 (1992) R1005.
- [3] T. Banks, A. Dabholkar, M.R. Douglas and M. O'Loughlin, Phys. Rev. D45 (1992) 3607.
- [4] J.G. Russo, L. Susskind and L. Thorlacius, Phys. Lett. B292 (1992) 13; preprint SU-ITP-92-17 (1992); preprint UTTG-19-92 (1992).
- [5] A. Biral and C. Callan, preprint PUPT-1320, hep-th/9205089 (1992).
- [6] S.P. de Alwis, preprint COLO-HEP-280, hep@xxx9205069 (1992); preprint COLO-HEP-284, hep@xxx9206020 (1992).
- [7] A. Strominger, preprint UCSBTH-92-18, hep-th/9205028 (1992).
- [8] K. Hamada, preprint UT-Komaba 92-7 (1992).
- [9] J. Soda, Elhime preprint (1992).
- [10] W. Fischler, D. Morgan and J. Polchinski, Phys. Rev. D42 (1990) 4042.
- [11] A. Tomimatsu, Phys. Lett. B289 (1992) 283.
- [12] V. P. Frolov, Phys. Rev. D46 (1992) 5383.

Quantum Gravity and Black Hole[†]

KEN-JI HAMADA AND ASATO TSUCHIYA

*Institute of Physics, University of Tokyo
Komaba, Meguro-ku, Tokyo 153, Japan*

Abstract

The quantum theory of the spherically symmetric gravity in 3+1 dimensions is investigated. The functional measures are explicitly evaluated and the physical state conditions are derived by using the technique developed in two dimensional quantum gravity. Then the new features which are not seen in ADM formalism come out. If $\kappa_s > 0$, where $\kappa_s = (N - 27)/12\pi$ and N is the number of matter fields, a singularity appears, while for $\kappa_s < 0$ the singularity disappears. The quantum dynamics of black hole seems to be changed by the sign of κ_s .

1. Introduction

Since the original work of Hawking,^[1] many authors study the quantum dynamics of black holes. Almost all of works are done within the semi-classical approximation.^[2,3,4,5] In this talk we discuss how the quantum gravity will influence the dynamics of black holes.^[6,7] As a model of gravity we consider the spherically symmetric gravity in 3+1 dimensions.

As a quantization method of gravitation, Arnowitt-Deser-Misner (ADM) formalism is well-known. This method, however, has some serious problems, which are the issues of measures and orderings. Here we explicitly evaluate the contributions from measures. Following the procedure developed in two dimensional gravity we determine the measures in conformal gauge. From the gauge fixed theory the physical state conditions are derived. Then the new features which are not seen in ADM formalism appear.

[†] Talk given by K.H. at "Workshop on General Relativity and Gravity", Waseda, Tokyo, Japan, 18-20 Jan 1993.

The spherically symmetric gravity in 3+1 dimensions is defined by reducing the Einstein-Hilbert action to the two dimensional one as

$$I_{EH} = \frac{1}{16\pi G} \int d^4x \sqrt{-g^{(4)}} R^{(4)} = \frac{1}{4} \int d^2x \sqrt{-g} \left(R_g \varphi^2 + 2g^{\alpha\beta} \partial_\alpha \varphi \partial_\beta \varphi + \frac{2}{G} \right). \quad (1)$$

The fields $g_{\alpha\beta}$ and φ are defined through the four dimensional metric $(ds^{(4)})^2 = g_{\alpha\beta} dx^\alpha dx^\beta + G\varphi^2 d\Omega^2$, where $\alpha, \beta = 0, 1$ and $d\Omega^2$ is the volume element of a unit 2-sphere. G is the gravitational constant. In the following we set $G = 1$. We couple N two dimensional conformal matter fields

$$I_M(g, f) = -\frac{1}{2} \sum_{j=1}^N \int d^2x \sqrt{-g} g^{\alpha\beta} \partial_\alpha f_j \partial_\beta f_j. \quad (2)$$

Some classical solutions of this system are known. For $f = 0$ the Schwarzschild geometry is well-known. The gravitational collapse geometry is given by^[6]

$$ds^2 = -\left(1 - \frac{2M\vartheta(\bar{v})}{r}\right) \frac{\bar{u}}{\bar{u} + 4M\vartheta(\bar{v})} d\bar{u} d\bar{v}, \quad \varphi = r, \quad (3)$$

where $ds^2 = g_{\alpha\beta} dx^\alpha dx^\beta$ and the coordinate (\bar{u}, \bar{v}) is defined through the relations, $d\bar{u} = du^*(\bar{u} + 4M)/\bar{u}$, $u^* = v - 2r^*$, $r^* = r + 2M \log(\frac{r}{2M} - 1)$ and $\bar{v} = v$. This geometry is derived by sewing the flat space time and the Schwarzschild black hole geometry along the shock wave line $\bar{v} = 0$, where the infalling matter flux is given by $T_{\bar{v}\bar{v}}^f = M\delta(\bar{v})$. In (\bar{u}, \bar{v}) coordinate the horizon locates at $\bar{u} = -4M$.

2. Quantization of Spherically Symmetric Gravity

Let us define the quantum theory of the spherically symmetric gravity. The partition function is expressed in terms of the path integral over the two dimensional metric $g_{\alpha\beta}$, the scale field φ and the matter fields f as

$$Z = \int \frac{D_g(g) D_g(\varphi) D_g(f)}{\text{Vol}(\text{Diff.})} e^{iI_{SSG}(g, \varphi, f)}, \quad I_{SSG} = I_{EH} + I_M, \quad (4)$$

where $\text{Vol}(\text{Diff.})$ is the gauge volume of diffeomorphism. The functional measures are defined

by the following norms

$$\begin{aligned}
\langle \delta g, \delta g \rangle_g &= \int d^2x \sqrt{-g} g^{\alpha\beta} g^{\gamma\delta} (\delta g_{\alpha\gamma} \delta g_{\beta\delta} + \delta g_{\alpha\beta} \delta g_{\gamma\delta}) , \\
\langle \delta \varphi, \delta \varphi \rangle_g &= \int d^2x \sqrt{-g} \delta \varphi \delta \varphi , \\
\langle \delta f_j, \delta f_j \rangle_g &= \int d^2x \sqrt{-g} \delta f_j \delta f_j \quad (j = 1, \dots, N) .
\end{aligned} \tag{5}$$

The measures explicitly depend on the dynamical field g . Therefore we must extract its contributions from the measures. They are evaluated by using the procedure of David-Distler-Kawai (DDK)^[9] in conformal gauge $g = e^{2\rho} \hat{g}$, where \hat{g} is the background metric. The final expression is given by

$$Z = \int D_{\hat{g}}(\Phi) e^{i\hat{I}(\hat{g}, \Phi)} , \tag{6}$$

where Φ denotes the fields ρ, φ, f and the reparametrization ghosts b and c . The gauge-fixed action \hat{I} is

$$\begin{aligned}
\hat{I} &= \kappa_s S_L(\rho, \hat{g}) + I_{EH}(e^{2\rho} \hat{g}, \varphi) + I_M(\hat{g}, f) + I_{gh}(\hat{g}, b, c) \\
&= \frac{1}{2} \int d^2x \sqrt{-\hat{g}} \left[\hat{g}^{\alpha\beta} \partial_\alpha \varphi \partial_\beta \varphi + 2 \hat{g}^{\alpha\beta} \varphi \partial_\alpha \varphi \partial_\beta \rho + \frac{1}{2} \hat{R} \varphi^2 + e^{2\rho} \right. \\
&\quad \left. + \kappa_s (\hat{g}^{\alpha\beta} \partial_\alpha \rho \partial_\beta \rho + \hat{R} \rho) - \sum_{j=1}^N \hat{g}^{\alpha\beta} \partial_\alpha f_j \partial_\beta f_j \right] + I_{gh}(\hat{g}, b, c)
\end{aligned} \tag{7}$$

with

$$\kappa_s = \frac{1}{12\pi} (1 + c_\varphi + N - 26) = \frac{N - 27}{12\pi} , \tag{8}$$

where $S_L(\rho, \hat{g})$ is the Liouville action defined by

$$S_L(\rho, \hat{g}) = \frac{1}{2} \int d^2x \sqrt{-\hat{g}} (\hat{g}^{\alpha\beta} \partial_\alpha \rho \partial_\beta \rho + \hat{R} \rho) . \tag{9}$$

The value of κ_s is given by setting $\xi = 1/2$ in ref.6. The functional measure of the Liouville field ρ is defined by the norm on \hat{g} as

$$\langle \delta \rho, \delta \rho \rangle_{\hat{g}} = \int d^2x \sqrt{-\hat{g}} \delta \rho \delta \rho \tag{10}$$

and also the measures for φ and f is defined by the norms (5) on \hat{g} instead of g .

The background metric \hat{g} is very artificial so that the theory should be independent of how to choose it. Really it is proved that the partition function is invariant under the conformal change of the background metric, or $Z(e^{2\sigma}\hat{g}) = Z(\hat{g})$, where σ is an arbitrary local function. This means that the theory is considered as a kind of conformal field theory defined on \hat{g} . The Virasoro algebra without central extension should be realized.* The physical state conditions are derived from the demand that the theory should be independent of how to choose the background metric,

$$\left. \frac{\delta Z}{\delta \hat{g}^{\alpha\beta}} \right|_{\hat{g}=\eta} = 0, \quad \text{or} \quad \langle \hat{T}_{\alpha\beta} \rangle = 0, \quad (11)$$

where $\eta_{\alpha\beta} = (-1, 1)$ and the energy-momentum tensor is defined by $\hat{T}_{\alpha\beta} = -\frac{2}{\sqrt{-\hat{g}}} \frac{\delta \hat{I}}{\delta \hat{g}^{\alpha\beta}}|_{\hat{g}=\eta}$.

Since the Liouville field ρ is transformed as $\rho'(x') = \rho(x) - \gamma(x)$ for the conformal coordinate transformation $x^{\pm'} = x^{\pm'}(x^{\pm})$, where $\gamma(x) = \frac{1}{2} \log |\frac{\partial x'}{\partial x}|^2$, $|x|^2 = x^+ x^-$ and $x^{\pm} = x^0 \pm x^1$, the energy-momentum tensor $\hat{T}_{\alpha\beta}$ is transformed as[‡]

$$\hat{T}'_{\pm\pm}(x') = \left(\frac{\partial x^{\pm}}{\partial x^{\pm'}} \right)^2 (\hat{T}_{\pm\pm}(x) + \kappa_s t_{\pm}(x)), \quad \hat{T}'_{+-}(x') = \left| \frac{\partial x}{\partial x'} \right|^2 \hat{T}_{+-}(x), \quad (12)$$

where $t_{\pm}(x)$ is the Schwarzian derivative $t_{\pm}(x) = (\partial\gamma(x)/\partial x^{\pm})^2 - \partial^2\gamma(x)/\partial x^{\pm 2}$. t_{\pm} is determined by the boundary condition that the coordinate system which is joined to the Minkowski space time (asymptotically) is considered as the coordinate system with $t_{\pm} = 0$.

3. Black hole dynamics

To derive the black hole dynamics we must solve the physical state conditions (11). But it is a very difficult problem so that we take an approximation. The original actions (1) and (2) are the order of $1/\hbar$, while the Liouville part of \hat{I} is the zeroth order of \hbar . However, if

* Note that in this case the theory does not reduce to the free-like theory. So it is quite different from the usual conformal field theory.

‡ More explicitly, $\hat{T}_{\alpha\beta}$ is transformed as

$$\hat{T}'_{\pm\pm}(x') = \left(\frac{\partial x^{\pm}}{\partial x^{\pm'}} \right)^2 (\hat{T}_{\pm\pm}(x) + \kappa_s t_{\pm}(x)) + \frac{c_{tot}}{12\pi} \left(\frac{\partial x^{\pm}}{\partial x^{\pm'}} \right)^2 t_{\pm}(x)$$

with $c_{tot} = 1 - 12\pi\kappa_s + c_{\varphi} + N - 26 = 0$. Note that if $\hat{T}'_{\pm\pm}(x')$ satisfies the usual form of the Virasoro algebra with central charge $c_{tot} = 0$, then in x coordinate the combination $\hat{T}_{\pm\pm}(x) + \kappa_s t_{\pm}(x)$, not $\hat{T}_{\pm\pm}(x)$ itself, just satisfies the same form of the Virasoro algebra. The importance of t_{\pm} in quantum gravity is stressed in ref.10.

$|\kappa_s|$ is large enough, then it is meaningful to consider the “classical” dynamics of \hat{I} . This is nothing but the semi-classical approximation, which is valid only in the case of $M \gg 1$ and $|\kappa_s| \gg 1$. The classical dynamics of \hat{I} is ruled by the equations $\hat{T}_{\alpha\beta} = 0$ and the φ field equation of motion. Then we set $\hat{T}_{\alpha\beta}^{gh} = 0$ because the ghost flux should vanish in the flat space time.

The gravitational collapse geometry is given as a solution with non-zero infalling matter flux. Giving the flux $\hat{T}_{\bar{v}\bar{v}}^f = M\delta(\bar{v})$, we can get the exact solution along the shock wave line $\bar{v} = 0$,

$$\partial_{\bar{v}}\varphi(\bar{v} = 0, \bar{u}) = \frac{1}{2} \left(1 - \frac{4M}{\sqrt{\bar{u}^2 - 4\kappa_s}} \right), \quad \varphi(\bar{v} = 0, \bar{u}) = r = -\frac{1}{2}\bar{u}. \quad (13)$$

The (apparent) horizon, which is defined by the equation $\partial_{\bar{r}}\varphi = 0$,^[11] locates at

$$\bar{u} = -4M\sqrt{1 + \frac{\kappa_s}{4M^2}}, \quad \bar{v} = 0. \quad (14)$$

If $\kappa_s > 0$, the location of the horizon initially shifts to the outside of the classical horizon $\bar{u} = -4M$ by quantum effects. Then the black hole evaporates and the horizon approaches to the singularity asymptotically. The location of the singularity is determined by the equation $\varphi^2 = \kappa_s$ (at $\bar{v} = 0$, it is $\bar{u} = -2\sqrt{\kappa_s}$). Note that at the singularity the curvature is singular, but the metric is finite. If $\kappa_s < 0$, the singularity disappears. The location of the horizon initially shifts to the inside of the classical horizon. If the effective mass of the black hole is defined by $M_{BH} = \frac{1}{2}\varphi|_{\text{horizon}}$, this means that the initial mass of the black hole is less than the infalling matter flux M . After the black hole is formed, the positive flux comes in through the horizon and the black hole mass increases. It seems that the horizon approaches to the classical horizon asymptotically and becomes stable.

For $\kappa_s > 0$, the classically forbidden region $\kappa_s > \varphi^2 > 0$ called “Lionville region” extends behind the singularity. To understand this region we must go back to the full quantum gravity. In the canonical quantization the physical state conditions are written as

$$\hat{T}_{00}\Psi = \hat{T}_{01}\Psi = 0, \quad (15)$$

where Ψ is a physical state and

$$\begin{aligned}\hat{T}_{00} = & \frac{1}{\varphi^2 - \kappa_s} \left(\frac{1}{2} \Pi_\rho^2 - \varphi \Pi_\varphi \Pi_\rho + \frac{\kappa_s}{2} \Pi_\varphi^2 \right) + \varphi \varphi'' + \frac{1}{2} \varphi'^2 - \varphi \varphi' \rho' - \frac{1}{2} \varphi^2 \rho^2 \\ & - \frac{\kappa_s}{2} (\rho'^2 - 2\rho'') + \frac{1}{2} \sum_{j=1}^N (\Pi_{f_j}^2 + f_j'^2) , \\ \hat{T}_{01} = & \rho' \Pi_\rho - \Pi'_\rho + \varphi' \Pi_\varphi + \sum_{j=1}^N \Pi_{f_j} f_j' .\end{aligned}\tag{16}$$

These correspond to the Hamiltonian and the momentum constraints. The conjugate momentums for ρ, φ and f_j are defined by

$$\Pi_\rho = -\kappa_s \dot{\rho} - \varphi \dot{\varphi} , \quad \Pi_\varphi = -\dot{\varphi} - \varphi \dot{\rho} , \quad \Pi_{f_j} = \dot{f}_j .\tag{17}$$

The notable point is the factor $(\varphi^2 - \kappa_s)^{-1}$ in front of the kinetic term of the Hamiltonian constraint, which does not appear in ADM formalism.⁽¹¹⁾ The region $\varphi^2 > \kappa_s$ is classically allowed, whereas the Liouville region $\kappa_s > \varphi^2 > 0$ is the classically forbidden region where the sign of the kinetic term changes. There may be some possibility of gravitational tunnelings through this region.

The problem of the information loss seems to come out in the case of $\kappa_s > 0$. Then the black hole evaporates and the information seems to be lost. However in this case the Liouville region extends behind the singularity. So it appears that there is a possibility that the informations run away through this region by gravitational tunneling. On the other hand, if $\kappa_s \leq 0$, the Liouville region disappears. But the black hole seems to be stable. In this case it appears that the problem of the information loss does not exist.

4. Discussions

The quantum model of spherically symmetric gravity discussed in this talk has some problems. Here we adopt the conformal matter described by the action (2). Strictly speaking, however, we should consider the action such as $I_M = -\frac{1}{2} \int d^2x \sqrt{-g} \varphi^2 g^{\alpha\beta} \partial_\alpha f \partial_\beta f$, which is derived by reducing the four dimensional action to the two dimensional one. Ignoring φ^2 -factor corresponds to ignoring the potential which appears when we rewrite the d'Alembertian in terms of the spherical coordinate. The black hole dynamics is determined by the behavior near the horizon so that it seems that this simplification does not change the nature of dynamics.

The other problem is in the definitions of measures. As the actions are derived from the four dimensional ones, the two dimensional measures also should be derived from the four dimensional one

$$<\delta g^{(4)}, \delta g^{(4)}>_{g^{(4)}} = \int d^4x \sqrt{-g^{(4)}} g^{(4)ab} g^{(4)cd} (\delta g_{ac}^{(4)} \delta g_{bd}^{(4)} + \delta g_{ab}^{(4)} \delta g_{cd}^{(4)}) . \quad (18)$$

From this definition we get

$$\begin{aligned} <\delta g, \delta g>_g = \int d^2x \sqrt{-g} \varphi^2 g^{\alpha\beta} g^{\gamma\delta} (\delta g_{\alpha\gamma} \delta g_{\beta\delta} + \delta g_{\alpha\delta} \delta g_{\beta\gamma}) , \\ <\delta\varphi, \delta\varphi>_g = \int d^2x \sqrt{-g} \delta\varphi \delta\varphi . \end{aligned} \quad (19)$$

And also for the matter fields,

$$<\delta f_j, \delta f_j>_g = \int d^2x \sqrt{-g} \varphi^2 \delta f_j \delta f_j \quad (j = 1, \dots, N) . \quad (20)$$

The difference between (5) and (19-20) is apparent. The factor φ^2 in the measures of g and f prevents us from quantizing the spherically symmetric gravity exactly. We expect that this factor also does not change the nature of quantum dynamics drastically.

REFERENCES

1. S. Hawking, Comm. Math. Phys. **43** (1975) 199; Phys. Rev. **D14** (1976) 2460.
2. P. Davies, S. Fulling and W. Unruh, Phys. Rev. **D13** (1976) 2720.
3. C. Callan, S. Giddings, J. Harvey and A. Strominger, Phys. Rev. **D45** (1992) R1005.
4. J. Russo, L. Susskind and L. Thorlacius, Phys. Lett. **B292** (1992) 13; T. Banks, A. Dabholkar, M. Douglas and M. O'Loughlin, Phys. Rev. **D45** (1992) 3607.
5. S. Hawking, Phys. Rev. Lett. **69** (1992) 406; L. Susskind and L. Thorlacius, Nucl. Phys. **B382** (1992) 123; B. Birnir, S. Giddings, J. Harvey and A. Strominger, Phys. Rev. **D46** (1992) 638.
6. K. Hamada, *Quantum Theory of Dilaton Gravity in 1+1 Dimensions*, preprint UT-Komaba 92-7, to appear in Phys. Lett. B.

7. K. Hamada and A. Tsuchiya, *Quantum Gravity and Black Hole Dynamics in 1+1 Dimensions*, preprint UT-Komaba 92-14, to appear in Int. J. Mod. Phys. A.
8. W. Hiscock, Phys. Rev. D **23** (1981) 2813.
9. J. Distler and H. Kawai, Nucl. Phys. B **321** (1989) 509; F. David, Mod. Phys. Lett. A **3** (1988) 1651.
10. N. Seiberg, Prog. Theor. Phys. Suppl. **102** (1990) 319.
11. P. Thoni, B. Isaak and P. Hajicek, Phys. Rev. D **30** (1984) 1168; P. Hajicek, Phys. Rev. D **30** (1984) 1178.

One-loop counterterms in 2d dilaton-Maxwell quantum gravity

E. ELIZALDE¹

*Department E.C.M., Faculty of Physics, University of Barcelona,
Diagonal 647, 08028 Barcelona, Spain*

S. NAFTULIN

*Institute for Single Crystals, 60 Lenin Ave., 310141 Kharkov, Ukraine
and*

S.D. ODINTSOV²

*Department of Physics, Faculty of Science, Hiroshima University,
Higashi-Hiroshima 724, Japan*

Abstract

The renormalization structure of two-dimensional quantum gravity is investigated in a covariant gauge. One-loop divergences of the effective action are calculated. All the surface divergent terms are taken into account thus completing previous one-loop calculations of the theory. It is shown that the on-shell effective action contains only surface divergences. The off-shell renormalizability of the theory is discussed and classes of renormalizable dilaton and Maxwell potentials are found.

¹E-mail address: eli @ ebubecm1.bitnet

²On sabbatical leave from Tomsk Pedagogical Institute, 634041 Tomsk, Russia. E-mail address: odintsov @ theo.phys.sci.hiroshima-u.ac.jp

The current activity in the study of the two-dimensional ($2d$) quantum gravity is motivated by the following (main) reasons. First of all, it is extremely difficult to study the physics of black holes and of the early universe in the ambitious frames of the modern models of four-dimensional quantum gravity. Solvable toy models like the $2d$ gravity simplify the considerations and hence can help in the study of more realistic situations. From another point of view, the $2d$ quantum gravity is interesting on its own as a good laboratory for developing formal methods of the quantum field theory. Moreover, a connection with very fundamental physics may be developed because some models of the $2d$ gravity are string-inspired models.

Recently, an investigation of the renormalization structure of the $2d$ dilaton gravity has been started [1-4]. The one-loop counterterms in covariant gauges have been calculated [1-4] and it has been shown that the theory may be renormalizable off-shell for some choices of the dilatonic potential (in particular, for the Liouville potential). The only one-loop divergences on shell are surface terms [1].

In the present paper we address the question of the calculation of the one-loop counterterms which appear in the dilaton-Maxwell $2d$ quantum gravity as given by the following action³ [5,6]

$$S = - \int d^2x \sqrt{g} \left[\frac{1}{2} g^{\mu\nu} \partial_\mu \varphi \partial_\nu \varphi + c_1 R \varphi + V(\varphi) + \frac{1}{4} f(\varphi) g^{\mu\alpha} g^{\nu\beta} F_{\mu\nu} F_{\alpha\beta} \right], \quad (1)$$

where $F_{\mu\nu} = \partial_\mu A_\nu - \partial_\nu A_\mu$ is the electromagnetic field strength, φ is the dilaton, $V(\varphi)$ is a general dilatonic potential and $f(\varphi)$ is an arbitrary positive valued function. Notice that for some choices of f and V this action corresponds to the heterotic string effective action. The theory admits black hole solutions. Properties of the $2d$ black holes associated with different variants of the theory (1) were studied in Refs.[5,9,10] along the same lines as developed for the pure dilaton gravity (without the Maxwell term) [7,8]. The model given by (1) is also connected (via some compactification) with the four-dimensional Einstein-Maxwell theory which admits charged black hole solutions [14].

The one-loop counterterms for the theory with the action (1) have been already calculated in Refs.[6,9] — but *not* taking into account the contributions of the divergent surface terms. In this paper we generalize those calculations in order to take into account all such terms in the effective action. It is well known that they are relevant, e.g. in the context of the Casimir effect calculations (see, for example, Ref.[15]).

³For a higher derivative generalization, see Ref.[12]

The classical field equations corresponding to (1) are

$$\begin{aligned} \nabla_\mu (f F^{\mu\nu}) &= 0, \quad -\Delta\varphi + c_1 R + V'(\varphi) + \frac{1}{4} f'(\varphi) F_{\mu\nu}^2 = 0, \\ -\frac{1}{2}(\nabla^\alpha\varphi)(\nabla^\beta\varphi) + \frac{1}{4}g^{\alpha\beta}\nabla^\mu\varphi\nabla_\mu\varphi + c_1(\nabla^\alpha\nabla^\beta - g^{\alpha\beta}\Delta)\varphi \\ + \frac{1}{2}g^{\alpha\beta}V + \frac{1}{8}g^{\alpha\beta}fF_{\mu\nu}^2 - \frac{1}{2}fF_\mu^\alpha F^{\beta\mu} &= 0. \end{aligned} \quad (2)$$

We will use Eqs.(2) below, in the analysis of the divergences of the theory.

The background field method is employed. The fields are split into their quantum and background parts,

$$\varphi \longrightarrow \bar{\varphi} = \phi + \varphi, \quad A_\mu \longrightarrow \bar{A}_\mu = A_\mu + Q_\mu, \quad g_{\mu\nu} \longrightarrow \bar{g}_{\mu\nu} = g_{\mu\nu} + h_{\mu\nu}, \quad (3)$$

where the second terms φ , Q_μ and $h_{\mu\nu}$ are the quantum fields. In what follows we shall use the dynamical variables $h = g^{\mu\nu}h_{\mu\nu}$ and $\bar{h}_{\mu\nu} = h_{\mu\nu} - \frac{1}{2}hg_{\mu\nu}$ rather than $h_{\mu\nu}$.

In order to make contact with Ref.[4] where the surface divergences in the absence of the Maxwell term are calculated, the following term is added to the initial action

$$\Delta S = c_1 \xi \int d^2x \sqrt{g} \left[\phi \bar{h}_{\mu\nu} (R^{\mu\nu} - \frac{1}{2}Rg^{\mu\nu}) \right], \quad (4)$$

where ξ is an arbitrary parameter. Owing to the $2d$ identity $R_{\mu\nu} - \frac{1}{2}Rg_{\mu\nu} = 0$, the expression (4) is obviously zero. (Notice that ΔS is very similar to a kind of Wess-Zumino topological term. The observation that the parameter ξ only appears in the surface on-shell counterterms and is in fact related to the trace anomaly, hints in this direction.) However, the second variation of (4) may be important for the removal of non-minimal contributions from the differential operator corresponding to $S^{(2)}$. A possible interpretation of this term is given in [4].

To fix both the abelian and general covariant invariances we use the following covariant gauge conditions

$$\begin{aligned} S_{GF} &= -\frac{1}{2} \int d^2x \left\{ \chi^A C_{AB} \chi^B \right\}, \\ \chi^* &= -\nabla^\nu Q_\nu, \quad \chi^\mu = -\nabla^\nu \bar{h}_\nu^\mu - [c_1/(2\gamma\phi)]\nabla^\mu\varphi, \quad \gamma = c_1(\xi - 1)/2. \end{aligned} \quad (5)$$

The index $A = \{*, \mu\}$ runs over the three-dimensional space of gauge transformations. The most convenient form for the matrix C_{AB} is

$$C_{AB} = \sqrt{g} \text{diag} (f, 2\gamma\phi g_{\mu\nu}).$$

If the identity (4) is absent then $\xi = 0$ and $\gamma = -c_1/2$.

As is well known, the divergences of the one-loop effective action are given by

$$\Gamma_{div} = \frac{i}{2} \text{Tr} \ln \widehat{\mathcal{H}} - i \text{Tr} \ln \widehat{\mathcal{M}}_{gh} \Big|_{div}, \quad (6)$$

where $\widehat{\mathcal{M}}_{gh}$ is the ghost operator corresponding to S_{GF} (5) and the second variation of the action defines the operator $\widehat{\mathcal{H}}$:

$$\frac{1}{2} \varphi^i \widehat{\mathcal{H}}_{ij} \varphi^j = S^{(2)} + \Delta S^{(2)} + S_{GF}. \quad (7)$$

Here φ^i stands for the set of the quantum fields, $\{Q_\mu, \varphi, h, \bar{h}_{\mu\nu}\}$. Making use of the background vs quantum fields splitting (3) one easily finds that

$$\widehat{\mathcal{H}} = -\widehat{K} \Delta + \widehat{L}^\lambda \nabla_\lambda + \widehat{\mathcal{M}}, \quad (8)$$

where

$$\widehat{K}^{-1} = \begin{pmatrix} \frac{1}{f} g_{\mu\alpha} & 0 & 0 & 0 \\ 0 & 0 & \frac{2}{c_1} & 0 \\ 0 & \frac{2}{c_1} & -\left(\frac{4}{c_1^2} + \frac{2}{\gamma\phi}\right) & 0 \\ 0 & 0 & 0 & \frac{1}{\gamma\phi} \widehat{P}_{\mu\nu, \alpha\beta} \end{pmatrix}, \quad (9)$$

the projector $\widehat{P}^{\mu\nu, \alpha\beta}$ being $\delta^{\mu\nu, \alpha\beta} - \frac{1}{2} g^{\mu\nu} g^{\alpha\beta}$, and

$$\begin{aligned} \widehat{L}_{11}^\lambda &= f'(\nabla^\alpha \phi) g^{\mu\lambda} - f'(\nabla^\mu \phi) g^{\alpha\lambda} - f'(\nabla^\lambda \phi) g^{\mu\alpha}, \\ \widehat{L}_{12}^\lambda &= -\widehat{L}_{21}^\lambda = f' F^{\mu\lambda}, \quad \widehat{L}_{13}^\lambda = -\widehat{L}_{31}^\lambda = -\frac{1}{2} f F^{\mu\lambda}, \\ \widehat{L}_{14}^\lambda &= -\widehat{L}_{41}^\lambda = f F_\omega^\lambda \widehat{P}^{\alpha\beta, \mu\omega} - f F_\omega^\mu \widehat{P}^{\alpha\beta, \lambda\omega}, \quad \widehat{L}_{22}^\lambda = \frac{c_1^2}{2\gamma\phi^2} (\nabla^\lambda \phi), \\ \widehat{L}_{23}^\lambda &= \widehat{L}_{32}^\lambda = 0, \quad \widehat{L}_{24}^\lambda = -\widehat{L}_{42}^\lambda = (\nabla_\omega \phi) \widehat{P}^{\alpha\beta, \lambda\omega}, \quad \widehat{L}_{33}^\lambda = -\frac{c_1}{2} (\nabla^\lambda \phi), \\ \widehat{L}_{34}^\lambda &= -\widehat{L}_{43}^\lambda = \frac{c_1}{2} (\nabla_\omega \phi) \widehat{P}^{\alpha\beta, \lambda\omega}, \\ \widehat{L}_{44}^\lambda &= \left(\frac{c_1}{2} - \gamma\right) (\nabla^\omega \phi) (\widehat{P}_{\omega\kappa}^{\mu\nu} \widehat{P}^{\alpha\beta, \lambda\kappa} - \widehat{P}^{\mu\nu, \lambda\kappa} \widehat{P}_{\omega\kappa}^{\alpha\beta}) - \frac{3c_1}{2} (\nabla^\lambda \phi) \widehat{P}^{\mu\nu, \alpha\beta}, \\ \widehat{M}_{11} &= \frac{1}{2} f R g^{\mu\alpha}, \quad \widehat{M}_{23} = \widehat{M}_{32} = \frac{1}{2} V' - \frac{1}{8} f' F_{\mu\nu}^2, \quad \widehat{M}_{33} = \frac{1}{8} f F_{\mu\nu}^2, \\ \widehat{M}_{44} &= \left(\gamma - \frac{3}{2} c_1\right) (\nabla_\lambda \nabla^\omega \phi) \widehat{P}^{\mu\nu, \lambda\kappa} \widehat{P}_{\omega\kappa}^{\alpha\beta} + (\nabla_\lambda \phi) (\nabla^\omega \phi) \widehat{P}^{\mu\nu, \lambda\kappa} \widehat{P}_{\omega\kappa}^{\alpha\beta} \\ &\quad - \frac{1}{4} (\nabla^\lambda \phi) (\nabla_\lambda \phi) \widehat{P}^{\mu\nu, \alpha\beta} + \gamma \phi R \widehat{P}^{\mu\nu, \alpha\beta} - \frac{1}{2} V \widehat{P}^{\mu\nu, \alpha\beta} \\ &\quad - \frac{1}{8} f F_{\mu\nu}^2 \widehat{P}^{\mu\nu, \alpha\beta} + f F_{\omega\lambda} F^{\rho\lambda} \widehat{P}^{\mu\nu, \omega\kappa} \widehat{P}_{\rho\kappa}^{\alpha\beta} + \frac{1}{2} f F^{\omega\kappa} F^{\lambda\rho} \widehat{P}_{\omega\lambda}^{\mu\nu} \widehat{P}_{\kappa\rho}^{\alpha\beta}. \end{aligned} \quad (10)$$

Now we can start the computation of the contribution of the gravitational-Maxwell part to the effective action divergences. First of all, one easily sees that

$$\text{Tr} \ln \widehat{\mathcal{H}}|_{\text{div}} = \text{Tr} \ln (-\widehat{K}^{-1}\widehat{\mathcal{H}})|_{\text{div}}, \quad (11)$$

because $\text{Tr} \ln(-\widehat{K})$ gives a contribution proportional to $\delta(0)$ which is zero in the dimensional regularization. However, in order to apply the standard algorithm

$$\begin{aligned} \Gamma_{\text{div}} &= \frac{i}{2} \text{Tr} \ln \widehat{\mathcal{H}}|_{\text{div}} = \frac{i}{2} \text{Tr} \ln (\widehat{1}\Delta + 2\widehat{E}^\lambda \nabla_\lambda + \widehat{\Pi})|_{\text{div}} \\ &= \frac{1}{2\varepsilon} \int d^2x \sqrt{g} \text{Tr} \left(\widehat{\Pi} + \frac{R}{6} \widehat{1} - \nabla^\lambda \widehat{E}_\lambda - \widehat{E}^\lambda \widehat{E}_\lambda \right), \end{aligned} \quad (12)$$

where $\varepsilon = 2\pi(n-2)$, one should take care that the operator $\widehat{\mathcal{H}}$ be hermitean, properly symmetrized, etc. Imprudent integrations by parts actually change the matrix elements which may lead to the breakdown of these compulsory properties.

In order to recover an operator $\widehat{\mathcal{H}}$ with the required properties the doubling procedure of 't Hooft and Veltman [13] is very useful. A clear explanation on how to do this in the present context can be found in Refs. [2-4] (for more details, see [13]). In fact, using this method amounts to the following redefinitions of the operator $\widehat{\mathcal{H}}$ given in (8):

$$\begin{aligned} \widehat{L}_\lambda &\longrightarrow \widehat{L}'_\lambda = \frac{1}{2}(\widehat{L}_\lambda - \widehat{L}_\lambda^T) - \nabla_\lambda \widehat{K}, \\ \widehat{\mathcal{M}} &\longrightarrow \widehat{\mathcal{M}}' = \frac{1}{2}(\widehat{\mathcal{M}} + \widehat{\mathcal{M}}^T) - \frac{1}{2} \nabla^\lambda \widehat{L}_\lambda^T - \frac{1}{2} \Delta \widehat{K}. \end{aligned} \quad (13)$$

Now, introducing the notation $\widehat{E}^\lambda = -\frac{1}{2}\widehat{K}^{-1}\widehat{L}'^\lambda$ and $\widehat{\Pi} = -\widehat{K}^{-1}\widehat{\mathcal{M}}'$, we have the operator $\widehat{\mathcal{H}}$ of the proper form and thus we can apply the algorithm (13).

The explicit form of the operators \widehat{E}^λ and $\widehat{\Pi}$ can be found from (11) and (13) to be the following

$$\begin{aligned} (\widehat{E}^\lambda)_1^1 &= \frac{f'}{2f} [(\nabla^\lambda \phi)g_\rho^\alpha - (\nabla^\alpha \phi)g_\rho^\lambda + (\nabla_\rho \phi)g^{\alpha\lambda}], \quad (\widehat{E}^\lambda)_2^1 = -\frac{f'}{2f} F_\rho^\lambda, \\ (\widehat{E}^\lambda)_3^1 &= \frac{1}{4} F_\rho^\lambda, \quad (\widehat{E}^\lambda)_4^1 = \frac{1}{2} F_{\rho\omega} \widehat{P}^{\alpha\beta, \lambda\omega} - \frac{1}{2} F^{\lambda\omega} \widehat{P}_{\rho\omega}^{\alpha\beta}, \\ (\widehat{E}^\lambda)_1^2 &= -\frac{f}{2c_1} F^{\alpha\lambda}, \quad (\widehat{E}^\lambda)_2^2 = (\widehat{E}^\lambda)_3^2 = 0, \quad (\widehat{E}^\lambda)_4^2 = -\frac{1}{2} (\nabla_\omega \phi) \widehat{P}^{\alpha\beta, \lambda\omega}, \\ (\widehat{E}^\lambda)_1^3 &= \left(\frac{f}{c_1^2} + \frac{f}{2\gamma\phi} + \frac{f'}{c_1} \right) F^{\alpha\lambda}, \quad (\widehat{E}^\lambda)_2^3 = -\frac{c_1}{2\gamma\phi^2} (\nabla^\lambda \phi), \quad (\widehat{E}^\lambda)_3^3 = 0, \\ (\widehat{E}^\lambda)_4^3 &= \frac{c_1}{2\gamma\phi} (\nabla_\omega \phi) \widehat{P}^{\alpha\beta, \lambda\omega}, \quad (\widehat{E}^\lambda)_1^4 = \frac{f}{2\gamma\phi} (F_\omega^\lambda \widehat{P}_{\rho\sigma}^{\alpha\omega} - F_\omega^\alpha \widehat{P}_{\rho\sigma}^{\lambda\omega}), \\ (\widehat{E}^\lambda)_2^4 &= \frac{1}{2\gamma\phi} (\nabla_\omega \phi) \widehat{P}_{\rho\sigma}^{\lambda\omega}, \quad (\widehat{E}^\lambda)_3^4 = \frac{c_1}{4\gamma\phi} (\nabla_\omega \phi) \widehat{P}_{\rho\sigma}^{\lambda\omega}, \end{aligned} \quad (14)$$

$$\begin{aligned}
(\hat{E}^\lambda)_4^4 &= \left(\frac{c_1}{4\gamma\phi} - \frac{1}{2\phi} \right) (\nabla^\omega \phi) \left(\hat{P}_{\omega\kappa}^{\alpha\beta} \hat{P}_{\rho\sigma}^{\lambda\kappa} - \hat{P}_{\rho\sigma,\omega\kappa} \hat{P}^{\alpha\beta,\lambda\kappa} \right) + \frac{1}{2\phi} (\nabla^\lambda \phi) \hat{P}_{\rho\sigma}^{\alpha\beta}; \\
\hat{\Pi}_1^1 &= -\frac{1}{2} R g_\rho^\rho, \quad \hat{\Pi}_2^2 = -\frac{1}{c_1} V' + \frac{f'}{4c_1} F_{\mu\nu}^2, \\
\hat{\Pi}_3^3 &= -\frac{1}{c_1} V' + \left(\frac{f}{2c_1^2} + \frac{f}{4\gamma\phi} + \frac{f'}{4c_1} \right) F_{\mu\nu}^2 + \left(\frac{1}{c_1} + \frac{c_1}{2\gamma\phi} \right) (\Delta\phi), \\
\hat{\Pi}_4^4 &= \left[\left(\frac{3c_1}{2\gamma\phi} - \frac{1}{\phi} \right) (\nabla_\lambda \nabla^\omega \phi) - \frac{1}{\gamma\phi} (\nabla_\lambda \phi) (\nabla^\omega \phi) - \frac{f}{\gamma\phi} F_{\lambda\nu} F^{\omega\nu} \right] \hat{P}_{\rho\sigma}^{\lambda\kappa} \hat{P}_{\omega\kappa}^{\alpha\beta} \\
&\quad - \frac{f}{2\gamma\phi} F^{\omega\kappa} F^{\lambda\nu} \hat{P}_{\rho\sigma,\omega\lambda} \hat{P}_{\kappa\nu}^{\alpha\beta} \\
&\quad + \left[\frac{1}{4\gamma\phi} (\nabla_\lambda \phi) (\nabla^\lambda \phi) + \left(\frac{1}{2\phi} - \frac{3c_1}{4\gamma\phi} \right) (\Delta\phi) - R + \frac{V}{2\gamma\phi} + \frac{f F_{\mu\nu}^2}{8\gamma\phi} \right] \hat{P}_{\rho\sigma}^{\alpha\beta}.
\end{aligned}$$

Applying the algorithm (13) and the matrix elements (15), after some tedious algebra we find the gravitation-Maxwell contribution to the effective action:

$$\begin{aligned}
\Gamma_{GM \text{ div}} &= -\frac{1}{2\varepsilon} \int d^2x \sqrt{g} \left[2R + \frac{2}{c_1} V' - \frac{V}{\gamma\phi} + \left(\frac{f'}{2c_1} + \frac{f}{4\gamma\phi} \right) F_{\mu\nu}^2 \right. \\
&\quad \left. + \left(\frac{f'}{f} + \frac{1}{\phi} - \frac{1}{c_1} - \frac{c_1}{2\gamma\phi} \right) (\Delta\phi) + \left(\frac{f''}{f} - \frac{f'^2}{f^2} - \frac{1}{\phi^2} + \frac{c_1}{2\gamma\phi^2} + \frac{c_1^2}{8\gamma^2\phi^2} \right) (\nabla^\lambda \phi) (\nabla_\lambda \phi) \right]. \quad (15)
\end{aligned}$$

To complete the calculations we should add the ghost contributions. The ghost operators corresponding to (5) are

$$\widehat{\mathcal{M}}_{gh}^* = \Delta, \quad \widehat{\mathcal{M}}_{gh\mu}^\mu = g_\mu^\mu \Delta + \frac{c_1}{2\gamma\phi} (\nabla_\nu \phi) \nabla^\mu + \frac{c_1}{2\gamma\phi} (\nabla^\mu \nabla_\nu \phi) + R_\mu^\mu. \quad (16)$$

Again, using the algorithm (13), we get the divergent ghost contributions of the effective action

$$\Gamma_{gh \text{ div}} = -\frac{1}{2\varepsilon} \int d^2x \sqrt{g} \left[3R + \frac{c_1}{2\gamma\phi} (\Delta\phi) + \left(\frac{c_1}{2\gamma\phi^2} - \frac{c_1^2}{8\gamma^2\phi^2} \right) (\nabla^\lambda \phi) (\nabla_\lambda \phi) \right]. \quad (17)$$

Note that the doubling procedure (14) should not be invoked.

Finally, the total divergent part of the one-loop effective action given by the sum of (16) and (18) becomes

$$\begin{aligned}
\Gamma_{div} &= -\frac{1}{2\varepsilon} \int d^2x \sqrt{g} \left[5R + \frac{2}{c_1} V' - \frac{V}{\gamma\phi} + \left(\frac{f'}{2c_1} + \frac{f}{4\gamma\phi} \right) F_{\mu\nu}^2 \right. \\
&\quad \left. + \left(\frac{f'}{f} + \frac{1}{\phi} - \frac{1}{c_1} \right) (\Delta\phi) + \left(\frac{f''}{f} - \frac{f'^2}{f^2} - \frac{1}{\phi^2} + \frac{c_1}{\gamma\phi^2} \right) (\nabla^\lambda \phi) (\nabla_\lambda \phi) \right]. \quad (18)
\end{aligned}$$

A few remarks are in order. First of all, in the absence of the Maxwell sector ($f = 0$) and when dropping the surface divergent terms, expression (19) (no surface divergences)

coincides with the results obtained in Refs.[2,3,4] in the same gauge,

$$\Gamma_{div} = -\frac{1}{2\varepsilon} \int d^2x \sqrt{g} \left[\frac{2}{c_1} V' - \frac{V}{\gamma\phi} + \frac{c_1}{\gamma\phi^2} (\nabla^\lambda \phi)(\nabla_\lambda \phi) \right]. \quad (19)$$

Notice that the term (4) was not introduced in Refs.[2,3] so that $\gamma = -c_1/2$. Besides, we actually disagree with Ref.[4] in the surface divergent terms. This stems from the fact that the term $-\widehat{\nabla}^\lambda \widehat{E}_\lambda$ corresponding to the algorithm (13) is missing in Ref.[4]. This term gives an additional contribution to the surface divergencies.

Secondly, dropping the surface divergent terms one can see that the divergencies of the Maxwell sector coincide with the ones previously obtained in Refs.[6,9].

Eq.(19) which contains the surface divergent terms of the theory (1), constitutes the main result of the present work, and completes the calculations done in Refs.[6,9]. It is interesting to notice that there is no dependence on γ in the terms which result from the Maxwell or the Maxwell-dilaton sectors (only in the pure dilaton sector does such dependence appear). Also to be remarked is the fact that the contribution from the Maxwell terms to the dilaton sector

$$-\frac{1}{2\varepsilon} \int d^2x \sqrt{g} \nabla_\lambda \left(\frac{f'}{f} \nabla^\lambda \phi \right), \quad (20)$$

is trivial: it is merely a surface term [6].

Let us now consider the result (19) on shell. Integrating (19) by parts, keeping all the surface terms and using the classical field equations (2) we obtain the on-shell divergences of the effective action

$$\Gamma_{div}^{on-shell} = -\frac{1}{2\varepsilon} \int d^2x \sqrt{g} \left\{ 5R + \frac{2}{c_1} \left(V' + \frac{f'}{4} F_{\mu\nu}^2 \right) + \Delta \left[\ln f + \left(1 - \frac{c_1}{\gamma} \right) \ln \phi - \frac{1}{c_1} \phi \right] \right\}. \quad (21)$$

Using the second of the field equations (2), we can rewrite Eq.(22) as follows:

$$\Gamma_{div}^{on-shell} = -\frac{1}{2\varepsilon} \int d^2x \sqrt{g} \left\{ 3R + \Delta \left[\ln f + \left(1 - \frac{c_1}{\gamma} \right) \ln \phi + \frac{1}{c_1} \phi \right] \right\}. \quad (22)$$

Hence, one can see that the on-shell divergences of the one-loop effective action are just given by the surface terms. If we are allowed to drop the surface terms we can conclude that the one-loop S -matrix is finite as in the pure dilaton gravity [1]. Note also that the surface counterterms on shell depend on the parameter γ (and hence on ξ). This is not surprising because by adding the term (4) one introduces a new parameter into the theory. (This parameter apparently can influence only surface counterterms because the triviality of Eq.(4) is a consequence of the Bianchi identities.)

Finally, let us discuss the renormalizability of the theory off shell. Dropping the surface terms in (19) we get

$$\Gamma_{div} = -\frac{1}{2\varepsilon} \int d^2x \sqrt{g} \left[\frac{2}{c_1} V' - \frac{V}{\gamma\phi} + \left(\frac{f'}{2c_1} + \frac{f}{4\gamma\phi} \right) F_{\mu\nu}^2 + \frac{c_1}{\gamma\phi^2} (\nabla^\lambda \phi)(\nabla_\lambda \phi) \right]. \quad (23)$$

For the case $\xi = 0$ this result has been obtained previously [9]. Adding to the counterterms (i.e. (24) with the opposite sign) to the initial action (1) we obtain the renormalized action. Choosing the one-loop renormalization of the metric $g_{\mu\nu}$ as

$$g_{\mu\nu} = \exp \left(-\frac{1}{2\varepsilon\gamma\phi} \right) \tilde{g}_{\mu\nu}, \quad (24)$$

we get the renormalized action in the following form

$$S_R = \int d^2x \sqrt{\tilde{g}} \left[\frac{1}{2} \tilde{g}^{\mu\nu} \partial_\mu \phi \partial_\nu \phi + c_1 \tilde{R} \phi + V(\phi) + \frac{1}{4} f(\phi) F_{\mu\nu}^2 - \frac{V'(\phi)}{\varepsilon c_1} - \frac{f'(\phi)}{4\varepsilon c_1} F_{\mu\nu}^2 \right]. \quad (25)$$

The dilaton and the coupling c_1 do not get renormalized in the one-loop approximation.

From (26) it follows that the theory under discussion is one-loop multiplicatively renormalizable for the families of potentials:

$$\begin{aligned} V(\phi) &= e^{\alpha\phi} + \Lambda, & f(\phi) &= e^{\beta\phi} \text{ or } f(\phi) = f_1, \\ V(\phi) &= A_1 \sin \phi + B_1 \cos \phi, & f(\phi) &= A_2 \sin \phi + B_2 \cos \phi, \end{aligned} \quad (26)$$

where $\alpha, \Lambda, \beta, f_1, A_1, B_1, A_2$ and B_2 are arbitrary constants.

The black hole solutions which appear for the Liouville-like potentials in (27) were discussed in Refs. [5,9,10]. It would be interesting to study the time-dependent solutions (the 2d cosmology) for the theory that has been considered here with the potentials (27) and taking into account the back reaction [11].

Summing up, we have investigated the renormalization structure of Maxwell-dilaton gravity and found all the one-loop counterterms including the surface counterterms. The on-shell limit of the effective action and the renormalizability off-shell have also been studied in detail.

Acknowledgments

S.D.O. wishes to thank the Japan Society for the Promotion of Science (JSPS, Japan) for financial support and the Particle Physics Group at Hiroshima University for kind hospitality. E.E. has been supported by DGICYT (Spain), research project PB90-0022, and by the Alexander von Humboldt Foundation (Germany).

References

- [1] S.D. Odintsov and I.L. Shapiro, *Phys. Lett. B* **263** (1991) 183; *Mod. Phys. Lett. A* **7** (1992) 437.
- [2] S.D. Odintsov and I.L. Shapiro, *Perturbative analysis of two-dimensional quantum gravity*, *Int. J. Mod. Phys. D*, to appear.
- [3] F.D. Mazzitelli and N. Mohammadi, *Classical gravity coupled to Liouville theory*, *Nucl. Phys. B*, to appear.
- [4] R. Kantowski and C. Marzban, *One-loop Vilkovisky-De Witt counterterms for 2D gravity plus scalar field theory*, *Phys. Rev. D*, to appear.
- [5] R.B. Mann, S. Morsink, A. Sikemma and T.G. Steele, *Phys. Rev. D* **43** (1991) 3948; O. Lechtenfeld and C. Nappi, *Phys. Lett. B* **288** (1992) 72; C. Nappi and A. Pasquinucci, *Mod. Phys. Lett. A* **7** (1992) 3337. R.B. Mann, *Conservation laws and 2D black holes in dilaton gravity*, preprint WATPHYS Th-92/03.
- [6] E. Elizalde and S.D. Odintsov, *JETP Lett.* **56** (1992) 185; *One-loop divergences in two-dimensional Maxwell-dilaton quantum gravity*, *Mod. Phys. Lett. A*, to appear.
- [7] C.G. Callan, S.B. Giddings, J.A. Harvey and A. Strominger, *Phys. Rev. D* **45** (1992) 1005; S.B. Giddings and W.M. Nelson, *Phys. Rev. D* **46** (1992) 2486.
- [8] S.P. de Alwis, preprint HEP-TH 9207095 (1992); A. Bilal and C. Callan, preprint PUPT-1320 (1992); J.G. Russo, L. Susskind and L. Thorlacius, *Phys. Lett. B* **292** (1992) 13; S.W. Hawking, *Phys. Rev. Lett.* **69** (1992) 406; K. Hamada, preprint UT-Komaba 92-7 (1992); G.W. Gibbons and M.J. Perry, preprint HEP-TH 9204090 (1992); T. Banks, A. Dabholkar, M.R. Douglas and M. O'Loughlin, *Phys. Rev. D* **45** (1992) 3607; K. Hamada and A. Tsuchiya, preprint UT-Komaba 92-14 (1992).
- [9] E. Elizalde and S.D. Odintsov, *One-loop renormalization in two-dimensional matter-dilaton quantum gravity and charged black-holes*, *Nucl. Phys. B*, to appear.
- [10] S. Nojiri and I. Oda, preprint HEP-TH 9207077 (1992).
- [11] F.D. Mazzitelli and J.G. Russo, preprint UTTG-28-92 (1992).
- [12] I.M. Lichtzier and S.D. Odintsov, *Mod. Phys. Lett. A* **6** (1991) 1953; T. Muta and S.D. Odintsov, preprint HUPD-92-13 (1992).
- [13] G. 't Hooft and M. Veltman, *Ann. Inst. H. Poincare* **20** (1974) 69.

- [14] G.W. Gibbons, *Nucl. Phys.* **B207** (1982) 337; G.W. Gibbons and K. Maeda, *Nucl. Phys.* **B298** (1988) 74; D. Garfinkle, G. Horowitz and A. Strominger, *Phys. Rev.* **D43** (1991) 3140.
- [15] E. Elizalde and A. Romeo, *Int. J. Mod. Phys.* **A5** (1990) 1653.

Role of the 5th Coordinate in Wesson's 5D STM Theory of Gravity

Takao Fukui

Faculty of Liberal Arts, Dokkyo University, Soka, Saitama, Japan

Abstract. It is shown that the physical quantities in the 4D world such as density, pressure and then an equation of state for a gravitating spherically symmetric fluid can be derived from the geometrical property of the fifth dimension of a spherically symmetric line-element in the Wesson's 5D STM theory of gravity.

1. Introduction

Since Wesson proposed a 5D Space-Time-Mass theory of gravity [1], the theory has physically been studied by various authors [2] besides finding cosmological solutions [3]. The authors made it possible to draw some physical properties only from the geometrical property of an extra dimension in the theory. From observational point of view, Coley [4] studied the nucleosynthesis and Wesson [5] presented some testable results, with applying the theory to the Universe. An equation of state in the early epoch of the Universe was derived by Fukui [6] with using the Chatterjee's cosmological solution [3]. This equation of state can be applied for studying baryon synthesis in the early Universe. These studies imply that the theory will be useful in describing the physical quantities of the 4D Universe in terms of the geometry of a higher dimensional world, when it is applied to cosmology.

While Wesson and Wesson & Lim [7] studied the effective properties of matter by applying the theory to a spherically symmetric 5D line-element, and showed that the theory can be useful also in studying solar system dynamics. Ma [8] derived expressions of the rest mass of a test body by applying the theory to Mach's principle in a quasi-static and spherically symmetric gravitational field.

Here we derive an equation of state and study the motion of a test particle in and around gravitating spherically symmetric systems.

2. 5th Coordinate and Energy-Momentum Tensor in 4D

A metric for 5D Space-Time-Mass is taken here as

$$d^{(5)}s^2 = d^{(4)}s^2 - e^{\mu} dm^2, \quad (1)$$

where $d^{(4)}s^2$ is a familiar standard form of the 4D Space-Time metric,

$$d^{(4)}s^2 = e^{\nu} dt^2 - e^{\lambda} dr^2 - r^2 (d\theta^2 + \sin^2 \theta d\phi^2), \quad (2)$$

and ν , λ , and μ are functions of t , r , and m .

According to the works of Wesson [2,5], Fukui [6], and Wesson & Ponce de Leon [9], 5D Einstein's field equations in vacuum ${}^{(5)}G^a_b=0$ are split here into ${}^{(4)}G^a_b$, the part which is proper to 4D ST, and the remainder H^a_b . Furthermore H^a_b is regarded as the energy-momentum tensor T^a_b in 4D ST. So the field equations are written as

$${}^{(5)}G^a_b = {}^{(4)}G^a_b + H^a_b = {}^{(4)}G^a_b + (8\pi k/c^4)T^a_b = 0. \quad (3)$$

Greek indices run from 0 to 4, while Latin from 0 to 3^(*).

The conservation laws in the energy-momentum tensor, $T^{ab}{}_{;b}=0$ of which only $T^{ab}{}_{;b}=T^{1b}{}_{;b}=0$ are not identically satisfied, put the following constraints. From $T^{ab}{}_{;b}=0$,

$$\begin{aligned} &(\dot{\nu} \dot{\lambda} \dot{\mu} - 2\ddot{\lambda} \dot{\mu} + \dot{\lambda} \dot{\mu}^2 - \dot{\lambda}^2 \dot{\mu})e^{-\nu} + (2\ddot{\mu}'\mu' - \dot{\lambda} \dot{\mu}'^2 - 4\dot{\lambda} \dot{\mu}'/r + \nu'^2 \dot{\mu} - \nu' \dot{\mu} \mu' - \lambda' \nu' \dot{\mu} + \\ &+ \lambda' \dot{\mu} \mu' + 2\nu'' \dot{\mu} - 2\ddot{\mu} \mu'' + 4\nu' \dot{\mu}/r - 4\dot{\mu} \mu'/r)e^{-\lambda} - (4\dot{\lambda}^* \dot{\mu} + 2\dot{\lambda}^2 \dot{\mu} - 2\dot{\lambda} \dot{\mu}^* \dot{\mu} - 4\dot{\lambda}^* - 4\dot{\lambda} \dot{\lambda}^* + \\ &+ 2\dot{\lambda}^* \dot{\mu} + 2\dot{\lambda} \dot{\mu}^* + 2\nu^* \dot{\lambda} + \nu^2 \dot{\lambda} - \nu^* \dot{\lambda}^* - 2\dot{\lambda} \dot{\lambda}^* - \dot{\lambda}^2 \dot{\lambda} + \dot{\lambda} \dot{\lambda}^* \dot{\mu})e^{-\mu} = 0, \end{aligned} \quad (4)$$

and from $T^{1b}{}_{;b}=0$,

$$\begin{aligned} &(-\dot{\nu} \dot{\lambda} \mu' + \dot{\nu} \dot{\mu} \mu' + \dot{\lambda}^2 \mu' - \dot{\lambda} \dot{\mu} \mu' + 2\ddot{\lambda} \mu' - 2\ddot{\mu} \mu' + 2\dot{\mu} \mu' - \nu' \dot{\mu}^2 - 4\dot{\lambda} \dot{\mu}/r)e^{-\nu} + (\nu' \lambda' \mu' + \\ &+ 4\lambda' \mu'/r - 2\nu'' \mu' + 4\mu'^2/r + \nu' \mu'^2 - \nu'^2 \mu')e^{-\lambda} - (-4\nu^* \mu' - 2\nu^2 \mu' + 2\nu^* \mu' \mu^* + 4\nu'^* + 4\nu' \nu^* - \\ &- 2\nu^* \mu^* - 2\nu^* \mu^* - 2\nu' \lambda^* - \nu' \dot{\lambda}^2 + \nu' \dot{\lambda} \mu^* + 2\nu' \nu^* + \nu' \nu^2 - \nu' \nu^* \mu^* - 8\dot{\lambda}^*/r - 4\dot{\lambda}^2/r - 4\nu^* \dot{\lambda}/r + \\ &+ 4\dot{\lambda} \dot{\mu}^*/r)e^{-\mu} = 0, \end{aligned} \quad (5)$$

where $(\dot{})$, (ν') , and $(*)$ represent partial differentials with respect to t , r , and m respectively. Thus Eqs. (1)-(5) are basic equations to be employed in the following sections.

3. Perfect Fluid

Since in the Universe as a whole and even inside star, the matter is a perfect fluid to high precision, the energy-momentum tensor is taken here as,

$$T^a_b = (\rho c^2 + p)U^a U_b - p \delta^a_b. \quad (6)$$

^(*) Refer to [1(1983)] for detail of Eq. (3).

Where ρ and p are the density and pressure respectively in the 4D Universe, and $U^a (=dx^a/d^{(4)}s)$ & U_b are the four velocities and its non-zero components are obtained from Eq. (2), i.e. $1=e^r(U^0)^2-e^\lambda(U^1)^2$. Then by using Eqs. (3) and (6), the density and pressure are given as

$$(8\pi k/c^4) \rho c^2 = (3\mu'/2r)e^{-\lambda} - (\dot{\nu} \ddot{\lambda} / 4)e^{-\mu}, \text{ and} \quad (7)$$

$$(8\pi k/c^4) p = (\mu'/2r)e^{-\lambda} - (\dot{\nu} \ddot{\lambda} / 4)e^{-\mu}. \quad (8)$$

Eqs. (7) and (8) lead to the following equation of state for gravitating spherically symmetric fluids.

$$p = (1/3) \rho c^2 - (c^4/48\pi k) \dot{\nu} \ddot{\lambda} e^{-\mu}. \quad (9)$$

In case of $U^1=0$, a co-moving coordinate, the following new conditions yielded from $T^1_1 = T^2_2 (=T^3_3)$ should be taken into account; from ${}^{(4)}G^1_1 = {}^{(4)}G^2_2$,

$$(2\ddot{\lambda} + \dot{\lambda}^2 - \dot{\nu} \ddot{\lambda})e^{-\nu} - (2\nu'' + \nu'^2 - \nu'\lambda' - 2\lambda'/r - 2\nu'/r - 4/r^2)e^{-\lambda} - 4/r^2 = 0, \quad (10)$$

and from $H^1_1 = H^2_2$,

$$\dot{\lambda} \dot{\mu} e^{-\nu} - (2\mu'' + \mu'^2 - \lambda' \mu' - 2\mu'/r)e^{-\lambda} - (2\ddot{\lambda} + \dot{\lambda}^2 + \dot{\nu} \ddot{\lambda} - \ddot{\lambda} \mu) e^{-\mu} = 0. \quad (11)$$

4. Motion of a Test Particle

The geodesic equation in 5D is calculated by

$$d^2x^\alpha/d^{(5)}s^2 + \Gamma^\alpha_{\beta\gamma} (dx^\beta/d^{(5)}s) (dx^\gamma/d^{(5)}s) = 0. \quad (12)$$

In the following $d^{(5)}s$ should be written just as ds .

For $\kappa=0$,

$$d^2t/ds^2 + (\dot{\nu}/2) (dt/ds)^2 + \nu' (dt/ds) (dr/ds) + \dot{\nu} (dt/ds) (dm/ds) + (e^{\lambda-\nu}/2) \dot{\lambda} (dr/ds)^2 + (e^{\mu-\nu}/2) \dot{\mu} (dm/ds)^2 = 0, \quad (13)$$

for $\kappa=1$ which represents the radial equation of motion,

$$d^2r/ds^2 + (e^{\nu-\lambda}/2) \nu' (dt/ds)^2 + \dot{\lambda} (dt/ds) (dr/ds) + (\lambda'/2) (dr/ds)^2 + \dot{\lambda} (dr/ds) (dm/ds) - re^{-\lambda} (d\theta/ds)^2 - r \sin^2 \theta e^{-\lambda} (d\phi/ds)^2 - (e^{\mu-\lambda}/2) \mu' (dm/ds)^2 = 0, \quad (14)$$

for $\kappa=2$,

$$d^2\theta/ds^2 + (2/r) (dr/ds) (d\theta/ds) - \sin \theta \cos \theta (d\phi/ds)^2 = 0, \quad (15)$$

for $\kappa=3$ which is the azimuthal equation of motion,

$$d\{r^2 \sin^2 \theta (d\phi/ds)\}/ds=0, \quad (16)$$

and for $\kappa=4$ which gives the rate of change of the mass of a test particle,

$$d^2 m/ds^2 + (e^{\nu-\mu}/2) \dot{\nu} (dt/ds)^2 + \dot{\mu} (dt/ds) (dm/ds) - (e^{\lambda-\mu}/2) \dot{\lambda} (dr/ds)^2 + \mu' (dr/ds) (dm/ds) + (\dot{\mu}/2) (dm/ds)^2 = 0. \quad (17)$$

In the "Newtonian limit", these equations reduce to those of 4D ST theory of gravity, and we can make identical discussion to that in 4D ST, on the motion of a test particle [1].

5. Wesson's solution and Comments

Here we take a spherically symmetric solution obtained by Wesson [1], and see what physical results the present scenario draws from the solution. The solution obtained by Wesson is as follows,

$$d(s^2) s^2 = (1-2a/r) c^2 dt^2 - dr^2 / (1-2a/r) - r^2 (d\theta^2 + \sin^2 \theta d\phi^2) - dm^2, \quad (18)$$

where "a" is a constant with the dimension of length. Since Gm/c^2 is constant on the surface of $dm=0$ of the 5D manifold, there the constant "a" can be equated to GM_0/c^2 where M_0 is the mass of the central body. This solution satisfies the conservation laws Eqs. (4) and (5) and the co-moving coordinate conditions Eqs. (10) and (11), and leads to $\rho=p=0$ in Eqs. (7) and (8). Then the metric Eq. (18) on the surface of $dm=0$ can be understood as the exterior Schwarzschild solution of a static spherically symmetric star in a co-moving coordinate system of the 4D ST i.e. a black hole of mass M_0 .

While Eqs. (7)-(8) imply that there may be possibility to give a radiation equation of state for a neutron star or a 'cold' electron gas [10] $p=(1/3)\rho c^2$, and an equation of state for a "stiff matter" $p=\rho c^2$. In case of the Chatterjee's cosmological solution [3], it was shown by Fukui [6] that our Universe experienced a stiff matter state before the radiation era.

From Eqs. (13) and (17), $dm/dt = \alpha (1-2a/r)$. The size of the constant α is expected to be small. This relation implies that the Wesson's theory can be studied in connection with Mach's Principle [8].

In conclusion, the present scenario shows that the Wesson's 5D STM theory of gravity which is within the framework of general relativity is useful in studying the inside and neighbourhood of a relativistic star as well as the origin of the Universe.

Acknowledgements

The author is grateful to P.S.Wesson for his useful comments and to J.Ponce de Leon for his calculations of Eqs. (7)-(9).

References

1. Wesson, P. S. (1983) *Astron. Astrophys.*, 119, 145.
Wesson, P. S. (1984) *Gen. Rel. Grav.*, 16, 193.
Wesson, P. S. (1985) *Astron. Astrophys.*, 143, 233.
2. Wesson, P. S. (1986) *Astron. Astrophys.*, 166, 1.
Wesson, P. S. (1988) *Astron. Astrophys.*, 189, 4.
Wesson, P. S. (1990) *Gen. Rel. Grav.*, 22, 707.
Wesson, P. S. (1992) *Mod. Phys. Lett.*, 7, 921.
Fukui, T. (1988) *Astron. Space Sci.*, 146, 13.
Grøn, Ø. (1988) *Astron. Astrophys.*, 193, 1.
Grøn, Ø., and Soleng, H. (1988) *Gen. Rel. Grav.*, 20, 1115.
Banerjee, A., Bhui, B. K., and Chatterjee, S. (1990) *Astron. Astrophys.*, 232, 305.
Ma, G. (1990) *Phys. Lett.*, A143, 183.
3. Chatterjee, S. (1987) *Astron. Astrophys.*, 179, 1.
Fukui, T. (1987) *Gen. Rel. Grav.*, 19, 43.
Ponce de Leon, J. (1988) *Gen. Rel. Grav.*, 20, 539.
4. Coley, A. (1990) *Astron. Astrophys.*, 233, 305.
5. Wesson, P. S. (1992) *Astrophys. Jour.*, in press.
6. Fukui, T. (1992) *Astron. Astrophys.* 253, 1.
7. Wesson, P. S. (1992) *Phys. Lett.*, B276., 299.
Wesson, P. S., and Lim, P. (1992) *Astron. Astrophys.*, in press.
8. Ma, G. (1990) *Phys. Lett.*, A146, 375.
9. Wesson, P. S., and Ponce de Leon, J. (1992) preprint, U. Waterloo.
10. Schutz, B. F. (1985) *A first course in general relativity* (Cambridge Univ. Pr., Cambridge) ch. 10.

Turns of General Relativity*

Humitaka SATO
Department of Physics, Kyoto University, Kyoto 606-01

Contents

I General Relativity: past and future

(1) Past

- (a) 1920; Heisenberg
- (b) 1939; Oppenheimer
- (c) 1963; QSO, Hoyle
- (d) Metamorphose of General Relativity; Texas Sympo.
- (e) "Problems of Cosmology" in 1967

(2) Future

- (a) After the boom of "Cosmology and Unified Theory"
- (b) Surroundings of General Relativity; manner of survival
- (c) Mathematical Physics vs Theoretical Physics

II Dynamics of Time

- (a) Dynamics of Manifold
- (b) Dynamics by Parametric Time
- (c) Arbitrariness in Types of Motion
- (d) An Example; q^{-2} potential vs harmonic oscillator,
closed time, local analysis of phase flow
- (e) Quantum mechanics and Time Variable
- (f) Symmetry for Time Variable; Schrodinger Group

* Japanese version of the manuscript is given at the end of this
Proceedings (p.469)

Energy, Momentum and Angular-Momentum Currents in General Relativity

KOICHI NOMURA AND KENJI HAYASHI

Institute of Physics, Kitasato University, Sagamihara, Kanagawa 228

and

TAKESHI SHIRAFUJI

Physics Department, Saitama University, Urawa, Saitama 338

ABSTRACT

Extending the tetrad formalism of General Relativity, we introduce a notion of *local translation* in addition to the local Lorentz transformation. By means of Noether's method applied to action integral with the local translation and local Lorentz invariance, we derive the energy-momentum and angular-momentum currents, $P^{k\mu}$ and $J^{kl\mu}$, which transform as four-vector densities under general coordinate transformations.

In a series of papers,¹⁾⁻⁵⁾ Kawai has developed a gauge theory of gravity on the basis of the principal fiber bundle over four-dimensional spacetime with the covering group of the proper orthochronous Poincaré group. In this theory, there exists an *internal Poincaré gauge group*, and the tetrad fields $e_{k\mu}$ are constructed from the connection coefficients $A_{k\mu}$ and $A_{kl\mu}$, and a Higgs type field X_k ; $e_{k\mu} = X_{k,\mu} + A_{kl\mu} X^l + A_{k\mu}$. Particularly noteworthy is the fact that conservations of the energy-momentum and of (orbital + spin) angular-momentum both follow from the internal Poincaré gauge invariance.

In this paper, we apply Kawai's formalism to general relativity. Namely, let us take $A_{k\mu}$ and a Higgs type field X_k as the basic fields, and assume that the tetrad fields $e_{k\mu}$ are constructed from X_k and $A_{k\mu}$ as follows: $e_{k\mu} = X_{k,\mu} + A_{k\mu}$. As for the spin connection $A_{kl\mu}$, we assume that it is expressed by the tetrad fields. In flat spacetime, X_k can be *globally* identified with the position vector, while in curved spacetime, X_k can only *locally* be identified with the position vector.

Now let us define a *local translation* by $\tilde{X}_k = X_k - \epsilon_k(x)$, and assume that the tetrad fields are kept invariant; $\tilde{e}_{k\mu} = e_{k\mu}$. Here $\epsilon_k(x)$ are four arbitrary functions. Then $A_{k\mu}$ are transformed as $\tilde{A}_{k\mu} = A_{k\mu} + \epsilon_{k,\mu}$. Matter fields ϕ are also assumed to be invariant under local translations; $\tilde{\phi} = \phi$. On the other hand, since the tetrad fields are changed like $e_{k'\mu} = L_{k'}^l e_{l\mu}$ under local Lorentz rotations, under which $A_{k\mu}$ are transformed as $A_{k'\mu} = L_{k'}^l A_{l\mu} - L_{k'}^l{}_{,\mu} X_l$.

We take the gravitational Lagrangian density L_G as follows:

$$L_G = \frac{1}{2\kappa} e (A^m A_m - A^{mnk} A_{knm}) \quad (1)$$

following Møller.⁶⁾ Here A_m is defined by $A_{mnk} \eta^{nk}$. It should be noticed that $A_{kl\mu}$ involves only first-order derivatives of X_k and $A_{k\mu}$. L_G can be obtained from the Einstein-Hilbert Lagrangian density $R/2\kappa$ by subtracting first-order derivatives of $A_{kl\mu}$ in the form of a total derivative;

$$\frac{1}{2\kappa} R = -L_G + D^\mu{}_{,\mu} \quad (2)$$

where the explicit form of D^μ is given by

$$D^\mu = \frac{1}{\kappa} \left(e e^{k\nu} e^{l\mu} A_{kl\nu} \right). \quad (3)$$

Since the total (gravitational + matter) Lagrangian density $L = L_G + L_M$ is local translation invariant, there are three Noether's identities, from which we can derive

$$\frac{\delta L}{\delta A_{k\mu}} \stackrel{\text{id}}{=} P^{k\mu} - F^{k\mu\nu}{}_{,\nu} \quad (4)$$

where the energy-momentum current $P^{k\mu}$ and its super-potential $F^{k\mu\nu}$ are defined by

$$P^{k\mu} \stackrel{\text{def}}{=} T^{k\mu} + t^{k\mu}, \quad T^{k\mu} \stackrel{\text{def}}{=} \frac{\delta L_M}{\delta A_{k\mu}}, \quad t^{k\mu} \stackrel{\text{def}}{=} \frac{\partial L_G}{\partial A_{k\mu}} \quad (5)$$

and

$$F^{k\mu\nu} \stackrel{\text{def}}{=} \frac{\partial L_G}{\partial A_{k\mu,\nu}} \stackrel{\text{id}}{=} -F^{k\nu\mu}, \quad (6)$$

respectively. Thus the differential conservation law $P^{k\mu}{}_{,\mu} = 0$ follows from the field equation $\delta L / \delta A_{k\mu} = 0$, which turns out to agree with the Einstein equation. As is shown by using Noether's identities mentioned above, the field equation $\delta L / \delta X_k = 0$ is automatically satisfied, if the Einstein equation and the field equation of ϕ are both satisfied.

Since the Lagrangian density L_G is changed by a total derivative under local Lorentz transformations; $\delta L_G = (\delta D^\mu)_{,\mu}$, there are four Noether's identities. From these identities, we obtain ^{*)}

$$2X^{[k} \frac{\delta L}{\delta A_{l]\mu}} \stackrel{\text{id}}{=} J^{kl\mu} - \Sigma^{kl\mu\nu}{}_{,\nu} \quad (7)$$

where the angular-momentum current $J^{kl\mu}$ and its super-potential $\Sigma^{kl\mu\nu}$ are de-

*) Here the symbol $\{ \quad \}$ denotes the antisymmetrization.

defined by

$$J^{kl\mu} \stackrel{\text{def}}{=} 2 \left(X^{[k} P^{\eta]\mu} + A^{[k}_{\nu} F^{\eta]\nu\mu} - e^{[k}_{\nu} \frac{\partial D^{\mu}}{\partial A_{\eta]\nu}} - A^{[k}_{\nu,\lambda} \frac{\partial D^{\mu}}{\partial A_{\eta]\nu,\lambda}} \right) \quad (8)$$

and

$$\Sigma^{kl\mu\nu} \stackrel{\text{def}}{=} 2 \left(X^{[k} F^{\eta]\mu\nu} + \frac{\partial D^{\nu}}{\partial A_{[k\mu,\lambda}} e^{\eta]_{\lambda}} \right) \stackrel{\text{id}}{=} -\Sigma^{kl\nu\mu}, \quad (9)$$

respectively. Thus, with the help of the Einstein equation and (7), we have the differential conservation law $J^{kl\mu}_{,\mu} = 0$.

Let us define P^k and J^{kl} by

$$P^k \stackrel{\text{def}}{=} \int P^{k\mu} d\sigma_{\mu} \quad \text{and} \quad J^{kl} \stackrel{\text{def}}{=} \int J^{kl\mu} d\sigma_{\mu}, \quad (10)$$

respectively. Then, it can be shown that for an isolated system P^k and J^{kl} agree with the total energy-momentum and the total angular-momentum, respectively.

It is worth mentioning that $P^{k\mu}$ and $J^{kl\mu}$ are transformed as tensors under global Lorentz rotations of tetrad fields and as vector densities under general coordinate transformations.

Details of this paper will be published elsewhere.

Acknowledgements: one of the author (K.N.) would like to thank Professor T. Kawai of Osaka City University for valuable discussions.

REFERENCES

- 1) T.Kawai, *Gen.Rel.Gravit.* 18 (1986), 995; 19 (1987), 1285 E.
- 2) T.Kawai, *Prog. Theor. Phys.* 76 (1986), 1166; 79 (1988), 920.
- 3) T.Fukui, T.Kawai, and H.Saitoh, *Prog. Theor. Phys.* 79 (1988), 1420.
- 4) T.Kawai, and H.Saitoh, *Prog. Theor. Phys.* 81 (1989), 280, 1119.
- 5) T.Kawai, *Prog. Theor. Phys.* 82 (1989), 850; 84 (1990), 993.
- 6) C.Møller, *Mat. Fys. Skr. Dan. Vid. Selsk.* 1 (1961), no.10.

Black Holes with Non-Abelian Hair and their Thermodynamic Properties

TAKASHI TORII and KEI-ICHI MAEDA^(a)

Department of Physics, Waseda University, Shinjuku-ku, Tokyo 169-50, Japan

Abstract

We present some black hole solutions of Einstein-Yang-Mills-dilaton system, and calculate their Hawking temperatures. We find that if the coupling constant of the dilaton is smaller than some critical value, the thermodynamic behavior of these black holes includes two phase transitions at points determined by the value of the mass parameter. The black holes with the mass between those two critical values have positive specific heat. This is also true for the known colored black hole solution. We also reanalyse Skyrme black holes and find that there exist two modes of solutions (stable mode and unstable excited mode) and they have a critical horizon radius beyond which there is no Skyrme black hole. Those stable black holes with small mass have two fates: One possible remnant is a particle-like solution (Skyrmion) through the Hawking's evaporation process and the other is a Schwarzschild black hole by matter accretion. When a Skyrme black hole evolves in a Schwarzschild black hole at some critical mass, its area increases by a finite amount, hence we may regard this change as the first order phase transition. The specific heat of stable Skyrme black holes is always negative, while there is one or three transition points for unstable modes.

1 Introduction

The discovery of the particle-like solution and the colored black hole solution of the Einstein-Yang-Mills(EYM) equations[1,2] has been received much attention. Because non-trivial solution was not known and the black hole solution may be a counter example to the "no-hair" conjecture. By recent works, however, it turns out that the colored black hole as well as the particle-like solution is unstable[3]. Although such instability may give a doubt in its reality, it never lose their importance as the black hole solution with non-Abelian hair. Furthermore, new class of non-Abelian black holes is found in the Einstein-Skyrme(ES) system[4], which is stable against linear radial perturbations[5]

Here, first we study static black holes in a theory that couples a scalar field to a Yang-Mills(YM) field. The theory we consider arises as the 4-dimensional effective theory corresponding to various higher dimensional unified theories of fundamental interactions, and the scalar field it contains, which we shall call the dilaton field, is an artifact of the scale invariance typical of these unified theories. We present dilatonic colored black hole solutions in Einstein-Yang-Mills-dilaton (EYMD) system numerically[6] and discuss the effect of the dilaton coupling on their structure (§.2). We also calculate their Hawking temperatures to see their thermodynamical properties (§.3).

Several years ago, in a simpler gravitational system, the Einstein-Maxwell-dilaton (EMD) system, a black hole solution and their thermal properties were discussed[7]. It was shown that a second order phase transition (change sign of the specific heat), which also appears in the case of a Reissner-Nordström black hole, does not occur when the coupling constant of the dilaton α is greater than

unity. From our numerical analysis, we find that a dilatonic colored black hole has similar phase transitions at two points, if α is smaller than a critical coupling constant $\alpha_{cr} \sim 0.5$ (§.3).

We also reanalyse the black hole solutions of the ES system and calculate its Hawking temperature. It turns out that the ES system has two modes of solutions: one is the stable mode discussed in ref.[5] and the other is an excited mode which is unstable[8]. They have the same critical horizon radius, above which there is no solution except for a Schwarzschild solution. This fact provides us a scenario of their evolution as will be discussed below (§.4). No phase transition occurs in stable mode, while the excited mode has one or three phase transition points (§.5). The concluding remarks will follow them.

2 Dilatonic Colored Black Holes

We consider models with the following action[9];

$$S = \int d^4x \sqrt{-g} \left[\frac{1}{2\kappa^2} R(g) - \frac{1}{2\kappa^2} (\nabla\Phi)^2 - \frac{1}{16\pi g_C^2} e^{-\alpha\Phi} \text{Tr} F^2 \right], \quad (1)$$

where $\kappa^2 = 8\pi G$, Φ is the dilaton field, and F and A are the YM field strength and its potential, respectively. g_C and $\alpha (\geq 0)$ are coupling constants for the YM field and the dilaton field, respectively. This type of action is reduced from various unified theories as discussed in [7]. For example, $\alpha = 1$ and $\alpha = \sqrt{3}$ are the models from a superstring theory and from the 5-dimensional Kaluza-Klein theory, respectively. Notice that $\alpha = 0$ with $\Phi = 0$ denotes the usual EYM system.

We now consider an SU(2)-YM field. We shall make the spherically symmetric ansatz. In the spherically symmetric static case the space-time metric can be written as

$$ds^2 = - \left(1 - \frac{2Gm}{r} \right) e^{-2\delta} dt^2 + \left(1 - \frac{2Gm}{r} \right)^{-1} dr^2 + r^2 (d\theta^2 + \sin^2 \theta d\phi^2). \quad (2)$$

For its potential, we consider only the purely ‘magnetic’ case, i.e.,

$$A = w\tau_1 d\theta + (\cos \theta \tau_3 + w \sin \theta \tau_2) d\phi, \quad (3)$$

where τ_i denote the generators of SU(2). m , δ and w are functions only of r .

Variation of the action (1) leads to the field equations,

$$\bar{m}' = \frac{\bar{r}^2}{4} \left(1 - \frac{2\bar{m}}{\bar{r}} \right) \Phi'^2 + \frac{1}{\lambda_H^2} e^{-\alpha\Phi} \left\{ \left(1 - \frac{2\bar{m}}{\bar{r}} \right) w'^2 + \frac{1}{2\bar{r}^2} (1 - w^2)^2 \right\} \quad (4)$$

$$\delta' = -\frac{\bar{r}}{2} \Phi'^2 - \frac{2}{\lambda_H^2} \frac{e^{-\alpha\Phi}}{\bar{r}} w'^2 \quad (5)$$

$$\left[e^{-\delta} \bar{r}^2 \left(1 - \frac{2\bar{m}}{\bar{r}} \right) \Phi' \right]' + \frac{2}{\lambda_H^2} \alpha e^{-(\delta+\alpha\Phi)} \left[\left(1 - \frac{2\bar{m}}{\bar{r}} \right) w'^2 + \frac{1}{2\bar{r}^2} (1 - w^2)^2 \right] = 0 \quad (6)$$

$$\left[e^{-(\delta+\alpha\Phi)} \left(1 - \frac{2\bar{m}}{\bar{r}} \right) w' \right]' + e^{-(\delta+\alpha\Phi)} \frac{1}{\bar{r}^2} w (1 - w^2) = 0, \quad (7)$$

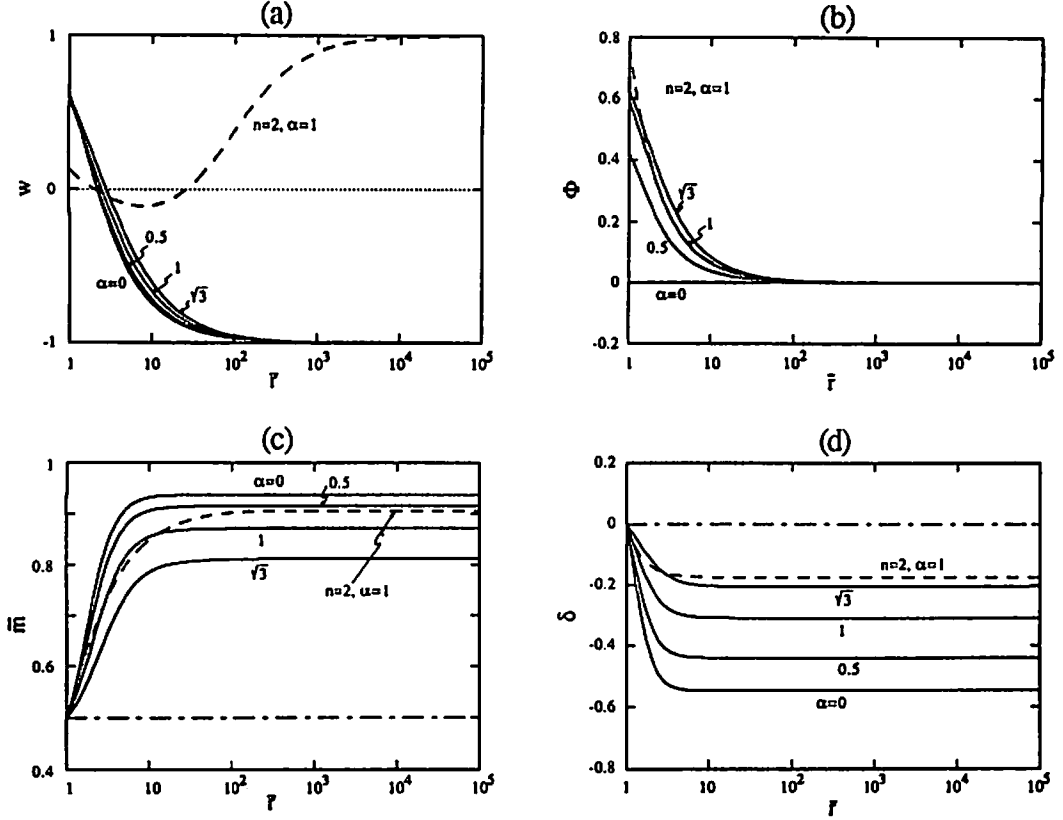


Figure 1: The solutions of (a) the Yang-Mills potential w , (b) the dilaton field Φ , (c) the mass function m and (d) the lapse function δ for dilaton colored black holes with one node ($n = 1$) and two nodes ($n = 2$). We set $\lambda_H = 1$. For $n = 2$ (dashed line) we show the model of $\alpha = 1$. In the limit of $\alpha \rightarrow \infty$, the solution approaches to the Schwarzschild solution (the dot-dashed line).

where we have introduced the dimensionless variables, \bar{r} and \bar{m} , normalized by the radius of the horizon r_H , i.e., $\bar{r} = r/r_H$ and $\bar{m} = Gm/r_H$. Λ prime denotes a derivative with respect to \bar{r} . $\lambda_H \equiv r_H/[l_P/g_C]$ with the Planck length $l_P \equiv \sqrt{\hbar G}$ denotes the ratio of the size of black hole to a typical scale length of the present theory ($\sim l_P/g_C$).

For the boundary conditions, first we assume a regular event horizon at $\bar{r} = 1$, i.e.,

$$\bar{m}_H = \frac{1}{2}, \quad |\delta_H| < \infty, \quad (8)$$

where the subscript H denotes the values of functions at the horizon. Outside the horizon, the condition $r > 2m(r)$ must be satisfied. To find asymptotically flat solutions, we have

$$m(r) \longrightarrow M = \text{const.} \quad \delta(r) \longrightarrow \delta_\infty = 0 \quad \text{as} \quad r \longrightarrow \infty, \quad (9)$$

where M is a gravitational mass of a black hole. As for Φ and w , we assume $\Phi \rightarrow 0$ and $w \rightarrow \pm 1$ as $r \rightarrow \infty$, which guarantee the finiteness of the energy of the system.

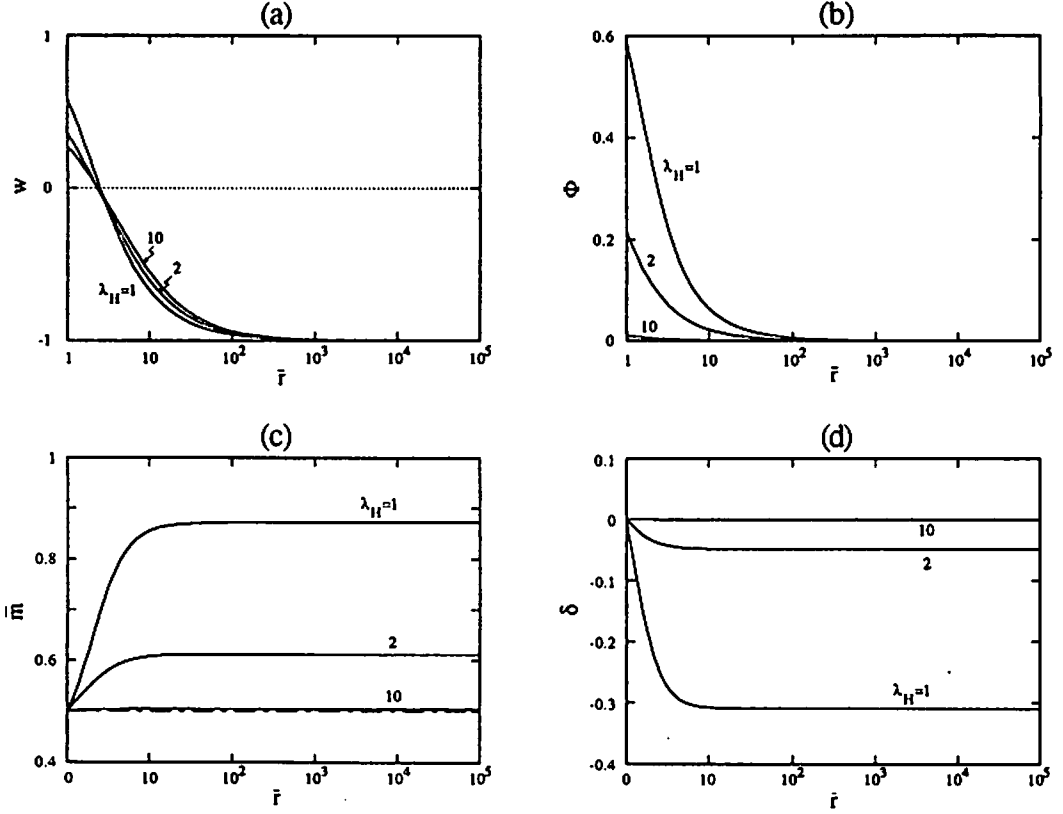


Figure 2: The solutions of (a) the Yang-Mills potential w , (b) the dilaton field Φ , (c) the mass function m and (d) the lapse function δ for dilaton colored black holes with one node ($n = 1$). We set $\alpha = 1$. We also plot the Schwarzschild solution by a dot-dashed line for comparison.

Under the above conditions, we solved Eqs. (4)-(7) numerically and found a discrete family of regular black hole solutions characterized by the node number (n) of the YM potential. For $\lambda_H = 1$, the solutions with one node ($n = 1$) and two node ($n = 2$) are shown in Fig.1. We can see that the dilaton field Φ increases as the coupling constant α increases. But α increases further, Φ decreases again. Because, in the limit of $\alpha \rightarrow \infty$, we recover a Schwarzschild solution ($\bar{m} = \frac{1}{2}$ and $\delta = 0$) with $\Phi = 0$ and $w = 1$. We confirmed those behaviours numerically. For the solution with $n = 2$ (two nodes) the YM field distributes to a larger distance.

In Fig. 2, we also show the solutions for various values of λ_H , setting $\alpha = 1$. When $\lambda_H \rightarrow \infty$, i.e., $r_H \rightarrow \infty$ (large black holes) or $y_C \rightarrow \infty$, we find that the space-time approaches the Schwarzschild solution, while the YM potential w is not trivial ($w \neq 1$). This is easy to understand, because in the limit $\lambda_H \rightarrow \infty$, the YM field decouples from gravity (See Eqs. (4)-(7)). The non-Abelian YM field can then have non-trivial configuration although it makes no contribution to black hole structure (see Fig. 2). What physically happens is as follows: The contribution in its mass energy from the

YM field itself may also be a kind of “quanta”. Although its value may depend on n , it may be a typical mass scale, m_P/g_C . When the black hole gets large, its energy may not increase so much and its contribution to the black hole structure becomes ignorable, resulting in the Schwarzschild black hole.

3 Thermodynamic Properties of Dilatonic Colored Black Holes

The black holes considered here may be rather small unless $g_C \ll 1$, because their typical size is probably l_P/g_C . Their quantum effects may be important in the context, hence we shall calculate the temperature of dilatonic colored black holes. The Hawking temperature is given as

$$T = \frac{1}{4\pi r_H} e^{-\epsilon_H} (1 - 2\tilde{m}'_H). \quad (10)$$

The results of $\beta \equiv 1/T$ v.s. the gravitational mass M are shown in Fig. 3. For the colored black hole case ($\alpha = 0$), as M increases, T increases within some range of black hole masses, i.e., for $M_{1,\text{cr}} = 0.905m_P/g_C < M < M_{2,\text{cr}} = 1.061m_P/g_C$ [10]. This means that the specific heat is positive in this mass range. This is hardly surprising, since a colored black hole has similar behavior near the horizon to the Reissner-Nordström black hole which has a kind of phase transition at $Q_{\text{cr}} \equiv \sqrt{3}GM/2$. We find, however, a new behavior: the specific heat change its sign again if M gets smaller than $0.905 m_P/g_C$. For $M < M_{1,\text{cr}}$, as M decreases β decreases again and vanishes at $M = 0.829m_P/g_C$, when the black hole disappears and a particle-like solution is recovered.

Similar behavior is found for the dilatonic colored black hole, if the coupling constant α is small enough. This behavior is similar to the EMD black hole, although in the EMD system, there is only one phase transition point. From Fig. 3, we see that the temperature has a tendency to approach that of the Schwarzschild black hole as α grows, and find that no phase transition occurs beyond some critical value of α ($\alpha_{\text{cr}} \sim 0.5$).

4 Skyrme Black Holes

The Skyrme black holes [4] are another type of black holes which have non-Abelian hair. Here we reanalyse the black hole solutions of ES system and study their thermodynamical properties.

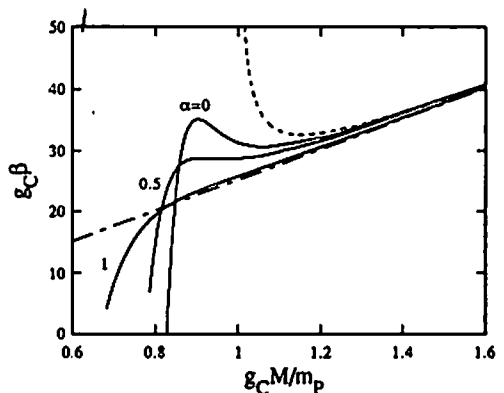


Figure 3: The inverse temperature $\beta (= 1/T)$ of dilatonic colored black hole ($n = 1$) as a function of M . For comparison, we also plot the Schwarzschild ($w \equiv 1, \Phi \equiv 0$) and the Reissner-Nordström black-hole cases ($w \equiv 0, \Phi \equiv 0$) by a dot-dashed and a dotted lines, respectively.

The $SU(2) \times SU(2)$ invariant action coupled to gravity is given by [13]

$$S = \int d^4x \sqrt{-g} \left[\frac{1}{2\kappa^2} R(g) + \frac{1}{4} f_S^2 \text{Tr} A^2 - \frac{1}{32g_S^2} \text{Tr} F^2 \right], \quad (11)$$

where F and A are the field strength and its potential, respectively, and f_S and g_S are coupling constants. A and F are expressed in terms of the $SU(2)$ -valued function U as $A = U^\dagger \nabla U$, $F = A \wedge A$. We are interested in spherically symmetric static solutions, so we make the hedgehog ansatz for U

$$U(x) = \cos \chi(r) + i \sin \chi(r) \sigma \cdot \hat{r}, \quad (12)$$

where the σ_i denote the Pauli matrices and χ is a function of the radial coordinate r . For the spherically symmetric static spacetime we take the same metric form (2) as in the EYMD case.

Varying the action (11), we obtain the following field equations,

$$\tilde{m}' = \kappa^2 f_S^2 \left[\frac{\tilde{r}^2}{4} \left(1 - \frac{2\tilde{m}}{\tilde{r}} \right) \chi'^2 + \frac{\sin^2 \chi}{2} + \frac{1}{2\lambda_H^2} \sin^2 \chi \left\{ \left(1 - \frac{2\tilde{m}}{\tilde{r}} \right) \chi'^2 + \frac{\sin^2 \chi}{2\tilde{r}^2} \right\} \right] \quad (13)$$

$$\delta' = -\kappa^2 f_S^2 \left[\frac{\tilde{r} \chi'^2}{2} - \frac{1}{\lambda_H^2} \frac{\chi'^2}{\tilde{r}} \sin^2 \chi \right] \quad (14)$$

$$\left\{ e^{-\delta} \tilde{r}^2 \left(1 - \frac{2\tilde{m}}{\tilde{r}} \right) \chi' \right\}' - e^{-\delta} \sin 2\chi + \frac{2}{\lambda_H^2} \sin \chi \left[\left\{ e^{-\delta} \left(1 - \frac{2\tilde{m}}{\tilde{r}} \right) \chi' \sin \chi \right\}' - e^{-\delta} \frac{1}{\tilde{r}^2} \cos \chi \sin^2 \chi \right] = 0, \quad (15)$$

where we have again normalized the scale length by the radius of the event horizon r_H . $\lambda_H \equiv r_H/[1/f_S g_S]$ describes the ratio of a radius of an event horizon to a typical scale of the present theory. Note that in the limit of $f_S \rightarrow 0$ the above equations are reduced to that of colored black hole case by replacement $\cos \chi$ with w and setting $g_S^2 = 4\pi g_C^2$ [13].

For the boundary conditions we demand the existence of a regular event horizon (8) and asymptotic flatness (9). We can restrict the value of χ at the horizon to the range $[-\pi, \pi]$ without loss of generality. Finiteness of the energy of the system gives us the asymptotic boundary condition for χ :

$$\chi(r) \longrightarrow 2n\pi \quad \text{as} \quad r \longrightarrow \infty, \quad (16)$$

where n is an integer. $|n|$ denotes the winding number of the Skyrmin solution. In the case of Skyrme black hole, as a topology is trivial, the winding number, defined by [8]

$$W_n \equiv \frac{1}{2\pi} [\chi(r_H) - \sin(\chi(r_H))], \quad (17)$$

is no longer an integer. But, since W_n is close to $|n|$, we also call n the “winding number”.

We solve the field equations (13)-(15) under the above boundary conditions, and find two modes of solution. One is a family of solutions which is stable against linear radial perturbations [5]. The other is another family of solutions which is an excited state of the first family and is unstable [8]. In the limit of $f_S \rightarrow 0$, the excited solution approaches the colored black hole in the EYM system [8].

The stable mode has critical values of $\lambda_{H,cr}$ for each coupling constant f_S and their “winding number” n . Beyond this value there is no non-trivial solution. For example $\lambda_{H,cr} = 340.85$ when $f_S/\sqrt{G} = 0.02$, $n = 1$. This means that the stable Skyrme black hole with large horizon radius (and then with large mass) does not exist. In the previous example, these critical values are $r_{H,cr} = 68.17l_P$ and $M_{cr} = 46.30m_P$ for $g_S = 0.1$ respectively. The critical value $\lambda_{H,cr}$ gets small as n increases ($\lambda_{H,cr} = 109.19$ for $f_S/\sqrt{G} = 0.02$, $n = 2$), (See also Fig. 4). The family of excited solutions also has the same critical value of λ_H , where two family coincide each other.

This non-existence of large stable black holes provides us a scenario for the evolution of the Skyrme black holes. Suppose we have a stable Skyrme black hole initially. When a matter fluid falls into the black hole, the mass increases and then the radius of the event horizon increases[12,13]. If the horizon radius exceeds the above critical value, the Skyrme black hole shifts to a Schwarzschild black hole. The Skyrme “hair” may have dropped into the black hole beyond the event horizon. In this sense, a Skyrme black hole may not be stable unless the surroundings are just in a vacuum. One interesting fact is that when the Skyrme black hole evolves into a Schwarzschild black hole, the area of the black hole increases discretely (Fig. 4), which may be regarded as a first order phase transition because the area can be interpreted as the black hole entropy.

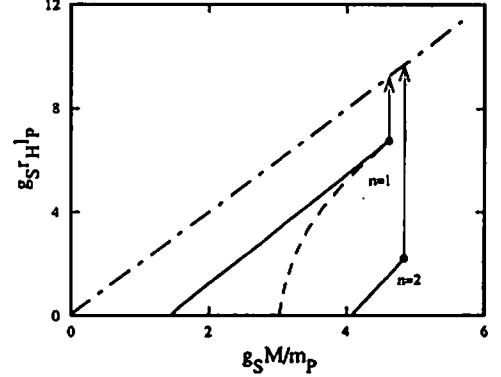


Figure 4: The relations between the mass and the horizon radius for the Skyrme black holes. We set $f_S/\sqrt{G} = 0.02$. The dots in right edges of the lines denote the limit of the solutions. Hence, by matter accretion, the black hole evolves into a Schwarzschild black hole (a dot-dashed line) as shown by the line with an arrow. This may be regarded as a first-order phase transition.

5 Thermodynamic Properties of Skyrme Black Holes

In Fig. 5 we show the temperature of Skyrme black holes. The stable mode has always negative specific heat and has no phase transition (Fig. 5(a)). In case of the excited mode (Fig. 5(b)), for large coupling constant f_S we find one phase transition point, but as f_S gets small, black holes has three phase transition points; $M_{1,cr}$, $M_{2,cr}$, $M_{3,cr}$. The critical point $M_{2,cr}$ is the same type as that of the Reissner-Nordström black hole and the smaller one ($M_{1,cr}$) corresponds to the lower critical point in the colored black hole type. Between $M_{1,cr}$ and $M_{2,cr}$, the specific heat becomes positive, when the Skyrme field becomes dominant. The largest critical point $M_{3,cr}$ appears only in the Skyrme black hole. Beyond $M_{3,cr}$, the specific heat becomes again positive. In the limit of $f_S \rightarrow 0$, the temperature of colored black hole is recovered. (Compare $\alpha = 0$ in Fig. 3 and $f_S/\sqrt{G} = 0.01$ in Fig. 5(b)).

From the above properties, we can speculate the following scenario for the evolution of Skyrme

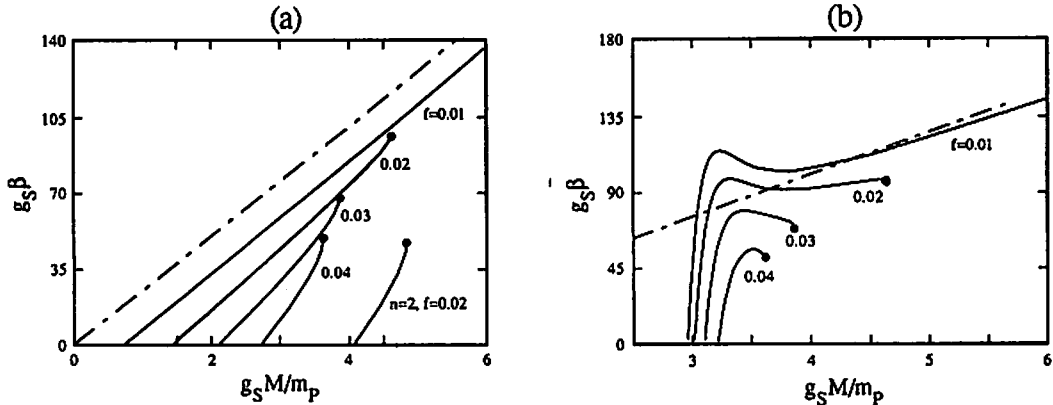


Figure 5: (a) The inverse temperature $\beta (= 1/T)$ of the Skyrme black hole with $n = 1$ as a function of M . The dots in right edges of the lines denote the limit of the solutions. We also show that of the Schwarzschild black hole by a dot-dashed line for comparison. (b) The inverse temperature $\beta = 1/T$ of excited modes of the Skyrme black holes as a function of M . The dots in right edges of the solid curves denote the limit of the solutions. The dot-dashed line is that of a Schwarzschild black hole.

black holes. If the surroundings of the black hole are just in a vacuum, those black hole will evaporate away by the Hawking's quantum process. The temperature of those black holes, however, becomes infinity when the mass approaches some non-zero finite value, e.g. $M = 14.50m_P$ for $f_S/\sqrt{G} = 0.02$, $g_S = 0.1$. Through the evaporation process, hence, the event horizon shrinks and eventually disappears, and the particle-like solution (Skyrmion) remains with a finite mass determined by the fundamental constants (g_S, f_S and m_P) and the "winding number" n .

6 Concluding Remarks – A Hair or A Wig –

We have shown the black hole solutions, with non-Abelian hair, in the Einstein-Yang-Mills-dilaton system, and study their temperatures and specific heats. If the dilaton coupling $\alpha < \alpha_{cr} \sim 0.5$, these dilatonic colored black holes have two phase transition points, between which the specific heat becomes positive. While the Skyrme black holes, which also have non-Abelian hair, do not have such a phase transition point and the specific heat is always negative in the stable mode, although the unstable excited mode has some phase transition points like a colored black hole. From the fact of the absence of the Skyrme black holes with a large mass, we conclude that either the black hole will evaporate away and leave a stable particle-like non-Abelian structure (Skyrmion) with a finite mass or the Skyrme black hole will evolve into the Schwarzschild black hole and lose its "Skyrme hair" by matter accretion. When the Skyrme black hole evolves into a Schwarzschild black hole, the area (the entropy) of black hole will increase by a finite amount, which may be regarded as a kind of first-order phase transition.

As for the stability of dilatonic colored black holes, they may be linearly unstable like a "pure"

colored black hole. Because the dilaton field Φ does not give a great change to the potential of first-order equations of linear perturbations compared with the colored black hole case, a bound state (a growing mode) may exist. This is now under investigation.

From the present analysis, we may extract a common property for both non-Abelian “hair”s. When the (dilaton) colored black hole becomes large, the YM “hair” will not give so much contribution on the black hole structure. We just find the Schwarzschild black hole with non-trivial YM structure. While, for the case of the Skyrme black hole, there is no large black hole with the Skyrme “hair”. In both cases, the mass energy of non-Abelian gauge field structure seems to be “quantized” by the fundamental constants just as for the particle-like solutions. In fact there is no such a particle-like structure with large mass. Rather its mass is “quantized” and this “discretized” mass is specified by the node number or the “winding number”. When the mass of the black hole gets large, hence, the contribution from those non-Abelian gauge field structure becomes small, finally finding the trivial Schwarzschild solution. In the case of the Skyrme black hole, we guess, such a structure may be hardly stretched because of its “winding number” and hence the size is also compactified. It cannot co-exist with the black hole structure because the size of those structure becomes smaller than the horizon scale. When the black hole gets large, the “Skyrme hair” may fall into the black hole. From those facts, it may be more suitable to call those non-Abelian structure as “a wig” instead of “a hair”. “A wig” is more unstable than a “hair” and it is easily put off.

– Acknowledgements –

We would like to thank T. Maki and T. Tachizawa for discussion and L.D. Gunnarsen for his critical reading of our report. This work was supported partially by the Grant-in-Aid for Scientific Research Fund of the Ministry of Education, Science and Culture (No. 04234211 and No. 04640312), by a Waseda University Grant for Special Research Projects, and by The Sumitomo Foundation.

References

- [1] R. Bartnik and J. McKinnon, Phys. Rev. Lett. 61 (1988) 141.
- [2] M.S. Volkov and D.V. Galt'sov, Sov. J. Nucl. Phys. 51 (1990) 747;
P. Bizon, Phys. Rev. Lett. 64 (1990) 2844;
H.P. Künzle and A.K. Masoud-ul-Alam, J. Math. Phys. 31 (1990) 928.
- [3] N. Straumann and Z.-H. Zhou, Phys. Lett. B 243 (1990) 33;
Z.-H. Zhou and N. Straumann, Nucl. Phys. B 360 (1991) 180;
P. Bizon, Phys. Lett. B 259 (1991) 53;
P. Bizon and R.M. Wald, Phys. Lett. B 267 (1991) 173.
- [4] S. Droz, M. Heusler and N. Straumann, Phys. Lett. B 268 (1991) 371.
- [5] M. Heusler, S. Droz and N. Straumann, Phys. Lett. B 271 (1991) 61.
- [6] We learned of the paper by G. Lavrelashvili and D. Maison, Phys. Lett. B 295 (1992) 67, in which the authors show the existence of particle-like solution in Yang-Mills-dilaton system.

- [7] G. W. Gibbons and K. Maeda, Nucl. Phys. B 298 (1988) 741.
For the recent works, see also D. Garfinkle, G. T. Horowitz and A. Strominger, Phys. Rev. D 43 (1991) 3140.
- [8] When we were writing this manuscript, we found the paper on the Skyrme black hole by P. Bizon and T. Chmaj, Phys. Lett. B 297 (1992) 55. They have found the similar results to ours, e.g. the existence of two modes and non-existence of a large black hole. Although they presented the stability analysis, which we have not studied, we have further discussed the dynamical evolution and the fate of the Skyrme black hole.
- [9] We use units such that $c = \hbar = k_B = 1$. As for notation and conversion we follow C. W. Misner, K.S. Thorne and J.A. Wheeler *Gravitation*, (Freeman, 1973).
- [10] The temperature of the colored black hole ($\alpha = 0$) which we calculate does not agree with I. Moss and A. Wray, Phys. Rev. D 46 (1992) R1215. The difference is exactly that from the term $e^{-\delta_H}$ in Eq.(10). They may set $\delta_H = 0$, which is not correct, when they calculate the temperature.
- [11] We adopt the coupling constant g_S in the ES system different from g_C in the EYMD system. In order to recover the basic equations in EYM case in the limit, we have to replace g_S with g_C .
- [12] D.Sudarsky and R. M. Wald, Phys. Rev. D 46 (1992) 1453.
- [13] I. Moss, Phys. Rev. Lett. 69 (1992) 1852.

Exact Solution for a Black Hole with a Thin Disk [†]

Takahiro Azuma *

Faculty of Liberal Arts, Dokkyo University

Soka, Saitama 340, Japan

ABSTRACT

The static soliton solutions to the vacuum Einstein equation with axial symmetry is considered. It is shown that the 6-soliton solution constructed from one pair of real pole trajectories and two pairs of complex conjugate pole trajectories describes the gravitational field with asymptotic flatness, which is produced by a black hole surrounded by a thin disk.

The soliton technique to solve the gravitational field equation[1] provides us an infinite series of exact solutions to the vacuum Einstein equation with axial symmetry. For example, the 2-soliton solution with asymptotic flatness is the Kerr black hole solution and a certain limit of the 4-soliton solution is the Tomimatsu-Sato solution in the stationary case. In the static case the 2-soliton solution corresponds to the Weyl solution and the solutions with higher soliton numbers are interpreted as the nonlinear superpositions of multi-Weyl solutions[2,3]. These solutions are

[†] Based on the work in collaboration with M. Endo and T. Koikawa.

* E-mail address: azuma@jpndokyo.bitnet

obtained by adopting only real pole trajectories in constructing the soliton solutions. The solutions with complex pole trajectories have been little considered and it is recently that they were shown to have interesting features[3,4,5]. In this report we consider the 6-soliton solution constructed from one pair of real pole trajectories and two pairs of complex conjugate pole trajectories. It will be shown that the solution describes the gravitational field with asymptotic flatness, which is produced by a black hole surrounded by a thin disk.

The solution is given by

$$-ds^2 = -f dt^2 + f^{-1}[Q(d\rho^2 + dz^2) + \rho^2 d\phi^2], \quad (1)$$

with

$$f = f_{BH} f_D, \quad Q = Q_{BH} Q_D Q_I, \quad (2)$$

where

$$f_{BH} = -\frac{\mu_a \mu_b}{\rho^2}, \quad (3)$$

$$f_D = \frac{|\mu_1|^2 |\mu_2|^2}{\rho^4}, \quad (4)$$

$$Q_{BH} = \frac{\rho^2 (\mu_a - \mu_b)^2}{(\mu_a^2 + \rho^2)(\mu_b^2 + \rho^2)}, \quad (5)$$

$$Q_D = \frac{\rho^8 |\mu_1 - \mu_2|^4 |\mu_1 - \bar{\mu}_2|^4 (\mu_1 - \bar{\mu}_1)^2 (\mu_2 - \bar{\mu}_2)^2}{2^8 \Sigma_1^2 \Sigma_2^2 |\mu_1^2 + \rho^2|^2 |\mu_2^2 + \rho^2|^2 |\mu_1|^4 |\mu_2|^4}, \quad (6)$$

$$Q_I = \frac{\rho^8 |\mu_a - \mu_1|^4 |\mu_a - \mu_2|^4 |\mu_b - \mu_1|^4 |\mu_b - \mu_2|^4}{2^8 (m^2 + \Sigma_1^2)^2 (m^2 + \Sigma_2^2)^2 |\mu_1|^4 |\mu_2|^4 (\mu_a \mu_b)^4}. \quad (7)$$

Here μ_a and μ_b are the real pole trajectories

$$\mu_a = -(m + z) + \sqrt{(m + z)^2 + \rho^2}, \quad (8a)$$

$$\mu_b = (m - z) - \sqrt{(m - z)^2 + \rho^2}, \quad (8b)$$

μ_1 and μ_2 are the complex pole trajectories

$$\mu_1 = i\Sigma_1 - z + [(i\Sigma_1 - z)^2 + \rho^2]^{1/2}, \quad (9a)$$

$$\mu_2 = i\Sigma_2 - z - [(i\Sigma_2 - z)^2 + \rho^2]^{1/2}, \quad (9b)$$

and $\bar{\mu}_1$ and $\bar{\mu}_2$ are the complex conjugate trajectories to μ_1 and μ_2 , respectively.

If we introduce the $(r - \theta)$ coordinates by

$$\rho = \sqrt{r(r - 2m)} \sin \theta, \quad z = (r - m) \cos \theta, \quad (10)$$

f_{BH} and Q_{BH} reduce to

$$f_{BH} = 1 - \frac{2m}{r}, \quad Q_{BH} = \frac{r(r - 2m)}{r^2 - 2mr + m^2 \sin^2 \theta}, \quad (11)$$

which shows that they describe a Schwarzschild black hole. In the spatial infinity $\rho, z \rightarrow \infty$, f_D , Q_D and Q_I tend to 1 and so the solution is asymptotically flat. On the event horizon and along the z -axis defined by $\rho = 0$, f_D stays finite and $Q_D = Q_I = 1$, which means that the event horizon evades defectiveness and the axis retains a locally Euclidean nature. We also find that $Q_D \rightarrow \infty$ at $z = 0$ and $\rho = \Sigma_k (k = 1, 2)$, which constitutes two rings located on the $z = 0$ plane outside the event horizon. In addition to this we find that there is discontinuity of the derivatives of f_D and Q_D on the $z = 0$ plane. In order to see this behavior let us assume that $\Sigma_1 < \Sigma_2$ and expand $\ln f_D$ and $\ln Q_D$ in the neighbourhood of $z = 0$. We obtain for $\rho > \Sigma_2$

$$\ln f_D = 2 \left(\frac{1}{\sqrt{\rho^2 - \Sigma_1^2}} - \frac{1}{\sqrt{\rho^2 - \Sigma_2^2}} \right) |z| + \mathcal{O}(|z|^3), \quad (12)$$

$$\ln Q_D = \ln \frac{(\sqrt{\rho^2 - \Sigma_1^2} + \sqrt{\rho^2 - \Sigma_2^2})^4}{2^4(\rho^2 - \Sigma_1^2)(\rho^2 - \Sigma_2^2)} + \mathcal{O}(z^2), \quad (13)$$

and for $\Sigma_1 < \rho < \Sigma_2$

$$\ln f_D = \ln \frac{(\Sigma_2 + \sqrt{\Sigma_2^2 - \rho^2})^2}{\rho^2} - \frac{2}{\sqrt{\rho^2 - \Sigma_1^2}} |z| + \mathcal{O}(z^2), \quad (14)$$

$$\ln Q_D = \ln \frac{\rho^2(\Sigma_2^2 - \Sigma_1^2)^2}{2^4(\rho^2 - \Sigma_1^2)(\Sigma_2^2 - \rho^2)\Sigma_2^2} + \frac{4\Sigma_2}{\sqrt{\rho^2 - \Sigma_1^2}\sqrt{\Sigma_2^2 - \rho^2}} |z| + \mathcal{O}(z^2). \quad (15)$$

The existence of the terms including $|z|$ in these expansions shows the discontinuity of the derivatives with respect to z . Note that there is not any kind of discontinuity

in the region $0 < \rho < \Sigma_1$ and so the solution is regular there. The components of the Einstein tensor, which consist of the derivatives of $\ln f$ and $\ln Q$, therefore include the terms with the $\delta(z)$. This means that the vacuum Einstein does not hold on the plane given by $\rho > \Sigma_1$ and $z = 0$ and a certain disk-like source exists there.

The properties of the disk-like source can be elucidated by calculating the energy-momentum tensor of the source, which is directly given by the calculation of the Einstein tensor. The results are for $\rho > \Sigma_2$

$$T_{D\nu}^\mu = \frac{2^6 \sqrt{\rho^2 - \Sigma_1^2} \sqrt{\rho^2 - \Sigma_2^2} (\Sigma_2^2 - \Sigma_1^2)}{(\sqrt{\rho^2 - \Sigma_1^2} + \sqrt{\rho^2 - \Sigma_2^2})^5} \delta(z) \text{diag}(-1, 0, 0, 0), \quad (16)$$

for $\Sigma_1 < \rho < \Sigma_2$

$$\begin{aligned} T_{D\rho}^\rho &= T_{Dz}^z = 0, \\ T_{Dt}^t &= \frac{2^6 \Sigma_2^3 (\Sigma_2 + \sqrt{\Sigma_2^2 - \rho^2})^3 \sqrt{\rho^2 - \Sigma_1^2} \sqrt{\Sigma_2^2 - \rho^2}}{\rho^4 (\Sigma_2^2 - \Sigma_1^2)^2} \delta(z), \\ T_{D\phi}^\phi &= \frac{2^6 \Sigma_2^3 (\Sigma_2 + \sqrt{\Sigma_2^2 - \rho^2})^2 \sqrt{\rho^2 - \Sigma_1^2} \sqrt{\Sigma_2^2 - \rho^2}}{\rho^4 (\Sigma_2^2 - \Sigma_1^2)^2} \delta(z), \end{aligned} \quad (17)$$

and for $\rho < \Sigma_1$ $T_{D\nu}^\mu = 0$. Note that we have taken only the disk part of the solution into account to obtain these expressions. There is of course contribution from the interaction between the black hole and disk but it does not change the essential behaviors of $T_{D\nu}^\mu$. From Eq. (16) we find that the outer part of the disk defined by $\rho > \Sigma_2$ and $z = 0$ has positive energy density and zero pressure. Therefore this part behaves like dust. As $\rho \rightarrow \infty$, the energy density decreases rapidly as

$$\epsilon \sim \frac{2(\Sigma_2^2 - \Sigma_1^2)}{\rho^3} \delta(z), \quad (18)$$

which assures the asymptotic flatness of the solution. On the other hand, Eq. (17) shows that the inner part defined by $\Sigma_1 < \rho < \Sigma_2$ and $z = 0$ has negative energy density and positive pressure. The equation of state is given by

$$\epsilon = -\frac{\Sigma_2 + \sqrt{\Sigma_2^2 - \rho^2}}{\Sigma_2} p. \quad (19)$$

We have shown that the solution considered here describes the asymptotically flat gravitational field produced by a black hole and disk. The black hole is surrounded by the disk which is composed of two parts. The outer part consists of dust and the inner part consists of the matter with negative energy density (Fig. 1). The negative energy density of the inner part may be unphysical. It is natural to guess that this comes from the static condition of the solution. Therefore the stationary case in which the rotation of the disk is taken into account might be worth studying to seek a physical solution.

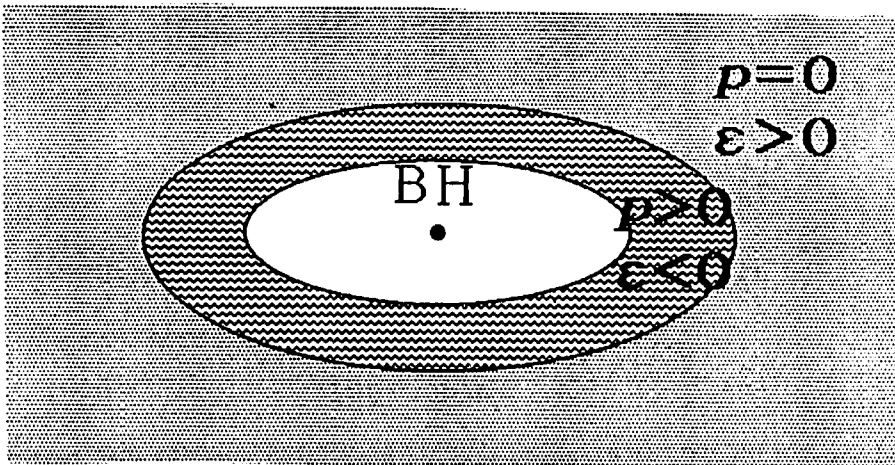


Fig. 1 A black hole surrounded by a thin disk.

REFERENCES

- [1] V.A. Belinskii and V.E. Zakharov, Sov. Phys. JETP 50(1979)1.
- [2] G.A. Alekseev and V.A. Belinskii, Sov. Phys. JETP 51(1980)655.
- [3] T. Azuma and T. Koikawa, preprint OTSUMA-HEP-9201 and DMP 92-2.
- [4] T. Azuma and T. Koikawa, Gen. Rel. Grav. 24(1992)1223.
- [5] T. Azuma, M. Endo and T. Koikawa, in preparation.

Exact Solutions to the Einstein Equation with Scalar Fields

Takao Koikawa

School of Social Information Studies, Otsuma Women's University

9-1 Kamioyamada-Machi, Tama, Tokyo 206, Japan

ABSTRACT

We study the axially symmetric static Einstein equation coupled with a scalar field. The parallelism between the scalar field and a part of the metric in the Einstein equation enables one to obtain the soliton solutions for both the scalar field and the metric. Of the infinite series of solutions we focus on the solution composed of 4-soliton solution of metric and 4-soliton solution of the scalar field. We give a physical interpretation of the solution that two Weyls with scalar charges are exactly sustained by the tension of a string which lies between the two Weyls.

In the preceding papers[1] the present author and Azuma have already exhausted the vacuum soliton solutions to the static Einstein equation and discussed their intriguing features. The solutions are classified by their soliton number together with the feature whether the poles are real or complex. In the last workshop on General Relativity and Gravitation held at Tokyo Metropolitan University in December 1991, we reported our result on the 4-soliton solution with real poles[2]. The physical interpretation of 2-soliton solution with real poles is the Weyl solution and the 4-soliton solution is the two Weyl connecte by a cosmic string with string tension μ . It is quite surprising that our investigation of the strenght of string tension shows the exact cancellation of the gravitational force between two Weyls. What is peculiar about this equation is that the string tension or the energy density per unit length becomes negative as far as two masses of the two Weyls are positive. In this paper we consider the case that the energy-momentum tensor is made up of a scalar field as a step toward the realistic situation of two rotating black holes connected by a cosmic string. We shall show an infinite series of soliton solutions of both the scalar field and the metric which are physically quite interesting. We focus on the 4-soliton solution of the scalar field and give the physical interpretation of it and then inquire the above difficulty of negative energy density. The metric is given by

$$-ds^2 = F(\rho, z)(d\rho^2 + dz^2) + g_{ab}(\rho, z)dz^a dz^b. \quad (a, b = 0, 1) \quad (1)$$

By introducing the 2×2 matrix $g = (g_{ab})$, the Einstein equation reads

$$(\rho g_{,\rho} g^{-1})_{,\rho} + (\rho g_{,z} g^{-1})_{,z} = 0, \quad (2a)$$

$$(\ln F)_{,\rho} = -\frac{1}{\rho} + \frac{1}{4\rho} \text{Tr}(U^2 - V^2) - \frac{2G}{c^4} \rho(\phi_{,\rho}^2 - \phi_{,z}^2), \quad (2b)$$

$$(\ln F)_{,z} = \frac{1}{2\rho} \text{Tr}(UV) - \frac{4G}{c^4} \rho \phi_{,\rho} \phi_{,z}, \quad (2c)$$

$$\frac{1}{\rho F} \{(\rho \phi_{,\rho})_{,\rho} + (\rho \phi_{,z})_{,z}\} = 0, \quad (2d)$$

where the 2×2 matrices U and V are defined by

$$U = \rho g_{,\rho} g^{-1}, \quad V = \rho g_{,z} g^{-1}. \quad (3)$$

In Eqs. (2a)-(2d) and thereafter $F_{,z}$ is a partial differentiation of F with respect to z . In Eqs. (2b) and (2c) $\phi(\rho, z)$ is a scalar field. The difference between the static and stationary conditions apperars in the diagonality of g . In the present static case g becomes diagonal and we express it as $g = \text{diag}(-f, f^{-1}\rho^2)$. We can simplify the equations by introducing $Q(\rho, z)$ and $\tilde{Q}(\rho, z)$ by

$$F = f^{-1}Q\tilde{Q}, \quad (4)$$

and require that Q satisfy the vacuum Einstein equation. We further introduce ψ by

$$f = \exp(2\psi). \quad (5)$$

Eventually we have

$$(\rho\psi_{,\rho})_{,\rho} + (\rho\psi_{,z})_{,z} = 0, \quad (6a)$$

$$(\ln Q)_{,\rho} = 2\rho(\psi_{,\rho}^2 - \psi_{,z}^2), \quad (6b)$$

$$(\ln Q)_{,z} = 4\rho\psi_{,\rho}\psi_{,z}, \quad (6c)$$

$$(\rho\phi_{,\rho})_{,\rho} + (\rho\phi_{,z})_{,z} = 0, \quad (6d)$$

$$(\ln \tilde{Q})_{,\rho} = -\frac{2G}{c^4}\rho(\phi_{,\rho}^2 - \phi_{,z}^2), \quad (6e)$$

$$(\ln \tilde{Q})_{,z} = -\frac{4G}{c^4}\rho\phi_{,\rho}\phi_{,z}. \quad (6f)$$

This shows the parallelism between ψ and ϕ .

The procedure of solving the Einstein equations is first obtaining ψ from Eq.(6a). Then by substituting them into Eqs.(6b) and (6c) and integrating them we obtain Q . In the similar way we obtain \tilde{Q} . The last step or the integration is not always easy but we do not encounter the difficulty in a special case. When $Q\tilde{Q} = 1$ we do not need to obtain Q and \tilde{Q} respectively. We shall illustrate this in the follwing (i)non-soliton case and also discuss it in the(ii)soliton case in connection with Papapetrou-Majumdar-Myers(PMM) solution[3].

(i)non-soliton case. It is easy to see that Eqs.(6a) and (6d) are solved by

$$\begin{aligned}\phi &= \sum_i \frac{e_i}{\sqrt{\rho^2 + (z - a_i)^2}}, \\ \psi &= \sum_i \frac{m_i}{\sqrt{\rho^2 + (z - a_i)^2}}.\end{aligned}\tag{7}$$

Though it is not easy to integrate Eqs.(6b) and (6c) to obtain Q and \tilde{Q} for these solutions, we do not need their explicit form as far as the following condition holds:

$$m_i = e_i. \quad (i = 1, \dots, n)\tag{8}$$

When this condition holds, the metric becomes

$$-ds^2 = -\Phi^{-2}dt^2 + \Phi^2 d\vec{z}^2,\tag{9}$$

with

$$\Phi = \exp\left(\sum_i m_i / |\vec{z} - \vec{z}_i|\right).\tag{10}$$

This solution should be compared with the PMM solution which expresses the maximally charged black holes. The four-metric and four-potential are given by

$$\begin{aligned}-ds^2 &= -\tilde{\Phi}^{-2}dt^2 + \tilde{\Phi}^2 d\vec{z}^2, \\ A &= -(1 - \tilde{\Phi}^{-1})dt,\end{aligned}\tag{11a}$$

where

$$\tilde{\Phi} = 1 + \sum_i m_i / |\vec{z} - \vec{z}_i|.\tag{11b}$$

In the limit $|\vec{z}| \gg 1$, the above two four-metrics coincide despite the difference of the energy-momentum tensor constituent: scalar field or electric field.

(ii)soliton case. We shall next consider the soliton solution. We note that Eqs. (6a) – (6c) are the same as those for the vacuum case. In the previous papers[3,4] we have already written down the exact vacuum solutions and discussed their intriguing physical interpretations. We can now make use of the solutions

not only to ψ but also to the scalar field ϕ . We can therefore write a series of exact soliton solutions of scalar field as

$$\phi = \frac{c^2}{\sqrt{G}} \ln \left(i^n \frac{\tilde{\mu}_1 \tilde{\mu}_2 \cdots \tilde{\mu}_n}{\rho^n} \right)^{-q}, \quad (12a)$$

with

$$\tilde{\mu}_k = \tilde{w}_k - z \pm \sqrt{(\tilde{w}_k - z)^2 + \rho^2}, \quad (k = 1, 2, \dots, n) \quad (12b)$$

where G is the Newtonian constant. In the above equation the coefficient c^2/\sqrt{G} is attached in order to give the due dimension to the scalar field. Here \tilde{w}_k 's are constants which could be real or complex. The \pm sign in front of the square root in $\tilde{\mu}_k$'s is to be determined so that the scalar field vanishes asymptotically. The behavior of the soliton type solution near the origin is quite different from the non-soliton type solution. Now we obtain \tilde{Q} by substituting the solution to r. h. s. of Eqs. (6e) and (6f) and then integrating the equations just as we obtain Q from Eqs. (6b) and (6c) by substituting the solution ψ . We thus obtain

$$\tilde{Q} = \left[\frac{\rho^{n^2/2} \prod_{k>l} (\tilde{\mu}_k - \tilde{\mu}_l)^2}{\prod_k (\rho^2 + \tilde{\mu}_k^2) \prod_l \tilde{\mu}_l^{n-2} \tilde{C}^{(n)}} \right]^{q^2}, \quad (13a)$$

with

$$\tilde{C}^{(n)} = 2^{\frac{n}{2}(n-2)} \prod_{k>l}^{n/2} (\tilde{w}_{2k-1} - \tilde{w}_{2l-1})^2 (\tilde{w}_{2k} - \tilde{w}_{2l})^2. \quad (13b)$$

Just as we classified the vacuum solutions according as the pole trajectories μ_k 's are real or complex for every soliton number, we can classify the above solutions by complexness of $\tilde{\mu}_k$'s. In the vacuum case, the physically interesting solutions appear in the 4-soliton solution with real poles and complex poles. We called the 4-soliton solution with complex poles the "2-ring solution" which is free from the divergence of the curvature invariants[3]. The further investigation showed that the solution corresponds to that obtained by the disk-like source on the surface determined by two rings and it ranges outside of the inner ring[4]. On the other hand the interpretation of the 4-soliton solution with real poles is

the two coalesced Weyls sitting on the z -axis with a certain distance. In this note we shall concentrate on this real pole case.

Before we discuss the 4-soliton solution of the scalar field, we first consider the 2-soliton solution. The solution is given by

$$\phi = \frac{c^2}{\sqrt{G}} \ln \left(-\frac{\tilde{\mu}_1 \tilde{\mu}_2}{\rho^2} \right)^{-q}, \quad (14)$$

with

$$\begin{aligned} \tilde{\mu}_1 &= \tilde{w}_1 - z + \sqrt{(\tilde{w}_1 - z)^2 + \rho^2}, \\ \tilde{\mu}_2 &= \tilde{w}_2 - z - \sqrt{(\tilde{w}_2 - z)^2 + \rho^2}. \end{aligned} \quad (15)$$

We assume that $\tilde{w}_1 < \tilde{w}_2$ and parametrize them as $\tilde{w}_1 = z_0 - \sigma$ and $\tilde{w}_2 = z_0 + \sigma$. By introducing the prolate spheroidal coordinates (x, y) by

$$\begin{aligned} \rho &= \sigma \sqrt{(x^2 - 1)(1 - y^2)}, \\ z - z_0 &= \sigma xy, \end{aligned} \quad (16)$$

Eq. (14) reads

$$\phi = \frac{-qc^2}{\sqrt{G}} \ln \left(\frac{x - 1}{x + 1} \right). \quad (17)$$

When the distance from the origin is large the spheroidal coordinate x is approximated to

$$x \sim \frac{\sqrt{\rho^2 + z^2}}{\sigma}. \quad (18)$$

Substituting this into Eq. (14), we obtain

$$\phi \sim \frac{2q\sigma c^2/\sqrt{G}}{\sqrt{\rho^2 + z^2}}, \quad (19)$$

for large $\sqrt{\rho^2 + z^2}$. This shows that the charge e of the scalar field is given by $e = 2q\sigma c^2/\sqrt{G}$.

We shall next consider the case that both ψ and ϕ are 4-soliton solution with real poles. In Eq. (9) the constants \tilde{w}_k 's and q are not necessarily the same as those in the poles constituting the metric. But here we assume that $\tilde{w}_k = w_k$.

Taking the boundary condition into account, we choose the \pm signs in μ_k 's to obtain the explicit solution:

$$\psi = \frac{1}{2} \ln \left(\frac{\mu_1 \mu_2 \mu_3 \mu_4}{\rho^4} \right)^\delta, \quad (20a)$$

$$\phi = \frac{c^2}{\sqrt{G}} \ln \left(\frac{\mu_1 \mu_2 \mu_3 \mu_4}{\rho^4} \right)^{-q}, \quad (20b)$$

with

$$\begin{aligned} \mu_1 &= w_1 - z + \sqrt{(w_1 - z)^2 + \rho^2}, \\ \mu_2 &= w_2 - z - \sqrt{(w_2 - z)^2 + \rho^2}, \\ \mu_3 &= w_3 - z - \sqrt{(w_3 - z)^2 + \rho^2}, \\ \mu_4 &= w_4 - z + \sqrt{(w_4 - z)^2 + \rho^2}. \end{aligned} \quad (21)$$

Assuming that $w_1 < w_2 < w_3 < w_4$, we shall parameterize w_k 's as $w_1 = z_1 - \sigma_1$, $w_2 = z_1 + \sigma_1$, $w_3 = z_2 - \sigma_2$ and $w_4 = z_2 + \sigma_2$. In order to clarify the structure of Eq. (20b) we introduce the prolate spheroidal coordinates (x, y)

$$\begin{aligned} \rho &= \sigma_1 \sqrt{(x^2 - 1)(1 - y^2)}, \\ z - z_1 &= \sigma_1 xy. \end{aligned} \quad (22)$$

Then we find that Eq. (20b) behaves as

$$\phi = -\frac{qc^2}{\sqrt{G}} \ln \left(\frac{z-1}{z+1} \left[1 + \mathcal{O} \left(\frac{1}{|z_2 - z_1|} \right) \right] \right). \quad (23)$$

This shows that the charge $e_1 = 2q\sigma_1 c^2 / \sqrt{G}$ of the scalar field sits at $z = z_1$ and $\rho = 0$ when $|z_2 - z_1| \gg 1$. Similarly we can show that another charge $e_2 = 2q\sigma_2 c^2 / \sqrt{G}$ sits at $z = z_2$ and $\rho = 0$ when $|z_2 - z_1| \gg 1$. It is interesting to observe the vicinity of the z -axis between two Weyls. It is not flat and we can measure the deviation from Euclidian metric by using P_0 defined by

$$P_0^2 \equiv \lim_{\rho \rightarrow 0} \left(\frac{g_{\phi\phi}}{\rho^2 g_{\rho\rho}} \right). \quad (24)$$

The difficulty in the physical interpretation of the vacuum solution is that the string tension or the energy density per unit length is negative as far as the

masses of two Weyls are both positive[3]. It can be positive only when one of the Weyls has the negative mass, though this might not be so serious because such a case occurs only when we consider the far separated limit. In the present case there is a way out.

P_0 is now given by

$$P_0 = \left[\frac{(z_2 - z_1)^2 - (\sigma_2 - \sigma_1)^2}{(z_2 - z_1)^2 - (\sigma_2 + \sigma_1)^2} \right]^{\delta^2 - 4q^2} \quad (25)$$

$$\rightarrow 1 - 4G \left(-G \frac{M_1 M_2}{|z_2 - z_1|^2} + \frac{e_1 e_2}{|z_2 - z_1|^2} \right), \quad \text{as } |z_2 - z_1| \rightarrow \infty,$$

where $M_i = \delta c^2 \sigma_i / G (i = 1, 2)$ and $e_i = 2qc^2 \sigma_i / \sqrt{G} (i = 1, 2)$. The comparison with the metric in the presence of the cosmic string[5] with the string tension μ yields

$$\mu = -G \frac{M_1 M_2}{|z_2 - z_1|^2} + \frac{e_1 e_2}{|z_2 - z_1|^2}. \quad (26)$$

We find that the sign of μ depends on the strength of two "charges" of the two Weyls, or the masses and the scalar charges. From the string tension view point the negative μ corresponds to the repulsive force and the positive μ to the attractive force. It is now possible to require that the energy density per unit length or μ be positive even when two Newtonian masses M_1 and M_2 are positive. The non negative energy condition reads

$$e_1 e_2 \geq (\sqrt{G} M_1) (\sqrt{G} M_2). \quad (27)$$

We consider the case that the string tension vanishes. This is satisfied by the condition

$$\delta^2 - 4q^2 = 0. \quad (28)$$

In this case the metric simplifies into

$$-ds^2 = -\Phi^{-2} dt^2 + \Phi^2 d\vec{x}^2, \quad (29a)$$

$$\phi = \frac{c^2}{\sqrt{G}} \ln \left(i^n \frac{\tilde{\mu}_1 \tilde{\mu}_2 \cdots \tilde{\mu}_n}{\rho^n} \right)^{-q},$$

with

$$\Phi = \left(i^n \frac{\mu_1 \mu_2 \cdots \mu_n}{\rho^n} \right)^{-q} \quad (29b)$$

This should be also compared with MMP solution[3]. We should note that conditions that the metric get simplified in the non-soliton and soliton cases are different(see Eq.(8) and Eq.(28)). Both conditions leads to the balancing between the gravitational and scalar field interaction forces. However, as far as we consider the balancing between them, the weaker conditon Eq.(28) in the soliton case is natural.

The author would like to thank all the organizers of the workshop. He acknowledges Prof.Azuma for discussion and needs to say that the present paper and his talk at the meeting partly depends on the preprint[6].

References

- [1] T. Azuma and T. Koikawa, Gen. Rel. Grav.24(1992)1223;
preprint OTSUMA-HEP-9201 and DMP 92-2.
- [2] T. Koikawa, In the Proceeding of the Workshop on General Relativity and Grav-
itation edited by K.Maeda and et al.(1991).
- [3] A.Papetrou, Proc.R.Irish Acad.A51(1947)191.
S.D.Majumdar, Phys.Rev.72(1947)930.
R.C.Myers, Phys.Rev.D35(1987)455.
- [4] T. Azuma, M. Endo and T. Koikawa, in preparation.
- [5] A. Vilenkin, Phys. Rev. D23(1981)852.
- [6] T. Azuma, T. Koikawa, preprint OTSUMA-HEP-9202 and DMP 92-3.

Inhomogeneities in the de Sitter Space-Time

Ken-ichi Nakao

Department of Physics, Kyoto University, Kyoto 606, Japan

1. Introduction

Our universe observed today is homogeneous and isotropic. The standard Big Bang scenario is based on this observational fact and can explain the important observational facts, i.e., the Hubble's expansion law, 2.7K cosmic microwave background radiation and the abundance of light elements. However, since the homogeneity is just the basic principle in the Big Bang scenario, we cannot get a natural answer within the framework of this scenario for the question why our universe is so homogeneous at present. The inflationary-universe scenario is one of the most favorable models to resolve the above question, the so-called homogeneity problem.^[1] In this scenario, the vacuum energy due to the phase transition by inflaton scalar field dominates at very early stage of the universe. Since the vacuum energy of the inflaton field behaves like as the cosmological constant, the universe undergoes the de Sitter-like rapid cosmic expansion. After a phase transition, the vacuum energy is converted into radiation and the standard Big Bang model is recovered. Initial inhomogeneities are stretched and go outside the horizon by the rapid cosmic expansion, resulting in the present homogeneity of the universe.

However, even though there is a positive cosmological constant exists, it is not obvious whether the de Sitter-like rapid cosmic expansion is always realized or not. Since the inhomogeneities have "energy" and generate the gravitational field by themselves, those may collapse into a black hole or a naked singularity. In connection with this problem, the "cosmic no hair conjecture" is proposed, which states that "all" space-times approach the de Sitter space-time asymptotically if a positive cosmological constant exists.^[2] If this conjecture is true or almost true, we can understand why the present universe is so homogeneous.

In the realistic inflationary scenario, the cosmological constant is given by the vacuum energy of the inflaton field and hence the inhomogeneity of the cosmological “constant” itself is important for the onset of the inflation. So several authors have investigated the inhomogeneities of the inflaton field both in analytic and numerical approaches.^[3–9] However, inhomogeneities except for the cosmological “constant” are important too. Because, when we discuss about the onset of inflation, such inhomogeneities may also not so small before the de Sitter-like rapid expansion.

In this literature, we consider the space-times with isolated inhomogeneities and a cosmological constant (called asymptotically de Sitter space-times). In Sec.2, we show the Schwarzschild-de Sitter space-time and the Oppenheimer-Snyder-type collapsing dust solution in the de Sitter space-time, which are the simplest examples of the asymptotically de Sitter space-time. In Sec.3, we investigate initial data for the gravitational waves and the Einstein-Rosen bridges. These examples show the important feature of the inhomogeneities in the de Sitter space-time. As already mentioned, since the inhomogeneities are equivalent to the energy, these produce the gravitational field by themselves and may collapse into the black holes or naked singularities. In reality, it is well known that in the case of the asymptotically flat space-time, the large and well localized inhomogeneities form apparent horizons and evolved into black holes. However, our examples show that even though the inhomogeneities are localized enough, these inhomogeneities with large “gravitational mass” can not collapse into black holes. Hence, the inhomogeneities form only the small black holes and those may be diluted by the de Sitter-like rapid cosmic expansion which will be realized later stage. As a result, the cosmic no hair conjecture seems to be valid for the practical inflationary scenario. In this literature, we adopt the units of $c = G = 1$.

2. The Schwarzschild-de Sitter and Oppenheimer-Snyder Space-Times

The simplest spherically symmetric examples of the asymptotically de Sitter space-time with a cosmological constant $\Lambda (= 3H^2)$ are given in this section.

2.1 THE SCHWARZSCHILD-DE SITTER SPACE-TIME

By the use of the Schwarzschild coordinates, the metric of the Schwarzschild-de Sitter space-time is written as,^[10]

$$ds^2 = -C(R)dT^2 + \frac{1}{C(R)}dR^2 + R^2(d\theta^2 + \sin^2\theta d\varphi^2), \quad (2.1)$$

with

$$C(R) = 1 - \frac{2M}{R} - H_0^2 R^2, \quad (2.2)$$

where M is the “gravitational mass”, which is often called Abbott-Deser (AD) conserved mass.^[11]

As the Schwarzschild space-time, $C = 0$ gives the positions of event horizons. However, there does not exist a positive root of $C = 0$ if $M > M_{crit} \equiv 1/(\sqrt{27}H)$. On the other hand, in the case of $M \leq M_{crit}$, we obtain the following positive roots,

$$\begin{aligned} R_B &= \frac{2}{H\sqrt{3}} \cos\left[\frac{1}{3}(\pi + \tan^{-1} \sqrt{\omega_e})\right], \\ R_C &= \frac{2}{H\sqrt{3}} \cos\left[\frac{1}{3}(\pi - \tan^{-1} \sqrt{\omega_e})\right], \end{aligned} \quad (2.3)$$

where

$$\omega_e \equiv \frac{1}{27M^2H^2} - 1. \quad (2.4)$$

It is always true that $R_B \leq R_C$. $R_B = R_C (= 3M)$ is realized if $M = M_{crit}$. Here it should be noted that when $M \geq M_{crit}$, the Schwarzschild-de Sitter space-time is no longer the black-hole solution. The Penrose diagrams for $M < M_{crit}$,

$M = M_{crit}$ and $M > M_{crit}$ are depicted in Fig.1(a), (b) and (c), respectively. In the case of $M < M_{crit}$, R_B is regarded as the position of the black-hole event horizon, while R_C is the position of the cosmological event horizon for timelike observers along $R = \text{constant}$ lines.

In the case of $M < M_{crit}$, there is the static timelike Killing vector and hence the Penrose diagram has a reflection symmetry with respect to the timelike direction. On the other hand, since there is no static timelike Killing vector in the case of $M \geq M_{crit}$, we should introduce a direction of the time evolution, in order to discuss the causal structure. Here we consider the inhomogeneities in the expanding de Sitter space-time. Under this circumstance, the direction of time-evolution is uniquely determined and is upward in Fig.1.^[13] Along this direction, the black-hole singularity is formed for $M < M_{crit}$, while the space-time approaches the de Sitter space-time asymptotically and there does not appear the black-hole singularity in the case of $M \geq M_{crit}$. Hence, in the case of $M \geq M_{crit}$, there is no black-hole event horizon. However, it should be noted that there is always an event horizon for any observer along a timelike curve λ , which is defined by the boundary of the causal past of λ , i.e., $J^-(\lambda)$,^[13] but, in general, this does not agree with the apparent horizon, in particular, for a dynamical problem.

2.2 THE OPPENHEIMER-SNYDER SPACE-TIME

The Oppenheimer-Snyder space-time with Λ describes the motion of a homogeneous dust sphere and is obtained by the junction between the interior closed Friedmann-Robertson-Walker (FRW) space-time and the exterior Schwarzschild-de Sitter space-time. This solution will give us more intuitive understanding about an inhomogeneity in the de Sitter space-time than the Schwarzschild-de Sitter space-time.

The metric of the interior closed FRW solution is written as

$$ds^2 = -d\tau^2 + a^2(\tau)(d\chi^2 + \sin^2 \chi d\Omega^2). \quad (2.5)$$

The Friedmann equation is given by

$$\left(\frac{da}{d\tau}\right)^2 = \frac{2m}{a} + H^2 a^2 - 1, \quad (2.6)$$

where

$$m \equiv \frac{4\pi}{3} \rho a^3, \quad (2.7)$$

with the energy density of the dust ρ .

In the interior space-time, the dust particles move along timelike geodesics. Since the metric and its first order derivative should be continuous across the surface of the dust sphere, the surface of the dust sphere moves along a timelike radial geodesic also in the exterior Schwarzschild-de Sitter space-time. Therefore, we can see the motion of a dust sphere by investigating geodesics in the Schwarzschild-de Sitter space-time. The radial geodesics in the Schwarzschild-de Sitter space-time obey the equation,

$$\left(\frac{dR_p}{dT_p}\right)^2 = \frac{1}{E^2}(E^2 - C(R)) \equiv -V(R), \quad (2.8)$$

where R_p and T_p are, respectively, the proper radius and proper time defined by

$$\begin{aligned} dT_p &= C^{1/2}(R) dT, \\ dR_p &= C^{-1/2}(R) dR. \end{aligned} \quad (2.9)$$

E is an integration constant which corresponds to the energy of a particle with unit mass. From the continuity of the metric and its first order derivative at the surface of the dust sphere $\chi = \chi_s$, we obtain the relation,

$$\begin{aligned} M &= m \sin^3 \chi_s, \\ E &= \cos \chi_s. \end{aligned} \quad (2.10)$$

Since Eq.(2.8) is the same form as the energy equation for a relativistic particle moving in the potential $V(R)$, the forbidden region for the motion of the

particle is given by $V(R) > 0$. The forbidden region $V > 0$ is depicted by the shaded region in Fig.2. It should be noted that there is no forbidden region for $M > M_{crit}$. Typical trajectories of the surface of the dust sphere is depicted in the Penrose diagram of the Schwarzschild-de Sitter space-time by solid lines with an arrow in Fig.1. Since, as already mentioned, the direction of time evolution is upward in Fig.1, there is no collapsing solution in the case of $M \geq M_{crit}$. Therefore, the dust sphere with large gravitational mass cannot collapse into black hole.

3. Analysis of Initial Data

Initial data for vacuum space-times with a cosmological constant $\Lambda (= 3H^2)$ must satisfy the Hamiltonian and momentum constraints, i.e.,

$$^{(3)}R - K_i^j K_j^i + K^2 = 6H^2, \quad (3.1)$$

$$D_j(K_i^j - \delta_i^j K) = 0, \quad (3.2)$$

where $^{(3)}R$ is the Ricci scalar of the three-dimensional spacelike hypersurface. K_i^j is the extrinsic curvature of the three-space and K is its trace part. D_j is the covariant derivative with respect to the intrinsic metric of the three-space.

Here we consider the case with the extrinsic curvature which has only a trace part, i.e.,

$$K_i^j = -H\delta_i^j. \quad (3.3)$$

Here, it should be noticed that, for isotropic and homogeneous space-time in which the scale factor a is spatially constant, the condition (3.3) turns out to be the Friedmann equation in terms of the cosmic time t , i.e., $a^{-2}(da/dt)^2 = H^2$, resulting in the de Sitter solution ($a = e^{Ht}$). Thus, the condition (3.3) is regarded as the assumption of the uniformly expanding background universe.

By virtue of the above condition, the Hamiltonian constraint reduces to the same as that of the time symmetric initial value for the vacuum space-time without Λ , i.e.,

$$^{(3)}R = 0, \quad (3.4)$$

and the momentum constraint is satisfied trivially.

We solve Eq.(3.4) in order to get initial data for localized nonlinear gravitational waves and Einstein-Rosen bridges. To get some physical insight to the cosmic no hair conjecture, we search for the apparent horizon which is determined by initial data only in contrast with the event horizon. Since the apparent horizon always exists within the event horizon (and coincides with the event horizon in the stationary space-time), the existence of the apparent horizon means the existence of the black hole.^[14]

The apparent horizon is a closed two-surface such that the expansion ρ of the future directed *outgoing* null geodesic congruence vanishes, where *outgoing* means the direction toward the asymptotically de Sitter region.^[15] Detailed formalism to obtain the apparent horizon was given by Sasaki et al.^[16]

3.1 NONLINEAR GRAVITATIONAL WAVES

The time symmetric initial data of localized gravitational waves without Λ were discussed by Brill^[17] and treated numerically by Eppley.^[18] The Brill's wave can be interpreted to a snap shot of an axisymmetric gravitational waves as a moment on maximum expansion (or minimum contraction). While, our wave solution corresponds to a snap shot of the waves in the uniformly expanding background because of the condition (3.3), although their procedure and discussion are almost valid in our case as well.

Following Brill, we write the intrinsic metric of the three-dimensional space-like hypersurface in the following form,

$$d\ell^2 \equiv \gamma_{ab}dx^a dx^b = \psi^4(R, z)[e^{Aq(R,z)}(dR^2 + dz^2) + R^2 d\varphi^2], \quad (3.5)$$

where A is a constant, which corresponds to the amplitude of the gravitational waves and $q(R, z)$ is an arbitrary function which satisfies the boundary conditions;

$$\begin{aligned} q = 0 = \partial_R q & \quad \text{at } R = 0, \\ q \rightarrow O(1/r^2) & \quad \text{or faster for } r \rightarrow +\infty, \end{aligned} \quad (3.6)$$

where $r = \sqrt{R^2 + z^2}$. q provides a localization of the waves. We, then, adopt the following function $q(R, z)$,

$$q(R, z) = \left(\frac{R}{r_0}\right)^2 \exp\left(-\frac{r^2}{2r_0^2}\right), \quad (3.7)$$

where r_0 is a constant, which corresponds to a width of the waves.

With Eqs.(3.5) and (3.7), the Hamiltonian constraint (3.4) is written as,

$$\partial_R^2 \psi + \frac{1}{R} \partial_R \psi + \partial_z^2 \psi + \frac{A}{8} U(R, z) \psi = 0, \quad (3.8)$$

where

$$U(R, z) = \left(\frac{2}{r_0^2} - \frac{6R^2}{r_0^4} + \frac{R^2 r^2}{r_0^6}\right) \exp\left(-\frac{r^2}{2r_0^2}\right). \quad (3.9)$$

We solve Eq.(3.8) numerically. In order to impose the asymptotic de Sitter boundary condition, we demand the ordinary asymptotically flat behavior for the conformal factor ψ as,

$$\psi \rightarrow 1 + \frac{M}{2r} \quad \text{for } r \rightarrow +\infty, \quad (3.10)$$

where M is constant. It is worthy to notice that M corresponds to the gravitational mass (AD mass) and, as shown by Brill, it is always positive for non-vanishing A .

From a regularity on the symmetric axis, $R = 0$, and from a reflection symmetry with respect to the equatorial plane, $z = 0$, the conformal factor ψ should satisfy the following boundary condition,

$$\partial_R \psi|_{R=0} = \partial_z \psi|_{z=0} = 0. \quad (3.11)$$

Here we search for the apparent horizon for various width r_0 of the gravitational waves for fixed cosmological constant, i.e., H . We expect that the gravitational waves localized enough becomes black hole. In the case of the asymptotically flat space-time ($H = 0$), we find the apparent horizon for $r_0 \leq r_{crit} \sim 1.3M$. This means that the large gravitational mass M produces the strong gravity and hence a black hole is formed in the case of the large gravitational mass M even if the gravitational waves are localized not so hard. On the other hand, in the case of $H > 0$, r_{crit} is not a monotonically increasing function of M as shown in Fig.3. As expected, for $M > M_{crit}$, there is no apparent horizon for all r_0 . Hence, it seems to be likely that the gravitational waves with large gravitational mass do not collapse into a black hole.

3.2 EINSTEIN-ROSEN BRIDGES

Initial data for N -Einstein-Rosen bridges with $H = 0$ were investigated by Brill and Lindquist^[19] and the more accurate analysis of two Einstein-Rosen bridges was performed by Cadez.^[20] Here we shall investigate two Einstein-Rosen bridges with $H > 0$.

Following Brill and Lindquist, in order to solve Eq.(3.4), we assume the conformally flat metric,

$$d\ell^2 = \psi^4 [dr^2 + r^2(d\theta^2 + \sin^2 \theta d\varphi^2)], \quad (3.12)$$

where $d\ell^2$ is the three-metric of the initial surface. With this metric, the Hamil-

tonian constraint (3.4) becomes the Laplace equation, i.e.,

$$\Delta\psi = 0, \quad (3.13)$$

where Δ is the flat Laplacian.

As for the time symmetric initial value problem without Λ , we know how to obtain the two-Einstein-Rosen-bridge (with equal mass) solution, which is just to set ψ as^[19]

$$\psi = 1 + \frac{M}{2\sqrt{r^2 + r_0^2 - 2r_0r \cos \theta}} + \frac{M}{2\sqrt{r^2 + r_0^2 + 2r_0r \cos \theta}}, \quad (3.14)$$

where M is an integration constant and r_0 is half of the Euclidean distance between two Einstein-Rosen bridges. $M \geq 0$ in order to guarantee the positivity of the gravitational mass (AD mass). Here (r, θ) is the spherical coordinates in the conformally flat three-space which origin is chosen to be the center of two Einstein-Rosen bridges. This solution has three asymptotically de Sitter regions, $r \rightarrow \infty$, $(r, \theta) \rightarrow (r_0, 0)$ and $(r, \theta) \rightarrow (r_0, \pi)$ (See Fig.4). We call the first asymptotic sheet S_0 and the others S_1 and S_2 , respectively.

The gravitational mass m of each Einstein-Rosen bridge and the total mass M_{tot} of those are, respectively, given by^[19]

$$m = M \left(1 + \frac{M}{4r_0} \right), \quad M_{tot} = 2M. \quad (3.15)$$

Then the “interaction energy” m_{int} is given by

$$m_{int} = M_{tot} - 2m = -\frac{M^2}{2r_0}. \quad (3.16)$$

The interaction energy is always negative and when the distance $2r_0$ between two bridges are infinite, the interaction energy vanishes.

If r_0 is enough large, i.e., $r_0 \gg M$, each Einstein-Rosen bridge can be seen as an isolated system with “mass” M . Hence, in such a circumstance, each Einstein-Rosen bridge has the same kinds of the apparent horizons as the one Einstein-Rosen bridge (a cross section of the Schwarzschild-de Sitter space-time by Buirkhoff’s theorem). On the other hand, if r_0 is not so large and “interaction energy” m_{int} is not negligible, each Einstein-Rosen bridge cannot be seen as an isolated system. We expect that there is some influence for the apparent horizons by the interaction between those Einstein-Rosen bridges. In fact, for the $\Lambda = 0$ case, as r_0 decreases and smaller than $r_{crit} = 0.766M$, the black-hole apparent horizon surrounding both Einstein-Rosen bridges appears.^[20] This means that the large gravitational mass produces the strong gravity, by which the black-hole apparent horizon enclosing two massive bridges appears even for large distance. Thus one may expect that one black hole is formed by observers on S_0 , if two Einstein-Rosen bridges are sufficiently close. However, as shown in Fig.5, in our case with $H > 0$, r_{crit} is not monotonically increasing function with respect to M but has a maximum value at $M \sim 0.35M_{crit}$. Hence, it seems that the Einstein-Rosen bridges with large “gravitational mass” are hard to coalesce with each other and to form a black hole if there exists Λ .

4. Discussion

We have investigated several examples of inhomogeneities in the de Sitter space-time (asymptotically de Sitter space-time). From these examples we may get some physical insight about dynamics of inhomogeneous space-time with a cosmological constant.

Although we have not shown in the preceding sections, one of the most important conjectures is that there is an upper bound on the areas of apparent horizons in space-time with a cosmological constant, i.e.,

$$A \leq 4\pi H^{-2}. \quad (4.1)$$

In fact, we can prove that the inequality (4.1) is true for initial data with $K_i^j = \frac{1}{3}K\delta_i^j$, where K is a constant.^[14] We can also conjecture that the area of event horizons in a stationary space-time has also the same bound. This is true for a static space-time with single cosmological horizon.^[21] We can also prove the black-hole area theorem in de Sitter background.^[14] The area of the black-hole event horizons must increase in time just as in the case of asymptotically flat space-time. Suppose that the universe approaches a stationary space-time. It is, then, likely to exist an upper bound also on the black-hole event horizon in de Sitter background, i.e., $A_{BH} \leq 4\pi H^{-2}$. This fact with the above area theorem, hence, yields a following expectation: Black holes in de Sitter background cannot coalesce each other beyond the critical area of the event horizon, resulting that many small black holes still remain in de Sitter background.

This expectation brings us to a desirable inflationary scenario in inhomogeneous space-times as follows. Initial inhomogeneities collapse into many small black holes, which areas are bounded as $A_{BH} \leq 4\pi H^{-2}$, but not into large-scale inhomogeneities which may prevent the global portion of the universe expanding exponentially, if the cosmic censorship hypothesis is true. Those small black holes are harmless in an inflationary scenario, because they will not only be diluted away by the exponential expansion of the universe but also be evaporated away soon by Hawking radiation (The typical mass of the black holes is $\sim 10^2 g$ for GUT-scale vacuum energy.). In order to confirm this scenario, the research along the above discussion is now in progress.

REFERENCES

1. A.H.Guth, Phys. Rev. **D23**, 347 (1981);
K. Sato, Mon. Not. Roy. Astron. Soc. **195**, 467 (1981);
A. Albrecht and P. J. Steinhardt, Phys. Rev. Lett. **48**, 1220 (1982);
A. D. Linde, Phys. Lett. **108B**, 389 (1982).
2. G. W. Gibbons and S. W. Hawking, Phys. Rev. **D15** 2738 (1977);
S. W. Hawking and I. G. Moss, Phys. Lett. **110B**, 35 (1982);
as for a review, see also *e.g.* K. Maeda, "*Inflation and Cosmic No Hair Conjecture*", in the Proceedings of 5th Marcel Grossmann Meeting, ed. by D. G. Blair and M. J. Buckingham (World Scientific, 1989) p.145.
3. K. Sato, M. Sasaki, H. Kodama, and K. Maeda, Prog. Theor. Phys. **65** 1443 (1981);
K. Maeda, K. Sato, M. Sasaki and H. Kodama, Phys. Lett. **108B**, 98 (1982);
K. Sato, in the Proceedings of I. A. U. Symposium No.130 "*The Large Scale Structure of the Universe*" (1987).
4. E. Calzetta and M. Sakellariadou, Phys. Rev. **D45**, 2802 (1992).
5. H. Kurki-Suonio, J. Centrella, R. A. Matzner and J. R. Wilson, Phys. Rev. **D35**, 435 (1987);
P. Laguna, H. Kurki-Suonio, and R. A. Matzner, Phys. Rev. **D44**, 3077 (1991);
K. A. Holcomb, S. J. Park and E. T. Vishniac, Phys. Rev. **D39**, 1058 (1989);
D. S. Goldwirth and T. Piran, Phys. Rev. **D40**, 3269 (1989);
D. S. Goldwirth and Piran, Phys. Rev. Lett. **64**, 2852 (1990).
6. D. Gerfinkle and C. Vuille, GRG **23**, 471 (1991)
7. K. Nakao, Kyoto University Preprint, GRG **24**, 1069 (1992).

8. K. Nakao, K. Maeda, T. Nakamura and K. Oohara, To be published in Phys. Rev. D.
9. K. Nakao, K. Yamamoto and K. Maeda, To be published in Phys. Rev. D.
10. B. Carter, Commun. Math. Phys. **17**, 1067 (1970);
 B. Carter, in *Black Holes* ed. C. DeWitt and B. S. DeWitt (Gordon and Breach, New York, 1972).
 G. W. Gibbons and S. W. Hawking (Ref.3).
11. L. F. Abbott and S. Deser, Nucl. Phys. **B195**, 76 (1982).
12. K. Nakao, K. Maeda, T. Nakamura, and K. Oohara, Phys. Rev. **D44**, 1326 (1991).
13. G. W. Gibbons and S. W. Hawking (Ref.3).
14. T. Shiromizu, K. Nakao, H. Kodama and K. Maeda, in preparation.
15. S. W. Hawking, in *Black Holes* ed. C. DeWitt and B. S. DeWitt (Gordon and Breach, New York, 1972).
16. M. Sasaki, K. Maeda, S. Miyama and T. Nakamura, Prog. Theor. Phys. **63**, 1051, (1980).
17. D. Brill, Ann. Phys. **7**, 466 (1959).
18. K. Eppley, Phys. Rev. **16**, 1609 (1977).
19. D. R. Brill and R. W. Lindquist, Phys. Rev. **131**, 471 (1963).
20. A. Cadez, Ann. Phys. **43**, 449 (1974).
21. W. Boucher and G. W. Gibbons, Phys. Rev. **D 30**, 2447 (1984).

FIGURE CAPTIONS

1. The Penrose diagrams of the Schwarzschild-de Sitter space-time are depicted. (a), (b) and (c) are the cases of $M < M_{crit}$, $M = M_{crit}$ and $M > M_{crit}$, respectively. The thin solid curves is $R = \text{const}$ curves. Typical trajectories of the surface of the dust sphere are depicted by solid line with an arrow.
2. The shaded region is the forbidden region in which $V > 0$.
3. We show the relation between the critical width τ_{crit} and the gravitational mass of the gravitational waves.
4. A two dimensional embedding of the initial spacelike hypersurface of a space-time containing Einstein-Rosen bridges.
5. We show the relation between the critical separation τ_{crit} , at which the black-hole apparent horizon enclosing two bridges appears first, and the “gravitational mass” M . For $M > 0.35M_{crit}$, τ_{crit} decreases as M increasing. The maximum value of τ_{crit} turns out to be $\sim 0.025H^{-1}$.

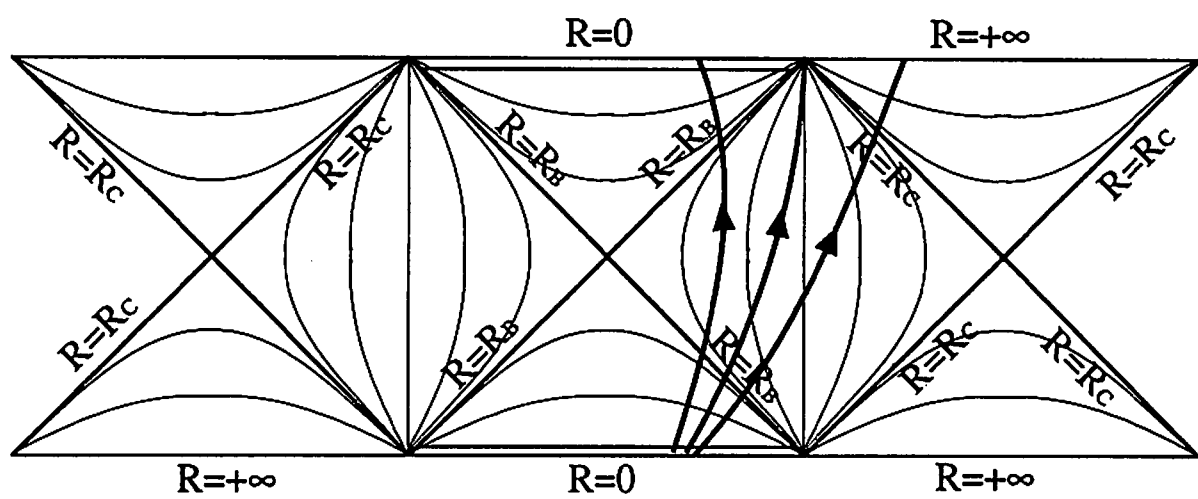


Fig.1(a)

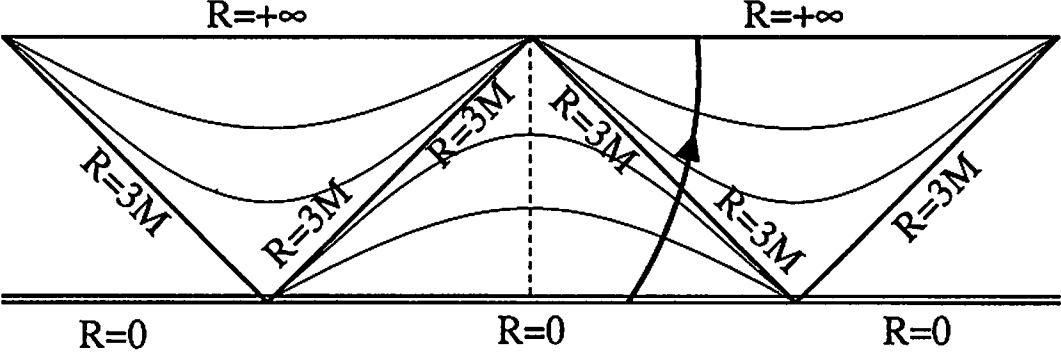


Fig.1(b)

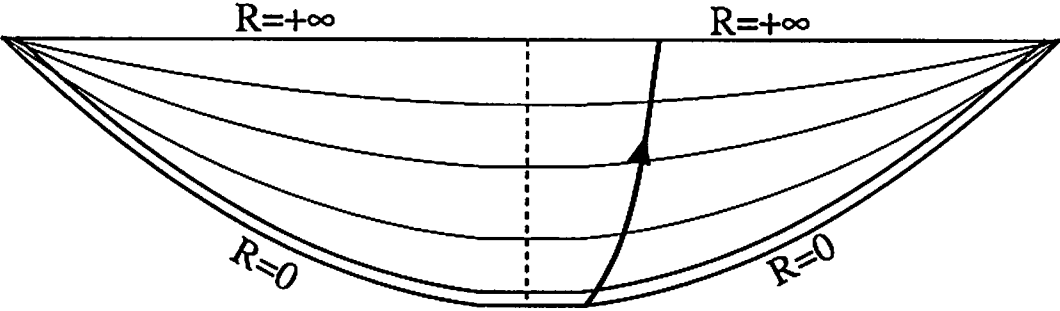


Fig.1(c)

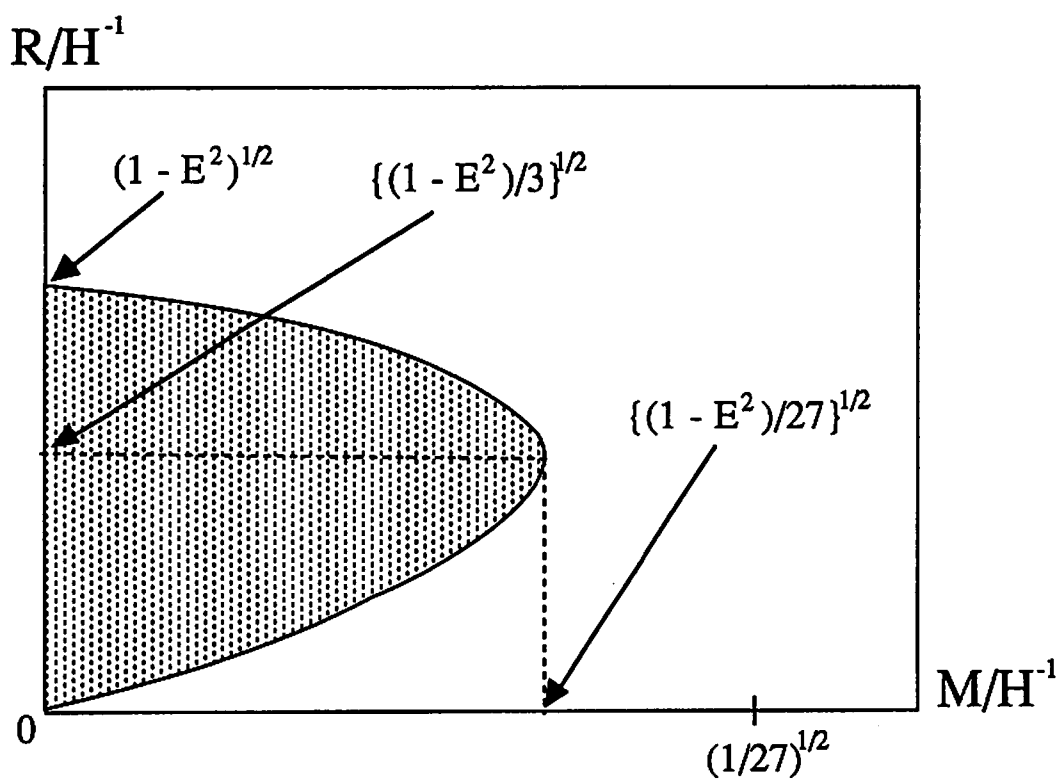


Fig.2

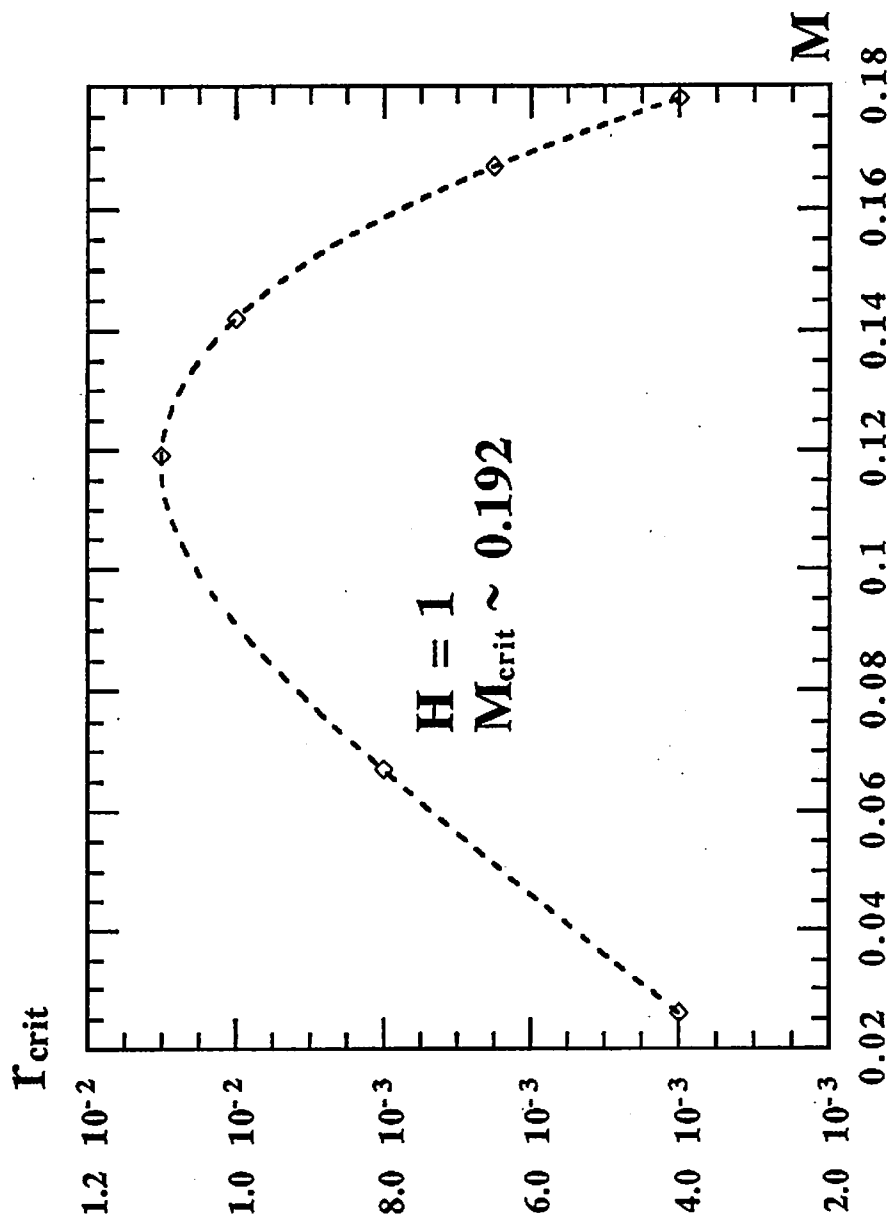


Fig.3

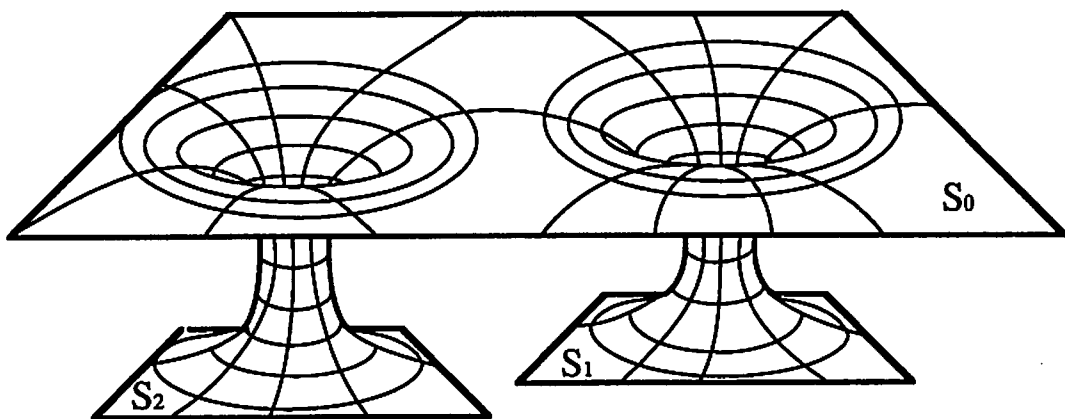


Fig.4

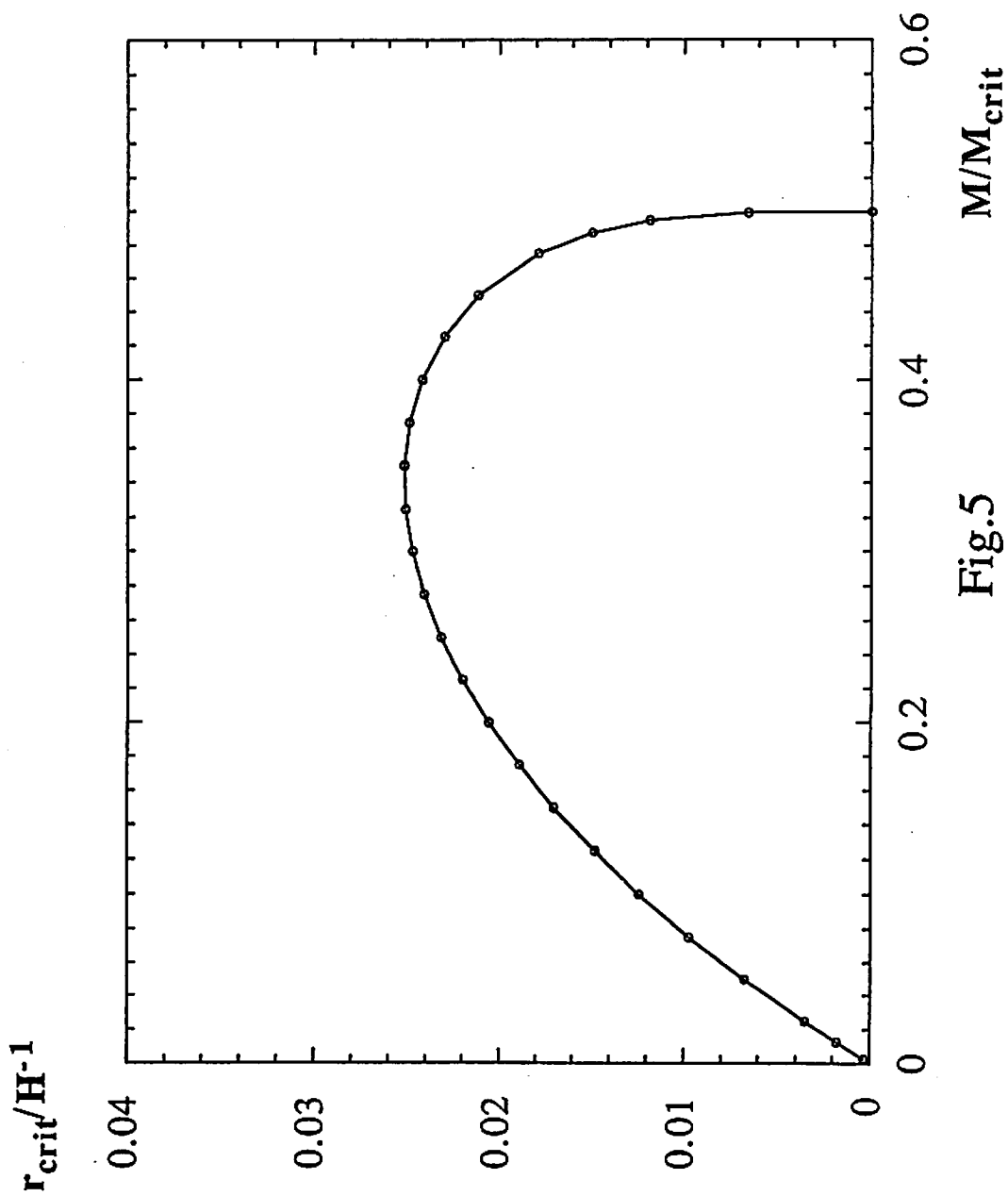


Fig.5

The Properties of Black Holes in the Asymptotically de Sitter Space-Time

Tetsuya Shiromizu¹, Ken-ichi Nakao², Hideo Kodama³ and Kei-ichi Maeda⁴

^{1,2}Department of Physics, Kyoto University,

³Department of Fundamental Sciences, FIHS, Kyoto University,
and

⁴Department of Physics, Waseda University

1. Introduction

The inflationary universe scenario^[1] is currently the most favorable model to explain the present homogeneity and isotropy of our universe. In this scenario, the vacuum energy of some fundamental field (the so-called “inflaton”) behaves as a positive cosmological constant during a period in the early universe. Although some fundamental problems in the standard big bang scenario are resolved by the idea of inflation, there may still be two unsolved problems in the inflationary scenario: One is what is the inflaton field, and the other is the isotropy-homogeneity problem. To answer for the former question, we may have to understand the final unified theory of fundamental forces, while the latter question might be solved in the context of the classical Einstein theory. If all or most space-times with a positive cosmological constant approaches the de Sitter space-time, we will find that the universe is isotropic and homogeneous just after inflationary era. This argument is closely related to “the so-called cosmic no hair conjecture”^[2]. This conjecture is true under some restrictions on space-times or on those initial conditions. However, we also know black hole space-time in de Sitter background. Schwarzschild-de Sitter space-time does never approach de Sitter one. Some dust sphere with a cosmological constant can evolve into the Schwarzschild-de Sitter space-time. Therefore, in the case of more inhomogeneous space-times without any symmetry, it is not clear whether or not the de Sitter-like cosmic expansion is realized even if there exists a positive cosmological constant. In particular, if the inhomogeneities are very “strong” and “localized” enough, some portions may gravitationally collapse into black holes or naked singularities. Hence, we propose that instead of proving the cosmic no-hair conjecture, we have to look for an inflationary scenario, in which many black holes could be formed but they are harmless, for inhomogeneous universes.

Motivated by these considerations, in the present paper, we study the behavior of black holes in space-times with a positive cosmological constant Λ . First, in order to make clear the meaning of black holes in such asymptotically non-flat space-times, we introduce a new class of space-times, called *asymptotically de Sitter space-time*. Then, we define black holes in asymptotically de Sitter

space-times and study their fundamental properties. We show that many of the theorems on black holes in the asymptotically flat space-times, including the area theorem, hold also in the asymptotically de Sitter space-times. Furthermore, we give an argument which strongly suggests the existence of an upper bound on the area of the event horizon of the black hole in the space-time with Λ . Our results obtained here may provide an inflationary scenario for inhomogeneous universes, as will be discussed later.

2. The Properties of Black Holes in the Asymptotically de Sitter Space-Time

First, we shall start with defining the asymptotically de Sitter space-time.^[3] A physical space-time (\mathcal{M}, g) is said to be *weakly future asymptotically simple* if there exists a strongly causal space-time $(\tilde{\mathcal{M}}, \tilde{g})$ and a conformal embedding, $\varphi : \mathcal{M} \rightarrow \varphi[\mathcal{M}] \subset \tilde{\mathcal{M}}$, such that $\varphi[\mathcal{M}]$ has a boundary $\partial\varphi[\mathcal{M}]$ and the following conditions are satisfied:

(1) There exists a C^∞ function Ω on $\tilde{\mathcal{M}}$, such that $\tilde{g} = \Omega^2 \varphi_*(g)$, where φ_* is the mapping induced from the embedding φ .

(2) $\Omega > 0$ on $\varphi[\mathcal{M}]$, and $\Omega|_{\mathcal{I}} = 0$ and $d\Omega|_{\mathcal{I}} \neq 0$ on the boundary of $\varphi[\mathcal{M}]$, $\mathcal{I} := \partial\varphi[\mathcal{M}]$. Further \mathcal{I} consists of two types of connected components, the future ones \mathcal{I}^+ (with $J^+(\mathcal{I}^+) \cap \varphi[\mathcal{M}] = \emptyset$) and the past ones \mathcal{I}^- (with $J^-(\mathcal{I}^-) \cap \varphi[\mathcal{M}] = \emptyset$) and $\mathcal{I}^+ \neq \emptyset$.

Remark: \mathcal{I} may have many connected components in general. For example, there exist an infinite number of connected components in the Schwarzschild-de Sitter space-time. Here we assume, however, that \mathcal{I}^\pm are both connected; this assumption holds in the applications that we have in mind. For the more general case in which \mathcal{I}^\pm have many connected components, we can apply the following theorems to the restricted space-time region in which \mathcal{I}^\pm are both connected.

Weakly future asymptotically simple space-times define a rather general category of space-times and include the asymptotically flat space-times as well. In order to remove such asymptotically flat cases and to restrict to those with de Sitter-like behavior in the future, we must assume the Einstein equations. A physical space-time (\mathcal{M}, g) is said to be *weakly future asymptotically simple and de Sitter* if (\mathcal{M}, g) is weakly future asymptotically simple and satisfies the following condition:

(3) g_{ab} satisfies $R_{ab} - \frac{1}{2}g_{ab}R + \Lambda g_{ab} = 8\pi GT_{ab}$ with $\Lambda > 0$, where $\Omega^{-3}T_b^a$ has a smooth limit on \mathcal{I}^+ .

From the point of view of causal structure, the above conditions are still too weak, since one can construct other space-times whose region outside black holes contain the closed timelike curves from these space-times by a perturbation. To eliminate such pathologies, we impose a further condition. A physical space-time (\mathcal{M}, g) which is weakly future asymptotically simple and de Sitter is said to be

strongly asymptotically predictable (from Σ) and de Sitter in the future if there exists a partial Cauchy surface Σ such that $\mathcal{I}^+ \subset \overline{D^+(\Sigma)}$, and $J^+(\Sigma) \cap \overline{J^-(\mathcal{I}^+)} \subset D^+(\Sigma)$. Hereafter, we shall call such space-times the *asymptotically de Sitter* space-times for brevity.

Let us pause for a moment to discuss the meaning of these conditions. First, though the condition (2) in general implies that the space-time has regular infinities \mathcal{I}^\pm , it alone does not restrict the structure of \mathcal{I}^\pm . If the condition (3) is imposed further, then \mathcal{I}^\pm are smooth three-dimensional space-like hypersurfaces in $\tilde{\mathcal{M}}$ because $\tilde{g}(\tilde{n}, \tilde{n})|_{\mathcal{I}^\pm} = -\frac{1}{3}\Lambda < 0$ where $\tilde{n}^a = \tilde{g}^{ab}\tilde{\nabla}_b\Omega$. \mathcal{I}^\pm represent the infinities in time, and Ω^{-1} can be regarded as the local scale factor near \mathcal{I}^\pm . The condition on T_{ab} in (3) implies that as the universe expands the energy density decreases at least as rapidly as the dust-like matter does. This condition is satisfied at least in all inflationary models. What is interesting here is that this requirement leads to a quite strong consequence, i.e., the space-time structure around \mathcal{I}^+ is locally de Sitter. To be precise, we can show from the conditions (2) and (3) that there exists a foliation of the space-time around \mathcal{I}^+ by space-like hypersurfaces whose expansion θ and shear $\sigma_{\mu\nu}$ behave as $\theta \rightarrow 3\sqrt{\Lambda/3}$ and $\sigma_{\mu\nu} \rightarrow 0$ toward \mathcal{I}^+ , respectively.

Now we proceed to the study of black holes. In analogy with the asymptotically flat case we define a black hole and its event horizon in an asymptotically de Sitter space-time to be the region $B = \varphi[\mathcal{M}] - J^-(\mathcal{I}^+)$ and its boundary $H = J^-(\mathcal{I}^+) \cap \varphi[\mathcal{M}]$, respectively. First, we show that the existence of a trapped surface guarantees the existence of a black hole, if there is no naked singularity.

Theorem 1: Let (\mathcal{M}, g) be an asymptotically de Sitter space-time such that $R_{ab}k^ak^b \geq 0$ for every null vector k^a . Let T be a trapped surface contained in $(\tilde{\mathcal{M}} - J^-(p)) \cap D^+(\Sigma)$, where p is a point on \mathcal{I}^+ . Then $T \subset B$, that is, the trapped surface is contained in a black hole.

Proof : Suppose $T \not\subset B$, that is, $J^-(\mathcal{I}^+) \cap T \neq \emptyset$. Let q be a point in $J^+(T) \cap \mathcal{I}^+$, and γ be a curve in \mathcal{I}^+ connecting q and p . Then, since $D^+(\Sigma)$ is globally hyperbolic, hence is causally simple, $J^+(T)$ is closed in $D^+(\Sigma)$ and its intersection with γ is a closed segment γ' containing q (or the single point q). Let r be the endpoint of γ' other than q if γ' is not the single point and otherwise be q . Then again from the causal simplicity of $D^+(\Sigma)$, r must be contained in $J^+(T)$. Then r lies on a future-directed null geodesic generator α of $J^+(T) \cap D^+(\Sigma)$ which starts from T , which is orthogonal to T and has no conjugate point to T between T and r , because $D^+(\Sigma)$ is globally hyperbolic. On the other hand, there must exist a conjugate point on α within a finite affine distance from $\alpha \cap T$, since the expansion rate of future directed null geodesic generators orthogonal to T is negative and the space-time satisfies the energy condition. This implies that α cannot be totally contained in $J^+(T)$ and leads to a contradiction. Thus $T \subset B$. QED.

In the above theorem we restricted the location of our trapped surface in order to guarantee that $J^+(T)$ intersects \mathcal{I}^+ . Dropping this restriction allows

us easily to construct counterexamples to the above theorem's conclusion (one is the Schwarzschild-de Sitter space-time).

Next we consider the properties of the event horizon. First, note that each geodesic generator of $J^-(\mathcal{I}^+)$ is either future inextendible or has a future end-point on \mathcal{I}^+ because, from condition (2), \mathcal{I}^+ is closed. If a generator intersects \mathcal{I}^+ , it must intersect at the edge of \mathcal{I}^+ . However, this is impossible since \mathcal{I}^+ does not have an edge. Hence, as in the asymptotically flat case, every null geodesic generator of $J^-(\mathcal{I}^+)$ is future inextendible in an asymptotically de Sitter space-time. This enables us to prove an area theorem for black holes in the asymptotically de Sitter case.

Theorem 2 (The Area Theorem in Asymptotically De Sitter Space-Time): Let (\mathcal{M}, g) be asymptotically de Sitter and such that $R_{ab}k^ak^b \geq 0$ for every null vector k^a . Let Σ_1 and Σ_2 be Cauchy surfaces of the globally hyperbolic region $D^+(\Sigma)$ with $\Sigma_2 \subset I^+(\Sigma_1)$. Furthermore suppose that there exists an event horizon $H = J^-(\mathcal{I}^+) \cap J^+(\Sigma)$. Then for $\mathcal{H}_1 := H \cap \Sigma_1$ and $\mathcal{H}_2 := H \cap \Sigma_2$, (Area of \mathcal{H}_1) \leq (Area of \mathcal{H}_2).

Proof: Suppose that the expansion rate θ of the future directed null geodesic generators of H is negative in an open set $U \subset H \cap D^+(\Sigma)$. Then there exist a compact closed two-surface $S \subset D^+(\Sigma) - J^-(\mathcal{I}^+)$ such that $S \cap U \subset H \cap D^+(\Sigma)$ and the trace K_{2a}^a of the second fundamental form K_{2ab} of S for the outgoing null geodesic coincides with θ in $S \cap U$. Let p be a point in \mathcal{I}^+ . Since $J^-(p)$ is closed in $D^+(\Sigma)$ because of causal simplicity, $D^+(\Sigma) - J^-(p)$ is open. Hence we can slightly deform S to a new surface S' inside $D^+(\Sigma) - J^-(p)$ so that $S' \cap J^-(\mathcal{I}^+) \neq \emptyset$, keeping K_{2a}^a negative on $S' \cap J^-(\mathcal{I}^+)$. Then by the same argument in the proof of Theorem 1 we can show that there exists a null geodesic generator α of $J^+(S') \cap D^+(\Sigma)$ which intersects \mathcal{I}^+ . Clearly $\alpha \cap S' \subset J^-(\mathcal{I}^+)$ and θ is negative therein. However, this implies that α has a conjugate point with a finite affine distance from $\alpha \cap S'$, hence goes into $I^+(S')$. This leads to a contradiction. Therefore θ is non-negative everywhere on H .

As Σ_2 is a partial Cauchy surface of $D^+(\Sigma)$, every future inextendible null geodesic μ through \mathcal{H}_1 must intersect with \mathcal{H}_2 at a single point. Through the correspond of these two intersecting-point, one can construct a natural mapping \mathcal{H}_1 to \mathcal{H}_2 . Taking account that the expansion of null geodesic generators of $J^-(\mathcal{I}^+) \cap J^+(\Sigma)$ is non-negative and the mapping is injective, one can obtain (Area of \mathcal{H}_2) \geq (Area of \mathcal{H}_1). *QED.*

One can also show in the asymptotically de Sitter case that the intersection of an event horizon with a partial Cauchy surface is a two-sphere. (The argument is exactly the same as in the asymptotically flat case.) This is also true of the apparent horizon in non-stationary space-times: Each connected component of the apparent horizon is homeomorphic to the two-sphere.

3. The Upper Bound on Event Horizons

We have shown so far that a black hole in an asymptotically de Sitter space-time has almost the same features as one in an asymptotically flat space-time. However, there is an important difference between black holes in an asymptotically de Sitter space-time and black holes in an asymptotically flat one. Here we shall give the upper bound on the event horizon at least for maximal slicing,^[4] by which some portion of space-time can be foliated.

Consider a three-dimensional spacelike maximal hypersurface (Σ, q) . Suppose that Σ can be foliated by a one-parameter family $\{S(r)\}_{r \in \mathbb{R}_+ \cup \{0\}}$ of two-spheres, and perform a (2+1)-decomposition of its geometry. The metric of Σ becomes

$$d\ell^2 = \nu^2 dr^2 + h_{AB}(dx^A + \nu^A dr)(dx^B + \nu^B dr), \quad (3.1)$$

where h_{AB} is the intrinsic metric of $S(r)$, and $A, B = 1, 2$. Defining the extrinsic curvature of $S(r)$ as

$$k_{AB} := \frac{1}{2\nu}(\partial_r h_{AB} - \mathcal{D}_A \nu_B - \mathcal{D}_B \nu_A), \quad (3.2)$$

we get

$$\begin{aligned} & \left(\partial_r + \frac{1}{2}k\nu \right) \left[h^{1/2} \left({}^{(2)}R - k^2 - \frac{4}{3}\Lambda - 4\mathcal{D}_A(\nu^{-1}\mathcal{D}^A\nu) \right) \right] \\ &= \nu k h^{1/2} \left({}^{(3)}R - 2\Lambda + k_{AB}k^{AB} - \frac{1}{2}k^2 + 2\nu^{-2}\mathcal{D}_A\nu\mathcal{D}^A\nu \right) \\ &+ 2\partial_r \left[h^{1/2} \left({}^{(2)}R - 2\mathcal{D}_A(\nu^{-1}\mathcal{D}^A\nu) \right) \right] - \mathcal{D}_A \left[h^{1/2} \left(k^2 + \frac{4}{3}\Lambda \right) \nu^A \right], \end{aligned} \quad (3.3)$$

where \mathcal{D}_A , ${}^{(2)}R$ and k are the covariant derivative induced on $S(r)$, the intrinsic curvature of $S(r)$ and the trace of k_{ab} , respectively. ${}^{(3)}R$ is the intrinsic curvature of Σ . Furthermore suppose that one can take ν and ν^A such that $\nu k > 0$ and

$$2\partial_r \left[h^{1/2} \left({}^{(2)}R - 2\mathcal{D}_A(\nu^{-1}\mathcal{D}^A\nu) \right) \right] - \mathcal{D}_A \left[h^{1/2} \left(k^2 + \frac{4}{3}\Lambda \right) \nu^A \right] = 0. \quad (3.4)$$

Define I by

$$I := \exp\left(\frac{1}{2} \int^r \nu k dr\right) h^{1/2} \left[{}^{(2)}R - k^2 - \frac{4}{3}\Lambda - 4\mathcal{D}_A(\nu^{-1}\mathcal{D}^A\nu) \right]. \quad (3.5)$$

Then, from eq.(4) and the Hamiltonian constraint, we see that $\partial_r I \geq 0$. Hence if $S(r)$ shrinks to a point as $r \rightarrow 0$, we obtain way the inequality $I \geq 0$. Thus,

integrating $e^{-\frac{1}{2} \int \nu k dr} I$ over $S(r)$, we get

$$16\pi - \int_{S(r)} k^2 dS - \frac{4}{3} \Lambda A(r) \geq 0, \quad (3.6)$$

where $A(r)$ is the area of $S(r)$. Hence, we obtain the upper bound A_{max} on the area of $S(r)$ as

$$A(r) \leq \frac{12\pi}{\Lambda} - \frac{3}{4\Lambda} \int_{S(r)} k^2 dS \leq A_{max} := \frac{12\pi}{\Lambda}. \quad (3.7)$$

The upper bound A_{max} is also applicable to the area of both the apparent and event horizons.

4. Discussion

The area theorem and the upper bound on the area of the event horizon, when put together, lead to a quite interesting consequence. Consider a collision of two black holes whose event horizons have areas A_1 and A_2 , respectively. As in asymptotically flat space-times, if these black holes merge to form a single black hole by collision, the area of the event horizon of the final black hole, A_f , should satisfy the inequality,

$$A_f \geq A_1 + A_2, \quad (4.1)$$

from the area theorem. However, in an asymptotically de Sitter space-time, A_f should be smaller than $A_{max} = 12\pi/\Lambda$, provided the space-time permits a foliation by maximal hypersurfaces. Hence, if $A_1 + A_2 > A_{max}$, the black holes cannot merge to a single black hole. This result, if it holds generally, suggests that the inflationary scenario works well even if the universe starts with strong inhomogeneities. In such case lots of small black holes will be formed from inhomogeneities at start, and some of them will merge or grow to larger black holes. However, since the area of each event horizon is bounded by $12\pi/\Lambda$, any region with scales much larger than the Hubble horizon radius $\sqrt{3/\Lambda}$ will never collapse. Hence the universe as a whole will continue to expand provide the initial size of the universe is much larger than the Hubble horizon size. Since the small black holes will eventually ease to be newly produced and be diluted away by this expansion, the universe will proceed to the standard inflationary stage soon or later.

This argument should be regarded as a suggestive one at present, since we do not prove the existence of maximal hypersurfaces which goes through event horizons and the partial foliation by maximal hypersurfaces in asymptotically de Sitter space-times. However, one can see easily that Schwarzschild-de Sitter space-time can be partially foliated by maximal surfaces^[4]. Hence, we expect that one may prove it.

Acknowledgment

We would like to thank H. Sato, M. Sasaki and L.D. Gurnnarsen for helpful discussions. T.S. is also grateful to T. Okamura and T. Tanaka for their stimulating discussions. This work was partly supported by the Grant-in-Aid for the Scientific Research Fellowship (No. 1526) and the Scientific Research Fund of the Ministry of Education, Science and Culture (No. 04234211 and No. 04640312), by a Waseda University Grant for Special Research Projects, by The Inamori Foundation, and by The Sumitomo Foundation.

REFERENCES

1. A.H.Guth, Phys. Rev. **D23**, 347 (1981);
K. Sato, Mon. Not. Roy. Astron. Soc. **195**, 467 (1981).
2. G. W. Gibbons and S. W. Hawking, Phys. Rev. **D15** 2738 (1977);
S. W. Hawking and I. G. Moss, Phys. Lett. **110B**, 35 (1982)
3. As for the asymptotically anti-de Sitter condition, see
S. W. Hawking, Phys. Lett. **126B**, 175 (1983);
A. Ashtekar and A. Magnon, Class. Quant. Grav. **1**, L39 (1984).
4. D. Brill and F. Flaherty, Commun. Math. Phys. **50**, 157(1976); Closed universes cannot be foliated by maximal hypersurfaces if $\int R_{ab}n^an^bdV > 0$, where the integral is performed over the maximal hypersurfaces. Furthermore, if $R_{ab}n^an^b > 0$, the space-time contains exactly one maximal hypersurface. However, we consider the case in which $\int R_{ab}n^an^bdV \leq 0$ or $R_{ab}n^an^b \leq 0$ due to the cosmological constant, so that this constraint does not render inconsistent with our assumption of a foliation by maximal hypersurfaces. (K. Nakao, T. Shiromizu, K. Maeda and H. Kodama, in preparation.)

Pattern Formation in the Expanding Universe

Jiro SODA

Department of Physics, Faculty of General Education
Ehime University, Matsuyama 790, Japan

January 26, 1993

Abstract

One dimensional cosmological model is studied from the point of view of the pattern formation. We show that the non-linear inertial term is crucial for the pattern formation. An infinite number of conserved quantities, which indicate the existence of the hidden symmetry, are newly founded. Those strongly constrain the power transfer of the density field. The above symmetry must be essential for explaining the scaling behavior at the epoch of the singularity formation.

1 Introduction

To understand the large scale structure is one of the important issues in the theoretical cosmology. First step to attack this problem is to characterize the pattern in the sky. Various statistics have been used for this purpose. The multi-point correlation functions are very popular [1]. Especially, the two-point correlation function for galaxies is well studied observationally. The result shows the power law behavior with the index about -1.8 . This scaling behavior is also observed in the cluster-cluster correlation with the same

index. One possible explanation is given by Peebles, however, his argument is not so convincing [1]. What we must reveal is the law hidden in the non-linear dynamics. This is essential for understanding the large scale structure of the universe.

With the above motivation, we shall study the one-dimensional cosmological equations which represent the flat universe with the dust fluid in one-dimension. In this case, the existence of the exact solution, the so-called Zeldovich solution, makes the analysis easy. Interestingly, the power spectrum of this model shows the universal scaling pattern with the index $-1/3$ at the epoch of the singularity formation [2,3,4]. This universality is expected to hold in the realistic case. Hence, to explain this universality is important to understand the large scale structure of the universe. Here, we will seek the law which governs this pattern formation.

2 Universality

One-dimensional cosmological equations are the following:

$$\frac{\partial}{\partial t}\delta(x, t) + \frac{1}{a(t)}\frac{\partial}{\partial x}[v(x, t)(1 + \delta(x, t))] = 0, \quad (1)$$

$$\frac{\partial}{\partial t}v(x, t) + \frac{1}{a(t)}v(x, t)\frac{\partial}{\partial x}v(x, t) + \frac{\dot{a}(t)}{a(t)}v(x, t) + \frac{1}{a(t)}\frac{\partial}{\partial x}\phi(x, t) = 0, \quad (2)$$

$$\frac{\partial^2}{\partial x^2}\phi(x, t) = \frac{3}{2}\left(\frac{\dot{a}}{a}\right)^2 a^2 \delta(x, t), \quad (3)$$

where δ and v are the density perturbation and the peculiar velocity field respectively. We assumed the flat universe, $a(t) = t^{2/3}$. Using the Lagrangian

picture, we can solve the above equation. As we would like to know the pattern formation in the real space, however, the Eulerian picture is appropriate for this aim. Hence, we will use the Eulerian picture throughout this paper. Before we examine the above equations, we must consider what causes the beautiful pattern. If we neglect the non-linear term, the pattern would never appear. Indeed, it is the mode coupling through the non-linear term that makes the pattern. Therefore, we can not discard the non-linear term. On the other hand, the cosmological expansion and the Newtonian gravity is not so crucial for the pattern formation. To make this fact manifest, we shall study the simplified model:

$$\frac{\partial}{\partial t}\delta(x, t) + \frac{\partial}{\partial x}[v(x, t)(1 + \delta(x, t))] = 0 , \quad (4)$$

$$\frac{\partial}{\partial t}v(x, t) + v(x, t)\frac{\partial}{\partial x}v(x, t) = 0 . \quad (5)$$

From now on, we will show that this almost trivial system belongs the same universal class with the cosmological model. To uncover the structure of this non-linear equations, we shall use the momentum space perturbation theory. Defining the new field $u(x) = \partial v(x)/\partial x$ and expanding the field like as

$$\delta(p) = \sum_{n=1}^{\infty} \delta_n(p), \quad (6)$$

$$u(p) = \sum_{n=1}^{\infty} u_n(p), \quad (7)$$

we obtain the perturbative equations

$$\frac{\partial}{\partial t}\delta_n(p) + u_n(p) = - \sum_{k=-\infty}^{\infty} \frac{p}{k} \sum_{m=1}^{n-1} u_m(k) \delta_{n-m}(p-k) , \quad (8)$$

$$\frac{\partial}{\partial t} u_n(p) = - \sum_{k=-\infty}^{\infty} \frac{p}{k} \sum_{m=1}^{n-1} u_m(k) u_{n-m}(p-k) . \quad (9)$$

By examining order by order, the time dependence of the variables become

$$\delta_n(k, t) = t^n \bar{\delta}_n(k) , \quad (10)$$

$$u_n(k, t) = -t^{n-1} \bar{u}_n(k) . \quad (11)$$

Thus the differential equations reduce to the algebraic recursion equations;

$$n \bar{\delta}_n(p) - \bar{u}_n(p) = \sum_{k=-\infty}^{\infty} \frac{p}{k} \sum_{m=1}^{n-1} \bar{u}_m(k) \bar{\delta}_{n-m}(p-k) , \quad (12)$$

$$(n-1) \bar{u}_n(p) = \sum_{k=-\infty}^{\infty} \frac{p}{k} \sum_{m=1}^{n-1} \bar{u}_m(k) \bar{u}_{n-m}(p-k) . \quad (13)$$

It is easy to prove the relation

$$\bar{\delta}_n(k) = \bar{u}_n(k) . \quad (14)$$

And the recursion equations are solved as

$$\bar{\delta}_n(p) = \frac{p^n}{n!} \sum_{k_i} \prod_{i=1}^n \frac{\bar{\delta}_1(k_i)}{k_i} \delta_{p, \sum_i k_i} . \quad (15)$$

Then the full non-perturbative mode becomes

$$\delta(p, t) = \sum_{n=1}^{\infty} t^n \bar{\delta}_n(p) = \frac{1}{2\pi} \int_0^{2\pi} dq \exp i p(q + v_1(q)t) , \quad p \neq 0. \quad (16)$$

It is natural to interpret the parameter q in the eq.(16) as a Lagrangian coordinate. Its relation to the Eulerian coordinate is given by

$$x = q + v_1(q)t , \quad (17)$$

where $v_1(q)$ is the linear velocity field. By the inverse Fourier transformation, we get

$$\rho(x, t) = \frac{\rho_b}{1 + v'_1(q)t}, \quad (18)$$

where ρ_b represents the mean density and the prime denotes the differentiation with respect to q . The zero-point of the Jacobian of the transformation from the Lagrangian coordinate to the Eulerian coordinate becomes the singularity of the density field (18). The singular point is given by the condition

$$v'_1(q_c) = -\frac{1}{t_c}, \quad (19)$$

$$v''_1(q_c) = 0. \quad (20)$$

Thus, the eq. (17) becomes

$$x = x_c + \alpha(q - q_c)^3 \quad (21)$$

in the leading order. Then we obtain

$$\rho(x, t) \sim (x - x_c)^{-\frac{1}{3}} \quad (22)$$

or, equivalently,

$$P(k, t) \sim k^{-\frac{1}{3}}. \quad (23)$$

This behavior coincides with that of the cosmological model [2]. Thus, we can fairly say that the cosmological expansion and Newtonian gravitational force is not essential for the pattern formation.

3 What is the law behind the non-linear dynamics?

Using the field variables, the relation (14) in the perturbative analysis can be written as

$$\delta(x, t) = -t \frac{\partial}{\partial x} v(x, t) . \quad (24)$$

This relation (24) reduces the basic equations (4) and (5) to the only one non-linear equation,

$$\frac{\partial}{\partial t} v(x, t) + v(x, t) \frac{\partial}{\partial x} v(x, t) = 0. \quad (25)$$

It is important to notice that there exist an infinite number of conserved quantities in the above systems,

$$\frac{d}{dt} \int_0^{2\pi} dx v^n(x, t) = 0 . \quad (26)$$

Equivalently,

$$\frac{d}{dt} \sum_{k_i} \langle v_{k_1}(t) \cdots v_{k_n}(t) \rangle \delta_{\sum_i k_i, 0} = 0 . \quad (27)$$

Denoting the initial n-th order moment of the velocity field as σ_n , the above equation is solved as

$$\sum_{k_i} \langle v_{k_1}(t) \cdots v_{k_n}(t) \rangle \delta_{\sum_i k_i, 0} = \sigma_n . \quad (28)$$

Using the relation (24) in the momentum space form

$$\delta(k, t) = iktv(k, t), \quad (29)$$

we obtain the law behind the non-linear dynamics as

$$\sum_{k_i} < \frac{\delta(k_1, t)}{k_1} \dots \frac{\delta(k_n, t)}{k_n} > \delta_{\sum_i k_i, 0} = \sigma_n (it)^n . \quad (30)$$

In particular, the power spectrum is constrained by the equation

$$\sum_k \frac{P(k, t)}{k^2} = \sigma_2 t^2 . \quad (31)$$

In the intermediate process of the non-linear evolution, the above infinite number of the equations constrain the power transfer strongly. This leads to the universal scaling behavior with the index $-1/3$. Although we do not yet understand the direct relation between our findings and the number $-1/3$, we believe the relation we found is the key for the analytic derivation of the miracle number. For supporting this expectation, we shall show that the same law also holds in the cosmological case which has the same miracle number $-1/3$.

Surprisingly, the equations (1),(2) and (3) reduce to one non-linear equation also in this case. Assuming the relation

$$\delta(x, t) = -\frac{3}{2} t^{\frac{1}{3}} \frac{\partial}{\partial x} v(x, t), \quad (32)$$

the seeking equation is

$$\frac{\partial}{\partial t} [t^{-\frac{1}{3}} v(x, t)] + \frac{1}{t} v(x, t) \frac{\partial}{\partial x} v(x, t) = 0 . \quad (33)$$

The eq.(33) leads to the infinite number of the conserved quantities again.

$$\frac{d}{dt} \int_0^{2\pi} dx [t^{-\frac{1}{3}} v(x, t)]^n = 0 . \quad (34)$$

This fact is highly non-trivial and yields the main result of this paper,

$$\sum_{k_i} < \frac{\delta(k_1, t)}{k_1} \dots \frac{\delta(k_n, t)}{k_n} > \delta_{\sum_i k_{i,0}} = \alpha_n a(t)^n, \quad (35)$$

where α_n is the constant determined by the initial n -th order moment of the velocity field. The special case of this law is previously obtained by us [5]. It should be noted that eq.(35) has the same form with the eq.(30). This fact is, of course, a refraction of the similarity between eq.(26) and eq.(34). These conserved quantities indicate the hidden symmetry. The large symmetry strongly constrains the dynamics. It must be this symmetry that yields the number $-1/3$.

4 Conclusion

We studied the one-dimensional cosmological pattern formation. It turns out that the cosmological expansion and the Newtonian gravity is not essential for the $-1/3$ pattern. Indeed we found the universal law (35) which holds for the universality class with the index $-1/3$. The pattern is related not to the detailed dynamics but to the non-linear inertial term. The existence of the infinite number of conserved quantities indicate the hidden symmetry behind this non-linear system. It is interesting to find it, however, we must understand the Hamiltonian structure before doing it. It should be noted that we do not yet understand two points. First point is how to calculate the number $-1/3$ from our formalism. Second one is how to extend our formulation to other situations, especially to the higher dimensional systems.

References

- [1] P. J. E. Peebles, *The Large Scale-Structure of the Universe* (Princeton: Princeton Univ. Press).
- [2] Ya. B. Zel'dovich, *Astrofizika* 6 (1970) 119.
- [3] T. Nakamura, *Prog. Theor. Phys.* 73 (1985) 657.
- [4] N. Gouda and T. Nakamura, *Prog. Theor. Phys.* 79 (1988) 765.
- [5] J. Soda and Y. Suto, *ApJ* 396 (1992) 379.

TIME VARIATIONS OF X-RAYS FROM BLACK HOLE CANDIDATES AND LOW MASS BINARY NEUTRON STARS.

Sigenori Miyamoto

Department of Earth and Space Science,
Faculty of Science, Osaka University.
Machikaneyama-cho 1-1, Toyonaka, Osaka, 560, Japan

ABSTRACT

Time variations of X-rays from a black hole candidate GS1124-683 are compared with those from other black hole candidates: Cyg X-1, GX339-4, GS2023+338 and low mass X-ray binary neutron stars: GX5-1 and X1608-522, and we get the following results.

- 1) In GS1124-683, four states, i.e. a high flare state, a high quiet state, a high-to-low transition state and a low state are recognized.
- 2) Normalized power spectrum densities (NPSDs) and phase lags between different energy X-rays from the black hole candidates in the same states are similar not only in the low state but also in the high flare state.
- 3) In the high flare state, the X-ray energy spectrum consists of two components: a disk black body component and a power law component. These two components have their inherent PSDs; a flat top shape noise (FTN) for the power law component and a power law shape noise (PLN) for the disk black body component. However, the NPSD values normalized to the corresponding component are not constant.
- 4) In the high quiet state, the main component is the disk black body component, and its NPSD is PLN.
- 5) In the low state, the X-ray energy spectrum consists of only a power law component. This component has a harder energy spectrum and shows different and larger time variations than those of the power law component in the high state. The NPSD of the power law component in the low state is larger than those in the high state and power law shaped, which saturate at the frequencies less than about 0.1 Hz. Thus the shape of the NPSD and the energy spectrum of the power law component in the low state are different from those in the high (flare and quiet) state.
- 6) GS2023+338 in its flare state has harder energy spectrum than that of GS1124-683 in the similar high flare state, and has the NPSDs rather similar to those in the low state of the black hole candidates, though in the low state GS2023+338 has the same X-ray energy spectrum and the same NPSD to the other black hole candidates.
- 7) A low mass X-ray binary neutron star GX5-1 has two component in its X-ray energy spectrum; a disk black body component and a hard black body component. In the horizontal branch, the fraction of the hard black body component is larger than that in the normal branch. In the horizontal branch, the NPSDs are the flat top shape noise (FTN) and are larger than the NPSDs in its normal branch, which are

the power law shape noise (PLN). These relations are similar to those of the black hole candidates in its high flare state and in its high quiet state. However, the phase lags of time variations between different energy X-rays from GX5-1 in its horizontal branch are different from those of the black hole candidates in the high flare state.

8) In the low state, a low mass X-ray binary neutron star X1608-522 has a power low X-ray energy spectrum and its NPSD is similar to those of the black hole candidates in the low state. Thus X-ray energy spectra and NPSDs of low mass X-ray binary neutron stars (GX5-1 and X1608-522) in the high and the low states are almost similar to those of the black hole candidates in the these states, though the phase lags between different energy X-rays seem to be different from those of the black hole candidates, and these are observed in different X-ray binary neutron stars.

Key words: X-ray star, black hole candidate, low mass X-ray binary neutron star, Nova Muscae 1991, time variations.

1. Introduction.

Mainly due to observations of Cyg X-1, it had been believed that black hole candidates had two states; a high state and a low state, and in the low state their X-rays had a power law energy spectrum and showed rapid time variations, and in the high state the X-rays had a soft energy spectrum and showed small time variations (for the reviews, see for instance, Oda, 1977, Liang and Nolan, 1984).

Recently, however, it was found that in the high state GX339-4 had two sub-states; a high flare state and a high quiet state. In the high flare state, X-rays have two components; a power law component and a disk black body component, and show rapid time variations including QPO and a peculiar peaked phase lag (Miyamoto et al. 1991). In the high quiet state of GX339-4, X-rays have a soft energy spectrum, and their time variations are smaller than those in the high flare state (Makishima et al. 1986).

Moreover, it was found that in the low state the energy spectra and time variations of X-rays from the black hole candidates, Cyg X-1, GX339-4, GS2023+338, were the same (Canonical time variation; Miyamoto et al. 1992), which were shown in Fig.1. The normalized power spectrum densities (NPSDs) and the phase lags in the low state of Cyg X-1, GX339-4 and GS2023+338 are the same. It was also shown by Miyamoto et al. (1988) that these phase (time) lag could not be explained by the Compton scattering model by Sunyaev and Trumper (1979), which was proposed to explain the power law X-ray component as a product of the inverse Compton scatterings in a very hot electron cloud.

An X-ray nova: Nova Muscae or GS1124-683 showed long term variations similar to a black hole candidate A0620-00 (Kitamoto et al.,1992) and optical observations showed that this X-ray source had a mass larger than about 3.8 Mo (Remillard et al.,1992) or had a mass of about 8 Mo (Cheng et al. 1992). These

strongly suggest that GS1124-683 is a black hole. Another X-ray nova: GS2023+338 showed rapid time variations and had a hard energy spectrum even in its flare state (Kitamoto et al. 1989; Tanaka 1989). Recently the mass of the compact star in this source was estimated to be 8-15.5 Mo, and shown to be a black hole candidate (Casares, Charles, and Naylor, 1992). However, the hard energy spectrum of this source in its flare state is quite different from those of GX339-4 in the same state mentioned above, though in the low state the normalized power spectrum density functions (NPSDs; Miyamoto et al. 1991), phase lags and X-ray energy spectrum of GS2023+338 are the same to other black hole candidates: Cyg X-1 and GX339-4 (Miyamoto et al. 1992) in the same state.

Thus it is of interest to investigate whether there are time variations in GS1124-683 in the high and the low states similar to those of other black hole candidates. Time variations of GS2023+338 in its high flare state are also interesting. Comparisons between X-ray time variations together with energy spectra of the black hole candidates and those of the low mass X-ray binary neutron stars are also very interesting.

2. Energy spectra, long term variations and four states of GS1124-683.

After the discovery of the Nova Muscae (GS1124-683) with the ASM (Makino and the Ginga team, 1991), this source was observed with the large area counter (LAC) on board Ginga (Turner et al., 1989) in the energy range of 1.2-36.8 keV from 1991 January 11 to September 24-25 when this source became undetectable with the LAC. The observed X-ray energy spectra were fitted with a two component model: a disk black body component and a power law component. The disk black body component is X-rays emitted from an accretion disk (Mitsuda et al. 1984). In addition to these two components, iron line components and absorption by interstellar gas and ionized iron atoms with spread excited energy levels (a smeared edge model) (Ebisawa, 1989) were taken into account. Evolution of these two components are shown in Fig.2 (Miyamoto et al. 1993a).

From Fig.2, one can discriminate four states in GS1124-683: a high flare state (about the 8-67th day), a high quiet state (about the 69-109th day), a high-to-low transition state (about the 109-164th days) and a low state (after about the 164th day). In the high flare state, X-rays had the two components mentioned above and showed rapid time variations including QPO, which were similar to those of GX339-4 in the same state (Miyamoto et al. 1991). In the high quiet state, the main X-ray component was the disk black body component and time variations were small. In the high (flare and quiet) state, the photon number index of the power law component was about $-(2.2-3.)$. In the low state, the energy spectrum could be represented by a power law and its photon number index was about -1.6 . Thus the photon number index in the low state is clearly different from those in the high state.

In long terms, the fluxes of the disk black body component and the power law component changed incoherently, but as if they were internally correlated together

as shown in Fig.2. Thus the X-ray flux from the disk should not be considered to be proportional to a rate of accreting matter. Gravitational energy released in the disk is partly used to produce the power law component, and the ratio of the energy flux of the power law component to the total flux changes with time. Thus superficially independent but internally related production process of these two components should be searched for, such as a jet model proposed by Miyamoto and Kitamoto (1991) to explain the time variation of X-rays from GX339-4 in the high flare state.

3. Short term variations of X-rays from GS1124-683.

To investigate short term variations of X-rays, we calculated the normalized power spectrum density (NPSD) and the phase lag (van der Klis et al. 1987; Miyamoto et al. 1988), and got following results.

1) In the high flare state, the NPSDs change with time, which are shown in Fig.3(a). For instance, on January 11, when a ratio of X-ray counts of the power law component to the total X-ray counts (a power law component ratio; PLR) was about 80%, the NPSD had a flat top shape (flat top shape noise (FTN)), which was similar to that on January 22 shown in Fig.3(a). However on January 17, when the power law component showed the local minimum and the PLR was about 15%, the NPSD changed to a power law shape (power law shape noise (PLN)) as shown in Fig.3(a). On January 18-22, when the PLRs were about 30-40%, it became FTN again. In this high flare state some data showed a mixed shape of these two type noises. In the high quiet state where the PLR was less than 3%, the NPSD was PLN as shown in Fig.3(a). Thus it is clear that the shape of the NPSD depends on the power law component ratio (PLR).

2) In the high flare state, the phase lags also changed with time. On January 11-12, time variations of 4.6-9.2 keV X-rays were the most advanced and the phase lags were about 0.02-0.1 radian. However, from January 16 to January 22, time variations of 2.3-4.6 keV X-rays were the most advanced. From January 16 to 22, the phase lags showed a peak around 2-3 Hz, though the peaks before January 22 were rather small, and on January 14-16, the peaks of the phase lags were about 0.1-0.3 radian. On January 22, the phase lags of X-rays had a clear peak around 2-3 Hz (Fig.4(a)), and the NPSD was the FTN which had a knee around 2-10 Hz (Fig.3(a)). These NPSDs and phase lags are similar to the C+D sub-state of the high flare state in GX339-4 observed by Miyamoto et al. (1991) (see Fig.3(b) and Fig.4(b)). Thus we could find another possible canonical time variations of X-rays in the high flare state. The energy spectra, the NPSDs and the phase lags are similar in these black hole candidates in their high flare state (Miyamoto et al. 1993a). These phase lags and the energy spectrum were explained by Miyamoto and Kitamoto (1991) with a jet model that the inverse Compton scatterings in large hot electron clouds were the production process of the power law component.

3) In the high quiet state, the NPSD had the lowest values. The NPSD in this state had a power law shape (PLN) and was similar to those of low energy X-rays from a

low mass X-ray binary neutron stars: GX5-1 in its normal branch as shown in Fig.3 (for the normal branch, see Lewin et al. 1988).

4) In the low state, except for frequencies below about 0.2 Hz, the NPSDs of the GS1124-683 became similar to those observed in Cyg X-1, GX339-4 and GS2023+338 as shown in Fig.5. They are the same not only on different occasions but also in different energy ranges. Thus canonical time variations in the low state discovered by Miyamoto et al. (1992) was confirmed also in GS1124-683. In this state the PSDs had a power law shape with the index of about -1 at the frequencies between 0.1-1.0 Hz.

5) The results described in 1) and 3) suggest that there are two kind of shapes in PSDs corresponding to the two energy spectrum components. To confirm this, we fitted the power spectrum density functions (PSDs) with a two component PSD model; one was a power law shape noise (PLN) and the other was a flat top shape noise (FTN) of a Lorentzian of zero central frequency. In the high state, we found that the PLN had the power law index of -0.7 and was consistent to be due to the disk black body component, and the FTN had a Lorentzian shape of the width of 8 Hz and was consistent to be due to the power law component. These parameters seemed to be constant throughout the high state. However, we also found that the values of these noises normalized to each corresponding component were not constant at all time. The PLN normalized to the disk black body component seems to become large with the increase of the PLR. The FTN normalized to the power law component also seems to change with PLR.

6) X-rays from GS2023+338 in the flare state had a hard energy spectrum, which was different from those of GX339-4 and GS1124-683 (Kitamoto et al. 1989; Tanaka 1989). The NPSD of GS2023+338 in the flare state is also different from those of GS1124-683 in the very high flare state, and is rather similar to that in the low state as shown in Fig.6 (Terada, 1991). Thus the X-rays from GS2023+338 in the flare state are not the same in the energy spectrum and in the time variations to those of GS1124-683 and GX339-4, though in the low state its energy spectrum, NPSD and phase lags are similar to those of Cyg X-1, GX339-4 (Miyamoto et al. 1992). Thus in the nova of GS2023+338 X-rays must be produced by a different process from that in other sources such as GX339-4 and GS1124-683.

4. Comparisons with low mass X-ray binary neutron stars GX5-1 and X1608-522.

X-rays from a low mass binary neutron star GX5-1 consist of the disk black body component and a hard black body component. In the horizontal branch the fraction of the hard black body component is larger than that in the normal branch. As mentioned in 3-3), the NPSD of X-rays from GX5-1 in the normal branch is similar to that of the GS1124-683 in the high quiet state. Both in GS1124-683 in the high quiet state and GX5-1 in the normal branch, the NPSDs of higher energy X-rays are larger than those of lower energy X-rays, though the NPSDs of high energy X-rays from GS1124-683 are much larger than those of the same energy X-rays from GX5-1. This is not only due to an increase of the ratio of the hard

component (the power law component or the hard black body component) at higher energy X-rays. In the normal branch of GX5-1, the NPSD of the disk black body component itself becomes larger at higher energy X-rays (Kamado, 1993).

The NPSD of GX5-1 in the horizontal branch is FTN, which is similar to that of the GS1124-683 on 1991 January 22 and GX339-4 in the C+D sub-state (in the high flare state) as shown in Fig.3. It is of interest to note that the above relation between the shape of the NPSD and a fraction of the hard black body component in GX5-1 is similar to the relation between the shape of the NPSD and PLR in GS1124-683 and GX339-4 mentioned in 3-1). The hard black body component in GX5-1 corresponds to the power law component in GS1124-683 and GX339-4. However the phase lags of time variations between different energy X-rays of the black hole candidates, GS1124-683 and GX339-4, are different from those of a low mass X-ray binary GX5-1, which are shown in Fig.7. GX5-1 does not show such a large peculiar phase lags observed in GS1124-683 and GX339-4, though it is possible that the peculiar peak of the phase lags may be produced only in a some part of the X-ray flare. These situations i.e. similar NPSDs and different phase lags, can be explained as followings. Both initial X-rays of hard components in these black hole candidates and those in the low mass X-ray binary neutron star are produced by the same process. However, in the black hole candidates, these X-rays have been transferred to higher energy X-rays by the inverse Compton scatterings in large very hot electron clouds and are observed as the power law component, which show the large peculiar phase lags (Miyamoto & Kitamoto 1991). In GX5-1, this component has not been processed by the inverse Compton scatterings in the large very hot electron cloud. This may be the reason why similar NPSDs are observed in the black hole candidates and in the low mass binary neutron star, and the phase lags between different energy X-rays from GX5-1 do not show the peculiar phase lags similar to those of GS1124-683 and GX339-4.

It is of interest to note that shapes of X-ray energy spectra of a low mass X-ray binary neutron star X1608-522 show similar change to those of the black hole candidates together with its X-ray intensity (Mitsuda et al. 1989). The shape changes from a thermal type at high luminosity to a power law type as the luminosity goes down. The energy spectrum of the X-rays from X1608-522 can be represented by a two component model i.e. the disk black body component or a black body component of kT of about 1.5 keV and a power law component with an exponential cut off. When the X-ray luminosity (2-20 keV) is less than about 2×10^{-9} erg s⁻¹ cm⁻², the main component of the energy spectrum is the power law component of the photon number index of about -1.7 with the exponential cut off at the X-ray energy larger than 20 keV and the luminosity of another component is less than about 1/10 of that of the power law component. When the X-ray luminosity is about $(2.5-3.5) \times 10^{-9}$ erg s⁻¹ cm⁻², the photon number index of the power law component is about -(2-3) (Mitsuda et al. 1989)

As for the NPSD, we have no results at high X-ray luminosity. However at the low X-ray luminosity of about $(2-6) \times 10^{-9}$ erg s⁻¹ cm⁻² (2-60 keV) $((3-9) \times 10^{36}$

erg s⁻¹ at the assumed source distance of 3.6 kpc), the NPSD was obtained by Yoshida et al. (1993) and the result is shown in Fig.8, together with that of Cyg X-1 in the low state. One can recognize that the NPSDs are similar to those of the black hole candidates in the low state. However there are some minor differences. In the black hole candidates, NPSDs are the same to each other at the frequencies above about 0.3 Hz (Miyamoto et al. 1992). But in X1608-522, NPSDs observed at different occasions are the same at the frequencies above 3 Hz. The values of NPSD of X1608-522 are smaller than those of the black hole candidates at the frequencies less than about 10 Hz.

5. Conclusions.

In the low state, time variations of GS1124-68 are similar to other black hole candidate: Cyg X-1, GX339-4, GS2023+338, and in the high flare state the time variations of GS1124-68 are also similar to those of GX339-4. These results strongly suggest that the canonical X-ray production process are going on in these black hole candidates not only in the low state but also in the high state. However, GS2023+338 is an exception. In the flare state, GS2023+338 has its energy spectrum and NPSD different from other black hole candidates.

In the high state, the PSDs of GS1124-683 and GX339-4 consist of a PLN which is due to the disk black body component and a FTN which is due to the power law component. The FTN normalized to the power law component is much larger than the PLN normalized to the disk black body component.

In the low state, X-rays have a power law energy spectrum and the PSD has a power law shape. In the high state the PSD of the power law component is FTN. The indexes of the energy spectra of these two power law components are also different in the low state and in the high state. Thus the production processes of the power law components in the high state and in the low state must be different.

The NPSD in the horizontal branch of GX5-1 is similar to those of the black hole candidates GS1124-68 and GX339-4 in their high flare state. However the phase lags of time variations between different energy X-rays of GX5-1 are different from those of GS1124-683, GX339-4. These suggest following situations. Initial X-ray of the hard component in GS1124-683, GX339-4 and GX5-1 are produced by the same process. However, in the black hole candidates, these X-rays have been transferred to higher energy X-rays by the inverse Compton scatterings and are observed as the power law component. In GX5-1, the hard component has not processed by the Compton scatterings and its phase lags do not show the peculiar peak lag.

In the high and the low state, X1608-522 has energy spectra similar to those of the black hole candidates. The NPSD of X1608-522 in its low state is similar to that of the black hole candidates in the same state. The phase lag of X1608-522 in its low state is not known yet.

In the nova of GS2023+338, X-rays must be produced by a different process from that in other black hole candidates, because its X-ray energy spectrum and NPSD in its flare state are different from those in other black hole candidates.

We would like to thank all the members of the Ginga team, who support this work through observations and data analysis. Thanks are also due to my colleagues, S.Kitamoto, K.Hayashida, K.Terada, Y.Kamado and S.Iga. This review is a summary of collaborative works with these people.

References.

- Casares, J., Charles, P.A., and Naylor, T. 1992, *Nature*, 355, 614.
Cheng, F. H., Horne, K., Panagia, N. Shrader, C. R., Gilmozzi, R., Paresce, F., and Lund, N. 1992, *ApJ*, 397, 664.
Lunde, N. and Brandt, S. 1991, *IAU Circ.*, No. 5161.
Ebisawa, K., 1989, Doctor Thesis, Univ. of Tokyo.
Kamado, T., 1993, private communication.
Kitamoto S. et al., 1989, *Nature*, 342, 518.
Kitamoto S. et al. 1992, *ApJ*, 394, 609.
Lewin, W. H. G., van Paradijs, J., and van der Klis, M., 1988, *Space Sci. Rev.*, 46, 273.
Liang, E.P. and Nolan, P.L., 1984, *Space Sci. Rev.* 38, 353.
Makino, F., and the Ginga team, 1991, *IAU Circ.* No. 5161.
Makishima, K., et al., 1986, *ApJ*, 308, 635.
Mitsuda, K., et al., 1984, *PASJ*, 36, 741.
Mitsuda, K., Inoue, H., Nakamura, N., and Tanaka, Y. 1989, *PASJ* 41, 97.
Miyamoto, S., Kitamoto, S., Mitsuda, K., and Dotani, T., 1988, *Nature* 336, 450.
Miyamoto, S. and Kitamoto, S. 1991, *ApJ*, 374, 741.
Miyamoto, S., Kimura, K., Kitamoto, S., Dotani, T. and Ebisawa, K., 1991, *ApJ*, 383, 784.
Miyamoto, S., Kitamoto, S., Iga, S., Negoro, H., Terada, K., 1992, *APJ*, 391, L21.
Miyamoto, S. Iga, S., Kitamoto, Kamado, Y., 1993a, *APJ*, 403, L39.
Miyamoto, S. et al. 1993b. (in preparation)
Oda, M. 1977, *Space Sci. Rev.* 20, 757.
Remillard et al., 1992, (preprint)
Sunyaev, R.A. & Trumper, J., 1979, *Nature*, 279, 506.
Tanaka Y. 1989, in *Proc. 23rd ESLAB Symp. on Two Topics in X-ray Astronomy*, ed. J. Hunt, B. Battrick (Paris: ESA Publication Division), 1, 3.
Terada, K. 1991, Master thesis, Osaka University.
Turner M. J. L., et al., 1989, *PASJ*, 41, 345.
Yoshida, K., et al. 1992, preprint.
van der Klis et al. 1987, *ApJ. Letter*, 319, L13.

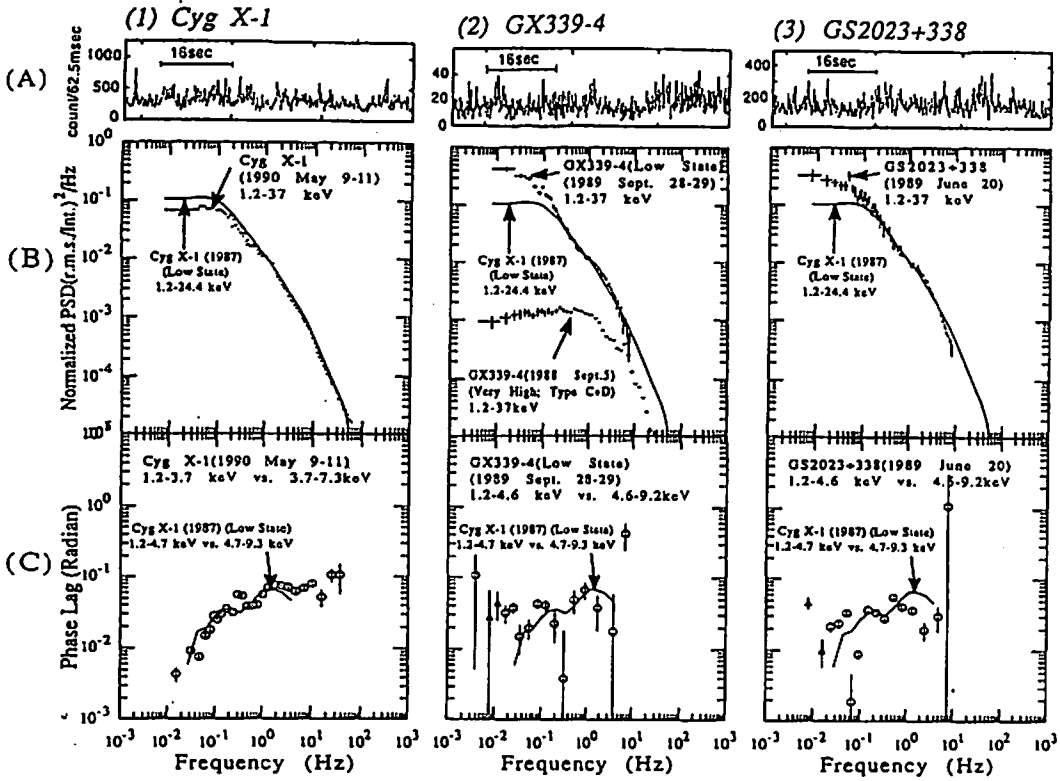


Fig.1. The normalized power spectrum densities (NPSDs) and the phase lags of the black hole candidates; *Cyg X-1*, *GX339-4*, and *GS2023+338* in the low state (Miyamoto et al. 1992).

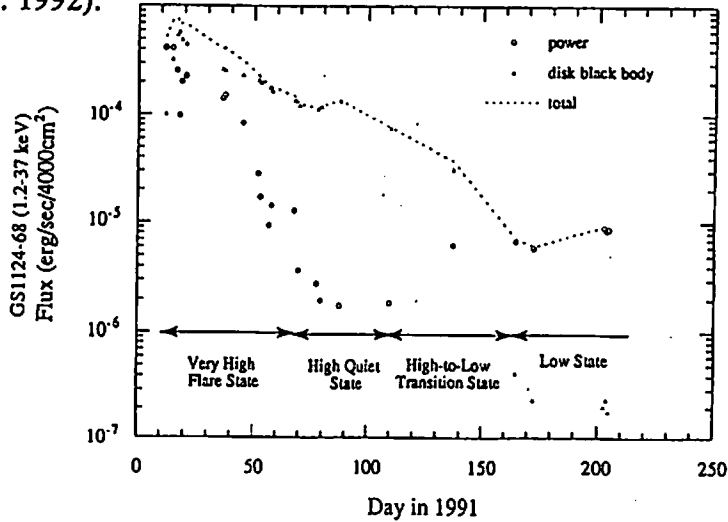


Fig.2. Evolution of X-ray fluxes of the disk black body component and the power law component of *GS1124-683* (Miyamoto et al. 1993a).

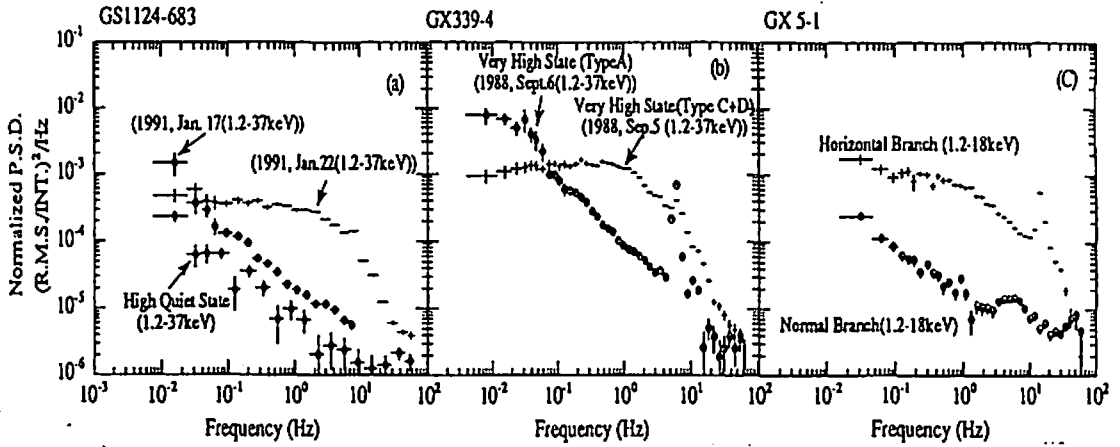


Fig.3. The NPSD of GS1124-683, GX339-4, and GX5-1. (a) GS1124-683 in the high (flare and quiet) state. (b) GX339-4 in the high flare state. (c) GX5-1 in the normal and the horizontal branch (Miyamoto et al, 1993a).

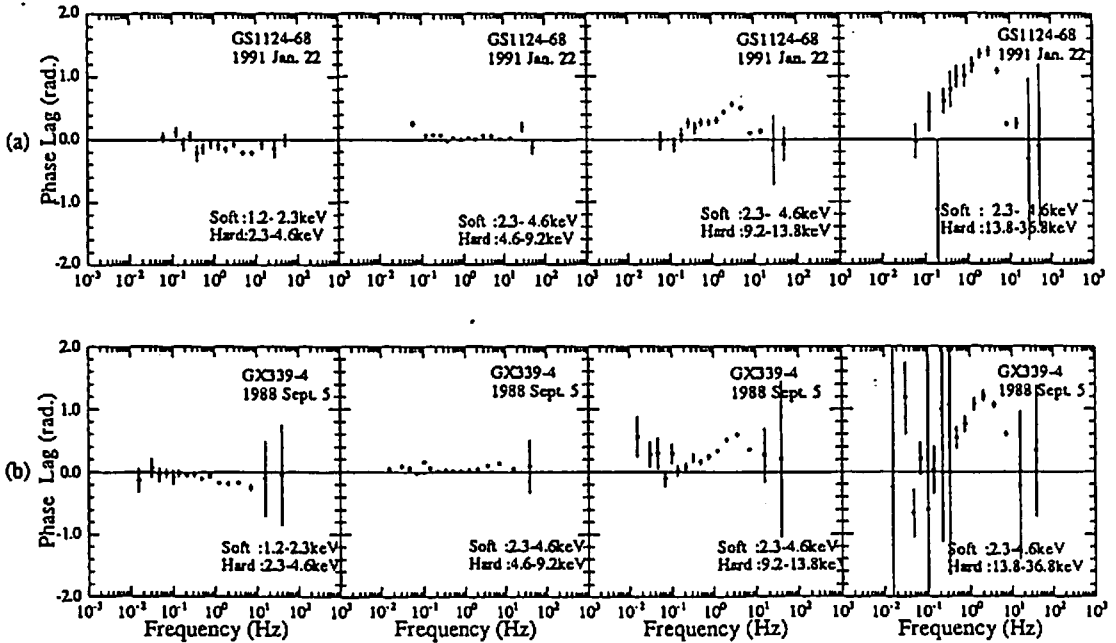


Fig.4. The phase lags. (a) GS1124-683 (1991 January 22). (b) GX339-4 (C+D sub-state (1988 Sept. 5)). Positive values of the phase lag correspond to hard lags (Miyamoto et al. 1993a).

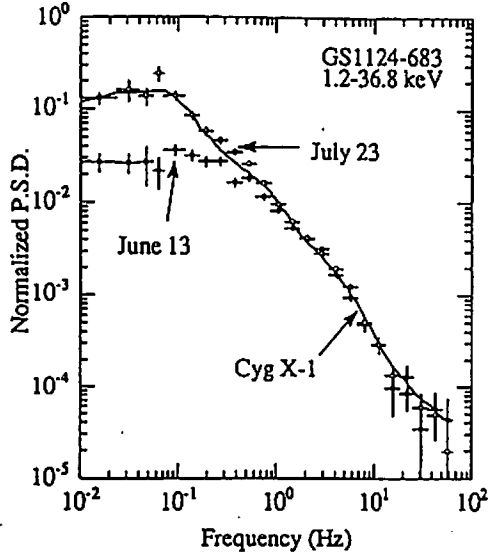


Fig.5. The normalized power spectrum density function of GS1124-683 in the low state. The values are compared with those of Cyg X-1.

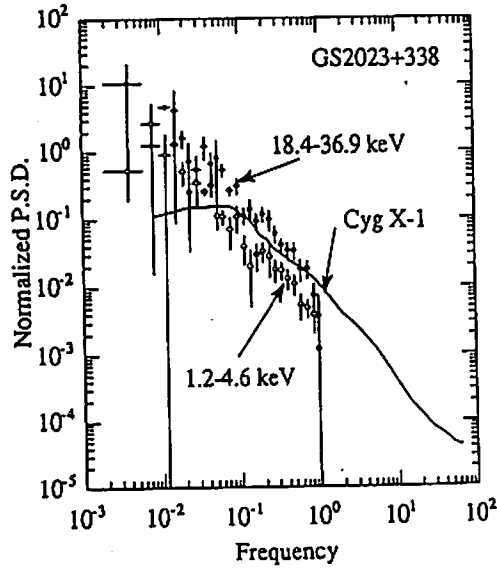


Fig.6 The normalized power spectrum density function of the GS2023+338 in its flare state. The values are compared with those of Cyg X-1 in the low state (Terada, 1991).

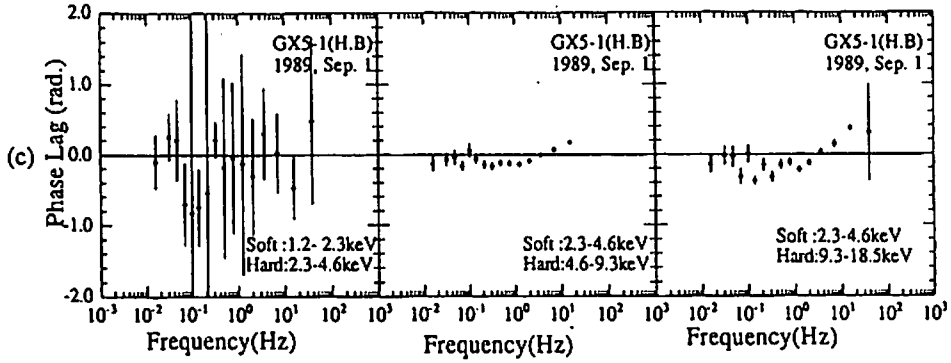


Fig.7. The phase lags of the GX5-1 in the horizontal branch (Kamado 1993).

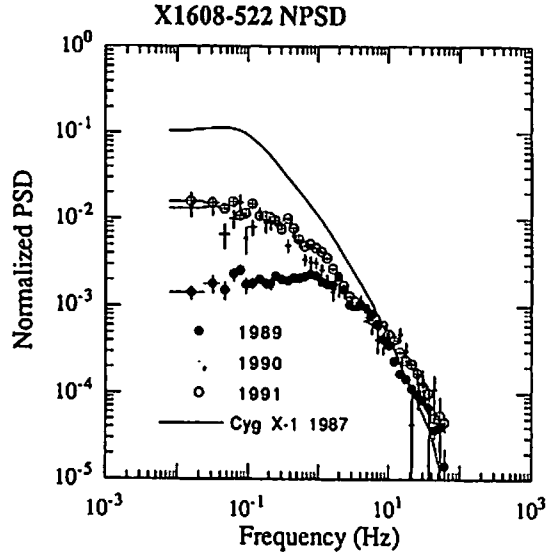


Fig.8. The NPSDs of X1608-522 in the low state. The values are compared with that of Cyg X-1 (Yoshida et al. 1992. Their results were compared with those of Cyg X-1 by Kitamoto).

Naked Singularity Dries up?

TAKASHI NAKAMURA

*Yukawa Institute for Theoretical Physics
Kyoto University, Kyoto 606, Japan*

MASARU SHIBATA AND KENICHI NAKAO

*Department of Physics, Kyoto University,
Kyoto 606, Japan*

ABSTRACT

We show a possibility of copious emission of gravitational waves from spindle like naked singularity which is formed dynamically from initially non-singular data as suggested in numerical relativity. We suggest that when the space-time approaches naked singularity, its gravitational mass may evaporate due to the emission of gravitational waves and therefore the mass of the resultant naked singularity almost vanishes. We also suggest a possibility of naked singularity formation as strong sources of gravitational waves.

1. Introduction

About ten years ago Nakamura and Sato^[1] performed numerical simulations of collapse of non-rotating deformed stars of mass $10M_{\odot}$. They used a phenomenological equation of state which becomes $P \propto \rho^2$ in the limit of $\rho \rightarrow \infty$. They started various simulations with oblate and prolate initial deformation and reduction of internal energy. They found that if the initial reduction of the internal energy is not large, the density distribution becomes almost spherically symmetric in the final stage and the apparent horizon is formed even though the density distribution is strongly deformed in the beginning. However if the initial reduction of the internal energy is large, the deformation of the distribution is enhanced for the large initial deformation. In these cases, no apparent horizon is identified. Rod-like or disk-like singularities which resemble naked singularities in Weyl metric^[2] seem to be formed. Nakamura and Sato, however, concluded such initial conditions are not realistic. Since a star should have evolved quasi-statically until the general relativistic instability sets in, the internal energy in the beginning should be near the virial value and the prolate and oblate deformation should not be so large. Recently, Shapiro and Teukolsky performed numerical simulations of general relativistic prolate and oblate collisionless spheroids.^[3] In a prolate collapse with large deformation, they showed the formation of spindle like singularity by measuring curvature invariant $I = R_{\mu\nu\rho\sigma}R^{\mu\nu\rho\sigma}$ and there are no apparent horizon, which suggests the singularity is naked.

As shown by Wald^[4] concretely, non existence of apparent horizons does not necessarily mean the non existence of the event horizon. Therefore spindle singularity suggested by above numerical examples may be covered by event horizons so that the cosmic censorship proposed by Penrose^[5] may be valid. What we like to discuss in this paper is, however, the converse case. If the formation of spindle-like singularity from non-singular initial data suggested by numerical relativity is naked, how should we understand this fact? The standard answer will be that the formation of singularity means only the breakdown of the Einstein's classi-

cal general relativity. If the quantum effects of gravity are taken into account, everything will be OK. In this paper, however, we try to analyze the formation of naked singularity within the classical gravity. In the formation of spindle singularity the curvature invariant, $I = R_{\mu\nu\rho\sigma}R^{\mu\nu\rho\sigma}$ diverges. If the singularity is naked, is there a special reason for non-propagation of the information of this increase to the null infinity \mathcal{I}^+ ? Intuitively at the formation of singularity, very short wave length disturbances of space-time will be created. If there is no event horizon, these disturbances may propagate as gravitational waves so that naked singularity may be a strong source of the very short wave length (i.e., $\lambda \ll M$, where M is the mass of naked singularity) gravitational waves, which suggests that the singularity itself should suffer strong back reaction.

In §2, we discuss the prolate dust collapse and generation of gravitational waves. In §3, we suggest a possibility of generation of the copious gravitational waves by the analytic solution of initial data for prolate dust collapse and its time evolution. In Appendix A, we show the Bel-Robinson Poynting vector for those data. §4 will be devoted to physical and astrophysical implications of the results. In this paper, we take the speed of light and the Newton's gravitational constant to be unity. Our convention for the Riemann and Ricci tensors are

$$\nabla_{[\mu}\nabla_{\nu]}w_{\rho} = \frac{1}{2}R_{\mu\nu\rho}{}^{\sigma}w_{\sigma}, \quad (1.1)$$

$$R_{\mu\nu} = R_{\mu\rho\nu}{}^{\rho}, \quad (1.2)$$

where ∇_{μ} is the covariant derivative. Greek tensor indices take values 0, 1, 2, 3, while latin indices take values 1, 2, 3.

2. Prolate Dust Collapse and Copious Generation of Gravitational Waves

As discussed in §1, several numerical simulations suggest the formation of spindle like naked singularity. If so, we like to ask how much gravitational waves are emitted in the formation process of naked singularity. Since the formation of naked singularity means the divergence of the curvature invariant, e.g., $R_{\mu\nu\rho\sigma}R^{\mu\nu\rho\sigma}$, very short wave length gravitational waves may be emitted. Therefore if one likes to estimate the amount of gravitational waves by numerical simulations, one needs extremely fine resolution of numerical grids (see discussion in §4). In this section, we estimate the amount of the gravitational radiation by using almost analytic solutions of prolate collapse. That is, we only solve ordinary differential equations.

Now if a spindle like naked singularity is formed from non-singular initial data, pressure or dispersion of collisionless matter should play a minor role. If they play a major role in dynamics, the singularity may not be formed. Therefore we here approximate the prolate collapse to a spindle singularity by the Newtonian dust collapse of the homogeneous prolate spheroid as a first step. We assume that the shape of the prolate spheroid is given as

$$\frac{x^2 + y^2}{a^2} + \frac{z^2}{c^2} = 1. \quad (2.1)$$

Then a and c obey^[6]

$$\ddot{a} = -\frac{3M}{2}\alpha(e)\frac{1}{ac}, \quad (2.2)$$

$$\ddot{c} = -\frac{3M}{2}\gamma(e)\frac{1}{a^2}, \quad (2.3)$$

$$\alpha(e) = \frac{1}{e^2} \left(1 - \frac{1-e^2}{2e} \ln \frac{1+e}{1-e} \right), \quad (2.4)$$

$$\gamma(e) = \frac{2(1-e^2)}{e^2} \left(-1 + \frac{1}{2e} \ln \frac{1+e}{1-e} \right), \quad (2.5)$$

where $e = \sqrt{1 - a^2/c^2}$ and M is the mass of the system. A dot is the time derivative. The luminosity of the gravitational waves in the frame of quadrupole formula is given as

$$L = \frac{1}{45} \ddot{D}_{\alpha\beta}^2 = \frac{2M^2}{375} (\ddot{a}^2 - \ddot{c}^2)^2. \quad (2.6)$$

We here ask the total amount of energy (ΔE) emitted until the prolate spheroid becomes a spindle singularity ($a = 0$ and $e = 1$).

ΔE is proportional to

$$I = \int (\ddot{a}^2 - \ddot{c}^2)^2 dt. \quad (2.7)$$

As discussed by Lin, Mestel and Shu^[6] a becomes zero for finite value of c . Then from Eq.(2.2), we have for $a \rightarrow 0$

$$\ddot{a} = -\frac{A}{a}, \quad (2.8)$$

where

$$A = \frac{3M}{2c}.$$

Eq.(2.8) means that velocity \dot{a} logarithmically diverges for $a \rightarrow 0$. Similarly, we have from Eq.(2-3)

$$\ddot{c} = B \left(1 + \frac{1}{2} \ln \frac{1-e}{2} \right), \quad (2.9)$$

where

$$B = \frac{3M}{c^2}.$$

From Eq.(2.9)

$$\dot{a} = -\sqrt{2A \ln(a_0/a)}, \quad (2.10)$$

where a_0 is a constant of integration.

Now defining t_c as a time when a becomes zero, we have

$$\int_0^{a(t)} \frac{da}{\sqrt{2A \ln(a_0/a)}} = t_c - t, \quad (2.11)$$

Changing an integration variable from a to $s = \sqrt{\ln(a_0/a)}$, we have

$$\frac{2a_0}{\sqrt{2A}} \int_s^\infty e^{-s^2} ds = t_c - t, \quad (2.12)$$

Now for $s \gg 1$, the Gauss's error function has asymptotic expansion as

$$\frac{2a_0}{\sqrt{2A}} e^{-s^2} \sum_{n=0}^{\infty} (-1)^n \frac{(2n-1)!!}{2^{n+1} s^{2n+1}} = t_c - t, \quad (2.13)$$

Therefore a is determined implicitly by

$$\frac{2a}{\sqrt{2A}} \sum_{n=0}^{\infty} (-1)^n \frac{(2n-1)!!}{2^{n+1} (\ln a_0/a)^{\frac{2n+1}{2}}} = t_c - t, \quad (2.14)$$

In the lowest order, Eq.(2.14) is approximated as

$$\frac{a}{\sqrt{2A \ln(a_0/a)}} = t_c - t, \quad (2.15)$$

and, hence,

$$a \sim (t_c - t) \sqrt{2A \ln\left(\frac{t_0}{t_c - t}\right)}, \quad (2.16)$$

where

$$t_0 \sim \frac{a_0}{\sqrt{2A}}, \quad (2.17)$$

Eq.(2.9) shows \ddot{c} diverges for $e \rightarrow 1$, However divergence is not strong but

logarithmical. At divergence \ddot{c} is approximated as

$$\ddot{c} \propto B \ln(t_c - t), \quad (2.18)$$

The integration of Eq.(2.18) yields

$$\dot{c} = \text{const.} - B(t_c - t)[\ln(t_c - t) + 1]. \quad (2.19)$$

That is, \dot{c} does not diverge. Now we are ready to estimate the integral of Eq.(2.7)

$$I \propto \int_0^{t_c} (a\ddot{a} + 3\dot{a}\ddot{a} - c\ddot{c} - 3\dot{c}\ddot{c})^2 dt, \quad (2.20)$$

Since \dot{a} , \ddot{a} and \ddot{c} diverge at $t = t_c$, we here mainly estimate the integral near $t \sim t_c$, that is, from $t = t_c - 0$ to $t = t_c$ as

$$I' = \int_{t_c-0}^{t_c} (a\ddot{a} + 3\dot{a}\ddot{a} - c\ddot{c} - 3\dot{c}\ddot{c})^2 dt, \quad (2.21)$$

Now \ddot{a} and \ddot{c} are estimated as

$$\ddot{a} = \frac{A}{a^2}\dot{a}, \quad \ddot{c} = B\left(1 + \ln \frac{a}{a'_0}\right), \quad \dot{c} = \frac{B}{a}\dot{a}. \quad (2.22)$$

where a'_0 is a constant. I' can be rewritten as

$$\begin{aligned} I' &= - \int_0^{0+} \frac{da}{\dot{a}} \left(-2A\frac{\dot{a}}{a} - B\frac{\dot{c}a}{a} - 3\dot{c}B(1 + \ln \frac{a}{a'_0}) \right)^2 \\ &= - \int_0^{0+} \frac{da}{a^2\dot{a}} \left(\frac{6GM\dot{a}}{c} + 3\dot{c}aB(1 + \ln \frac{a}{a'_0}) \right)^2 \\ &= + \int_0^{0+} \frac{36M^2\sqrt{2A\ln(a_0/a)}}{a^2c^2} da \\ &= + \infty. \end{aligned} \quad (2.23)$$

Eq.(2.23) means that under the Newtonian hydrodynamics with the quadrupole formula an infinite energy is radiated before the formation of spindle like singularity. If this is real even in the general relativistic treatment, the gravitational mass of the naked spindle like singularity may evaporate and the resultant singularity is dried up due to the copious emission of gravitational waves.

3. Momentarily Static Initial Data

Initial data of a momentarily static prolate spheroid give us some insight to how much gravitational waves are emitted in the course of the formation of the spindle singularity in general relativity. This was discussed by Nakamura, Shapiro and Teukolsky (NST).^[7] We consider the time symmetric initial data ($K_{ij} = 0$), with conformally flat 3-space as

$$d\ell^2 = \phi^4 f_{ij} dx^i dx^j, \quad (3.1)$$

where f_{ij} is the flat metric. The Hamiltonian constraint equation becomes

$$\Delta\phi = -2\pi\rho_H\phi^5, \quad (3.2)$$

where Δ and ρ_H are the flat Laplacian operator and the energy density measured by the normal line observer, respectively. NST^[7] set ρ_H as

$$2\pi\phi^5\rho_H = 4\pi\rho_N, \quad (3.3)$$

$$\rho_N = \begin{cases} M_N/(4\pi a^2 c/3), & R^2/a^2 + Z^2/c^2 \leq 1 \\ 0, & \text{elsewhere} \end{cases} \quad (3.4)$$

so that ϕ has an analytic solution as

$$\phi = 1 + \left(\frac{3M_N}{2ce}\beta + \frac{1}{2}(RK_R + ZK_Z) \right), \quad (3.5)$$

$$K_R = \frac{3M_N}{2(ce)^3} R(\beta - \sinh\beta \cosh\beta), \quad (3.6)$$

$$K_Z = \frac{3M_N}{(ce)^3} Z(\tanh\beta - \beta), \quad (3.7)$$

where β is given by

$$\sinh\beta = \frac{c}{a}e \quad \text{for} \quad \frac{R^2}{a^2} + \frac{Z^2}{c^2} \leq 1, \quad (3.8)$$

and

$$R^2\sinh^2\beta + Z^2\tanh^2\beta = c^2e^2 \quad \text{for} \quad \frac{R^2}{a^2} + \frac{Z^2}{c^2} > 1. \quad (3.9)$$

NST^[7] obtained the relation of the total rest mass energy defined by

$$M_0 = \int \rho \phi^6 d^3x, \quad (3.10)$$

to the gravitational mass M as

$$M = \frac{2M_0}{1 + (1 + \alpha M_0)^{1/2}}, \quad (3.11)$$

where

$$\alpha = \frac{6}{5ce} \ln \frac{1+e}{1-e}. \quad (3.12)$$

Eq.(3.11) shows that for the fixed total rest mass M_0 , the gravitational mass decreases as a function of the eccentricity e . In the limit of spindle singularity, M goes to zero. This means that the gravitational binding energy becomes just the total rest mass. Thus if we model the late stages of a collapse of a prolate spheroid to a spindle singularity by a sequence of above initial data with fixing M_0 and increasing eccentricity e , we expect the copious emission of gravitational waves so that the naked singularity itself might become zero gravitational mass.

One may say that the sequence of initial data is different from its true evolution. To argue against this objection, we shall discuss the evolution of the above initial data analytically for $t/M \ll 1$. As a coordinate condition we take $\alpha = 1$ and $\beta^i = 0$, where α and β^i are the lapse function and the shift vector, respectively. Further, we consider the dust fluid ($P = 0$). Then outside the prolate

spheroid, the evolution of the space-time is determined by

$$\frac{\partial}{\partial t} K_{ij} = {}^{(3)}R_{ij}, \quad (3.13)$$

and

$$\frac{\partial}{\partial t} \gamma_{ij} = -2K_{ij}, \quad (3.14)$$

where ${}^{(3)}R_{ij}$ is Ricci tensor with respect to the intrinsic metric γ_{ij} . Now we seek after the solution in a power series of $t \ll M$ as

$$\gamma_{ij} = \gamma_{ij}^{(0)} + \gamma_{ij}^{(2)}t^2 + \gamma_{ij}^{(4)}t^4 + \dots, \quad (3.15)$$

and

$$K_{ij} = K_{ij}^{(1)}t + K_{ij}^{(3)}t^3 + \dots. \quad (3.16)$$

In the lowest order we find

$$K_{ij}^{(1)} = 6\phi^{-2}\partial_i\phi\partial_j\phi - 2\phi^{-1}\partial_i\partial_j\phi - 2\phi^{-2}f_{ij}(\partial_t\phi)(\partial^t\phi) \equiv \Sigma_{ij}, \quad (3.17)$$

where ∂_i is the covariant derivative with respect to f_{ij} .

$$\gamma_{ij}^{(0)} = \phi^4 f_{ij}, \quad (3.18)$$

and

$$\gamma_{ij}^{(2)} = -\Sigma_{ij}. \quad (3.19)$$

It is easy to observe that $K_{ij}^{(1)}$ is traceless and divergence free respect to $\gamma_{ij}^{(0)}$ because of the Bianchi identity. Here it should be noticed that $K_{ij}^{(1)}$ does not include the longitudinal part which is determined by the momentum constraint. Since our coordinate is determined by the geodesic time slicing ($\alpha = 1$) and the co-moving spatial coordinate ($\beta^i = 0$) conditions, the momentum density J_m of

the dust fluid vanishes for all time if $J_m = 0$ initially. Hence, the longitudinal traceless part L_{ij} of the extrinsic curvature K_{ij} is determined by the momentum constraint as

$$D_j L_i^j = \frac{2}{3} D_i K = O\left(\frac{t^3}{M^3}\right). \quad (3.20)$$

Eq.(3.20) means that L_{ij} does not include the first order term with respect to t/M and therefore $K_{ij}^{(1)}$ is transverse traceless(TT), i.e., just the degree of freedom of the gravitational waves. Hence one may say that in reality emission of gravitational waves occurs from the prolate collapse to a spindle singularity, because TT part of K_{ij} exists.

We shall estimate roughly how much gravitational radiation is generated. The total energy (ADM energy) $E_{tot} = M$ of the system is given by

$$E_{tot} = -\frac{1}{2\pi} \int \tilde{\Delta} \phi \sqrt{\tilde{\gamma}} d^3x, \equiv \int \rho_{eff} \sqrt{\tilde{\gamma}} d^3x, \quad (3.21)$$

where $\tilde{\Delta}$ is the Laplacian operator with respect to the conformal metric $\tilde{\gamma}_{ij} = \phi^{-4} \gamma_{ij}$.^[8] By the use of the Hamiltonian constraint, the effective energy density ρ_{eff} is written as

$$\rho_{eff} = \rho_H \phi^5 + \frac{1}{16\pi} [(K_i^j K_j^i - K^2) \phi^5 - {}^{(3)}\tilde{R} \phi] \equiv \rho_H \phi^5 + \rho_G, \quad (3.22)$$

where ${}^{(3)}\tilde{R}$ is the Ricci scalar with respect to $\tilde{\gamma}_{ij}$. Here it should be noticed that, in the case of $t/M \ll 1$, the lowest order contribution to ρ_G comes from $K_{ij}^{(1)} t$ and $\gamma_{ij}^{(2)} t^2$. From Eqs.(3.17) and (3.19), we obtain ρ_G for the vacuum part as

$$\begin{aligned} \rho_G = & \frac{t^2}{\pi \phi^5} [(\partial^i \partial^j \phi)(\partial_i \partial_j \phi) - 9\phi^{-1}(\partial^i \phi)(\partial^j \phi)(\partial_i \partial_j \phi) \\ & + 12\phi^{-2}\{(\partial^i \phi)(\partial_i \phi)\}^2] + O\left(\frac{t^3}{M^3}\right). \end{aligned} \quad (3.23)$$

For the case of $a = 10^{-2}$, $c = 1$ and $M = 1$, we depict ρ_G on $Z = 0$ and $Z = c$ planes in Fig.1. ρ_G is very large irrespective of Z since we are using the unit of $M = 1$.

For $e \rightarrow 1$, ϕ diverges as $(3M/2c) \ln(c/R)$ near the spheroid, so that ρ_G becomes as

$$\rho_G \simeq \frac{1}{\pi} \left(\frac{2c}{3M} \right)^3 \frac{t^2}{R^4}. \quad (3.24)$$

Since the collapsing time of the prolate spheroid to a spindle singularity t_c is estimated as^[6]

$$t_c \sim 0.5\rho^{-1/2} \sim \left(\frac{M}{a^2 c} \right)^{-1/2}. \quad (3.25)$$

Then, the “energy” E_G produced until $t \sim t_c$, which comes from the transverse traceless part, i.e., the degree of gravitational waves, becomes

$$E_G \simeq \frac{1}{\pi} \left(\frac{2c}{3M} \right)^3 \frac{t_c^2}{R^4} \times \frac{4\pi}{3} a^2 c \simeq M \left(\frac{c}{M} \right)^5. \quad (3.26)$$

In the case that the naked singularity appears, $c/M \gtrsim 1.0$,^[7] so that E_G becomes almost equal to the total energy $E_{tot} = M$ of this system. The above estimate suggests that almost all E_{tot} is converted into the gravitational waves.

At this stage, it is not clear whether the “energy” of the gravitational waves E_G propagates away to \mathcal{I}^+ or collapses into the singularity. In order to see the propagation direction of gravitational waves, the Poynting vector proposed by Bel and Robinson P_i^{Bel} is often used in the numerical simulation since this is defined locally and covariantly.^[11] The lowest order of P_i^{Bel} for $t \ll M$ is directed toward the Z -axis. This feature seems to suggest that the gravitational waves collapse into the singularity. However, as shown in Appendix A, the lowest order contribution to P_i^{Bel} does not come from dominant TT part, $\gamma_{ij}^{(2)} t^2$ and $K_{ij}^{(1)} t$. Furthermore, the dimension of P_i^{Bel} is different from the physical energy flux. Hence, in our case, P_i^{Bel} does not seem to correspond to the energy flux of the gravitational waves.

Since there are no trapped surface, no apparent horizon and no event horizon, the gravitational waves seem to propagate away to \mathcal{I}^+ . Of course, even though the event horizon does not exist, there is a possibility that the outgoing

gravitational waves suffer the back scattering by some potential barrier like as the Regge-Wheeler one of the Schwarzschild space-time, which exists outside the event horizon. It is not known whether it exists or not in the axisymmetric space-time with the spindle singularity. However in the cylindrical space-time such a potential barrier does not exist to a gravitational wave variable ψ .^[9] Since we can regard the space-time with highly eccentric configuration with $c \gg M$ as the cylindrical one locally, gravitational waves emitted near the spindle will propagate to infinity. If so, the large amount of the gravitational radiation is emitted, which is comparable with the total energy of the system and the mass of the resultant naked singularity almost vanishes. However, since it is not clear whether the gravitational mass of naked singularity is non-negative, there is a possibility that the resultant naked singularity produces infinite gravitational waves and its mass diverges negatively. Recently, Echeverria shows that the cylindrical dust shell collapse produces finite gravitational waves even though the naked singularity is formed.^[10] This fact suggests that the spindle naked singularity does not have negative infinite value.

4. Discussions

Detailed fully general relativistic numerical simulations are needed to confirm the naked singularity dried up conjecture proposed in this paper. If we use Eq.(3.11), 50% of the total rest mass is radiated by the time when e becomes $e_{1/2}$ where $e_{1/2}$ is defined by

$$e_{1/2} = 1 - 2 \exp\left(-\frac{20c}{3M_0}\right). \quad (4.1)$$

At this time, a is only $2 \exp(-10c/3M_0) \times c$. For $c \sim M_0$, $a = 0.07c$. In order to resolve one wave length of gravitational waves in numerical relativity, we need ~ 20 grids per wave length. Since the wave length of the radiated gravitational waves may be $\sim a$ or so, we need ~ 200 grid along the spindle like

object with $a/c \sim 10^{-2}$. To resolve the structure of spindle like singularity up to asymptotically flat region, $R_{\max} \simeq Z_{\max} \simeq 10c$. Therefore needed number of grids becomes $\sim 2000 \times 2000$, which is barely possible by the most powerful super computers at present. Furthermore, in the course of the singularity formation, the energy density of matter grows up and very high temperature will be realized. Hence we have to take into account the effect of QCD and furthermore that of GUT, in order to investigate whether the naked singularity is formed or not finally.

If the naked singularity dried up conjecture is true, naked singularity formation in such as the galactic center, will be one of the most powerful source of gravitational waves, i.e. the conversion rate can be 100% (cf. for black hole collision, maximum possible is 29%, in practice $\lesssim 10\%$).^[12] In the case of the black hole formation, the shortest wave length of gravitational waves is limited to $\lambda \gtrsim 20M$.^[13] However in the naked singularity drying up λ can be $2 \exp(-10c/3M) \times c$ as shown in the previous paragraph. For $c = 5M$, λ can be $5.7 \times 10^{-7}M$. Thus naked singularity formation of mass $10^8 M_{\odot}$, may emit gravitational waves with wave length $8.7 \times 10^6 \text{cm}$, i.e., 3.4kHz . For the hypothetical event of naked singularity drying up at the distance of 1Gpc , the amplitude of the gravitational wave h can be $\sim 2.0 \times 10^{-18}$.

Acknowledgment

This work was partly supported by the Grant-in-Aid for Scientific Research on Priority Area of the Ministry of Education (04234104) and for Scientific Research Fellowship (1526).

APPENDIX A

The Poynting vector proposed by Bel and Robinson^[11] is often used in order to see the propagation direction of the gravitational waves in numerical simulations since it is constructed locally from the Weyl tensor and its definition is covariant. Fix a three dimensional spacelike hypersurface with the unit normal vector n_μ and set,

$$E_{\mu\nu} = C_{\mu\rho\nu}{}^\sigma n_\sigma n^\rho, \quad (A1)$$

$$B_{\mu\nu} = \frac{1}{2} \epsilon_{\mu\rho}{}^{\alpha\beta} C_{\alpha\beta\nu}{}^\sigma n_\sigma n^\rho, \quad (A2)$$

where $C_{\mu\rho\nu}{}^\sigma$ is the Weyl tensor of the space-time and $\epsilon_{\mu\rho}{}^{\alpha\beta}$ is the anti-symmetric tensor, respectively. The tensor fields $E_{\mu\nu}$ and $B_{\mu\nu}$ are purely spatial and can be written by the quantities on the three dimensional spacelike hypersurface as,

$$E_{ij} = {}^{(3)}R_{ij} + K K_{ij} - K_i^L K_{Lj}, \quad (A3)$$

$$B_{ij} = \epsilon_{lm(i} D^L K_{j)}^m, \quad (A4)$$

where ϵ_{lmn} and D_L are anti-symmetric tensor and the covariant derivative within the three dimensional spacelike hypersurface, respectively. The Bel-Robinson Poynting vector is given by

$$P_i^{Bel} = \epsilon_i^{ab} B_a^c E_{cb}. \quad (A5)$$

On the time symmetric hypersurfaces given in §3, P_i^{Bel} vanishes since B_{ij} is equal to zero. Then, as performed in §3, we consider the time evolution of those hypersurface and calculate P_i^{Bel} . For $t \ll M$, the intrinsic metric γ_{ij} and the extrinsic curvature K_{ij} are given by,

$$\gamma_{ij}(t) \simeq \gamma_{ij}^{(0)} - \Sigma_{ij} t^2, \quad (A6)$$

$$K_{ij}(t) \simeq \Sigma_{ij}t + \frac{1}{6}(\gamma_{ij}^{(0)}\Sigma_l^m\Sigma_m^l - 7\Sigma_i^l\Sigma_{lj})t^3, \quad (A7)$$

where we use the relation

$${}^{(3)}\ddot{R}_{ij}(t=0) = -3\left(\Sigma_i^l\Sigma_{lj} - \frac{1}{3}\gamma_{ij}^{(0)}\Sigma_l^m\Sigma_m^l\right). \quad (A8)$$

The lowest order of E_{ij} and B_{ij} are then obtained as

$$E_{ij} \simeq \Sigma_{ij}, \quad (A9)$$

$$B_{ij} \simeq -\frac{7}{12}t^3\Sigma_{km}(\epsilon^{lm}{}_i\overset{(0)}{D}_l\Sigma_j^k + \epsilon^{lm}{}_j\overset{(0)}{D}_l\Sigma_i^k), \quad (A10)$$

where $\overset{(0)}{D}_i$ is the covariant derivative with respect to $\gamma_{ij}^{(0)}$. Here, it should be noticed that the lowest order contribution to E_{ij} and B_{ij} does not come from the lowest TT part, $\gamma_{ij}^{(2)}t^2 = -\Sigma_{ij}t^2$ and $K_{ij}^{(1)}t = \Sigma_{ij}t$ because of $\overset{(0)}{D}_i\Sigma_{jk} = \overset{(0)}{D}_j\Sigma_{ik}$. Then, we get P_i^{Bel} as

$$P_i^{Bel} = \frac{7}{12}t^3\epsilon_i{}^{ab}\Sigma_a^c\Sigma_{dm}(\epsilon^{lm}{}_c\overset{(0)}{D}_l\Sigma_b^d + \epsilon^{lm}{}_b\overset{(0)}{D}_l\Sigma_c^d) + O\left(\frac{t^4}{M^4}\right). \quad (A11)$$

We can see that the lowest order of P_i^{Bel} is directed toward the Z -axis. This feature seems to suggest that the gravitational waves collapse into the singularity. However, the lowest order contribution to P_i^{Bel} does not include the lowest order of TT part, $\gamma_{ij}^{(2)}t^2$ and $K_{ij}^{(1)}t$. Furthermore, the dimension of P_i^{Bel} is different from the physical energy flux. Hence, in our case, P_i^{Bel} does not represent the energy flux of the gravitational waves.

REFERENCES

1. T. Nakamura and H. Sato, Prog. Theor. Phys. **67**(1982), 346.
2. Weyl metric is a solution to non-rotating vacuum Einstein Equations.
B. H. Voorhees, Phys. Rev. **D2**(1970), 2119;
D. M. Zipoy, J. Math. Phys. **7**(1966), 1137.
3. S. L. Shapiro and S. A. Teukolsky, Phys. Rev. Lett. **66** (1991), 994.
4. R. M. Wald, Phys. Rev. **D45**(1992), 2006.
5. R. Penrose, Riv. Nouvo. Cim. **1** (Numero Special) (1969), 252.
6. C. C. Lin, L. Mestel and F. H. Shu, Ap J. **142**(1965), 1431.
7. T. Nakamura, S. L. Shapiro and S. A. Teukolsky, Phys. Rev. **D38**(1988), 2292.
8. N. Ó Murchadha and J. W. York, Phys. Rev. **D10**(1974), 2345.
9. K. S. Thorne, Rhys. Rev. **B138**(1965), 251;
T. Piran, in *Sources of Gravitational Radiation*, ed. L. Smarr(Cambridge Univ. Press, Cambridge, 1979).
10. F. Echeverria, Caltech preprint, GRP-322(1992).
11. V. Zakharov, *Gravitational Waves in Einstein's Theory* (Halsted Press, Jerusalem, 1973).
12. T. Nakamura, K. Oohara and Y. Kojima, Prog. Theor. Phys. Suppl. **90**, (1987).
13. R. F. Stark and T. Piran, Phys. Rev. Lett. **55**(1985), 891.

FIGURE CAPTIONS

1. The effective energy density of the gravitational waves defined in §3 are depicted for the case of $a = 10^{-2}$, $c = 1$ and $M = 1$. In Fig.1(a), ρ_G on $Z = 0$ plane is depicted, while in Fig.1(b) that on $Z = c$.

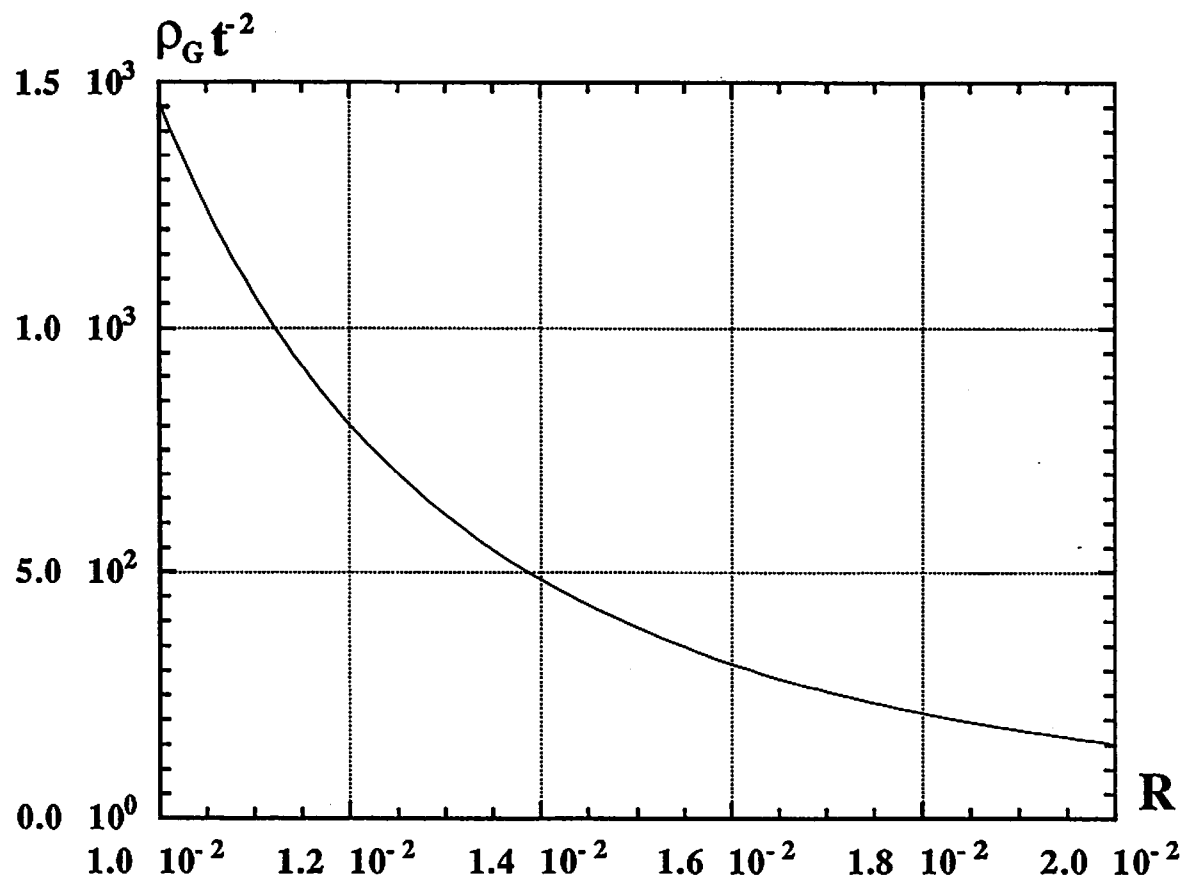


Fig.1(a)

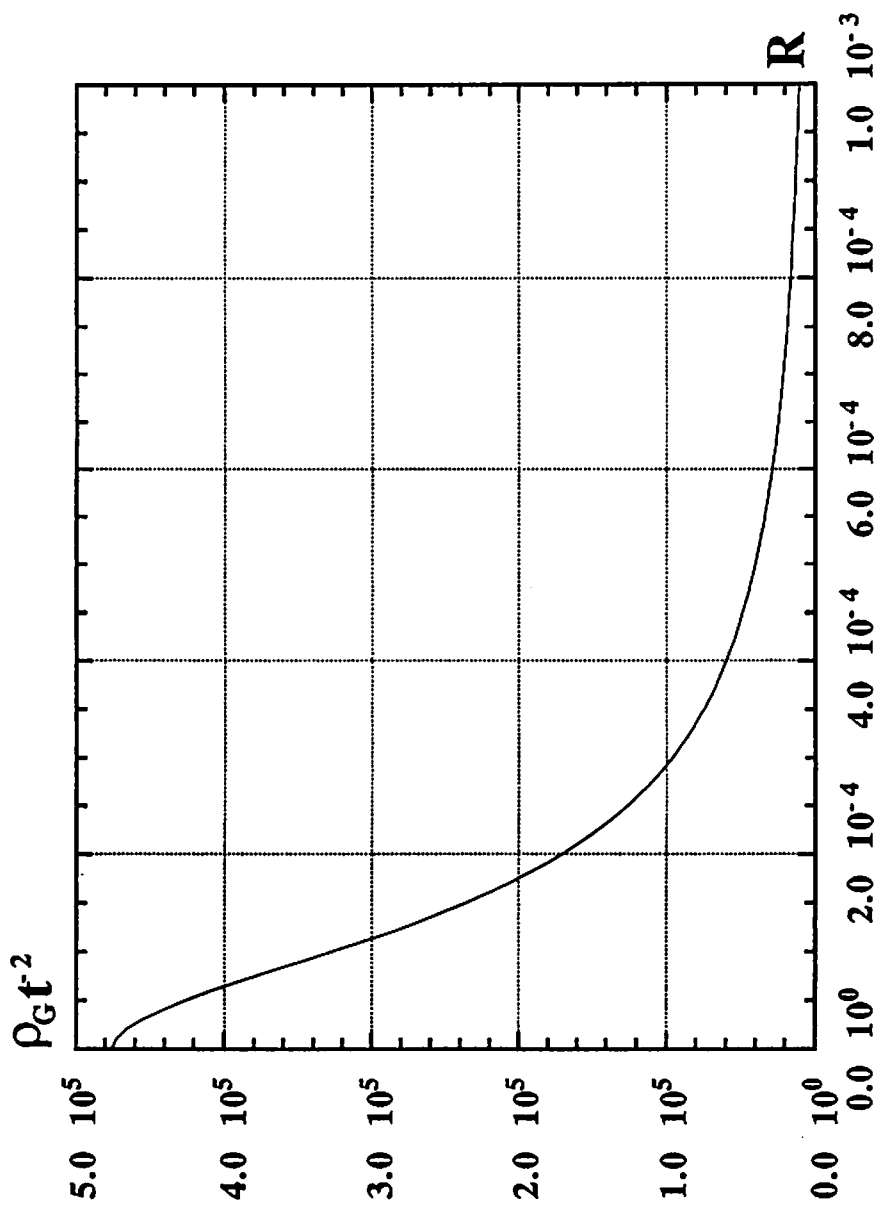


Fig.1(b)

Scattering of Maximally-Charged Dilaton Black Holes^{1,2}

Kiyoshi Shiraishi³

Akita Junior College
Shimokitade-Sakura, Akita-shi, Akita 010, JAPAN

The action for the Einstein-Maxwell-Dilaton system we consider in (N+1) dimensions is: [1]

$$S = \int d^{N+1}x \frac{\sqrt{-g}}{16\pi} \left[R - \frac{4}{N-1} (\nabla\phi)^2 - e^{(4a/(N-1))\phi} F^2 \right] \quad (N \geq 3), \quad (1)$$

where we fix the Newton constant to unity. The coupling constant a is the parameter which determines the strength of the coupling between the Maxwell field F and the dilaton field ϕ .

It is known that static forces among extreme black holes in this system are totally cancelled with one another. Therefore, there can exist multi-centered static solutions describing many-body systems of extreme charged black holes. We find n -black-hole solution in the following form:

$$ds^2 = - U^2(\vec{x}) dt^2 + U^{2/(N-2)}(\vec{x}) d\vec{x}^2, \quad (2)$$

where

$$U(\vec{x}) = \{ F(\vec{x}) \}^{(N-2)/(N-2+a^2)}, \quad (3)$$

¹Talk given at the Workshop on General Relativity and Gravitation (Waseda Univ., Tokyo, Japan), 18-20 January 1993.

²This talk is based on refs. [0].

³e-mail: g00345@jpnac.bitnet. or g00345@sinet.ad.jp.

and

$$F(\vec{x}) = 1 + \sum_{i=1}^n \frac{\mu_i}{(N-2)|\vec{x} - \vec{x}_i|^{N-2}} . \quad (4)$$

Using these expressions, the (Maxwell) vector one-form and the dilaton configuration are written as

$$A = \pm \sqrt{\frac{N-1}{2(N-2+a^2)}} [1 - \{F(\vec{x})\}^{-1}] dt , \quad (5)$$

and

$$e^{-\{4a/(N-1)\}\phi} = \{F(\vec{x})\}^{2a^2/(N-2+a^2)} . \quad (6)$$

In this solution, the asymptotic value of ϕ is fixed to be zero.

If we set $a=0$ in the solution, we find that the solution reduces to the Papapetrou-Majumdar-Myers solution in $(1+N)$ dimensions [2].

We anticipate that an addition of a small amount of kinetic energy to this static system can be treated by perturbation. This also presents the situation that radiation reactions can be ignored. We apply the method of Ferrell and Eardley [3] to the system of extreme charged dilaton black holes to get the information on the slow motion of the holes at arbitrary distances.

We first calculate the classical fields in the presence of the slow motion of the black-hole sources perturbatively. Secondly substituting the perturbative solutions into the action for the classical field, we obtain the effective action for maximally charged dilaton black holes as point sources.

Synthesizing all the contributions of small velocity perturbation, we obtain the effective lagrangian up to $O(v^2)$ for n maximally charged dilaton black holes:

$$L = - \sum_{i=1}^n m_i + \sum_{i=1}^n \frac{1}{2} m_i (\vec{v}_i)^2 + \frac{(N-1)(N-a^2)}{16\pi(N-2+a^2)^2} \int d^N x \{F(\vec{x})\}^{2(1-a^2)/(N-2+a^2)} \sum_{i,j}^n \frac{(\vec{n}_i \cdot \vec{n}_j) [\vec{v}_i \cdot \vec{v}_j]^2 \mu_i \mu_j}{2|\vec{r}_i|^{N-1} |\vec{r}_j|^{N-1}} , \quad (7)$$

where $\vec{r}_i = \vec{x} - \vec{x}_i$ and $\vec{n}_i = \vec{r}_i / |\vec{r}_i|$. $F(x)$ is defined by (3).

The integration must be carried out with care for the regularization

of divergences and seemingly-divergent integrals.

If we set the dilaton coupling to zero and set $N=3$ in the above expression, we reproduce the result of ref. [3]. Furthermore, in the large-separation limit (where we approximate $F(x)$ by 1), we find exactly the same result obtained by the Lienard-Wiechert method [0].

An interesting point we soon become aware of is the existence of many-body interactions. In general, we obtain infinite species of many-body interactions by expanding the function $F(x)$. Some special cases arise: (1) when $a^2=0$ and $N=3$, the black holes are governed only by two-body, three-body, and four-body interactions [3], (2) when $a^2=0$ and $N=4$, there are only two-body and three-body interactions, (3) when $a^2=1$ (and any N), there are only two-body interactions, and (4) when $a^2=N$, there is no interactions to this order.

The slow motion of classical lumps or solitons in many kind of field theoretical models is expressed by geodesic motion on the moduli space, which is the space of the parameters in the static configuration.

In the presense case, the moduli space metric can be obtained from the expression (7). Now we further focus our attention on the two-body problem. Then the metric of the 2-dimensional moduli space for the two-body system turns out to be

$$ds_{MS}^2 = \gamma(r) \{ dr^2 + r^2 d\Omega_{N-1}^2 \} , \quad (8)$$

where

$$\begin{aligned} \gamma(r) = & \frac{A_{N-1}(N-1)}{8\pi(N-2+a^2)} \times \left[\frac{\mu_a \mu_b}{\mu_a + \mu_b} + \mu_a \left(1 + \frac{\mu_b}{(N-2)r^{N-2}} \right)^{(N-a^2)/(N-2+a^2)} \right. \\ & \left. + \mu_b \left(1 + \frac{\mu_a}{(N-2)r^{N-2}} \right)^{(N-a^2)/(N-2+a^2)} - \mu_a - \mu_b - \frac{N-a^2}{N-2+a^2} \frac{\mu_a \mu_b}{(N-2)r^{N-2}} \right] \end{aligned} \quad (9)$$

Moreover, we consider two-dimensional intersection of the moduli space for simplicity. The two parameters are the distance between two black holes (r) and the azimuthal angle (θ) on the scattering plane.

The shape of this surface of the moduli space depends on the spatial dimension N as well as a^2 . The reduced metric can be written in the form:

$$\begin{aligned}
ds_{MS}^2 &= \gamma(r) \{ dr^2 + r^2 d\theta^2 \} \\
&= h(R) dR^2 + R^2 d\theta^2 \\
&= dR^2 + dz^2(R) + R^2 d\theta^2
\end{aligned} \tag{10}$$

where $R(r)$ is a new radial coordinate. We can realize the surface immersed in the three dimensional Euclidean space spanned by the coordinates R , θ , and $z(R)$. The surfaces for some case are sketched in Figs. 1 and 2. The "throat" of the surface is located at the distance where $h(R(r))$ diverges.

Suppose that the two black holes approach each other from spatial infinity with low relative velocity and impact parameter b , the two black holes coalesce if b is smaller than a certain critical value which is in the same order of the radius of the throat. If $a^2 > (N-2)^2/N$, moduli surface has no throat, and then two black holes never coalesce.

For $N=3$ and $a^2=1$, The black holes never coalesce according to the geodesic approximation on the moduli space. The differential cross section in this $N=3$ and $a^2=1$ case turns out to be written in the form of the Rutherford scattering:

$$\frac{d\sigma}{d\Omega} = \frac{1}{4} \frac{M^2}{\sin^4(\Theta/2)} \tag{11}$$

This behavior can be expected by observing the geometry of the moduli space -- deficit angle $= \pi$ near the origin for $N=3$ and $a^2=1$.

To summarize: We have studied the interaction among the maximally charged dilaton black holes in the low-velocity limit.

The nature of the interaction depends on the value of the dilaton coupling " a ", in quality as well as in quantity.

$a=1$ is a special value, in any dimensions, for realizing a simple 2-body interactions.

There is another critical value, for coalescence of two maximally charged dilaton black holes: it is $a^2 = (N-2)^2/N$. (for $N=3$, $a^2=1/3$). The global structure of moduli space depends on a^2 .

The geodesic approximation has been justified in the small mass and low velocity limit, by using the test particle/wave analyses. The

quantization on the moduli space have also been examined. For further detail, see refs. [0]. Other aspects on charged dilaton black holes are studied in refs. [00].

References

- [0] "Multi-Centered Solution for Maximally CDBHs in Arbitrary Dimensions", to appear in J. Math. Phys. 34; "Moduli Space Metric for Maximally CDBHs", AJC-HEP-8, to appear in Nucl. Phys. B; "Classical and Quantum Scattering of Maximally CDBHs", AJC-HEP-10, to appear in Int. J. Mod. Phys. D.
- [00] "Multi-Black Hole Solutions in Cosmological Einstein-Maxwell-Dilaton Theory", AJC-HEP-15; "Spinning a CDBH", Phys. Lett. A 166 (92) 298; "Superradiance from a CDBH", Mod. Phys. Lett. A 7 (92) 3449; "Quantum Effects near CDBHs", Mod. Phys. Lett. A 7 (92) 3569; "Motion of Test Particles around a CDBH", AJC-HEP-13.
- [1] G. W. Gibbons and K. Maeda, Nucl. Phys. B298 (1988) 741.
D. Garfinkle, G. Horowitz and A. Strominger, Phys. Rev. D43 (1991) 3140.
- [2] A. Papapetrou, Proc. R. Irish Acad. A51 (1947) 191.
S. D. Majumdar, Phys. Rev. 72 (1947) 930.
R. C. Myers, Phys. Rev. D35 (1987) 455.
- [3] R. C. Ferrell and D. M. Eardley, Phys. Rev. Lett. 59 (1987) 1617.

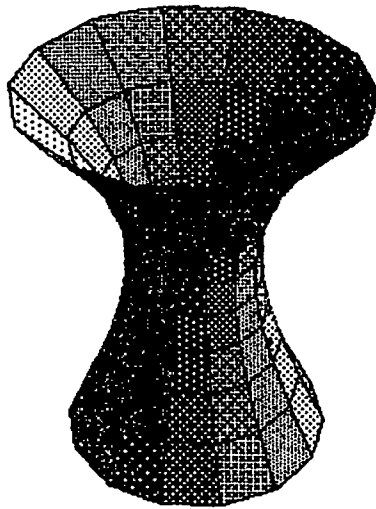
Figure Captions

Fig. 1: The surface of the moduli space for the two-body system of extreme charged dilaton black holes in three dimensional space ($N=3$). (a) for $a=0$, (b) for $a^2=1/3$, and (c) for $a^2=1$.

Fig. 2: The surface of the moduli space for the two-body system of extreme charged dilaton black holes in string theory ($a^2=1$). (a) for $N=5$, (b) for $N=4$, and (c) for $N=3$.

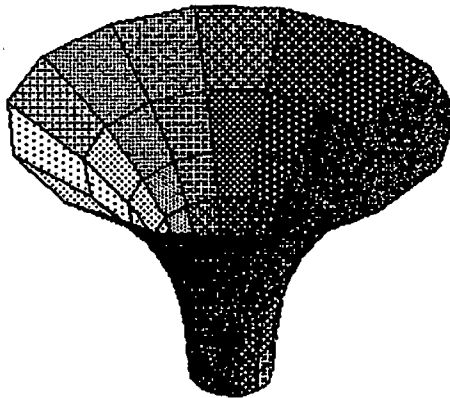
$N=3$

(a)



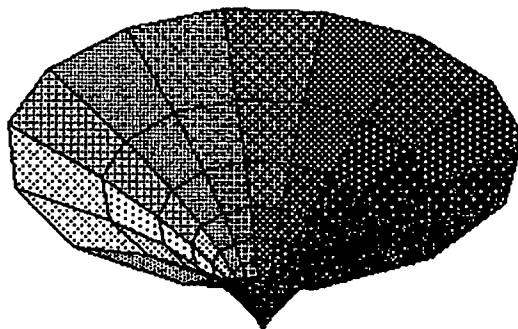
$a^2=0$

(b)



$a^2=1/3$

(c)

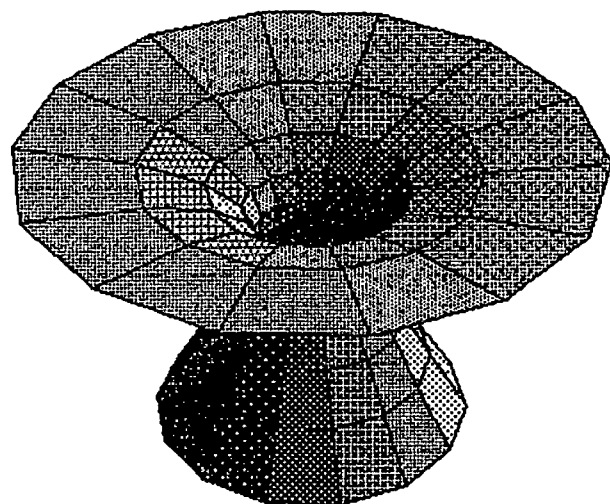


$a^2=1$

Fig. 1

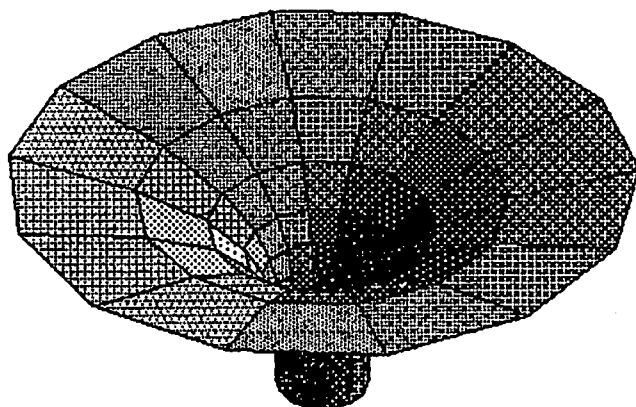
$$a^2=1$$

(a)



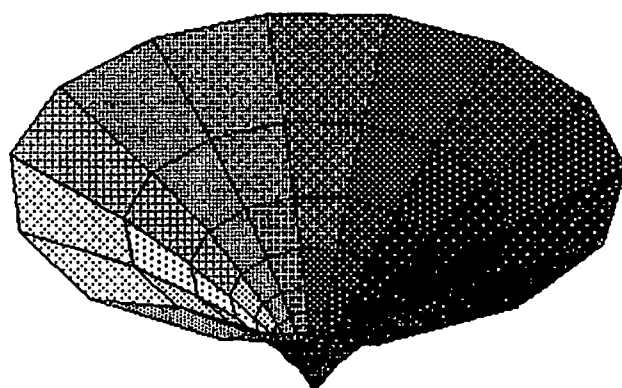
N=5

(b)



N=4

(c)



N=3

Fig. 2

Non-Equilibrium Thermodynamic Fluctuations of Black Holes

Osamu Kaburaki

Astronomical Institute, Faculty of Science, Tohoku University, Sendai 980, Japan

Slow evolutions of Kerr black holes due to quantum particle-emission in a vacuum are examined from a viewpoint of non-equilibrium thermodynamics. The spin-down process of a Kerr hole takes place much faster than the mass evaporation process. It is stressed that although the former is a relaxation process toward an equilibrium, the latter is not. The non-equilibrium fluctuation theory by Landau and Lifshitz is applied to the former and the correlation of the spin-down fluctuations are calculated. However, this method does not seem to be as powerful as suggested in investigating the thermodynamic properties of extreme Kerr holes which are expected to show a laser-like phase transition.

1. Introduction

There are divergences, for instance, in the heat capacities of black holes: e. g. the heat capacity of Kerr holes for constant angular-momentum diverges at $a_* \approx 0.68$ and that of Reissner-Nordström holes for constant charge does at $Q/M \approx 0.86$ [1]. Here, M , J and Q denote the mass, angular momentum and charge of a black hole, respectively, and $a_* = a/M = J/M^2$. These divergences have once interpreted as representing some kinds of phase transition at that points [1]. It has been shown, however, that they are actually the points of stability changes in certain ensembles of black holes in various circumstances [2].

The existence of another kind of phase transition has been proposed by Curir [3] for rotating holes based on an analogy between the holes and laser systems. She speculates that spontaneous particle emission in the super-radiant mode, which is random as long as hole's temperature is non-zero, becomes coherent when the temperature reaches zero. This means that the threshold temperature of Kerr holes as a laser system is absolute zero (i. e. holes are then in the extreme Kerr states) and they may experience a phase transition there.

From the analysis of equilibrium sequence of Kerr holes, it is difficult to check this point since the extreme states are located at the end of these sequences. A seemingly promising method to attack this problem in the regime of thermodynamics is to examine the thermodynamic fluctuations around the critical point. This has been done by Pavón and Rubi [4]. Since black holes in the universe are open systems which are evaporating continuously, the relevant fluctuations are those in non-equilibrium states. They insist that some of the correlations in the fluctuations of thermodynamic variables diverge in the limit of zero temperature with finite mass.

However, there is a serious problem about their calculations. They applied the Landau-Lifshitz theory [5] to the cases in which it is not allowed, and hence their conclusion should be suspended until a correct treatment appears. We reconsider this problem here.

2. Evolution of Kerr Holes in a Vacuum

Hereafter we restrict our attention to Kerr holes in a vacuum, for definiteness. Their states are specified by only two independent-variables and evolve slowly as particles evaporate from them, provided that their masses are not too small (the evaporation time is longer than the present age of the universe for holes of $M \geq 10^{15}$ g). We consider only such slow evolutions.

To this purpose it is convenient to adopt, for a set of variables, hole's mass M and rotation parameter h introduced in reference [6]: $h = a/r_H$, where r_H is the radius of inner or outer horizon (r_- or r_+) and $a = J/M$. Therefore h satisfies

$$h^2 - 2\frac{M^2}{J}h + 1 = 0, \quad (1)$$

with $0 \leq h \leq 1$ for outer horizons and $1 \leq h \leq \infty$ for inner horizons. However, the inner horizons are of no relevance in the present discussion. The expressions for various thermodynamic variables in terms of M and h are found also in reference [6].

From dimensional considerations we obtain the formulae for the rates of change of mass and angular momentum:

$$\dot{M} = -f(h) M^{-2}, \quad (2)$$

$$\dot{J} = -g(h) J M^{-3}, \quad (3)$$

where $f(h)$ and $g(h)$ are some positive functions of h only. Page [7] has calculated the behaviours of these functions for mass-less particles of spin 1/2, 1, and 2, in the whole range of rotation parameter $a_* \equiv a/M$. His parameter coincides with ours both in the limits of no rotation (Schwarzschild holes, $h = a_* = 0$) and maximal rotation (extreme Kerr holes, $h = a_* = 1$).

Here we note important points about the mass evaporation.

- *The process of mass evaporation is not the one toward an equilibrium.* Indeed, mass evaporation under fixed h (e. g. at $h = 0$) results in the increase in black-hole temperature while an equilibrium with surrounding vacuum space requires zero temperature.
- *\dot{M} is not proportional to M .*

Pavón and Rubi [4] adopt M as a parameter which represents the degree of departure from the equilibrium but this is not justified as we see above. They further apply the Landau-Lifshitz theory to \dot{M} while this is possible only when $\dot{M} \propto M$. Therefore they treat $f(h)/M^3$ as if it were the proportional constant. Of course, this is wrong.

3. Relaxation to Mechanical Equilibrium

The equation for the rate of change of the rotation parameter is derived by differentiating Eq. (1) with respect to time and substituting Eqs. (2) and (3):

$$\dot{h} = -(g - 2f) \frac{h(1 + h^2)}{1 - h^2} M^{-3}. \quad (4)$$

It has been shown by Page [7] that, for sufficiently massive holes ($M > 10^{19}$ g), $g - 2f$ is positive in the whole range of h (i. e. $0 \leq h \leq 1$). Here, we deal with only such holes. Further, Eq. (4) contains a diverging factor at $h = 1$ and \dot{h} is proportional to h near $h = 0$. Thus we have the following results:

- *The evolution of hole's rotation due to particle emission is a relaxation process toward a mechanical equilibrium (i. e. to $h = 0$).*
- *Time scale for the mechanical relaxation is much smaller than that for thermal evaporation.*
- *The third law of black-hole thermodynamics has a tendency to be kept valid by particle emission.*
- *The fluctuation theory of Landau and Lifshitz is applicable to the mechanical relaxation process only when $h \ll 1$.*

The change rates for other thermodynamic quantities are also calculated easily:

$$\dot{S} = \frac{-1}{1+h^2} \left[f - (g-2f) \frac{h^2}{1-h^2} \right] M^{-1}, \quad (5)$$

$$\dot{T} = \left[f(1-h^2) + 2(g-2f) \frac{h^2(1+h^2)}{1-h^2} \right] M^{-4}, \quad (6)$$

$$\dot{\Omega} = \frac{1}{2} \left[f - (g-2f) \frac{1+h^2}{1-h^2} \right] h M^{-4}. \quad (7)$$

It is interesting to note that the entropy (and hence the area of the event horizons) first increases as particles are emitted near $h = 1$ but decreases near $h = 0$. Therefore, it has a maximum in the course of spin-down (see also Page [7]). Both the rates for temperature and angular velocity contain divergence at the extreme Kerr states.

4. Correlation of the Fluctuations in Spin-Down Rate

In this section we regard a Kerr hole of mass M and rotation h as an excited state of a Schwarzschild hole of the same mass. Therefore the Kerr hole is in a non-equilibrium state whose deviation from an equilibrium state is expressed by non-zero h and, if this value is sufficiently small, the Landau-Lifshitz theory is applicable to this spin-down process. According to Landau and Lifshitz, we rewrite Eq. (4) around equilibrium states (i. e. $h \ll 1$) in the form

$$\dot{h} = -\lambda h + \delta\dot{h}, \quad (8)$$

where $\lambda \equiv (g_0 - 2f_0) M^{-3}$ is a coefficient of h , and $\delta\dot{h}$ represents stochastic fluctuations in the spin-down process.

Then the auto-correlation of the fluctuations in \dot{h} is given by

$$\langle \delta\dot{h}(t) \delta\dot{h}(t + \tau) \rangle = 2\lambda \langle h^2 \rangle \delta(\tau), \quad (9)$$

and its spectrum is

$$[(\delta\dot{h})^2]_{\omega} = \frac{\lambda}{\pi} \langle h^2 \rangle, \quad (10)$$

where the bracket $\langle \rangle$ denotes the time average which may be replaced by the ensemble average.

Since the probability that a state with h is realized, $w(h)$, is proportional to $\exp[S(M, h)]$ and $(\partial S/\partial h)_{h=0} = 0$, $(\partial^2 S/\partial h^2)_{h=0} = -M^2$, we have

$$w(h) = -\frac{M}{\sqrt{2\pi}} \exp \left[-\frac{M^2}{2} h^2 \right]. \quad (11)$$

Performing the average with this distribution function, we finally obtain

$$\langle h^2 \rangle = M^{-2} \quad \text{and} \quad [(\delta\dot{h})^2]_{\omega} = \frac{g_0 - 2f_0}{\pi} M^{-5}, \quad (12)$$

where f_0 and g_0 mean $f(0)$ and $g(0)$, respectively.

Although we have applied the Landau-Lifshitz theory to mechanical relaxation processes of Kerr black holes near equilibrium, it does not have the ability to predict about fluctuations near the extreme-Kerr states which are of our real interest.

References

- [1] P. C. W. Davies, Proc. R. Soc. Lond. A. **353** (1977) 499.
- [2] O. Kaburaki, I. Okamoto and J. Katz, Phys. Rev. D (1993), in press; J. Katz, I. Okamoto and O. Kaburaki, submitted to Class. Quant. Grav.
- [3] A. Curir, IL Nuovo Cimento **51B** (1979) 262; *ibid.* **52B** (1979) 165.

- [4] D. Pavón and J. M. Rubi, Phys. Rev. D 37 (1988) 2052; *ibid.* D 43 (1991) 2495.
- [5] L. Landau and E. M. Lifshitz, *Statistical Physics* (Pergamon, New York, 1980).
- [6] I. Okamoto and O. Kaburaki, Mon. Not. R. Astron. Soc. 255 (1992) 539.
- [7] D. N. Page, Phys. Rev. D 13 (1976) 198; *ibid.* D 14 (1976) 3260.

Thermodynamics of Kerr black hole and its applications to two hole coalescence problem and inner horizon dynamics

Shinji Horiuchi

Geophysical Institute, Faculty of Science, Tohoku University, Sendai 980, Japan

Isao Okamoto

Division of Theoretical Astrophysics, National Astronomical Observatory, Mizusawa 023, Japan

ABSTRACT The coalescence of two bare rotating uncharged black holes is examined on the thermodynamic grounds. We regard two Kerr holes before finding each other to begin gravitational interactions as being respectively in thermodynamic equilibrium. Using rotational parameter h (angular momentum per unit mass normalized by gravitational radius) the nature of inner horizon is discussed. After the coalescence the total area of inner horizons can be shown to be strictly subadditive. The situation is the same for charged holes that also have inner horizons. Further application to thermodynamical stability problem in systems containing Kerr black holes and radiation is developed with rotational parameters' treatment.

1 INTRODUCTION

The no-hair theorem of black holes insures holes' mass M , angular momentum J and charge Q to be regarded as *extensive* state variables in black hole equilibrium thermodynamics, with the aid of ideas that the black hole entropy is proportional to the surface area of the event horizon and black hole temperature is proportional to the hole's surface gravity. In this formalism the surface temperature is *intensive* variable together with holes' angular velocity and electric potential.

If two bare rotating (Kerr) black holes of masses M_1 and M_2 with angular momentum J_1 and J_2 collide each other to coalesce a new Kerr hole of mass M_3 with angular momentum J_3 , we can impose following conditions:

$$M_1 + M_2 \geq M_3 \tag{1}$$

$$S_1 + S_2 \leq S_3 \quad (2)$$

$$|J_1| + |J_2| \geq |J_1 + J_2| \geq |J_3| \quad (3)$$

where S_i denotes the entropy of the i -th hole.

The condition (1) is self-explanatory, because the mass of the third hole can never exceed the sum of the masses of the initial two holes. The condition (2) comes from Hawking's area law, or equivalently from the second law of black hole thermodynamics (Hawking 1976). The holes' angular momentum axes will not generally coincide with each other; they may be in the same direction in some case, but in the opposite in others. Thus, the case of $J_3=0$ may happen. One can thus express the situation about the holes' angular momenta as given in (3). The above three conditions will in general hold for any kind of coalescence of two bare Kerr holes, irrespective of after head-on collision or after at first the formation of a binary system and then gradual release of orbital energy in the form of gravitational wave.

We use units in which $c=G=\hbar=8\pi k_B=1$.

When we actually make some thermodynamic calculation on rotating or charged black holes it is often useful to introduce non-dimensional parameters instead of some of extensive variables, say, J or Q . To investigate the evolution of Kerr black holes Okamoto and Kaburaki (1990) first introduced a non-dimensional parameter $h \equiv a/r_H$, where $a \equiv J/M$ is angular momentum radius and r_H is gravitational radius. [As for charged holes, independently, Braden *et al* (1990) introduced a parameter $q \equiv e/r_H$, where $e \equiv Q^2/M$, to find stationary point with analysis of so-called "reduced action." See also Katz, Okamoto and Kaburaki (1993).] Okamoto and Kaburaki showed that a hole's entropy and the angular momentum can be written as

$$S = \frac{M^2}{2(1+h^2)} \quad (4)$$

$$J = \frac{2h}{1+h^2} M^2. \quad (5)$$

The rotating Kerr black holes and charged Reissner-Nordstrom black holes have the inner horizons that are known as the Cauchy horizons. It has been shown by Curir (1979) that in the case of a rotating hole, the inner horizon may be interpreted as a sort of *negative* temperature surface, satisfying a type of area theorem dissimilar to

(2), and bearing some relation to the concept of the *spin* temperature and entropy on the analogy of thermodynamics of the magnetic spin systems (e.g., Ramsey 1956). She interpreted the surface area of inner horizon as *spin* entropy of the rotating black hole, and expressed the sum of the both spin and thermal entropy with the entropy of a Schwarzschild black hole having mass corresponding to the total mass of the system:

$$S_{\text{spin}} + S_{\text{therm.}} = S_- + S_+ = M^2/2.$$

It is, however, worth remarking that this 'spin' temperature is quite different from the usual 'thermal' temperature. Because the inner horizons of black holes suffer from similar quantum mechanical divergence of the energy momentum tensor the quantum radiation from the outer horizon will pile up on the inner horizon, which will be at a different temperature. So it seems that there has to be an exact quantum gravitational definition of 'thermal temperature' measured locally on the inner horizon, which may be quite different from the negative spin temperature. The inner horizon's temperature may not be so simple in physical interpretation.

Let us next write down the spin entropy using the rotational parameter h . The surface of the inner horizon is a kind of mirror image of the event horizon (Okamoto and Kaburaki 1992). If we write S_+ the entropy of a black hole, and S_- the spin entropy, which is proportional to the surface area of inner horizon, relation $S_+ S_- = (J/4)^2$ holds, and the outer horizon and inner horizon have respective h 's satisfying relations $h_{\pm} = a/r_{\pm}$ and $h_+ h_- = 1$. So S_- is given by

$$S_- = \frac{M^2 h^2}{2(1 + h^2)} \quad (6)$$

for $0 \leq h < 1$. It is easy to see that solving (5) yields the two roots for h , one for the outer horizon, satisfying $0 \leq h_+ = h < 1$ and the other for inner horizon, given by $h_- = 1/h$ and hence satisfying $1 < h_- \leq \infty$.

2 MERGING OF TWO KERR BLACK HOLES

2.1 The case of $h_3 = h_1 = h_2 = 0$ (Two Schwarzschild holes' merging)

In the coalescence of two Schwarzschild holes, we need not take into account the angular momentum problem. So we first make a simple vision with this non-rotating case. Let's introduce notations $[X] \equiv X_3 - (X_1 + X_2)$ for an arbitrary physical quantity X , and then we can rewrite the conditions (1) and (2)

$$[M] \leq 0, \quad [M^2] \geq 0, \quad (8)$$

where (4) is used. Similarly we have in terms of entropy

$$[S^{1/2}] \leq 0, \quad [S] \geq 0. \quad (9)$$

One can draw these conditions on the M_1 - M_2 and S_1 - S_2 planes (see Fig. 1a,b). In Fig. 1a, the pair of two masses M_1 and M_2 must be inside the region of $M_1^2 + M_2^2 \leq M_3^2$. The farther the sum of the masses of the two holes from the line of $M_1 + M_2 = M_3$, the greater the energy release in the form of gravitational energy, and therefore there is the upper limit of energy release from the coalescence of two Schwarzschild holes. This is given by well-known value $(\sqrt{2} - 1)M_3$ in the adiabatic case with no increase of entropy, i.e., $M_1 = M_2 = M_3/\sqrt{2}$. We can see the same situation in the S_1 - S_2 plane. In the case of $S_1 = S_2 = S_3/2$, i.e., $[S] = 0$, we see the initial two holes lying in the middle of the line of $S_1 + S_2 = S_3$.

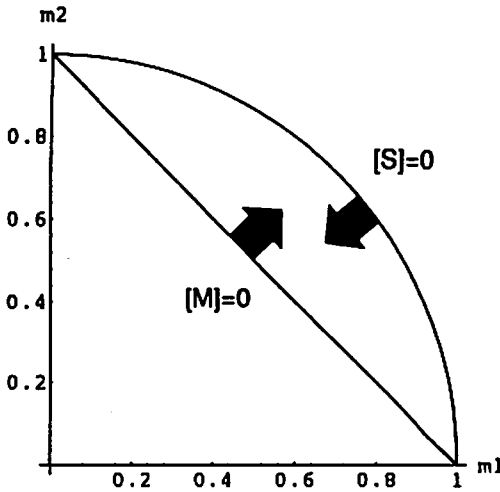


Fig.1a. (m_1, m_2) plane. Here $m_1 = M_1/M_3$, $m_2 = M_2/M_3$. Intersection between $m_1^2 + m_2^2 \leq 1$ and $m_1 + m_2 \geq 1$ is physically accepted area.

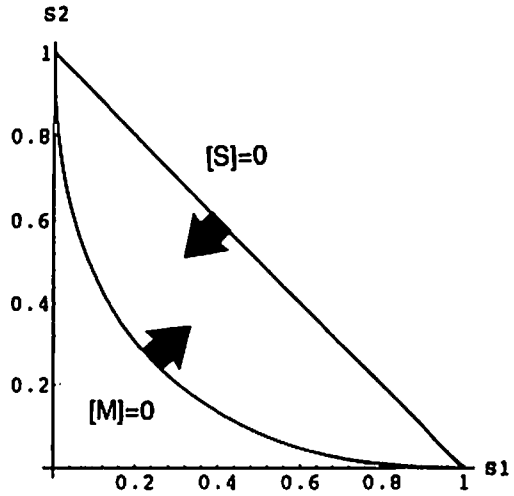


Fig.1b. (s_1, s_2) plane. $s_1 = S_1/S_3$, $s_2 = S_2/S_3$. Intersection between $s_1 + s_2 \leq 1$ and $\sqrt{s_1} + \sqrt{s_2} \geq 1$ is physically accepted area.

On the other hand, we have the maximum increase of entropy in coalescence in the case of $M_1=M_2=M_3/2$, i.e., $[S]=S_3/2$, because $S_1=S_2=S_3/4$. One can thus conclude that when the two holes lie on the line of $M_1+M_2=M_3$ in the M_1 - M_2 plane, one obtains no release of gravitational energy, but the hole 3 gains the maximum increase of entropy, which is given by the horizontal difference from the point (S_1, S_2) of the point where the horizontal line from (S_1, S_2) crosses the line $S_1+S_2=S_3$ on the S_1 - S_2 plane (see Fig. 1b). That is, $[S]=M_1M_2$.

We thus see that the region where coalescence can take place is given by the domain $[M]<0<[M_2]$ in the (M_1, M_2) plane or by the domain $[S]>0>[S_1/2]$ in the (S_1, S_2) plane.

2.2 The case of $h_3 > h_1, h_2$ or $h_3=h_1=h_2$

We can prove an important fact that if one requires condition (2) and (3) to hold for merging of two Kerr holes, the spin parameter of the hole 3 cannot be larger than both h_1 and h_2 , that is, $h_3 < h_1$ or $h_3 < h_2$. To prove this, we show that if $h_3 > h_1$ and $h_3 > h_2$, conditions (2) and (3) are incompatible. From (2), (3), (4) and (6), we have

$$\frac{1}{2}[J] = \frac{h_3 M_3^2}{1+h_3^2} - \left(\frac{h_1 M_1^2}{1+h_1^2} + \frac{h_2 M_2^2}{1+h_2^2} \right) > \frac{h_3 M_3^2}{1+h_3^2} - h_3 \left(\frac{M_1^2}{1+h_1^2} S + \frac{M_2^2}{1+h_2^2} \right) = 2h_3[S] \quad (10)$$

For $h_3 > h_1, h_2$, we thus see that if $[S]>0$, $[J]>0$ and if $[J]<0$, $[S]<0$, that is, two conditions $[S]>0$ and $[J]<0$ do not hold at the same time (See Fig. 2a,b and c).

We then conclude without losing generality that either

$$h_1 > h_3 > h_2 \text{ or } h_1 > h_2 > h_3 \quad (11)$$

must always hold for coalescence of two Kerr holes.

We finally mention the case of $h_3=h_1=h_2$, for which we have

$$[J]/2 = 2h_3[S_+]. \quad (12)$$

For both conditions (2) and (3) to be compatible, we obtain $[S_+]=[J]=0$. This means that angular momentum must conserve in an adiabatic process of coalescence. Energy release in this case occurs. This is given by

$$-[M] = M_1 + M_2 - \sqrt{M_1^2 + M_2^2}.$$

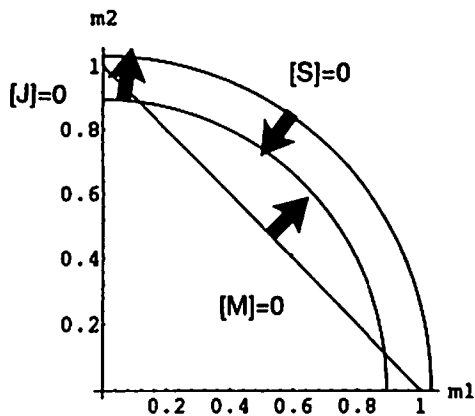


Fig.2a. $h_1, h_2 > h_3$. $[M] < 0, [S] > 0$, and $[J] < 0$ can coincide.

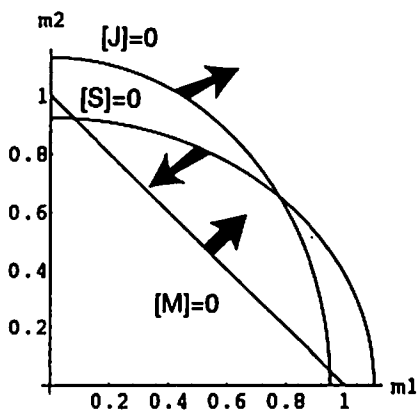


Fig.2b. $h_1 > h_3 > h_2$. A reasonable cross section exists.

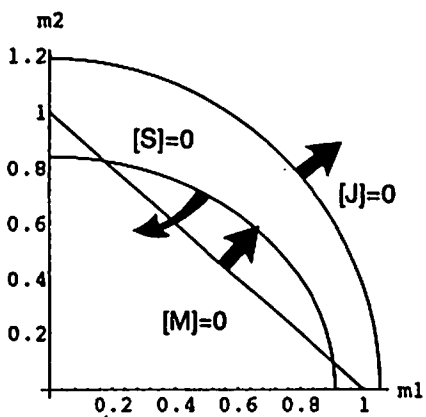


Fig.2c. $h_3 > h_2 > h_1$. $[J] < 0$ and $[S] > 0$ can not coincide.

3 CHANGING OF STATE OF THE INNER HORIZON AFTER MERGING

Recently Curir (1989) argued the subadditivity property of entropy function, in contrast to the superadditivity of the black hole entropy that had been pointed out before (e.g., Landsberg & Tranah 1980). She claimed that the behavior of spin entropy, i.e., the area of inner horizon's surface of a Kerr hole, is neither superadditive, nor subadditive. Now we will show that this is incorrect, and the area of inner horizon's surface must strictly subadditive for any type of merging.

Let us first give the proof in the former case of (11). From (2)–(6) we have

$$J_1 + J_2 = J_3 - [J], \quad J_1/h_1 + J_2/h_2 = J_3/h_3 - 4[S_+].$$

Solving these simultaneous equations for J_1 and J_2 , we obtain

$$J_1 = \frac{h_1(h_3 - h_2)}{h_3(h_1 - h_2)} J_3 + \frac{h_1 h_2}{h_1 - h_2} \left(4[S_+] - \frac{[J]}{h_2} \right), J_2 = \frac{h_2(h_1 - h_3)}{h_3(h_1 - h_2)} J_3 - \frac{h_1 h_2}{h_1 - h_2} \left(4[S_+] - \frac{[J]}{h_1} \right).$$

Substituting J_1 and J_2 into $4[S_-] = h_3 J_3 - (h_1 J_1 + h_2 J_2)$ yields

$$[S_-] = -h_1 h_2 [S_+] + (h_1 - h_2) \frac{[J]}{4} - \frac{(h_1 - h_2)(h_3 - h_2)}{4h_3} J_3.$$

Because $[J] < 0 < [S_+]$, we see that $[S_-] < 0$ for $h_1 > h_3 > h_2$.

For the latter case of (11), we have from (2), (3) and (6),

$$2[S_-] = \frac{h_3^2 M_3^2}{1 + h_3^2} - \left(\frac{h_1^2 M_1^2}{1 + h_1^2} - \frac{h_2^2 M_2^2}{1 + h_2^2} \right) < \frac{h_3^2 M_3^2}{1 + h_3^2} - h_3 \left(\frac{h_1 M_1^2}{1 + h_1^2} - \frac{h_2 M_2^2}{1 + h_2^2} \right) = \frac{h_3}{2} [J] \leq 0. \quad (13)$$

One can conclude that the inner horizon's surfaces are *always* decrease after coalescence. If we interpret following Curir (1979) that S_- stands for the spin entropy of a Kerr black hole, it is reasonable that if angular momentum decrease after coalescence, the inner horizon's entropy also decrease. In this meaning the area of inner horizon's surface of a Kerr hole must be subadditive.

For the case of $h_3 = h_1 = h_2$ we have an analogous equation to (12):

$$2[S_-] = h_3^2 [J]/2 < 0. \quad (14)$$

4 PROBLEM WITH RADIATION BACKGROUND

The equilibrium of systems containing one Schwarzschild black hole and black-body radiation in a box have been discussed by many authors (e.g., Gibbons & Perry 1978). Bishop & Landsberg extended the problem to that of two black holes (Bishop & Landsberg 1987) or n identical black holes (Landsberg & Bishop 1988) in a box separated by partitions. They estimated limits on the amount of gravitational wave energy being emitted after removing the separating partitions. Here we discuss the prospect to extension to the problem of the rotating black holes in a box.

In the following we assume that a single rotating black hole exists in a box. Normally the hole will be spin down as its radiation carries angular momentum into environment unless the box is rotating. At equilibrium, the black hole must radiate and accrete angular momentum at the same time. Therefore, the environment must also be rotating (Schumacher *et al* 1992). However, for simplicity, we neglect the contribution of the rotating box to the total energy of the system, it will be given by just the sum of the hole's mass and the energy of radiation.

First we assume the total energy in the box $E=M+E_{\text{rad}}=M+aVT^4$ is constant. Here a is Stefan-Boltzman constant, which depends upon the number of radiation fills in the heat bath. The total entropy in the box $S=S_H+S_{\text{rad}}=S_H(M)+S_{\text{rad}}(E-M)$ can be expressed with the rotational parameter h :

$$S = \frac{M^2}{2(1+h^2)} + \frac{4}{3}aVT^3. \quad (15)$$

If we introduce following scale transformations $V \rightarrow \lambda^5 V$, $T \rightarrow \lambda^{-1} T$, both E and S are modified homogeneously, $E \rightarrow \lambda E$ and $S \rightarrow \lambda^2 S$, with maintaining consistency. Thus, the extensive variables E and V have the scale invariance for the quantity E^5/V . If we write $x=M/E$ and $y=(4/3)(aV/E^5)^{1/4}$, then the entropy can be given simply with x and y :

$$S = E^2 \left[\frac{x^2}{2(1+h^2)} + y(1-x)^{3/4} \right] = E^2 s(x, h). \quad (16)$$

The shapes of the normalized entropy function $s(x, h)$ decide the equilibrium states for arbitrary value of y . Stable equilibrium state is at global maximum point of $s(x, h)$. Unstable equilibrium is at local maximum. The changing of state from the unstable equilibrium to the stable equilibrium is first order phase transition as was pointed out by Gibbons and Perry. At $y=0.7133$, a saddle point exists on only $h=1$ (maximally

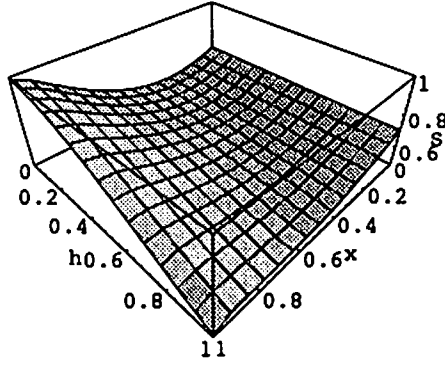


Fig.3.a. Entropy s as a function of x and h at $y < 0.7133$. Global maximum states exist at non zero x (BH phase).

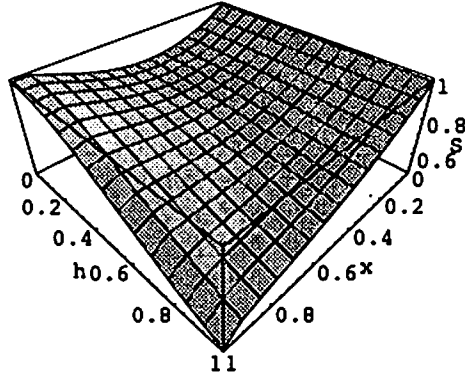


Fig.3.b. Entropy s as a function of x and h at $y = 1$. The stable black hole phases are just locally stable. A saddle point exists.

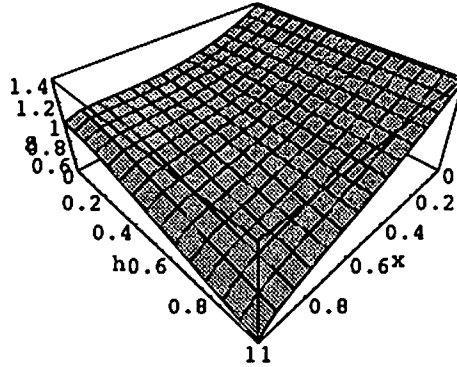


Fig.3.c. Entropy s as a function of x and h at $y = 1.4$. There is no local stable hole state. Saddle point doesn't exist at $h < 1$.

rotating state) (see Fig. 3a). In this case the unstable equilibrium can always exist in either the hole or radiation phase. There is a border line between the hole dominant state and the radiation dominant state. At $y < 1$ there exist such states that the black hole phase are dominant for some rotational parameter h (Fig. 3b). At $y = 1.4$ every state must be the radiation dominant phase (Fig. 3c). In this case, every black hole must be unstable and will evaporate gradually, or rapidly.

References

- Bishop, N. T. & Landsberg, P. T. 1987, *Gen. Relativity Gravitation* **19**, 1083
 Braden, H. W. , Brown, J. D., Whiting, B. F. & York, Jr., J. W. 1990, *Phys. Rev. D* **42**, 3376
 Curir, A. 1979, *Nuovo Cim.* **51**, 165
 Curir, A. 1989, *Europhys. Lett.* **9** (6), 609
 Gibbons, G. W. & Perry, M. J. 1978, *Proc. R. Soc. Lond. A*, **358**, 467
 Hawking, S. W. 1976, *Phys. Rev. D* **13**, 191
 Katz, J. , Okamoto, I. & Kaburaki, O. 1993, *Class. Quantum Grav.* (submitted)
 Landsberg, P. T. & Bishop, N. T. 1988, *Gen. Relativity Gravitation* **20**, 723
 Landsberg, P. T. & Tranah, D. 1980, *Phys. Lett. A* **78**, 219
 Okamoto, I. & Kaburaki, O. 1990, *Mon. Not. R. Astron. Soc.* **247**, 244
 Okamoto, I. & Kaburaki, O. 1992, *Mon. Not. R. Astron. Soc.* **255**, 539
 Ramsey, N. 1956, *Phys. Rev.* **103**, 20
 Schumacher, B. , Miller, W. A. & Zurek, W. H. 1992, *Phys. Rev. D* **46**, 1416

Evaporation of a Collapsing Shell with Scalar Field Production

Yoshimi Oshiro, Shigelu Konno, Kouji Nakamura,
and Akira Tomimatsu

*Department of Physics, Nagoya University
Chikusa-ku, Nagoya 464-01, Japan*

We consider gravitational collapse of a spherically symmetric dust shell coupled with a massless scalar field. The rest mass can decrease as a result of the scalar wave production. Our purpose is to discuss the backreaction problem in the context of classical general relativity. We construct junction conditions at the shell including the scalar field. Possible final fates of the gravitational collapse are found by solving them when the shell is close to the apparent horizon. Interestingly, as the collapsing shell shrinks to a point, it can completely evaporate without forming a black hole and naked singularity. The mass-loss rate measured by a static observer turns out to remain finite even at the final stage of the shell evaporation.

1 Introduction

Hawking has discovered that a black hole emits radiation like a blackbody with temperature proportional to its surface gravity [1]. This discovery has stimulated many researches on quantum gravity and quantum field theory on curved space time. The black hole evaporation is expected as a backreaction of the Hawking radiation. Although some Wheeler-DeWitt approach has been developed in recent papers [2], a main approach to the backreaction problem has been based on the semiclassical Einstein equations $G_{\mu\nu} = 8\pi G\langle T_{\mu\nu} \rangle$, where $\langle T_{\mu\nu} \rangle$ is the expectation value of the stress-energy tensor of quantized matter fields, $G_{\mu\nu}$ is the Einstein tensor, and G is the gravitational constant. (Units are chosen so that $c = 1$.) Unfortunately, it is very difficult to give the expectation value $\langle T_{\mu\nu} \rangle$ in a self-consistent manner, and any solutions representing evaporating black holes have not been found as yet.

As a preliminary step to discuss the quantum dynamics, it will be important to understand possible backreaction effects in a classical level. This motivates us to study gravitational collapse of classical matter coupled with a massless scalar field. We treat the matter as a thin dust shell. The quantum backreaction is mimicked by considering dynamical production of outgoing scalar waves from the collapsing shell. The shell's mass will be carried away by the radiation as the collapse goes on. Our main purpose is to discuss whether the evaporating shell can radiate away all of its mass before a black hole has a chance to form. We have a good model to observe the backreaction effect due to the emission of scalar waves.

In §2 we start with junction conditions for embedding the timelike 3-hypersurface of a thin shell. This formalism was first elaborated by Israel [3] and has been extensively applied to various problems [4]. The key point of our analysis is that we construct the junction

conditions for the scalar field coupled to the gravitational field and the dust shell. To see a shell evaporation, in §3, we introduce a locally defined gravitational mass [5] and calculate its loss rate just outside the shell. In this paper our treatment is limited to a local geometry near the shell. to check a black hole formation. In §4 we solve the junction conditions, when the shell collapses close to the apparent horizon. Usually the collapsing shell will cross the apparent horizon at a finite radius. However, we find the solutions representing a rapidly evaporating shell which shrinks to a point without crossing the apparent horizon. Our conclusion is that the classical scalar wave production can prevent some collapsing shell from forming a black hole. Section 5 contains discussions on the naked singularity, and the mass loss rate in the shell evaporation is compared with the backreaction of the Hawking radiation.

2 Dust shell model and junction conditions

Now let us give equations which describe the evolution of a dust shell coupled with a massless scalar field. These equations are derived from the classical Einstein equations and are called junction conditions.

We follow the usual procedure of the (3+1) splitting of spherically symmetric metric by introducing a Gaussian normal coordinate system. The time coordinate is the proper-time variable τ . The spatial coordinate η is taken as the proper distance from the shell.

In these coordinates the metric can be written as

$$ds^2 = -\alpha^2 d\tau^2 + L d\eta^2 + R^2(d\theta^2 + \sin\theta d\phi^2) \quad (2.1)$$

where α, L, R are functions of τ, η . Hereafter the partial derivatives with respect to τ and η are denoted by dots and primes, respectively. Since the coordinates τ and η are co-moving along with shell, we can set α to be equal to unity on the shell. (Note that the derivative α' is not assumed to be zero there.) The extrinsic curvature of the hypersurface is a 3-dimensional tensor whose components are defined by

$$K_{ij} = -n_{i;j} = -\frac{1}{2\sqrt{L}} g_{ij,\eta}. \quad (2.2)$$

where n_μ is the normal unit vector to a $\eta = \text{const}$ hypersurface, and the semicolon and comma denote 4-dimensional covariant derivative and ordinary derivative respectively.

The energy-momentum tensor $T_{\mu\nu}$ is composed of a dust shell and a massless scalar field ψ . Since we use the approximation of a thin shell, $T_{\mu\nu}$ can be written as

$$T_{\mu\nu} = S_{\mu\nu} \delta(\eta) + \frac{1}{4\pi} (\partial_\mu \psi \partial_\nu \psi - \frac{1}{2} g_{\mu\nu} \partial^\rho \psi \partial_\rho \psi). \quad (2.3)$$

The part of the shell contains the surface stress-energy $S_{\mu\nu}$ given by

$$S^{\mu\nu} = \sigma U^\mu U^\nu, \quad (2.4)$$

where σ is the surface energy density, and U^μ is the 4-velocity of the shell.

By virtue of the (3+1) splitting of the metric the Einstein equations have the form

$$G^\eta{}_\eta = \frac{1}{2}(K^2 - K^i{}_{;j}K^j{}_{;i}) - \frac{1}{2}{}^{(3)}R = 8\pi GT^\eta{}_\eta, \quad (2.5)$$

$$G^\eta{}_{;i} = K_{||i} - K^j{}_{;i||j} = 8\pi GT^\eta{}_{;i}, \quad (2.6)$$

$$\begin{aligned} G^i{}_{;j} &= {}^{(3)}G^i{}_{;j} + \frac{1}{\sqrt{L}}(K^i{}_{;j} - \delta^i{}_{;j}K)_{, \eta} - K K^i{}_{;j} + \frac{1}{2}\delta^i{}_{;j}(K^2 + K^k{}_{;l}K^l{}_{;k}) \\ &= 8\pi GT^i{}_{;j}, \end{aligned} \quad (2.7)$$

where the subscript vertical bar denotes 3-dimensional covariant derivative, and ${}^{(3)}R$ and ${}^{(3)}G^i{}_{;j}$ are the Ricci scalar and the Einstein tensor, respectively, on the $\eta = \text{const}$ hypersurface. We assume that the metric components α , R , L and the scalar field ψ are continuous at the shell $\eta = 0$. Then, the integration of Eq. (2. 7) with respect to η leads to the junction conditions

$$\gamma^i{}_{;j} = 8\pi G\sqrt{L} \left(S^i{}_{;j} - \frac{1}{2}\delta^i{}_{;j} \text{Tr } S \right). \quad (2.8)$$

where $\gamma^i{}_{;j}$ is the discontinuity of the extrinsic curvature

$$\gamma^i{}_{;j} = [K^i{}_{;j}] \equiv \lim_{\epsilon \rightarrow 0} \{ (K^i{}_{;j}(\eta = +\epsilon) - K^i{}_{;j}(\eta = -\epsilon)) \}. \quad (2.9)$$

From Eq. (2. 3) the equations for the energy-momentum conservation, we obtain

$$S^{ij}{}_{||j} + [T^i{}_\eta] = 0, \quad (2.10)$$

$$\bar{K}_{ij}S^{ij} + [T^\eta{}_\eta]\sqrt{L} = 0, \quad (2.11)$$

where $[T^\mu{}_\nu]$ is the discontinuity of the energy momentum tensor of the scalar field, and

$$\bar{K}_{ij} = \lim_{\epsilon \rightarrow 0} \frac{1}{2} \{ K_{ij}(\eta = +\epsilon) + K_{ij}(\eta = -\epsilon) \}. \quad (2.12)$$

Eqs. (2. 8), (2. 10) and (2. 11) give the full set of the junction conditions. We have a coordinate freedom to choose $L' = 0$ on the shell. Then these conditions can be written as follows

$$[R'] = -4\pi GL\sigma R, \quad (2.13)$$

$$[\alpha'] = 4\pi GL\sigma, \quad (2.14)$$

$$\partial_\tau(4\pi\sigma R^2) = \frac{R^2}{L}\dot{\psi}[\psi'], \quad (2.15)$$

$$4\pi\sigma\tilde{\alpha}' = -\frac{1}{2L}[\psi'^2], \quad (2.16)$$

where $\tilde{\alpha}'$ is defined in similar manner to Eq. (2. 12). The quantities in these equations should be understood as functions of τ only, which are defined on the shell $\eta = 0$. The remaining equations (2. 5) and (2. 6) may be solved in outer and inner spacetimes. However we focus

our attention on a local geometry near the shell. In the limit $\eta \rightarrow 0$ at each side of the shell, Eqs. (2. 5) and (2. 6) reduce to

$$\frac{R'_\pm \dot{L}}{2L} + \dot{R}\alpha'_\pm - \dot{R}'_\pm = GR\dot{\psi}\psi'_\pm, \quad (2.17)$$

$$\ddot{R} - \frac{R'_\pm \alpha'_\pm}{L} + \frac{1}{2R} + \frac{\dot{R}^2}{2R} - \frac{R'^2_\pm}{2RL} = -\frac{G}{2}R\left(\frac{1}{L}\dot{\psi}^2 + \psi'^2_\pm\right). \quad (2.18)$$

where the subscripts ' \pm ' mean respectively the quantities at the outer and inner sides of the shell. If taking the difference of Eq. (2. 17) between the inner and outer sides, we obtain $\dot{L} = 0$. Here we set $L = 1$ on the shell. The same difference of Eq. (2. 18) does not generate any new condition. In the following we use Eq. (2. 17) and Eq. (2. 18) only for the outer boundary.

The scalar field considered here must be generated through interaction with the shell, i.e.,

$$\psi^{\nu}{}_{;\nu} = \kappa\sqrt{G}S^\mu_\mu\delta(\eta), \quad (2.19)$$

where κ is a dimensionless coupling constant. Then, the integration of Eq. (2. 19) with respect to η leads to

$$[\psi'] = -\kappa\sqrt{G}\sigma, \quad (2.20)$$

In summary, we have the seven independent equations (2. 13) \sim (2. 18), and (2. 20), which holds in the limit $\eta \rightarrow 0$. The dynamical variables are functions of τ . To discuss a shell evaporation due to scalar wave production, we must introduce a concept of the gravitational mass in the τ - η coordinate system. This is the problem in the next section.

3 Gravitational mass

In the spherically symmetric system the gravitational mass can be locally defined as follows [5]

$$M = \frac{R}{2G}(1 - g^{\mu\nu}\partial_\mu R\partial_\nu R), \quad (3.1)$$

which becomes constant if the vacuum Einstein equations holds. Let us estimate it at the outer side of the shell. From Eq. (2. 17) and Eq. (2. 18), we obtain

$$\dot{M} = \frac{1}{4}R^2\{ (R'_+ - \dot{R})(\dot{\psi} + \psi'_+)^2 - (R'_+ + \dot{R})(\dot{\psi} - \psi'_+)^2 \}. \quad (3.2)$$

This clearly shows the time variation of the gravitational mass through the scalar wave production.

As the collapse goes on, the shell may cross the apparent horizon, where the expansion for outgoing null rays vanishes. The expansions denoted by θ_+ and θ_- at the outer and inner sides of the shell become

$$\theta_\pm = \frac{1}{R}(\dot{R} + R'_\pm). \quad (3.3)$$

Then we have $\theta_- = \theta_+ + 4\pi G\sigma > \theta_+$. The apparent horizon will appear at the outer side rather than the inner side. When $\theta_+ = 0$, the time variation of M becomes positive. This is

analogous to the area law of the event horizon [7]. However, we can find the condition that \dot{M} becomes negative. Let us assume that the scalar field at the outer side of the shell is purely outgoing,

$$\dot{\psi} + \psi'_+ = 0. \quad (3.4)$$

Since $\dot{R} + R'$ is always positive in the exterior region of the apparent horizon [8], \dot{M} can take a negative value even if the shell is close to it. We expect that such an effective emission of scalar waves can occur as a semiclassical backreaction of quantum shell evaporation induced by an ingoing negative-energy flux.

In the following we will study the shell evaporation under the outgoing condition (3. 4).

4 Shell evaporation

Does an evaporating shell can always cross the apparent horizon to form a black hole? To answer this question, let eliminate ψ'_\pm, α'_\pm and R'_\pm from Eqs.(2. 13) \sim (2. 18) and Eq. (2. 20) with the outgoing condition (3. 4), and solve them near the apparent horizon, where the expansion θ_+ for the outgoing null rays will have the approximate form

$$\theta(\tau)_+ \simeq \theta_0 \epsilon^\beta, \quad (4.1)$$

with a constant θ_0 . The time coordinate ϵ is defined by $\epsilon \equiv \tau_0 - \tau$, and is assumed to be very small. The shell may cross the apparent horizon at $\tau = \tau_0$. The dynamical variables can be solved in the power of ϵ . The approximate solutions valid up to the leading order are found as follows

$$R(\tau) \simeq R_0 \epsilon^\delta, \quad (4.2a)$$

$$\dot{\psi}(\tau) \simeq \psi_0 \epsilon^{-1}, \quad (4.2b)$$

$$R'(\tau) \simeq R'_0 \epsilon^{\delta-1}, \quad (4.2c)$$

$$\alpha'(\tau) \simeq \alpha'_0 \epsilon^{-1}, \quad (4.2d)$$

$$m(\tau) \simeq m_0 \epsilon^n, \quad (4.2e)$$

where $\psi_0, \alpha'_0, R_0, R'_0$ are constants. The powers δ and n are related to the arbitrary positive parameter β in Eq. (4. 1) as follows,

$$\delta = \frac{1}{2}(1 - \beta), \quad (4.3a)$$

$$n = \frac{\kappa}{2}(\sqrt{\kappa^2 \delta^2 + 4\delta(1 - \delta)} - \kappa\delta). \quad (4.3b)$$

All of δ, n, ψ_0 and α'_0 vanish in the limit $\beta \rightarrow 1$. This limit means that the shell crosses the apparent horizon at $R = R_0$. If β is in the range $0 < \beta < 1$, the shell shrinks to a point without crossing the apparent horizon. The gravitational mass given by

$$M = \frac{R}{2G}(1 + \dot{R}^2 - R'^2) \simeq \frac{R_0}{2G}(1 - 2\delta\theta_0 R_0^2)\epsilon^\delta, \quad (4.4)$$

decreases in proportion to the radius R and finally vanishes. This is a complete evaporation of the shell.

In this paper the parameter β is not determined. It of course depends on the initial conditions of the shell collapse. If the initial radius is sufficiently small, β will be equal to unity. If the initial value of $|\dot{\psi}|$ is sufficient large, the complete evaporation will be possible. This interesting initial value problem can be solved from the global Cauchy data on the Cauchy surface including the spatial infinity $R \rightarrow \infty$. Therefore it is beyond the scope of our local analysis. In the final section β is assumed to be in the range $0 < \beta < 1$ and the evaporating process is discussed in some detail.

5 Discussions

First let us see the scalar-modified junction conditions in the neighborhood of the apparent horizon. The discontinuities at the shell are estimated by equations

$$\frac{[R']}{R} = -4\pi\sigma, \quad (5.1)$$

$$[\alpha'] = 4\pi\sigma, \quad (5.2)$$

$$[\psi'] = -\kappa\sqrt{G}\sigma. \quad (5.3)$$

The surface energy density σ is approximately given by

$$\sigma = \frac{m}{4\pi R^2} \simeq \frac{m_0}{4\pi R_0^2} \epsilon^{n-2\delta}, \quad (5.4)$$

where $n - 2\delta > -1$. The right-hand sides of Eqs. (5. 1)~(5. 3) become much smaller than R'_\pm/R , α' , ψ'_\pm which are of the order of ϵ^{-1} . Therefore these quantities are continuous up to the leading order. We can neglect the effect of the shell on the junction conditions. Recall that Eq. (5. 3) is derived from Eq. (2. 20) in which the shell works as a source of the scalar field. The explosive scalar field production is mainly driven by the time variation of the gravitational field. If the shell crosses the apparent horizon at a finite radius ($\delta \rightarrow 0$), both sides of Eqs. (5. 1)~(5. 3) are of the order of ϵ^0 . The effect of the shell remains important to form a black hole.

Next, in the exterior of the shell, we introduce new coordinates t and r which give the metric

$$ds^2 = -\gamma^{-1} dt^2 + \gamma dr^2 + R^2 d\Omega^2, \quad (5.5)$$

where $\gamma^{-1} = 1 - 2GM_S(t, r)/r$. When the shell shrinks to a point, the time dilation becomes $d\tau/dt \sim \epsilon^{1-\delta}$. The collapsing speed and the mass loss rate measured by t are given by

$$\frac{dR}{dt} \sim -\theta_0 R_0^2, \quad (5.6)$$

$$\frac{dM}{dt} \sim -\frac{\theta_0 R_0^2}{2G} (1 - 2\delta\theta_0 R_0^2). \quad (5.7)$$

The static observer can see the shell approaching to the origin with a finite speed. The gravitational collapse with the mass evaporation terminates in a finite coordinate time t even

for the static observer. The mass loss is not so explosive, because dM/dt remains finite in the limit $M \rightarrow 0$. It will be a natural result that the mass loss rate is suppressed to a constant value in the limit $M \rightarrow 0$.

If a shell with conserved mass collapses to the origin $R = 0$, a singularity appears there. For the evaporating shell, the geometrical structure of the origin is not clear. Since the energy-momentum tensor and the Ricci-scalar ${}^{(4)}R$ of the spacetime contain the term $\delta(\eta)$, we consider the integration

$$\lim_{\epsilon \rightarrow 0} \int_{-\epsilon}^{\epsilon} d\eta {}^{(4)}R = 8\pi G\sigma \quad (5.8)$$

This means that a singularity appears when σ diverges. We have $\sigma \sim \epsilon^{n-2\delta}$ in the limit $\epsilon \rightarrow 0$. The condition $n > 2\delta$ leads to $\delta < \kappa^2/(3\kappa^2 + 4)$. The coupling constant κ must be large to generate efficiently scalar waves and to avoid the naked singularity.

Finally, let us give a brief summary. We have analyzed the behavior of a spherically symmetric dust shell interacting with a scalar field in the neighborhood of the apparent horizon by constructing the junction conditions. The junction conditions admits the solutions representing the spacetime with no black hole and no naked singularity. In the final stage of the shell evaporation, the scalar wave production is mainly driven by a time variation of the gravitational field, though the formation of naked singularity crucially depends on the coupling constant between the shell and the scalar field. The mass loss rate measured by a static observer becomes finite even in the limit $M \rightarrow 0$. To confirm the validity of the results in terms of a global analysis of the spacetime remains in future works.

Acknowledgement

We would like to thank Dr. Nambu for helpful discussions.

References

- [1] S. W. Hawking, *Commun. Math. Phys.* **43**, 199, (1974).
- [2] L.M.C.S.Rodrigues, I.D.Souares and J.Zanelli, *Phys. Rev. Lett.* **62**, 989, (1989); A.Tomimatsu, to appear in *Phys. Lett. B*.
- [3] W. Israel, *Nuovo Cimento* **44 B**, 463 (1966).
- [4] S.K.Blau, E.I.Guendelman and A.H.Guth, *Phys. Rev. D* **35**, 1747, (1987); J.Ipser and P.Silkvie, *Phys. Rev. D* **30**, 712, (1984); K.Sato, H.Kodama, M.Sasaki and K.Maeda, *Phys. Lett. B* **108**, 103, (1982).
- [5] W. Fischer, D. Morgan and J. Polchinski, *Phys. Rev. D* **42**, 4042, (1990); C.W.Misner and D.H.Sharp, *Phys. Rev.* **136**, B571, (1964); C.W.Hernandez and C.W.Misner, *Astrophys. J.* **143**, 452, (1966).
- [6] C.H.Brance and R.H.Dicke, *Phys. Rev.* **124**, 925,(1961).

- [7] S.W.Hawking, Phys. Rev. Lett. 26, 1344, (1971); Commun. Math. Phys. 25, 152, (1972).
- [8] P. Thoni, B. Isaak, and P. Hajicek, Phys. Rev. D30, 1168, (1984).
- [9] P. C. Vaidya, Proc. Indian Acad. Sci. A33, 264, (1951); R.W.Lindquist, R.A.Schwartz and C.W.Misner, Phys. Rev. 137, 1364, (1965).

STABILITY OF MAGNETOHYDRODYNAMICAL ACCRETION ONTO A BLACK HOLE

Masayoshi YOKOSAWA

Department of Physics, Ibaraki University, Mito 310

Abstract

The formation of shock wave triggered by magnetic stress is studied by numerical calculation. The radially symmetric accretion onto a black hole is possible to produce the shock wave near the event horizon. The magnetohydrodynamical accretion produces the distribution of the Alfvénic Mach number M_A that the upper stream is super-Alfvénic and the down stream is sub-Alfvénic. A perturbation near the Alfvén point nonlinearly grows and evolves to a shock wave. The asymmetry of the flow increases the critical Mach number M_{AC} ; the flow with $M_A \leq M_{AC}$ is unstable and produces the discontinuity front of the shock wave. We calculate the magnetohydrodynamical accretion with an initially uniform magnetic field directed along the rotation axis of the hole. The peak of the magnetic pressure appears at the rotation axis. The perturbations at the peak nonlinearly grow at $M_{AC} = 10$. After the slowdown of the radial motion the violent expansion starts to the azimuthal direction. The expanding the shock wave reflects at the equatorial plane and propagates into the up stream. Even the weak magnetic field whose energy density is one-thousandth of the energy density of the gas perturbs the flow and generates the shock wave. The temperature behind the shock front reaches the virial temperature. The shock waves produced near the event horizon may generate the large amount of X-ray radiation.

1. Introduction

According to the standard accretion disk model (Shakura and Sunyaev 1973), the effective temperature T_e of the emission from the optically thick disk decreases with increasing mass M_* of a central collapsed object, $T_e \propto M_*^{-1/4}$ (Rees 1984). The X-ray emission from the binary star systems can be explained by the standard model. On the other hand this model can not directly account for the X-ray emission from active galactic nuclei with a massive black hole, $M_* \approx 10^6 M_\odot$. Babul, Ostriker and Mészáros (1989) proposed the standing shock model for the radiation mechanism of the hard X-ray and γ -ray in quasars and active galactic nuclei. They showed that the steady state solution with shock can exist in a spherically symmetric accretion onto a black hole including nonadiabatic radiative losses and gains, heat transport processes and pair processes. The preheating of the infalling gas by emergent X-rays can suppress the accretion flow (Ostriker et al 1976; Mészáros and Ostriker 1983; Chang and Ostriker 1985). We consider here an other suppressing mechanism of the accretion flow due to the magnetic stress.

Yokosawa et al.(1991) obtained an exact nonstationary solution for the variation of the magnetic field with a given motion of particles falling into a rotating black hole. They considered the simple case that initially the gas and magnetic field are uniformly distributed around a hole. At first, the magnetic field is so weak that the gas falls freely into the black hole with no specific angular momentum. The gas and the frozen-in magnetic field near the event horizon increases with the matter falling. The proper gas density, ρ , and the radial, azimuthal and toroidal components of the the magnetic field in the comoving frame of particles, \tilde{B}^r , \tilde{B}^θ and \tilde{B}^ϕ , increas with the proper time τ of the infalling particle such as $\rho \propto \tau$, $\tilde{B}^r, \tilde{B}^\theta, \tilde{B}^\phi \propto \tau^{4/3}$. The frozen-in magnetic field has a smaller compressibility than the gas. The magnetic stress $\tilde{B}^i \tilde{B}^j$ grows with higher rate than the inertial force ρc^2 acting on the infalling gas. The infalling flow near the event horizon will be suppressed by the magnetic stress in a finite time.

Williams(1975) showed that if the magnetohydrodynamical flow is super-Alfvénic at infinity but sub-alfvénic further in, a smooth transition at the Alfvén surface would be unstable. With a Newtonian treatment

of the accretion onto a star, the spherically symmetric steady flow has the approximate relations such as in the supersonic region the flow density ρ , velocity v , and the strength of the magnetic field B are $\rho \sim r^{-3/2}$, $v \sim r^{-1/2}$ and $B \sim r^{-2}$. Thus the Alfvén velocity v_A is $v_A \sim r^{-5/4}$ and the Alfvénic Mach number M_A becomes $M_A \sim r^{3/4}$. The Alfvénic Mach number M_A decreases monotonically as the matter falls in to a collapsed object. The C_- characteristics which correspond to disturbances moving outwards against the flow converge to a Alfvén surface. The wavefronts of the Alfvén waves steepen, amplitudes increase exponentially and so does the wave energy: the flow is thus unstable. The smooth trans-Alfvénic flow is locally unstable, which is called as the piling-up instability. The unstable flow might produce the discontinuity surface of the shock wave front at the up-stream region.

The flow with nonradiality may require the different conditions for the formation of the shock wave. We examine the calculation of the accretion flow in which the gas falls quasi-radially and the weak magnetic field is a little different from the spherically symmetric field. The magnetohydrodynamical accretion with an initially uniform magnetic field directed along the rotation axis of the hole produces the gentle peak of the magnetic pressure at the rotation axis. The force balance of the flow in the azimuthal direction is kept by the magnetic stress in the case of the cool flow. The wave energy of the perturbations produced near the peak increases with the work done by the falling gas. The disturbances in the azimuthal direction easily grow and result in the shock waves propagating in to the azimuthal direction. The disturbances grow exponentially with the very small ratio of the energy density of the magnetic field to the kinetic energy density of the gas flow in comparison with the spherically symmetric flow.

The numerical method for the general-relativistic magnetohydrodynamics was developed by Yokosawa(1993). I proposed a new simulation method in which the Maxwell's equations are solved with the 3+1 formalism and the momentum equations are solved with the four-dimensional form. Using the method of the transformation law, the 3+1 components of the electro-magnetic field are transformed to the four dimensional components. This algorithm of the simulation is very simple. With this method I calculate the accretion flows which are spherically symmetric or the accretion with a bit of nonsphericity. I study the conditions and the processes of the formation of the shock wave near a black hole.

2. Calculation Methods of General-Relativistic Magnetohydrodynamics

The calculation method of MHD accretion and the accuracy of the numerical code were described in Yokosawa(1993). Here I explain the calculation method in brief. The magnetohydrodynamic calculations are performed in a fixed gravitational field; for accretion problems this field is represented by the Kerr metric in the coordinates of Boyer and Lindquist(1967)

$$ds^2 = g_{tt}dt^2 + 2g_{t\varphi}dtd\varphi + g_{\varphi\varphi}d\varphi^2 + g_{rr}dr^2 + g_{\theta\theta}d\theta^2. \quad (1)$$

We use geometric units in which $G = c = M = 1$ (M = black hole mass). The motion of the fluid is governed by the equation of motion

$$T^{\alpha\beta}_{;\beta} = 0, \quad (2)$$

where $T^{\alpha\beta}$ is the total energy-momentum tensor for the fluid and electromagnetic field. The baryon number is conserved :

$$(\rho u^\alpha)_{;\alpha} = 0, \quad (3)$$

where ρ and u^α are the fluid density and four velocity. The magnetic field according to a comoving observer is defined as

$$B_\alpha = \frac{1}{2} \epsilon_{\alpha\beta\gamma\delta} u^\beta F^{\gamma\delta}, \quad (4)$$

where u^β is a four-velocity of fluid and $\epsilon_{\alpha\beta\gamma\delta}$ is the Levi-Civita antisymmetric tensor. The corresponding electric field, $E_\alpha = F_{\alpha\beta} u^\beta$, vanishes in the highly conducting fluid. When one is not interested in the dissipative effects in the plasma, it is appropriate to regard it as a perfect fluid. Then one can write the total energy-momentum tensor as

$$T^{\alpha\beta} = (\rho + p)u^\alpha u^\beta + p g^{\alpha\beta} - \frac{B^2}{4\pi} g^{\alpha\beta} + \frac{B^\alpha B^\beta}{4\pi}, \quad (5)$$

where ϵ and P are the specific internal energy and the pressure of the fluid.

To express the time variation of the magnetic field we use the 3+1 formalism. Latin letters i, j, k, \dots represent indices in absolute space and greek letters $\alpha, \beta, \gamma, \dots$ represent indices in spacetime. The physical quantities, electromagnetic field E^i, B^i and fluid velocity v^i , are measured by the observers in the locally non-rotating frames(LNRF)(Bardeen, Press and Teukolsky, 1972) whose world lines are orthogonal to the hypersurfaces of constant t . Faraday's law becomes

$$(\frac{\partial}{\partial t} - L_{\vec{\beta}})B^i = -\epsilon^{ijk} \frac{\partial}{\partial x^j} (\alpha E_k), \quad (6)$$

where $L_{\vec{\beta}}$ is the Lie derivative along the shift vector $\vec{\beta}$. The flux-freezing condition gives $E_i = -\epsilon_{ijk} v^j B^k$. Then the *general relativistic* magnetic induction equation has the form

$$\partial_t B^i = \epsilon^{ijk} \partial_j \epsilon_{klm} (\alpha v^l - \beta^l) B^m. \quad (7)$$

The four-vector of the magnetic field B^α is derived from the electromagnetic field E^i, B^j measured in LNRF by using the standard transformation law between the LNRF and the Boyer-Lindquist coordinate frame. We introduce the set of LNRF basis vectors, $e^{\hat{\alpha}}$. The electro-magnetic tensor $F_{\hat{\alpha}\hat{\beta}}$ consisting of E^i and B^i is transformed into the coordinate tensor $F_{\alpha\beta}$ as

$$F_{\alpha\beta} = e^{\hat{\alpha}}_{\alpha} e^{\hat{\beta}}_{\beta} F_{\hat{\alpha}\hat{\beta}}. \quad (8)$$

Thus the magnetic four-vector B^α is given by the relation (3).

The above equations, (2),(3),(7) and the equation of state, $P = \rho\epsilon(\Gamma - 1)$, where Γ is the ideal gas adiabatic exponent, determine the evolutions of fluid and magnetic field. Our formalism, the time variation of the magnetic field described in LNRF, and the fluid motion described in the frame of the Boyer-Lindquist coordinate, is remarkably simple in all.

We use the numerical technique of the flux-corrected transport for evolving the fluid equations, which is developed from the numerical code for the special relativistic hydrodynamics (Yokosawa, Ikeuchi and Sakashita 1982). The magnetic induction is solved with the technique of the constrained transport (Evans and Hawley 1988). We use the two types of spatial grids. In the maximum case, we take the spatial grids in the spherical coordinates as 200 grids in the r -direction and 150 grids in the quarter of a circle. The three grids are used for each boundary. The geometrical values of the curved space are given at 1000 points in the r -direction and 150 points in the θ -direction. In the usual case, we take 125 grids in the r -direction and 100 grids in the quarter of a circle. The geometrical values are given at 625 points in the r -direction and 100 points in the θ -direction. The intermediate values of the geometry are calculated by the interpolation. The inner edge of the calculation domain is taken as $r_{in} = 1.04r_h$, where r_h is the radius of the event horizon. The outer edge is taken as $r_{out} = 10r_h$ or $20r_h$.

3. Formation Processes of Shock Wave in Magnetohydrodynamical Accretion

The evolution of perturbations in flow is described by a second-order quasilinear differential equation(Landau and Lifshitz 1959). For the spherically symmetric accretion in the Newtonian case the perturbation equations were derived by Williams(1975). The potential function Φ of the axisymmetric perturbations is written as

$$\Phi_{tt} + 2v\Phi_{rt} + (v^2 - v_A^2)\Phi_{rr} = v^2(\log v' - \log B')\Phi_r + v\log B'\Phi_t, \quad (9)$$

where $\Phi_t = \partial\Phi/\partial t$ etc., r denotes the radial derivative, $\log v' = \partial \log v / \partial r$, v and B are the unperturbed values of the flow velocity and the strength of radial magnetic field, and v_A is the Alfvén velocity. The perturbations of the toroidal component of the flow velocity and the magnetic field, $v_\phi^{(1)}$ and $B_\phi^{(1)}$, are derived from the derivatives of the potential, i.e. $B_\phi^{(1)} = \partial\Phi/r\partial r$ and $v_\phi^{(1)} = (\partial\Phi/\partial t + v\partial\Phi/\partial r)/rB$.

Since the above differential equation (9) is a hyperbolic type, the characteristics are given by

$$\frac{dr}{dt} = v \pm v_A. \quad (10)$$

The characteristics with the minus sign, C_- , correspond to disturbances moving inwards with the flow, while the characteristics with the plus sign, C_+ , correspond to disturbances moving outwards against the flow. The radially symmetric accretion flow has the radial dependences at the super-sonic region such as the flow velocity, $v \propto r^{-1/2}$, the density, $\rho \propto r^{-3/2}$ and the strength of magnetic field, $B \propto r^{-2}$. The Alfvén velocity is then $v_A \propto r^{-5/4}$. Thus the Alfvénic Mach number M_A becomes $M_A \propto r^{3/4}$, i.e. the fluid passes from super-Alfvénic to sub-Alfvénic speeds. The C_+ -characteristics converge to the Alfvén surface, $r = r_A$. The wave energy of the disturbances increase exponentially and the amplitudes of the physical variables are divergent at the surface. This is called the 'piling-up instability'. The magnetohydrodynamical accretion may be unstable at the Alfvénic surface.

We examine numerically the stability of the magnetohydrodynamical accretion onto a black hole. The initial conditions of the fluid flow and the magnetic field are given by the following consideration. In view of the stationary and spherical magnetic field in a spherically symmetric spacetime, the Maxwell equations, $F_{[\alpha\beta,\gamma]} = 0$, give

$$F_{\theta\varphi}, r = 0. \quad (11)$$

With reasonable asymptotic conditions we get

$$F_{\theta\varphi} = B_0 \sin \theta, \quad (12)$$

where B_0 is a constant, and other components, $F_{\alpha\beta} (\neq F_{\theta\varphi})$, can be taken to vanish. The radial magnetic field is expressed by the equation (3)

$$B^r = B_0 \left(\frac{r_h}{r} \right)^2. \quad (13)$$

The spherical accretion flow without the magnetic field was solved by Michel(1972). The hypersonic flow has the asymptotic forms

$$u^r \approx \sqrt{\frac{r_h}{r}}, \quad \rho \approx \rho_0 \left(\frac{r_h}{r} \right)^{3/2}, \quad \epsilon_0 \left(\frac{r_h}{r} \right)^{3(r-1)/2}. \quad (14)$$

The parameter to determine the stability of the flow is the Alfvénic Mach number. The Alfvénic Mach number M_A is defined as

$$M_A^2 = \frac{u_p^2}{u_A^2}, \quad (15)$$

where u_p is the poloidal velocity of the fluid measured in a locally inertia frame, $u_p^2 = u^r{}^2 + u^\theta{}^2$, and u_A is the Alfvén velocity (Lichnerowicz 1967), $u_A^2 = B_p^2 / (4\pi\rho h + B^2 - B_p^2)$. Here ρh is the density of the total inertia-carrying mass energy, $\rho h = \rho + \rho\epsilon + P$, and $B_p^2/4\pi$ is the energy density of the magnetic field in the poloidal direction, $B_p^2 = B_r B^r + B_\theta B^\theta + B_t B^t$.

We calculate the accretion by using the initial distributions (13) and (14). The specific internal energy ϵ is taken to be so small that the pressure of the fluid can be negligible, $P \ll \rho, B^2$. The parameters, ρ_0 and B_0 , are taken such as the Alfvén surface is located near the horizon. Initially the flow and the magnetic field are slightly disturbed in the azimuthal direction such as the initial values of the azimuthal components of the flow velocity and the magnetic field are taken to be $v^\theta = 10^{-9}$ and $B^\theta = 10^{-9}$, where v^θ is the convective velocity, $v^\theta \equiv u^\theta/u^t$. The results of the numerical calculations with the initial Alfvén surface, $r_A = 3r_H$, are shown in figure 1, where the specific angular momentum of the black-hole, a , is $a = 0.001$, and the other parameters are $\rho_0 = 1, B_0 = 30$ and $\epsilon_0 = 10^{-9}$. The evolution of the disturbances is shown in figure 2. Here the distributions of the flow and the magnetic field along the constant azimuthal angle $\theta = \pi/4$ are represented. In the early stage the wavy disturbances in the azimuthal direction are generated (see figure 2a). The disturbances near the Alfvén surface begin to grow (figure 2b). The large disturbances alter the

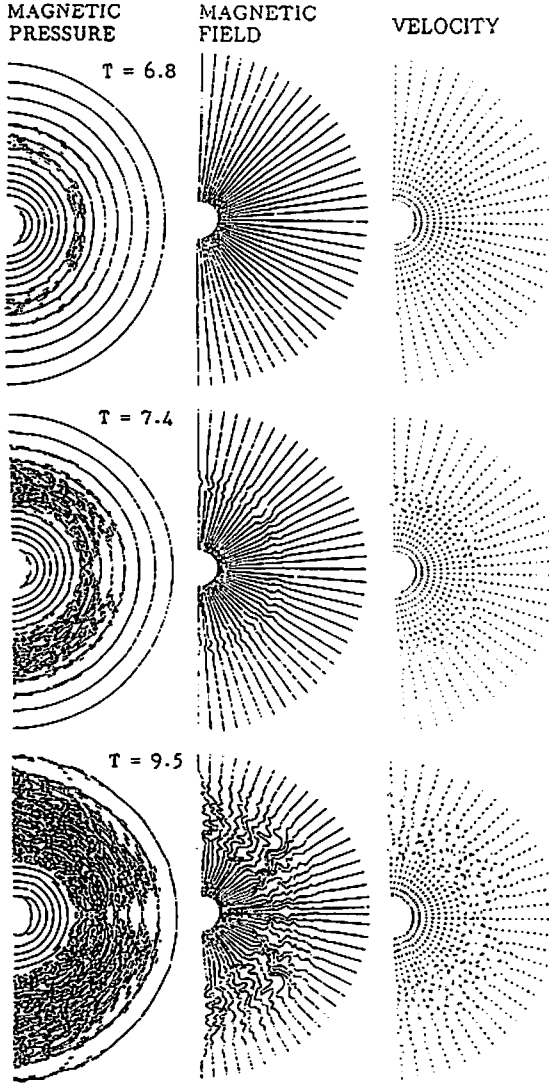


Figure 1.

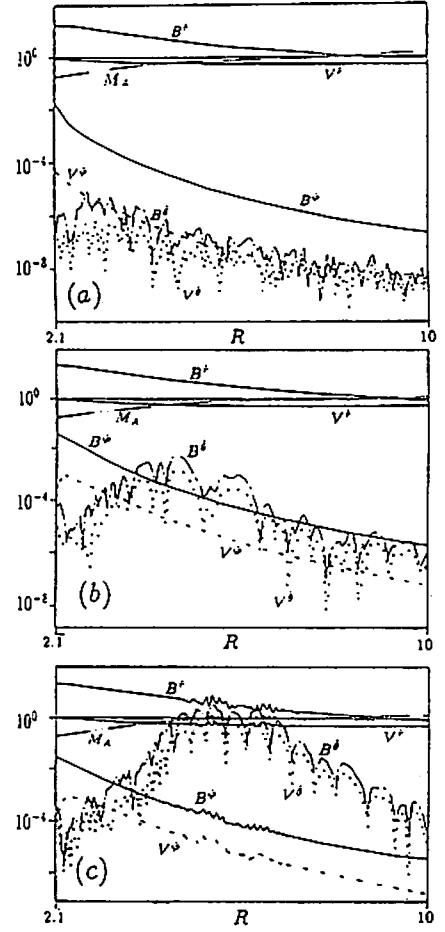


Figure 2.

Figure 1. Dynamical evolution of MHD accretion onto a black hole with $a = 0.001M$, $\rho_0 = 1$, $T_0 = 10^{-9}$, $B_0 = 30$. The initial geometry of the magnetic field lines are radial.

Figure 2. Evolutions of perturbations along the radius with $\theta = \pi/4$. The profiles of the magnetic field, B^r, B^θ, B^ϕ , the fluid velocity, v^r, v^θ, v^ϕ , and the Alfvénic Mach number M_A are shown for the times (a) $t = 0.8$, (b) $t = 4$, and (c) $t = 7$. The initial parameters are same as in figure 1.

radial components of the flow and the magnetic field (figure 2c). The radial flow begins to tremble near the Alfvén surface (figure 1a-b).

The position of the most growing disturbances depends on the radius of the Alfvén surface. When the strong magnetic field is taken as $B_0 = 10^2$ and the other parameters are fixed, the Alfvén surface locates at $r_A = 9.5r_h$. The numerical calculation shows that the disturbances more rapidly grow at the larger radius in the domain of the calculation, $r_{in} < r < 5r_h$. When the weak magnetic field is taken as $B_0 = 10$, the Alfvén surface is $r_A = 1.5r_h$. The disturbances at the inner radius grow more rapidly. When the still more weak field is taken as $B_0 = 1$, all over the flow becomes super-Alfvénic. The disturbances little grow. Though the wavy disturbances are generated at the early stage, they are suppressed by the accreting flow. While there are small disturbances near the horizon, these flickering lines become smooth lines after tenth dynamical time, $t \geq 10^2 M$. The black hole swallows all fluctuations. These calculations show that the evolution of the disturbances is determined by the magnitude of the Alfvénic Mach number.

The disturbed region expands in the outward direction (figure 1a-c). The accreting matter is wavyly disturbed in the early stage of the expansion. The dynamical evolution of the disturbed region is easily seen in the expansion starting from the inner edge (figure 2), where $B_0 = 10$, $\rho_0 = 1$, $\epsilon_0 = 10^{-9}$, $a = 0.001$ and $r_A = 1.5r_h$. After the expanding wave propagates to the radius, about twice the starting radius, the expanding front becomes a shock wave front. The accreting gas is rapidly decelerated and compressed at the front. The discontinuities of the density ρ , the pressure P , and the magnetic pressure P_B are produced. Their jumped values are approximately consistent with the Hugoniot relation for the magnetohydrodynamics (Lichnerowicz 1967 ; Hoffmann and Teller 1950). The expanding shell with the high density is formed and the accreting gas accumulates onto the shell. The shock wave propagates in the outward direction against the accreting MHD flow.

4. Shock Formation in MHD Accretion with Nonsphericity

We investigate the formation process of the shock wave in the MHD accretion with a bit of nonsphericity. In the case of the spherically symmetric accretion the magnetic field induces the unstable flow at the Alfvén surface where the energy density of the magnetic field is comparable with the density of the kinetic energy of the accreting fluid. There the distributions of the magnetic field and the fluid are spherically symmetric. If the nonsphericity is included in the magnetic field, even the weak magnetic field may induce the meridian motion because the force balance in the azimuthal direction is kept by the magnetic stress and the gas pressure and not by the inertia force. The evolution of the meridian motion will cause the disturbance on the quasi-radial accretion. The nonsphericity of the magnetic field may exchange the critical Mach number M_{AC} that causes the shock formation in the accretion flow. The shock wave formed in the accretion may exchange the flow pattern near the black hole.

We consider the accretion that initially the gas and the magnetic field are homogenous around a black hole. When the magnetic field is so weak that the magnetic stress is negligible for the gas falling, the cool gas may radially fall into a black hole. In this approximation the time evolutions of the gas density $\rho(t, r, \theta)$ and the magnetic field $B^a(t, r, \theta)$ are analytically solved (Yokosawa et al. 1991). The approximate expressions at the Newtonian region, $r \gg r_h$, are written as

$$\begin{aligned}\rho &\approx \rho_0 \left(1 + \frac{3}{2} \frac{t\sqrt{2M}}{r^{3/2}}\right) \propto t r^{-3/2}, \\ B^r &\approx B_0 \cos \theta \left(1 + \frac{3}{2} \frac{t\sqrt{2M}}{r^{3/2}}\right)^{4/3} \propto t^{4/3} r^{-2}, \\ B^\theta &\approx -B_0 \sin \theta \left(1 + \frac{3}{2} \frac{t\sqrt{2M}}{r^{3/2}}\right)^{1/3} \propto t^{1/3} r^{-1/2}, \\ B^\phi &\approx -B_0 \sin \theta \cos \theta \frac{3\sqrt{2} M a t}{r^3}.\end{aligned}\tag{16}$$

Since the radial component B^r increases most rapidly, the configuration of the magnetic field becomes a quasi-radial. At the distant region $r \gg r_h$, the azimuthal component B^θ becomes comparable with the

radial component B^r . Thus the magnetic pressure $P_B = B_\alpha B^\alpha / 4\pi$ may have a peak away from the axially symmetric line. The velocities of the freely falling fluid at large radii are expressed approximately as

$$u^r \approx -\frac{\sqrt{2M}}{r^{1/2}}, \quad u^\theta \approx 0, \quad u^\varphi \approx \frac{2aM}{r^3}. \quad (17)$$

The Alfvénic Mach number is

$$M_A \approx \frac{\sqrt{\rho_0}}{B_0 \cos \theta} t^{-5/6} r^{3/4}. \quad (18)$$

Initially the super-Alfvénic flow may produce the Alfvénic surface at first on the axially symmetric axis near the horizon.

We calculate numerically the accretion with nonsphericity. The fluid is initially static in LNRF and the magnetic field is homogenous around the black hole. The pressure of the fluid is taken as $P \ll \rho u^\alpha u^\beta, B^\alpha B_\beta$. Thus the initial parameters are adopted such as $B_0 = 0.02, \rho_0 = 1, T_0 = 10^{-12}$ and the rotating parameter of the black hole is $a = 0.999$. In a short time of the calculation the fluid begins to fall and its radial velocity becomes steady. The typical Alfvénic Mach number at the early stage of the accretion is about $M_A \approx 30$. At the early stage of the evolution the accretion produces a peak of the magnetic pressure off the central axis. The fluid near the axis slowly approaches to the central axis. The azimuthal components of the magnetic field B^θ and the fluid velocity v^θ are not wavyly disturbed but smoothly distributed. The azimuthal velocity $v^\theta(r, \theta)$ of the fluid is dynamically determined mainly by the magnetic pressure $P_B(r, \theta)$. Its value is very small and its sign is negative near the axis except for the vicinity of the horizon.

The approaching of the fluid to the central axis brings about the redistribution of the magnetic field and produces the peak of the magnetic pressure on the central axis. When the Alfvénic Mach number M_A reduces to about fifteen, the repulsion of the magnetic field begins to expand the fluid from the central axis. The azimuthal velocity v^θ is negative in early stage, $0 < t < 13.5$, and returns to be positive at $t = 13.5$. In the expansion stage of the fluid, $v^\theta > 0$, the wavy structures of the azimuthal components $v^\theta(r), B^\theta(r)$ are produced. The other components $B^r, B^\varphi, v^r, v^\varphi$ remain smooth. When $M_A \approx 10$ and $t \approx 27$, the radial and the toroidal components, B^r, B^φ , and v^φ , are also wavyly disturbed, while the radial velocity of the fluid v^r remains steady. From that time on the wavy magnetic field increases exponentially. The energy density of the magnetic field at a point on the central axis becomes comparable with the kinetic energy density of the fluid. The falling fluid is decelerated by the magnetic stress. The magnetized fluid rapidly expands in the azimuthal direction. The azimuthal motion produces the shock wave.

The nonradial propagation of the shock wave drastically exchanges the flow structure of the accretion. Figures 8 and 9 show the dynamical evolution of the MHD structures near the black hole. The primary force of the shock drive is the magnetic pressure since $P_{B \text{ at shock front}} \gg P_{\text{at shock front}}$. The shock wave starting from the central axis propagates down the hill of the magnetic pressure. The shock wave is so strong that the fluid and the magnetic field concentrate behind the shock front. The shock wave propagates to the equatorial plane and the disc with high density is formed.

Since the magnetic pressure of the accretion flow distributes approximately as $P_B \propto r^{-4}$, the strength of the shock wave is weak at the outer region. The weak shock wave can not sweep up the fluid and some fluid continues to fall. The falling fluid interacts with the equatorial disc. The MHD accretion with a bit of nonsphericity produces the complexly shocked structure around the black hole.

5. Discussion

The shock formation in the spherically symmetric accretion is driven by the waves induced at the Alfvén surface. On the other hand the accretion with nonsphericity produces the shock formation caused mainly by the dynamical effect. In the latter case the magnetic field near the symmetric axis is wavyly disturbed. It is necessary to discuss the physics of the expansion caused by the wavyly disturbed magnetic field. In the above both cases the energy of the MHD waves is enhanced by the falling fluid. The mechanism of this energy variation is satisfactorily understood by the split of the MHD flow into two compositions, which are the smooth MHD flow and the assembly of wave trains (Bretherton 1970; Dewar 1970; Jacques 1977).

The momentum equation of the azimuthal component and the Farady equation are approximately expressed at the Newtonian region on the assumption that the pressure of the fluid is negligible, $P \ll P_B$, and the radial component of the magnetic field is dominant, $B^r \gg B^\theta \gg B^\phi$.

$$\rho \frac{\partial v^\theta}{\partial t} \approx \frac{1}{r} \frac{\partial}{\partial \theta} \left(\frac{B^2}{8\pi} \right) - \rho v^r \frac{1}{r} \frac{\partial}{\partial r} (r v^\theta) + B^r J^\phi, \quad (19)$$

$$\frac{\partial B^\theta}{\partial t} = \frac{1}{r} \frac{\partial}{\partial r} r (v^\theta B^r - v^r B^\theta), \quad (20)$$

$$\frac{\partial B^r}{\partial t} = \frac{1}{r \sin \theta} \frac{\partial}{\partial \theta} (\sin \theta [v^r B^\theta - v^\theta B^r]), \quad (21)$$

where $J^\phi = \frac{1}{4\pi r} \frac{\partial}{\partial r} (r B^\theta)$. When the magnetic field with the radially symmetry is perturbed in the azimuthal direction such as the perturbation of the Alfvénic type, by the WKB approximation the linear theory drives the wave solution from the equations (19) and (20):

$$\begin{aligned} \delta v^\theta &= \frac{C_1}{r} e^{i(\omega t - \kappa r)}, & \delta B^\theta &= \frac{C_2}{r} e^{i(\omega t - \kappa r)}, \\ \omega &= (v^r \pm v_A) \kappa, \end{aligned} \quad (22)$$

where C_1, C_2 are constants and $v_A = B^r / \sqrt{4\pi\rho}$. The both perturbations, $\delta v^\theta, \delta B^\theta$, have the same phase. The small perturbations generated in the spherical or nonspherical accretion are approximately Alfvénic type. Since $\delta B^r / B^r \approx \delta v^\theta$, the fluctuation in the radial component B^r becomes remarkable at the large azimuthal perturbation, $\delta v^\theta > 0.1$ (figure 2c, figure 6c?). In the case of the accretion with nonsphericity the azimuthal motion is determined mainly by the gradient of the magnetic pressure. The expanding velocity near the symmetry axis $v^\theta(t)$ increases with the radial component of the magnetic field $B^r(t)$ (figure 7). After the remarkable fluctuation in B^r , the gradient of the magnetic pressure rapidly increases. The increased velocity v^θ accelerates the variation of B^r .

The increase of the energy of the wavy motion is brought about by the falling motion of the fluid. The fluid equation in the presence of MHD waves have been studied in the solar wind theory (Jacques 1977). The equations of the flow with waves are expressed in the Newtonian form (Yokosawa 1982) as

$$\rho \frac{dv}{dt} + \nabla \left(P + \frac{B^2}{8\pi} \right) - \frac{(B \cdot \nabla) B}{4\pi} - \rho \frac{GM}{r^3} r = -\nabla \cdot P_{\omega\pm} \quad (23)$$

$$\begin{aligned} \frac{\partial}{\partial t} \left(\frac{1}{2} \rho v^2 + \frac{P}{\Gamma-1} + \frac{B^2}{8\pi} \right) + \nabla \cdot \left\{ \left(\frac{1}{2} \rho v^2 + \frac{\Gamma P}{\Gamma-1} - \rho \frac{GM}{r} \right) v \right. \\ \left. + \frac{(v \times B) \times B}{4\pi} \right\} = -v \cdot \nabla \cdot P_{\omega\pm}, \end{aligned} \quad (24)$$

$$\frac{\partial}{\partial t} \epsilon_{\pm} + \nabla \cdot (\epsilon_{\pm} V_{g\pm} + P_{\omega\pm} \cdot v) = v \cdot \nabla \cdot P_{\omega\pm}, \quad (25)$$

where $d/dt = \partial/\partial t + v \cdot \nabla$; $\epsilon_{\pm}, P_{\omega\pm}$ and $V_{g\pm}$ are the energy density, stress tensor and group velocity of MHD waves propagating upward(+) and downward(-). In the case of the spherically symmetric accretion the smoothed magnetic field on the left side of the equations (23), (24) can do no effect on the fluid. The pressure of the waves, $\nabla \cdot P_{\omega\pm}$, accelerates or decelerates the fluid. When $v \cdot \nabla \cdot P_{\omega\pm} > 0$, the work by the falling fluid increases the energy of the waves ϵ_{\pm} . The gradient of the pressure, $\nabla \cdot P_{\omega\pm}$, depicted in figure 2b is negative at the outer region and positive at the inner region. Since $v < 0$, the wave energy at the outer region rapidly increases and thus the peak of the wave energy shifts to the outer radius (figure 2c). In the case of the accretion with nonsphericity the rapid increase of the wavy energy may be also given by the falling fluid.

6. Conclusions

The magnetic field could produce the shock wave in the accretion onto a black hole. The spherically symmetric accretion results in the shock formation near the Alfvénic surface. The nonsphericity of the MHD accretion may reduce the critical strength of the magnetic field at which the shock wave can be produced. In the case of the initial condition with homogeneous magnetic field, the critical Alfvénic Mach number is $M_{AC} \approx 10$. The energy density of the magnetic field is about one-hundredths of the falling fluid. The accretion with nonsphericity may produce the complexly shocked structure near the black hole. If the strength of the magnetic field in the accretion flow is larger than the critical value, the high luminous X-ray may be emitted from the vicinity of the black hole.

References

- Babul, A., Ostriker, F. P., and Mészáros, P. 1989, *Astrophys. J.*, **347**, 59.
Bardeen, J. M., Press, W. H., and Teukolsky, S. A. 1972, *Astrophys. J.*, **178**, 347.
Bretherton, F. P. 1970, in *Mathematical Problems in the Geophysical Sciences*, "The General Linearised Theory of Wave Propagation", (Providence: American Mathematical Society), pp61-102.
Chang, K. M., and Ostriker, K. M. 1985, *Astrophys. J.* **288**, 428.
Dewar, R. L. 1970, *Phys. Fluid* **13**, 2710.
Evans, C. R. and Hawley, J. F. 1988, *Astrophys. J.*, **332**, 659.
Hoffmann, F. de, and Teller, E. 1950, *Phys. Rev.*, **80**, 692.
Jacques, S. A. 1977, *Astrophys. J.*, **215**, 942.
Landau, L. D., and Lifshitz, E. M. 1963, in *Fluid Mechanics*, (Pergamon: Oxford), p381.
Lichnerowicz, A. 1967, in *Relativistic Hydrodynamics and Magnetohydrodynamics* (W. A. Benjamin, Inc., New York), p110.
Mészáros, P., and Ostriker, J. P. 1983, *Astrophys. J.* **273**, L59.
Ostriker, J. P., McCray, R., Weaver, R., and Yahil, A. 1976, *Astrophys. J.* **208**, L61.
Rees, M. J. 1984, *Ann. Rev. Astrophys.* **22**, 471.
Shakura, N. I., and Sunyaev, R. A. 1973, *Astron. Astrophys.* **24**, 337.
Sloan, J., and Smarr, L. L. 1985, in *Numerical Astrophysics*, ed. J. Centrella, J. LeBlance, and R. Bowers (Boston : Jones and Bartlett), p52.
Takahashi, M., Nitta, S., Tatematsu, Y., and Tomimatsu, A. 1990, *Astrophys. J.*, **363**, 206.
Yokosawa, M., Ikeuchi, S., and Sakashita, S. 1982, *Publ. Astron. Soc. Japan* **34**, 461.
Yokosawa, M., Ishizuka, T., and Yabuki, Y. 1991, *Publ. Astron. Soc. Japan*, **43**, 427.
Yokosawa, M. 1993, *Publ. Astron. Soc. Japan*, **45**, No. 2.
Williams, D. J. 1975, *Mon. Not. R. astr. Soc.*, **171**, 537.

Slow Evolution of Black Hole Magnetospheres

Toshio Uchida

Astronomical Institute, Faculty of Science, Tohoku University, Sendai 980, Japan

1. Introduction

Studies on black hole magnetospheres are important to understand activities of galactic nuclei. For this purpose, we have developed a Lagrangian perturbation theory of the relativistic ideal magnetohydrodynamics (Uchida 1993). By using this method, we will consider infinitesimally slow (quasi-static) evolutions of axisymmetric magnetospheres in this work.

The situation we will consider is as follows; Suppose a small axisymmetric change takes place in a stationary and axisymmetric magnetosphere and the magnetosphere settles in a nearby stationary and axisymmetric configuration. If this change takes place slowly enough, one can disregard time derivatives of the perturbation and it is sufficient to consider stationary axisymmetric solutions for small perturbations.

In the following, changes in gravitational field are neglected and we assume that the metric of the background spacetime is

$$ds^2 = -\alpha^2 dt^2 + \varpi^2 (d\phi - \omega dt)^2 + g_{rr} dr^2 + g_{\theta\theta} d\theta^2. \quad (1)$$

2. Basic equation

In the following, we will consider only the cold (massless) limit. In this limit, the energy density ρ is given by $\rho = nm$ (we use the units in which $c = G = 1$) and the basic equations of the relativistic ideal magnetohydrodynamics reduce to

$$\nabla_\mu n^\mu = 0, \quad (2)$$

$$F_{\mu\nu} u^\nu = 0, \quad (3)$$

$$\partial_\lambda F_{\mu\nu} + \partial_\mu F_{\nu\lambda} + \partial_\nu F_{\lambda\mu} = 0, \quad (4)$$

$$\nabla_\lambda F^{\mu\lambda} = 4\pi J^\mu, \quad (5)$$

$$m n u^\nu \nabla_\nu u_\mu = F_{\mu\nu} J^\nu, \quad (6)$$

where equation (2) is the equation of continuity ($n^\mu = n u^\mu$), equation (3) is the degenerate (ideal MHD) condition, equations (4) and (5) are Maxwell equation and equation (6) is Euler equation.

3. Stationary and axisymmetric configuration

In stationary and axisymmetric case, the electromagnetic field $F_{\mu\nu}$ is written as

$$\begin{aligned} F_{tr} &= \Omega_F \partial_r \Psi, & F_{t\theta} &= \Omega_F \partial_\theta \Psi, & F_{t\phi} &= 0 \\ F_{r\phi} &= \partial_r \Psi, & F_{\theta\phi} &= \partial_\theta \Psi, & F_{r\theta} &= \frac{\sqrt{-g}}{\alpha^2 \varpi^2} B_T, \end{aligned} \quad (7)$$

where Ψ is the stream function and chosen so as to coincide with the Boyer-Lindquist components of A_ϕ . The poloidal components of velocity are

$$u^r = \frac{\eta}{\sqrt{-g}n} \partial_\theta \Psi, \quad u^\theta = -\frac{\eta}{\sqrt{-g}n} \partial_r \Psi. \quad (8)$$

Then equations (2)~(6) yields the integrals on the poloidal field surface (surface on which $\Psi = \text{const.}$ in $r - \theta$ space) and there remains one equation to be solved. For the derivation of the following results, see e.g. Phinney (1983) or Carmenzind (1989).

The integrals are as follows;

- η ; magnetic flux/ particle flux ,
- Ω_F ; angular velocity of the magnetic field ,
- E ; energy at infinity ,
- L ; angular momentum at infinity ,

where E and L are given respectively by

$$E = -mu_t - \Omega_F \frac{B_T}{4\pi\eta}, \quad (9)$$

$$L = mu_\phi + \frac{B_T}{4\pi\eta}. \quad (10)$$

Further, there is a relation

$$u^\phi - \Omega_F u^t = \frac{\eta}{\alpha^2 \varpi^2 n} B_T. \quad (11)$$

By equations (9), (10) and (11), u^t , u^ϕ and B_T are given by the integrals and the metric. Further, by $u^\mu u_\mu = -1$, n is also written by Ψ , the integrals and the metric. The poloidal components of Euler equation yield

$$\begin{aligned} &\partial_A \left\{ \frac{\sqrt{-g}}{\alpha^2 \varpi^2} [\alpha^2 - \varpi^2 (\Omega_F - \omega)^2 - \frac{4\pi m \eta^2}{n}] \partial^A \Psi \right\} + \\ &+ \partial_A \left\{ \frac{\sqrt{-g}}{\alpha^2 \varpi^2} [\varpi^2 (\Omega_F - \omega) \frac{d\Omega_F}{d\Psi} + \frac{4\pi m \eta^2}{n} \frac{d\eta}{d\Psi}] \right\} |\nabla \Psi|^2 \\ &- n u^t \kappa_1 + n u^\phi \kappa_2 = 0, \end{aligned} \quad (12)$$

where

$$\kappa_1 = \frac{dE}{d\Psi} + \frac{B_T}{4\pi\eta} \frac{d\Omega_F}{d\Psi} - \frac{\Omega_F B_T}{4\pi\eta^2} \frac{d\eta}{d\Psi}, \quad (13)$$

$$\kappa_2 = \frac{dL}{d\Psi} - \frac{1}{4\pi\eta^2} \frac{d\eta}{d\Psi} \quad (14)$$

Then eliminating u^t , u^ϕ , B_T and n from equation (12), we have a closed set of equation for Ψ (for the explicit expression of this equation, see Nitta (1991)). This transfield equation (Grad-Shafranov equation) has regular singularity at the Alfvén and the fast magnetosonic surface and the critical condition is necessary to ensure regularity of solutions. To summarize, construction of the models of the stationary axisymmetric magnetosphere mathematically equivalent to obtain solutions of transfield equation for given η , Ω_F , E and L as functions of Ψ .

4. Linear perturbation theory of the relativistic MHD

When treating small perturbations, there are two theories. That is, the Eulerian perturbation theory and the Lagrangian perturbation theory. Here we choose the Lagrangian approach. In the Lagrangian perturbation theory, the dynamical variable is a vector field called the Lagrangian displacement and the perturbations of the physical quantities are expressed by the Lagrangian displacement. By the Lagrangian displacement ζ^μ the first order changes in the physical quantities are expressed as follows;

$$\delta n = -\nabla_\lambda (n\zeta^\lambda) - nu^\lambda u^\tau \nabla_\lambda \zeta_\tau, \quad (15)$$

$$\Delta n = -n\gamma^{\lambda\tau} \nabla_\lambda \zeta_\tau, \quad (16)$$

$$\delta u^\mu = -\gamma^\mu_\lambda \mathcal{L}_\zeta u^\lambda, \quad (17)$$

$$\Delta u^\mu = (u^\lambda u^\tau \nabla_\lambda \zeta_\tau) u^\mu, \quad (18)$$

$$\delta F_{\mu\nu} = \nabla_\mu (F_{\nu\lambda} \zeta^\lambda) - \nabla_\nu (F_{\mu\lambda} \zeta^\lambda), \quad (19)$$

$$\Delta F_{\mu\nu} = 0, \quad (20)$$

where $\gamma^{\mu\nu} = g^{\mu\nu} + u^\mu u^\nu$, δ denotes the Eulerian changes and Δ denotes the Lagrangian changes. Their relation is given by

$$\Delta = \delta + \mathcal{L}_\zeta, \quad (21)$$

where \mathcal{L}_ζ is the lie derivative with respect to the Lagrangian displacement ζ^μ . Further, it can

be shown that the component of ζ parallel to u^μ does not contribute to the physical quantities at all. Thus we can impose the condition $\zeta^\mu u_\mu = 0$ without the loss of generality.

The advantage of the Lagrangian approach lies in the fact that it reduces the number of equations to be solved greatly. In fact, as easily verified, the first order changes in the physical quantities given above automatically satisfy

$$\nabla_\mu \delta n^\mu = 0, \quad (22)$$

$$F_{\mu\nu} \delta u^\nu + \delta F_{\mu\nu} u^\nu = 0, \quad (23)$$

$$\partial_\lambda \delta F_{\mu\nu} + \partial_\mu \delta F_{\nu\lambda} + \partial_\nu \delta F_{\lambda\mu} = 0, \quad (24)$$

(or equivalent equations for the Lagrangian changes). Thus the equation which we must solve is only perturbed Euler equation given by

$$m n u^\nu \nabla_\nu \delta u_\mu + m (\delta n u^\nu + n \delta u^\nu) \nabla_\nu u_\mu = F_{\mu\nu} \delta J^\nu + \delta F_{\mu\nu} J^\nu. \quad (25)$$

This equation has three independent components. Thus our basic equation is a three-components equation for three independent components of ζ^μ .

5. Changes in Ψ, η and Ω_F

Before treating perturbed Euler equation, let us examine some consequences of equation (15)~(20). By equation (), $\delta F_{A,\phi}$ and δF_{tA} ($A = r\theta$) are given by

$$\delta F_{A,\phi} = -\partial_A (\zeta^\lambda \partial_\lambda \Psi), \quad (26)$$

$$\delta F_{tA} = -\partial_A (\zeta^\lambda \partial_\lambda \Omega_F) \partial_A \Psi - \Omega_F \partial_A (\zeta^\lambda \partial_\lambda \Psi). \quad (27)$$

By comparing these expressions with equation (7), we see that

$$\delta \Psi = -\zeta^\lambda \partial_\lambda \Psi, \quad \Delta \Psi = 0, \quad (28)$$

$$\delta \Omega_F = -\zeta^\lambda \partial_\lambda \Omega_F, \quad \Delta \Omega_F = 0. \quad (29)$$

Further, by equation (15), δn^r and δn^θ are written as

$$\sqrt{-g} n^r = -(\zeta^\lambda \partial_\lambda \eta) \partial_\theta \Psi - \eta \partial_\theta (\zeta^\lambda \partial_\lambda \Psi), \quad (30)$$

$$\sqrt{-g} n^\theta = +(\zeta^\lambda \partial_\lambda \eta) \partial_r \Psi + \eta \partial_r (\zeta^\lambda \partial_\lambda \Psi). \quad (31)$$

This implies that

$$\delta \eta = -\zeta^\lambda \partial_\lambda \eta, \quad \Delta \eta = 0. \quad (32)$$

That is, in the quasi-static axisymmetric changes of the ideal MHD systems, the values of η and Ω_F on one poloidal field surface assigned by the value of Ψ are invariant.

6. Reduction of perturbed Euler equation

In order to treat Euler equation, it is convenient to rewrite equation (25) as

$$m\sqrt{-g}n u^\nu (\partial_\nu \Delta u_\mu - \partial_\mu \Delta u_\nu) = \frac{1}{4\pi} F_{\mu\nu} \partial_\lambda (f^{\nu\lambda}), \quad (33)$$

where $f^{\mu\nu}$ is defined by

$$f^{\mu\nu} = \delta F^{\mu\nu} + 4\pi (J^\mu \zeta^\nu - J^\nu \zeta^\mu). \quad (34)$$

Thus $f^{\mu\nu}$ is an antisymmetric tensor. It is to be noted that $f^{r\theta}$ is written as

$$f^{r\theta} = \delta B_T + \zeta^\lambda \partial_\lambda B_T = \Delta B_T, \quad (35)$$

where B_T is given in equation (7) and $\delta B_T = \sqrt{-g} \delta F^{r\theta}$.

Then t and ϕ components of equation (33) respectively lead to

$$u^A \partial_A (m \Delta u_t + \frac{\Omega_F}{4\pi\eta} \Delta B_T) = 0, \quad (36)$$

$$u^A \partial_A (m \Delta u_\phi - \frac{1}{4\pi\eta} \Delta B_T) = 0. \quad (37)$$

Thus we have

$$-m \Delta u_t - \frac{\Omega_F}{4\pi\eta} \Delta B_T = \Delta E(\Psi), \quad (38)$$

$$m \Delta u_\phi - \frac{1}{4\pi\eta} \Delta B_T = \Delta L(\Psi), \quad (39)$$

where ΔE and ΔL are functions of Ψ . That is, contrary to η or Ω_F , Lagrangian changes in E and L change during the quasi-static evolution.

Two poloidal components of equation (33) are not independent. In fact, some manipulations they read

$$\begin{aligned} & \frac{1}{4\pi} \{ \partial_A (f^{\phi A}) - \Omega_F \partial_A (f^{tA}) \} + m\eta (\partial_\theta \Delta u_r - \partial_r \Delta u_\theta) \\ & - \sqrt{-g} n^t \frac{d\Delta E}{d\Psi} + \sqrt{-g} n^\phi \frac{d\Delta L}{d\Psi} \\ & - \frac{\sqrt{-g}}{4\pi\eta} \left[\frac{B_T}{\alpha^2 \varpi^2} \frac{d\eta}{d\Psi} + n^t \frac{d\Omega_F}{d\Psi} \right] \Delta B_T = 0. \end{aligned} \quad (40)$$

Further, by tedious manipulations this equation is rewritten as

$$\begin{aligned}
& \partial_A \left\{ \frac{\sqrt{-g}}{\alpha^2 \varpi^2} [\alpha^2 - \varpi^2 (\Omega_F - \omega)^2 - \frac{4\pi m \eta^2}{n}] \partial^A \delta \Psi \right\} + \partial_A \left\{ \frac{\sqrt{-g}}{\alpha^2 \varpi^2} \frac{4\pi m \eta^2}{n^2} \delta n \partial^A \Psi \right\} \\
& - 2 \partial_A \left\{ \frac{\sqrt{-g}}{\alpha^2 \varpi^2} [\varpi^2 (\Omega_F - \omega) \frac{d\Omega_F}{d\Psi} + \frac{4\pi m \eta^2}{n} \frac{d\eta}{d\Psi}] \delta \Psi \partial^A \Psi \right\} \\
& + 2 \frac{\sqrt{-g}}{\alpha^2 \varpi^2} [\varpi^2 (\Omega_F - \omega) \frac{d\Omega_F}{d\Psi} + \frac{4\pi m \eta^2}{n} \frac{d\eta}{d\Psi}] \partial^A \Psi \partial_A \delta \Psi \\
& + \frac{\sqrt{-g}}{\alpha^2 \varpi^2} \left\{ [\varpi^2 (\Omega_F - \omega) \frac{d^2 \Omega_F}{d\Psi^2} + (\frac{d\Omega_F}{d\Psi})^2] + \frac{4\pi m \eta}{n} [\frac{d^2 \eta}{d\Psi^2} + (\frac{d\eta}{d\Psi})^2] \right\} |\nabla \Psi|^2 \delta \Psi \\
& + 4\pi \sqrt{-g} [\delta n^t \kappa_1 - \delta n^\phi \kappa_2] + 4\pi \sqrt{-g} [n^t \delta \kappa_1 - n^\phi \delta \kappa_2] = 0.
\end{aligned} \tag{41}$$

By comparing above equation with equation (12), it is evident that this equation is nothing but perturbed transfield equation. Although equation (41) contains perturbed quantities which are not expressed explicitly by $\delta \Psi$, we can show that these quantities can be expressed by $\delta \Psi$, ΔE , ΔL and background quantities and eliminated from equation (41). As a result, equation (41) becomes a equation for $\delta \Psi$.

7. Conclusion

In this work, we showed following results.

- (1) $\Delta \eta$ and $\Delta \Omega_F$ vanish.
- (2) ΔE and ΔL are also functions of Ψ .
- (3) The poloidal components of perturbed Euler equation yield equation for $\delta \Psi$, which can be regarded as perturbed transfield equation.

Reference

- Carmenzind, M., 1989 In *Accretion Disk and Magnetic Field in Astrophysics*,
ed. Belevredre, G. Kluwer, Dordrecht.
- Nitta, S., 1991 Phys. Rev. 44, 2295.
- Phynney, E.S., 1983. In *Proceedings of the Trino Workshop on Astrophysical Jet*
p201, eds. Ferrari, & Pacholczyk, A.G., Reidel Pordrect, Holland.
- Uchida, T., 1993 in preparation

Plasma Accretion in the Vicinity of a Black Hole

Kouichi HIROTANI and Akira TOMIMATSU

Department of Physics, Nagoya University Chikusa-ku, Nagoya 464-01, Japan
and

Masaaki TAKAHASHI

Department of Physics and Astronomy, Aichi University of Education
Hirosawa, Igaya-cho, Kariya 448, Japan

Abstract

We study a magnetohydrodynamic (MHD) interaction between the accreting matter and the magnetic field in a Kerr black hole magnetosphere. Adopting the magnetically dominated limit, we analyze in detail the critical condition that the MHD ingoing flows must pass through the fast magnetosonic point. It is clearly shown that energy and angular momentum transport processes between the fluid and the magnetic field should be sufficiently effective in the accretion. Furthermore, studying non-stationary perturbations of MHD accretion in the short wave-length limit, we find that the fluid becomes highly variable compared with the electromagnetic field near the horizon. This is due to the effects of a critical point and the existence of the horizon. This result may be responsible for the variability of higher energy X-rays observed from active galactic nuclei.

1. Introduction

It is widely believed that an active galactic nucleus (AGN) contains a supermassive black hole in the central region (Elliot & Shapiro 1974; e.g., Rees 1984). The black hole will work as a central engine for producing the power output of an AGN, if its rotational energy is efficiently extracted. Then, during the active lifetime of an AGN, the total mass M and angular momentum J of the black hole should evolve with time. This evolutionary process of the central black hole may derive the luminosity evolution observed in AGNs (Park & Vishniac 1988;1990).

We expect that such an active black hole is surrounded by a magnetosphere and an accretion disk. Plenty of plasma can be supplied from the disk into the magnetosphere.

The plasma will be nearly neutral and can be treated by the perfect MHD approximation. In order to understand the long-term evolution of M and J , we must investigate the MHD accretion onto the black hole in the magnetosphere.

The MHD energy and angular momentum flux carried across the event horizon $r = r_H (\equiv M + \sqrt{M^2 - a^2})$ consists of electromagnetic and matter parts, where a is the spin parameter defined by $a \equiv J/M$. If the magnetospheric structure is assumed to be stationary and axisymmetric, some useful results for the general relativistic MHD flows have been obtained (see, e.g., Phinney 1983b). We can introduce the angular velocity Ω_F of the magnetic field lines, which may thread the horizon. If Ω_F is smaller than the hole's angular velocity $\omega_H \equiv a/2Mr_H$, the toroidal field can furnish an outgoing Poynting flux of electromagnetic energy and angular momentum (Blandford & Znajek 1977). This electromagnetic process induces a mass loss and a spin-down of the black hole. However the matter accretion carries an ingoing flux of positive energy and angular momentum, unless the Penrose mechanism becomes important. In the cold limit that thermal energy and pressure of fluid elements are negligible, the fluid's energy and angular momentum per unit rest mass are defined by the covariant components U_t and $-U_\phi$ of fluid four-velocity U^μ , respectively. If no magnetic field is present, U_t and $-U_\phi$, which are conserved along the flow line in this case, should be evaluated at the innermost stable circular orbit which corresponds to the inner edge of the disk. As a result of the accretion, the black hole is spun up to a limiting state (Bardeen 1970; Thorne 1974). In a magnetosphere this spin-up process is more complex. Plasma particles interacting with the magnetic field can flow from a more extended region of the disk towards the horizon, and U_t and $-U_\phi$ evolve along the flow line during its accretion owing to the MHD transport. In this paper we focus our attention on a MHD interaction in the black hole magnetosphere especially on the critical condition that the accretion should pass through the fast-magnetosonic point, and present first a general relativistic calculation of U_t and $-U_\phi$ in section 2. We show that the MHD interaction is so effective that typically 10% of the rest-mass energy of infalling plasma will be transported to the magnetic field and be carried outwards as Poynting flux.

If a small-amplitude perturbation is superposed on such an active stationary black hole magnetosphere, then a substantial perturbation energy may be transported between the plasma and the magnetic field; a very small perturbation in the field may cause a significant influence on the plasma flow. Therefore, it is attractive to consider a time-dependent accretion onto a black hole, because short-term variabilities of X-rays which are expected to be emitted from a very central region of an AGN are observed.

It is to this end that we turn in section 3 to the investigation of nonstationary and nonaxisymmetric perturbation superposed on a stationary and axisymmetric black hole magnetosphere. Adopting the magnetically dominated limit, we show that the fluid energy, angular momentum and poloidal velocity become highly variable near the fast-magnetosonic point in the magnetically dominated limit, even if perturbations in the electromagnetic field are very small. This result may be responsible for the observed short-term variations of X-ray emission from AGNs; this will be discussed in the final section.

2. MHD Interaction Between Plasma and Magnetic Field

2.1. Stationary Flows

In order to set the stage for our investigation of black hole magnetosphere and to prepare us with a feeling for the physical principles involved, it is helpful to consider for a moment what is known about stationary MHD flows in Kerr geometry. Before coming to this point, however, let us first present basic equations for general relativistic MHD flows.

Since the self-gravity of electromagnetic field and plasma around the black hole is very weak, the background geometry of the magnetosphere is described by the Kerr metric

$$ds^2 = \frac{\Delta - a^2 \sin^2 \theta}{\Sigma} dt^2 + \frac{4Mar \sin^2 \theta}{\Sigma} dt d\phi - \frac{A \sin^2 \theta}{\Sigma} d\phi^2 - \frac{\Sigma}{\Delta} dr^2 - \Sigma d\theta^2, \quad (1)$$

where $\Delta \equiv r^2 - 2Mr + a^2$, $\Sigma \equiv r^2 + a^2 \cos^2 \theta$, $A \equiv (r^2 + a^2)^2 - \Delta a^2 \sin^2 \theta$. Throughout this paper we use geometrized units such that $c = G = 1$.

Under ideal MHD conditions the electric field vanishes in the fluid rest frame, thus we have $F_{\mu\nu} U^\mu = 0$, where $F_{\mu\nu}$ is the electromagnetic field tensor satisfying the Maxwell equations $F_{[\mu\nu,\rho]} = 0$. The motion of the fluid in the cold limit is governed by the equations of motion $[m_p n U^\mu U^\nu + (F^{\mu\rho} F_\rho{}^\nu g^{\mu\nu} F_{\alpha\beta} F^{\alpha\beta} / 4) / (4\pi)]_{;\nu} = 0$, where the proper rest-mass energy density $m_p n$ obeys the continuity equation $(m_p n U^\mu)_{;\mu} = 0$.

From the analysis of stationary and axisymmetric ideal MHD equations, it is known that there exist four integration constants conserved along each flow line (e.g. Camenzind 1986a,b). These conserved quantities are the angular velocity of a magnetic field

line (Ω_F), particle flux per magnetic flux tube (η), total energy (E) and total angular momentum (L). A poloidal flow line is identical with a poloidal magnetic field line and is given by $\Psi(r, \theta) = A_\phi = \text{constant}$, where A_ϕ is the electromagnetic vector potential. The conserved quantities are functions of Ψ only; the discussion in this paper is valid for arbitrary Ψ .

We next describe a stationary plasma accretion in a black hole magnetosphere. In a black hole magnetosphere, there are two light surfaces. One is called the outer light surface which is formed by centrifugal force in the same manner as in pulsar models. The other is called the inner light surface which is formed by the gravity of the hole. In a region between the horizon and the inner light surface plasma must stream inwards, while in a region beyond the outer light surface it must stream outwards. The plasma source where both inflows and outflows start with low poloidal velocity will be located between these two light surfaces. This injection region ($r = r_I$) of the accretion may be a pair creation zone above the disk or the disk surface whose inner edge corresponds to the innermost stable circular orbit in Kerr geometry. Before reaching the horizon, plasma inflows must pass through the fast-magnetosonic point ($r = r_F$). At $r = r_F$, the fluid velocity coincides with the propagation speed of the fast-magnetosonic wave. The wave propagates outwards (inwards) in the r -coordinate at $r > r_F$ ($r < r_F$). Such a situation is illustrated in figure 1. From now on, we will use the subscript I and H to indicate that the quantities are to be evaluated at $r = r_I$ and $r = r_H$, respectively.

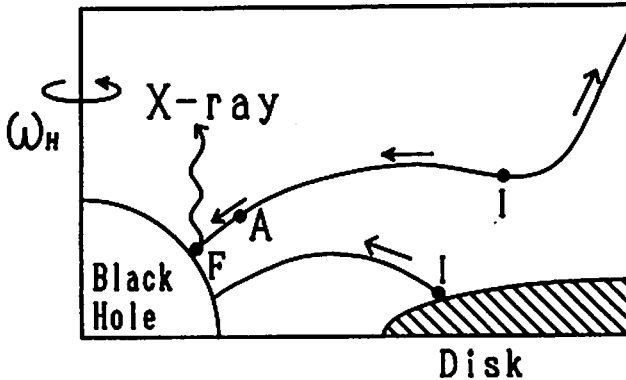


Fig. 1. Schematic figure (side view) of a stationary axisymmetric black hole magnetosphere. The accretion starts from a disk surface or a pair creation zone above it. The points I , and F correspond to the injection, and fast-magnetosonic points, respectively.

In the next subsection, we will analyze the critical condition that the accretion must pass through $r = r_F$ in the magnetically dominated limit, in which the MHD interaction will exert a significant influence on fluids.

2.2. Critical Conditions for Magnetically Dominated Accretion

To elucidate MHD interactions between the accreting plasma and the magnetic field, we shall first focus our attention on the problem of energy and angular momentum transport between them. The accretion onto the black hole occurs along the field lines which originates from a thin disk and threads the horizon; such a situation is depicted in Figure 1. The transport from the plasma to the field during the accretion can be expressed as $U_{tH} - U_{tI}$ and $-U_{\phi H} - (-U_{\phi I})$. Since the fluid is assumed to be in a general relativistic Keplerian motion at $r = r_I$, the initial values U_{tI} and $-U_{\phi I}$ can be calculated from geometry at $(r = r_I, \theta = \theta_I)$ as $U_{tI} = (g_{tt}^I + g_{t\phi}^I \Omega_F) m_p / e$ and $-U_{\phi I} = -(g_{t\phi}^I + g_{\phi\phi}^I \Omega_F) m_p / e$, where $e \equiv E - \Omega_F L \approx m_p$. Let us next consider the final values U_{tH} and $-U_{\phi H}$. If the plasma dominates the field ($E/m_p = U_t \approx 0.9$), then no transport occurs, i.e., $U_{tH} = U_{tI}$ and $-U_{\phi H} = -U_{\phi I}$ hold. On the contrary, if the field dominates the plasma ($E/m_p \gg 1$), the transport process will occur most effectively. In the intermediate case, the transport is expected to be written in terms of magnetized parameter (Hirotani et al. 1992), if its upper limit is known in the magnetically dominated limit. We will therefore consider the magnetically dominated limit in this paper to estimate the maximum value of the transport.

Analyzing the critical condition, we can calculate fluid's energy (U_t) and angular momentum ($-U_\phi$) at $r = r_F$. In particular, in the magnetically dominated limit, the fast-magnetosonic point is located close to the horizon ($[r_F - r_H]/r_H \approx m_p/E \ll 1$). Therefore, we can compute $U_t^H \approx U_t^F$ and $-U_\phi^H \approx -U_\phi^F$ by analyzing the critical condition; the result is

$$U_{tH}(r_I, \theta_I) = \frac{1}{\omega_H - \Omega_F} \left(\omega_H \sqrt{K_I} - \frac{1 - a\omega_H \sin^2 \theta_H}{1 - a\Omega_F \sin^2 \theta_H} \frac{1}{W} \Omega_F \sqrt{K_I - K_H} \right), \quad (2)$$

$$-U_{\phi H}(r_I, \theta_I) = \frac{1}{\omega_H - \Omega_F} \left(\sqrt{K_I} - \frac{1 - a\omega_H \sin^2 \theta_H}{1 - a\Omega_F \sin^2 \theta_H} \frac{1}{W} \sqrt{K_I - K_H} \right), \quad (3)$$

where W and $K \equiv g_{\phi\phi} \Omega_F^2 + 2g_{t\phi} \Omega_F + g_{tt}$ are of order unity. Note that both U_{tH} and $-U_{\phi H}$ do not depend on m_p/E , which contains the strength of the magnetic field. These quantities depend on the position of the injection point ($r = r_I, \theta = \theta_I$) through the function K_I .

If we consider the accretion from a thin disk, we can choose $\theta_I = \pi/2$. Then both U_{tI} and U_{tH} (and also both $-U_{\phi I}$ and $-U_{\phi H}$) can be described in terms of r_I only. In

Figure 2 we present a comparison between U_{tH} and U_{tI} for the case $a = 0.5M$. Since the result does not depend on Ω_F very much, we present here the case $\Omega_F = 0.5\omega_H$ only. The plasma begins to fall from the injection point with $U_{tI} < 1$ (denoted by the dashed curve) because of the contribution of binding energy. In the same manner as in Figure 2, we present $-U_{\phi H}(r_I)$ and $-U_{\phi I}(r_I)$ in Figure 3. The angular momentum transport depends on Ω_F significantly, so we present three typical cases, $\Omega_F = 0.8\omega_H, 0.5\omega_H, 0.2\omega_H$.

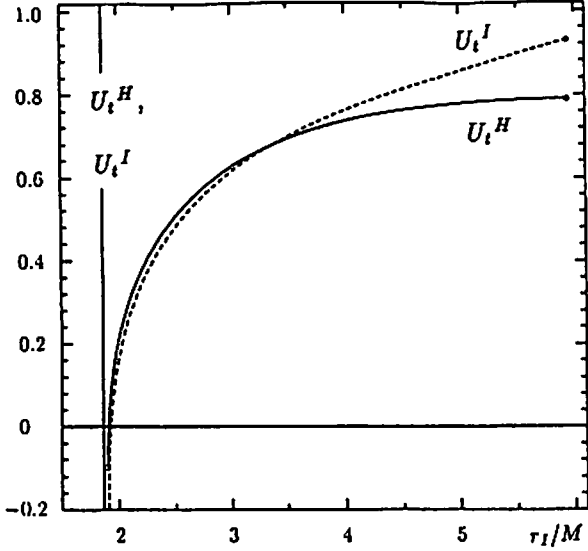


Fig. 2. Curves for U_{tH} (solid) and U_{tI} (dashed) as a function of the position of r_I for $\theta_H = \theta_I = \pi/2$, $\Omega_F/\omega_H = 0.5$ and $a/M = 0.5$.

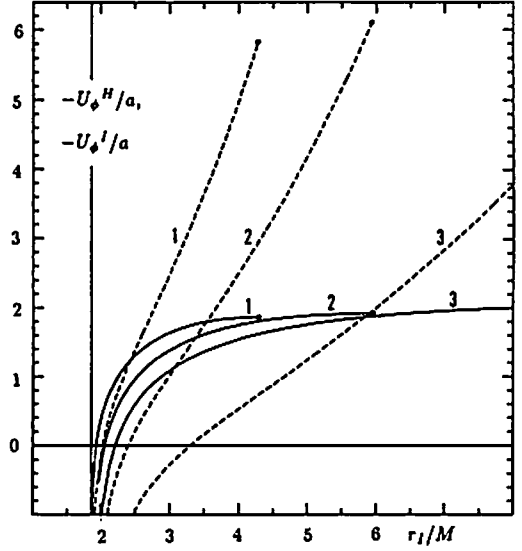


Fig. 3. Curves for $U_{\phi H}$ (solid) and $U_{\phi I}$ (dashed) as a function of the position of r_I for $\theta_H = \theta_I = \pi/2$, $\Omega_F/\omega_H = 0.8, 0.5, 0.2$ and $a/M = 0.5$.

It is demonstrated in Figure 2 and 3 that the MHD interactions occur very effectively in a magnetically dominated magnetosphere. Provided that the accretion starts from a relatively outer region (with a large value of r_I), typically 10% of the fluid's energy and substantial part of its angular momentum are transported to the magnetic field. In the next section, we describe variabilities of fluid's motion owing to such an active MHD interaction.

3. Highly Variable Accretion

As we have seen, in a stationary and axisymmetric magnetically dominated black hole magnetosphere, interactions between the plasma and the magnetic field are very

effective. The next question now arises: will the plasma accretion become highly variable if the magnetic field is slightly perturbed? It is worth while examining the subject more closely, because highly variable accretion is favourable with X-ray observations. We thus study non-stationary and non-axisymmetric perturbations and investigate relative amplitude among fluid quantities (velocity, energy and angular momentum) and electromagnetic field.

Since we wish to examine the relative amplitude at each point along a flow line, we shall henceforth adopt the short wave-length limit in which the characteristic scale of radial and meridional variations are taken to be much shorter than any characteristic radial and meridional scale in the unperturbed state, respectively. In the frame of this approximation, neither the acceleration due to gravity nor the curvature of the unperturbed magnetic field will be taken into account, because all covariant derivatives can be replaced by normal derivatives and all the derivatives of unperturbed magnetic field will not contribute. In this limit, every perturbed quantity is proportional to $\exp(ik_\mu x^\mu) = \exp[i(-\omega t + m\phi + k_r r + k_\theta \theta)]$.

In the frame of this short wave-length limit, we obtain two MHD wave modes, the Alfvén mode and the fast-magnetosonic mode. For reasons that we shall go into later, the fluid becomes highly variable for the outgoing fast-magnetosonic mode. We shall therefore concentrate on this mode afterwards.

Before describing relative amplitude, let us briefly describe the dispersion relation for the outgoing fast-magnetosonic mode, which is essential for the description of relative amplitude. Near the horizon, the dispersion relation becomes

$$\omega - m\omega_H = \frac{\Delta - \Delta_F}{\Delta_F + \Delta} \frac{\Delta}{2Mr_H} k_r = \frac{\Delta - \Delta_F}{\Delta_F + \Delta} k_{r_*} \quad (4)$$

in the magnetically dominated limit. It is convenient to introduce the tortoise coordinate r_* satisfying $dr_*/dr = (r^2 + a^2)/\Delta$. In this coordinate, we can easily express that the characteristic scale of radial variations are much shorter than that of the gravitational field ($|Mk_{r_*}| \gg 1$), because the interval (r_H, ∞) in the r -coordinate is stretched to $(-\infty, \infty)$ in r_* .

At very close to the horizon ($\Delta \ll \Delta_F$), it follows from (4) that the outgoing fast-magnetosonic wave propagates nearly with the velocity of light as $\omega - m\omega_H = -k_{r_*}$, or equivalently as $k_\mu k^\mu = 0$. We can also see that the outgoing fast-magnetosonic wave propagates outwards (inwards) in the sub(super)-fast-magnetosonic region $r_F < r < r_I$ ($r_H < r < r_F$). At the fast-magnetosonic point ($\Delta = \Delta_F$), it stagnates as expected.

Let us now examine the relative amplitude. Inserting the dispersion relation (4) in the expression of relative amplitude, we obtain

$$\frac{\tilde{u}^r}{U^r} = A \frac{x}{(1+x)^2} \frac{-E}{m_p} \frac{\tilde{b}^\theta}{B^r} \quad (5)$$

near the horizon $\Delta \ll M^2$ (, or equivalently $x \ll |E/m_p|$), where

$$A \equiv \frac{4(2Mr_H)^2}{\Sigma_H^2} \frac{\omega_H - \Omega_F}{\Omega_F} \frac{(1 - a\Omega_F \sin^2 \theta)W}{\sqrt{K_I - K_H}} \frac{(k_{r*})^2}{[m(\omega_H - \Omega_F) - k_{r*}]k_\theta} \approx 1,$$

$$x \equiv \frac{\Delta}{\Delta_F} = \frac{r - r_H}{r_F - r_H};$$

\tilde{u}^r and \tilde{b}^θ are perturbed fluid radial velocity U^r and the meridional component B^θ of the magnetic field in the orthonormal frame, respectively. Note that the factor $x/(1+x)^2 \cdot (E/m_p)$ crucially determines the relative amplitude and that $|E/m_p| \gg 1$ holds for the magnetically dominated limit. The function $f(x) \equiv x/(1+x)^2$ becomes maximum at $x = 1$. Therefore the fluid will become most variable at the fast-magnetosonic point in the frame of the short wave-length limit. In the somewhat extended region $|m_p/E| \ll x \ll |E/m_p|$, we have $|\tilde{u}^r/U^r| \gg |b^\theta/B^r|$. In addition, fluid energy and angular momentum have same order amplitude as \tilde{u}^r at an arbitrary point along the flow line. Furthermore, \tilde{b}^θ has the maximum amplitude among all components of the electromagnetic field. Therefore, in the somewhat extended region $|m_p/E| \ll x \ll |E/m_p|$ near $r = r_F$, fluid velocity, energy and angular momentum become highly variable if the electromagnetic field is slightly perturbed. For another (Alfvén, and ingoing fast-magnetosonic) wave modes, all perturbed quantities have same order amplitude, and such amplification never occurs.

In summary, The analysis of the critical condition at the fast magnetosonic point is very important, because it determines the fluid's energy and angular momentum accreted onto the black hole. Their initial values ϵ_I and l_I at the injection point crucially depend on the position $r = r_I$ and the angular velocity $\Omega_F(r_I)$. The MHD transport of ϵ and l between the fluid and the magnetic field occurs efficiently along the field lines connecting the disk with the horizon. Considering nonstationary perturbations, we can further determine the relative amplitude of perturbed quantities and find that the fluid becomes highly variable in the somewhat extended region near $r = r_F$, even if the fluctuations in the magnetic field is very small. This is due to the effects of a critical point and strong gravity near the horizon. However, the fluid quantities are not perturbed at all just at the horizon because of the regularity condition.

4. Summary and Discussion

Let us first discuss the energy and angular momentum transport between the plasma and the magnetic field in the magnetically dominated limit. Since $U_{tI} - U_{tH}$ and $-U_{\phi I} - (-U_{\phi H})$ are described only by (r_I, θ) , the transport do not depend on the global field line shape. It is surprising, because U_t and $-U_\phi$ are not conserved along a flow line. From this fact we may say that the event horizon regulates the accretion with the help of the magnetic field and makes the fluid energy and angular momentum certain values there. This is a new conjecture on the property of the horizon.

Next discuss how the critical point and the horizon play an important role on the fluid variability in the somewhat extended region near $r = r_F$. Equation (5) can be rewritten as

$$\frac{\tilde{u}^r}{U^r} = C \frac{(\omega - m\omega_H + k_{r*})^2}{\Delta} \frac{\tilde{b}^\theta}{B^r}, \quad (6)$$

where C is of order unity. The denominator Δ^{-1} describes the effect of redshift and the numerator $\omega - m\omega_H + k_{r*}$ crucially depends on the propagation speed of the outgoing fast-magnetosonic wave. In the close vicinity of the horizon $x \ll |m_p/E|$, we have $\omega - m\omega_H + k_{r*} = O(\Delta)$ and hence $\tilde{u}^r/U^r \approx \Delta \cdot \tilde{b}^\theta/B^r$. Since fluid disturbance cannot propagate with light velocity owing to its inertia, electromagnetic disturbance decouples with fluid disturbance. As a consequence, only the electromagnetic field is perturbed. That is, the boundary condition at the horizon makes the fluid be unperturbed. Near the fast-magnetosonic point $x \approx 1$ on the contrary, we have $\omega - m\omega_H + k_{r*} \approx 1$ and hence $\tilde{u}^r/U^r \approx E/m_p \cdot \tilde{b}^\theta/B^r$ because of the redshift factor $\Delta_F^{-1} \approx |E/m_p|$. Far from the horizon, the amplification factor damps, because the redshift factor behaves as $(1/x)(E/m_p)$ in this region.

Such amplification never occurs for the outflows even in the magnetically dominated limit. Therefore, the existence of the horizon is essential for the amplification of the fluid. In addition, if the magnetically dominated limit breaks down, fluid will never be amplified at an arbitrary point. That is, the amplification occurs only when the fast-magnetosonic point is located close to the horizon. Therefore, we can safely say that the fluid inertia, the magnetic field, and the horizon are essential for the amplification of the fluid. The amplification will never occurs in the Newtonian theory.

Let us next discuss briefly the possibility of emission around the hole. Since we did not take the effect of any dissipative processes into account, the results derived in

this paper are not directly applicable for the interpretation of X-ray emission observed from AGNs. To connect the results with observation, we must further consider the mechanisms which convert fluid's kinetic energy into radiation. It is therefore important to consider whether dissipative processes work effectively or not (see Nobili et al. 1991 for self-consistent treatment of radiative transfer and spherical plasma accretion; Hanawa 1990, Hirotani et al. 1990 for Comptonization due to bulk motion of accreting electrons). It needs future consideration.

The authors would like to thank Prof. Kato and Dr. Hanawa for helpful suggestions, and to acknowledge discussion with Mr. S. Nitta on several points in this article. This work is partially supported by the Grant-in-Aid for Scientific Research from the Ministry of Education, Science and Culture (04640268).

References

- Bardeen, J. M. 1970, *Nature*, **226**, 64.
 Blandford, R. D., & Znajek, R. L. 1977, *Monthly Notices Roy. Astron. Soc.*, **179**, 433.
 Camenzind, M. 1986a, *Astron. Astrophys.*, **156**, 137.
 Camenzind, M. 1986b, *Astron. Astrophys.*, **162**, 32.
 Elliott, J. L., and Shapiro, S. L. 1974, *Astrophys. J.*, **192**, L3.
 Hanawa, T. 1990, *Astrophys. J.*, **355**, 585.
 Hirotani, K., Hanawa, T., & Kawai, N. 1990, *Astrophys. J.*, **355**, 577.
 Hirotani, K., Takahashi, M., Nitta, S., & Tomimatsu, A. 1992, *Astrophys. J.*, **386**, 455.
 Hirotani, K., Takahashi, and Tomimatsu, A. 1992b, *submitted to Publ. Astron. Soc. of Japan*
 Nobili, L., Turolla, R., & Zampieri, L. 1991, *Astrophys. J.*, **383**, 250.
 Park, S. J., & Vishniac, E. T. 1988, *Astrophys. J.*, **332**, 135.
 Park, S. J., & Vishniac, E. T. 1990, *Astrophys. J.*, **353**, 103.
 Phinney, E. S. 1983, *Ph. D. thesis, University of Cambridge* .
 Rees, M. J. 1984, *Ann. Rev. Astron. Astrophys.*, **22**, 471.
 Thorne, K. D. 1974, *Astrophys. J.*, **191**, 507.

ACCRETION OF A HOT PLASMA ONTO THE CENTRAL BLACK HOLE: FOKKER-PLANCK FORMULATION

F.Yabuki and F.Takahara

Department of Physics, Tokyo Metropolitan University,
Minamiohsawa 1-1, Hachioji, Tokyo 192-03, Japan

ABSTRACT

We report on a preliminary study the accretion process of a hot plasma onto a central black hole. We consider the steady-state distribution and consumption rate of particles orbiting a Schwarzschild hole assuming the spherical symmetry. We take account of only ion-ion Coulomb scattering and neglect effects of electrons except that they assure the charge neutrality. We assume that diffusion approximation can be adopted. Under these assumptions, we formulate relativistic Fokker-Planck equation in a general form and derive the Fokker-Planck coefficients which are related to the velocity diffusion coefficients measured by observer in local Lorentz frame.

Keywords: black hole, relativistic kinetic equation, accretion, hot plasma

1 INTRODUCTION

Accretion onto a central hole is believed to be a reasonable model of active galactic nuclei and black hole candidates to explain the powerful radiative flux emerging from a very small volume. If a particle falls into the hole from the innermost stable circular orbit, the released energy is estimated as 0.0572 and $0.4235mc^2$ for Schwarzschild and extreme Kerr black hole, respectively (m :rest mass of a particle, c :light velocity)(Ref.1). This estimation is appropriate only for a cold disk. However, it is quite probable that the accreting matter becomes hot and that the particle orbit is non-circular in the vicinity of

the central hole. The particles interact each other, change their momentum and energy by binary Coulomb scattering and their orbits are also changed. Such processes may play an important role in the formation of jets or extraction of rotation energy of the black hole. The distribution function of infalling particles into the hole and the released energy are an open problem at present. In this paper, for the first step, we formulate Fokker-Planck equation which treat accretion of a hot plasma onto the central hole taking account for interaction between particles. One of the objectives is to determine the steady-state distribution and consumption rate of particles orbiting a hole. We adopt the relativistic kinetic theory derived by Kandrup(Refs.2-4). Section 2 presents basic assumptions and focuses upon the derivation of relativistic Fokker-Planck equations appropriate for weak and short range interaction between particles. Section 3 discusses the direction of future research. In this paper we employ geometrized units($G = c = 1$) and $M = 1$ (M : mass of a black hole).

2 MODEL

2.1 Assumptions

We make the following assumptions for accreting particles to which we apply the kinetic theory. The assumptions are as follows:

- (1) The distribution of particles is spherically symmetric.
- (2) The background geometry is described by the Schwarzschild metric, and selfgravitation is neglected.
- (3) The interaction between particles is described by ion-ion binary Coulomb scattering and effects of electrons are neglected except that they assure the charge neutrality of plasma.
- (4) Diffusion approximation can be adopted.

Under these assumptions, we derive a relativistic Fokker-Planck equation for accreting particles.

2.2 Relativistic Fokker-Planck equation for accreting particles

When we ignore the effects of electrons on interactions between particles, the evolution of the system is described by a kinetic equation for ions. Many authors have exten-

sively studied about relativistic kinetic theory (Refs.2-7). Here, we adopt the formalism of general relativistic kinetic theory derived by Kandrup(Refs.2-4). Kandrup formulated a relativistic Fokker-Planck equation in a general form, which is appropriate for a collection of N identical particles, evolving in some fixed background spacetime. The most important assumption in his formalism is that the system is evolved via experiencing elastic binary collisions and these collisions may be modeled as instantaneous pointlike events, characterized by a transition probability. In other words, he supposed that these interactions are sufficiently short range, or very weak. In this case, we may use analysis of a one-particle distribution function as a reasonable first approximation to the exact solution, which is frequently adopted for an analysis of collisionless systems.

Following Kandrup, we define a distribution function as a number density in the phase space, characterized by the cotangent bundle over the spacetime manifold. The eight-dimensional phase space volume element takes the form

$$d^8V = d^4V_p d^4V_x = (-g)^{1/2} d^4p (-g)^{1/2} d^4x = p^\alpha d\sigma_\alpha d\omega dm d\tau \equiv d^7V d\tau. \quad (1)$$

Here $d^\alpha V$ stands for α -dimensional volume element. $p^\alpha, d\sigma_\alpha, \tau$ and m denote a four-momentum, an element of spacelike hypersurface, the proper time and the particle's mass. Because of the mass shell constraint $m^2 = -p_\alpha p^\alpha$, only three of the four momentum components are independent and $d\omega$ is a three-dimensional momentum space element on the mass shell.

The distribution function $\tilde{f}(x^\alpha, p_\alpha)$ is defined as

$$DN(x^\alpha, p_\alpha) = \tilde{f}(x^\alpha, p_\alpha) d^7V = f(x^\alpha, p_\alpha) \delta[m - \sqrt{-p_\alpha p^\alpha}] dm d^3x d^3p. \quad (2)$$

Here $DN(x^\alpha, p_\alpha)$ denotes the number of particles with mass m passing through the element $d\sigma_\alpha$ with momentum p^α in the element $d\omega$ at proper time τ . Under the mass shell constraint, \tilde{f} is rewritten by f , a function of seven independent variables. Introducing the transition probability, the relativistic Chapman-Kolmogorov equation is given by

$$\begin{aligned} & DN(x^\alpha + p^\alpha \Delta\tau/m, p_\alpha + K_\alpha \Delta\tau) \\ &= \int (-g)^{-1/2} d^4\delta p DN(x^\alpha, p_\alpha - \delta p_\alpha) \chi(x^\alpha, p_\alpha - \delta p_\alpha; \delta p_\alpha, \Delta\tau), \end{aligned} \quad (3)$$

where $K_\alpha \equiv \frac{1}{m} \Gamma_{\alpha\mu}^\lambda p_\lambda^\mu$. Here, δp_α stands for the random increment in p_α induced by the inter particle forces and χ is the probability that a particle located at the phase space point (x^α, p_α) experiences a random increment δp_α in the time interval $\Delta\tau$. We expand the left hand side of Eq.(3) about $DN(x^\alpha, p_\alpha)$ to first order in $\Delta\tau$ and the right hand side, to second order in δp_α . Using the normalization of probability χ

$$\int (-g)^{-1/2} d^4 p \chi(x^\alpha, p_\alpha; \delta p_\alpha, \Delta\tau) = 1, \quad (4)$$

we derive the relativistic Fokker-Planck equation which takes the form

$$\begin{aligned} & \frac{Df(x^\alpha, p_\alpha)}{d\tau} \\ &= -\frac{\partial}{\partial p_\alpha} [f(x^\alpha, p_\alpha) \langle \delta p_\alpha \rangle_\tau] + \frac{1}{2} \frac{\partial^2}{\partial p_\alpha \partial p_\beta} [f(x^\alpha, p_\alpha) \langle \delta p_\alpha \delta p_\beta \rangle_\tau] \end{aligned} \quad (5)$$

where

$$\begin{aligned} \langle \delta p_\alpha \rangle_\tau &\equiv \int (-g)^{-1/2} d^4 p \frac{\chi(x^\alpha, p_\alpha; \delta p_\alpha, \Delta\tau)}{\Delta\tau} \delta p_\alpha \\ \langle \delta p_\alpha \delta p_\beta \rangle_\tau &\equiv \int (-g)^{-1/2} d^4 p \frac{\chi(x^\alpha, p_\alpha; \delta p_\alpha, \Delta\tau)}{\Delta\tau} \delta p_\alpha \delta p_\beta. \end{aligned}$$

On the analogy of stellar dynamics (Ref.8), we regard that f is a function of two isolated integrals E and L , here E and L are energy and angular momentum per unit mass, respectively. Following Kandrup (Ref.9), we take orbital averages of Eq.(5),

$$\begin{aligned} \oint \frac{d\tau}{u} \frac{Df}{d\tau} &= -\frac{\partial}{\partial E} [f \langle \delta_p E \rangle] - \frac{\partial}{\partial L} [f \langle \delta_p L \rangle] \\ &+ \frac{1}{2} \left\{ \frac{\partial^2}{\partial E^2} [f \langle (\delta_p E)^2 \rangle] + \frac{\partial^2}{\partial L^2} [f \langle (\delta_p L)^2 \rangle] + 2 \frac{\partial^2}{\partial E \partial L} [f \langle \delta_p E \delta_p L \rangle] \right\} \end{aligned} \quad (6)$$

where

$$\langle \delta_p E \rangle = \oint d\tau \langle \delta E \rangle_\tau, \quad \langle \delta_p L \rangle = \oint d\tau \langle \delta L \rangle_\tau.$$

Here, $\delta_p E$ and $\delta_p L$ are defined as the changes of E and L during one orbital period. The quantities $\langle \delta E \rangle_\tau$ and $\langle \delta L \rangle_\tau$ represent the mean value of δE and δL per unit time. $\langle \delta_p E \rangle$ and $\langle \delta_p L \rangle$ stand for the mean values of $\delta_p E$ and $\delta_p L$ averaged over many orbits, with a similar definition for $\langle (\delta_p E)^2 \rangle$, $\langle (\delta_p L)^2 \rangle$ and $\langle \delta_p E \delta_p L \rangle$.

We rewrite these Fokker-Planck coefficients in terms of quantities measured by an observer in the local Lorentz frame.

E and L are rewritten as

$$E = \gamma \sqrt{-g_{tt}} \quad (7)$$

$$L = r u_T = \sqrt{-g_{tt}} E v_T \quad (8)$$

$$(15) \quad \langle z(\tau u \nabla) \rangle \left(\frac{z^2}{z^2 T} - \frac{z}{z} \right) \frac{z}{1} + \langle z(\tau u \nabla) \rangle \frac{z}{z^2 T} = \langle z(TN) \rangle$$

$$(14) \quad \langle z(\tau u \nabla) \rangle \frac{z^2 T}{z^2} + \langle z(\tau u \nabla) \rangle \frac{z}{z^2 T} = \langle z(TN) \rangle$$

$$T_N = \tau u$$

where

$$(13) \quad \langle \delta E \delta L \rangle = \sqrt{-g} [T_N \langle \delta E \rangle + E \langle \delta E \delta L \rangle]$$

$$(12) \quad \langle \delta L \rangle = -\sqrt{-g} [T_N \langle \delta E \rangle + E \langle \delta E \delta L \rangle]$$

$$(11) \quad \langle \delta L \rangle = \sqrt{-g} [T_N \langle \delta E \rangle + E \langle \delta L \rangle]$$

$$(10) \quad \langle \delta E \rangle = -\sqrt{-g} [T_N \langle \delta E \rangle + E \langle \delta E \delta L \rangle]$$

$$(9) \quad \langle \delta E \rangle = \sqrt{-g} [T_N \langle \delta E \rangle + E \langle \delta E \delta L \rangle] + \frac{z}{1} \langle \delta E \rangle + \frac{z}{1} \langle \delta E \delta L \rangle$$

Here $v^{(i)}$ are the components of the three-velocity measured in the local Lorentz frame. Using Eqs. (7) and (8), the Fokker-Planck coefficients are described as

$$\begin{aligned} u^{(\phi)} &= \left(-\frac{g_{\phi\phi}}{g_{\phi\phi}} \right) \frac{n}{z^{1/2}} \\ u^{(\theta)} &= \left(-\frac{g_{\theta\theta}}{g_{\theta\theta}} \right) \frac{n}{z^{1/2}} \\ u^{(r)} &= \left(-\frac{g_{rr}}{g_{rr}} \right) \frac{n}{z^{1/2}} \\ u_z &= u_z^{(r)} + u_z^{(\theta)} + u_z^{(\phi)} \\ \gamma &= 1 - u_z^{(r)} - u_z^{(\theta)} - u_z^{(\phi)} \\ \tau &= u_z^{(r)} + u_z^{(\theta)} + u_z^{(\phi)} \\ n &= u_z^{(r)} + u_z^{(\theta)} + u_z^{(\phi)} \end{aligned}$$

where

Here $\langle \Delta v_{\parallel} \rangle$, $\langle (\Delta v_{\parallel})^2 \rangle$ and $\langle (\Delta v_{\perp})^2 \rangle$ are the velocity diffusion coefficients. The symbols \parallel and \perp stand for the directions parallel and perpendicular to \vec{v} , respectively. We assume that related velocity diffusion coefficients are given by the Newtonian value. The velocity diffusion coefficients are calculated by giving the distribution of field particles and the Fokker-Planck coefficients are then determined (Ref.8). To be self-consistent, the distribution of field particles should be also described by $f(E, L)$. We solve Eq.(6) for the steady-state distribution function $f(E, L)$ ($\frac{Df}{dt} = 0$) by the following procedure. We give a certain initial distribution function of field particles, from which we compute the velocity diffusion coefficients and the Fokker-Planck coefficients. For these coefficients, we solve $f(E, L)$ which is then used as a new field-particle distribution to compute a new Fokker-Planck coefficients. This procedure is iterated until a converging solution is obtained. The numerical code is now being developed.

2.3 Boundary Conditions

As mentioned in section 1, the objective of our work is to investigate the steady state distribution of a hot plasma around a hole. To solve the Fokker-Planck equation derived in subsection 2.2, we set four boundary conditions in E-L-space as shown in Fig.1. Though each particle travels in various orbits determined by E and L , we pay attention to particles in bound orbits around a hole. For Schwarzschild geometry, bound particles have energy in the region, $\sqrt{8/9} \leq E < 1$, and angular momentum, $J_{\min}(E) < L < J_{\max}(E)$ for each E . $J_{\min}(E)$ corresponds to a particle which travels in the marginally impinging orbit and particles with $L \leq J_{\min}(E)$ fall into the hole. $J_{\max}(E)$ corresponds to a particle which has Keplerian circular orbit and no particles with $L > J_{\max}(E)$ exist. $J_{\min}(E)$ and $J_{\max}(E)$ are given as follows, respectively.

$$E = \sqrt{\left(1 - \frac{2}{r}\right) \left(1 + \frac{L^2}{r^2}\right)} \quad (16)$$

where

$$r = \frac{L^2}{2} \left(1 \pm \sqrt{1 - \frac{12}{L^2}}\right) \text{ for } \begin{matrix} J_{\max}(E) \\ J_{\min}(E) \end{matrix}$$

Under the above constraint, bound particle is subject to the following boundary conditions:

- (1) The distribution function $f(E, L) = 0$ at $L = J_{\min}(E)$.

(2) The distribution function $f(E, L) = 0$ at $E = 1$.

(3) Flux of particles in the direction perpendicular to $J_{\max}(E)$ equal to zero, that is, $\vec{n} \cdot \vec{\nabla} f(E, L) = 0$. Here \vec{n} is normal vector to $J_{\max}(E)$.

In addition to the above boundary conditions, we should give an appropriate condition on incident particles at $L = L_{\max}$.

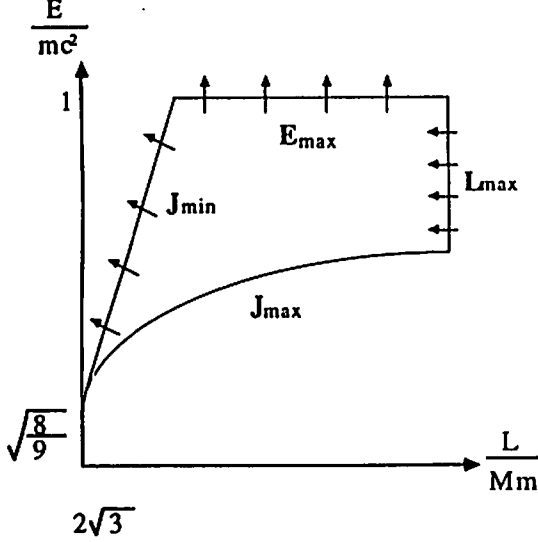


Fig.1 The boundary conditions in E-L-space

3 CONCLUDING REMARKS

In this paper, we have formulated the Fokker-Planck equation for a hot plasma around a massive black hole with the boundary conditions to solve it numerically. We formulated the Fokker-Planck coefficients for the particles under assumption of spherical symmetry. Numerical calculations is now under way. In future, we will study more realistic problems. For example, in order to treat an accretion disk, it is necessary to improve these coefficients for the case of axisymmetric systems. Although we ignored effect of electrons on interaction between particles, this must be taken into account to know behavior of a

plasma in realistic situations. When a hole rapidly rotates, particle orbits can be located still more close to a hole. It is one of interesting problems how rotation of a hole affects on a surrounding hot plasma.

REFERENCES

1. C.W.Misner, K.S.Thorne and J.A.Wheeler 1972, *Gravitation*, p885.
2. W.Israel and H.E.Kandrup 1984, *Ann.Phys.*, **152**, 30.
3. H.E.Kandrup 1984, *Ann.Phys.*, **153**, 44.
4. H.E.Kandrup 1986, *Ann.Phys.*, **169**, 352.
5. J.L.Synge 1957, *The Relativistic Gas*, (North-Holland, Amsterdam)
6. R.W.Lindquist 1966, *Ann.Phys.* **37**, 487.
7. W.Isarel 1972. in *General Relativity: Papers in Honour of J.L.Synge*, edited by L.O'Raifeartaigh (Oxford University Press, Oxford, England) p.201.
8. A.P.Lightman and S.L.Shapiro 1977, *Ap.J.* **211**, 244.
9. H.E.Kandrup 1985, *Astrophys.Space.Sci.* **109**, 215.

Particle Acceleration around Neutron Stars with Comets, Planets and Black Hole

Hitoshi HANAMI

Physics Section, College of Humanities and Social Sciences,
Iwate University, Morioka 020, Japan

abstract : We studied a magnetosphere interaction model with orbiting objects for γ -ray bursts with the picture of a current circuit which consists of the magnetosphere and the surface of a neutron star. The motion of objects, which is a good conductor and rotating in the magnetosphere, works as the battery in the circuit system. The physical condition on the surface of the neutron star is important to make a closed current circuit inducing good conversion from the kinetic energy of a rotating objects to that of the magnetosphere oscillation. An old and cooled neutron star with the temperature $\simeq 10\text{eV}$ can prepare the condition for closing the current circuit in the surface of the neutron star. The magnetosphere system is unstable to feedback instability related to the variability of the γ -ray bursts.

Introduction

Gamma-ray bursts have been still a unsolved problem in astrophysics for fifteen years since their discovery of Klebesadel et al. (1973). Recent observations show the sources have strong magnetic field $\sim 10^{12}\text{G}$ which is consistent with the model of cyclotron absorption for the observed spectrum feature (e.g. Murakami et al. 1988). Neutron star is only one object whose magnetic field is strong enough to explain these strong field evidence in our known objects in the universe. It suggests that gamma-ray bursts occur around the neutron star with strong magnetic field. It was investigated that the magnetospheric plasma oscillations accelerate energetic electrons which can produce γ -ray (Melia 1990). Some possibilities for excitation mechanism of the transient magnetospheric perturbations have been proposed to account a starquake (Blaes et al. 1990), neutron star rotation or a episodic accreting object (Harwit and Salpeter 1973). However, the total picture for these magnetospheric oscillations and gamma-ray bursts still stands as an open question in front of astrophysical theorists.

Recently some discoveries of planets around pulsars were reported. Wolszczan and Frail (1992) observed the evidence for the existence of planets around the millisecond pulsar PSR1257-12. These planets are about several times the mass of the Earth.

This discovery encourages us to consider that neutron stars can have planets around itself generally (e.g. Nakamura and Piran 1991). This picture naturally arrows us to an interesting speculation, in which planets and also comets, rotating in the magnetosphere of the neutron stars, drive gamma-ray bursts. We find similar situation to Jovian decametric radiation related to the interaction between strong magnetic field of Jupiter and one of its

satellite Io. One popular interpretation is that electrons or ions are somehow accelerated in this system with plasma instabilities (Goldreich and Lynden-Bell 1969). This view point for the Jovian decametric radiation may be expanded to the picture of the electrodynamics of neutron star with the objects orbiting in it.

This paper deals with the electromagnetic coupling using current circuit analogy between the magnetosphere and the objects rotating around a neutron star and the possibility of strong particle acceleration for gamma-ray bursts.

Current Circuit with Magnetosphere

The starting point is that owing to the motion of a object with relative velocity v_p through the corotating magnetosphere, an induced electric field $E_{ind} = \frac{v_p}{c} \times B$ appears in the frame of the object. If the object is a good conductor, the electric field will be screened by induced surface charges, so that the magnetic field in the column through the object is zero. In the neutron star frame, there is an electric field due to these charges which is uniform inside the column and given by $E_p = -E_{ind}$. We can understand the rotating motion of the object produces the electric potential gap in the circuit which is connected by the magnetic field column between the objects and the surface of the neutron star. It is shown schematically in Figure 1. We will assume that the axes of the magnetic moment of the neutron star is perpendicular to the plane of the object orbit.

The circuit is closed by currents in the surface of the neutron star which should have Pedersen conductance sufficient to carry current across the magnetic field. The closed circuit with Pedersen current may work for a particle acceleration.

For the collisionless plasma, then, we can easily see that the current cannot flow along the electric field even if we have strong perpendicular electric field to the magnetic field. Since the plasma in magnetosphere is collisionless, there exists no Pedersen current in the magnetosphere. On the other hand, for the collisional plasma, we should point out that the current can flow along the electric field even if it is perpendicular to the magnetic field. Especially, the Pedersen current takes the maximum when the collision frequency $\nu_{ei} = 3 \times 10^{19}(n_e/3 \times 10^{26}cm^{-3})\ln\Lambda(T/10eV)^{-3/2}$ has the same order of the gyrotron frequency $\omega_c = 1.8 \times 10^{19}(B/10^{12}G)$ for electrons. These results show us that Pedersen current can flow most efficiently in the surface layer ($n_e \simeq 3 \times 10^{26}cm^{-3}$) of neutron star cooled with its temperature $T = 10eV$.

From the consideration of the mobility, we consider two zone model which consists of the magnetosphere and the surface layer, which are approximated to ideal MHD current and Pedersen current system, respectively.

It shows that the coupling process between the magnetosphere and the surface generally induces the spontaneous excitation of Alfvén wave with a AC current in the magnetosphere.

High Energy Particle Acceleration with Alfvén wave

The coherency of the excited wave takes an advantage for the particle acceleration. Moreover, the accelerated particle can be converted to the high energy photon like observed γ -ray. Then, using the numerical simulation code (Hoshino et al. 1992), we are try-

mirrors reflect the beams back to recombine at the beam splitter forming an interference pattern.

In the proper reference frame of an observer, where the speed of light is nearly constant, the force of gravitational waves on a mass is proportional to the mass's coordinate position. Therefore we can consider that end masses are shaken back and forth by gravitational waves, whereas the beam splitter is at rest. The relative change in the position of the end mirrors is then measured by the light whose speed is constant, resulting in a change in the interference pattern. This description of gravitational wave forces is accurate only if the region of interest is spatially small enough compared to a wavelength of the gravitational wave.

When the arm length is larger, TT coordinate system should be used, where the spacetime metric can be regarded as the Minkowski metric with a small perturbation due to gravitational waves. In the TT coordinate system, gravitational waves don't impart any force on masses which are falling freely, while they modify the speed of light. Consequently the optical path difference, measured by such modulated light, is altered and the interference pattern is changed.

Laser interferometers are ideally suited for detecting gravitational waves, because changes of opposite sign will be induced in the arms for a suitable gravitational wave. And the difference in phase between the reflected beams can be increased by scaling up the arm length. However, above an optimum total optical path length, which is equal to half of the wavelength of the gravitational wave, the gravitational wave changes its sign and the difference in phase between two beams caused by the gravitational wave is partially or totally canceled.

The optimum arm length for a 1kHz gravitational wave is 75km. Since it is rather money-consuming to build a 75km vacuum tank, two methods for achieving long storage time with a short arm length have been tested: delay line type and Fabry-Perot type.

In the delay line type interferometer, a beam is folded many times in the arms using additional mirrors; the gravitational-wave signal can be multiplied by the number of reflections of the light. The other method employs resonant Fabry-Perot cavities in each arm.

On the other hand, Rainer Weiss and several other researchers had come to seize on the idea of using light beams to detect gravitational waves ³⁾. The first detector that used laser interferometers was build by Robert Forward ⁴⁾. Since then, several groups over the world have developed laser interferometer detectors ^{5) 6) 7)}, and most experimentalists have come to believe that interferometers should ultimately be more sensitive to gravitational waves than bar detectors.

At present a several projects for constructing km-class laser interferometer detectors are going on or will soon start in the world. Among them the most promising and the most advanced one is the Laser Interferometer Gravitational-Wave Observatory (LIGO) project. In near future LIGO is likely to open a totally new window onto the Universe -- a window based on gravitational waves rather than electromagnetic waves.

2. Principle of Laser Interferometer Detectors

The simplified layout of a Michelson interferometer is shown in figure 1. A beam splitter splits a beam of light into two beams of equal amplitude propagating in orthogonal directions. All components are suspended by wires so that they respond as practically free masses above the resonant frequency of the pendula. End

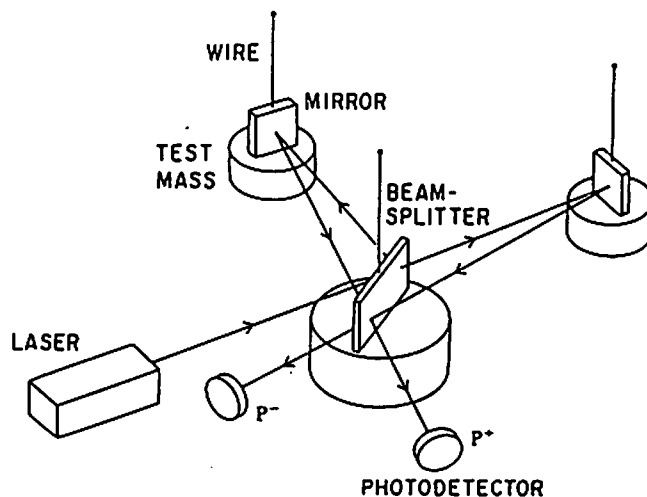


Fig.1 Principle of laser interferometer antennas for detecting gravitational waves.

5. The 40m Prototype ⁷⁾

A 40m prototype on the Caltech campus is an important testbed for full scale LIGO interferometer. Figure 4 shows a schematic diagram of the 40m prototype interferometer. An argon ion laser is servo prestabilized in frequency by the RF modulation technique to a mode cleaner cavity, which serves as a spatial mode filter as well as frequency reference. A power stabilizer samples and controls the amplitude of the light transmitted through the mode cleaner. The beam is then directed to the beam splitter, each resulting beam enters one 40m cavity. The frequency of the light is stabilized by the RF technique to the primary cavity, and then the secondary cavity is locked to the stabilized light. The required correction in the secondary cavity servo is proportional to the difference in natural lengths of the primary and secondary cavities, and thus to the gravitational wave strain.

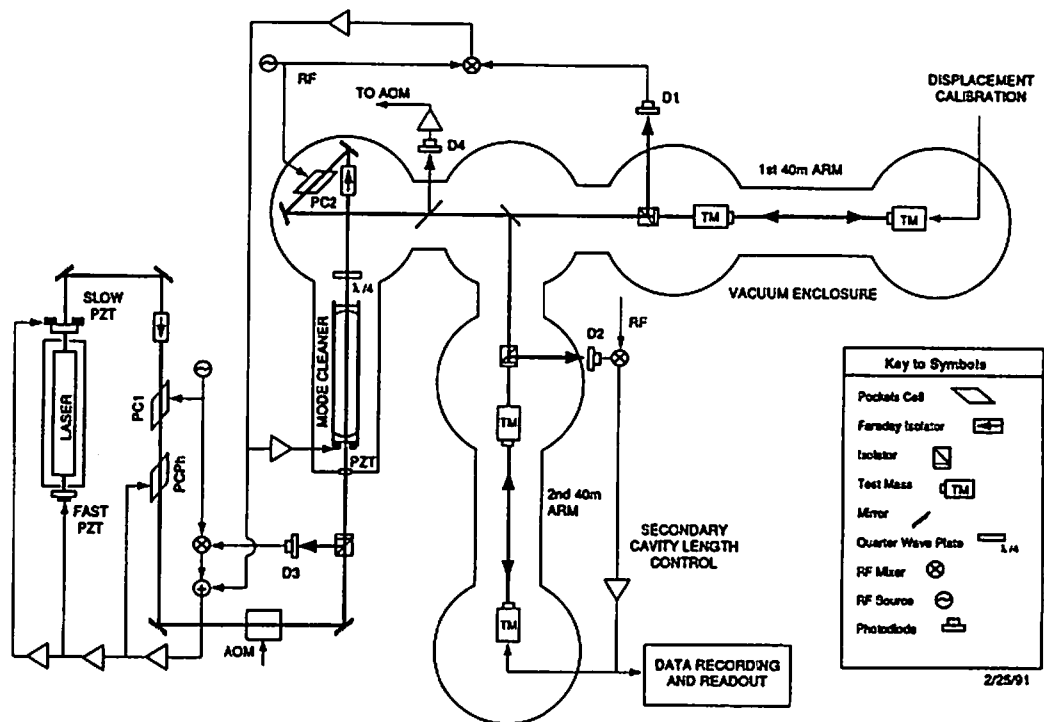


Figure 4. Schematic diagram of the 40m prototype.

The bottom spectrum in Figure 5 is the 40m prototype's displacement performance in June 1992. Progress of the sensitivity since 1984 is also illustrated. The 1992 spectrum shows a number of peaks, superimposed on a smooth background. All of these peaks can be removed with further work, except peaks due to thermally excited vibrational modes of the test masses' suspension wires. At high frequencies (above 1kHz), the noise is dominated by shot noise and is consistent with the level predicted for the current laser power and interferometer optical configuration. At low frequencies (below 120Hz), the observed noise is due to ground vibrations coupling through the suspensions to the test masses. In the intermediate region, the noise spectrum contains contributions from a number of sources, whose relative importance varies with frequency.

Experiments performed on the 40m prototype together with other special purpose set-ups give us confidence that the fundamental noise sources are understood and the LIGO noise performance goals can be achieved.

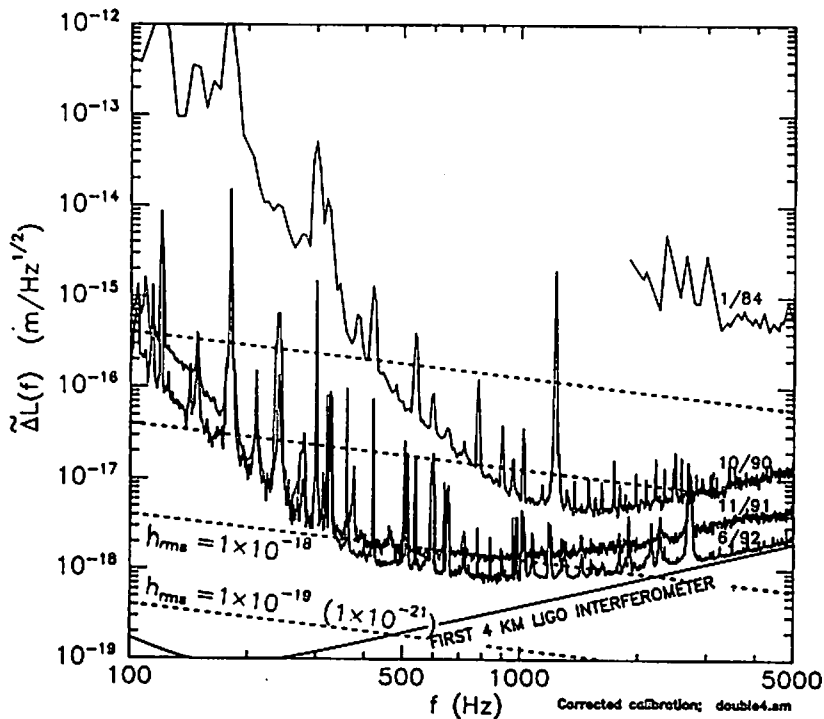


Figure 5. Displacement noise of the 40m prototype.

6. LIGO Facility

LIGO will consist of two widely separated facilities (Hanford in Washington and Livingston in Louisiana). It is necessary to cross correlate data from the detectors at the two sites to distinguish real gravitational-wave bursts from local noise. Each LIGO facility will consist of a $4\text{km} \times 4\text{km}$ L-shaped vacuum system with access ports to the vacuum at corner-, end-, and mid-station. The laser beams must travel through a high vacuum in order to avoid spurious phase shifts due to fluctuations in the scattering by gas molecules. LIGO construction is proposed to be staged over three phases. LIGO's Phase A configuration is the minimum that can house a three-interferometer detector system, consisting of two full-length and one half-length interferometers (Figure 6-a). This Phase A configuration has been designed to permit an upgrade into the configuration. The upgraded LIGO (Phase C), as shown in Figure 6-b, can house three independent such detector systems that operate simultaneously without interfering with the operations of the others, and without breaking the main vacuum. Figure 7 shows how this capability is designed in the vacuum chambers housing the test masses.

7. Detectability of Astrophysical Signals

The capability to measure waveforms from astrophysical events depends on both the strength of the signals and the rate of their occurrence in order for the signal to be distinguished from detector noises. The only amplitude that presently can be calculated with reasonable certainty is that of coalescing neutron stars or black holes. With the rate of neutron star coalescences, which is reasonably well known, Figure 8 shows that LIGO's initial detectors will be about good enough to detect three neutron star inspiral events per year with the "optimistic" event rate, and the advanced detectors will be about good enough with the "ultraconservative" rate.

SYMBOLS

- Test Mass
- ⊙ Test Mass Chamber (Type1)
- ⊙ Test Mass Chamber (Type2)
- / Beam Splitter
- ⊙ Beam Splitter Chamber
- Laser & Input Optics
- Output Optics
- Laser Beam

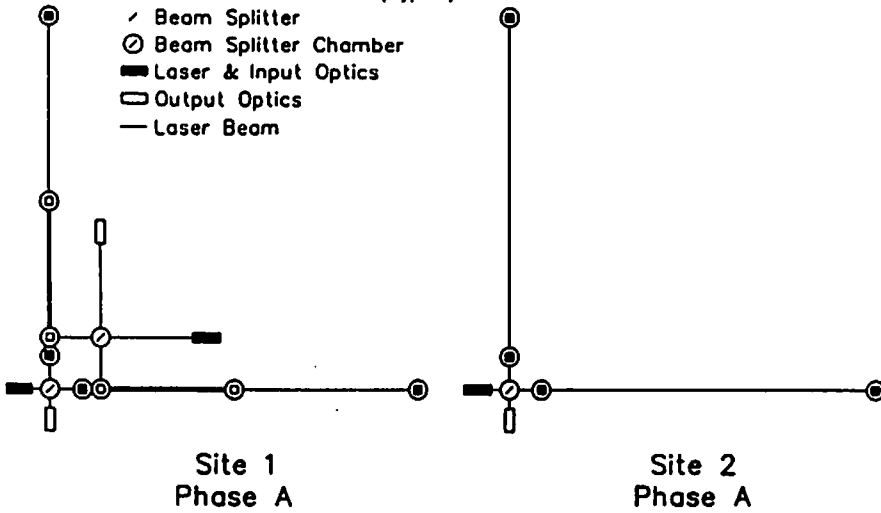


Figure 6-a. LIGO Phase A configuration

SYMBOLS

- Test Mass
- ⊙ Test Mass Chamber (Type1)
- ⊙ Test Mass Chamber (Type2)
- / Beam Splitter
- ⊙ Beam Splitter Chamber
- Laser & Input Optics
- Output Optics
- Laser Beam

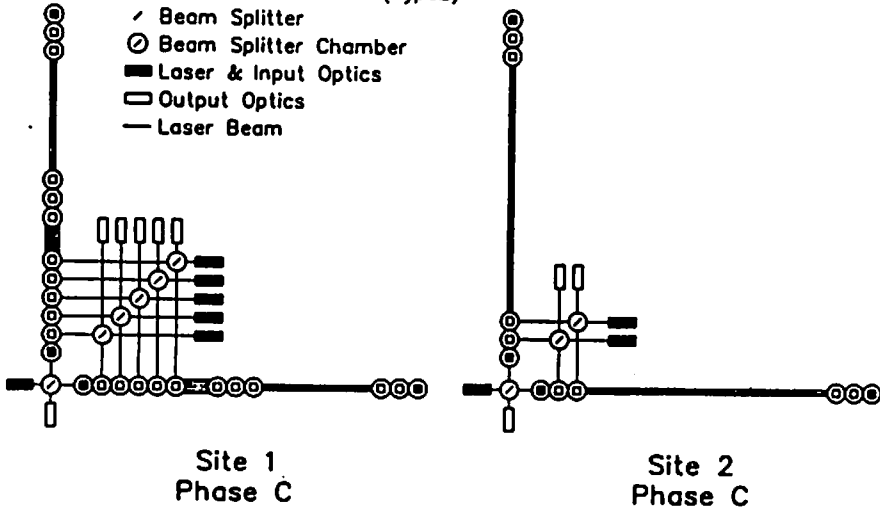
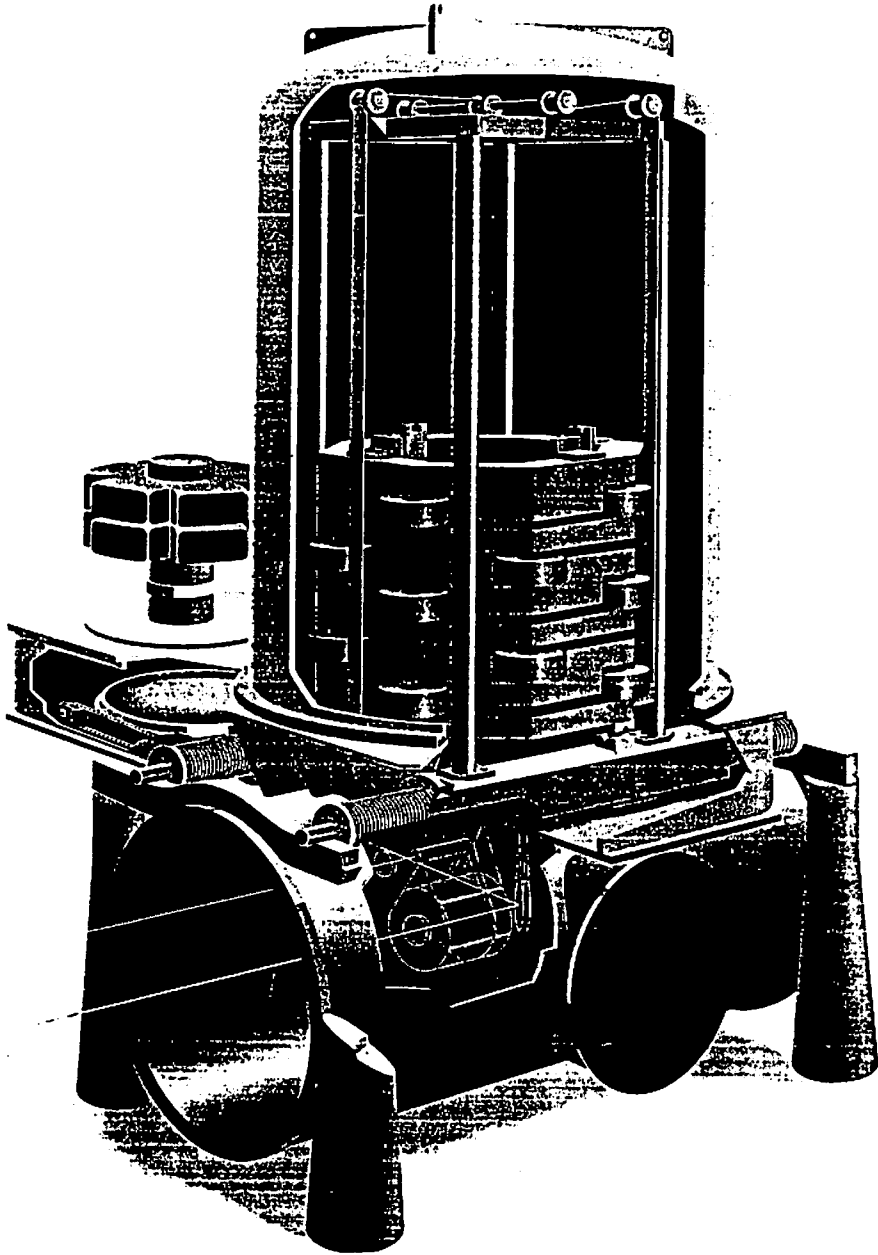


Figure 6-b. LIGO Phase C configuration



Rendering by J. H. Lindemann © 1993 Caltech

Figure 7. Concept of LIGO test mass chamber.

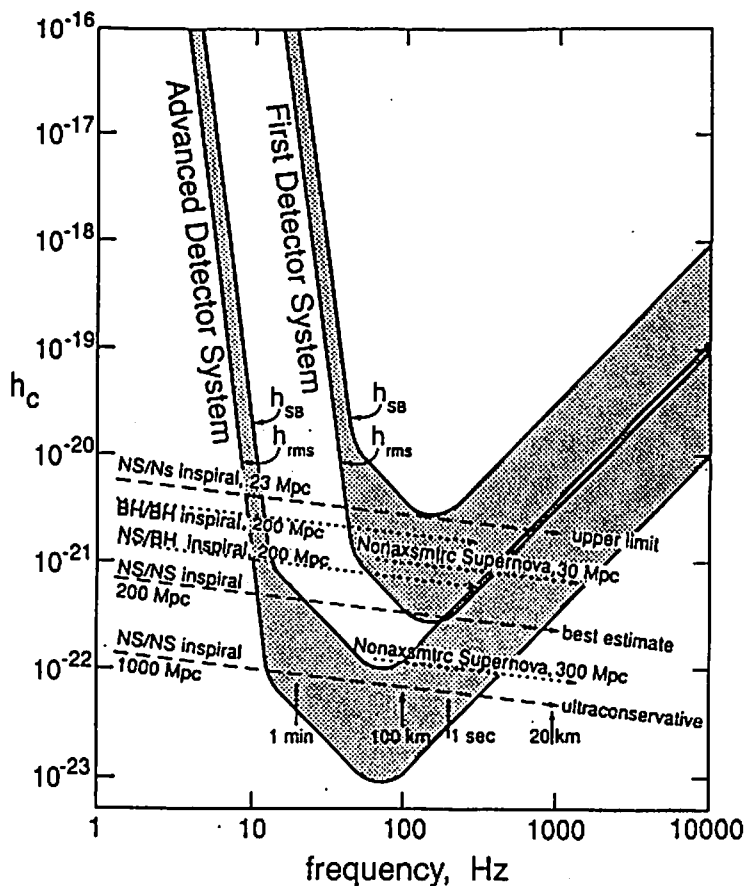


Figure 8. Expected gravitational wave signal and noise in LIGO detector.

8. Conclusion

The initial LIGO, that will use only the technology now in hand, will be operational in 1998 under the current schedule. This initial LIGO detector may discover gravitational waves. If not, then experimenters will press forward with detector improvements (for which development is already underway), leading toward the advanced LIGO. These improvements are expected to lead to the detection of waves from many sources each year. The scientific community can then begin to harvest the rich information carried by the waves.

References

1. J. Weber, Phys. Rev. Lett. 22 (1969) 1320
2. F. Ricci, Proc. of MG6 (1991)
3. R. Weiss, MIT Quarterly Progress Report (Research Laboratory of Electronics) 105 (1972) 54
4. R. L. Forward, Phys.Rev. D17 (1978) 379
5. D. Shoemaker et.al., Phys.Rev. D38 (1988) 423
6. S. Kawamura et.al., ISAS Report 637 (1989)
7. M. Zucker, Proc. of MG6 (1991)
8. A. Abramovici et.al., Science 256 (1992) 325
9. R. Vogt, Proc. of MG6 (1991)

Direct Imaging Interferometer - 2D to 5D Signal Processing -

T.Daishido, K.Asuma¹⁾, K.Nishibori²⁾, J.Nakajima, E.Otobe, N.Watanabe,
Y.Aramaki, H.Kobayashi, T.Saito, N.Tanaka, T.Hoshikawa, S.Komatsu,
H.Ohara, S.Iwase²⁾

Astrophysics Group, Department of Science, School of Education,
Waseda University, 1-6-1 Nishiwaseda, Shinjuku-ku, Tokyo 169, Japan
(Phone: +81-3-3203-4141 ext71-3858, Telefax: +81-3-3208-1032)

¹⁾Soka High School, Soka City, Saitama, Japan

²⁾SONY Corporation, Atsugi City, Kanagawa, Japan

Introduction

64 element Radio Patrol Camera at Waseda University is observing the radio sky with a 200 GOPS direct imaging processor - FFT based Digital Lens-[1]. Since each element of the array antenna is a $2.4\text{m}\phi$ dish, the total collective area is the same as a $20\text{m}\phi$ single dish. The processor generates 64 pixels in every 50 ns. Thus, it surveys the sky 64 times fast as a $20\text{m}\phi$ single dish. At first, we will search transient radio sources like Cyg X-3 or SS 433. In next step, we will extend the present 2D processor to a 5D processor for the pulsar survey.

Ergodic and Non-ergodic Signal in Imaging[2]

Our system is a direct imaging one for both ergodic and non-ergodic signals. It requires the maximum redundant configuration in the array design. This means the strategy of sensitivity maximum. Algorithm in our Digital Lens is a spatial FFT, and it preserves the phase of the radio waves processed. Signals of pulsars or communications are non-ergodic. So, Digital Lens could be used for pulsar survey.

2D to 3D, 5D Signal Processing - Spatial and Temporal and more -

Phase rotation is done by the complex multiplications before 2D spatial FFT in Digital Lens, and each pixel(or beam) could track pulsars independently. The present Digital Lens transforms 8×8 complex amplitude data of $E(u,v)$ in the real space(array plane) to 8×8 complex amplitude $E(\alpha,\delta)$ in momentum space(k space), every 50 ns. This 2D processor has capability to be extended to a 3D processor. That is, combining the two Digital Lens could transform $8\times 8\times 64$ 3D complex data of $E(u,v,t)$ to 3D complex data of $E(\alpha,\delta,f)$, every 50 ns. After squaring and integrating the data, they will be analysed by the floating point 2D FFT processors for searching the periods and the dispersion measure. This is 5D signal processing for pulsar survey, which we are designing. When we use $15\text{m}\phi \times 64$ array, the sensitivity is better than Arecibo.

References

- [1]T.Daishido, XXIII URSI General Assembly(Prague), Abstracts Vol.2, J1, 689, 1990
- [2]T.Daishido, K.Asuma, K.Nishibori, J.Nakajima, M.Yano, E.Otobe, N.Watanabe, A.Tsuchiya, S.Iwase, Radio Interferometry: Theory, Technique, and Applications, A.S.P.Conf.Series, Vol. 19, 86, 1991

Survey of the galactic transient radio sources with the Spatial FFT Interferometer

Eiichiro Otoe * *Junichi Nakajima* * *Tomohiro Saito* *
Naoki Tanaka * *Hiromi Kobayashi* * *Naoki Watanabe* †
Yoshitaka Aramaki ‡ *Tuneaki Daishido* ‡

1 Introduction

We have constructed the two-dimensinal Spatial FFT Interferometer using Digital Lens(the complex amplitdue equalizer + 2D FFT) at Waseda University to survey transient radio sources such as Cyg.X-3,SS433, LSI61°+303 and radio supernovae at frequency range 10.6 ~ 10.7GHz. The Large Array (overall size 22.9*m* (north-south) × 21.5*m* (east-west)) is consituted of $8 \times 8 = 64$ equally spaced array antennas,so that this interferometer is a maximum redundant array. Two dimesional images are obtained as the convolution of point spread function and the switched-beams synthesized by the Digital Lens. Hence , the complete system will provide $0.07^\circ \times 0.07^\circ$ angular resolution and sensitivity of $\sim 500\text{mJy}$. We have obtained the first

*Department of Physics, Graduate School of Science and Engineering, Waseda University, 3-4-1 Ohkubo , Shinjuku-ku , Tokyo 169.

†Department of Electronics and Communications, Graduate School of Science and Engineering, Waseda University, 3-4-1 Ohkubo , Shinjuku-ku , Tokyo 169.

‡Department of School of Sciece and Education, Waseda University , 1-6-1 Nishiwaseda Shinjuku-ku, Tokyo 169.

This papaer is the preprint for the 37th Yamada Conference "Evolution of the Universe and its Observational Quest" on 1993 June 8-12.

two-dimensional switched image of Tau.A with the the partially completed arrays.

2 Two dimensional Imaging

Fourier synthesis radio telescopes are designed to obtain the fine angular structure of radio sources by a minimum redundant array. They are indirect imaging system. However, the Digital lens can synthesize the two-dimensional sixty-four fan beam simultaneously; the digital lens is the facility of direct imaging [T.Daishido91]. The electric fields $E(\mathbf{x}, t)$ distributed on the Large Array are superimposed radiation from the whole sky. Correspondingly with the directional vector \mathbf{k} , the electric fields $E(\mathbf{k}, t)$ have the different spatial frequency on the array, where $\mathbf{k} = (2\pi/\lambda_x, 2\pi/\lambda_y)$. The radiowaves $E(\mathbf{x}, t)$ are spatially sampled with the array where $\mathbf{x} = (mD, nD)$ (D : minimum baseline) and using the spatial FFT, we can directly obtain the electric fields $E_{j,l}(\mathbf{k}, t)$ in momentum space. Because $E_{j,l}(\mathbf{k}, t)$ is related with $E(\mathbf{x}, t)$ by Fourier transform

$$E_{j,l}(\mathbf{k}, t) = \frac{1}{N} \cdot \frac{1}{N} \sum_{n=0}^N \sum_{m=0}^N E(\mathbf{x}, t) \exp(i\mathbf{k} \cdot \mathbf{x} - i\frac{2\pi jn}{N} - i\frac{2\pi lm}{N}) \quad (1)$$

$E_{j,l}(\mathbf{k}, t)$ and the intensity $I(\mathbf{k}) = \langle E^*(\mathbf{k}) \cdot E(\mathbf{k}) \rangle$ are the direct observable value, while $I(\mathbf{k})$ are indirectly observed in Fourier synthesis telescopes. Therefore, two dimensional image of 8×8 pixels is obtained in the present system.

3 Observation and Results

The observation of Tau.A were made on 1992 December 30, using the 5 east-west arrays each of which is composed of 8 elements. Each element is a $2.4m\phi$ cassegrain antenna of which the feed is equipped with the low noise receiver of 200K system temperature. The integral time is 2.048sec and the center frequency and the bandwidth is 10.65GHz and 20MHz, respectively. The phase errors in analogue transmission lines from antenna to baseband, including PLO, can be controlled by the complex equalisers on FFT boards. [K.Asuma91]. The relative phase error of two elements were measured from the fringe period and peak shift value of time from transit

time of Cas.A, observed on 1992 December 29. The complex equalizer is also used in phase switching for reducing gain fluctuation effects in the receivers. Figure.1 is the two-dimensional image of Tau.A. It is seen that Tau.A passes over the synthesized beams.

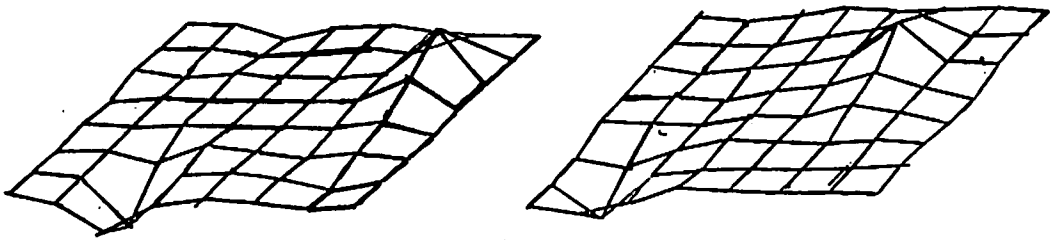


Fig.1 Two Dimensional Image of Tau.A. 64-pixels correspond to the 64 direction. The right figure shows the 10sec later image of Tau.A than that in the left figure.

References

- [T.Daishido91] Tuneaki Daishido., Kuniyuki Asuma., Kazuhiko Nisibori., Junichi Nakajima., Motoko Yano., Eiichiro Otobe., Naoki Watanabe., Akira Tuchiya., *Direct imaging Digital Lens for transient radio source. A.S.P Conf. Ser., Vol.19 (1991),pp. 86-89.*
- [K.Asuma91] Kuniyuki Asuma., Seiichiro Iwase., Kazuhiko Nisibori., Junichi Nakajima., Eiichiro Otobe., Naoki Watanabe., Akira Tuchiya., *Phase control in the Digital Lens. A.S.P Conf. Ser., Vol.19 (1991),pp. 90-91.*

Coalescence of Spinning Binary Neutron Stars

MASARU SHIBATA, TAKASHI NAKAMURA¹ AND KEN-ICHI OOHARA²

Department of Physics, Kyoto University, Kyoto 606-01, Japan

¹ *Yukawa Institute for Theoretical Physics
Kyoto University, Kyoto 606-01, Japan*

² *National Laboratory for High Energy Physics
Oho-machi, Tsukuba-shi, Ibaraki-ken, 305, Japan*

ABSTRACT

We have performed numerical simulations of coalescence of binary neutron stars using a Newtonian hydrodynamics code including radiation reaction by gravitational waves^[1]. In order to examine the effect of spin and plunging velocity, we start the simulations from three distinct types of the initial conditions.

1) To see the dependence of results on the initial separation of binary, a Roche solution of separation $27km$, each mass $\sim 1.5M_{\odot}$ and each radius $\sim 9km$, respectively, is given as the initial condition. We found that the evolution sequence and the wave form of gravitational waves are essentially the same as those in the previous simulations in which computations are started when two neutron stars just contact.

2) We include spin of each star with $-\Omega$, where Ω is Keplerian angular velocity of orbital motion, which is required from the conservation of the circulation. We found that the wave pattern has high amplitude oscillation after coalescence contrary to the former case. This means that it will be possible to determine the spin of coalescing neutron stars from the observed wave form of gravitational waves. The maximum amplitude of gravitational waves is 3.4×10^{-21} for a hypothetical event at the distance of 10Mpc.

3) We include the plunging velocity half times as large as the Keplerian velocity. The plunging velocity is realistic at the final coalescence phase because in binary neutrons system the last stable circular orbit will exist. We found that at first two neutron stars coalesce like a head on collision and then the coalescing object becomes the double core structure. This structure is kept considerably long time because the angular momentum is not lost so efficiently until contact. The wave pattern of gravitational waves is also at first similar to that in the case of the head on collision and then similar to that in the coalescence of spinning neutron stars. The maximum amplitude of gravitational waves is 3.6×10^{-21} for a hypothetical event at the distance of 10Mpc.

1. Introduction

There are at least three neutron star-neutron star binaries, PSR 1913+16, PSR 2127+11C and PSR 1534+12 in our galaxy. This suggests that about one percent of neutron stars are in the binary system. These binaries will coalesce within $10^8 \sim 3 \times 10^9$ yr due to the emission of gravitational waves. The statistical analysis shows that the binary coalescence may occur ~ 1 event per year within the distance of ~ 100 Mpc^[2]
^[3] . Therefore coalescing binary neutron stars is one of the most promising sources of gravitational waves. Nakamura and Oohara performed the post-Newtonian three dimensional simulations including the radiation reaction of gravitational waves to know the amplitude and the wave form of gravitational waves at coalescing events^[4] ^[5] ^[6]
^[7] . They found that the maximum amplitude of gravitational waves is $\sim 10^{-21}$ for a hypothetical event at a distance of 50 Mpc. This suggests that the sensitivity of LIGO(Laser Interferometric Gravity Wave Observatory) project will enable us to know the final phase of the coalescence.

Calculations by Nakamura and Oohara were performed for the various initial conditions, but we must argue the following two points. In the calculations of Nakamura and Oohara, the initial neutron stars are rigidly rotating around the center of mass. However as recently suggested by Kochanek^[8] , if there is no or small viscosity in the system, the neutron stars must have spin from the conservation of the circulation while their separation decreases due to the emission of gravitational waves. Accordingly the initial conditions of Nakamura and Oohara is correct only when the viscosity works sufficiently in the system until the coalescence. If the sufficient viscosity does not exist

in the system, we must consider the initial condition in which the neutron stars are spinning.

There is another point to consider in coalescence of binary neutron stars. Recently Lincoln and Will^[9] and Kidder et al^[10] showed that taking into account the general relativistic effect, there exists the last stable circular orbit for binary neutron stars similar to that for a test particle in Schwarzschild space-time. According to them, if the separation of binary shrinks within $\sim 4 - 5M_{tot}^*$, where M_{tot} is the total mass of the system, the binary cannot keep the circular orbit and each neutron star must plunge into each other. They also showed that in the final phase of the coalescence, approaching velocity of binary becomes comparable to the orbital velocity.

Considering the above points, we use the initial condition in which each neutron star has spin angular momentum assuming that the viscosity does not exist in the system. We also use the initial condition, in which binary neutron stars initially have approaching velocity comparable to the orbital one using the present code in this paper although in our code the effects of general relativity except for radiation reaction are not included. In section 2 we show the basic equations. In section 3 the initial models are shown. In section 4 we show the numerical results. In section 5 we discuss the astrophysical implications of our results.

2. Basic Equations

The basic equations are the three dimensional hydrodynamics equations with a back reaction potential proposed by Blanchet et al^[11]. Although we should evaluate post-Newtonian terms up to 2.5PN order^[12], in this paper we only include the radiation reaction terms.

The basic equations are as follows^{[6][7]}.

$$\frac{\partial \rho}{\partial t} + \frac{\partial \rho v^i}{\partial x^i} = 0, \quad (2.1)$$

* Note that in the Newtonian approximation, the isotropic coordinate are used as a radial coordinate. Hence these values are in the unit of the isotropic radial coordinate. In the Schwarzschild radial coordinate, these become $\sim 6 - 7M_{tot}$.

$$\frac{\partial \rho w^i}{\partial t} + \frac{\partial \rho w^i v^j}{\partial x^j} = -\frac{\partial P}{\partial x^i} - \rho \frac{\partial(\psi + \psi_{react})}{\partial x^i}, \quad (2.2)$$

$$\frac{\partial \rho \epsilon}{\partial t} + \frac{\partial \rho \epsilon v^j}{\partial x^j} = -P \frac{\partial v^i}{\partial x^i}, \quad (2.3)$$

$$P = (\Gamma - 1)\rho\epsilon, \quad (2.4)$$

$$\Delta\psi = 4\pi G\rho, \quad (2.5)$$

$$\Delta R = 4\pi G \left(\frac{d^3}{dt^3} D_{ij} \right) x^j \frac{\partial \rho}{\partial x^i}, \quad (2.6)$$

$$v^i = w^i + \frac{4G}{5c^5} \left(\frac{d^3}{dt^3} D_{ij} \right) w^j, \quad (2.7)$$

$$\psi_{react} = \frac{2G}{5} \left(R - \left(\frac{d^3}{dt^3} D_{ij} \right) x^j \frac{\partial \psi}{\partial x^i} \right), \quad (2.8)$$

The symmetric trace-free part of the quadrupole moment D_{ij} and its third time derivative can be obtained by

$$D_{ij} = STF \left(\int \rho x^i x^j dV \right)$$

and

$$\frac{d^3}{dt^3} D_{ij} = STF \left[2 \int \left(2P \frac{\partial v_i}{\partial x^j} - 2\rho v_i \frac{\partial \psi}{\partial x^j} + x_i \frac{\partial \psi}{\partial x^j} \frac{\partial \rho v^k}{\partial x^k} - \rho x_i \frac{\partial \dot{\psi}}{\partial x^j} \right) dV \right], \quad (2.9)$$

where the notation STF means

$$STF(Q_{ij}) = \frac{1}{2}(Q_{ij} + Q_{ji}) - \frac{1}{3}\delta_{ij}Q_{kk}.$$

The time derivative of the gravitational potential $\dot{\psi}$ is determined by

$$\Delta \dot{\psi} = -4\pi G \frac{\partial \rho v^k}{\partial x^k}, \quad (2.10)$$

We take the units of

$$M = M_\odot, \quad L = \frac{GM_\odot}{c^2} = 1.5\text{km}, \quad T = \frac{GM_\odot}{c^3} = 5 \times 10^{-3}\text{msec}. \quad (2.11)$$

We fix the polytropic index $\Gamma = 2$.

3. Initial Conditions

We consider the following two points to set the initial conditions.

1) In the absence of the viscosity, the circulation of the system should be conserved. If the neutron stars are assumed to rotate rigidly around the center of mass at first, the circulation in the $z = \text{constant}$ plane is $2\Omega_0 S$, where Ω_0 and S are the initial angular velocity and the area of the cross section of the neutron stars, respectively. While the two neutron stars approach each other by radiation reaction, the area of the cross section of the neutron stars does not change so much, but the angular velocity Ω becomes much larger than Ω_0 because $\Omega \propto a^{-3/2}$. Therefore to conserve the circulation, the neutron stars must have spin with the angular velocity $-\Omega$, i.e., retrograde to the orbital motion ^[8].

2) Taking into account the general relativistic effect, there exists the last stable orbit for binary neutron stars ^{[9][10]}. Therefore the separation of binary shrinks within $\sim 5M_{tot}$, each neutron stars of the binary has the plunging velocity as large as the orbital velocity.

To take into account above points, we perform following three simulations.

	Model I	Model II	Model III
Spin	no	yes, $-\Omega_K$	yes, $-\Omega_K$
Orbital frequency	Roche Model(Ω)	Keplerian(Ω_K)	Keplerian(Ω_K)
Plunging velocity	no	no	yes, $v_K/2$
Major Axis, Separation(l_0)	8.8km, 27km	9km, 27km	9km, 27km
$(v^x, v^y)(x > 0)$ $(v_x, v_y)(x < 0)$	$(-y\Omega, x\Omega)$	$(0, l_0\Omega_K/2)$ $(0, -l_0\Omega_K/2)$	$(-l_0\Omega_K/4, l_0\Omega_K/2)$ $(l_0\Omega_K/4, -l_0\Omega_K/2)$
Mass(M_\odot)	1.5×1.5	1.4×1.4	1.4×1.4
Grid Number	$141 \times 141 \times 131$	$121 \times 121 \times 121$	$121 \times 121 \times 121$

A Roche equilibrium model is determined by the method given by Oohara and Nakamura ^[6]. It is obtained by solving the following equations;

$$\psi + h - \frac{1}{2}R^2\Omega^2 = C, \quad (3.1)$$

and

$$\Delta\psi = 4\pi G\rho. \quad (3.2)$$

Eq.(3.1) is the integrated representation of equation of motion and $h = 2K\rho$. To determine the solution, we must fix three parameters. We fix the innermost points of the stars, the centers of the neutron stars and the density there. Solving the above equations by the iteration, we obtain an equilibrium model. In this case, the mass of two neutron stars and the orbital angular velocity are determined only from the equilibrium model.

In the case that two neutron stars have spin, we do not know how to determine an equilibrium model because this is a similar problem to determine the Dedekind configuration^[13]. However as for an axisymmetric rotating star, we can obtain the equilibrium configurations. We here consider axisymmetric equilibrium rotating stars as the initial condition for each spinning neutron star. This initial condition is consistent if the tidal force is much smaller than the self-gravity. An equilibrium axisymmetric rotating star is determined by

$$\rho = \frac{1}{2K} \left[\frac{1}{2} R^2 \Omega^2 + C - \psi \right], \quad (3.3)$$

and

$$\frac{1}{r^2} \frac{\partial}{\partial r} \left(r^2 \frac{\partial \psi}{\partial r} \right) + \frac{1}{r^2} \frac{\partial}{\partial x} \left[(1 - x^2) \frac{\partial \psi}{\partial x} \right] = 4\pi G\rho, \quad (3.4)$$

where $x = \cos\theta$. To solve these equations, we must fix three quantities. In the absence of viscosity, the circulation should be conserved, so that each neutron star should have spin angular velocity the same as the Keplerian angular velocity with opposite sign. Hence the angular velocity is fixed contrary to the usual case. We also fix the density at the center and the major axis of the star. A numerical method to solve the above equations is as follows. 1) We expect the trial density configuration and using this we solve the axisymmetric Poisson equation (3.4). 2) The constant C and the polytropic constant K are determined by

$$\begin{aligned} \psi_c + 2K\rho_c &= C \\ \psi_e - \frac{1}{2} R_e^2 \Omega^2 &= C, \end{aligned} \quad (3.5)$$

where ψ_c , ψ_e , ρ_c and R_e are the Newtonian potential at the center, the Newtonian

potential at the surface of the star in equatorial plane, the density at the center and the major axis of the star, respectively. 3) Using Eq.(3.3), we determine the new trial density configuration. The procedure 1), 2) and 3) is repeated until convergence. We use an axisymmetric rotating star determined by the above method as each neutron star of the binary. As a result, it is found that the virial equilibrium is almost satisfied. This means that the solution seems to be almost in a true equilibrium.

4. Numerical Results

4.1 EVOLUTION SEQUENCES FOR DENSITY CONTOURS

We show the contours of the density and the velocity vectors on the $x - y$ plane for Model I, II and III in Figs.1, 2 and 3. In both Model I and Model II, at $t \lesssim 1\text{msec}$, the orbit of the neutron stars shrinks radiating almost periodic gravitational waves. After the coalescence, however, two models show the different evolution sequences. In Model I, in the outer region the spiral arms are formed and in the inner region the ellipsoidal core is formed($t > 1\text{msec}$). Then the spiral arms gradually wind round the core by differential rotation and become axially symmetric disk. On the other hand, in Model II, in the outer region, there is no spiral arm, so the configuration becomes a nearly axially symmetric disk soon. This result seems to be reasonable. Since the velocity of the outer region is smaller than in Model I due to the spin retrograde to the orbital motion for each neutron star, the centrifugal force is weaker than in Model I. In the inner region, the neutron stars are gradually coalescing because of the enhanced centrifugal force, so that the double core structure is kept for a long time. By the radiation reaction, the double cores merge at last. It does not become the rotating ellipsoid, but the ring. At $t \sim 3\text{msec}$, $\beta \equiv T/|W|$ of the system is 0.143. This value is slightly larger than that at the secular instability limit^[14] ($\beta \lesssim 0.14$). In the model EQ8 of ref.[5] the ring slowly evolved to a disk, so that it is expected that the disk is formed in the subsequent evolution.

In Model III we put the approaching velocity half times as large as the Keplerian velocity. Due to the approaching velocity, two neutron stars coalesce soon ($t \sim 0.2\text{msec}$). After the coalescence, the cores of the neutron stars not only rotate around the center of mass, but also oscillate radially like in a head on collision of the neutron stars^[15]

Because of the large centrifugal force, they behave like a binary until $t \sim 1\text{ms}$. Due to the emission of gravitational waves they merge, but in the inner region the double core structure is formed ($t \sim 1 - 1.5\text{ms}$) and this structure is kept for a long time. In particular for $t \gtrsim 2\text{ms}$ the nearly stationary state can be seen. For $t \gtrsim 2\text{ms}$, β converges at ~ 0.15 and for $t \sim 3\text{ms}$ the system becomes almost in virial equilibrium, that is $(2T + W + 3\Pi)/(2T + |W| + 3\Pi) \sim 10^{-3}$, where Π is the thermal energy. However β is larger than the value at the secular instability limit ~ 0.14 ^[16]. Therefore the double core will evolve the axially symmetric structure radiating gravitational waves in the much longer time scale than the dynamical time scale. Let us estimate the time scale for the system to become axially symmetric. β will become less than 0.14 if about 5% of the angular momentum is lost by the emission of gravitational waves. The time scale of this process is expressed as^{[6][7]}

$$\tau \sim 0.05 J \Omega \left(\frac{dE}{dt} \right)^{-1}, \quad (4.1)$$

where J is the angular momentum of the system, Ω is the rotational period of the double core and dE/dt is the luminosity of gravitational waves. At the end of the calculation, $J = 3.4$, $\Omega \sim 0.025$ and $dE/dt \sim 5 \times 10^{-6}$, so that $\tau \sim 750$ in non-dimensional unit. Therefore we stopped our simulation at $t \sim 670$ to save the computational time. β is also larger than that in Model II. This is because the angular momentum is not lost so efficiently until contact.

4.2 GRAVITATIONAL WAVES

In Figs.4, 5 and 6 we show the wave forms h_+ and h_\times of gravitational waves observed on the z-axis at 10 Mpc in Model I, II and III. They are defined by

$$\begin{aligned} h_+ &= \frac{1}{r} (\ddot{D}_{xx} - \ddot{D}_{yy}) \\ h_\times &= \frac{2}{r} \ddot{D}_{xy}. \end{aligned} \quad (4.2)$$

In Figs.7, 8 and 9 we also show the luminosity of gravitational waves calculated by

$$\frac{dE}{dt} = \frac{1}{5} \left(\frac{d^3 D_{ij}}{dt^3} \right)^2. \quad (4.3)$$

In Model I the wave forms are made of the three part. One is the periodic wave part ($t \lesssim 1\text{msec}$). The second is the burst part induced by the coalescence of the neutron

stars($t \sim 1\text{msec}$). The third is the damping part($t \gtrsim 1\text{msec}$). Contrary to Model I, the wave form of Model II is composed of the four part. The first, the second and the last part have the same tendency as Model I. However after the coalescence($t \gtrsim 1\text{msec}$), it shows different tendency: The high amplitude oscillation continues for several times. This difference of the wave form also affects the time variation of the luminosity. In Fig.7 the peak of luminosity appears at the moment of the contact of the neutron stars and then the luminosity decrease exponentially. On the other hand, in Fig.8 after the first peak appears, the second large peak appears again. This is because in Model II the double core structure is formed after the coalescence and it oscillates before merging.

In Fig.6 we show the wave forms of Model III. It is found that the wave forms are at first similar to that in the case of the head on collision^[15] and then similar to those in the coalescence of the spinning neutron stars with no plunging velocity(Model III). In particular for $t \lesssim 1\text{ms}$, the wave forms are quite similar to that in the head on collision: At first a burst peak is observed($t \sim 0.2\text{msec}$) and then the small peaks induced by the radial oscillation are found. After $t \sim 1\text{ms}$, the wave forms resemble those in Model II. Because the binary-like structure is kept till $t \sim 1\text{ms}$, the peaks of the periodic waves are found. For $t > 2\text{ms}$, the nearly stationary double core structure is formed, so the periodic waves are emitted. Because of the emission of gravitational waves, the amplitude of gravitational waves dumps little by little.

In Fig.9 we also show the luminosity of gravitational waves calculated by

$$\frac{dE}{dt} = \frac{1}{5} \left(\frac{d^3 D_{ij}}{dt^3} \right)^2. \quad (4.4)$$

At $t \sim 0.2\text{ms}$, the large peak is found. As mentioned above, it occurs at the moment of the contact of each neutron star. In the case of Model II, the second large peak was found after the contact. However in Fig.9, such peak is not found and instead, several small peaks are found till $t \sim 1\text{ms}$. This tendency is also similar to that in the case of the head on collision of two neutron stars^[15]. However for $t \gtrsim 1.5\text{ms}$, the luminosity curve is similar to that in Model II. This is because in both model the double core is formed at the late stage of the evolution.

In conclusion, the wave forms are considerably different in the case that the effects of the conservation of the circulation and the plunging velocity are included. Inversely

if gravitational waves from coalescing binary neutron stars are detected, we may know whether each neutron star had spin and plunging velocity before the coalescence or not. If the spin is not so large, this means that the viscosity was very effective before the coalescence.

5. Discussion and Summary

The maximum amplitude of gravitational waves observed on the z -axis at 10 Mpc is 4.0×10^{-21} , 3.4×10^{-21} and 3.6×10^{-21} for Model I, II and III. The efficiency of the gravitational wave emission amounts to 2.6%, 2.3% and 1.4% for Model I, II and III. The efficiency in Model III is smaller than those in Model I and II. This is because the angular momentum is not lost so efficiently until coalescence. In Model II and III, a fraction of the angular momentum loss is 38% and 32%, respectively. More angular momentum is lost, more gravitational waves are emitted, so that our results are reasonable. $J/M^2 (= a/m) \sim 0.4$ in all models and total mass of the coalescing objects exceed the neutron star mass limit, so the final products are expected to be slowly rotating black holes. In conclusion, the amplitudes of gravitational waves are not changed if the effects of the spin and plunging velocity are included. However the wave form and the efficiency of the emission of gravitational waves is not the same in each model. Therefore if gravitational waves from coalescing binary neutron stars are detected, we may know whether each neutron star had spin and plunging velocity before the coalescence.

The numerical calculations were performed on HITAC S820/80 at the Data Handling Center of National Laboratory for High Energy Physics (KEK) and FACOM VP2600 of Data Proceeding Center of Kyoto University. This work was partly supported by a Grant-in-Aid for Scientific Research on Priority Area of Ministry of Education, Science and Culture(04234104).

REFERENCES

1. M. Shibata, T. Nakamura and K. Oohara, Prog. Theor. Phys. **88**(1992), 1079; Preprint YITP/K 989
2. R. Narayan, T. Piran and A. Shemi, Astrophys. J. **379**(1991), L17

3. E. S. Phinney, *Astrophys. J.* **380**(1991), L17
4. K. Oohara and T. Nakamura, *Prog. Theor. Phys.* **82** (1989), 535
5. T. Nakamura and K. Oohara, *Prog. Theor. Phys.* **82** (1989), 1066
6. K. Oohara and T. Nakamura, *Prog. Theor. Phys.* **83** (1990), 906
7. T. Nakamura and K. Oohara, *Prog. Theor. Phys.* **86** (1991), 73
8. C. S. Kochanek, *Astrophys. J.* **398** (1992), 234
9. C. W. Lincoln and C. M. Will, *Phys. Rev.* **42**(1990), 1123
10. L. E. Kidder, C. M. Will and A. G. Wiseman, *Class. Quantum Grav.* **9** (1992), L125
11. L. Blanchet, T. Damour and G. Schafer, *Mon. Not. R. Astron. Soc.* **242** (1990), 289
12. K. Oohara and T. Nakamura, *Prog. Theor. Phys.* **88**(1992), 291
13. J. Ipser and R. Managan, *Astrophys. J.* **250** (1981), 362
14. S. Chandrasekhar, *Ellipsoidal Figures of Equilibrium*(1969), Dover
15. D. L. Gilden and S. L. Shapiro, *Astrophys. J.* **287**, 728
16. S. Chandrasekhar, *Ellipsoidal Figure of Equilibrium*(1969),Dover

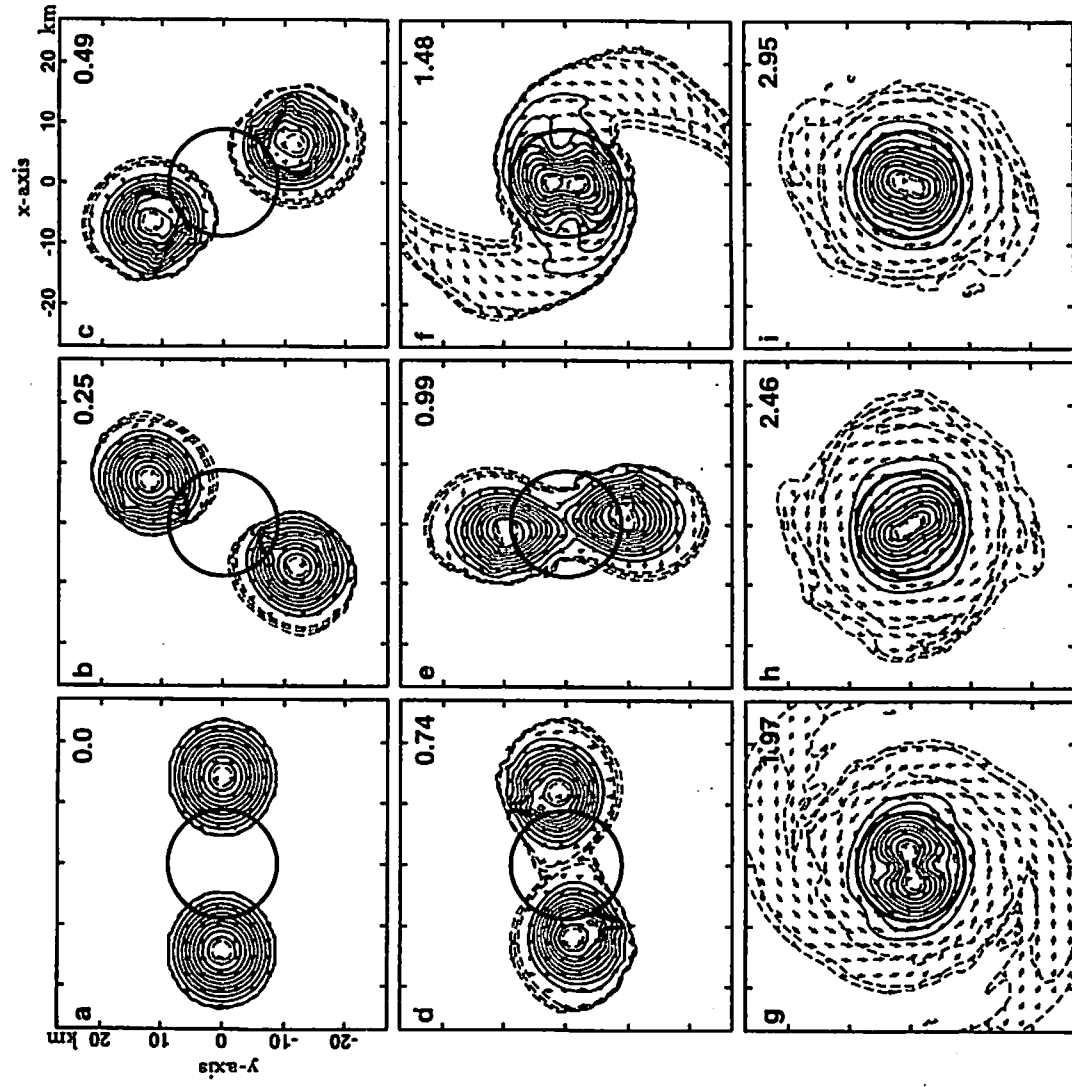


Figure 1.

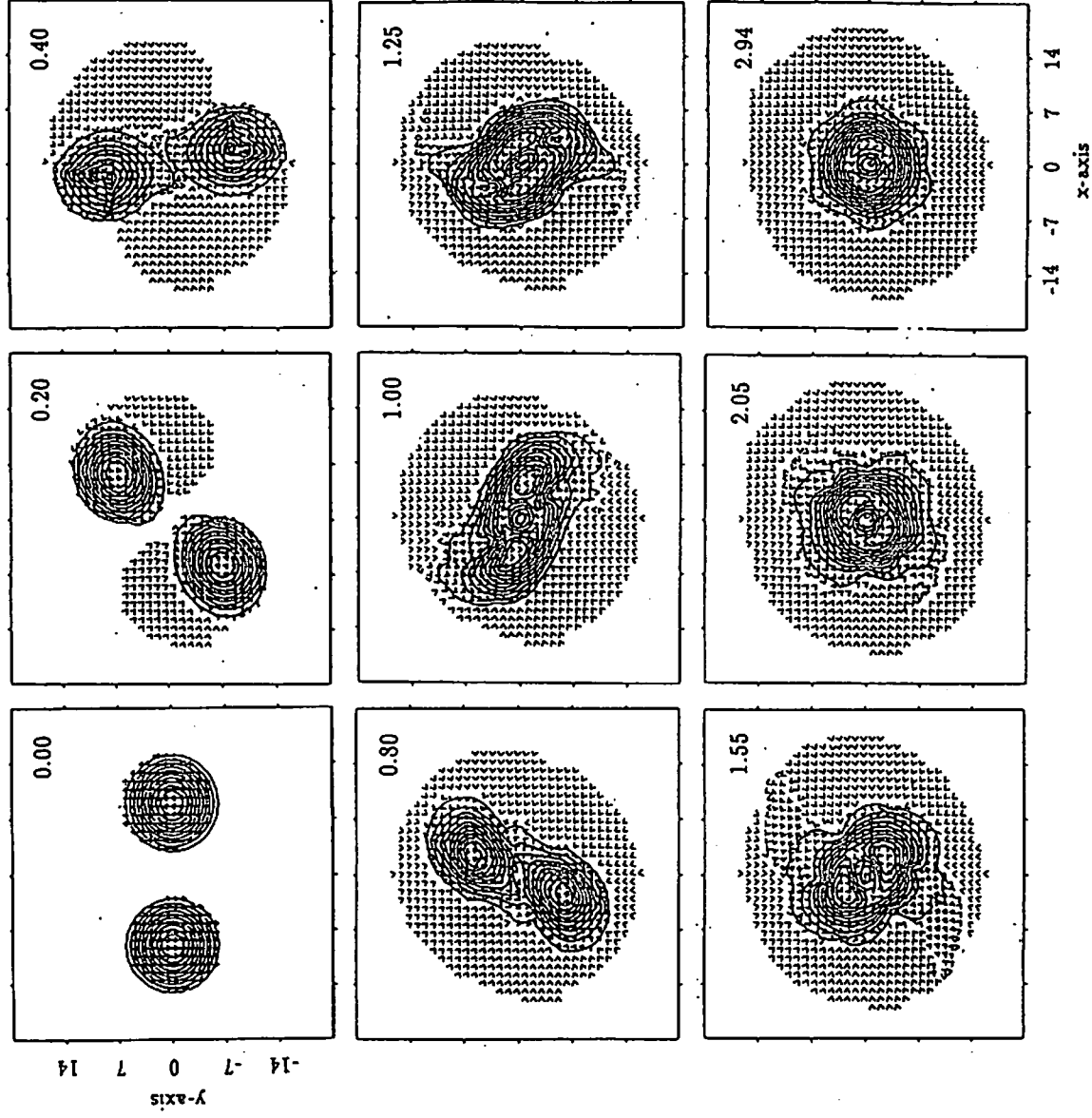


Figure 2.

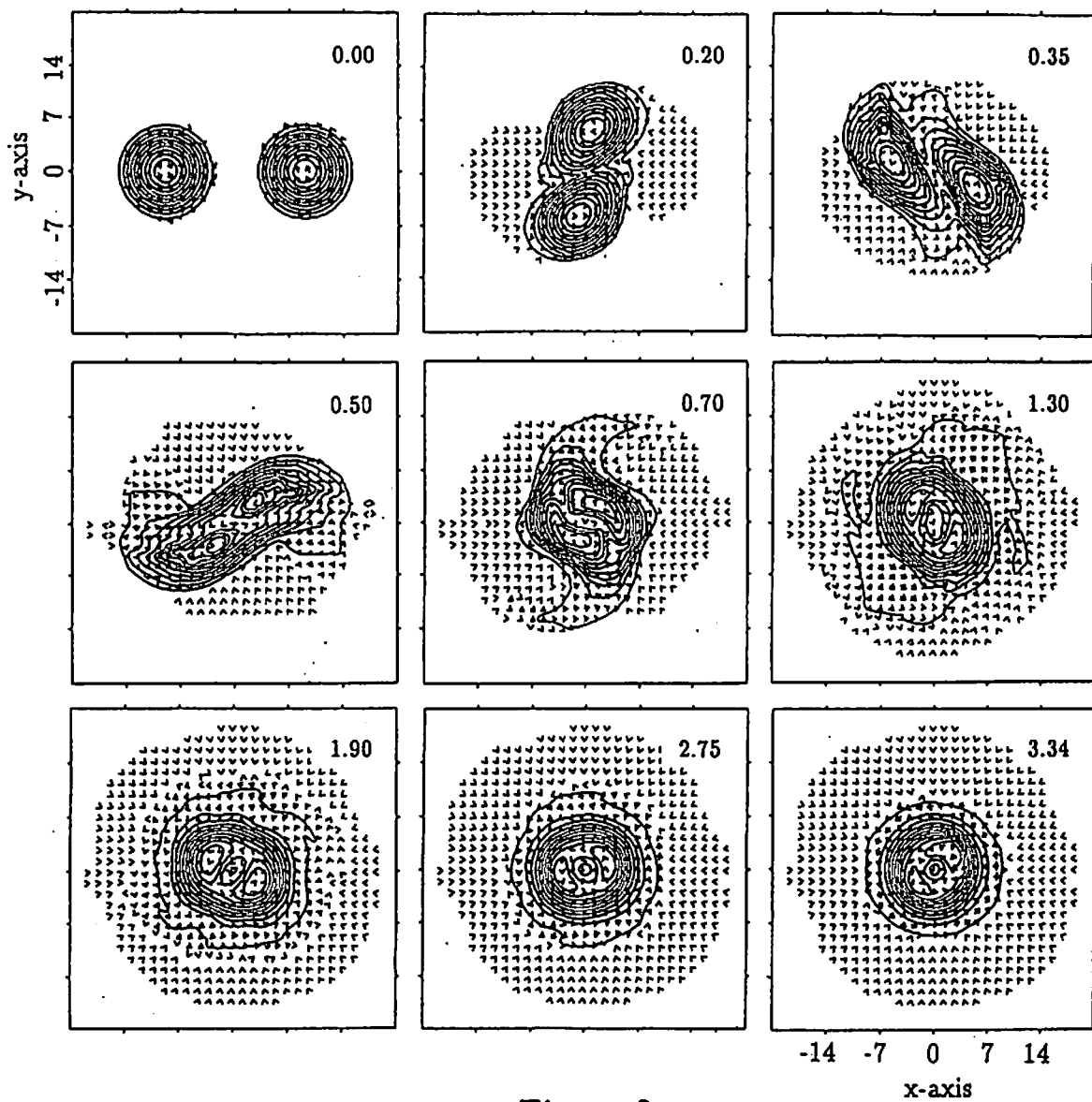


Figure 3.

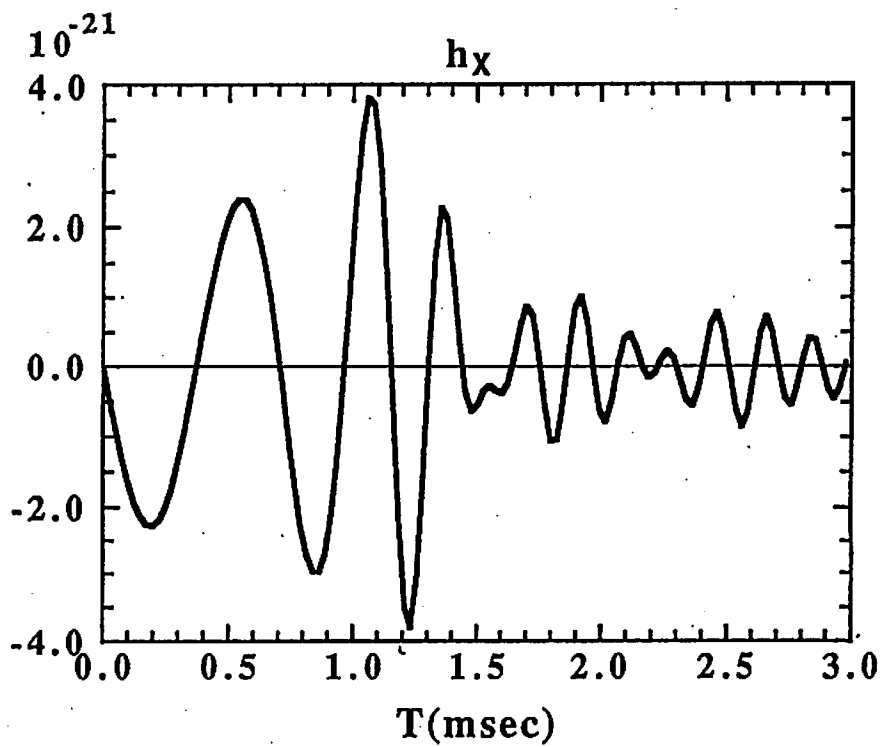
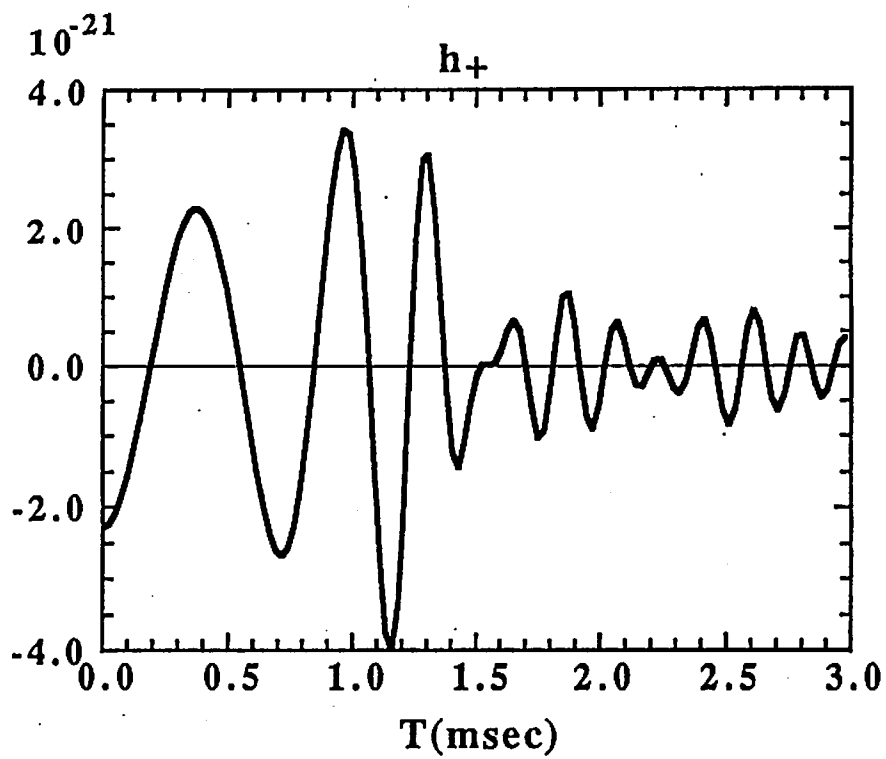


Figure 4.

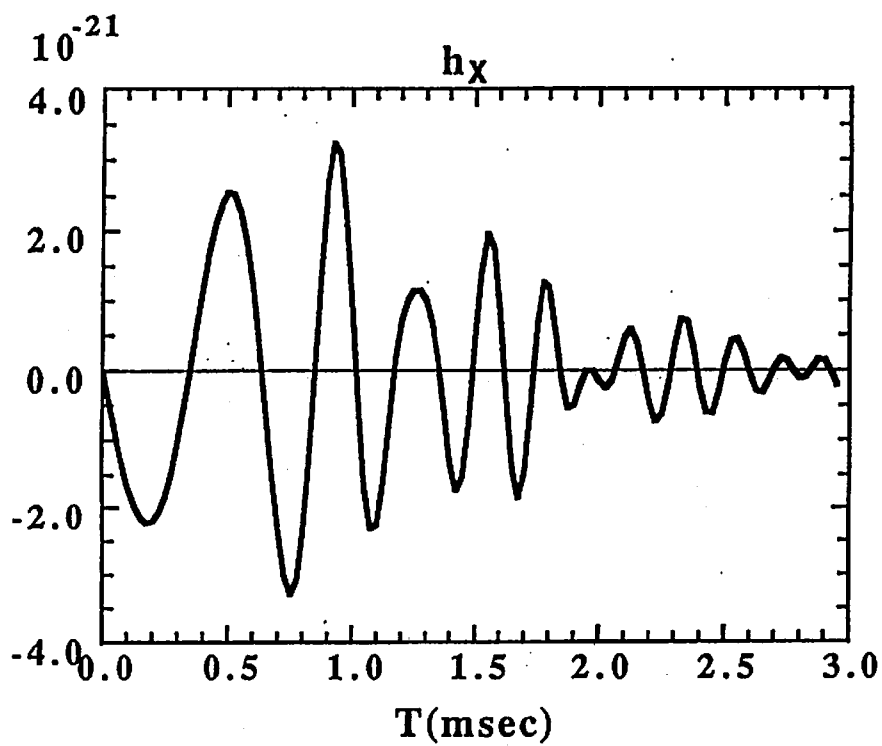
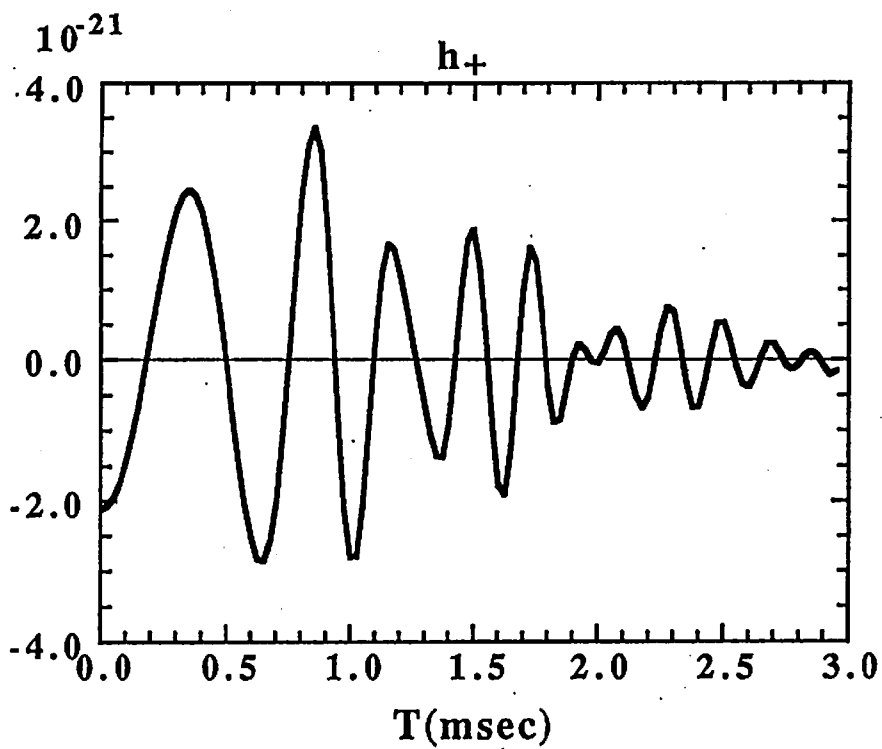


Figure 5.

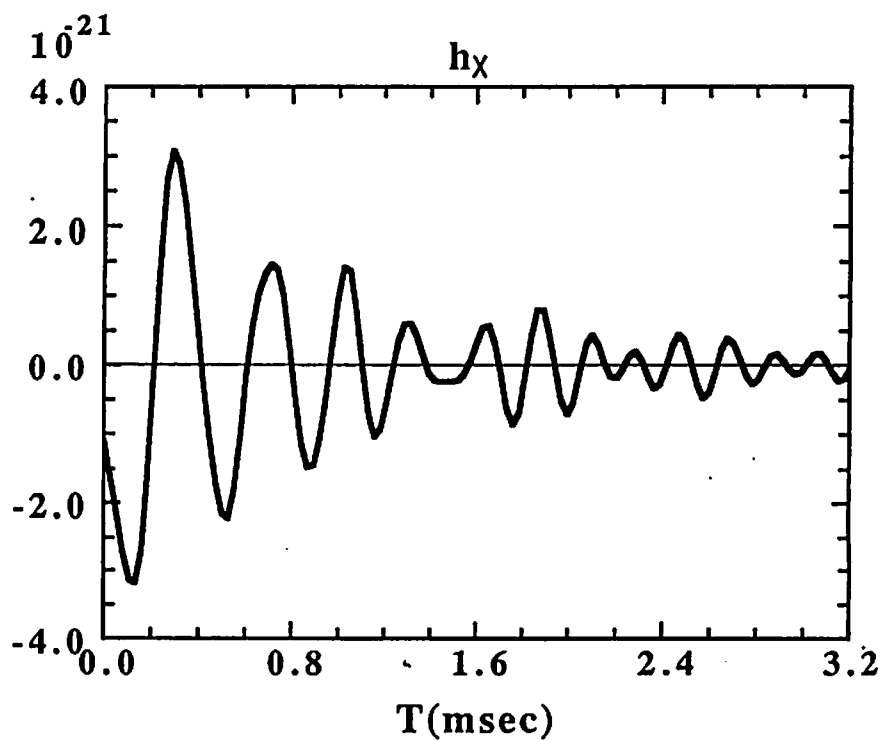
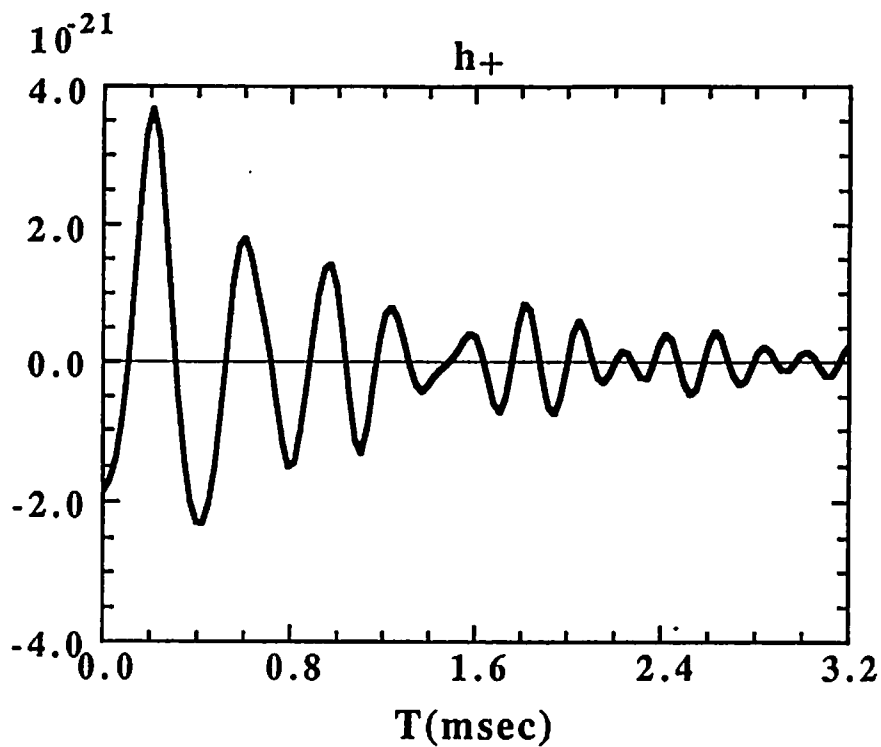


Figure 6.

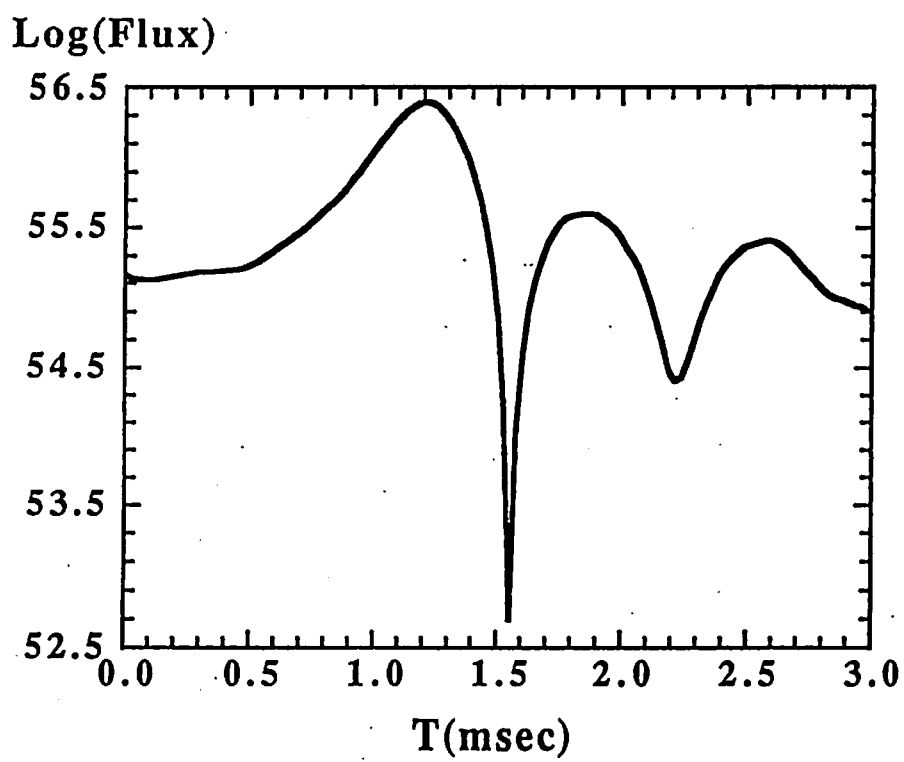


Figure 7.

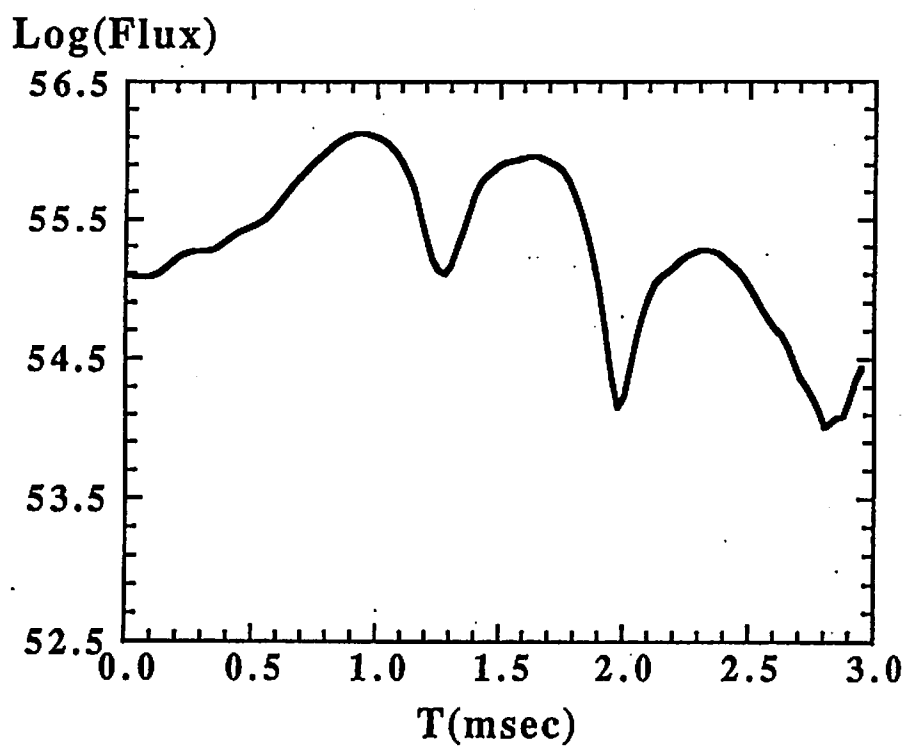


Figure 8.

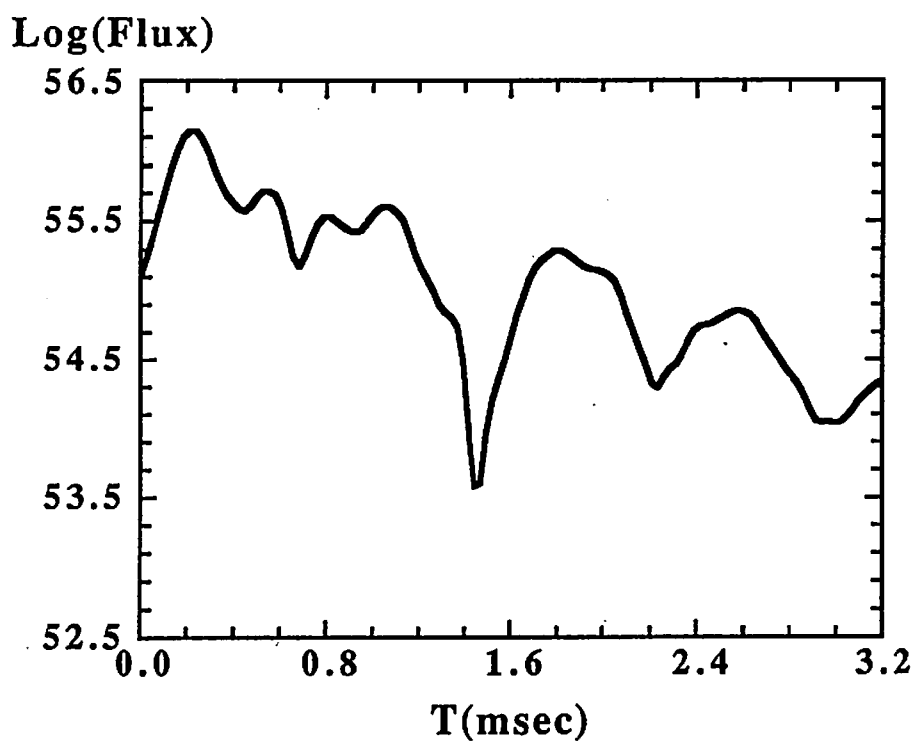


Figure 9.

Gravitational Wave Induced by a Particle Orbiting around a Schwarzschild Black Hole

Takahiro. Tanaka¹, Masaru. Shibata¹, Misao. Sasaki¹,

Hideyuki. Tagoshi¹ and Takashi. Nakamura²

¹Department of Physics, Kyoto University, Kyoto 606-01, Japan

²Yukawa Institute for Theoretical Physics Kyoto University, Kyoto 606-01, Japan

1 Introduction

Coalescence of two compact objects, such as Black Hole-Black Hole, Black Hole-Neutron star and/or Neutron star-Neutron star binary is one of the promising source of gravitational waves. To investigate the gravitational waves radiated in this process, the completely relativistic numerical calculation will be necessary. But now there are many technical problems to be overcome to achieve the 3D fully relativistic numerical calculation.

Instead, different approaches ,i.e., A) hydrodynamical simulation in Post-Newtonian approximation , B) two body problem in Post-Newtonian approximation, and C) relativistic perturbation by the test particle approximation are studied extensively. As for A), Nakamura, Oohara and Shibata^[1,2,3] performed 3D calculation of coalescence of neutron stars with a wide range of initial conditions. They showed how the gravitational wave emission depends on the post-Newtonian effect, the spin of each neutron star and the plunging velocity. However their simulations do not give the final answer because the reality of the initial conditions they used, though seems plausible, has not been justified, not to mention the need of a fully general relativistic treatment. As for the evolution of the orbit before merging, there is the approach B). Lincoln and Will,^[4] and Wiseman^[5] performed $P^{5/2}N$ calculations with radiation damping using the point particle approximation. They found that for two equal mass particles, the final plunge orbit begins around $r = 8M_{tot}$ where the radial velocity becomes equal to the circular velocity. However, as is pointed out by Cutler *et al.*,^[6] to improve the

signal-to-noise ratio in the detection of gravitational waves from a coalescing binary, we need to know the more accurate wave form theoretically, and to prepare reasonable initial conditions for future 3D relativistic numerical simulations of a coalescing binary we need to know the orbital parameters of the plunging orbit more in detail.

As a first step toward the above goal, we consider another approach C) here^[8]. Although perturbations of a black hole by a test particle have been extensively studied,^[9] the gravitational radiation from general bound orbits has not been investigated, except for circular ones. In our approach, although the nonlinear effect of gravity is neglected, characteristic features of the gravitational radiation induced by the fast motion in the strong gravitational field can be investigated. Therefore the test particle calculations are still quite meaningful and in a sense complementary to the approach B) for the study of the gravitational radiation.

2 Formulation

We calculate the perturbation by a test particle on the Schwarzschild geometry

$$ds^2 = -(1 - r/2M)^{-1} dt^2 + (1 - r/2M) dr^2 + r^2 d\Omega^2. \quad (1)$$

Here, we skip the detail of the formulation^[9], and just comment on what is different in our case of bounded orbit from the other which have ever been done.

The equation to be solved is the generalized Regge-Wheeler equation;

$$\left[\frac{d^2}{dr^{*2}} + \omega^2 - \frac{r-2}{r^4} \{(\lambda+2)r-6\} \right] X_{lm\omega}(r) = S_{lm\omega}(r), \quad (2)$$

where $r^* = r + 2 \log(r/2 - 1)$, and $X_{lm\omega}(r)$ and $S_{lm\omega}(r)$ are something like metric perturbation and projection of the energy momentum tensor of a test particle which is Fourier transformed with respect to t and expanded by the spherical

harmonics $Y_{lm}(\Omega)$. The quantity $S_{lm\omega}(r)$ has the form like

$$S_{lm\omega}(r) = \int_{-\infty}^{\infty} dt e^{i\omega t} T_{lm}(t, r), \quad (3)$$

schematically. As the time interval which has the dominant contribution to the integration is $(-\infty, \infty)$, this integration is divergent. Therefore the numerical estimate can not be done directly in this form. But, by virtue of the symmetry of the orbit like

$$r(t + \Delta t) = r(t), \quad \varphi(t + \Delta t) = \varphi(t) + \Delta\varphi, \quad (4)$$

as for $T_{lm}(t, r)$, the relation;

$$T_{lm}(t + \Delta T, r) = e^{-im\Delta\phi} T_{lm}(t, r), \quad (5)$$

holds. Therefore, the integration of the eq.(3) is reduced to the integration on finite time interval;

$$S_{lm\omega}(r) = \mu \sum_n \frac{2\pi}{\Delta t} \delta(\omega - \omega_n) \int_0^{\Delta T} dt e^{i\omega_n t} T_{lm}(t, r), \quad (6)$$

where ω_n is defined by

$$\omega_n = (2n\pi + m\varphi)/\Delta t. \quad (7)$$

3 Results and Discussions

Using the method which was outlined above, we study gravitational waves emitted by a test particle moving in the Schwarzschild metric. We introduce the semi-relativistic approximation here and show our main results in comparison with those evaluated by this approximation. In this approximation, the orbit of test particle is determined by the geodesic motion and is represented by the Schwarzschild coordinate like $r(t), \phi(t)$. By regarding this orbit as that

in flat space-time, i.e. $x_1(t) = r \cos \phi$, $x_2(t) = r \sin \phi$, $x_3(t) = 0$, we define the quadrupole moment $Q_{ij} = \mu x_i x_j$, where μ is the mass of a test particle. When we want to know the energy flux of gravitational waves, for example, it can be estimated by using the ordinary quadrupole formula

$$P = \frac{1}{5} \left(Q_{ij}^{(3)} Q_{ij}^{(3)} - \frac{1}{3} Q_{ii}^{(3)} Q_{jj}^{(3)} \right). \quad (8)$$

The ordinary quadrupole formula does not contain the following four effects, i.e., a) the effect that the orbit is determined not in fully relativistic manner but in Newtonian one, b) the gravitational redshift effect, c) contribution from the higher multipoles other than quadrupole, d) the curvature scattering and amplification effects. The effects a) and b) are included in the semi-relativistic approximation introduced here. Of course, it is difficult to distinguish the effects a) and c). So we consider that the definition of the distinction of a) and c) is given by the semi-relativistic approximation.

We show the ratio of the energy flux of the fully relativistic calculation to that in the semi-relativistic approximation for many orbits of various eccentricity in Fig.1. The horizontal axis represents the perihelion radius. As was known in the case of circular orbit, the relative error of the semi-relativistic approximation is less than 8% at $r_{min} \gtrsim 10M$ for general bounded orbits. However, this coincidence does not indicate that the semi-relativistic approximation is rather good.

We pointed out that there are two effects which are not taken into the semi-relativistic approximation, i.e., c) and d). To see the effect of c), in Fig. 2, we show the same plot as in Fig. 1 replacing the total energy flux of the fully relativistic calculation by its quadrupole component. Now we can see there is more than 10% discrepancy at $r_{min} \sim 30M$. To see the effect of d), in Fig. 3, we show the ratio of the quadrupole component to the total energy flux. The discrepancy is about 6% at $r \gtrsim 30M$. These results show that the agreement of the approximation is not so good as is expected from Fig. 1.

Here, we did not consider the back action to the orbit by gravitational wave emission, but our final aim is to calculate the wave pattern including the back action. We can calculate the averaged energy and angular momentum flux radiated as gravitational waves. If those values are known at each time, the orbit of a test particle is completely determined and so the back action by the gravitational wave emission is. However, since the energy and the angular momentum of the gravitational waves are non-local quantities, the orbit of the test particle including the effect of back action can not be determined directly from this calculation. However, it can be easily shown that it is possible to include the back action approximately as long as something like semi-relativistic approximation works in the way analogous to the standard method in Post-Newtonian approximation by virtue of its resemblance to the ordinary quadrupole formula. We have shown above that the semi-relativistic approximation is not good enough, but it seems possible to give an empirical good approximation by a small modification. On the point c), we used a natural identification between the point in the Schwarzschild geometry and that in the flat space-time, but we can replace it with an empirical relation. Since the relative error shown in Fig. 2 is almost independent of the eccentricity of the orbit, it can be reduced by changing the identification of the radial coordinates. As for the point d), if we include the octapole component, the approximation will be much improved. Our next step is to estimate the orbit and the wave pattern approximately with back action effect, taking into account those discussed above.

REFERENCES

1. K. Oohara and T Nakamura, Prog. Theor. Phys. **82**(1989), 535;
 — **83**(1990), 906;
 — **88**(1992), 307
2. T Nakamura and K. Oohara, Prog. Theor. Phys. **82**(1989), 1006;
 — **86**(1991), 73
3. M. Shibata, T Nakamura and K. Oohara, Prog. Theor. Phys. **88**(1992) in
 press;
 — YITP/K 989
4. C. W. Lincoln and C. M. Will, Phys. Rev. **D42** (1990), 1123
5. A. G. Wiseman, Phys. Rev. **D46** (1992), 1517
6. C. Cutler, L. S. Finn, E. Poisson and G. J. Sussman, Caltech preprint
 GRP-316, GRP-317
7. T. Tanaka, M. Shibata, M. Sasaki, H. Tagoshi, T. Nakamura, preprint
 KUNS-1175, YITP/K 1004, submitted to Prog. Theor. Phys.
8. T. Nakamura, K. Oohara and Y. Kojima, Prog. Theor. Phys. suppl. **90**

FIGURE CAPTIONS

- Fig. 1 :* Plot of relative errors in the semi-relativistic estimation of (a) the average energy flux and (b) the average angular momentum flux, against the periastron radius r_{min} . The vertical coordinate is $\delta Q = (\dot{Q}_{semi-rel} - \dot{Q}_{true})/\dot{Q}_{true}$, where $Q = E$ or J_z . All orbits in Table 1 are plotted. The closed circles denote the cases of almost circular orbits.
- Fig. 2 :* Plot of the ratio of the quadrupole component to the total energy flux. The closed circles are the same as above mentioned.
- Fig. 3 :* Same plot as Fig. 5(a) but compared with the energy flux where only the quadrupole contribution is accounted.

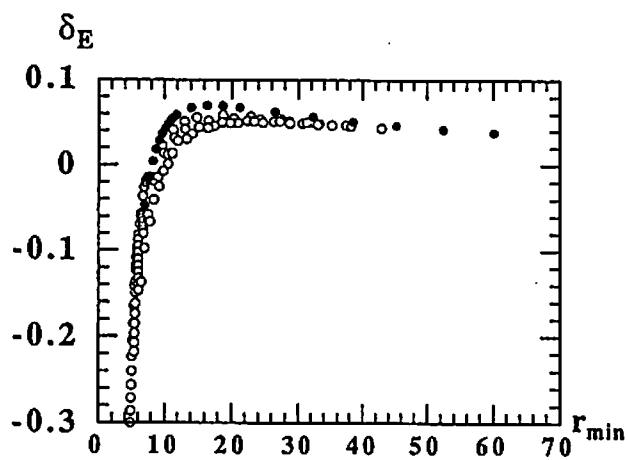


Fig.1

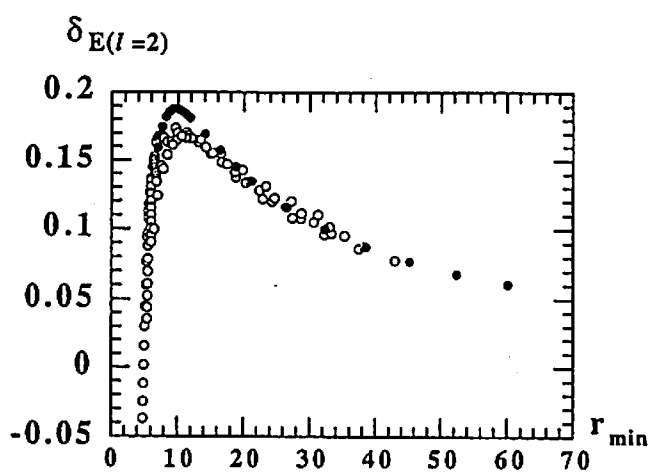


Fig.2

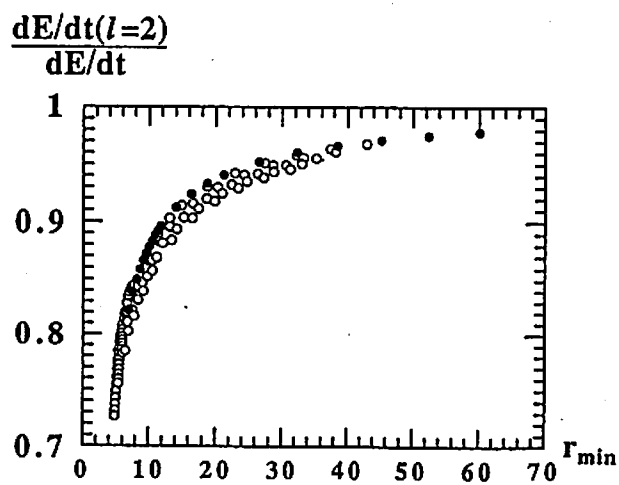


Fig.3

GRAVITATIONAL WAVE BURST PRODUCED BY MERGING OF CENTRAL BLACK HOLES OF GALAXIES

Toshikazu Ebisuzaki¹, Toshiyuki Fukushige¹, and Junichiro Makino²

¹ *Department of Earth Science and Astronomy,*
² *Department of Information Science and Graphics,*
College of Arts and Sciences, University of Tokyo
Komaba 3-8-1, Meguro-ku, Tokyo 153, Japan

Abstract

When galaxies merge, the central black holes rapidly sink toward the center of the system, and make a binary. We found that this black hole binary merges within $\lesssim 10^9$ years. This merging of black holes produces an intense burst of the gravitational wave. We investigated the nature of these gravitational wave bursts and found that the dimensionless amplitude at the earth is as high as 10^{-15} if black holes with the mass of $10^8 M_\odot$ merge at the distance of 2 Gpc. The mean time between burst is about 2 years if the elliptical galaxies are the merger remnants of galaxies having central black holes. In previous studies, the time scale of merging of black hole binary was estimated to be much longer than Hubble time ($\sim 10^{10}$ yr.). In those studies, the orbit of binary was assumed to be circular. We found, however, that the dynamical friction makes the orbit highly eccentric. The life time of a binary with a highly eccentric orbit is much shorter than that with a circular orbit, because the emission of the gravitational wave is much stronger for shorter periastron distance.

1. Introduction

Thorne and Braginsky (1976; hereafter TB) suggested that the formation and the collision of supermassive black holes ($M > 10^6 M_\odot$) produce bursts of the gravitational wave strong enough to be detectable at the earth. The dimensionless amplitude, h , and the period of the burst, P , are estimated as $h \sim 2 \times 10^{-15} \times (M/10^8 M_\odot)$ and $P \sim 150 \times (M/10^8 M_\odot)$ minutes, respectively. Such bursts can be detectable by, e.g., the Doppler tracking of a spacecraft (TB; Hellings 1979). TB estimated that the mean time between bursts is in the range of 1 week to 300 years, assuming that quasar activities are associated with the formation and the collision of black holes. The large uncertainty in their estimate mainly comes from ambiguity in the number of quasars.

We estimate the mean time between bursts from the number of elliptical galaxies (Fukushige, Ebisuzaki, and Makino 1992b). A significant fraction of elliptical galaxies are believed to have massive central black holes (Sargent *et al.* 1978; Young *et al.* 1978; Dressler 1989; Sadler 1984; Rees 1984). These central black holes would have experienced several bursts of the gravitational wave through their growth. For example, when galaxies merge, their central black hole also merge to produce a gravitational wave burst. Many theoretical works (Toomre and Toomre 1972; Toomre 1978; Barnes 1988; Okumura, Ebisuzaki and Makino 1991) and observations (Schweizer 1982; Bergvall, Rönnebeck and Johansson 1989; Wright *et al.* 1990) suggested that most elliptical galaxies have formed by merging. Therefore, such merging of black hole are expected to be fairly frequent.

Begelman, Blandford and Rees (1980) argued that the lifetime of a black hole binary formed in the core of a merger remnant is longer than the Hubble time ($\sim 10^{10}$ yr.). However, they overestimated the lifetime by a large factor, because they assumed that the orbit became circular. Ebisuzaki, Makino and Okumura (1991) suggested that their assumption is not correct and that the orbit of the black hole binary become highly eccentric. The

evolution of the black hole binary is driven by the dynamical friction from field stars. The strength of the dynamical friction is proportional to v^{-3} , where v is the velocity of the black hole. Therefore, the dynamical friction is strongest at the apocenter of the orbit, and the eccentricity of the binary increase through the evolution. As a result, the periastron distance of the black hole binary decreases much faster than the mean separation. Since the energy loss rate through the emission of the gravitational wave is determined by the periastron distance, the lifetime of the black hole binary would be much shorter than the estimate of BBR.

Fukushige, Ebisuzaki, and Makino (1992a) investigated the orbital decay of the black holes in a uniform distribution of field stars. They found that the orbital angular momentum decreases much faster than the orbital separation. They concluded that the central black holes merges within several dynamical times ($\sim 10^7 \text{ yr}$) of the core of the parent galaxy. Makino *et al.* (1992) performed self-consistent N-body simulations of the black hole binary in the core of a galaxy. According to their simulations, the time scale of the merging is as short as 10^9 years, although the decrease of the angular momentum slows down when the core begins to rotate in the same direction as that of black hole binary. One might think that the core of the merger would be rotating rapidly, if two galaxies merged with relatively large initial angular momentum. This rapid rotation of the core, if it would occur, might suppress the decrease of the angular momentum of the central black hole binary. However, such a rapidly rotating core is not likely to be found, since numerical simulations of mergers have shown that the inner half mass of the merger is rotating roughly rigidly. (Sugimoto and Makino 1989; Okumura, Ebisuzaki and Makino 1991).

We show that the mean time between bursts is in range of 2 to 5 years, assuming that elliptical galaxies are the merger remnants of galaxies that have central black holes (Fukushige, Ebisuzaki, and Makino 1992b). This mean time between bursts is consistent with the estimate of TB, who used the number of quasars in the universe. In section 2, we describe the expected character of the gravitational wave burst produced by the merging of central black holes. In section 3, we estimate the burst frequency. In section 4, we briefly discuss the detectability of these bursts.

2. Expected Character of The Burst

The period of the wave, P , is estimated as

$$\begin{aligned} P &\approx \frac{3\sqrt{3}\pi GM}{c^3}(1+z), \\ &= 8.1 \times 10^3 \left(\frac{M}{10^8 M_\odot} \right) (1+z) \quad (\text{s}), \end{aligned} \quad (1)$$

where M is the mass of the black hole, G is the gravitational constant, c is the light velocity and z is the redshift. According to TB, the dimensionless amplitude, h , is obtained by

$$h \approx \left(\frac{8\pi G P^2 F}{c^3} \right)^{\frac{1}{2}}, \quad (2)$$

where F is the energy flux of the gravitational wave at the earth. The energy flux, F , is given by

$$F = \frac{\epsilon M c^2}{4\pi R^2 P(1+z)}, \quad (3)$$

where ϵ is the efficiency of the energy release and R is the distance to the source from the earth. Assuming that the universe is flat, the distance, R , is calculated by

$$R = \frac{z}{1+z} \frac{c}{H_0}, \quad (4)$$

where H_0 is the Hubble constant. Using equations (2)(3)(4), the dimensionless amplitude, h , is estimated as

$$h \approx 2.1 \times 10^{-15} \left(\frac{1+Z}{Z} \right) \left(\frac{\epsilon}{0.05} \right)^{\frac{1}{2}} \left(\frac{M}{10^8 M_\odot} \right) \left(\frac{H_0}{100 \text{ km} \cdot \text{s}^{-1} \cdot \text{Mpc}^{-1}} \right). \quad (5)$$

The efficiency ϵ is estimated as about 0.05 by Nakamura, Oohara and Kojima (1987).

3. The Burst Frequency

The burst frequency, ν , is calculated as

$$\nu = \int_0^{H_0/c} 4\pi R^2 N_m(R) dR \quad (\text{yr}^{-1}) \quad (6)$$

where R is the distance to the burst source in the unit of Mpc , $N_m(R)$ is the frequency of merging per Mpc^3 .

In the following, we estimate $N_m(R)$ from the number of observed elliptical galaxies. The total number, n_{merge} , of merging that have occurred per Mpc^3 , is given by

$$n_{\text{merge}} = n_{\text{el}} \cdot N, \quad (7)$$

where n_{el} is the number density of the elliptical galaxies, and N is the average number of bursts that one elliptical galaxy experienced. Using $N_m(R)$, n_{merge} is calculated as

$$n_{\text{tot}} = \int_0^{t_H} N_m[c(t_H - t)] dt, \quad (8)$$

where t_H is the Hubble time. Here, we assume that most merging events happened after $z=2.5$. This assumption is consistent with the observation that the distribution of quasars has a sharp peak around $z \approx 2.5$ (e.g. Rees 1990). We consider two limiting cases for $N_m(R)$. First, we assume that all mergings have occurred at $z=2.5$, that is,

$$N_m(R) = cn_{\text{el}} N \cdot \delta(R - R_{2.5}), \quad (9)$$

where $\delta(R)$ is the delta function. From equations (6) and (9), we get

$$\nu \simeq 5.2 \times 10^{-1} \left(\frac{n_{\text{el}}}{3 \times 10^{-3} \text{ Mpc}^{-3}} \right) \left(\frac{N}{10} \right) \left(\frac{H_0}{100 \text{ km s}^{-1} \text{ Mpc}^{-1}} \right) (\text{yr}^{-1}). \quad (10)$$

Second, we assume that $N_m(R)$ is constant from $z=2.5$ to $z=0$, that is,

$$N_m(R) = \begin{cases} \frac{cn_{\text{el}} N}{R_{2.5}}, & (R \leq R_{2.5}) \\ 0, & (R > R_{2.5}) \end{cases} \quad (11)$$

where $R_{2.5}$ is the distance to the source at $z=2.5$. From equations (6) and (11), we get

$$\nu \simeq 1.7 \times 10^{-1} \left(\frac{n_{\text{el}}}{3 \times 10^{-3} \text{Mpc}^{-3}} \right) \left(\frac{N}{10} \right) \left(\frac{H_0}{100 \text{km s}^{-1} \text{Mpc}^{-1}} \right) (\text{yr}^{-1}). \quad (12)$$

From equations (10) (12), equation (6) becomes

$$\nu \simeq (1.7 - 5.2) \times 10^{-1} \left(\frac{n_{\text{el}}}{3 \times 10^{-3} \text{Mpc}^{-3}} \right) \left(\frac{N}{10} \right) \left(\frac{H_0}{100 \text{km s}^{-1} \text{Mpc}^{-1}} \right) (\text{yr}^{-1}). \quad (13)$$

The above equation shows that the burst occurs every 2 or 5 years. The burst frequency, ν , is insensitive to the assumption of functional form of $N_{\text{m}}(R)$.

We estimate the number density of ellipticals as $3 \times 10^{-3} \text{Mpc}^{-3}$ using the CfA survey data (Huchra *et al.* 1990). They made a complete sample of galaxies brighter than 15.5 mag. in the sky area of $\pi/13 \text{ str.}$, and found 384 elliptical galaxies in this volume. If we select the area of $z < 0.03$, n_{el} becomes 3.3×10^{-3} . Since the brightness of 15.5 mag. corresponds to the absolute magnitude of -19.5 at $z=0.03$, the sample in the volume of $z < 0.03$ would give reasonable estimate for fairly bright ellipticals.

4. Detectability

Gravitational wave bursts produced by supermassive black holes are detectable by the Doppler tracking of interplanetary spacecraft (Thorne and Braginsky 1976; Hellings 1979). Using Voyager I, Hellings *et al.* (1981) performed one observation of 500 second long and obtained an upper limit of $h = 3 \times 10^{-14}$. Recently, Bertotti *et al.* (1992) performed the measurement for much longer time using Ulysses, and they plan to continue their experiment using subsequent planetary missions such as Galileo and CRAF/Cassini. Continuous observations are essentially important to detect one event which may take place in several years. Simultaneous observations with several spacecraft are also important to increase the reliability of detections. The LAGOS project (Thorne 1992) aims at the detection of the gravitational wave of $h \sim 10^{-20}$ by means of laser interferometer in space. The burst produced by merging of the black hole is much stronger than this detection limit.

We thank Daiichiro Sugimoto, Yoshiharu Eriguchi for helpful discussions.

Reference

- Barnes, J. E. 1988, *Ap. J.*, **331**, 699
 Begelman, M. C., Blandford, R. D., and Rees, M. J. 1980, *Nature*, **287**, 307
 Bergvall, N., Rönnebeck, J., and Johansson, L. 1989, *A. & Ap.*, **222**, 49.
 Bertotti, B., Ambrosini, R., Asmar, S. W., Brenkle, J. P., Comoretto, G., Iess, L., Messeri, A. and Wahlquist, H. D., 1992, *A. & Ap.*, **92**, 431
 Dressler, A. 1989, in *Active Galactic Nuclei*, ed Osterbrock, D. E. and Miller, J. S., IAU Simp. No.139, 217
 Ebisuzaki, T., Makino, J., and Okumura, S. K., 1991, *Nature*, **352**, 212
 Fukushima, T., Ebisuzaki, T., and Makino, J., 1992a, *Publ. Astron. Soc. Japan*, **44**, 281.
 Fukushima, T., Ebisuzaki, T., and Makino, J., 1992b, *Ap. J. (Letters)*, **396**, L62.
 Hellings, R. W., 1979, *Phys. Rev. Lett.*, **43**, 470

- Hellings, R. W., Callahan, P. S., Anderson, J. D., and Moffet, A. T., 1980, *Phys. Rev. D*, **23**, 844
- Huchra, J. P., Geller, M. J., de Lapparent, V., and Corwin, Jr., H. G., 1990, *Ap. J. Suppl.*, **72**, 433
- Nakamura, T., Oohara, K., Kojima, Y., 1987, *Prog. Theor. Phys. Suppl.*, **90**, 135
- Makino, J., Fukushige, T., Okumura, S. K., and Ebisuzaki, T., 1992, *Publ. Astron. Soc. Japan*, in press.
- Okumura, S. K., Ebisuzaki, T., and Makino, J., 1991, *Publ. Astron. Soc. Japan*, **43**, 781
- Press, W. H. 1971, *Ap. J. (Letters)*, **170**, L105
- Rees, M. J., 1984, *Ap & A.*, **22**, 471
- Rees, M. J., 1990, *Science*, **247**, 817
- Sadler, E. M., 1984, *A. J.*, **89**, 53
- Sargent, W. L. W., Young, P. J., Boksenberg. A., Shortridge, K., Lynds, C. R., and Hartwick, F. D. A., 1978, *Ap. J.*, **221**, 731
- Schweizer, F. 1982, *Ap. J.*, **252**, 455
- Sugimoto, D. and Makino, J., 1989, *Publ. Astron. Soc. Japan*, **41**, 117
- Thorne, K. S., and Braginsky, V. B., 1976. *Ap. J. (Letters)*, **204**, L1
- Thorne, K. S. 1992. in *Recent Advance in General Relativity*, ed. J. Janis and J. Porter, Birkhauser, Boston, in press
- Toomre, A. 1977, in *Evolution of Galaxies and Stellar Populations*, ed. B. M. Tinsely and R. B. Larson, Yale Observatory, New York
- Toomre, A. and Toomre, J. 1972, *Ap.J.*, **178**, 623
- Wright, G. S., James, P. A., Joseph, R. D., and McLean, I. S. 1990, *Nature*, **344**, 417
- Young, P. J., Westphal, J., Kristian, J., Wilson, C. P., and Landauer, F. P. 1978, *Ap. J.*, **221**, 721

Implications of the COBE-DMR and South-Pole Experiments on CMB Anisotropies to Inflationary Cosmology

MISAO SASAKI

*Department of Physics, Faculty of Sciences,
Kyoto University, Kyoto 606*

Submitted to Prog. Theor. Phys.

ABSTRACT

We discuss implications of the discovery of the cosmic microwave anisotropy at 10° scale by COBE-DMR and the null result at 1° scale from the South-Pole experiment to inflationary universe models. In doing so, we derive an approximate analytic formula which relates the anisotropies at 10° and at 1° without a heavy numerical computation. The formula, when tested against the known numerical results, turns out to reproduce those results quite accurately, and gives us a clear insight into cause and effect of the intermediate and large angular CMB anisotropies. Then applying the formula to models with adiabatic density perturbations based on the inflationary universe scenario, we find that the only model compatible with the claimed observational data is either (i) a power-law (or extended) inflation model which predicts the power spectrum of density fluctuations with the power-law index $n \lesssim 0.8$, in which case the gravitational wave contribution to the CMB anisotropies on $\theta > 5^\circ$ FWHM is significant, or (ii) a natural inflation model with $n \lesssim 0.7$, in which case the gravitational wave contribution is negligible on all angular scales. In both of these cases, if the universe is dominated by cold dark matter, the resulting bias factor turns out to be $b \gtrsim 2$, i.e., a relatively large bias is unavoidable.

§ 1. Introduction

The first detection of cosmic microwave background (CMB) anisotropies by COBE-DMR [1] has given much excitement in the field of cosmology [2]. From the analysis of the data, Smoot *et al.* [1] concluded that the rms value of the anisotropy at 10° scale is

$$(\Delta T/T)_{10^\circ \text{FWHM}} = (1.1 \pm 0.2) \times 10^{-5}, \quad (1.1)$$

and the autocorrelation function is consistent with a power-law spectrum of the primordial density fluctuation; $P(k) \propto k^n$ with $n = 1.1 \pm 0.5$. Smoot *et al.* also claimed a finite detection of the quadrupole moment; $(\Delta T/T)_Q = (6 \pm 1.5) \times 10^{-6}$. However, here we disregard the reported value, since it may be an overestimate [3] or at least it is subject to a large cosmic variance. At any rate, unless one considers a rather eccentric scenario, Eq.(1.1) implies the existence of density fluctuations on super-horizon scales in the very early universe with an almost scale-invariant spectrum, a natural explanation of which is possible only in the context of the inflationary universe scenario.

However, soon after the discovery of CMB anisotropy by COBE-DMR, Gaier *et al.* [4] reported no detection of CMB anisotropy above $(\Delta T/T)_{\text{noise}} = 10^{-5}$ at 1° scale in the sky near the South Pole. This result is rather controversial, since the predicted rms temperature fluctuation at 1° scale for the scale-invariant spectrum, which is the case of the standard exponential inflationary scenario, is $\sim 2 \times 10^{-5}$. Hence one would naively expect that the probability of no signal detection is small. In fact, assuming $(\Delta T/T)_{10^\circ \text{FWHM}} = 1 \times 10^{-5}$, Gorski *et al.* [5] performed a detailed statistical analysis and concluded that all conceivable $\Omega = 1$ universe models with $n = 1$ spectrum are excluded at 95% C.L..

In this respect, the possible dominance of the tensor mode contribution to the CMB anisotropy and its relation to the scalar mode power spectrum has been discussed already by Davis *et al.* [6] and Lucchin *et al.* [7]. However, Davis *et al.* relies their analysis on the value of quadrupole moment detected by COBE, which is subject to large cosmic variations as mentioned above. Further, they seem to place too much emphasis on the tensor mode contribution to the CMB anisotropy.

On the other hand, Lucchin *et al.* gives a detailed analysis but only for power-law inflation models.

In this paper, we investigate all conceivable inflation models with adiabatic curvature perturbations having the spectral index $n \leq 1$ in a semi-quantitative but analytically tractable way and derive the constraint on these models from the results of 10° COBE-DMR and 1° South-Pole experiments. By doing so, we clearly demonstrate the essential factors that determine the intermediate and large angular CMB anisotropies.

§ 2. Scalar and tensor contributions to CMB anisotropy

If both of the results of COBE-DMR and South-Pole experiments should be taken seriously, one has to abandon at least the simplest scenario of exponential inflation. It is then a matter of great concern if this means the death of the inflationary universe scenario. Fortunately, it is not so but indeed there are other viable inflationary scenarios in which the power spectrum of density perturbations differs appreciably from $n = 1$. Among them are the scenarios of power-law inflation [8], extended inflation [9] and natural inflation [10]. In particular, the former two predict not only the matter density fluctuations but also a significant amplitude of fluctuations in the transverse-traceless part of the metric, *i.e.*, the gravitational wave perturbations, which may be actually the ones detected by COBE-DMR [6,7].

In what follows, we briefly review the origin of these fluctuations in the inflationary universe and give an estimate of the predicted amplitude of CMB anisotropy. Concerning the possible types of density perturbations, there is yet another possibility, namely isocurvature perturbations. However, here we focus on the curvature, (*i.e.*, the so-called adiabatic type) perturbations.

2.1 ORIGIN OF FLUCTUATIONS

In almost all of the inflationary scenarios, inflationary expansion of the universe is driven by the potential energy of some scalar field ϕ . At the stage when the universe is under inflation, the quantum fluctuations of the scalar field are rapidly redshifted to a macroscopic scale and give rise to super-horizon scale fluctuations in the matter density and hence the scalar-type perturbations in the metric which eventually turns into large scale structures of the universe.

The power spectrum of thus generated perturbation is given by [11,12]

$$\frac{4\pi k^3}{(2\pi)^3} P_{\mathcal{R}}(k) \equiv \langle \mathcal{R}^2 \rangle_k = \frac{H^4}{4\pi^2 \dot{\phi}^2} \Big|_{t=t_k}, \quad (2.1)$$

where \mathcal{R} is the spatial curvature perturbation measured on the comoving hypersurface and t_k is the time at which the comoving scale k leaves the Hubble horizon scale H^{-1} during the inflation. After the inflation, this in turn gives rise to perturbations in the Newtonian potential Ψ as

$$\langle \Psi^2 \rangle_k = \begin{cases} \left(\frac{3}{5}\right)^2 \langle \mathcal{R}^2 \rangle_k : & \text{matter-dominated stage;} \\ \left(\frac{2}{3}\right)^2 \langle \mathcal{R}^2 \rangle_k : & \text{matter-dominated stage.} \end{cases} \quad (2.2)$$

On the other hand, the quantum fluctuations of the gravitational wave modes are also redshifted to a macroscopic scale and give rise to the transverse-traceless (i.e., tensor-type) perturbations in the metric h_{ij}^{TT} . The power spectrum is given by [13]

$$\frac{4\pi k^3}{(2\pi)^3} P_T(k) \equiv \left\langle \left(h_{ij}^{TT} \right)^2 \right\rangle_k = 64\pi \frac{H^2}{4\pi^2 m_{pl}^2} \Big|_{t=t_k}, \quad (2.3)$$

where m_{pl} is the planck mass.

2.2 CMB ANISOTROPY

The CMB anisotropy induced by the perturbations discussed above can be calculated by solving the photon propagation equation in the perturbed Friedmann universe. Assuming the universe is spatially flat, matter-dominated after the baryon-photon decoupling, it is approximately given by [14]

$$\frac{\Delta T}{T}(\gamma^i; \eta_0) \approx \frac{1}{2} \int_{\eta_d}^{\eta_0} d\eta \left(\frac{\partial h_{ij}^{TT}}{\partial \eta} \gamma^i \gamma^j \right) + \frac{1}{3} \Psi(\eta_d) + \gamma^i \left(V_i(\eta_d) - V_i(\eta_0) \right), \quad (2.4)$$

where $\eta = \int^t dt/a(t)$ is the conformal time, η_d and η_0 are the decoupling time and the present time, respectively, γ^i is the direction cosine and V_i is the matter velocity perturbation. As it is clear, the first term in the right-hand-side of Eq.(2.4) is due to tensor-type perturbations, and the second and third to scalar-type ones. Following conventional terminology, we call the second the Sachs-Wolfe effect and the third the Doppler effect.

When discussing the CMB anisotropy, it is often convenient to express it in terms of its multipoles with respect to the spherical harmonics:

$$\frac{\Delta T}{T} = \sum_{\ell, m} a_{\ell m} Y_{\ell m}(\Omega_{\vec{\gamma}}). \quad (2.5)$$

Quadrupole

Among the multipoles, the lowest non-trivial one is the dipole, but it is generally believed (and is true for most of viable cosmological models) that the dipole is dominated by our peculiar velocity at present, i.e., $V_i(\eta_0)$. Hence, the lowest non-trivial multipole which carries the direct information of the early universe is the quadrupole. The mean square of it can be estimated from Eqs.(2.1)– (2.3), and (2.4) as

$$\begin{aligned} 4\pi Q_S^2 &\equiv \sum_m \langle a_{2m}^2 \rangle_S \approx \left. \frac{H^4}{60\pi\phi^2} \right|_{t_*}, \\ 4\pi Q_T^2 &\equiv \sum_m \langle a_{2m}^2 \rangle_T \approx 0.93 \left. \frac{H^2}{m_{pl}^2} \right|_{t_*}, \end{aligned} \quad (2.6)$$

where $k = H_0$, H_0 is the present value of the Hubble parameter and the scale factor at present has been normalized to unity; $a_0 = 1$. From Eq.(2.6), one finds

$$\frac{Q_T^2}{Q_S^2} \approx 56\pi \frac{\dot{\phi}^2}{m_{pl}^2 H^2} = 42 \left. \frac{\frac{1}{2}\dot{\phi}^2}{\frac{1}{2}\dot{\phi}^2 + V(\phi)} \right|_{t_1}. \quad (2.7)$$

Thus, the tensor mode contribution can dominate the quadrupole only if the kinetic energy of the scalar field is comparable to the potential energy of it at the inflationary stage.

Intermediate scales

At intermediate angular scales ($1^\circ \sim 10^\circ$), it is convenient to express the degree of anisotropy in terms of the temperature auto-correlation function,

$$C(\theta) = \left\langle \frac{\Delta T}{T}(\vec{\gamma} + \vec{\theta}) \frac{\Delta T}{T}(\vec{\gamma}) \right\rangle = \frac{1}{4\pi} \sum_l \langle a_l^2 \rangle P_l(\cos \theta),$$

where $\langle a_l^2 \rangle = \sum_m \langle a_{lm}^2 \rangle$. In the present case, $\langle a_l^2 \rangle$ can be approximately expressed as

$$\langle a_l^2 \rangle \approx \langle a_l^2 \rangle_{GW} + \langle a_l^2 \rangle_{SW} + \langle a_l^2 \rangle_{Doppler}, \quad (2.8)$$

where the first, second and third terms are the contributions from the gravitational waves, the Sachs-Wolfe effect, and the Doppler effect, respectively. For inflation models considered later, the primordial power spectrum is well approximated by a power-law. In such a case, the Sachs-Wolfe contribution can be analytically evaluated [15]. Further, for models of power-law (or extended) inflation, in which case the tensor contribution can become significant, one may assume $P_{\mathcal{R}}(k) \propto P_{\mathcal{T}}(k) \propto k^{n-4}$ [6,7]. In this case, one approximately has

$$\langle a_l^2 \rangle_{GW} \propto \langle a_l^2 \rangle_{SW} \simeq \frac{12}{5} \langle a_l^2 \rangle_{SW} \ell^{n-2}; \quad \ell \gg 1. \quad (2.9)$$

As for the Doppler term, noting that the Fourier component is given by

$$(\gamma^i V_i)_{\vec{k}} \doteq \frac{1}{3} \mu_k k \eta_d \Psi_{\vec{k}}; \quad \mu_k = \frac{\vec{k} \cdot \vec{\gamma}}{k}, \quad (2.10)$$

it may be approximated as

$$\langle a_l^2 \rangle_{Doppler} \sim \frac{\ell^2}{1+z_d} \langle a_l^2 \rangle_{SW} = \left(\frac{\ell}{\ell_d} \right)^2 \langle a_l^2 \rangle_{SW}, \quad (2.11)$$

where $z_d \sim 10^3$ is the redshift at decoupling and hence $\ell_d \sim 30$, which corresponds to the angular scale $\theta_d \sim 2^\circ$ ($= 5^\circ$ FWHM) or to the horizon scale at decoupling.

From Eqs.(2.9) and (2.11), one finds:

(a) $(\Delta T/T)_{10^\circ}$ is dominated by $\langle a_l^2 \rangle_{GW}$ and/or $\langle a_l^2 \rangle_{SW}$,

and

(b) $(\Delta T/T)_{1^\circ}$ is dominated by $\begin{cases} \langle a_l^2 \rangle_{Doppler} & \text{if } Q_T \ll Q_S, \\ \langle a_l^2 \rangle_{GW} \text{ and/or } \langle a_l^2 \rangle_{Doppler} & \text{if } Q_T \gtrsim Q_S. \end{cases}$

§ 3. $(\Delta T/T)$ -test of power spectrum

In order to evaluate the CMB anisotropy predicted in a given cosmological model in a quantitatively accurate way, one of course has to do numerical integrations. However, it is always useful to have an analytic formula to do a semi-quantitative analysis, not only because we may gain more clear understanding of cause and effect, but also we can obtain predictions of other models without a heavy numerical computation by simply varying the parameters in the formula. Furthermore, considering uncertainties in the observational data, it is sometimes meaningless to require a high accuracy in the resulting numbers. In this section, we give such a formula for cosmological models with a power-law spectrum discussed above and compare the result with the observations.

3.1 $(\Delta T/T)_{10^\circ}$ VERSUS Q_{rms}

According to Smoot *et al.*[1], the relevant theoretical formula which corresponds

to the mean square temperature fluctuation at 10° discovered by COBE-DMR is

$$\begin{aligned} \left(\frac{\Delta T}{T}\right)_{10^\circ}^2 &= C_{COBE}(0) = \frac{1}{4\pi} \sum_{\ell \geq 2} \langle a_\ell^2 \rangle e^{-\ell^2/\ell_0^2} \\ &\approx Q_{rms}^2 \times \frac{12}{5} \int_3^\infty \frac{d\ell}{\ell} \ell^{n-1} e^{-\ell^2/\ell_0^2} \\ &\approx Q_{rms}^2 \times \frac{12}{5} e^{-3^2/\ell_0^2} \frac{3^{n-1}}{1-n} \left(1 - \left(\frac{\ell_0}{3}\right)^{n-1}\right), \end{aligned} \quad (3.1)$$

where $Q_{rms} = \sqrt{Q_T^2 + Q_S^2}$ is the rms quadrupole moment, $\ell_0 = 17.8$ is the smearing scale relevant for COBE-DMR, and Eq.(2.9) has been used to approximate $\langle a_\ell^2 \rangle$. The above formula gives

$$\left(\frac{\Delta T}{T}\right)_{10^\circ} \approx \begin{cases} 2.0 Q_{rms}; & n = 1, \\ 1.6 Q_{rms}; & n = 0.8, \\ 1.4 Q_{rms}; & n = 0.6, \end{cases} \quad (3.2)$$

which are in good agreement with more accurate numerical results [1]. This shows our approximation is reasonable after all.

3.2 $(\Delta T/T)_{10^\circ}$ VERSUS $(\Delta T/T)_{1^\circ}$

Given the evidence that our approximation works fairly well, let us now turn to the anisotropies on intermediate angular scales.

The Sachs-Wolfe and tensor contributions

First consider contributions from the Sachs-Wolfe effect and gravitational waves. Again, from Eq.(2.9), one has

$$\begin{aligned} \left(\frac{\Delta T}{T}\right)_{1^\circ, SW+GW}^2(n) &\approx Q_{rms}^2 \times \frac{12}{5} \int_0^\infty \frac{d\ell}{\ell} \ell^{n-1} e^{-\ell^2 \sigma^2} f(\ell; \theta_0); \\ f(\ell; \theta_0) &= 2 \left(1 - P_\ell(\cos \theta_0)\right) \approx 2 \left(1 - J_0(\ell \theta_0)\right); \quad \theta_0 \ll 1, \ell \gg 1, \end{aligned} \quad (3.3)$$

where $\theta_0 = 0.037$ (2.1°) and $\sigma = 0.011$ (0.63°) are the beam separation and smearing angles, respectively, and f is the filter function, relevant for the South-Pole

experiment [4]. Unfortunately, the above integral cannot be done exactly. However, for $n = 1$, it may be evaluated as

$$\begin{aligned} \left(\frac{\Delta T}{T}\right)_{1^\circ, SW+GW}^2 &\approx \frac{12}{5} Q_{rms}^2 \int_0^{\frac{\theta_0^2}{4\sigma^2}} \frac{1-e^{-x}}{x} dx \\ &\approx \frac{12}{5} Q_{rms}^2 \left(\ln \frac{\theta_0^2}{4\sigma^2} + \gamma \right) \lesssim (10^{-5})^2, \end{aligned} \quad (3.4)$$

where $\gamma = 0.577 \dots$ is the Euler constant and the last figure is obtained from Eqs.(1.1) and (3.2) with $n = 1$. Now for a fixed value of $(\Delta T/T)_{1^\circ}$, $(\Delta T/T)_{1^\circ}(n)$ is apparently a decreasing function of n since the dominant contribution to the integral (3.3) comes from $\ell \gtrsim \theta_0^{-1} = 27 > \ell_0 = 17.8$. Hence we may conclude that the Sachs-Wolfe and gravitational wave contributions to the CMB anisotropy at 1° scale will not make a conflict with the observational upper bound for all values of $n \leq 1$.

The Doppler contribution

The above result tells us that the only contribution to the 1° anisotropy which we have to worry about is the one due to the Doppler effect. Using Eq.(2.11), it is approximately given by

$$\begin{aligned} \left(\frac{\Delta T}{T}\right)_{1^\circ}^2(n) &\approx \alpha Q_S^2 \int_0^\infty \frac{d\ell}{\ell} \left(\frac{\ell}{\ell_d}\right)^2 \ell^{n-1} e^{-\ell^2 \sigma^2} f(\ell; \theta_0) \\ &\approx \sigma^{1-n} \left(\frac{\Delta T}{T}\right)_{1^\circ}^2(1), \end{aligned} \quad (3.5)$$

where α is a constant of $O(1)$. Since the approximation (2.11) for the Doppler contribution is very crude, we should regard ℓ_d as an adjustable parameter rather than a given one, by absorbing the factor α . The adjustment can be done by using the fact that $(\Delta T/T)_{1^\circ}(1) \approx 3Q_S$ [5]:

$$\left(\frac{\Delta T}{T}\right)_{1^\circ}^2(1) \approx \frac{Q_S^2}{(\ell_d \sigma)^2} \left(1 - e^{-\frac{\theta_0^2}{4\sigma^2}}\right) = 3^2 Q_S^2. \quad (3.6)$$

This happens to give $\ell_d \sim 30$; an interesting coincidence that errors due to the

crudeness of Eq.(2.11) are canceled somehow by that of Eq.(3.5).

Combining the formulas (3.1) and (3.5) with Eq.(3.6), we obtain the final formula,

$$\left(\frac{\Delta T}{T}\right)_{1^\circ}(n) \approx 1.5 R F(n) \left(\frac{\Delta T}{T}\right)_{10^\circ}; \quad R = \sqrt{\frac{S}{T+S}}, \quad (3.7)$$

where

$$F(n) = \sqrt{\frac{(1-n)(3\sigma)^{1-n}}{1-(3/\ell_0)^{1-n}} \ln(\ell_0/3)} = \begin{cases} 1.00; & n = 1.0, \\ 0.77; & n = 0.8, \\ 0.60; & n = 0.6. \end{cases} \quad (3.8)$$

For the COBE-normalization; $(\Delta T/T)_{10^\circ} = 1.1 \times 10^{-5}$, the above formula gives

$$\left(\frac{\Delta T}{T}\right)_{1^\circ} \approx \begin{cases} 1.6 \times 10^{-5} R; & n = 1.0, \\ 1.3 \times 10^{-5} R; & n = 0.8, \\ 1.0 \times 10^{-5} R; & n = 0.6. \end{cases} \quad (3.9)$$

Comparing these numbers with the rms noise level of the South-Pole experiment; $(\Delta T/T)_{noise} = 10^{-5}$ [4], and taking into account the inaccuracy of our approximation (which we estimate as $\lesssim 10\%$), we conclude that (i) if $Q_T \gtrsim Q_S$, all models with $n \leq 1$ are consistent with the observational bound, but (ii) if $Q_T \ll Q_S$, even a model with $n = 0.8$ seems marginally excluded and a moderate allowable range would be $n \lesssim 0.7$.

§ 4. Models of inflation with $n < 1$

Now, let us examine models of inflation which can explain the observational data.

4.1 POWER-LAW (OR EXTENDED) INFLATION

Although the extended inflation is basically different from the power-law inflation in that the former is based on the Brans-Dicke type gravity theory [9] while the latter on the conventional Einstein gravity [8], both of them gives effectively the same law of inflationary expansion, i.e., the power-law expansion of the universe. Hence, here we focus on the proto-type power-law inflationary model.

The power-law inflation is driven by a scalar field with an exponential potential [8];

$$V(\phi) = V_0 \exp(\lambda \kappa \phi); \quad \kappa = \frac{\sqrt{8\pi}}{m_{pl}}. \quad (4.1)$$

The cosmic scale factor then approaches asymptotically to

$$a(t) \propto t^p; \quad p = \frac{2}{\lambda^2} (> 1), \quad (4.2)$$

At this asymptotic stage of inflation, both fluctuations in the scalar and tensor parts of the metric are produced with the same power-law index $n = (p - 3)/(p - 1)$. The ratio of the kinetic energy to the total energy density is given by

$$\frac{\frac{1}{2}\dot{\phi}^2}{\frac{1}{2}\dot{\phi}^2 + V(\phi)} = \frac{6}{\lambda^2} = \frac{1}{3p} = \frac{1-n}{3(3-n)}, \quad (4.3)$$

which, together with Eq.(2.7), implies

$$\frac{Q_T^2}{Q_S^2} \approx \frac{14}{p} = 14 \frac{1-n}{3-n}. \quad (4.4)$$

Hence $Q_T \gtrless Q_S$ for $p \lesg 14$, or $n \lesg 0.85$.

Thus, according to the power-law inflationary scenario, the conclusion of the previous section implies that the detected anisotropy at 10° by COBE-DMR must be dominated by the tensor mode contribution with the power-law index $n \lesg 0.8$. For cold dark matter (CDM) models, this implies the bias factor $b \gtrsim 2$ as mentioned in Davis *et al.* [6] and Lucchin *et al.* [7].

4.2 NATURAL INFLATION

In the scenario of natural inflation [10], the potential has the form,

$$V(\phi) = M^4 \left(\frac{1 + \cos(\phi/f)}{2} \right), \quad (4.5)$$

and inflation is assumed to occur when the scalar field is at $|\phi| \ll f$. In this case, the expansion is exponential;

$$a(t) \propto e^{Ht}; \quad H = \sqrt{\frac{8\pi}{3}} \frac{M^2}{m_{pl}}, \quad (4.6)$$

and $\phi^2 \ll V(\phi)$ so that the tensor mode contribution is negligible, but the power-law index of the density perturbation can differ appreciably from unity [10,12];

$$n \approx 1 - 2\delta; \quad \delta(\delta + 3) = \frac{3m_{pl}^2}{16\pi f^2}. \quad (4.7)$$

For example, for a typical GUT scale; $M \sim 10^{15}\text{GeV}$, a reasonable amplitude of the scalar perturbation; $\Psi \lesssim 10^{-4}$, is realized for $f \sim 5 \times 10^{18}\text{GeV}$. This value implies $\delta \sim 0.1$, hence $n \sim 0.8$.

Since the tensor perturbation must be necessarily negligible in this scenario, we conclude that $n \lesssim 0.7$ if the natural inflation should be adopted. In this case, the corresponding bias factor for CDM models is again $b \gtrsim 2$ [16].

§ 5. Summary

In this paper, we discussed the implications of the results of COBE-DMR and South-Pole experiments to inflationary universe models. For this purpose we derived a semi-analytic formula which relates the CMB anisotropies at 10° and 1° scales. In the context of inflationary cosmology, we found that only a power-law inflation models with the spectral index $n \lesssim 0.8$ and a natural inflation models with $n \lesssim 0.7$ are allowed, provided that the primordial power spectrum is of adiabatic

type. In both of these cases, the resulting bias factor b for CDM models is found to be $b \gtrsim 2$. This coincidence happens because the difference in the scalar mode amplitude at 10° , which corresponds to a scale $\sim 200 \text{ Mpc} h^{-1}$, is compensated by the difference in the rate of increase in the power spectrum as the scale goes down to $8 \text{ Mpc} h^{-1}$. Of course, to justify the above conclusion in the strict sense, we have to perform detailed numerical computations. However, as noted before, errors due to the crudeness of our approximation are expected to be buried well under uncertainties of the observational data.

Finally we note that if the existence of large-scale flow; $V(40 \text{ Mpc} h^{-1}) \sim 400 \text{ km}$, is proved and if it is found to be a typical value everywhere in the universe, it will be a clear contradiction to the null result of the South-Pole experiment, provided one relies on the standard gravitational instability scenario of large-scale structure formation [17]. A possible resolution is to assume reionization of the universe soon after decoupling until quite recently which smears out the CMB anisotropies on 1° scales. For this to occur, it seems necessary to have baryon isocurvature perturbations of a large amplitude on small scales [18], and interestingly enough there exists such a scenario in the context of power-law inflation models [19]. Therefore it may be worthwhile to investigate the predictions of such a model in more detail, or a hybrid model which includes *everything* necessary, though one cannot deny the feeling that the latter is too *ad hoc*.

I would like to thank K.M. Gorski and E.D. Stewart for stimulating conversations. This work was supported in part by the Grant-in-Aid for Scientific Research on Priority Areas of Ministry of Education, Science and Culture, No.04234104.

REFERENCES

1. G.F. Smoot *et al.*, *Astrophys. J.* 396 (1992) L1.
2. For implications of the COBE data to general cosmological models, see *e.g.*, N. Sugiyama and N. Gouda, *Prog. Theor. Phys.* 88 (1992) 803.
3. A. Gould, *Astrophys. J.* 403 (1993) L51.
4. T. Gaier *et al.*, *Astrophys. J.* 398 (1992) L1.
5. K.M. Gorski, R. Stompor and R. Juszkievicz, preprint YITP/U-92-36 (1992).
6. R.L. Davis *et al.*, *Phys. Rev. Lett.* 69 (1992) 1856.
7. F. Lucchin, S. Matarrese and S. Mollerach, preprint FERMILAB-Pub-92/185-A (1992).
8. F. Lucchin and S. Matarrese, *Phys. Rev. D* 32 (1985) 1316.
9. D. La and P.J. Steinhardt, *Phys. Rev. Lett.* 62 (1989) 376.
10. K. Freese, J.A. Frieman and A.V. Olinto, *Phys. Rev. Lett.* 65 (1990) 3233.
11. M. Sasaki, *Prog. Theor. Phys.* 76 (1986) 1036.
12. E.D. Stewart and D.H. Lyth, to be published in *Phys. Lett. B* (1993).
13. L. Abbott and M. Wise, *Nucl. Phys. B* 244 (1984) 541.
14. H. Kodama and M. Sasaki, *Prog. Theor. Phys. Suppl.* 78 (1984); *Int. J. Mod. Phys. A* 1 (1986) 265.
15. J.R. Bond and J. Efsthathiou, *MNRAS* 226 (1987) 655.
16. R. Cen *et al.*, *Astrophys. J.* 399 (1992) L11.
17. K.M. Gorski, *Astrophys. J.* 398 (1992) L5.
18. P.J.E. Peebles, *Astrophys. J.* 315 (1987) L73.
19. M. Sasaki and J. Yokoyama, *Phys. Rev. D* 44 (1991) 970;
K. Yamamoto *et al.*, *Phys. Rev. D* 46 (1992) 4206.

The Anisotropy of Cosmic Microwave Background Radiation produced by Gravitational Wave

Shin-ichi NAKAMURA[†], Noriaki YOSHINO^{*},
Shiho KOBAYASHI^{*1} and Akio HOSOYA^{*2}

[†] *Department of Applied Physics*

^{*} *Department of Physics*

Faculty of Science

Tokyo Institute of Technology,

Oh-Okayama 2-12-1, Meguro-ku, Tokyo 152, Japan

January, 1993

Abstract

We calculate the CMB anisotropy which is induced from gravitational wave. As for the gravitational wave, we consider the gravitational wave which arises from inflation. To compare with COBE's measurements directly, we estimate the correlation function with 7° FWHM.

As the results, we get constraint on GUT mass, that is, $M_{GUT} \leq 3 \times 10^{16}$ GeV. We emphasize that the contribution to the CMB anisotropy from gravitational wave cannot be ignored.

E-mail address: [†] snakamur@geo.titech.ac.jp

E-mail address: ^{*1} gewa@phys.titech.ac.jp

E-mail address: ^{*2} ahosoya@phys.titech.ac.jp

1. Introduction

Recently magnitude of an anisotropy of the cosmic microwave background (here after CMB) radiarion was reported by COBE's group [1]. Its observation clarified that the CMB anisotropy $\Delta T/T$ has a quite small value 10^{-5} at 10° scale (large scale). For such large scale, it has been said that the CMB anisotropy is mainly induced from the Sachs-Wolfe effect [2].

The relation between the CMB anisotropy and the Sachs-Wolfe effect concernd with an initial density perturbation and a formation of the large scale structure was investigated by Gouda and Sugiyama [3]. However, many authers [4] suggested that cosmic gravitational wave would make the CMB anisotropy through the Sachs-Wolfe effect.

Now we consider the contribution to the CMB anisotropy from only gravitational wave. As for cosmic gravitational wave, we are going to consider the one which arises from inflation. Because the inflationary theory predicts the production of the gravitational wave [5]. The initial quantum tensor perturbation grows to the gravitational wave due to the huge redshift by the exponential expansion of the universe.

Many authers [6] calculated the expectation values and variances of the lowest multipole moments of the $\langle (\Delta T/T)^2 \rangle$. However, it is difficult to compare their results of calculation with the mesurements of COBE directry. In order to compare with COBE'e mesurements, it is necessary to calculate the correlation function $\langle \Delta T/T \Delta T/T \rangle_{(\Theta=10^\circ)}$ with 7° FMHW. We shall calculate the correlation function as accurate as possible.

Note that ,in our paper, k and p are the momentum of photon and graviton, respectively.

2. Basic equations

We consider for a spatially flat FRW universe with metric;

$$ds^2 = a_{(\eta)}^2(-d\eta^2 + \gamma_{ij}dx^i dx^j), \quad (2.1)$$

where $\eta = \int dt/a$ is the conformal time and γ_{ij} is the metric of flat space. The full three metric which contains the deviation from the FRW metric is given by

$$g_{ij} = a_{(\eta)}^2(\gamma_{ij} + h_{ij}), \quad (2.2)$$

where h_{ij} describes a small deviation from FRW metric. As is well known, this deviation exhibits the gravitayional wave under the weak field approxmation. Now we consider only the gravitational wave, so h_{ij} is regarded as the gravitational wave.

Graviton

The gravitational wave is governed by the equation of motion;

$$h''_{ij} + 2\frac{a'}{a}h'_{ij} - \Delta^{(3)} h_{ij} = 0, \quad (2.3)$$

where prime denotes $\partial/\partial\eta$, and $\Delta^{(3)}$ denotes the Laplacian. As the same manner of canonical quantization, we can quantize the gravitational wave. The quantized gravitational wave which aries from inflation is expanded in terms of mode function $\psi_p(\eta)$ as

$$h_{ij} = \sqrt{16\pi G} \sum_{B=+,x} \int \frac{d^3p}{(2\pi)^{3/2}} (\epsilon_{ij(B)} \hat{A}_{p(B)} \psi_p e^{i\mathbf{p}\cdot\mathbf{x}} + h.c.), \quad (2.4)$$

with

$$\begin{aligned} [\hat{A}_p \hat{A}_{p'}^\dagger] &= \delta_{(p-p')}, \\ [\hat{A}_p \hat{A}_p] &= [\hat{A}_p^\dagger \hat{A}_p^\dagger] = 0. \end{aligned} \quad (2.5)$$

In the above $\hat{A}_{p(B)}$ and $\hat{A}_{p(B)}^\dagger$ are the annihilation and creation operators, respectively, $\epsilon_{ij(A)}$ the time-independent polarization tensor which satisfies $\epsilon_{ij(A)} p^i = 0$, $\epsilon_{ii(A)} = 0$ and $\epsilon_{ij(A)} \epsilon_{ij(B)} = 2\delta_{AB}$.

In order to calculate the gravitational wave which exists in the matter-dominated universe, we consider a simple cosmological model, which describes the three stages of the expanding universe: the inflation, the radiation-dominated and the matter-dominated epochs. We choose the Bunch-Davies vacuum for the initial condition in the inflatiuon epoch. We calculate time evolution of the Bunch-Davies vacuum in our simple cosmological model. The mode functions in the matter-dominated epoch is

$$\psi_p^M(\eta) = \alpha^{IM} u_p^M + \beta^{IM} (u_p^M)^*. \quad (2.6)$$

Here α, β are the Bogoliubov coefficients and u_p^M is the positive frequency part of the mode function which is written in terms of the Hankel function. Concrete forms for the

mode functions and the Bogoliubov coefficients are given by Nakamura et al [7]. Using this mode function, ψ_p^M , we can estimate the power spectrum of gravitational wave. The power spectrum is shown in Fig.1.

Sachs-Wolfe formula

We consider the light (photon) propagation in the FRW universe. The photon is described by

$$\text{null eq.} \quad g_{\mu\nu} k^\mu k^\nu = 0, \quad (2.7)$$

$$\text{geodesic eq.} \quad k^\mu{}_{;\nu} k^\nu = 0. \quad (2.8)$$

We carry out the linear perturbation theory with setting $\tilde{k}_\mu = k_\mu + \delta k_\mu$ and $\tilde{g}_{ij} = a^2(\gamma_{ij} + h_{ij})$. From the perturbed null equation, $\tilde{g}_{\mu\nu} \tilde{k}^\mu \tilde{k}^\nu = 0$, and the perturbed geodesic equation, $\tilde{k}^\mu{}_{;\nu} \tilde{k}^\nu = 0$, we obtain the fluctuation of temperature:

$$\begin{aligned} \frac{\Delta T}{T} &= \frac{\delta k^0}{k^0}, \\ &= -\frac{1}{2} \int_{\eta_d}^{\eta_0} \frac{\partial h_{ij}}{\partial \eta} \frac{k^i k^j}{k^2} d\eta, \end{aligned} \quad (2.9)$$

where η_d and η_0 are the conformal time at decoupling and present times, respectively. Generally the CMB anisotropy induced from the Sachs-Wolfe effect is related to the formation of the large scale structure. However, the CMB anisotropy from cosmic gravitational wave also is evaluated by the same Sachs-Wolfe formula.

Correlation function

We calculate a correlation function directly. The correlation function is given by

$$\left\langle \frac{\Delta T}{T} \frac{\Delta T}{T} \right\rangle = \frac{1}{4} \int_{\eta_d}^{\eta_0} d\eta \int_{\eta_d}^{\eta_0} d\eta' \left\langle \frac{\partial h_{ij}}{\partial \eta} \frac{\partial h_{kl}}{\partial \eta'} \frac{k^i k^j k^k k^l}{k^4} \right\rangle. \quad (2.10)$$

Substituting Eq.(2.4) into Eq.(2.10), we find

$$\left\langle \frac{dh_{ij}}{d\eta} \frac{dh_{kl}}{d\eta'} \right\rangle \frac{k^i k^j k^k k^l}{k^4} = \frac{G}{\pi^2} \int d^3 p \frac{\partial \psi_p}{\partial \eta} \frac{\partial \psi_p^\dagger}{\partial \eta'} P_{ij,kl} \frac{k^i k^j k^k k^l}{k^4} e^{i \mathbf{p} \cdot (\mathbf{x} - \mathbf{x}')} \quad (2.11)$$

where $P_{ij,kl} = \sum_{A=\pm, \times} \epsilon_{ij(A)} \epsilon_{kl(A)} = \hat{\delta}_{ik} \hat{\delta}_{jl} + \hat{\delta}_{il} \hat{\delta}_{jk} - \hat{\delta}_{ij} \hat{\delta}_{kl}$ with $\hat{\delta}_{ij} = \delta_{ij} - p_i p_j / p^2$.

In order to calculate above integral, we set up coordinate system (Fig.2). At first, we perform average over ϕ and θ , i.e. $(\int \dots \sin \theta d\phi d\theta) / 2\pi^2$. We obtain

$$\begin{aligned} \left\langle \frac{\Delta T}{T} \frac{\Delta T}{T} \right\rangle_{(\Theta)} = \frac{G}{\pi^3} \int_{\eta_d}^{\eta_0} d\eta \int_{\eta_d}^{\eta_0} d\eta' \int_0^\infty p^2 dp \frac{\partial \psi_p}{\partial \eta} \frac{\partial \psi_p^1}{\partial \eta'} (C_4 j_4(pr) \\ + C_2 j_2(pr) + C_0 j_0(pr)), \end{aligned} \quad (2.12)$$

with

$$\begin{aligned} C_4 &= -\frac{8}{35}(1 - 3 \cos^2 \Theta) + \frac{2}{7}(9 \cos^2 \Theta + 7) \frac{x^2 x'^2}{r^4} - \frac{16}{7} \cos \Theta \sin^2 \Theta \frac{x^3 x' + x x'^3}{r^4}, \\ C_2 &= \frac{16}{21}(1 - 3 \cos^2 \Theta) + \frac{16}{7} \cos \Theta \sin^2 \Theta \frac{x x'}{r^2}, \\ C_0 &= -\frac{8}{15}(1 - 3 \cos^2 \Theta). \end{aligned} \quad (2.13)$$

In the above, $j_4(pr)$, $j_2(pr)$ and $j_0(pr)$ are the spherical bessel functions. The relation between x, x', r and η is given by $x = \eta = \eta_d$, $x' = \eta' - \eta_d$ and $r^2 = x^2 + x'^2 - 2xx' \cos \Theta$, respectively. Note that the above formula is written in any gravitational wave.

Here we use the mode function derived from inflation theory, i.e., eq.(2.6). First, we perform the momentum integral ($\int \dots dp$) exactly. Next we perform η -integral numerically. As a result we get Fig.3. Moreover the correlation function smoothed by 7° FWHM is Fig.4.

3. Conclusion and Discussions

It is possible to make constraint on any model of inflation. The GUT mass during the inflation phase must be less than 3×10^{16} GeV, or else there gravitational wave will produce unacceptably large CMB anisotropy.

Through the contribution to the CMB anisotropy from gravitational wave was ignored, we emphasize that its contribution must not ignore. The CMB anisotropy measured by COBE originate in not only primordial density perturbation but also gravitational wave. It is practically impossible to separate them. If we take the GUT mass to be 10^{16} GeV, which is a characteristic value, the contribution from gravitational wave is dominant rather than the one from density perturbation.

More detailed discussion will be published by Kobayashi et al [6].

4. Acknowledgments

We wish to thank Dr. K.Watanabe and Dr. Y.Nambu for extremely helpful discussion and comments.

5. References

- [1] G.F.Smoot et al., Ap.J.Lett. 396 (1992) L1
C.L.Bennet et al., Ap.J.Lett. 396 (1992) L7
G.F.Smoot et al., Ap.J. 360 (1990) 685
J.C.Mather et al., Ap.J.Lett. 354 (1990) L37
- [2] R.K.Sachs and A.M.Wolfe, Ap. J. 147 (1967) 73
- [3] N.Sugiyama and N.Gouda, Prog.Theo.Phys. 88 (1992) 803
N.Gouda and N.Suguyama, Ap.J.Lett. 395 (1992) L59
- [4] A.Starobinsky, JEPT Lett. 30 (1979) 682
V.Rubakov, M.Sazhin and A.Veryaskin, Phys. Lett. 115B (1982) 189
R.Fabbri and M.Pollock, Phys. Lett. 125B (1983) 445
L.F.Abbot and M.B.Wise, Nucl. Phys. B244 (1984) 541
L.F.Abbot and M.B.Wise, Phys. Lett. 135B (1984) 279
K.Tomita and K.Tanabe, Prog.Theo.Phys. 69 (1983) 828
- [5] L.F.Abbot and D.D.Harari, Nucl. Phys. B264 (1986) 487
- [6] V.A.Rubakov, M.V.Sazhin, and A.V.Veryaskin, Phys. Lett. 115B (1982) 189
R.Fabbri and M.D.Pollock, Phys. Lett. 125B (1983) 445
L.F.Abbot and R.Schaefer, Astrophys. J. 308 (1986) 546
- [7] S.Nakamura, N.Yoshino and S.Kobayashi, Prog. Theo. Phys. 88 (1992) 1107
- [8] S.Kobayashi, S.Nakamura, N.Yoshino and A.Hosoya, 1993, in preparation

6. Figure captions

Fig.1 the geometry and coodinate system.

Fig.2 The power spectrum of the gravitational wave $h_{(k)}$ is plotted as a function of the frequency ν . Here we identify the present Hubble horizon with 6000Mpc ($\simeq 1.6 \times 10^{-18}$

Hz).

Fig.3 The bare correlation function $\langle \Delta T/T \Delta T/T \rangle_{(\Theta)}$ is plotted as a function of Θ .

Fig.4 The correlation function $\langle \Delta T/T \Delta T/T \rangle_{(\Theta)}$ with 7° FWHM is plotted as a function of Θ .

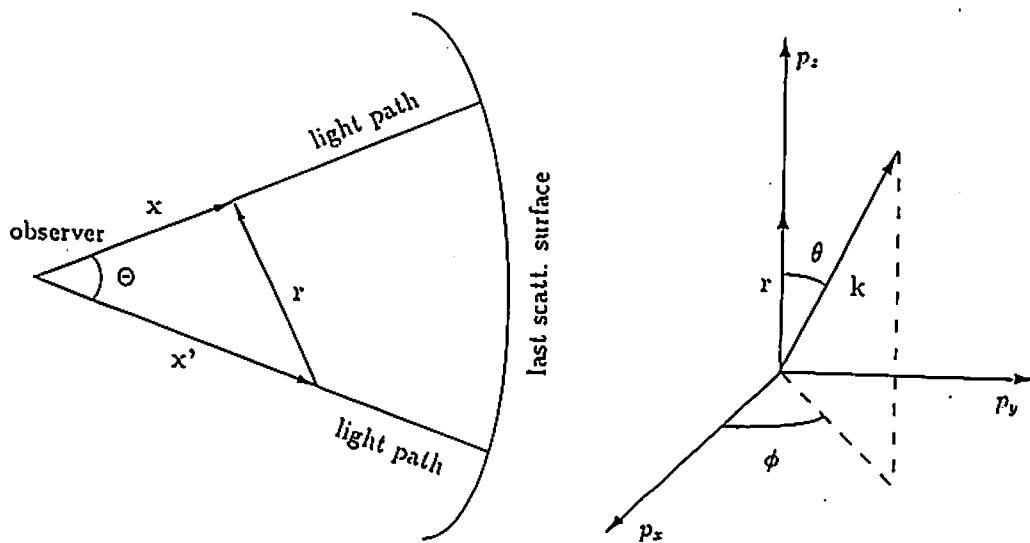
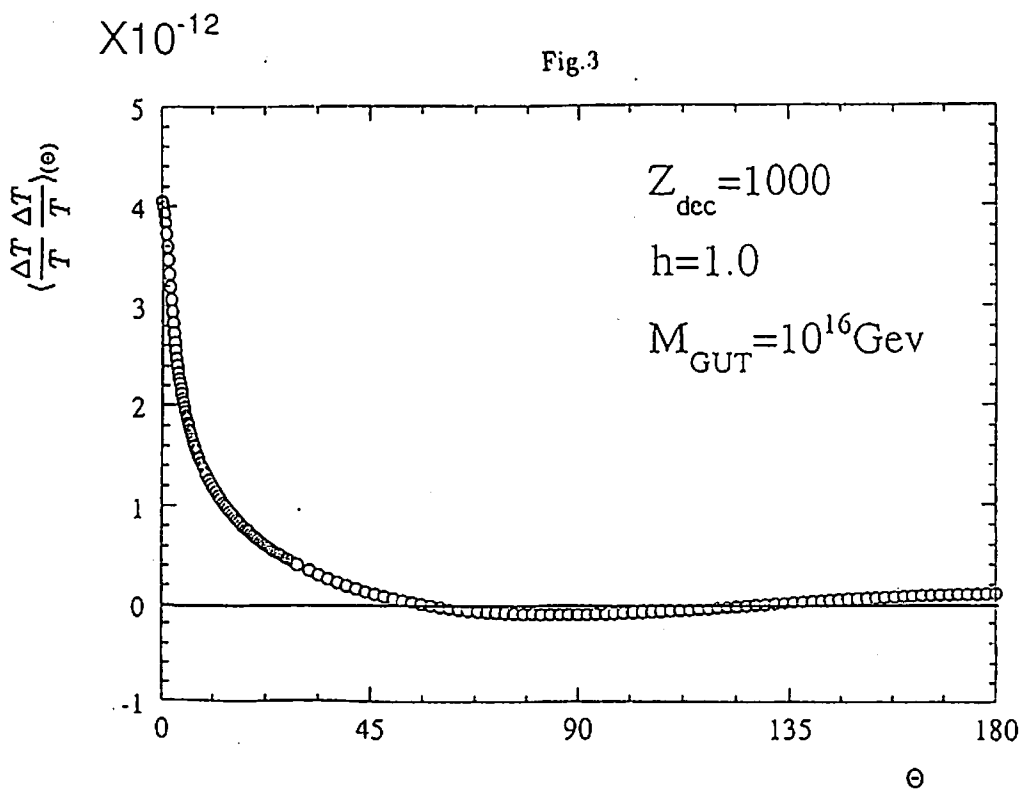
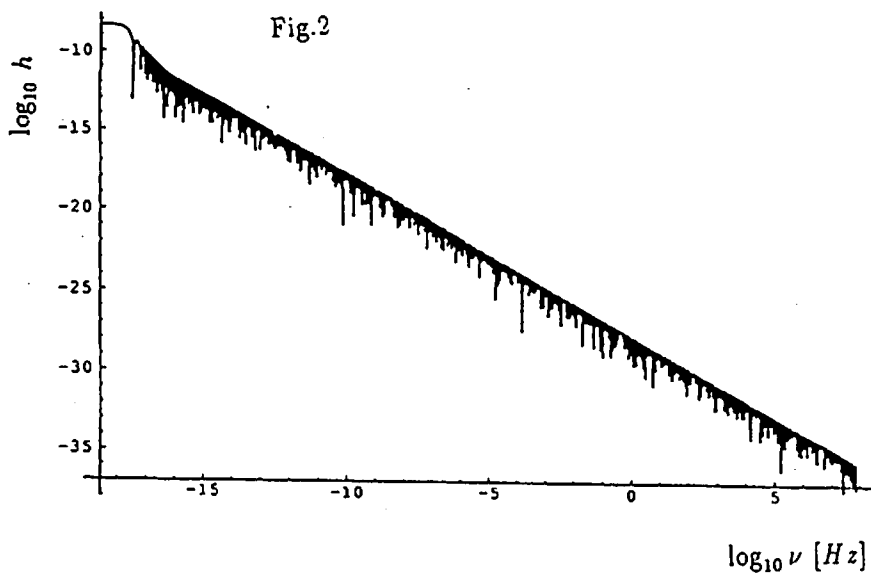
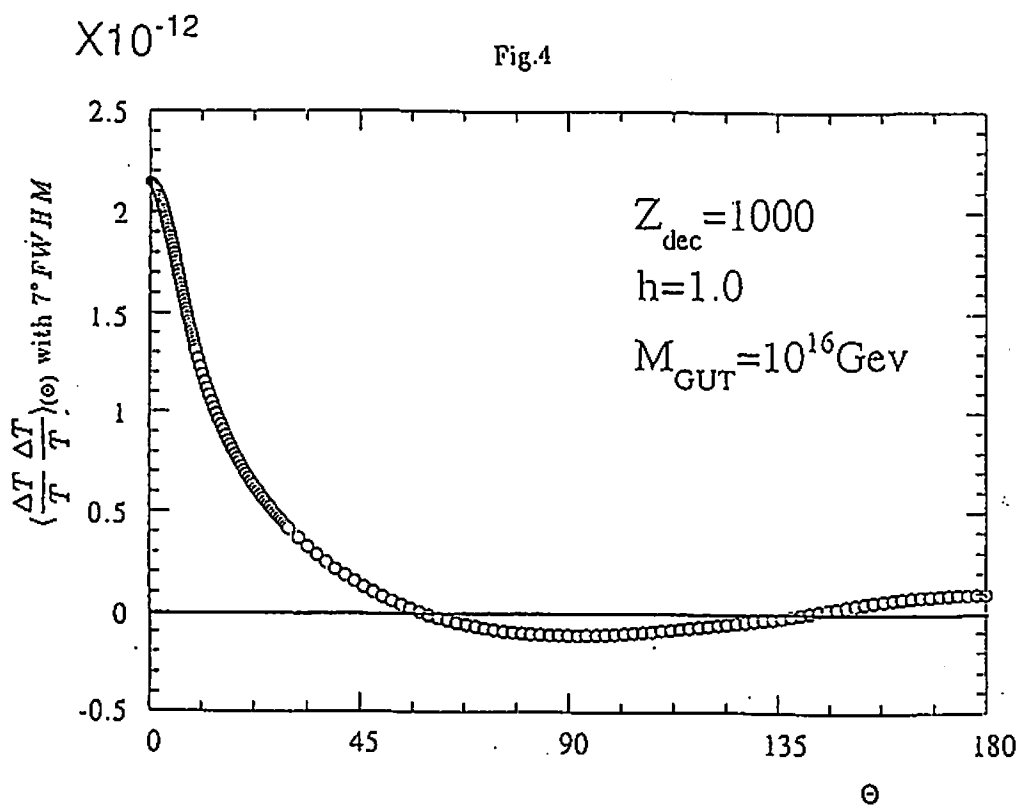


Fig.1





Smoothing of the Anisotropy of the Cosmic Background Radiation by gravitational scattering

Toshiyuki Fukushima*, Junichiro Makino† and Toshikazu Ebisuzaki*

**Department of Earth Science and Astronomy,*

†Department of Information Science and Graphics,

College of Arts and Sciences, University of Tokyo,

3-8-1 Komaba, Meguro-ku, Tokyo 153, Japan

Abstract

The homogeneity of the cosmic microwave background radiation (CBR) is one of the most severe constraint for the theory of the structure formation in the universe. We investigated the effect of the gravitational scattering of galaxies, clusters of galaxies, and superclusters on the anisotropy of the CBR by numerical simulations. Although this effect was thought to be unimportant, we found that the gravitational scatterings by superclusters reduce the anisotropy of the CBR significantly. We took into account the exponential growth of the distance between two rays due to multiple scatterings. This exponential growth is caused by coherent scatterings, and was neglected in previous studies. The gravitational scattering by superclusters reduces the observed temperature anisotropy of the CBR at present time approximately by 30 % from that at the recombination time, for angular scale up to a few degrees.

1. Introduction

Observations have shown that the cosmic microwave background radiation (CBR) is extremely isotropic. Observed upper limit of the temperature fluctuation, $\Delta T/T$, of the CBR is $\sim 4.5 \times 10^{-5}$ at $4'.5$ [1], and $\sim 2.1 \times 10^{-5}$ at $7'.15$ [2]. Recent observation with COBE shows that the temperature fluctuation is $(1.1 \pm 0.18) \times 10^{-5}$ at 10 degrees [3], and the observation at South Pole shows that the upper bound is 1.4×10^{-5} at a degree scale [4]. If the density fluctuation is actually small as suggested by these observations, the structure formation models which are consistent with the "observed" temperature anisotropy are rather few. For example, baryon dominant model is ruled out [5][6]. In addition, the standard CDM model is only marginally acceptable [7].

During its travel from the last scattering surface, the CBR is gravitationally scattered by astronomical objects such as galaxies, clusters of galaxies, and superclusters. We investigate this effect of gravitational scattering on the anisotropy of the CBR, taking into account the exponential growth of the distance between nearby rays through multiple scatterings. We found that the temperature anisotropy of the CBR can be reduced by 30% through scatterings by superclusters.

The smoothing of CBR by the gravitational lensing has been investigated by many researchers [8]-[14]. Sasaki [11] and Linder [12] gave the mathematical formula of the gravitational lensing on angular correlation function of the temperature anisotropy.

Kashlinsky [9] derived the equation that describes the multiple gravitational lensing of the CBR, and concluded that the original fluctuation was smoothed out on scales up to several arcminutes. Cole and Efstathiou [10] pointed out that Kashlinsky overestimated this effect because he modeled galaxy clusters as point masses. They argued that the effect is negligible using the formula of the increase of the beam width derived by Gunn [15]. Blanchard and Schneider [8] and Watanabe and Tomita [13] also obtained similar results. Tomita and Watanabe [14] performed numerical simulations of the propagation of light, and concluded that the effect of the gravitational lensing by clusters of galaxies was small.

Gunn [15] derived the formula for the change of the beam width under the assumption that the total effect of increase of the beam width is expressed by a superposition of that of small scatterings. However, this assumption is not appropriate. If the distance between two rays is small, they are scattered coherently. In the case of two dimensional space, the average increase of the distance between rays by one scattering is proportional to its width, since the difference in the deflection angle is caused by the tidal force. As a result, the distance increases exponentially by multiple scatterings. This exponential growth continues until the scattering becomes incoherent. Therefore, the increase of the distance between beams evidently cannot be expressed by a simple superposition.

In the three-dimensional space, the behavior of the rays is more complicated than what is described above. The angle increases, if the rays and the scattering object are in the same plane; the angle decreases, if the impact parameter vector is perpendicular to its distance vector between two rays. The net change is positive and proportional to the initial angle, if the amount of the change in the angle is averaged over the position angle of encounters.

In the field of stellar dynamics, this exponential growth of a small difference of initial condition has been well known [16]-[21]. However, a clear theoretical understanding of this exponential growth was given only recently by Goodman, Heggie and Hut [22].

In this paper, we investigate this exponential growth of the distance between nearby

rays by numerical calculations, and evaluate its effect on the anisotropy of the CBR. We calculate sets of path of two photons in a uniform distribution of scattering objects. We use the post-Newtonian equations of motion for photon [23] given by

$$\frac{d^2\mathbf{x}}{dt^2} = 2\nabla\phi - 4\mathbf{n}(\mathbf{n} \cdot \nabla\phi), \quad (1)$$

where \mathbf{x} is the position of photon, ϕ is the gravitational potential, and \mathbf{n} is the initial direction vector which satisfies $|\mathbf{n}| = 1$. This post-Newtonian approximation is always valid in a real universe, unless we consider a universe dominated by supermassive black holes. The maximum deflection angle of a scattering by an object is determined by the depth of its potential well. The depth of the potential well of galaxies, clusters of galaxies or superclusters are by far smaller than c^2 . In the numerical calculation, we ignore the second term of right hand-side of equation (1), since the purpose of our calculation is to obtain the trajectory of a photon. The second term changes the deflection angle through the change of the light velocity. Since the change of the velocity and the deflection are both $O(\phi/c^2)$, the contribution of the second term to the deflection is $O[(\phi/c^2)^2]$, which is negligible.

Our calculation showed that the angle between two rays increases exponentially up to an angle θ_{pr} given by

$$\theta_{\text{pr}} = \sqrt{4\pi} N^{-\frac{1}{2}}, \quad (2)$$

where N is the number of the scattering objects within the horizon of the present universe, in the case of a flat universe. When the angle becomes larger than θ_{pr} , it increases in proportion to $t^{1/2}$. This is because the scattering becomes incoherent within a beam [19].

The angle grows exponentially only when the size of the scattering objects, ϵ , is smaller than the projected mean particle distance d_{pr} :

$$d_{\text{pr}} = \sqrt{4\pi} N^{-\frac{1}{2}} R_H, \quad (3)$$

where R_H is the distance to the horizon. We found that superclusters satisfies this condition of exponential growth, $\epsilon < d_{\text{pr}}$, and that θ_{pr} is a few degrees for superclusters. We, therefore, conclude that the anisotropy of the CBR is smoothed up to a scale of a few degrees. We evaluated the angular correlation function using the formula derived by Wilson and Silk[24], and Sasaki[11]. We found that the gravitational scattering due to superclusters can decrease the anisotropy of the CBR approximately by 30% if the beam width of antenna is not much smaller than the intrinsic angular scale of the fluctuation.

2. Numerical Simulations

We calculate the trajectory of a photon using the gravitational potential expressed as

$$\nabla\phi = -Gm_{s,j} \sum_j^N \frac{\mathbf{x} - \mathbf{x}_{s,j}}{[|\mathbf{x} - \mathbf{x}_{s,j}|^2 + \epsilon^2]^{\frac{3}{2}}} + \frac{GM}{R^3} \mathbf{x}, \quad (4)$$

where G is the gravitational constant, N and M are the number and the total mass of the scattering objects, $\mathbf{x}_{s,j}$ and $m_{s,j}$ are the position and mass of the j -th scattering object, R is the radius of the sphere in which scattering objects are uniformly distributed, and ϵ is the size of the scattering object. We used the system of the unit in which $G = R = 1$ and $M = 1/2$, and we used the unit of time determined by this system of the unit.

The masses of the scattering objects are set to be equal to each other, i.e., $m_{s,j} = M/N$. The second term of the right hand side of equation (4) is introduced to cancel the global harmonic potential due to scattering objects. We started the numerical integration of the trajectory of photons at the surface of the sphere. The initial velocity vector, \mathbf{v}_0 , of a photon points to the center of the sphere and its length is unity. To calculate the growth of the width of an initially narrow beam, we calculated the trajectory of a photon from slightly different initial condition. We performed simulations for three cases: $N = 128, 1024, 8192$. We used GRAPE-2A [25], a special-purpose computer for N -body problem, for the calculation of the gravitational force. We integrated the orbits with the 4-th order Runge-Kutta scheme with an automatic timestep adjustment [26]. The details of our discussion are presented elsewhere [27].

Figure 1 shows the growth of the angle, θ , between the velocity vectors of two photons in the case of $N = 1024$ and $\epsilon = 0$ for eight different values for the initial angle between velocity vectors. Each curve represents the median value of 200 orbit pairs. This angle grows exponentially until θ becomes close to θ_{pr} .

In figure 2, growth factor, $\alpha = \theta_{1.5}/\theta_0$, is plotted against θ_0/θ_{pr} where θ_0 and $\theta_{1.5}$ are the values of θ at $t = 0$ and 1.5, respectively. Figure 2 is divided into three regions, depending on the value of θ_0/θ_{pr} , i.e., exponential, transitional, and diffusive region. If $\theta_0/\theta_{pr} < 0.1$, the growth factor, α , is about 10, independent of the initial condition. In this region, the beam width grows exponentially. If $0.1 < \theta_0/\theta_{pr} < 1$, the growth factor α is almost proportional to θ_0^{-1} . The growth factor α is roughly θ_{pr}/θ_0 . In this region, θ increases up to θ_{pr} . If $\theta_0/\theta_{pr} > 1$, the growth factor, α , is order of unity. This behavior is independent of the number of the scattering objects, N .

The growth factor, α^* , in an expanding universe is calculated as

$$\alpha^* = \exp \left[\int_{t(z=z^*)}^{t(z=0)} \frac{1}{\tau^*(t)} dt \right], \quad (5)$$

where z^* is the redshift at which the scattering objects were formed, and $\tau^*(t)$ is the e -folding time of the angle [21][22], which is calculated from the results of our calculations:

$$\tau^*(t) = \tau_0 \left[\frac{\rho(t)}{\rho_0} \right]^{-\frac{1}{2}}, \quad (6)$$

where $\rho(t)$ is the density of scattering objects, and τ_0 and ρ_0 are the e -folding time and density in our calculation. The value of τ_0 is estimated by the relation; $\theta = \theta_0 \exp(t/\tau_0)$. We estimate $\rho(t)$ assuming that the universe is flat. The growth factor α^* becomes

$$\alpha^* = (1 + z^*)^\eta, \quad (7)$$

where

$$\eta = \frac{\Omega_s^{1/2}}{\tau_0}.$$

Here, Ω_s is density parameter of scattering objects. The growth factor, α_{LS} , of the angle between two photons that come from the last scattering surface is calculated as

$$\alpha_{LS} = \frac{1}{\theta_0 R_{LS}} \left[\int_0^{R^*} \theta dR + \alpha^*(R_{LS} - R^*) \right] \simeq \frac{\eta}{\eta - 1} (1 + z^*)^{\eta-1} - \frac{1}{\eta - 1}, \quad (8)$$

where R_{LS} is the distance to the last scattering surface from $z = 0$, and R^* is to $z = z^*$

In figure 3, the growth factor, α , is plotted against ϵ/d_{pr} . The initial angle is chosen so that $\theta_0/\theta_{pr} < 1$. Figure 3 is again divided into three regions, depending on ϵ/d_{pr} . If $\epsilon/d_{pr} < 0.08$, the growth factor, α , is about 10, independent of ϵ/d_{pr} . In this region, the beam width grows exponentially. If $0.08 < \epsilon/d_{pr} < 0.3$, the growth factor is proportional to ϵ^{-1} . If $\epsilon/d_{pr} > 0.3$, the growth factor, α , is the order of unity.

In table 1, we summarize the estimate of ϵ/d_{pr} for galaxies, clusters of galaxies, and superclusters. Here, we gave the value of ϵ , d , and calculated the distance, d_{pr} , using the relation $(4\pi/3)(R_H \Omega_s^{-1/2}/d \Omega_s^{-1/3})^3 = 4\pi(R_H \Omega_s^{-1/2}/d_{pr})^2$ where R_H is the distance to the horizon and d is the mean particle distance between the scattering objects. We adopt R_H of 3Gpc. For the cases of superclusters ($\Omega_s = 1$), $\epsilon/d_{pr} \ll 1$ and $\alpha^* \gg 1$. It increases the angle of the CBR by a large factor. Here, we assume that the superclusters have a large fraction of the mass in the Universe. This can be justified by the observation showing that the universe consists of the void with very low density and the structures of the scale of supercluster. Whether galaxies ($\Omega_s=0.1$) and clusters of galaxies ($\Omega_s=0.2$) have significant effect or not is unclear. This result is consistent with the result of Tomita and Watanabe [14]. They considered the clusters of galaxies as scattering objects and concluded that the clusters of galaxies had relatively small effect on the anisotropy of CBR.

3. Angular correlation of the temperature anisotropy

In the following, we give a quantitative estimate of the anisotropy of CBR in terms of the angular correlation function using the formula derived by Wilson and Silk [24] and Sasaki[11]. Temperature fluctuation of the CBR averaged over antenna beam pattern is given by

$$\left\langle \left(\frac{\delta T}{T}(\theta; \sigma) \right)^2 \right\rangle \equiv 2[C(0; \sigma) - C(\theta; \sigma)], \quad (9)$$

where

$$C(\theta; \sigma) \simeq \frac{1}{2\sigma^2} \int_0^\infty \phi C(\phi) \exp \left[-\frac{1}{4\sigma^2}(\theta^2 + \phi^2) \right] I_0 \left(\frac{\theta\phi}{2\sigma^2} \right) d\phi,$$

and σ is the beam width of antenna and I_0 is the 0th order modified Bessel function. The angular correlation function, $C(\theta)$, is calculated as

$$C(\theta) = C(0) \left[1 + \frac{G(\theta)\theta^2}{\theta_c^2} \right]^{-\frac{1}{2}} \exp \left[-\frac{\theta^2}{2(\theta_c^2 + G(\theta)\theta^2)} \right], \quad (10)$$

where $G(\theta) = [\alpha^*(\theta) - 1]^2$. Here, θ_c represents the coherence angle of the intrinsic temperature fluctuation determined by the Silk damping [29]. We use an interpolation formula of $G(\theta)$:

$$G(\theta) \simeq \frac{\theta_{\text{pr}}^2}{\theta^2 + \theta_{\text{pr}}^2 G(0)^{-1}}. \quad (11)$$

This formula well expresses the behavior of $G(\theta)$ in the entire region of θ . In figure 4, the average temperature anisotropy is plotted against θ for the cases of $\theta_c = 4'$, $\sigma = 1'$, $z^* = 2, 4$ and 10. For the case of $z^* = 4$, the observed temperature anisotropy is smaller than the intrinsic one approximately by 30%.

4. Summary

We found that the anisotropy of the CBR is reduced by the gravitational scatterings due to superclusters. This smoothing occurs because the distance between nearby rays increases exponentially through multiple scatterings. In previous studies, the effect of gravitational scatterings was argued to be small, since the effect of the exponential growth was neglected.

Acknowledgment

We thank Tomoyoshi Ito, who developed GRAPE-2A, and Shaun Cole for many critical comments on the original manuscript.

Reference

- [1] Uson, J. M. & Wilkinson, D. T. *Nature*, **312**, 427-429 (1984).
- [2] Readhead, A. C. S., Lawrence, C. R., Myers, S. T., Sargent, W. L. W., Hardebeck, H. E. & Moffet, A. T. *Astrophys. J.* **346**, 566-587 (1989).
- [3] Smoot, G. F., et al. *Astrophys. J.*, **396**, L1-L5 (1992).
- [4] Gaier, T., Schuster, J., Gundersen, J., Koch, T., Seiffert, M., Meinhold, P., & Lubin, P. *Astrophys. J.*, **398**, L1-L4 (1992).
- [5] Peebles, P. J. E. & Silk, J. *Nature*, **346**, 233-239 (1990).
- [6] Gouda, N., Sasaki, M., & Suto, Y. *Astrophys. J.*, **341**, 557-574 (1989).
- [7] Gouda, N., & Sugiyama, N. *Astrophys. J.*, **395**, L59-L63 (1992).
- [8] Blanchard, A. & Schneider, J. *Astr. Astrophys.*, **184**, 1-6 (1987).
- [9] Kashalinsky, A. *Astrophys. J.* **331**, L1-L4 (1988).
- [10] Cole, S. & Efstathiou, G. *Mon. Not. R. astr. Soc.*, **239**, 195-200 (1989).
- [11] Sasaki, M. *Mon. Not. R. astr. Soc.*, **240**, 415-420 (1989).
- [12] Linder, E. V. *Mon. Not. R. astr. Soc.*, **243**, 353-361 (1990).
- [13] Watanabe, K. & Tomita, K. *Astrophys. J.* **370**, 481-486 (1991).
- [14] Tomita, K. and Watanabe, K. *Prog. Theor. Phys.*, **82**, 563-580 (1989).
- [15] Gunn, J. E. *Astrophys. J.* **147**, 61-72 (1967).
- [16] Miller, R. H. *Astrophys. J.* **140**, 250-256 (1964).
- [17] Lecar, M. *Bull. Astron.*, **3**, 91-104 (1968).
- [18] Gurzadyan, V. G. & Savvidy, G. K. *Astr. Astrophys.*, **160**, 203-210 (1986).
- [19] Sakagami, M. & Gouda, N. *Mon. Not. R. astr. Soc.* **249**, 241-247 (1991).
- [20] Kandrup, H. E. & Smith, H. *Astrophys. J.* **374**, 255-265 (1991).
- [21] Suto, Y. *Publ. Astron. Soc. Japan.* **43**, L9-L15 (1991).
- [22] Goodman, J., Heggie, D. C. & Hut, P., submitted to *Astrophys. J.*.
- [23] Will, C. M. *Theory and experiment in gravitational physics*. (Cambridge Univ. Press, London/New York, 1981).
- [24] Wilson, M. L., & Silk, J. *Astrophys. J.* **243**, 14-25 (1981).
- [25] Ito, T., Makino, J., Fukushige, T., Ebisuzaki, T., Okumura, S. K., & Sugimoto, D. *Publ. Astron. Soc. Japan*, in press.
- [26] Press, W. H., Flannery, B. P., Teukolsky, S. A. & Vetterling, W. T. *Numerical Recipes*. (Cambridge Univ. Press, London/New York, 1986).
- [27] Fukushige, T., Makino, J., Nishimura, O., & Ebisuzaki, T. submitted to *Publ. Astron. Soc. Japan*.
- [28] Geller, M., & Huchra, J., *Science*, **246**, 897-903 (1989).
- [29] Silk, J. *Astrophys. J.* **151**, 459-471 (1968).

Table 1. The growth of the beam width due to different astronomical objects.

object	ϵ	d	Ω_b	d_{pr}	ϵ/d_{pr}	θ_{pr}	τ_0	η	$\alpha^{LS}(z^* = 4)$
galaxy	20kpc	5Mpc	0.1	530kpc	0.04	0.7'	0.63	0.50	1.68
cluster of gal.	2Mpc	20Mpc	0.2	4.5Mpc	0.44	4.5'	2.16	0.21	1.19
supercluster	10Mpc	200Mpc	1.0	90Mpc	0.11	100'	0.68	1.5	5.35

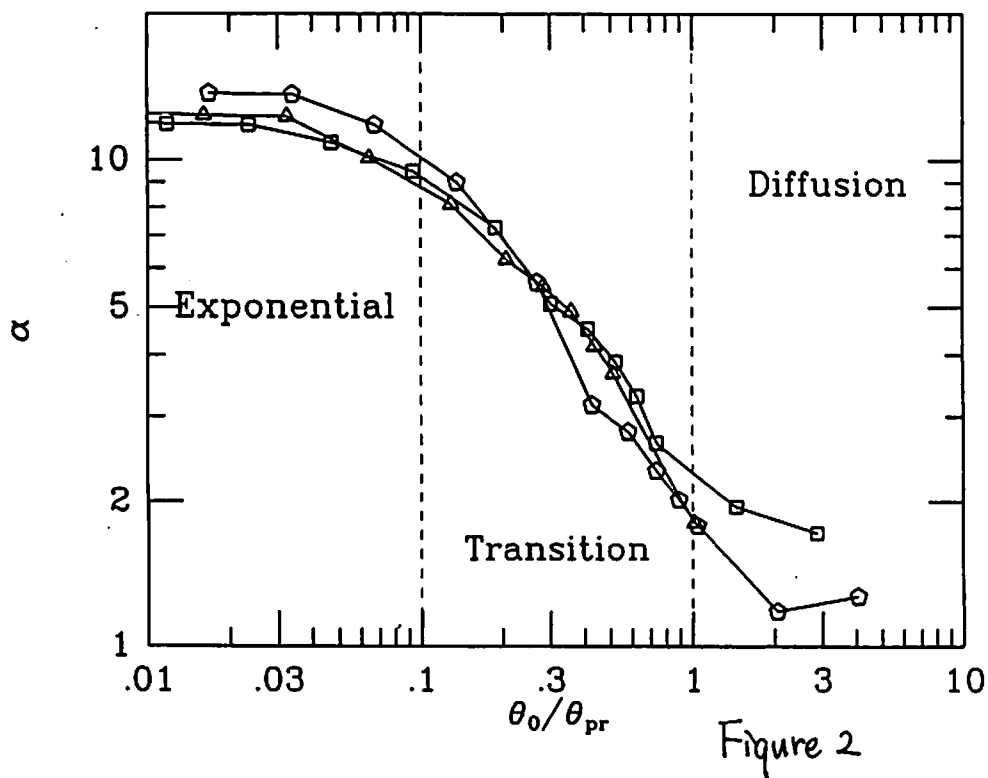
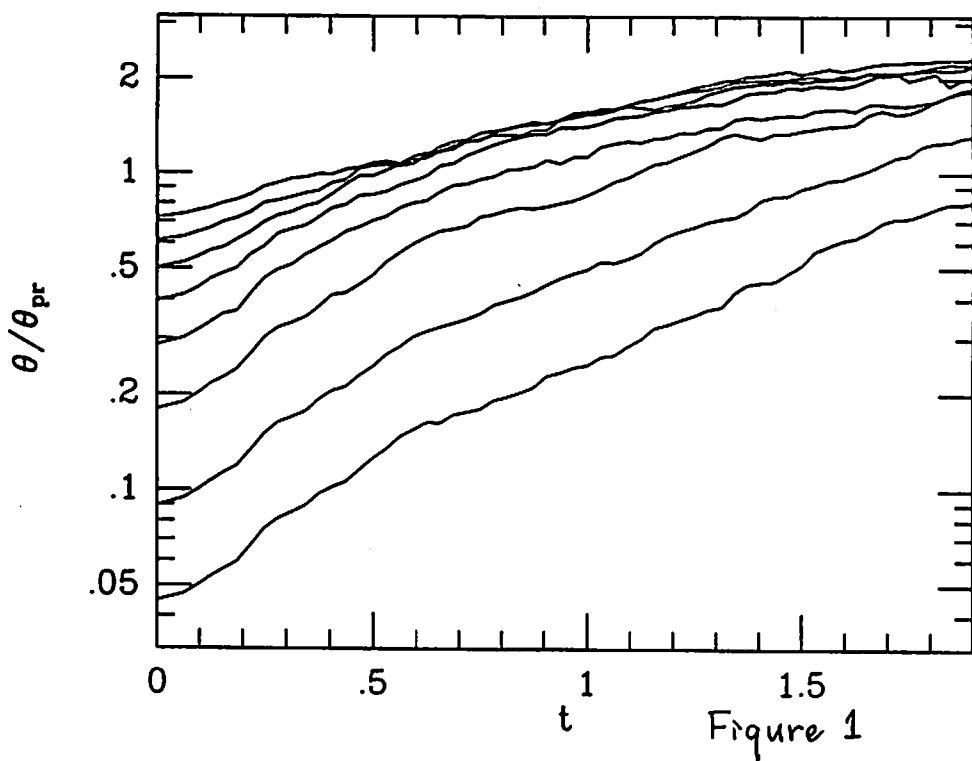
Figure Caption

Fig.1 The growth of the angle between the velocity vectors of two photons for the case of $N = 1024$ and $\epsilon = 0$. Each curve represents the median value calculated over 200 orbit pairs.

Fig.2 Growth factor, $\alpha = \theta_{1.5}/\theta_0$, plotted against θ_0/θ_{pr} . The triangles, squares and pentagons are for $N = 128, 1024$, and 8192 , respectively. The softening parameter, ϵ , is set to be 0.

Fig.3 Growth factor, α , plotted against ϵ/d_{pr} . The meanings of symbols are the same as in figure 2.

Fig.4 Averaged temperature fluctuation plotted against the chopping angle, θ , for $\theta_c = 4'$. The thin curve indicates the intrinsic temperature fluctuation for the beam width of antenna, $\sigma = 1'$. The thick curves indicate the observed temperature fluctuation for $z^* = 2, 4$ and 10 .



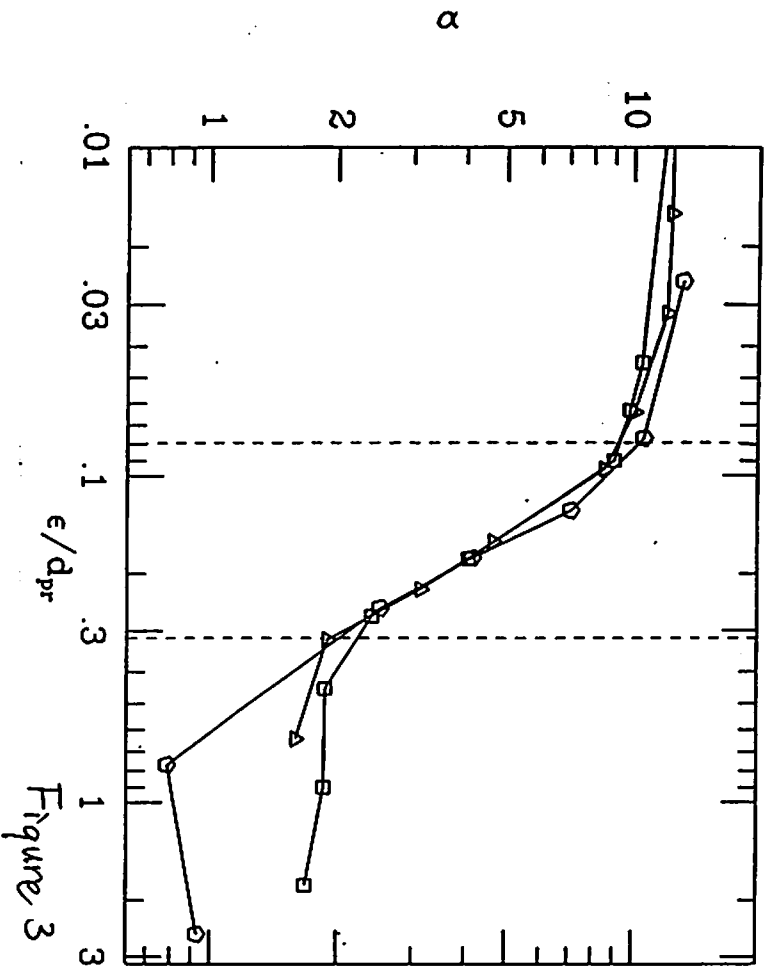


Figure 3

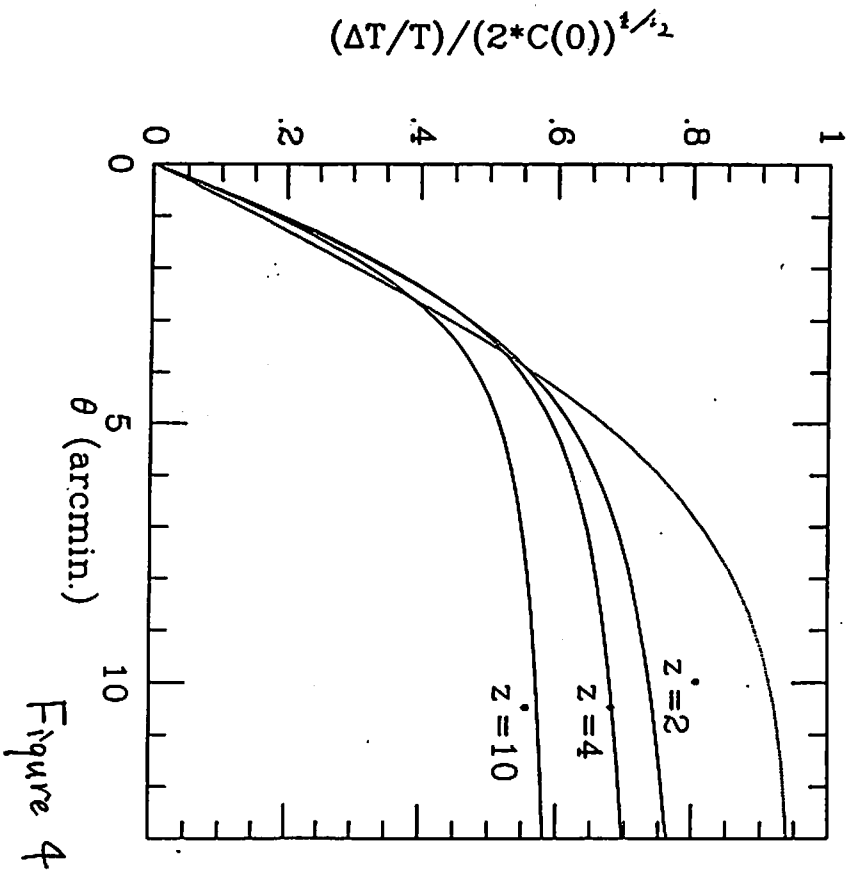


Figure 4

IMAGE DEFORMATION DUE TO GRAVITATIONAL LENSING IN A UNIVERSE WITH HIGH-REDSHIFT QUASAR CLUSTERING

KENJI TOMITA

*Uji Research Center, Yukawa Institute for Theoretical Physics
Kyoto University, Uji 611*

ABSTRACT

The observational evidence for high-redshift quasar clustering has recently been reported. In this note gravitational lens effect in a cosmological model with such a clustering is considered. It is shown that the image deformation due to lensing is too large compared with the observational average images of galaxies, if the clustering means the real inhomogeneity of density perturbation of all matter at the stage $0 \leq z \leq z_i$ (~ 5).

I. INTRODUCTION

The existence of clustering of high-redshift quasars has so far been reported by many workers (Shanks et al. 1987; Anderson, Kunth, & Sargent 1988; Andreani, Cristiani, & La Franca 1991). Recently its observational evidence has been shown more clearly by Andreani & Cristiani (1992), with the remarkable property that the two point correlations of the quasars have no or weak evolutionary change. At present it does not seem clear whether this clustering is associated with the real inhomogeneity of the total density distribution of matter, and how the correlation can be kept to be constant, in the case when it is associated with the real inhomogeneity.

With respect to the density perturbations associated with the quasar clustering we can consider following two cases. In the first case the real density perturbations of all matter are assumed to be associated with the quasar clustering at all epochs of $z \leq z_i$ ($z_i \sim 5$). In the second case it is assumed that the real density perturbations of all matter are associated with it transiently at the interval $z_i \leq z \leq z_f$ ($z_f \sim 10$) and at epoch z_i the real perturbations disappeared leaving only an apparent inhomogeneity corresponding the quasar clustering.

In this note we derive in the first case the image deformation of galaxies due to gravitational lens effect brought by the real perturbations, and examine whether the resulting deformation is allowed in comparison with the observational optical galactic images.

In §II the gravitational potentials corresponding to density perturbations with constant correlation length are first derived in the linear approximation using the part of the Einstein equations. Next in the above first case the image deformation is derived using our theory of gravitational lensing in the linear approximation (Tomita 1989), which has been proposed to study the deformation of the cosmic microwave radiation in a cosmological model with the usual density perturbations.

II. NON-EVOLUTIONAL DENSITY PERTURBATIONS CORRESPONDING TO QUASAR CLUSTERING AND IMAGE DEFORMATION

a) *Non-evolutional density perturbations*

As the background universe at the matter-dominant stage we assume the Einstein-de Sitter model with the line-element

$$ds^2 = R^2(\tau)[-(dx^0)^2 + (dx^1)^2 + (dx^2)^2 + (dx^3)^2], \quad (1)$$

where $x^0 = \tau$, $R(\tau) = (\tau/\tau_0)^2$ and τ_0 is the present value of τ . The metric tensors of the perturbed universe are expressed in Bardeen's notation (Bardeen 1980) as

$$g_{00} = -R^2[1 + 2 \int dk A(k)Q], \quad g_{0i} = -R^2 \int dk B(k)Q_{,i},$$

$$g_{ij} = R^2[\delta_{ij} + \int dk (2H_L(k)\delta_{ij}Q + 2H_T(k)Q_{ij})] \quad (2)$$

for scalar (density) perturbations, where $dk = dk_1 dk_2 dk_3$, $Q = \exp(ik_j x^j)$ and $i, j = 1, 2$, and 3 ($\alpha, \beta = 0, 1, 2$, and 3). The gauge-invariant metric perturbations ($\tilde{\Phi}_A, \tilde{\Phi}_H$) and density perturbations $\tilde{\epsilon}_m$ are given by

$$\tilde{\Phi}_A = \int dk \Phi_A(k)Q, \quad \tilde{\Phi}_H = \int dk \Phi_H(k)Q, \quad \tilde{\epsilon}_m = \int dk \epsilon_m(k)Q, \quad (3)$$

where $\Phi_A = A + k^{-1}[\dot{B} + (\dot{R}/R)B] - k^{-2}[\ddot{H}_T + (\dot{R}/R)\dot{H}_T]$, $\Phi_H = H_L + \frac{1}{3}H_T + k^{-1}(\dot{R}/R)[B + k^{-1}\dot{H}_T]$.

Here it is assumed that all matter has the same density perturbations corresponding to quasar clustering from an epoch $z = z_i (\simeq 5)$ to the present, and they have a non-evolutional power form as

$$\epsilon_m(k) = \tau_0^2 \epsilon(k) a(k), \quad \epsilon(k)^2 = A_0 k^n, \quad (4)$$

where A_0 and $n (\sim 1)$ are positive constants, and $a(k)$ is a random variable with $a^*(k) = a(-k)$ whose average satisfies the relation

$$\langle a(k) a^*(k') \rangle = \delta(k - k'). \quad (5)$$

The above behavior is clearly different from that of density perturbations for the perfect fluid shown in the ordinary theory of gravitational instability, and is brought by the support of hypothetical non-gravitational forces. Since we concerned only with the gravitational influence upon the light rays, we will not touch upon these forces and derive only the gravitational potentials associated with the density perturbations (4), assuming that the following part of the Einstein equations are satisfied at least approximately :

$$2(k/R)^2 \tilde{\Phi}_H = E \tilde{\epsilon}_m, \quad -(k/R)^2 (\Phi_A + \Phi_H) = P \pi_T, \quad (6)$$

where the background energy density E is $12/(\tau R)^2$ and the anisotropic stress in the latter equation is regarded here as being negligibly small. Then from these two equations we obtain

$$\Phi_H = -\Phi_A = 6(\tau_0/\tau)^2 \int dk k^{-2} \epsilon(k) a(k) Q, \quad (7)$$

The density perturbation is normalized as follows using the window function $w(x)$ defined by

$$w(x) = \exp \left[-\frac{1}{2} \left(\frac{2}{9\pi} \right)^{1/3} x^2 \right]. \quad (8)$$

The average of square mass perturbation at the radius r is

$$\langle (\delta M/M)^2 \rangle_r = 2\pi \tau_0^4 \int_0^\infty dk k^2 \epsilon(k)^2 w^2(kr). \quad (9)$$

Here we normalize as $\langle (\delta M/M)^2 \rangle_{(r=8h^{-1} \text{ Mpc})} = 1$. Then we have

$$A_0 = (2\pi\tau_0^4)^{-1} \left(\frac{2}{9\pi}\right)^{\frac{n+3}{6}} (8h^{-1} \text{ Mpc})^{n+3} / f(n), \quad (10)$$

where $f(n) = \sqrt{\pi}(n+1)!!/2^{\frac{n}{2}+1}$, $(\frac{n+1}{2})!$ for even, odd n , respectively, with $f(0) = \sqrt{\pi}/2$ and $f(1) = 1$. The average of the density perturbations is

$$\langle (\epsilon_m)^2 \rangle = \tau_0^4 \int dk \epsilon(k)^2 = \frac{4\pi}{n+3} \tau_0^4 A_0 (k_{\max}^{n+3} - k_{\min}^{n+3}), \quad (11)$$

where k_{\max} and k_{\min} correspond to the maximum and minimum wavenumbers and the corresponding linear sizes are $L_{\max} = 2\pi/k_{\max}$ and $L_{\min} = 2\pi/k_{\min}$. The linear approximation is valid for $L_{\max} \geq 8h^{-1} \text{ Mpc}$. Here we take the values $L_{\max} = 8h^{-1} \text{ Mpc}$ and $L_{\min} = 30h^{-1} \text{ Mpc}$. Since $k_{\max}^{n+3} \gg k_{\min}^{n+3}$, the following results are not sensitive to the value of L_{\min} for $n > 0$.

b) Lens effect and image deformation

Next we consider the deflection of light rays with wave vector $\tilde{k}^\mu (\equiv dx^\mu/d\lambda)$ satisfying the basic equations:

$$\tilde{k}^\mu \tilde{k}_\mu = 0, \quad \tilde{k}^\mu_{;\nu} \tilde{k}^\nu = 0.$$

The solutions in the linear approximation are expressed as

$$\tilde{k}^0 = R^{-2}(\tau)(1+l), \quad \tilde{k}^i = R^{-2}(\tau)(e^i + l^i), \quad (12)$$

where $e^i (\equiv e_i)$ is the three-dimensional unit vector $[\sum_{i=1}^3 (e^i)^2 = e^i e_i = 1]$ representing the directions of light rays, and the perturbations l and l^i are small. From the basic equations we obtain (Tomita 1989)

$$dl/d\tau = \dot{l} + l_{,i} e^i = (2\dot{R}/R)F - \int dk [\dot{A}Q + 2A_{,i} e^i Q + B e^i e^j Q_{i,j} + \dot{H}_L Q + \dot{H}_T e^i e^j Q_{ij}], \quad (13)$$

$$dl^i/d\tau = (\dot{l}^i) + l^i_{,j} e^j = \int dk \{ (H_L - A)Q_{,i} + \dot{B}Q_i$$

$$-2\dot{H}_L e_i Q - 2H_L Q_{,j} e^j e_i + H_T e^m e^j (Q_{mj,i} - 2Q_{ij,m}) + e^j [B(Q_{i,j} - Q_{j,i}) - 2\dot{H}_T Q_{ij}] \}, \quad (14)$$

where $\dot{l} = \partial l / \partial \tau$, $l_{,i} = \partial l / \partial x^i$.

For the gauge-invariant quantities \tilde{l}, \tilde{l}^i such that $\tilde{l} = l, \tilde{l}^i = l^i$ in the Newtonian gauge with $B = H_T = 0$, we obtain from eqs. (13)~(14)

$$d\tilde{l}/d\tau = - \int dk (\dot{\Phi}_A + 2ik_j e^j \Phi_A + \dot{\Phi}_H) Q, \quad (15)$$

$$d\tilde{l}^i/d\tau = \int dk [-ik_i \Phi_A - 2e_i \dot{\Phi}_H + i(k_i - 2k_j e^j e_i) \Phi_H] Q. \quad (16)$$

The integration of these equations leads to

$$\tilde{l} = 2 \int dk [\Phi_H Q + 2 \int_{\tau_0}^{\tau} d\tau \tau^{-1} \Phi_H Q], \quad (17)$$

$$\tilde{l}^i = 2 \int dk [-e^i (\Phi_H Q)]|_{\tau_0}^{\tau} + ik_i \int_{\tau_0}^{\tau} d\tau \Phi_H Q \quad (18)$$

and

$$\tilde{\delta}x^i = \int_{\tau_0}^{\tau_e} \tilde{l}^i d\tau + e^i (\delta\tau_e - \int_{\tau_0}^{\tau_e} \tilde{l} d\tau). \quad (19)$$

Of the components of $\tilde{\delta}x^i$, we are interested in the components $\tilde{\delta}_\perp x^i$ on the two-dimensional plane perpendicular to $k^\mu (= R^{-2}(1, e^i))$ and the matter velocity $u^i (= R^{-1}\delta_0^\mu)$. By the use of the projection tensor $h_{\mu\nu}$ (Tomita 1989), it is defined as $\tilde{\delta}_\perp x^i = h_\nu^i \tilde{\delta}x^\nu$ and expressed as

$$\tilde{\delta}_\perp x^i = 12i\tau_0^2 \int dk (k_i - k_e e^i) k^{-2} \epsilon(k) a(k) I(e^i), \quad (20)$$

where $k_e \equiv k_j e^j$, $Q = \exp(ik_e(\tau - \tau_e))$,

$$I(e^i) \equiv \int_{\tau_0}^{\tau_e} d\tau' \int_{\tau_0}^{\tau'} d\tau'' \tau''^{-2} Q$$

$$= \tau_e/\tau_0 - \cos k_e \Delta\tau - C(k_e \tau_e) - k_e \tau_e S(k_e \tau_e) + i[\sin k_e \Delta\tau - k_e \tau_e C(k_e \tau_e) - S(k_e \tau_e)] \quad (21)$$

with $\Delta\tau \equiv \tau_0 - \tau_e$. Here $C(k_e \tau_e)$ and $S(k_e \tau_e)$ are defined and expressed in terms of the integral

sine and cosine functions as follows:

$$C(k_e \tau_e) = \cos k_e \tau_e [ci(k_e \tau_e) - ci(k_e \tau_o)] + \sin k_e \tau_e [si(k_e \tau_e) - si(k_e \tau_o)] \quad (22)$$

and

$$S(k_e \tau_e) = \cos k_e \tau_e [si(k_e \tau_e) - si(k_e \tau_o)] - \sin k_e \tau_e [ci(k_e \tau_e) - ci(k_e \tau_o)]. \quad (23)$$

If we notice two neighbouring rays with the directional vectors e^i and $\bar{e}^i (\equiv e^i + \Delta e^i)$ and put the difference of $\bar{\delta}_\perp x^i$ as $\Delta_\perp(\bar{\delta}_\perp x^i)$, it is defined as

$$\Delta_\perp(\bar{\delta}_\perp x^i) \equiv h_j^i [\bar{\delta}_\perp x^j(\bar{e}^m) - \bar{\delta}_\perp x^j(e^m)] \quad (24)$$

and using (20) we obtain

$$\Delta_\perp(\bar{\delta}_\perp x^i) = 12i\tau_0^2 \int dk k^{-2} \epsilon(k) a(k) \xi_i, \quad (25)$$

where

$$\xi_i \equiv (k_i - \bar{k}_e \bar{e}^i) I(\bar{e}^m) - (k^i - k_e e^i) I(e^m) \quad (26)$$

and $\bar{k}_e \equiv k_j \bar{e}^j$. If we put $e^i = (1, 0, 0)$ and $\bar{e}^i = (\sqrt{1 - \Delta_e^2}, \Delta_e, 0)$ for a small separate angle Δ_e , we have

$$\bar{k}_e = \sqrt{1 - \Delta_e^2} k_1 + \Delta_e k_2. \quad (27)$$

The ratio of the average relative angular displacement of neighbouring two rays to the separate angle Δ_e is given by

$$\beta^2 \equiv \langle \sum_i [\Delta_\perp(\bar{\delta}_\perp x^i)]^2 \rangle / \Delta_e^2 = 12^2 (\tau_0 / \Delta_e)^2 \int dk k^{-4} \epsilon(k)^2 \sum_i |\xi_i|^2, \quad (28)$$

where the integration is performed for $k_{min} \leq k \leq k_{max}$, and $\epsilon(k)$ is given by (4) and (10). The quantity β shows the degree of the image deformation.

The values of β were numerically calculated for various sets of n and L_{max} . The result is shown in Table 1 for a representative case : $n = 1$ and $L_{max} = 8h^{-1}$ Mpc. It is found in these examples that β is about $0.12z_e$ for $\Delta \simeq 0$ arcmin. Observational quasar clustering seems to have $L_{max} < 8h^{-1}$ Mpc, and for such smaller L_{max} the values of β are larger than in those in Table 1. Since the average change in the ellipticity due to deformation is 2β , these values of β show too much deformation, compared with observational images of high-redshift galaxies. This result means that there are no real density perturbations of all matter associated with the high-redshift quasar clustering, while it may exist as a non-dynamical pattern at present.

Table 1 Average relative angular displacement (β) of neighbouring two rays to the separate angle Δ_e arcmin at the emission epochs $z_e = 1.0, 2.0, 3.0, 4.0$. The power index n is 1.

Δ_e	$z_e = 1.0$	$z_e = 2.0$	$z_e = 3.0$	$z_e = 4.0$
0.0	0.117	0.244	0.357	0.457
7.2	0.111	0.218	0.303	0.372
14.1	0.097	0.166	0.211	0.245
21.0	0.080	0.123	0.149	0.169
27.8	0.066	0.095	0.113	0.128
34.7	0.054	0.076	0.091	0.102
41.6	0.046	0.064	0.075	0.084
48.5	0.040	0.055	0.064	0.072

REFERENCES

- Anderson, N., Kunth, D., & Sargent, W.L.W. 1988, AJ, 95, 644
 Andreani, P., Cristiani, S., & La Franca, F. 1991, MNRAS, 253, 527
 Bardeen, J.M. 1980, Phys. Rev. D22, 1882
 Shanks, T., Fong, R., Boyle, B. J., & Peterson, B.A. 1987, MNRAS, 227, 739
 Tomita, K. 1989, Phys. Rev., D40, 3821

Expanding Surface of a Void and Universe Model

NOBUYUKI SAKAI^{*1}, KEI-ICHI MAEDA^{*2} and HUMITAKA SATO^{**3}

^{*}*Department of Physics, Waseda University, Shinjuku-ku, Tokyo 169-50, Japan*

^{**}*Department of Physics, Kyoto University, Kyoto 606-01, Japan*

Abstract

Under the thin-shell approximation, we study the expansion of the shell formed around a single spherical void in the dust universe. We find that the peculiar velocity of the shell is determined mostly by the density parameter Ω_0 . It also depends on the interior dust energy density, but is not so sensitive to a cosmological constant. This feature may open a possibility of determining the universe model from the surface motion of voids.

1 Introduction

The enlargement of a less-dense region (void) was considered with the motivation to explain the large voids in galaxy distributions [1,2,3]. In the non-linear stage of density perturbation, the less-dense region behaves like an explosive source because the less-dense region expands faster than the outer region, and a dense thin shell is formed behind the shock front by a snow-plow mechanism. The formation of a thin shell is demonstrated by numerical simulation [2]. These studies on shell expansion may also be relevant to the theory of explosive galaxy formation [4], where such a shell is generated by an explosion of pregalactic objects.

In Ref.[3], by using the metric junction method given by Israel [5], a relativistic motion of the void's shell was investigated. In the flat universe, the shell radius R expands asymptotically as $R \propto t^{(15+\sqrt{17})/24}$, that is, its peculiar velocity with respect to the background cosmic expansion, v , approaches to $[(\sqrt{17} - 1)/16]HR$, where H is the Hubble parameter. For other universe models, the motion of the shell was calculated numerically. In the open universe, the shell expansion is eventually frozen to the background expansion, while, in the closed universe, the surface expands much faster and its velocity finally approaches the speed of light. Thus, the peculiar velocity of the void's shell is sensitively dependent on the background universe model. Then, from the observation of the less dense region in the universe, we may be able to determine the universe model. This method can be contrasted to that of determining the universe model from the Virgo infall, in which the peculiar velocity of the lower dense region is used [6].

In this paper, we re-examine the dynamics of the expanding shell to see a relation between the expansion law of a void and the universe models. In particular we discuss the dependency of the peculiar velocity on the cosmological parameters. In Sec.2, we present the fully

^{1,2,3}electric mail: ¹62L506@jpnwas00.bitnet, ²maeda@jpnwas00.bitnet, ³MG6@jpnyitp.bitnet

relativistic equations for a thin shell, which will be solved later numerically. In Sec.3, we discuss general features of the motion of the shell, including the explosion cases. In Sec.4, we show the relation between the present peculiar velocity of the shell and the universe model parameters at present, such as the density parameter, a cosmological constant and interior dust energy.

2 Basic Equations

Here we give the equations of motion for a spherical shell, by applying Israel's method [5]. For the dust homogeneous universe model, the basic equations were derived in Ref.[2,3], and the equations are extended to the homogeneous space-time with general matter fluid in Ref.[7]. In those papers the equations of motion were written with the proper time of the shell τ , but it is often convenient to use the cosmic time of the outer region t in discussing the evolution of a void in the expanding universe, in particular, when we observe the void's shell from outside. Hence in this paper, we present simpler and more tractable equations than the previous ones, by applying the equation obtained by Berezin, Kuzumin and Tkachev [8], which is expressed in terms of the outside physical variables except the density of inner matter fluid and its velocity. In Ref.[9], we have applied those equations to analyze dynamics of an inhomogeneous bubble in an inflationary scenario. We find that those equations are also useful in our case where the metrics of both sides are given, as we will see below.

Let a time-like hypersurface Σ , which denotes a world-surface of a spherical shell, divide a space-time into two regions, V^+ (outside) and V^- (inside). We define a unit space-like vector N_μ , which is orthogonal to Σ and pointing from V^- to V^+ . It is convenient to introduce a Gaussian normal coordinate system (n, x^i) [10] in such a way that the hypersurface of $n = 0$ corresponds to Σ . From the assumption that a shell is infinitely thin, the surface energy-momentum tensor of the shell is defined as

$$S_{\mu\nu} \equiv \lim_{\epsilon \rightarrow 0} \int_{-\epsilon}^{\epsilon} T_{\mu\nu} dn. \quad (2.1)$$

Using the extrinsic curvature tensor of the hypersurface of the shell, $K_{ij} \equiv N_{i;j}$, and the Einstein equations, we can write down the jump conditions on the shell as [8]

$$[K_j^i]^\pm = -8\pi G \left(S_j^i - \frac{1}{2} \delta_j^i \text{Tr} S \right), \quad (2.2)$$

$$-S_{i;j}^\pm = [T_i^n]^\pm, \quad (2.3)$$

$$K_j^i S_i^j + 4\pi G \left\{ S_j^i S_i^j - \frac{1}{2} (\text{Tr} S)^2 \right\} = [T_n^n]^\pm. \quad (2.4)$$

where we have denoted the value of any field variable Ψ on Σ on the side of V^\pm by Ψ^\pm and defined a bracket as $[\Psi]^\pm \equiv \Psi^+ - \Psi^-$. $|$ denotes the covariant derivative with respect to the three metric of Σ . By using Eq.(2.4), we can obtain a simple expression of the basic

equation, because it does not contain the metric in V^- . Notice that the above equations do not change their forms even if the Einstein equation contains a cosmological constant term $\Lambda g_{\mu\nu}$.

We assume the homogeneous space-times both in V^+ and in V^- . The space-times are described by the Friedman-Robertson-Walker metric as

$$ds^2 = g_{\mu\nu}^\pm dx_\pm^\mu dx_\pm^\nu = -dt_\pm^2 + a_\pm^2(t_\pm)\{d\chi_\pm^2 + f_\pm^2(\chi_\pm)(d\theta^2 + \sin^2\theta d\phi^2)\}, \quad (2.5)$$

where

$$f_\pm(\chi_\pm) = \begin{cases} \sin \chi_\pm & (k_\pm = +1, \text{ closed universe}) \\ \chi_\pm & (k_\pm = 0, \text{ flat universe}) \\ \sinh \chi_\pm & (k_\pm = -1, \text{ open universe}) \end{cases}$$

The direct calculation of K_j^{\pm} yields [9]

$$K_\theta^{\pm} = \frac{\gamma_\pm(f'_\pm + v_\pm H_\pm R)}{R}, \quad K_r^{\pm} = \gamma_\pm^3 \frac{dv_\pm}{dt_\pm} + \gamma_\pm v_\pm H_\pm, \quad (2.6)$$

where $f'_\pm \equiv df_\pm/d\chi_\pm$, and the circumference radius of the shell R , the peculiar velocity of the shell v , its Lorentz factor γ and the Hubble expansion parameter H are defined as

$$R \equiv a_+ f_+ = a_- f_-, \quad v_\pm \equiv a_\pm \frac{d\chi_\pm}{dt_\pm}, \quad \gamma_\pm \equiv \frac{1}{\sqrt{1 - v_\pm^2}}, \quad \text{and} \quad H_\pm \equiv \frac{da_\pm/dt_\pm}{a_\pm}. \quad (2.7)$$

As the energy momentum tensor, we consider a dust fluid on Σ and in V^\pm , i.e.,

$$S_{\mu\nu} = \sigma v_\mu^\pm v_\nu^\pm, \quad T_{\mu\nu}^\pm = \rho_d^\pm u_\mu^\pm u_\nu^\pm, \quad (2.8)$$

where σ and v_μ are the surface density and the four velocity of the shell, ρ_d and u_μ are the density and the four velocity of background dust, respectively.

The background expansion obeys the following relation,

$$H_\pm^2 + \frac{k_\pm}{a_\pm^2} = \frac{8\pi G}{3} \rho_d^\pm + \frac{\Lambda}{3}. \quad (2.9)$$

The effect of a cosmological constant appears only through this equation.

Now, with the help of Eqs.(2.6) and (2.8), we can write down Eqs.(2.3) and (2.4) explicitly as

$$\gamma_+ \frac{d(4\pi R^2 \sigma)}{dt_+} = [4\pi R^2 \gamma^2 v \rho_d]^\pm, \quad (2.10)$$

$$\frac{d(\gamma_+ v_+)}{dt_+} = -\gamma_+ v_+ H_+ + 2\pi G \sigma - \frac{[\gamma^2 v^2 \rho_d]^\pm}{\sigma}. \quad (2.11)$$

The relationship between dR/dt_+ and v_+ is given by

$$\frac{dR}{dt_+} = f'_+ v_+ + H_+ R. \quad (2.12)$$

Further, the conditions of the continuity of the metric;

$$d\tau^2 = dt_+^2 - a_+^2(t_+)d\chi_+^2 = dt_-^2 - a_-^2(t_-)d\chi_-^2, \quad (2.13)$$

$$\frac{dR}{d\tau} = \frac{d}{d\tau}(a_+f_+) = \frac{d}{d\tau}(a_-f_-), \quad (2.14)$$

are reduced to

$$\frac{dt_-}{dt_+} = \frac{\gamma_-}{\gamma_+}, \quad (2.15)$$

$$\gamma_+(f'_+v_+ + H_+R) = \gamma_-(f'_-v_- + H_-R). \quad (2.16)$$

The equations of motion for the shell are designed by Eqs.(2.9), (2.10), (2.11) and (2.12). In the case where the inside region is not vacuum ($\rho_d^- \neq 0$), we have to know the values of v_- and ρ_d^- . Then we use the above supplementary equations (2.15) and (2.16), which give t_- and v_- , respectively. Once we know t_- , we can also find ρ_d^- .

The angular component of the jump condition (2.2);

$$[\gamma(f' + vHR)]^\pm = -4\pi G\sigma R, \quad (2.17)$$

gives a constraint for the value of surface density σ , which guarantees both V^+ and V^- are homogeneous.

In what follows, we omit the subscript + for variables in V^+ unless one may be confused. The subscripts i and 0 denote initial and present values, respectively. Here, the initial time just means the time when we start our calculations. Free parameters we can choose initially are v , R , $\Omega \equiv 8\pi G\rho_d/3H^2$, $\lambda \equiv \Lambda/3H^2$, and ρ_d^-/ρ_d^+ . In the case where V^- is not the Minkowski space-time ($\Lambda \neq 0$ or $\rho_d^- \neq 0$), we have chosen the spatial curvature of V^- and the time t_i so as to satisfy $H_i^- = H_i^+$. v_i^- and σ_i are determined from Eqs.(2.16) and (2.17), respectively. Setting up initial data, we numerically integrate the equations of motion for a shell by Runge-Kutta method. Since we are interested in a dependence of the shell motion on the universe model parameters at present, we will give our conclusion mainly in terms of the present values, Ω_0 , λ_0 and $(\rho_d^-/\rho_d^+)_0$, rather than the initial values, Ω_i , λ_i and $(\rho_d^-/\rho_d^+)_i$.

3 Void and Explosion

Before we are going to discuss the relation between the shell motion around the void and the universe model, first we show a dependency of the shell motion on the initial velocity v_i . If the void is formed from the less-dense region, the initial peculiar velocity v_i may be negligible. However, if the void structure is formed by the explosion of pregalactic objects, v_i will take a large value. In this section we restrict our analysis to the case that $\Lambda = 0$ and $\rho_d^- = 0$.

In Fig.1 and Fig.2, the time-variation of v and its ratio to the Hubble velocity, $\tilde{v} \equiv v/HR$, are shown, respectively. We find that after the universe expands by several times from its

initial value, the effect of the background expansion gets more important rather than the initial velocity v_i . Although the void size and v vary depending on v_i , the asymptotic behavior of \tilde{v} is determined only by the universe model. This is a useful feature which we can utilize for the determination of the universe model from observation.

In the Newtonian approximation, we can discuss the dynamics of the shell analytically. Setting $\gamma \approx 1$ and $4\pi\sigma R^2 \approx (4/3)\pi\rho_d R^3$ in Eq.(2.11), we get

$$\frac{dv}{dt} = H^2 R \left(\frac{\Omega}{4} - \tilde{v} - 3\tilde{v}^2 \right), \quad (3.1)$$

This shows how the shell is accelerated or decelerated depending on \tilde{v} and Ω . Then the stationary velocity v where $dv/dt = 0$ is attained when

$$\tilde{v}_{cr} = \frac{-1 + \sqrt{1 + 3\Omega}}{6}. \quad (3.2)$$

The existence of the maximum value of $v(t)$ at $\tilde{v} = \tilde{v}_{cr}$ is seen in Fig.1(a).

4 Void and Universe Model

For the determination of the universe model parameters from the shell motion, it is convenient to give the relation between the present expansion velocity of the void's shell and the present values of the universe model parameters. As we show in Sec.3, the dimensionless value of the shell velocity \tilde{v} is sensitive to Ω . Thus its present value \tilde{v}_0 may be a key value. Furthermore the asymptotic value of \tilde{v}_0 is $(\sqrt{17} - 1)/16 \approx 0.195$ for the flat model in the Newtonian limit. This value may verify the flat model.

In this section, first, we will investigate the dependence of \tilde{v}_0 on Ω_0 , which is the parameter we hope to estimate in the observational cosmology. Later, we will discuss the effect of a cosmological constant and of interior dust density.

(1) Void and the Density Parameter

In Fig.3 we show the Ω_0 - \tilde{v}_0 relation for the case that $\Lambda = 0$ and the interior of the void is empty ($\rho_d = 0$). \tilde{v}_0 is an increasing function of Ω_0 . We also find that, for the voids which are much smaller than the horizon scale and are generated at $z_i \gtrsim 4$, \tilde{v}_0 depends mainly on Ω_0 , although the value of \tilde{v}_0 in general depends on R_0 and z_i .

As long as $z_i \gtrsim 4$ and $R_0 \lesssim 0.1 H_0^{-1}$, which may be true for the observed voids, thus, we can estimate Ω_0 from the observation of v_0 and $H_0 R_0$. It should be remarked that these values are observable at present. Hence we think there may be possibility of evaluating Ω_0 by observation of an expanding void.

(2) Effect of a Cosmological Constant

Some observational analysis for the number count of faint galaxies has suggested the existence of a non-vanishing cosmological constant [11]. Besides, in the context of the particle physics cosmology, it is natural to include a cosmological constant as a vacuum energy.

In Fig.4(a) we show the time-variation of \tilde{v} for various λ_i for $\Omega_i = 1$. Now, the background expansion equation (2.9) includes Λ . Here we again assume that the interior of the void is vacuum. We find that when a cosmological constant exists, the shell expansion is decelerated and frozen soon to the background expansion regardless of the value of Ω_i . This feature is similar to that in the open universe model with $\Lambda = 0$.

We can discuss the above effect of a cosmological constant in terms of Eqs.(2.9) and (3.1). From Eq.(2.9), Ω is expressed as

$$\Omega = \frac{8\pi G\rho_d}{8\pi G\rho_d + \Lambda - 3k/a^2}. \quad (4.1)$$

This shows that Ω gradually decreases independent of the initial value of spatial curvature if $\Lambda \neq 0$, because the density ρ_d decreases when the universe expands. That is, Λ term works to reduce Ω . If Ω decreases, \tilde{v}_{cr} also decreases, as we can see in Eq.(3.2). Hence, Λ term has an effect to reduce the shell expansion.

The λ_0 - \tilde{v}_0 relation is presented in Fig.4(b). We find that the present value \tilde{v}_0 has a little dependency on λ_0 for a fixed value of Ω_0 , although temporal behaviour of \tilde{v} in the past are quite sensitive to the value of λ_0 . Notice that we can distinguish the dust energy density Ω_0 from the cosmological constant even if the universe model is flat ($k = 0$). (See the solid line in Fig.4(b).)

(3) Effect of Interior Dust Energy

So far we have assumed that the interior of a void is vacuum. However, the darkness does not necessarily imply its emptiness. Here we, therefore, examine the effect of the interior matter density.

We present time-variation of \tilde{v} for several values of $(\rho_d^-/\rho_d^+)_i$ in Fig.5(a). As we may expect, the expansion velocity of a shell is smaller for larger value of $(\rho_d^-/\rho_d^+)_i$. Since ρ_d^- decreases faster than ρ_d^+ , ρ_d^-/ρ_d^+ approaches 0, and hence the asymptotic behaviour gets similar to the previous model ($\rho_d^- = 0$).

The relation between $(\rho_d^-/\rho_d^+)_0$ and \tilde{v}_0 is presented in Fig.5(b). We find that \tilde{v}_0 is approximately proportional to $1 - (\rho_d^-/\rho_d^+)_0$.

5 Summary and Discussions

We have investigated the expanding shell around a spherical void in the expanding dust universe. Our main purpose is to relate the expansion law of a void to the universe model parameters. \tilde{v}_0 , the ratio of the peculiar velocity v to the background Hubble expansion HR , is determined mainly by the present value of the density parameter Ω_0 . It also depends on the

ratio of the inside dust density to the outside one $(\rho_d^-/\rho_d^+)_0$. As long as $z_i \gtrsim 4$ and $R_0 \lesssim 0.1 H_0^{-1}$, however, it has little dependency on a cosmological constant Λ , the initial redshift z_i and the present size of void R_0 . Our result is summarized in Fig.6. From this contour map, we can evaluate the value of Ω_0 from the observation of $(v/HR)_0$ and $(\rho_d^-/\rho_d^+)_0$.

In the actual situation, however, even if voids are formed by explosion mechanism or from the less dense fluctuation, most of them may have already collided with each other, and hence a simplified single void expansion may not be realistic. Further, it may also be difficult to identify the peculiar velocity of a shell because of its finite thickness. Although there are many problems for the application to realistic situation at present, an intrinsic relation of the shell expansion to the universe model could be used in the future.

Acknowledgements

This work was supported partially by the Grant-in-Aid for Scientific Research Fund of the Ministry of Education, Science and Culture (No.04234211 and No.04640312), by a Waseda University Grant for Special Research Projects, and by The Sumitomo Foundation.

References

- [1] H. Sato, Prog. Theor. Phys. **68** (1982), 236;
K. Maeda, M. Sasaki and H. Sato, Prog. Theor. Phys. **69** (1983), 89;
H. Sato and K. Maeda, Prog. Theor. Phys. **70** (1983), 119.
- [2] Y. Suto, K. Sato and H. Sato, Prog. Theor. Phys. **71** (1984), 938.
- [3] K. Maeda and H. Sato, Prog. Theor. Phys. **70** (1983), 772; 1273.
- [4] S. Ikeuchi, Publ. Astron. Soc. Japan **33** (1981), 221;
J.P. Ostriker and L.L. Cowie, Astrophys. J. **243** (1981), L127.
- [5] W. Israel, Nuovo Cim. **44B** (1966), 1.
- [6] M. Davis and P.J.E. Peebles, Ann. Rev. Astron. Astrophys. **21** (1983), 109.
- [7] K. Maeda, Gen. Rel. Grav. **18** (1986), 9.
- [8] V.A. Berezin, V.A. Kuzumin and I.I. Tkachev, Phys. Rev. **D36** (1987), 2919.
- [9] N. Sakai and K. Maeda, preprint, WU-AP/23/92 (1992).
- [10] In this paper, Greek letters run from 0 to 3, and Latin letters run in 0, 2, 3.
- [11] M. Fukugita, F. Takahara, K. Yamashita and Y. Yoshii, Astrophys. J. **361** (1990), L1.

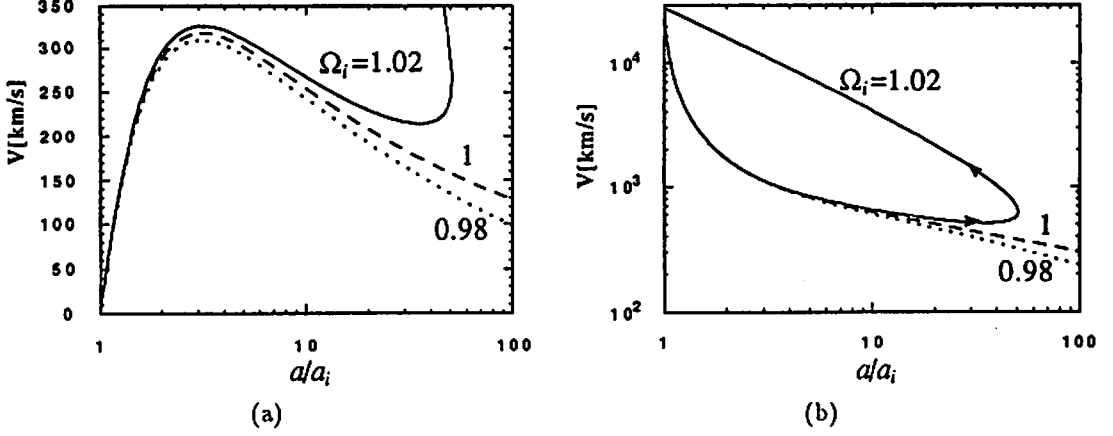


Fig.1. Time-variation of the shell velocity v for $\Omega_i = 0.98, 1, 1.02$. The abscissa is the scale factor $a(t)$ in units of its initial value. We assume $\rho_d^- = 0$, $\Lambda = 0$ and $R_i = 10^{-2}H_i^{-1}$. The case (a) corresponds the void formed from a less-dense region, i.e., $v_i = 0$. The case (b) is the explosion case, where we have chosen as $v_i = 10H_i R_i = 0.1$, as an example. For the closed universe model, there exist turning points where $a(t)$ starts to decrease. When the universe recollapses, the shell expansion velocity becomes very large. For each universe model in the expanding phase, v takes the maximum value at $v_{cr} \approx (-1 + \sqrt{1 + 3\Omega})/6$ (see text).

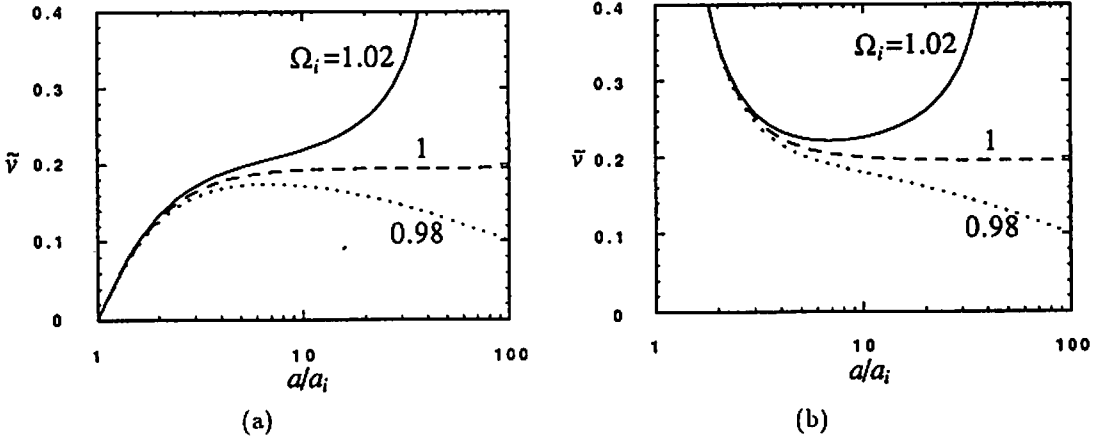


Fig.2. Time-variation of $\bar{v} = v/HR$ is shown for the same models in Fig.1. The asymptotic behaviour for each value of Ω_i is quite different, but they do not depend on the initial expansion velocity v_i .

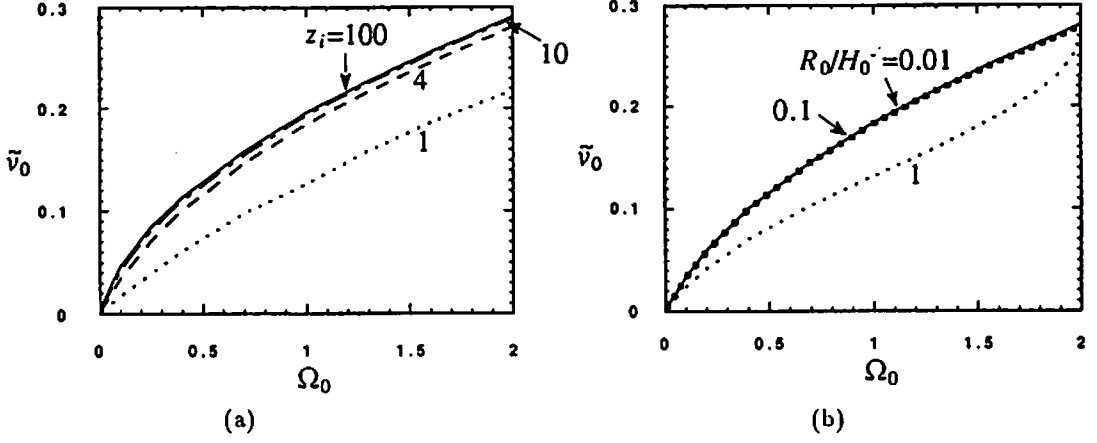


Fig.3. Ω_0 - \tilde{v}_0 relation. (a) We change the value of z_i , setting $\Lambda = 0$, $\rho_d^- = 0$, $v_i = 0$ and $R_i = 0.1 H_i^{-1}$. \tilde{v}_0 is monotonically increasing with respect to Ω_0 . We find that all curves for $z_i \geq 4$ converge to the same one. (b) We change the value of R_0 , setting $\Lambda = 0$, $\rho_d^- = 0$, $v_i = 0$ and $z_i = 4$. For $R_0 \leq 0.1 H_0^{-1}$, all curves coincide with each other.

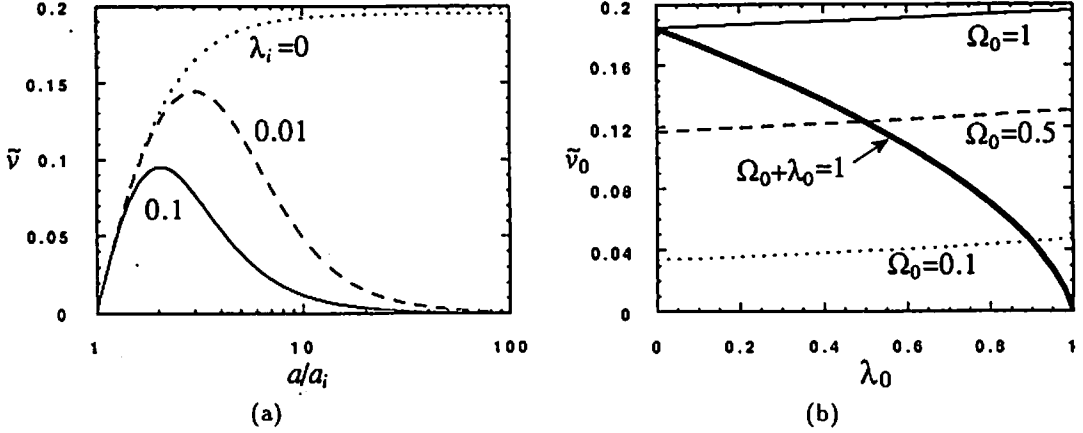


Fig.4. Effect of a cosmological constant. (a) Time-variation of \tilde{v} for several values of λ_i . We assume that $\Omega_i = 1$, $\rho_d^- = 0$, $v_i = 0$ and $R_i = 0.1 H_i^{-1}$. If $\Lambda = 0$, \tilde{v} approaches to a constant, while, if $\Lambda \neq 0$, \tilde{v} increases once and then eventually decreases to zero. Hence, such a model becomes similar to the open universe (see Fig.2). (b) λ_0 - \tilde{v}_0 relation for several values of Ω_0 . The bold line corresponds to values for the spatially flat universe; $\Omega_0 + \lambda_0 = 1$. The solid, dashed and dotted lines denote the relations for $\Omega_0 = 1$, 0.5 and 0.1, respectively. We set $\rho_d^- = 0$, $v_i = 0$, $R_i = 0.1 H_i^{-1}$ and $z_i = 4$. We find that the value of \tilde{v}_0 depends just on the present density parameter Ω_0 , but not on λ_0 .

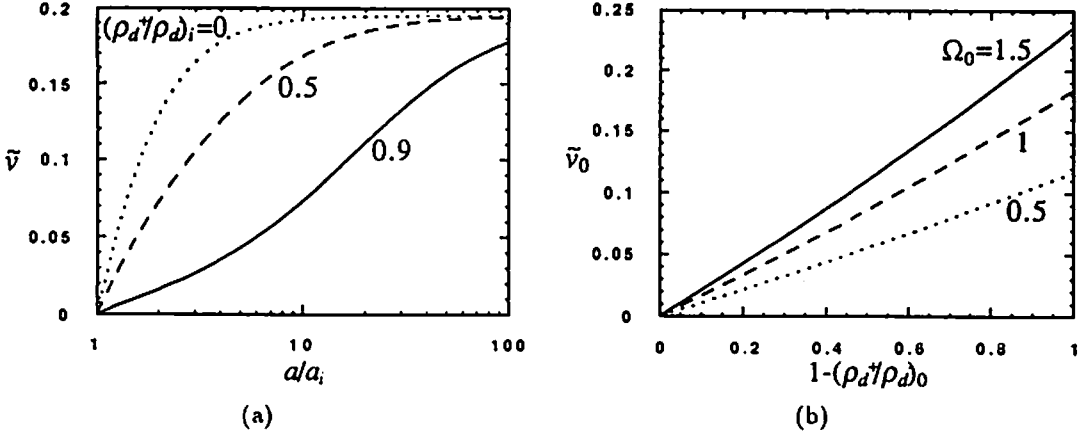


Fig.5. Effect of interior dust energy. (a) Time-variation of \tilde{v} for several values of $(\rho_d^-/\rho_d^+)_i$. We set $\Lambda = 0$, $v_i = 0$ and $R_i = 0.1H_i^{-1}$. \tilde{v}_0 approaches to the case of empty void, because the interior density ρ_d^- decreases faster than ρ_d^+ , and then ρ_d^-/ρ_d^+ asymptotically (b) The relation between $(\rho_d^-/\rho_d^+)_0$ and \tilde{v}_0 for several values of Ω_0 . We set $\Lambda = 0$, $v_i = 0$, $R_i = 0.1H_i^{-1}$ and $z_i = 4$. We find that \tilde{v}_0 is proportional to $1 - (\rho_d^-/\rho_d^+)_0$.

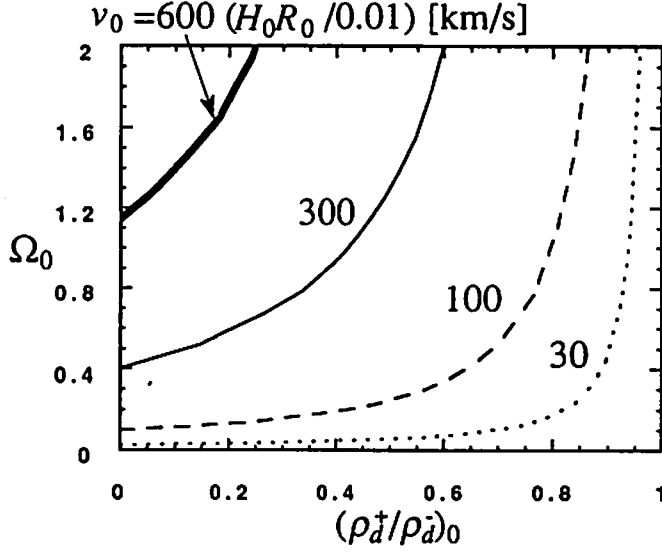


Fig.6. The contour map of \tilde{v}_0 with respect to $(\rho_d^-/\rho_d^+)_0$ and Ω_0 . If we observe v_0 , $H_0 R_0$ and $(\rho_d^-/\rho_d^+)_0$, we can determine the value of Ω_0 .

CHAOTIC INFLATION DRIVEN BY A SNEUTRINO FIELD

H. Murayama, Hiroshi Suzuki, T. Yanagida, and Jun'ichi Yokoyama[†]

Department of Physics, Faculty of Science,
Tohoku University, Sendai 980, Japan

[†]Uji Research Center, Yukawa Institute for Theoretical Physics,
Kyoto University, Uji 611, Japan

Abstract

We present a model of chaotic inflation driven by the superpartner of the right-handed neutrino (sneutrino). This model naturally gives the correct order of magnitude of the density perturbation observed by COBE with a mass of the right-handed neutrino $\sim 10^{13}$ GeV, which is also preferred by the Mikheyev-Smirnov-Wolfenstein solution to the solar neutrino problem. The reheating process is the decay of the coherently oscillating right-handed sneutrino. The reheating temperature is around 10^{10} GeV, and hence gravitino problem is solved. This decay process also generates lepton number asymmetry via CP-violation, which will be converted to baryon number asymmetry thanks to the electroweak anomaly. This model can incorporate the mass of the τ -neutrino around 10 eV.

The inflationary expansion in the early universe is a desirable ingredient of modern cosmology to solve the horizon and the flatness puzzles [1] as well as the monopole [2], the domain-structure [3] and the gravitino problems [4]. Recently, COBE satellite [5] detected an anisotropy of the cosmic microwave background, and found that it is consistent with the almost scale-invariant density perturbation generated by the quantum fluctuations during the inflation era [6]. Furthermore, the observed temperature fluctuation at the level of $\delta T/T \sim 10^{-5}$ allows us to fix the scale of chaotic inflation around $H \sim 10^{13}$ GeV [7].

Even though we have sound motivations for inflation as above, it is very difficult to make a convincing particle physics model which naturally predicts a scalar field driving inflation (inflaton) with Einstein gravity. This is because it must be a gauge singlet, and should be very weakly interacting, to have a very flat potential. The necessity of baryogenesis at or after the reheating stage makes it even harder since the reheating

temperature is constrained to be much lower than the typical grand unification scale at which baryogenesis takes place in the conventional scenario [8]. Furthermore, the baryon asymmetry, if generated at all, would be washed out due to the electroweak anomalous process [9] if there were no $B - L$ asymmetry as in $SU(5)$ grand unification. Thus we have to search for a model which generates $B - L$ asymmetry at lower temperature in the post-inflationary universe [10].

On the other hand, supersymmetry (SUSY) is regarded as a necessary ingredient in constructing models beyond the Standard Model, in order to stabilize the large hierarchy between the weak and the unification or the Planck scales [11]. Combined with the SUSY breaking induced by the supergravity interactions, it also gives a natural framework to break the electroweak symmetry radiatively [12]. Furthermore, the only candidate of the quantum gravity, the superstring, requires SUSY for its consistency. The discovery at LEP [13] that all the three gauge coupling constants meet at a single point in the SUSY Standard Model is also a strong support for the SUSY. Once we regard the SUSY as the correct low-energy symmetry of the nature, we have to take the SUSY Standard Model as a serious candidate to describe the nature below the Planck (or unification) scale. It is natural to seek for a candidate of the inflaton among scalar partners of the fermion species whose existence is known or suggested by experimental basis.

In the present letter we propose a scenario of chaotic inflation [14] by identifying the inflaton with the scalar partner of a right-handed Majorana neutrino. Being gauge-singlet, its scalar component can have large values at the Planck epoch, and automatically induces chaotic inflation. Then the primordial density perturbation is proportional to its mass,

$$\frac{\delta T}{T} \simeq 10 \frac{M}{M_P}, \quad (1)$$

at the scales reflecting the anisotropy of the cosmic microwave background, with M_P being the Planck mass. The beautiful data by COBE $\delta T/T \simeq 10^{-5}$ has fixed the mass at 10^{13} GeV [7]. The reheating process is nothing but the decay of the coherently oscillating right-handed sneutrinos. If CP violation exists, the decay process generates lepton number asymmetry, since the Majorana mass of the right-handed neutrino breaks the lepton number conservation. This lepton number asymmetry will be subsequently partially converted to baryon number asymmetry due to the electroweak anomalous process [15]. On the other hand, the existence of the right-handed neutrino is strongly supported by recent confirmation of the deficit of solar neutrino flux at Homestake, Kamiokande and GALLEX [16], at more than two sigma level. The Mikheyev-Smirnov-Wolfenstein (MSW) solution [17], combined with seesaw model [18], predicts the right-handed neutrino mass around 10^{10} to 10^{15} GeV. Thus the mass preferred by the COBE data $M \sim 10^{13}$ GeV naturally fit into this window [19].

Now we begin to describe our model in more detail. We assume the existence of the right-handed neutrinos N_i for each generation, with a common mass at 10^{13} GeV for simplicity. Their only possible interactions are the Yukawa couplings with the lepton and

Higgs fields l_i , H_u and H_d , with the superpotential

$$W = \frac{1}{2} M N_i^c N_i^c + \mu H_u H_d + h^{ij} N_i^c l_j H_u + k^{ij} e_i^c l_j H_d. \quad (2)$$

Here we have assigned the odd R -parity for the right-handed sneutrinos, which inhibits $(N^c)^3$ term in the superpotential.

At the Planck epoch ($t \sim M_P^{-1}$) when the classical description of spacetime becomes possible, we expect that the universe was in a highly non-equilibrium state, since there was not enough time for the thermal equilibrium to be realized. The only criterion at that time is that every term in the Lagrangian can have the order of magnitude M_P^4 , varying from one horizon to another [14]. Allowing each term in the potential to be $\sim M_P^4$, all the scalar fields can have values $\sim M_P$. However, only those fields with values larger than $\sim M_P$ can act as an inflaton. Any gauge non-singlet fields cannot have values larger than $\sim M_P$ due to the D -terms [20]. Thus the right-handed sneutrinos are the unique candidates of the inflaton, and that with smallest Yukawa coupling (presumably right-handed electron sneutrino \tilde{N}_1) acts as an inflaton. We will only deal with \tilde{N}_1 hereafter, and assume that its largest Yukawa coupling is that to the τ -doublet, of the order of $h_{13} \simeq 10^{-4}$ to 10^{-5} . Then it can have an initial value as large as $|\tilde{N}_1(0)| \simeq M_P/h_{13}$. If the Yukawa couplings are larger than $\sqrt{8\pi/3} M/M_P \simeq 10^{-6}$, the slepton and Higgs fields get larger masses from $\langle \tilde{N}_1 \rangle$ than the Hubble parameter H . Then those scalar fields oscillate and the amplitudes will be damped away exponentially within the inflation era.

The field equation is very simple after the slepton and Higgs fields died away,

$$\ddot{\tilde{N}}_1 + 3H\dot{\tilde{N}}_1 + \Gamma_1\dot{\tilde{N}}_1 + M^2\tilde{N}_1 = 0, \quad (3)$$

with

$$H^2 = \frac{8\pi}{3M_P^2} \left[M^2 |\tilde{N}_1|^2 + |\dot{\tilde{N}}_1|^2 \right] \quad (4)$$

and $\Gamma_1 \simeq |h_{1j}|^2 M/4\pi \sim 10^2$ to 10^4 GeV. Until the time $H \sim M$, the sneutrino field is simply rolling down the potential,

$$|\tilde{N}_1(t)| = |\tilde{N}_1(0)| - \frac{MM_P}{\sqrt{24}\pi} t, \quad (5)$$

$$R(t) = R(0) \exp \left[\sqrt{\frac{8\pi}{3}} \frac{M}{M_P} |\tilde{N}_1(0)| t \left(1 - \frac{MM_P t}{4\sqrt{6\pi} |\tilde{N}_1(0)|} \right) \right]. \quad (6)$$

After the time $H \sim M$, the sneutrino field oscillates around its minimum, $\tilde{N}_1 = 0$, with frequency M . This coherent oscillation will be slowly damped due to the expansion. Once $H \sim \Gamma_1$, the coherent oscillation starts to decay into light particles, which will “reheat” the universe up to the temperature $T_{RH} \simeq 0.1\sqrt{M_P\Gamma_1} \simeq 10^9$ GeV to 10^{10} GeV, sufficiently low to avoid the gravitino problem [21]. Simultaneously, the decay of \tilde{N}_1 produces lepton

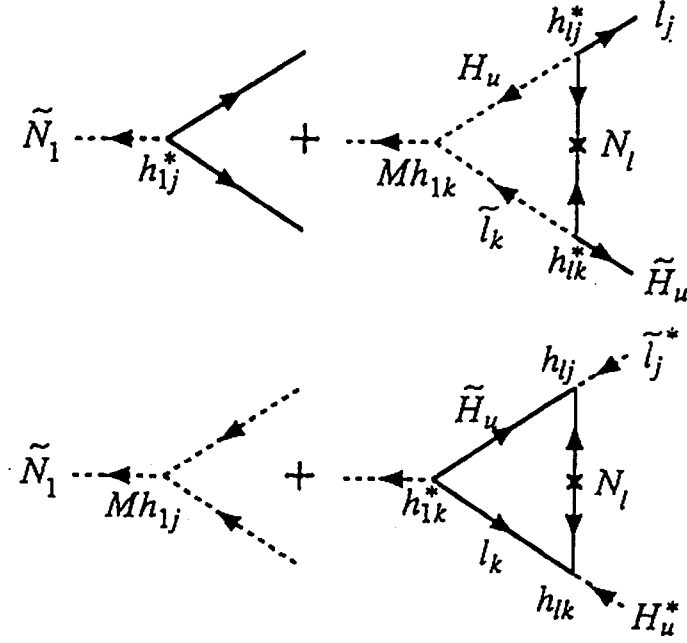


Figure 1: The diagrams for decay of the right-handed sneutrino \tilde{N}_1 into lepton $l_j \tilde{H}_u$ and anti-slepton $\tilde{l}_j^* H_u^*$ at tree and one-loop levels.

number asymmetry due to the CP-violation. This reheating period can be described by the following equations.

$$\dot{\rho}_N + 3H\rho_N + \Gamma_1\rho_N = 0, \quad (7)$$

$$\dot{\rho}_R + 4H\rho_R = \Gamma_1\rho_N, \quad (8)$$

$$H^2 = \frac{8\pi}{3} \frac{\rho_N + \rho_R}{M_P^2}, \quad (9)$$

where ρ_N is the energy density of the coherently oscillating right-handed sneutrino field, and ρ_R is the energy density of the produced radiation. The generated lepton number asymmetry can be evaluated by the equation

$$\begin{aligned} n_L + 3Hn_L &= \epsilon\Gamma_1 \frac{\rho_N}{M} - \frac{9}{2\pi} \left| \frac{h_{33}^2}{M_3} \right|^2 \frac{1}{\zeta(3)} n_\gamma n_L \\ &= \epsilon\Gamma_1 \frac{\rho_N}{M} - \frac{9}{2\pi} \frac{2G_F^2 m_{\nu\tau}^2}{\sin^4 \beta} \frac{1}{\zeta(3)} n_\gamma n_L. \end{aligned} \quad (10)$$

This equation may require some explanations. The parameter ϵ is the asymmetry in the \tilde{N}_1 decay between that into leptons $l \tilde{H}_u$ and that into anti-sleptons $\tilde{l}^* H_u^*$ (see Fig. 1),

$$\epsilon = \frac{\ln 2}{8\pi} \frac{\Im m(h_{1j} h_{1k} h_{lj}^* h_{lk}^*)}{h_{1j} h_{1j}^*} \sim \frac{\ln 2}{8\pi} \Im m h_{33}^2. \quad (11)$$

Here we have assumed that h_{13} dominates over h_{11} and h_{12} , and took the convention that both h_{13} and right-handed neutrino masses are real. The first term in the right-hand side of Eq. (10) is the production of lepton number asymmetry due to this CP-violating decay of \tilde{N}_1 . The second term represents the destruction of the lepton number due to the lepton-number violating scattering process via the N_3 exchange. The seesaw formula $m_{\nu_\tau} = |h_{33}|^2 \sin^2 \beta / (\sqrt{2} G_F M)$ has been used to demonstrate that the rate of the destruction is proportional to the square of the mass of ν_τ . Here β is defined by the ratio of two vacuum expectation values, $\tan \beta = \langle H_u \rangle / \langle H_d \rangle$, and G_F is the Fermi constant.

The maximum lepton number to entropy ratio ($Y_L \equiv n_L/s$) generated in this process is

$$Y_L^{\max} \simeq \epsilon \frac{3}{4} \frac{T_{RH}}{M}. \quad (12)$$

The produced lepton number asymmetry will be rapidly converted to baryons with the rate $\sim \alpha_{\psi}^4 T^4$ [22], reaching the chemical equilibrium [22, 23]

$$Y_B = \frac{8n_g + 4}{22n_g + 13} Y_L \simeq 0.35 Y_L \quad (13)$$

with the number of generations $n_g = 3$. This maximum value gives the correct baryon to entropy ratio $4 \times 10^{-11} \leq Y_B \leq 14 \times 10^{-11}$ required from nucleosynthesis only if we take unnaturally small values $\epsilon \sim 10^{-8}$ to 10^{-6} depending on T_{RH} .

However, there are two processes which suppress the baryon number asymmetry. The first one is the destruction of the lepton number asymmetry due to the N_3 -exchange scattering process appearing in Eq. (10). It gives a suppression factor of roughly

$$\exp \left[-0.012 \frac{G_F^2 m_{\nu_\tau}^2}{\sin^4 \beta} M_P T_{RH} \right] \quad (14)$$

and is important for $m_{\nu_\tau} \gtrsim 2$ eV. For example, $\epsilon \sim 10^{-3}$, $T_{RH} \sim 10^9$ GeV and $m_{\nu_\tau} \sim 10$ eV gives the correct baryon to entropy ratio. The second one is the dilution effect due to the decay of scalar field in the flat direction of the potential. It is a general phenomenon in the supersymmetric models that there are flat directions in the scalar potential. From the chaotic configuration of the initial scalar fields, it may be occasionally possible that the scalar fields will drop into the flat direction with values of $\sim M_P$ during the inflation. It will begin to oscillate only at the time $H \sim m$, where m denotes the mass along the flat direction, expected to be the order of the weak-scale. Since the decay rate of our inflaton is also of the same order, the cold oscillation begins soon after the reheating. However then the energy density will be dominated by the cold oscillation. Its decay will generate a large amount of entropy, giving a dilution factor [24, 25] roughly of

$$\left(\frac{\alpha_s}{\pi} \frac{m}{M_P} \right)^{1/3} \left(\frac{\chi}{M_P} \right)^{-3/2} \sim 10^{-6} \left(\frac{\chi}{M_P} \right)^{-3/2}, \quad (15)$$

where χ is the initial value when the flat direction begins the oscillation. Then the CP-violating parameter ϵ should be at its maximum possible value $\epsilon \sim 10^{-2}$, and we will

obtain an upperbound on m_{ν_τ} of the order of 2 eV so that the lepton number asymmetry generated will not be suppressed further.

Now we discuss several points in our scenario.

1. It is not clear whether the scalar fields will drop into one of the flat directions during the inflation. Note that the lepton doublets \tilde{l}_i and Higgs field H_u cannot have a large value due to the coupling to the inflaton \tilde{N}_1 in the potential. Thus only the squark fields and right-handed sleptons can have large values. Such flat directions may be too special to be realized. If the scalar fields do drop into one of those flat directions, one may question whether the decay of the flat direction will produce baryon number asymmetry via the Affleck-Dine mechanism [24]. However, there are no terms in the tree-level potential which violates $B - L$ symmetry along this flat direction. We have also checked that the higher order correction can generate $B - L$ violating potential only at a negligible magnitude. Thus the only effect of the flat direction, if present, is to dilute the generated lepton number asymmetry.

2. During the reheating process, the lepton and Higgs fields mix due to the oscillating right-handed sneutrino background, and one may worry that the produced lepton number will be destroyed due to the mixing [26]. At the reheating period, the amplitude of the oscillation is $\sim \Gamma_N M_P / M$, and the mixing mass is $m_{\text{mix}} \sim h_{13} \Gamma_N M_P / M \sim 10^3$ GeV. On the other hand, the right-handed sneutrino background is oscillating with the frequency of $M = 10^{13}$ GeV $\gg m_{\text{mix}}$. Then the mixing is estimated to be only of $16 m_{\text{mix}}^2 / M^2 \sim 10^{-18}$, and hence negligible.

3. Our scenario can easily be incorporated in the $SU(5)$ grand unification, since right-handed neutrino is singlet under the $SU(5)$ gauge group. The analysis in this letter applies without any modifications. On the other hand, the right-handed sneutrino field cannot have a large initial value if the $U(1)_{B-L}$ symmetry is gauged, like in $SO(10)$ models.

4. This model can naturally incorporate a τ -neutrino mass $m_{\nu_\tau} \sim 10$ eV as seen above. Then ν_τ can contribute to the energy density of the present universe $\Omega_{\nu_\tau} \sim 0.1$ as a hot dark matter (HDM). On the other hand, the lightest superparticle (LSP) can account for the cold dark matter (CDM) component. Thus our model can provide both CDM and HDM, as a mixed dark matter model recently favored in the literatures [27].

In summary, we have demonstrated that the right-handed neutrino, combined with SUSY, gives a natural model of chaotic inflation. This model also generates baryon number asymmetry by the decay of the inflaton. The mass of the right-handed neutrino $M \sim 10^{13}$ GeV is consistent both with the COBE data and the MSW solution to the solar neutrino problem.

References

- [1] A.H. Guth, *Phys. Rev. D* **23**, 347 (1981).
- [2] K. Sato, *Mon. Not. R. astr. Soc.* **195**, 467 (1981); M.B. Einborn and K. Sato, *Nucl. Phys. B* **180** [FS2], 385 (1981).
- [3] K. Sato, *Phys. Lett.* **99B**, 66 (1981).
- [4] S. Weinberg, *Phys. Rev. Lett.* **48**, 1303 (1982).
- [5] G.F. Smoot *et al.*, *Astrophys. J. Lett.* **396**, L1 (1992).
- [6] S.W. Hawking, *Phys. Lett.* **115B**, 295 (1982); A.A. Starobinsky, *Phys. Lett.* **117B**, 175 (1982); A.H. Guth and S-Y. Pi, *Phys. Rev. Lett.* **49**, 1110 (1982).
- [7] D.S. Salopek, *Phys. Rev. Lett.* **69**, 3602(1992).
- [8] M. Yoshimura, *Phys. Rev. Lett.* **41**, 281 (1978); A.Yu. Ignatiev, N.V. Krasnikov, V.A. Kuzmin and A.N. Tavkhelidze, *Phys. Lett.* **76B**, 436 (1978).
- [9] V.A. Kuzmin, V.A. Rubakov, and M.E. Shaposhnikov, *Phys. Lett.* **155B**, 508 (1985).
- [10] There are attempts to generate baryon number asymmetry at the electroweak scale (see, for example, A. Cohen, D.B. Kaplan, and A.E. Nelson, *Nucl. Phys. B* **373**, 453 (1992), and references therein). However, it requires a first-order phase transition of the electroweak symmetry breaking, and there should be a light Higgs boson ($\lesssim 35$ GeV) in the minimal Standard Model (M. Dine *et al.*, *Phys. Rev. D* **46**, 550 (1992)) which contradicts the lower bound from LEP ($\gtrsim 65$ GeV). A large CP-violating phase is also necessary in the Higgs potential. Thus at least two doublets of Higgs bosons should be introduced. Moreover, the resulting baryon number asymmetry depends on the details of the dynamics of phase transition, and it is still not clear whether the desired baryon number asymmetry can be generated. Though SUSY predicts two doublets of Higgs bosons, such a large CP-violation is difficult to achieve (N. Maekawa, *Phys. Lett.* **B282**, 387 (1992)). Other sources of CP-violation in SUSY models are also strongly constrained from the neutron electric dipole moment (A.G. Cohen and A.E. Nelson, UCSD-PTH-92-32, Aug 1992).
- [11] M. Veltman, *Acta Phys. Pol.* **B12**, 437 (1981); L. Maiani, *Proc. Summer School of Gif-sur-Yvette* (Paris, 1980) p.3; S. Dimopoulos and S. Raby *Nucl. Phys. B* **192**, 353 (1981); E. Witten, *Nucl. Phys. B* **188**, 513 (1981); M. Dine, W. Fischler and M. Srednicki, *Nucl. Phys. B* **189**, 575 (1981).
- [12] K. Inoue, A. Kakuto, H. Komatsu, and S. Takeshita, *Prog. Theor. Phys.* **68**, 927 (1982); L.E. Ibanez and G.G. Ross, *Phys. Lett.* **110B**, 215 (1982).

- [13] LEP Collaborations, *Phys. Lett.* **B276**, 247 (1992).
- [14] A.D. Linde, *Phys. Lett.* **129B**, 177 (1983).
- [15] M. Fukugita and T. Yanagida, *Phys. Lett.* **B174**, 45 (1986).
- [16] For a combined analysis of three experiments, see P. Anselmann *et al*, *Phys. Lett.* **B285**, 390 (1992).
- [17] L. Wolfenstein, *Phys. Rev.* **D17**, 2369 (1978); P. Mikhayev and A. Smirnov, *Nuovo Cimento* **9C**, 17 (1986); H. Bethe, *Phys. Rev. Lett.* **56**, 1305 (1986).
- [18] T. Yanagida, in *Proceedings of Workshop on the Unified Theory and the Baryon Number in the Universe*, Tsukuba, Japan, 1979, edited by A. Sawada and A. Sugamoto (KEK, Tsukuba, 1979), p. 95; M. Gell-Mann, P. Ramond and R. Slansky, in *Supergravity*, proceedings of the Workshop, Stony Brook, New York, 1979, edited by P. Van Nieuwenhuizen and D.Z. Freedman (North-Holland, Amsterdam, 1979), p. 315.
- [19] Identifying the deficit of the solar neutrino with ν_e - ν_μ oscillation *à la* MSW, we need a Dirac mass $\simeq 3$ GeV for the second generation, which is larger than the charm quark mass.
- [20] It is quite unnatural to expect that the gauge non-singlet fields sit precisely on the flat direction from the beginning with a huge value $\gg M_P$.
- [21] R. Juskiewicz, J. Silk, and A. Stebbins, *Phys. Lett.* **158B**, 463 (1985); J. Ellis, D.V. Nanopoulos, and S. Sarkar, *Nucl. Phys.* **B259**, 175 (1985); M. Kawasaki and K. Sato, *Phys. Lett.* **B189**, 23 (1987); J. Ellis, G.B. Gelmini, J.L. Lopez, D.V. Nanopoulos, and S. Sarkar, *Nucl. Phys.* **B373**, 399 (1992).
- [22] S.Yu. Khlebnikov and M.E. Shaposhnikov, *Nucl. Phys.* **B308**, 885 (1988).
- [23] J.S. Harvey and M.S. Turner, *Phys. Rev.* **D42**, 3344 (1990).
- [24] I. Affleck and M. Dine, *Nucl. Phys.* **B249**, 361 (1985).
- [25] J. Ellis, K. Enqvist, D.V. Nanopoulos, and K. Olive, *Phys. Lett.* **B191**, 343 (1987).
- [26] We thank T. Moroi for pointing out this problem.
- [27] M. Davis, F.J. Summers, and D. Schlegel, *Nature* **359**, 393 (1992); A.N. Taylor and M. Rowan-Robinson, *Nature* **359**, 396 (1992).

Generation of Gravitational Wave in the First Order Phase Transition

Y.Suzuki,

Department of Physics, Tohoku University

Abstract

We point out a possibility that the JBD field radiation from true vacuum bubble may exist without any collision process in the context of extended inflation.

1 Introduction

The inflationary model based on the first order phase transition has recently been reviewed in the context of extended inflationary scenario. Extended inflation was proposed as a solution to the “graceful exit” problem by La and Steinhardt[1]. The essential difference with old inflation is that gravity is described by the Jordan-Brans-Dicke(JBD) type theory with a scalar field ϕ and the scale factor in the false vacuum grows according to a power law in time rather than the exponential one. This “softened” behavior of the scale factor allows percolation of the true vacuum. In the first order inflation the transition proceeds via the nucleation of true-vacuum bubbles, and the reheating of the Universe may be caused by the collision of bubbles. As pointed out by Turner and Wilzek, this collision may produce a large amount of gravitational wave[2]. Recently the amount of gravitational radiation from bubble collision has been computed[3].

In the following we will study the effect of the JBD type scalar field ϕ on the generation of the gravitational wave. This is based on a work in progress in collaboration with Y. Tamiya and M. Yoshimura[4].

2 Conservation law

We consider the theory described by the action

$$S = \int d^4x \sqrt{-g} (AR - B \nabla_\lambda \phi \nabla^\lambda \phi - U + \mathcal{L}_M), \quad (1)$$

where ϕ is a real scalar field corresponding to the JBD field and A, B , and U are some functions depending only on ϕ . \mathcal{L}_M is the matter Lagrangean which includes the inflaton field Ψ of which the true vacuum bubble is composed. The field equations in this theory are written as

$$G_{\mu\nu} - \frac{1}{A} (\nabla_\mu \nabla_\nu - g_{\mu\nu} \square) A = \frac{1}{2A} (T_{\mu\nu} + T_{\mu\nu}^{(\phi)}), \quad (2)$$

$$2B \square \phi = -A' R + U' - B' \nabla_\lambda \phi \nabla^\lambda \phi, \quad (3)$$

$$\frac{\delta S}{\delta \Psi} = 0, \quad (4)$$

where $T_{\mu\nu}$ is the energy-momentum tensor of the matter field, $T_{\mu\nu}^{(\phi)}$ is defined by

$$T_{\mu\nu}^{(\phi)} \equiv 2B \nabla_\mu \nabla_\nu \phi - g_{\mu\nu} (B \nabla_\lambda \phi \nabla^\lambda \phi + U), \quad (5)$$

and the prime denotes the ϕ derivative. The choice $A = \phi/16\pi$, $B = \omega/16\pi\phi$, and $U = 0$ corresponds to the original JBD theory. It is important to bear in mind that the covariant conservation law $\nabla_\mu T^{\mu\nu} = 0$ holds if \mathcal{L}_M does not depend on ϕ .

In the Einstein theory ($A = 1/16\pi G$, $B = 0$, and $U = 0$), the ordinary conservation law is obtained by rewriting the Einstein equation[5] as follows:

$$(-g) \left(T^{\mu\nu} + \frac{1}{16\pi G} \tau^{\mu\nu} \right) = \frac{1}{16\pi G} \partial_\lambda \partial_\rho H^{\mu\lambda\nu\rho}, \quad (6)$$

where $H^{\mu\lambda\nu\rho} \equiv (-g)(g^{\mu\nu}g^{\lambda\rho} - g^{\mu\rho}g^{\lambda\nu})$ and $\tau^{\mu\nu}$ is defined by

$$(-g)\tau^{\mu\nu} \equiv \partial_\lambda \partial_\rho H^{\mu\lambda\nu\rho} - 2(-g)G^{\mu\nu}. \quad (7)$$

The conservation law $\partial_\mu (-g)(T^{\mu\nu} + \tau^{\mu\nu}/16\pi G) = 0$ follows immediately from the antisymmetry of indices μ and λ of $H^{\mu\lambda\nu\rho}$. It can be shown that $\tau^{\mu\nu}$ has two significant properties, that is, it is symmetric and contains no second derivatives of the metric.

As concerns the generalized JBD type theory(1), we can also obtain the conservation law by means of eq.(7)[6]. There are an infinite number of conservation laws as pointed out by

D.L.Lee [7]. To see this, multiplying eq.(2) by some function F of ϕ , we obtain

$$\begin{aligned} & (-g)F\tau^{\mu\nu} + (-g)\frac{F}{A}(T^{\mu\nu} + T_{\mu\nu}^{(\phi)}) + \partial_\lambda F \cdot \partial_\rho H^{\mu\lambda\nu\rho} + \partial_\rho F \cdot \partial_\lambda H^{\mu\lambda\nu\rho} \\ & + H^{\mu\lambda\nu\rho}\partial_\lambda\partial_\rho F + 2(-g)\frac{F}{A}(\nabla^\mu\nabla^\nu - g^{\mu\nu}\square)A = \partial_\lambda\partial_\rho(FH^{\mu\lambda\nu\rho}), \end{aligned} \quad (8)$$

after using eq.(7). The conservation law of the form

$$\partial_\mu[(-g)FZ^{\mu\nu}] = 0, \quad (9)$$

follows from the antisymmetric property of $FH^{\mu\lambda\nu\rho}$ in the right hand side of eq.(8) and where $Z^{\mu\nu}$ is a complicated expression involving derivatives of $g_{\lambda\rho}$, ϕ , and $T^{\mu\nu}$. The point to observe is that $Z^{\mu\nu}$ is symmetric for arbitrary F , but generally contains second derivatives of ϕ . From eq.(8), the requirement for $Z^{\mu\nu}$ not to contain second derivatives of ϕ uniquely determines $F = A^2$ up to a constant factor. This requirement is natural in the sence of the energy-momentum tensor for the ordinary matter field in the flat space-time, so we shall concentrate on this choice below.

3 Radiation from one bubble

Let us leave the generality of the conservation law and turn to the generation of the gravitational wave from bubble. Especially to clarify the difference between the Einstein theory and the JBD type theory which contains a scalar field ϕ , we consider the following case:

$$\begin{aligned} g_{\mu\nu} &= \eta_{\mu\nu} + h_{\mu\nu} & (h_{\mu\nu} \ll 1), \\ \phi &= \phi_0 + \varphi & (\phi/\varphi \ll 1), \\ T_\alpha^\alpha &\gg U_0, U'_0, U''_0, \end{aligned}$$

where ϕ_0 is constant, the subscript "0" denotes the value at ϕ_0 , and $\eta_{\mu\nu}$ is the Minkowski metric. Such conditions are not always met in extended inflation senario; especially $g_{\mu\nu}$ will be far from $\eta_{\mu\nu}$. Nevertheless, we will make the weak field approximation since we discuss only qualitative aspects in this article. Formulation for generation of gravitational wave in general space-time background is very difficult. Thus, the lowest order field equations[8] are

$$\square(h_{\mu\nu} + \frac{A'_0}{A_0}\eta_{\mu\nu}\varphi) = -\frac{1}{A_0}(T_{\mu\nu} - \frac{1}{2}\eta_{\mu\nu}T_\alpha^\alpha), \quad (10)$$

$$\square\varphi = \beta_0 T_\alpha^\alpha \quad \left(\beta_0 \equiv \frac{A'_0}{4A_0} \left(B_0 + \frac{3}{2} A'_0 \frac{A'_0}{A_0} \right)^{-1} \right), \quad (11)$$

where $\square \equiv \eta^{\mu\nu} \partial_\mu \partial_\nu$, and we impose the gauge condition

$$\partial_\mu (\sqrt{-g} A g^{\mu\nu}) \approx A_0 \partial_\mu \left(\frac{1}{2} h \eta^{\mu\nu} + \frac{A'_0}{A_0} \eta^{\mu\nu} \varphi - h^{\mu\nu} \right) = 0, \quad (12)$$

where $h \equiv \eta^{\mu\nu} h_{\mu\nu}$. These linearized equations can be solved using the retarded potential and $T_{\mu\nu}$ is determined by solving eq.(4) in flat space-time with appropriate boundary conditions. The expression of the energy emitted from the source $T_{\mu\nu}$ is obtained by substituting above solution into $Z^{\mu\nu}$. If $T_{\mu\nu}$ vanishes at infinity, using Fourier components of $T_{\mu\nu}$, the energy per solid angle emitted in a direction \hat{k} is

$$\frac{dE}{d\Omega} = \frac{1}{8\pi A_0} \int_0^\infty d\nu \nu^2 (\Lambda_{ij,lm} + \beta_0 A'_0 V_{ij,lm}) \tilde{T}^{ij}(\mathbf{k}, \nu) \tilde{T}^{lm*}(\mathbf{k}, \nu), \quad (13)$$

$$\Lambda_{ij,lm} \equiv \delta_{ij} \delta_{lm} - 2\hat{k}_j \hat{k}_l \delta_{im} + \frac{1}{2} \hat{k}_i \hat{k}_j \hat{k}_l \hat{k}_m - \frac{1}{2} \delta_{ij} \delta_{lm} + \frac{1}{2} \delta_{ij} \hat{k}_l \hat{k}_m + \frac{1}{2} \hat{k}_i \hat{k}_j \delta_{lm},$$

$$V_{ij,lm} \equiv (-\hat{k}_i \hat{k}_j + \delta_{ij})(-\hat{k}_l \hat{k}_m + \delta_{lm}),$$

$$\tilde{T}^{ij}(\mathbf{k}, \nu) \equiv \frac{1}{2\pi} \int d^4x \exp(i\nu t - i\mathbf{k} \cdot \mathbf{x}) T^{ij}(\mathbf{x}, \nu),$$

where (\mathbf{k}, ν) is null vector, $\hat{k}^i \equiv k^i/\nu$ (i.e. unit vector), and we have expressed $\tau^{\mu\nu}$ with the purely spacelike components T^{ij} by means of the flat space-time conservation law $\partial_\mu T^{\mu\nu} = 0$. In the Einstein theory, the second term of eq.(13) which is proportional to A'_0 vanishes.

Consider one growing bubble. The corresponding field configuration will be spherically symmetric, that is, \tilde{T}^{ij} is of the form

$$\tilde{T}^{ij}(\mathbf{k}, \nu) = c_1(\nu) \delta^{ij} + c_2(\nu) \hat{k}^i \hat{k}^j, \quad (14)$$

where c_1 and c_2 are some functions depending only upon ν . From definition of $\Lambda_{ij,lm}$ and $V_{ij,lm}$,

$$\delta^{ij} \Lambda_{ij,lm} = 0, \quad \hat{k}^i \hat{k}^j \Lambda_{ij,lm} = 0,$$

$$\delta^{ij} V_{ij,lm} = 2(-\hat{k}_l \hat{k}_m + \delta_{lm}), \quad \hat{k}^i \hat{k}^j V_{ij,lm} = 0.$$

Here we can see the difference between the Einstein theory and the JBD theory. That is, in the Einstein theory no gravitational wave is emitted from a spherically symmetric source (it is known as Birkhoff's theorem), but in the JBD type theory ($A'_0 \neq 0$) the radiation may exist even for a spherically symmetric source. It is a remarkable difference.

4 Discussions

Finally we shall discuss the effect on extended inflation. First, the energy stored in a bubble wall is liberated not only into the gravity wave but also into the scalar ϕ wave, since the gravitational wave generated by the bubble wall will be reduced in comparison with the Einstein theory. Second, when the back reaction is taken into account the velocity of the wall will not become very large. If this is the case, the suppression of large bubbles will be achieved, which may reduce inhomogeneity caused by large bubbles[9].

References

- [1] D. La and P.J. Steinhardt, *Phys.Rev.Lett.***62**(1989)376
- [2] M.S. Turner and F. Wilczek, *Phys.Rev.Lett.***65**(1990)3080
- [3] M. Shibata and Y. Nambu, Kyoto University preprint 1095, A. Kosowski, M.S. Turner, and R. Watkins, *Phys.Rev.Lett.***69**(1992)2026
- [4] Y. Suzuki, Y. Tamiya, and M. Yoshimura, in preparation.
- [5] L. Landau and E. Lifshitz, *The Classical Theory of Fields* (Addison-Wesley Press, Cambridge 1951)
- [6] Y. Nutku, *Astrophys.J.***158**(1971)991 and J. Dykla, Ph.D. thesis, Caltech, 1972, unpublished.
- [7] D.L. Lee, *Phys.Rev.D***10**(1974)2374
- [8] S. Weinberg, *Gravitation and Cosmology* (Wiley, New York, 1972)
- [9] E.J. Weinberg, *Phys.Rev.D***40**(1989)3950

Annihilation of Domain Walls

Michiyasu Nagasawa

*Department of Physics, Faculty of Sciences,
The University of Tokyo, Tokyo 113, Japan*

Abstract

The dynamical evolution of a wall-string system is investigated. Walls intersect each other and collapse at about ten percent of the light velocity. Such moving walls attract matter as positive gravitational sources. They annihilate with few oscillation so that the lost energy radiates as a scalar mode. Thus although the decays are non-spherical, the production of gravitational waves is expected to be rare. As for the $N = 1$ axion domain wall model, walls prove to be harmless in the standard cosmology since they do not dominate the universe.

1 Introduction

The union of cosmology and high energy physics has brought some interesting ideas to the events in the very early universe. Topological defects stem from such ideas. They come into existence at phase transitions accompanied by some symmetry breakings. Such a phase transition takes place when the symmetries between elementary interactions vanish away. For this process to occur, the restoration of the symmetries which are now broken is indispensable. The high energy density state in the early part of the cosmic history enables this revival so that topological defects are produced during the thermal phase transition[1]. Thus it is natural that the energy scale of defects generation should be a unification scale. In the GUT era, however, the universe must not be in the thermal equilibrium[2], which makes the Kibble mechanism impossible. Even in that case, the inflationary expansion[3] saves the symmetry recovery due to the curvature correction and the quantum phase transition generates topological defects[4]. Hence the creation of defects is a fairly general phenomenon and its effect to the cosmological evolution is worth to notice. By the degree number of the homotopy group concerning the true vacuum manifold, they can be classified to various types such as domain walls, cosmic strings, monopoles or textures. Particularly, global textures provide a promising scenario of the structure formation in the universe[5]. On the other hand, domain walls were considered to be disastrous since they would soon grow to dominate the energy density of the universe[6]. To avoid this problem, the wall producing transition has to happen on the sufficiently late time. Such a phase transition after the recombination may explain the cosmological large-scale structure[7].

In the present paper, we concentrate on complex defects, that is, walls bounded by strings. This kind of walls arises in various axion models[8]. Two different transitions are

included in these theories. First, the Peccei-Quinn $U(1)$ symmetry is broken and global strings are produced. Then the second phase transition at QCD energy scale comes about and the strings turn to be surrounded by N walls that spring out from each string. For the axion model to work successfully, these walls should annihilate not to dominate the universe with their energy. It is believed that in the cases of $N > 1$ the network of walls survives too long so that the model fails, although $N = 1$ walls rapidly disappear, which means the axion postulation does not conflict with the cosmology[9]. Ryden et al. got this result by numerical simulations but they used a modified equation. Here we investigate the dynamics of an individual string-wall system and confirm the justification of the $N = 1$ axion model. Moreover, the detailed aspect of wall collapses is roughly reported.

2 Model and Method

We employ a complex scalar field of a single component that obeys a following Lagrangian

$$\mathcal{L} = \frac{1}{2}(\partial_\mu \phi)(\partial^\mu \phi) - V_s(\phi) - V_w(\phi), \quad V_s(\phi) = \frac{\lambda}{4}(|\phi|^2 - v^2)^2, \quad V_w(\phi) = V_a(1 - \cos \theta), \quad (1)$$

where θ signifies the phase of ϕ . The first term of the potential, V_s , gives rise to strings and domain walls ($N = 1$) are originated from the second term, V_w , at $\theta = \pi$. The line energy density of strings, μ , and the core radius of them, δ_s , are

$$\mu \sim v^2, \quad \delta_s \sim 2(\lambda v^2)^{-1/2}, \quad (2)$$

respectively. The surface energy density of walls, σ , and the width scale of them, δ_w , are

$$\sigma \sim v\sqrt{V_a}, \quad \delta_w \sim \frac{v}{\sqrt{V_a}}. \quad (3)$$

To follow the time evolution of walls numerically, we have to solve the field evolution under a certain space-time. As the most simple hypothesis, we assume that the background should be a flat Robertson-Walker universe. Then the field equation is written by

$$\frac{\partial^2 \phi}{\partial \tau^2} + \frac{2}{a} \left[\frac{da}{d\tau} \right] \frac{\partial \phi}{\partial \tau} - \nabla^2 \phi = -a^2 \frac{\partial V}{\partial \phi}, \quad (4)$$

where $a = a(\tau)$ is a scale factor and τ is conformal time defined by $d\tau = dt/a$. When we pay attention to a single hybrid string-wall system well inside the cosmological horizon, we can make use of the Minkowski metric, that is, the effect of the expansion can be neglected. Then the evolution equation is expressed as

$$\frac{\partial^2 \phi}{\partial t^2} - \nabla^2 \phi = -\frac{\partial V}{\partial \phi}. \quad (5)$$

In numerical steps, the factor, a^2 , on the right-hand-side term of the equation (4) spoils the calculations. The physical meaning of this breakdown is that the resolution becomes

lower with the increase of the expansion factor, a , since the lattice separation of the simulation box is constant in comoving size although the wall width is constant in physical length. To keep away from this restriction, Ryden et al.[9] dropped the a^2 factor and replaced the coefficient, 2, in the second term of the left-hand-side in the equation (4) with 3. We are not confident whether this modification alters the dynamics of walls fatally so we have used two equations (4) and (5) without any reformation.

Numerical simulations are performed in 100^2 two-dimensional boxes and 64^3 three-dimensional boxes. In both cases, the equations are solved by the discretized method in the second order accuracy. The parameters are set such that $\delta_s \sim 2$ meshes and $\delta_w \sim 10$ meshes. As a result, the ratio of the string vacuum energy to the wall vacuum energy, $\lambda v^4/V_w$, becomes ~ 100 . We have found that the change of μ has little effect on the wall dynamics since there is extremely small region where the field stays in the false vacuum of V_s . When the cosmic expansion is taken into consideration, the scale factor is normalized as $a = 1$ at the equipartition time of radiation and matter.

3 Evolution of Wall Area

At first we look over the time evolution of the wall area in the expanding universe. For this purpose, we have to find a way to determine the total amount of walls in the simulation box. This can be carried out by counting the number of cells in which the phase of the field, θ , takes π , that is, where the false vacuum of V_w remains. However, we can get the value of θ only at grid points. Thus it is rather difficult to find out the place at which θ equals π exactly. Instead, we have identified sides where the sign of $\sin \theta$ changes from plus to minus and yet $\cos \theta < 0$ at the same time as the position where walls cross. Using this method, we have calculated the evolution of domain walls numerically in the 64^3 box.

Initially the amplitude of the field equals v at every cell and the phase is chosen randomly. The difference in the initial condition has no effect on the field evolution sufficiently after the stabilizing era. Of course our following results are acquired from the analysis in this post-stabilization period. Figure 1 shows the result in the radiation dominated universe. Evidently the amount of walls has a tendency to decrease with time promptly. Figure 2 depicts the case that the expansion law is that in the matter universe. The same trend as the previous figure is also observed here.

Hence the prediction that the $N = 1$ axion domain wall should not bother the cosmological framework seems to be right. However, these simulations are executed for a few expansion time. This is because the resolution of the wall width becomes worse with the growth of the scale factor as we have mentioned. Moreover, we have solved the field equation precisely so that the viewpoint that we regard walls as rigid is not necessary. We can understand the dynamics of walls by using the distribution of the potential energy that is related with domain walls, V_w , in the simulation box. Following two sections treat such cases and the fact that walls surely collapse and disappear is examined in detail.

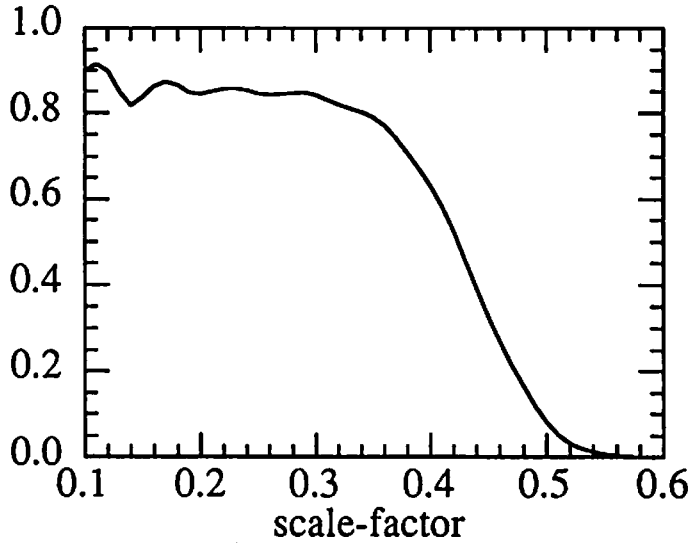


Figure 1 This figure shows the evolution of the volume ratio of the cells that contain walls to 64^3 , i.e., the number of the total cells in the comoving simulation box. The scale factor is normalized such as $a = 1$ at the equality time.

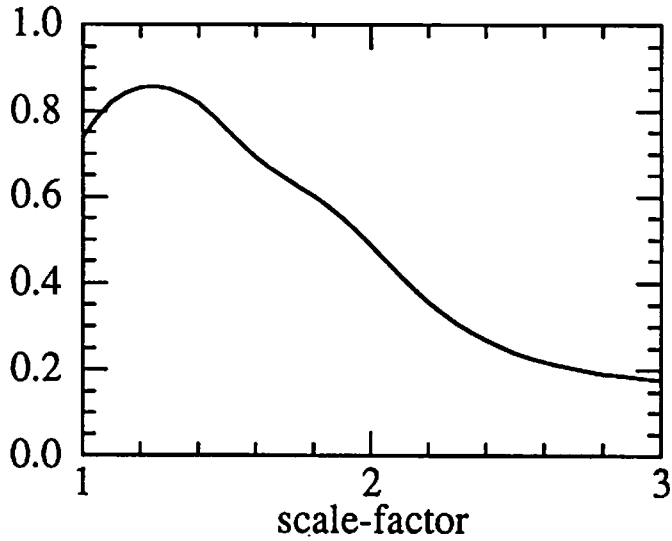


Figure 2 The same quantity as Figure 1 is plotted but in the matter dominated era.

4 Two Walls

In this section, we consider the interaction between two walls. Since defects fairly inside the horizon are our concern, we can ignore the cosmic expansion and the equation (5) is adopted. The initial condition is set so that one wall and one string-wall exist in the simulation box. Here "one wall" means the wall that has no end in the simulation box. And "one string-wall" means the wall that has only one end in the simulation box. They are arranged such that the edge of the string-wall faces one side of another wall. The distance between them is 10 meshes. Thus the translational symmetry in the z -direction is imposed on the configuration in the 100^2 box. This initial distribution of V_w at the z -slice is shown in Figure 3. This figure picks up the 50×50 meshes in the central principal part. The string-wall has an initial velocity whose magnitude is equal to the light velocity, c , toward the edgeless wall. Figure 4 shows the same quantity at the same slice as Figure 3 after the period of $10\Delta x/c$, where Δx represents the lattice separation. In this figure, the wall is cut by the string-wall and a kind of intercommutation of walls happens. When $t = 20\Delta x/c$, the wall potential energy is almost dissipated away, which we can see in Figure 5. The speed of wall motion is estimated to be about $0.1c$. We have done these computation under the periodic boundary. Other conditions, for example the reflective one, cause any deformation to our conclusions since the box size is so large that the influence of the boundaries cannot reach the main part where defects interact.

We have also checked how the behavior of walls is altered when the expansion of the universe is taken into account. The value of V_w after the scale factor grows 20 times larger than the initial one is shown in Figure 6. This calculation in the radiation dominant era starts from the same initial setup as the non-expanding one. The configuration of ϕ is practically unchanged from the outset and the collapse of walls is still on the way at this time. The walls move at almost the speed of light but the introduction of the expansion decelerates the disintegration process. In the matter era, this reduction becomes stronger.

When we suppose that walls may construct the cosmological large-scale structures, it is important how such wall decays work as a gravitational source. It is generally believed that an infinite plane wall acts as a repulsive sheet[10]. This solution of the Einstein equation is obtained under the approximation that the wall thickness is neglected. We have the original field configuration of walls so we can calculate the source density directly. The energy momentum tensor of a scalar field is written by

$$T_{\mu\nu} = \partial_\mu\phi\partial_\nu\phi - \frac{1}{2}g_{\mu\nu}g^{\alpha\beta}\partial_\alpha\phi\partial_\beta\phi + g_{\mu\nu}V(\phi). \quad (6)$$

Then using the Minkowski metric as $g_{\mu\nu}$ the gravitational source density, ρ , can be defined as

$$\rho = 2\dot{\phi}^2 - 2V(\phi), \quad (7)$$

under the Newtonian approximation. We have plotted this quantity in Figure 7 at the same time and slice as Figure 4. In the region where the wall is shrinking into, ρ has a positive value. Thus the contracting wall operates as a seed of attractive force. Unlike a simple static wall whose thickness is zero, moving walls are quite natural gravitational sources.

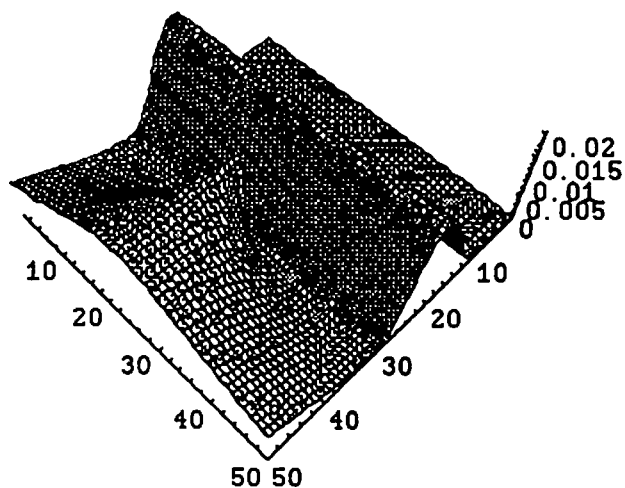


Figure 3 Two-dimensional distribution of the potential energy, V_w , in 50×50 z -slice is shown. This is the initial configuration for the crash of a wall and a string-wall. The vertical axis is normalized as $V_a = 0.01$.

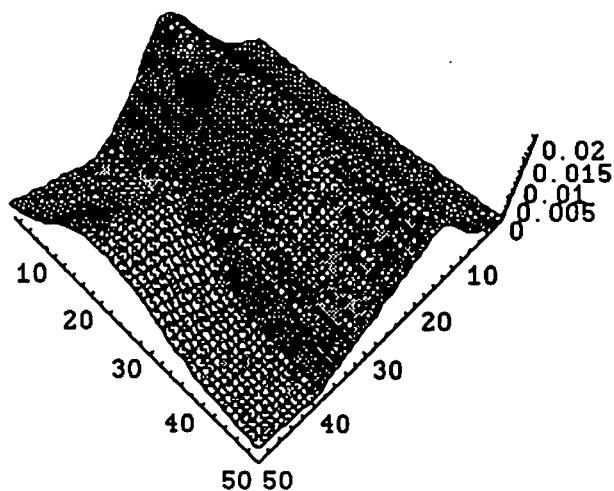


Figure 4 The value of V_w when the time, $t = 10\Delta/c$, has passed from Figure 3 is depicted.

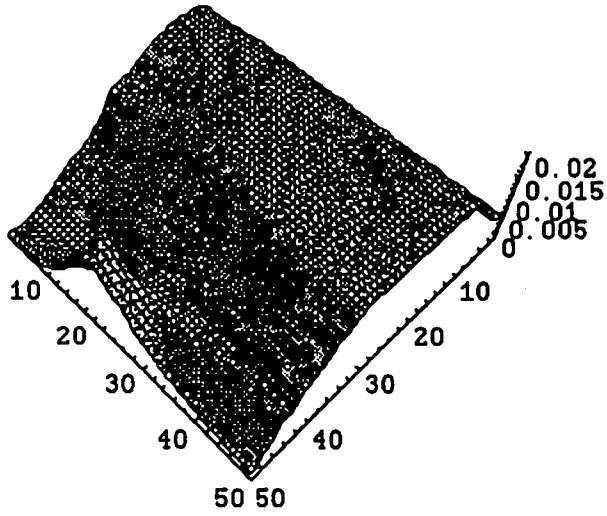


Figure 5 The value of V_w when the time, $t = 20\Delta/c$, has passed from Figure 3 is depicted.

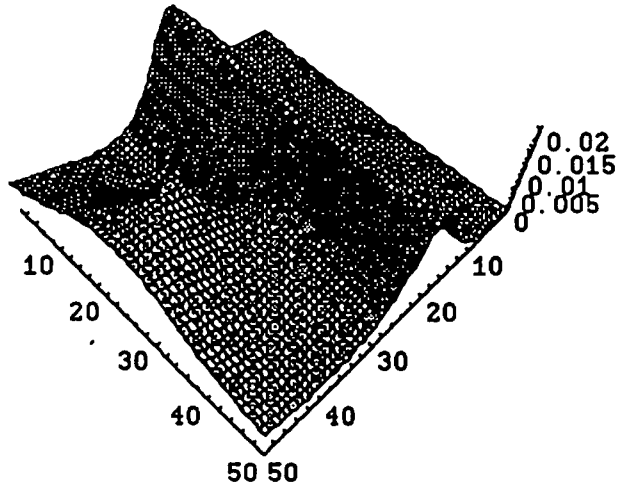


Figure 6 The case in which the cosmic expansion is included is shown. The calculation begins at $a = 0.05$ from the same configuration as Figure 3 and when $a = 1$ this figure is drawn.

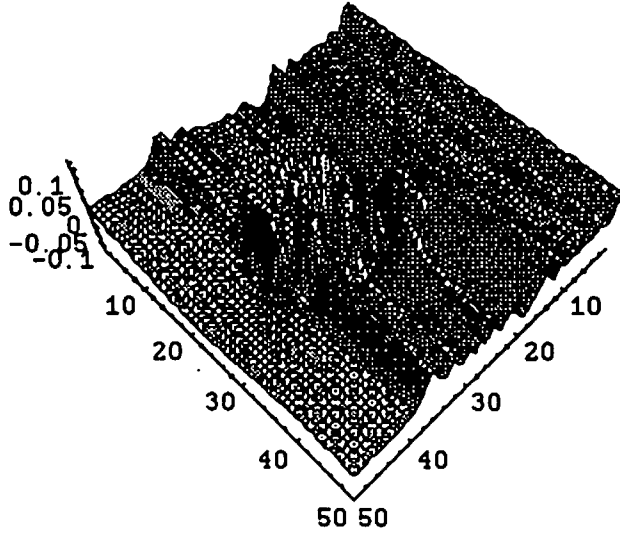


Figure 7 The distribution of the source energy density, ρ , at the same time and space as Figure 4 is demonstrated. The peaks correspond to the wall contracting region.

5 Disk Wall

Finally we have simulated the motion of a disk wall, a wall that is surrounded by a string loop. A collision of a wall and a string-wall which we have surveyed in the previous section is practically a two-dimensional simulation. On the other hand, a full three-dimensional simulation becomes possible in this case. When the computations start, the wall whose radius equals 15 meshes is placed in the x, z -plane centered on the 64^3 box. Therefore the coordinate of the circular string that encloses the wall is expressed by

$$y = 32, \quad (x - 32)^2 + (z - 32)^2 = 15^2. \quad (8)$$

The direction of the wall motion is that of the y -axis. Its magnitude is the speed of light at the ends where $(x, z) = (17, 32), (47, 32)$ and is zero at the middle of the wall, $x = 32$. The distribution of V_w at $y = 32$ when $t = 0$ is shown in Figure 8. At $t = 20\Delta x/c$ this evolves to Figure 9. Apparently the energy of the wall has diffused and the division to multiple wall pieces is proceeding. Also in these situations, we have calculated the distribution of ρ that is described in Eq. (7). The fact that the source density is positive in the wall interacting region is verified as well.

When such loops decay, it is supposed that they oscillate many times and may radiate gravitational waves[11]. Our simulations, however, cannot reproduce clear oscillations. The intercommutations of walls are so frequent that there is not enough time for them to pursue the global motion like fluttering or wriggling.

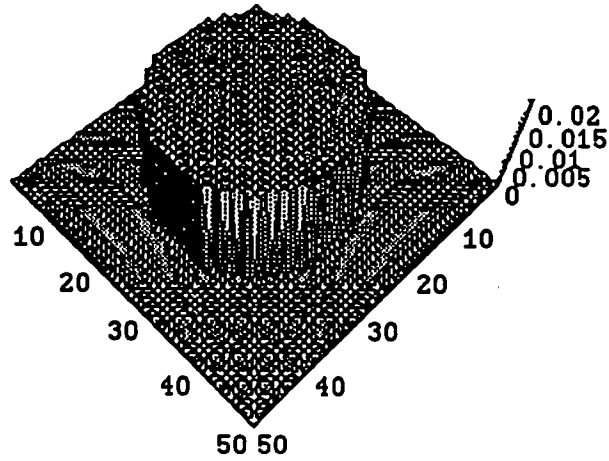


Figure 8 The initial V_w potential energy distribution of the disk wall simulation is shown at $y = 32$, $(x, z) = (8, 8) - (57, 57)$ slice. In this and the next figures, $V_a = 0.01$.

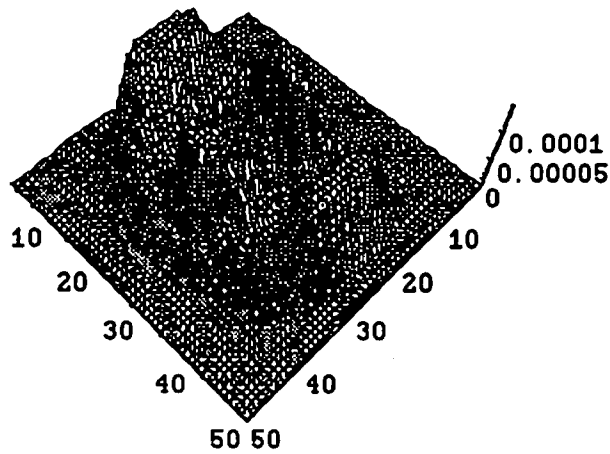


Figure 9 After $20\Delta/c$ from Figure 8 is plotted. The left-hand-side of the numbered axes is x -one. The height of this graph is magnified compared with the previous figure. The real value of the potential energy is much smaller than that in Figure 8 since most of it is transferred to the time derivative of the field.

6 Summary

We have investigated the dynamics of the scalar field that obeys a potential in (1). When it settles on a true vacuum, a connected string-wall system develops. Thus the motion of the hybrid topological defects has been understood. When the wall joined to the string is only one, such walls annihilate and dissipate the energy at the speed of $\sim 0.1c$ although this process is slowed down by the expansion of the universe. This means the $N = 1$ domain wall does not contradict the observation of our universe so that this gives a unique valid axion model.

The gravitational source density is calculated from the field configuration in various cases. All the results show that the interacting walls generate positive gravitational energy and produce attractive force. This feature may help the scenario of the large-scale structure formation by walls. It is an important distinction from an infinite static wall.

The interactions between walls are very violent. The oscillations of loops are hardly observed. It indicates that the false vacuum energy of domain walls is released mainly by a scalar field mode rather than by gravitational waves. Such a statement may be also realized in the case of pure strings. Whether it is true or not depends on the further study.

References

- [1] T.W.B. Kibble, J. Phys. **A9**(1976)1387.
A. Vilenkin, Phys. Rep. **121**(1985)263.
- [2] J. Ellis and G. Steigman, Phys. Lett. **B89**(1980)186.
- [3] K. Sato, Mon. Not. R. astr. Soc. **195**(1981)467.
A.H. Guth, Phys. Rev. **D23**(1981)347.
- [4] M. Nagasawa and J. Yokoyama, Nucl. Phys. **B370**(1992)472.
- [5] A. K. Gooding, C. Park, D. N. Spergel, N. Turok and R. Gott III, Ap. J. **393**(1992)42.
M. Nagasawa and K. Sato, Int. J. of Mod. Phys. **D1**(1992)427.
- [6] Y. B. Zel'dovich, I. Y. Kobzarev and L. B. Okun, JETP **40**(1975)1.
- [7] C. T. Hill, D. N. Schramm and J. N. Fry, Comments Nucl. Part. Phys. **19**(1989)25.
- [8] R. D. Peccei and H. R. Quinn, Phys. Rev. Lett. **38**(1977)1440.
- [9] B. S. Ryden, W. H. Press and D. N. Spergel, Ap. J. **357**(1990)293.
- [10] J. Ipser and P. Sikivie, Phys. Rev. **D30**(1984)712.
- [11] A. Vilenkin, Phys. Rev. Lett. **46**(1981)1169.

FALSE VACUUM DECAY IN GENERALIZED EINSTEIN GRAVITY

Takuya Maki

Department of Physics, Tokyo Metropolitan University,
Minami-ohsawa, Hachioji-shi, Tokyo 192-03

ABSTRACT

Bubble nucleation rate in theories including Brans-Dicke type scalar gravity is discussed. The Euclidean action is obtained in thin-wall approximation to calculate the rate. BD-scalar used in the estimate is seemed to be consistent in four-dimensional Euclidean space-time.

Many works for investigating to effects of gravity on the false vacuum decay have done (e.g. for non-zero vacuum energy [1] and for $O(3)$ symmetric bubble associate with a local gravitational source [2]). The decay rate in the generalized Einstein gravity has also been studied in some approximation, motivated by the extended inflation that avoids the so-called "graceful exit problem" without any fine-tuning [3][4]. The aim of this paper is to study $O(4)$ symmetric bubble solution in four-dimensional Euclidean space-time and discuss the effects of the generalized Einstein gravity on the bubble nucleation rate. For simplicity we consider the system including Brans-Dicke type scalar gravity (Einstein-BD scalar-Higgs system):

$$S = \frac{1}{16\pi} \int dx^4 \sqrt{-g} \left[-\phi R + \frac{\omega}{\phi} \partial^\mu \phi \partial_\mu \phi + 16\pi \left(\frac{1}{2} \partial^\mu \sigma \partial_\mu \sigma - V(\sigma) \right) \right], \quad (1)$$

where ϕ denotes BD-scalar and σ is the scalar (hereafter denoted σ -field). The σ -field undertakes the phase transition with potential $V(\sigma)$ which possesses double minima.

Making use of Euclidean Path Integral(EPI) formalism, the decay rate of the false vacuum per unit four-volume in the first WKB approximation can be expressed by

$$\Gamma=A\exp(-B), \quad (2)$$

where

$$B=S_E(\sigma)-S_E(\sigma_-).$$

The coefficient B is the difference between the Euclidean action for the bubble solution and that of the space-time with no bubble [5]. The coefficient A embodies the first order($O(\hbar)$) quantum correction to the action, which is of dimension of (mass)⁴. In this paper we are concerned with only evaluating the effect on the coefficient B .

We consider the scalar in metastable state with no local gravitational sources. Not that in the system there is no static background solution corresponding to the deSitter phase in Einstein-Higgs system (In extended inflation it is the fact that can solve the graceful exit problem i.e., power-law expansion). The investigation of the false vacuum decay in such a non-static background is in progress, so that we assume that the time-dependence can be neglected in the transition. Then the bounce solution with least action that make the dominant contribution to the rate Γ may have $O(4)$ symmetry, viz. scalar and BD-type scalar depend only on the four-radial coordinate ζ in four dimensional Euclidean space-time. The metric has the form

$$ds^2=d\zeta^2+a^2(\zeta)d\Omega^2, \quad (3)$$

where $d\Omega^2$ represents the unit 3-sphere. The Euclidean action is reduced to the simple form

$$S_E=\int d\zeta\{a^3(\zeta)V(\sigma)-\frac{3}{8\pi}a(\zeta)\phi(\zeta)\} \quad (4)$$

The $O(4)$ symmetric bounce solution satisfies the Euclidean field equations obtained by variation of Euclideanized action (1). The boundary conditions

for σ -field are the same as in the presence of conventional Einstein gravity: $\dot{\sigma}(\zeta=0)=\dot{\sigma}(\zeta=\zeta_{\max})=0$ and $\sigma(\zeta_{\max})=\sigma_-$ where ζ_{\max} denotes a maximum value for ζ (one of zeros of $a(\zeta)$). That for BD-scalar is not clear and is assumed that $\dot{\phi}=0$ at $\zeta=0$.

We consider the thin-wall approximation with BD-type scalar: the frictional term in the equation of motion is assumed to be neglect for σ -field. The scalar field remains near to v.e.v of the true vacuum state σ until ζ becomes large and then the field change its expectation value. This means that the field can be treated as a constant (vacuum value) both outside and inside the bubble. Then if ϕ -field is also a constant in Euclidean space-time as in previous works, the bubble solution in Euclidean space-time is not consistent because the energy-momentum tensor for σ -field should have δ -functional peak at the bubble wall in the thin-wall approximation. Indeed BD-scalar is affected by the wall and should obey the junction condition at the wall,

$$\dot{\phi}_-(\bar{\zeta})-\dot{\phi}_+(\bar{\zeta})=-\frac{8\pi}{2\omega+3}3s, \quad (5)$$

where s is the surface energy in the absence of BD-scalar. There is a trivial solution when the true vacuum energy vanishes: $\phi=\text{const.}=\phi_-$, $\sigma=\sigma_-$, $a=\zeta$, while outside the wall the solution with bubble is equivalent to that without bubble. Thus we may concern with only difference of Euclidean action with and without bubble inside the wall. In order to see the effect of BD-scalar, the solution of ϕ without bubble is approximated as

$$\phi=\phi_- - \frac{1}{2}\left(\frac{8\pi}{2\omega+3}4V_-\right)\zeta^2.$$

The difference of Euclidean action inside the bubble may be written as

$$S_E(\sigma)-S_E(\sigma_-)=-\frac{3\pi}{4}\phi_+a^2(\bar{\zeta})-\frac{3}{16V_-}\phi_-\left(1-\frac{8\pi}{3\phi_-}V_-a^2(\bar{\zeta})\right)^{3/2}-\frac{9s}{2\omega+3}\int_0^{\bar{\zeta}}d\zeta a(\zeta)\zeta^2. \quad (6)$$

ϕ_+ is determined by using the junction condition. The first and second terms are the same as those obtained by ref.[3]. The third term arises from

the fact that ϕ is not a constant in the presence of vacuum energy. When contribution of the derivative of ϕ to the equation of motion for $a(\zeta)$ can be neglected in the state without bubble and $(\phi - \phi_-) \ll \phi_-$, $a(\zeta)$ is of conventional Einstein-Higgs system. Then the third term is written as

$$I_3 = \frac{9s}{2\omega+3} \frac{1}{H^4} \{ (-H^2\zeta^2 + 2)\cosh H\zeta + 2H\zeta \sinh H\zeta - 2 \} \quad (7)$$

where $H_- = (8\pi V_-/3\phi_-)^{1/2}$. This result, together with contribution from bubble wall, gives the coefficient B.

The consistent bubble solution involving BD-scalar in four-Euclidean space-time has been taken account in thin-wall approximation for σ -field. In order to estimate the nucleation rate, We have used the $O(4)$ symmetric configuration of ϕ that satisfies the junction condition (5). Since understanding of behavior of BD-scalar in EPI formalism is lack, it is not clear that the result obtained by Eq.(6) determines really the nucleation rate. The problem is left for future work.

REFERENCES

- [1] Coleman and De Luccia, Phys. Rev. D21, 3305 (1980).
- [2] Hiscock, Phys. Rev. D35, 1161 (1987); Berezin, Kuzmin and Tkachev, *ibid.* 43, R3112 (1991).
- [3] Accetta and Romanelli, Phys. Rev. D41, 3024 (1990).
- [4] La and P.J.Steinhardt, Phys. Rev. Lett. 62,376 (1989).
- [5] Coleman, Phys. Rev. D15, 2929 (1977); C.Callan and S. Coleman, *ibid.* 16, 1762 (1977).

Fate of Inhomogeneity in Schwartzshild-deSitter Space-time

Sigeru Konno and Yasusada Nambu

Department of Physics, Nagoya University
Chikusa, Nagoya 464-01, Japan

February 22, 1993

1 Introduction

The inflationary scenario is a favorable model to explain the homogeneity and isotropy of the present universe. In this scenario, the vacuume energy of the matter field plays a role of the cosmological constant, and the universe enters the phase of deSitter expansion. Initial inhomogeneity of the universe damps due to the rapid cosmological expansion. To utilize these aspects of inflation, it is necessary to discuss whether the universe can enter the inflationary phase from the wide range of the initial condition. "Cosmic no hair conjecture" states that if a positive cosmological constant exists, all space-times approach deSitter space-time asymptotically. But it is difficult to prove and formulate this conjecture for general situation and we do not know whether it is true.

In the case of spherical symmetric space-time with cosmological constants, it is shown that the space-time does not necessarily approaches deSitter but a black hole and a worm hole may be created[1, 2]. The final global structure of the space-time depends the scale and the amplitude of the initial inhomogeneity. In a practical sense, a whole universe does not need to inflate but only a portion of our universe has to inflate(weak no hair conjecture)[3]. We can say that inflation works well if the "measure" of the initial condition, from which the universe has a inflating region, is large.

To tackle this problem, we investigate the evolution of the inhomogeneity in the Schwartzshild-deSitter space time. As a source of inhomogeneity, we use a false vacuume bubble. Our purpose is to classify the parameter space that represents the degree of the initial inhomogeneity, and check the effectiveness of "weak no hair conjecture".

2 Metric Junction

We assume that the inside space-time of the bubble is described by deSitter metric with cosmological constant Λ_1 , the outside is described by Schwartzshild-deSitter metric with

mass m and cosmological constant Λ_2 :

$$ds_{in}^2 = -(1 - \chi_1^2 r^2) dt^2 + (1 - \chi_1^2 r^2)^{-1} dr^2 + r^2 d\Omega^2, \quad (1)$$

$$ds_{out}^2 = -(1 - \frac{r_g}{r} - \chi_2^2 r^2) dt^2 + (1 - \frac{r_g}{r} - \chi_2^2 r^2)^{-1} dr^2 + r^2 d\Omega^2, \quad (2)$$

where $\chi_1^2 = 8\pi G\Lambda_1/3$, $\chi_2^2 = 8\pi G\Lambda_2/3$ and $r_g = 2Gm$. The motion of the bubble can be determined by the junction condition:

$$K_j^i(in) - K_j^i(out) = 4\pi\sigma G\delta_j^i, \quad (3)$$

where K_j^i is the extrinsic curvature of $(2+1)$ -dimensional hypersurface swept out by the domain wall. σ is the surface energy of the bubble and is a constant for the scalar field domain wall. θ - θ component of this equation gives the equation of motion of the bubble's radius $r(\tau)$ where τ is the proper time on the wall. By introducing the dimensionless variable[4], our basic equation becomes

$$\left(\frac{dz}{d\tau}\right)^2 + V(z) = E, \quad (4)$$

where

$$\begin{aligned} z &= r/r_0, & r_0^3 &= 2G|m|/\chi_+^2, & \kappa &= 4\pi G\sigma \\ \chi_+^2 &= [(\kappa^2 + \chi^2 - \chi_2^2)^2 + (2\kappa\chi_2)^2]^{1/2}, \\ V(z) &= -\left(z - \frac{1}{z}\right)^2 - \gamma^2/z, \\ \gamma^2 &= 2 + 2\text{sgn}(m)(\kappa^2 + \chi_2^2 - \chi^2)/\chi_+^2, \\ E &= -\left(\frac{2\kappa}{\chi_+}\right)^2 (2G|m|\chi_+)^{-2/3}. \end{aligned}$$

θ - θ component of the extrinsic curvature of the bubble interior and exterior are given by

$$\beta_{in} = \left(\frac{G|m|}{r_0^2\kappa}\right) \frac{1}{z^2} \left[\text{sgn}(m) - \left(\frac{\chi^2 - \chi_2^2 + \kappa^2}{\chi_+^2}\right) z^3 \right], \quad (5)$$

$$\beta_{out} = \left(\frac{G|m|}{r_0^2\kappa}\right) \frac{1}{z^2} \left[\text{sgn}(m) - \left(\frac{\chi^2 - \chi_2^2 - \kappa^2}{\chi_+^2}\right) z^3 \right]. \quad (6)$$

3 Classification of the space-time

We can classify the global structure of the space-time using Eq.(4) and Eq.(6). The result is shown in Fig.1. The horizontal axis is the ratio of the cosmological constant χ_2/χ_1 , and the vertical axis is the gravitational mass $2Gm\chi_1$. The parameter space (χ_2, m) is divided to regions R1~R14. R1~R9 corresponds to the positive gravitational mass. In R1,R2, Schwarzschild horizon disappears and the space-time becomes deSitter like. R4 and R5 also correspond to a deSitter like space-time. R2 is to a worm hole space-time. R4,R5,R6 corresponds to a black hole space-time. If we take the limit $\kappa \rightarrow 0$, the motion of the bubble

becomes null and we get the same result of Maeda *et al*[1]. In this limit, R3,R4,R5,R10 and R11 disappear. Non zero value of the surface energy gives the same effect as to make χ_1 large (make χ_2/χ_1 small) and make the gravitational mass small. We found that the motion with the negative gravitational mass is possible for the all value of χ_2/χ_1 except $\chi_2/\chi_1 = 0$. In this case, the singularity becomes time-like and is not hidden by the event horizon. But if we use the spatially flat time slice to foliate this space-time, this naked singularity does not appear to our universe.

Now let us consider the situation of the chaotic inflation at the Planck energy scale. During the inflation, the effective vacuum energy varies spatially by the quantum fluctuation of the inflaton field. The spatial correlation scale of the fluctuation is $L \sim H^{-1}$, and the amplitude is $\delta\rho \sim m^2\delta\phi^2$ ($\delta\phi \sim H$) where m is the mass of the inflaton field. The gravitational mass of the fluctuation is $GMH \sim (8\pi/3)(m/m_{pl})^2$ and the cosmological constant is $\chi_1/\chi_2 \sim 1 + (4\pi/3)(m/m_{pl})^2$. Combining this value and the result of Fig.1, we can say that the probability of a black hole formation in the chaotic inflation is less than 12% and the most universe evolves to the globally deSitter like space-time.

References

- [1] K. Maeda, K. Sato, M. Sasaki and H. Kodama, *Phys.Lett.*108B (1982) 98.
- [2] Y. Nambu and M. Shiino, *Phys. Rev.D*(1993).
- [3] D. Garfinkle and C. Vuille, *Gen. Rel. Grav.*23(1991) 471.
- [4] S. K. Blau, E. I. Guendelman and A. H. Guth, *Phys. Rev.D*35(1987) 1747.

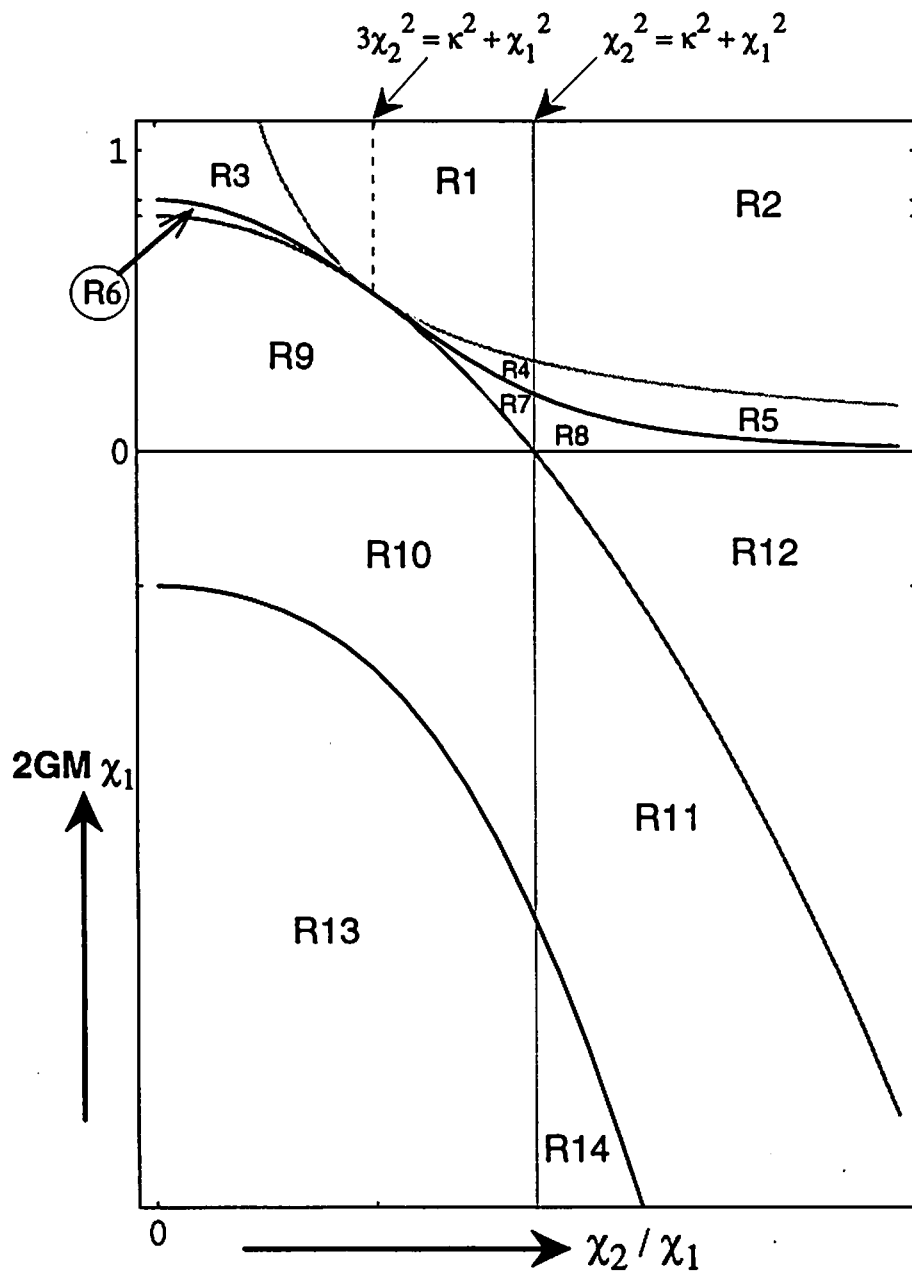


Fig.1 Graph of the classification of the global structure of the space-time, for $\kappa/\chi_1 = 0.8$.

The global structures
of the space-time.

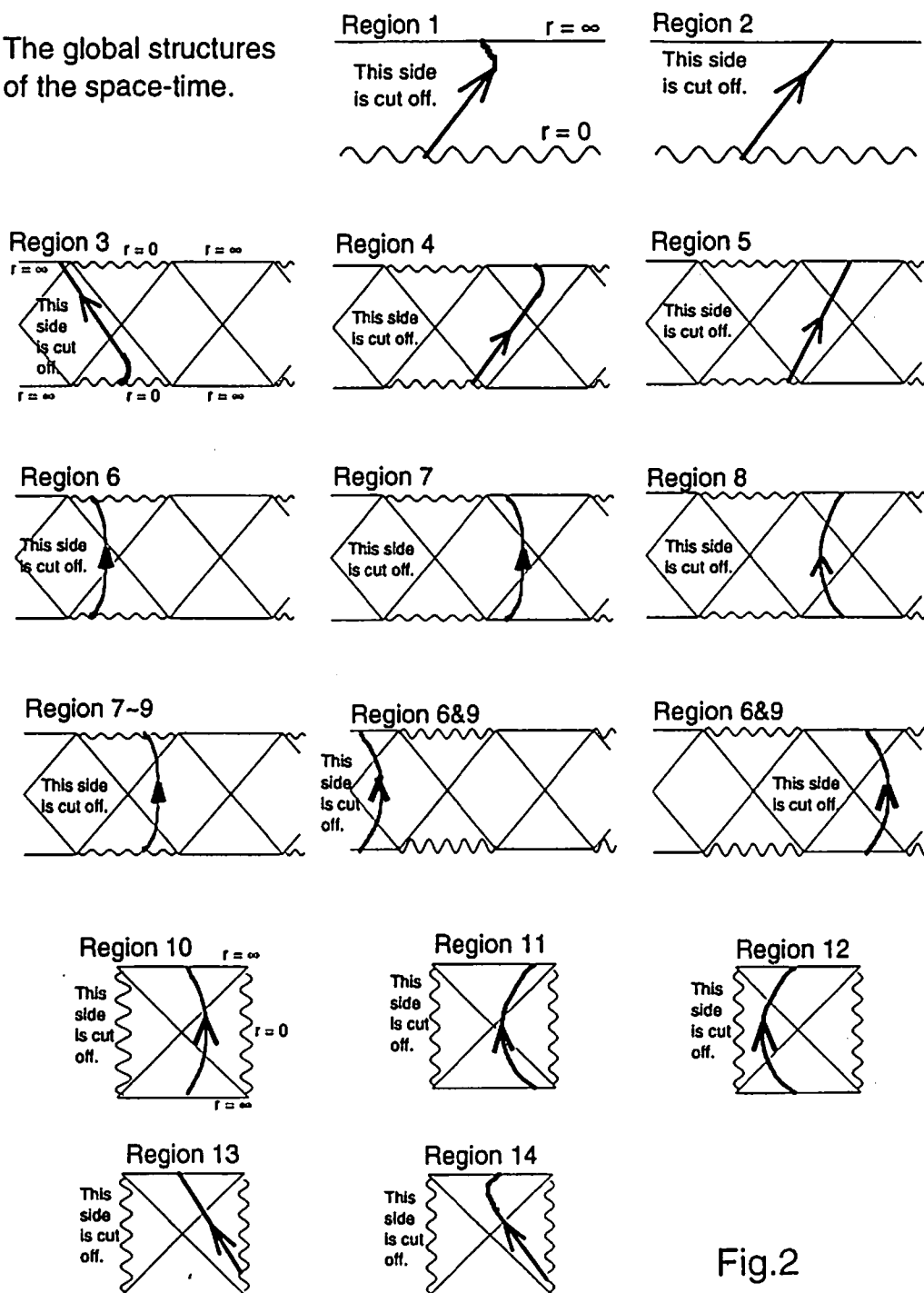


Fig.2

1. 一般相対論の過去と未来

(イ) 過去

(a) 「1920年」

ハイゼンベルグの「部分と全体」¹⁾という自叙伝の第2章は「物理学研究への決定—1920年」となっている。1920年は1901年12月生まれの彼が大学に入って何を専攻するかを決める年であった。彼は高校の最後の数カ月病気で隔離され、その時に「数学者」ワイルの「空間、時間、物質」に接し、熱中した。数学に自身のあった彼は、同じ大学のギリシャ語の教授であった父の紹介でまず数学者のリンデマンを訪ね、ワイルの本の挙げたら「数学をやってもどうせだめでしょう」とあっさり断われた。次に父はゾンマーフェルドを紹介した。話がまた「空間、時間、物質」におよんだとき、ゾンマーフェルドは「あなたはむずかしいことを求めすぎている」「相対論に引きつけられるのはわかる。しかし現代物理は他のところでも、哲学的な根本命題をとりあげており、…」 「ですが、そこへの道はあなたがいま考えているよりずっと遠いのです。あなたは伝統的な物理学の領域の中の、もっと手ごろな、細かな仕事からはじめなくてはいいません」と諭した。ハイゼンベルグが「小さな問題よりも背後にある哲学的な問題に興味がある」というと、ゾンマーフェルドは「でもあなたはシラーがカントとその注釈者についてどういったか知っているでしょう。」王様が土木工事に着手すると人夫たちは仕事にありつける”。はじめは、われわれはみんな人夫なのですよ。」

ゾンマーフェルドのグループで1才半年上のパウリに会う。彼は一般相対論の大きな論文を書いたところだった。(これは後に単行本になったもので20才のときの作品である)しかし「おそらくそのために僕には原子論の方が根底においてもっと面白そうに思えるんだ。」というアドバイスをした。こうして一般相対論の“誘惑”を振り切ったハイゼンベルグは量子力学から素粒子へとつづく物理学の主役になっていくのである。

(b) 「1939年」

前記の話が象徴的に示しているように、一般相対論は量子力学の存在しない時代からある古いのである。現在では電磁気学並に大学生の必須科目のようになった量子力学はワイルやパウリが一般相対論の教科書を書いた当時にはこの世にまだ無かったのである。”ひきつけて止まない魅力があるが、近づいたら危険”といった、一風変わったイメージが一般相対論に長い間つきまとっていたのは当然といえる。こういうことは内山先生などからよく聞いたことであり、1960年に大学院に入った私自身も知っている雰囲気である。内山先生は素粒子との境にいたからこの雰囲気強烈に意識していたようだが、どっぷり浸かっていた成相先生にはそうした気配はなかった。

一般相対論は現在まで約77、8年も経過している。25年を区切りに見ると、1915—1940年の第一期はアインシュタインの存在感も手伝ってそれなりに賑やかであった。シュワルツシルド解、ド・ジッター宇宙、フリードマン宇宙などは最初の成果である。特に1929年の膨張宇宙の発見は第三期の開花を予言するものであった。第一期の最後をかざった星の終末としての重力崩壊は、量子力学と原子核の成果が一般相対論を“物理にした”ものであった。しかしこの流れは、1939年、オッペンハイマーが重力崩壊の論文を書いた直後にマンハッタン・プロジェクトでロスアラモスに赴いたように、戦争で中断する。

戦争はそう長い期間ではないが第二期の大半1940—1960年には一般相対論が物理学界の大きな話題になることは無かったといえよう。戦争への貢献で政府とコネの出来た物理学は次々と核・素粒子・宇宙の巨大科学を生み出し、また量子力学は産業技術に広がっていった。物理学は50年代じつにダイナミックな展開をした。一般相対論の理論的進展はほそぼそこの時期にもあるが、物理学は他のダイナミックな話題で活気づいていた。「物理帝国主義」という言葉はこの時期のものである。「中断」はこの「活気」のためであった。

(c)「1963年」

重力の量子化といった純理論的課題に端を発するもの(ADM等)と平行して、実験も含む一般相対論の話題が1950年代末から現れだした。会議やサマースクールなどのテーマで登場するようになる。私の推測では当時のハイテクを駆使した実験が報告されたことが学界の雰囲気を変えたのだと思う。こうして“あぶない”一般相対論の理論家にも他分野の物理学者から声がかかるようになった。

こういった背景をもとに、一般相対論をサイエンスの表舞台に引き出すきっかけになったのはクエーサー(準星)の発見だった。これはその前から話題の牽引役であった電波天文学の成果で1960年代はじめのNatureの誌面を毎回彩ったものである。”驚き”は二つあって(1)赤方変位 z の大きな天体の発見、(2) z が宇宙膨張ならおこるエネルギー発生量の大きさ、である。二番目の問題が核エネルギーでない重力エネルギー説を生み、重力崩壊研究の復活につながったことはよく知られている。しかし同時に第一の膨張宇宙の観測的拡大でもあったことを見落としてはいけない。

クエーサーと重力崩壊の結び付けで影響力があったのはHoyle達の論文²⁾である。私はそこで

Oppenheimer-Snyderに初めて出会った。その頃プレプリントというものはまだ一般的でなかったがCalTech天体物理のオレンジの表紙のついたプレプリが沢山だされ、まさにアメリカの豊かさの象徴のようだった。1963年だったと思うが、林先生がHoyle達のそのプレプリントを見せてくれた。私は宇宙線、シンクロトン放射、電波銀河という流れでクエーサーのことを追いかけていた。この少し前にでたsupermassive starモデルでのポスト・ニュートン効果での不安定性が話題になり(私の学位論文はこれがテーマ)、その辺から私は一般相対論を勉強始めた。ころ論文を私がコロキウムで紹介したときには、林先生が湯川先生を呼んできたのを憶えている。

60年代の中期は準星の他、3K放射、パルサー、X線星、重力波(?)、等等と目まぐるしく観測的な大発見が続いた時期だった。63年暮れのテキサス・シンポジウムで造られたrelativistic astrophysicsという分野が飛躍的に拡大した。1970年の前後はCalTechとプリンストンにアメリカ中の秀才達が集まったと言われた時期である。きっかけは準星だったが、すぐに主役は星の終末としてのコンパクト星(中性子星、ブラックホール)になり、観測もX線が主になりこの話題を引っ張った。

(d)一般相対論の変身

テキサス・シンポは準星が生み出したもので、人脈的には一般相対論と宇宙線からはじまった。シンクロをつうじて電波天文は宇宙線に結び付いていたし、一時代前の花形だった宇宙線屋が新しい宇宙観測に挑戦していった時期だった。提唱者の一人は相対論のSchuckingであるが彼も、Robinson, Schild, Kerrなど皆テキサスにいた。「何故、テキサスに一般相対論なのか?」ということ調べれば、相対論専門家が、その頃、大大学でいかに扱われていたかが見えてくる。石油と宇宙産業の景気が”文化果てる地”のテキサスにポストにあぶれていた専門相対論屋が職をえていたのである。アメリカに流れたドイツの相対論屋を育てたハンブルグは何故あったかという、ボスのP.Jordanがナチ時代にゲルマン物理優位のシンボルにされたため、戦後、彼は学界の主流と交わらず独自の路をいったことの結果だという話を聞いたことがある。何れの話も物理の主流からずれた姿が見えてくる。60年代の初めにはそんな状態だったのが、60年代の終わりには大大学の花形分野に変身していたのである。

(e)1967年「宇宙論の諸問題」

私自身もこの宇宙物理との関連で興隆しつつあった一般相対論の研究に参加したものである。当時の意識を語るものに1967年に基研での宇宙論研究会の世話人として当時の一般相対論を含む宇宙論の状況を勉強してまとめた文章が残っている。³⁾内容は省略するが、特徴は当時の話題がバリエイティに富むことである。最近と違って堅実な主流的な問題と自由なアイデアでの相対論を拡張するような議論の見境があまり明確でなく、気楽な時期だったということである。物理定数変化の話題に多く触れており、また最近この話題が復活している。これはこの間に真空転移の挿話あるから現実味が増して現在受け取られているということだろう。相対論がらみでは同じ話題でも周囲の物理学の状況がかわってれば違って見えてくるよい例である。

(ロ) 未来

少し説教的なことをいえるというのが世話人の意図のようなので、以下それを述べる。但し、これは普通人向けのアドバイスで、天才は我が道をいけばよい。

(a) 「衰」がすすんで

60年代の宇宙物理、70年代の素粒子物理の進展によって一般相対論が物理学の前面に出てきた。その結果として一般相対論の研究会にこのように多くの人が集まる状況が生まれている。量子重力も含めれば素粒子の相当部分も入り規模はもっと大い。この“繁栄して見える”「現代」には何もいう必要がない。「未来」について述べる。

過去約二十年間、「宇宙論と統一理論の展開」⁴⁾は時代の寵児であった。私自身大変“いい気”になって振舞ったが、「未来」はこうはいかないと思う。いささか“こけおとし”の大言壮語で周囲を威圧した部分が無きにしてもあらずであったからである。「寵児」である期間は同時にそれに反発する批判を育ててきたということもある。実際、反発を持ったり、訝しく思ったりしている物理学者や周辺の科学者が増えているのは事実である。

反発はポストをめぐるレベルのものから、物理学、ひいてはサイエンスとは何であるかというレベルの大問題にまで及ぶものである。

私は「宇宙論と統一理論の展開」という路線が誤りであったとかいっているのではない。ただ、一般相対論に何の欠陥もないのにそれが物理になるには半世紀を要し、その間、科学愛好家の間では別にして、学界的にはずっと「寵児」であったのではなかった、という「過去」を想起し必要がある。実験もなく、数学と大言壮語だけでは半世紀はもたない。また、一般相対論の場合がそうであったように、大言壮語が実現するためには間に別の一幕が必要なきもあるのである。

(b) 一般相対論の展開図：生き残りのマナー

まず、当然の事だが一般相対論関連の研究で他分野の研究にも意味のあるもの、すなわち、他のサイエンス並に実証性が云々出来る（計画も含め）もの及び他の分野での問題と共通性のある理論問題、を正確に（正直に！）語ることである。その際注意すべきは、もろもろの話題の性格を各々正確にメリハリをつけていうことだ。もちろん、この“線びき”は人によって違うグレイゾーンがあるの当然だ。「寵児」時代の感覚は戒め、数年して足が出るような大言壮語は止めることである。

次には他の分野から孤立しないように積極的に関連を探ることである。一般相対論の展開図は「宇宙」「素粒子」だけでなく「数学」「物性（宇宙と素粒子以外の物理の意味）」に囲まれていると考えよう。「宇宙」には実証性が期待してよい課題が、重力波だけでなく天文学にも、いくつもあり、理論家も積極的にそうした発想をもてば心配ない。日本では余り実績がない物理実験との関連も積極的に発想すべきだろう。

関連は単に実証性の程度だけで決まるものではない。三十数年まえの Everett の仕事がそうであったように動機は高踏的でも広い普遍性をもつ場合もある。量子宇宙は量子力学そのものの革新の動機を与えており、視点を変えれば決して荒唐無稽ではない。あまりリアルに考えず問題を普遍的なかたち、道具としての量子力学というかたちに表現する努力をすれば、他分野と関係も強いものだ。⁵⁾

(c) 数理解物理と理論物理

今でも英国系では一般相対論屋は大体「数学」で職を得ている。理論物理という概念は19世紀後半にドイツ系でつくられたらしい。⁶⁾（数学を分けたことが純粋数学をもドイツ系で強くしたとも言われている）数学で書かれた法則は力学だけかと思っていたら、熱も電気も数学で書くことが出来ることがわかって両者の関係が狭まった。「純粋」数学の成果もその内に物理現象に役立つという構図が19世紀末に出来上がった。一般相対論はまさにその路線の成果だった。その後“数学現象”は物理から工学その他あらゆるものに拡大し数理科学が有用科学になった。かつて力学が解析の発祥であったように、量子重力が数学に本質的な貢献をするという、意見もある。統一理論と聞くと「実験もないのに」となるが量子重力の古典近似で古典重力を導く問題と表現すれば、すでに攻略可能な問題設定であって、数理解物理の課題である。順番としてそちらが先にあるべきで、弦理論は具体的に過ぎ若干先走りし過ぎた感がある。数理解物理としての整理整頓の作業（lattice など）が先と位置づける方がよいと思う。

量子宇宙や量子重力が「大言壮語」でないなら何が控えるべき「大言壮語」かと訝しく思う人もあろう。要点は関連の関心を「対象」から「方法」「道具」に移すことではないかと思う。これが実証サイエンスとは別な意味で、理論家が生き延びる道である。

11. 時間の力学

2 回生に解析力学を教えて数年過ぎたが、この科目は奥が深い。最近、相対論学者の Matzner と Shepley の力学の教科書⁷⁾を手に入れた。斜面の演習問題などが付いた普通の教科書であるが、第 1 章には一般相対論の教科書と同じ様な多様体、座標、ベクトル、フォームといったことがならぶ。一般相対論屋も、対象を離れても通用する、「方法」「道具」観を見せなければならぬと思う。以下に述べることはこの教科書とは関係ないし、かならずしも良い例とは思わないが、最近気になっている題材なので未完成だが記しておく。

(a) 多様体の力学

一次元の広がった対象である弦の運動軌跡は二次元の world sheet を構成する。これを target space の中の二次元面として描かれることもあるが、同時に面上に座標 (σ, τ) を持ち込んで、面から出ずにその二次元多様体を記述することもできる。面を base space として各点上に物理量が載っている fiber を考えることもできる。

一次元の弦が 3 次元の体積になったのが一般相対論で、world sheet の代わりに 4 次元の時空多様体となる。そこでは target space にこれをはめ込むことはせず、何時も時空多様体の上に物理量を載せてみる習慣になっている。

次に次元を下げて、一次元の代わりに 0 次元の質点を考えると、出来上がったものが world line という一次元の多様体である。時空と違ってこの場合には、何時も target space の中にこの多様体を書いて議論する。これが質点の力学である。以下で議論しようというのは質点力学を一般相対論的に一次元多様体上に物理量が載っているという見方に徹して見ようということである。

(b) パラメータ時間での力学

この視点は決して新しいものではなく特殊相対論での質点力学で遭遇した問題がある。今は、相対論特有の問題との混同を避けるため、非相対論で考える。ところがそうなると Lagrangian を書き下ろす原理は何なのか問題になる。“物理的”に相対論の近似だというのが一つの立場である。ただそれだけでなく理論的にはガリレオ群の non-linear realization とか、場に徹してソリトン中心の運動で決めるといった立場もありえる。このような問題は非相対論的弦の Lagrangian をどう奮くかに関連して、現代的な問題でもある⁸⁾。ここではそれがユニークかどうかといった問題は回避して、勝手に例を与えて議論を進める。

多様体ではどの座標も本来的なものでないから、Lagrangian はその一般座標変換に対して不変でなければならない。この座標を時間方向にとるのでこの不変性は time reparametrisation 不変性と呼ばれている。そして次の二通りの書き方がされる⁹⁾。

$$S = \int L(q, t, q', t') d\tau, \quad L = \frac{1}{2} \frac{q'^2}{t'} - t' V(q, t). \quad (1)$$

$$S = \int L(q, q', N) d\tau, \quad L = \frac{1}{2} \frac{q'^2}{N} - NV(q). \quad (2)$$

ここで $t = \int N(\tau) d\tau$ とすれば古典的には同じものである。(1) 式は時間を変数として他と同等にあつかうが、何故か Lagrangian には時間変数は別の形で入っている、という見方である。 t 変数についての運動

方程式は

$$\frac{d}{d\tau} \left(\frac{1}{2} \frac{q'^2}{t'^2} + V \right) = 0$$

というエネルギー保存を与えるに過ぎない。一方、(2) 式は次のような gauge 変換に対し不変である。

$$\delta\tau = \epsilon, \quad \delta q = \epsilon q', \quad \delta N = (\epsilon N)'.$$

この変換での lapse N の変換は自明でないが、 N が $dt = N d\tau$ だから 1-form の成分であることに注意すれば、Lie 微分の定義からわかる。

$$\delta N = L_\epsilon N = \epsilon \frac{dN}{d\tau} + N \frac{d}{d\tau} \epsilon = \frac{dN\epsilon}{d\tau}.$$

この不変性に由来して次の Hamilton constraint が出る。

$$\frac{1}{2} \frac{q'^2}{N} + NV = 0.$$

よく知られているようにこれは電磁場の Lagrangian に ϕ' がいないので $\nabla E = 0$ が出るのに対応する。

(c) 運動形態の任意さ

一次元多様体上の物理量として q と t を対等に扱って例題をといてみる。運動方程式を $\frac{\delta L}{\delta q_i} = 0$ ($q_1 = q, q_2 = t$) と書けば

$$\frac{q'}{t'} \left(\frac{\delta L}{\delta q} \right) = \frac{\delta L}{\delta t}.$$

だから $q'/t' \neq 0$ なら、運動方程式は一つしかない。従って、 q か t の何れかを勝手に "gauge fixing" して残りのを解けばよい。こういう言い方をすれば普通は $t = \tau$ という gauge fixing をしている訳である。また宇宙モデルでの conformal time は $t = \int a(\tau) d\tau$ なる non-trivial な gauge を用いている。ここでは $a(\tau)$ が勝手に選ばれている。 t が τ の単調関数なら、 t を変数と見なすことは何も問題はないが、 $t' = 0$ を含む場合にはそこでどう接続するか若干心配がのこる (後述)。しばらくこの路線を徹底してみる。

ここで gauge fixing とは t に τ の任意関数をもってくるような印象を与えるが、それは違う。何故なら τ 自体が何の固有な意味がないのだから勝手な他の座標 (パラメータ時間) λ に変えて、 t や q 、あるいはその combination、が λ に対して適当に与えられている、としてよい。こうすれば一見勝手な運動形態に map することが可能になる。例えば

$$\lambda = \int \sqrt{2(E - V)} dt, \quad \frac{1}{2} \left(\frac{dq}{d\lambda} \right)^2 = 1$$

とすれば、どんな運動も自由運動になる。運動形態というのには固有の意味がないことになる。gauge 依存の区別ということになる。

こうすると $q(\lambda)$ はトリビアルに解け、それを λ の定義式に入れて $\lambda(t)$ を出し、 $q(t)$ が出るという順序になる。これは多変数に一般化でき、Jacobi の変分原理というのがこの路線である。また運動をトリビアルなもの ($H \rightarrow H = 0$) に変換する、Hamilton-Jacobi の形式というのもこの思想上にある¹⁰⁾。自由運動とか調和振動とかいう運動の区別は gauge 依存の概念に過ぎない。それなのに、何故かわれわれは時間については何時までも特定の gauge での記述を後生大事にしているのである。

(d) 例題

たしかにこのような運動形態の map は滅多にやっていないが、宇宙モデルの式をとくときは実はそれを行っている。輻射優勢、閉空間モデルの運動は $q = a$ として

$$\left(\frac{q'}{t'}\right)^2 - \frac{C^2}{q^2} = -1.$$

$t = \tau$ とすればこれは $V \sim -1/q^2$ での運動となる。ところが変形すれば

$$q^2 \left(\frac{q'}{t'}\right)^2 + q^2 = C^2.$$

ここで $q/t' = 1$ となる τ をとれば、運動は調和振動となり $q = C \sin \tau$ 、 $t = C \int \sin \tau d\tau = C(1 - \cos \tau)$ なるパラメータ解を普通使う。

ところでこのパラメータ解で τ を消去すると、 $q^2 + (C - t)^2 = C^2$ なる円となる。(C は正、負) いまの問題では q はスケールファクターではないから、 $q = 0$ を通過して負の値になる。しかし時間が逆行することになるのはどこかおかしい。これは一つの座標で多様体全部を覆えないことに起因し、シュバルツシルド時空で座標の maximal extension が必要性であったことに対応する。

位相空間での flow

位相空間は (q, q', t, t') の 4 次元空間で、問題は $t' = 0$ での流れであるからこの点近傍での local analysis を見てみる。 $q = 0$ を横切るときの t の振舞いが問題なのだから、その近傍で $q \sim C\tau$ という gauge ($q = C \sin \tau$ の $\tau \sim 0$ でのかたち) をとって t に関する運動方程式を解くことにする。 $q \sim 0$ では

$$t'' = \frac{q''}{q'} t' + \frac{\frac{dV}{dq}}{2q'} t'^3 \sim \frac{1}{2} \frac{dV}{dq} t'^3.$$

$V \sim -1/q^2$ では、 $x = t, y = t'$ として

$$x' = y, \quad y' = \frac{y^3}{\tau^3}$$

だから、この解は 4 通りあって

$$y = \tau, \quad -\tau, \quad |\tau|, \quad -|\tau|.$$

したがって接続の仕方はユニークには定まらない。

winding number?

いま $q = \sin \tau$ にとったとすれば τ は角変数であり、一次元多様体は S^1 である。しかしそしてこの上への物理量の載せ方がユニークでなく、 t' というベクトルの置き方に自由度があるということである。各点で (q', t') なる大きさ 1 ($q'^2 + t'^2 = 1$) のベクトルを考えると、 S^1 上を一周するあいだにこれがどう振舞うかで「載せ方」が決まる。一回転するようにも出来るし、半周して戻る場合もありえる。 $q \sim \sin n\tau$ (n は整数) とすれば、一周の間に n 回転するようにも出来るし、その他いろいろの場合がありえる。

そして t が単調に変動する場合には時間変数として採用出来る。

(e) 量子力学と時間変数

q と t を対等に扱う Hamilton 形式は次のようになる。(1) 式の Lagrangian では Hamiltonian をつくと ($\pi = \partial L / \partial t'$)

$$H = pq' + \pi t' - L = t'(h + \pi) = 0, \quad h = \frac{1}{2} p^2 + V$$

という constraint が導かれる。ここで拘束系の Dirac の量子化に従えば状態は次の条件を満たすべしとなる。

$$\left[-i \frac{\partial}{\partial t} + h(-i \frac{\partial}{\partial q}, q) \right] \psi = 0$$

というシュレーディンガー方程式がでる。結局パラメータ時間 τ は出る幕がなかった。

ところがシュレーディンガー方程式の t は物理変数らしい振舞いをしないことが以前から指摘されている。(energy unbound, diffusion 項なし、など) これは対等に扱ったつもりでも Lagrangian の中で明確な区別があったからである。そこで t は変数でなくパラメータだと見なせば、量子的な状態は parameterization の仕方について対称化しておかねばならない。同一粒子系の波動関数の対称化にあたる。その結果、状態は $\Psi = \int \psi dt$ で表されるとなり、 Ψ は

$$h(-i \frac{\partial}{\partial q^A}, q^A) \Psi = 0$$

という Wheeler-DeWitt 型の方程式を満たすことになる。

量子宇宙が提起したシュレーディンガー方程式の見方は q^A の何れかが古典的に振舞う特殊な状態に宇宙が現在あるのでそれが時間の役目をしている、というものである。時間は内部変数から調達した「宇宙の部分品 (parts)」であるという観点である。変数の部分的古典化は Born-Oppenheimer 近似で扱え、Wheeler-DeWitt 型からシュレーディンガー型が出る¹¹⁾。もし時間がこうした本来的に古典変数なら、量子力学にいくとときに対等に扱うのはおかしいとなる。

(f) 時間変数変換と運動形態

非相対論的系の (q, t) を変数とした場合、それらの間に存在する最大対称性を考えてみよう。自由運動ではまづ空間回転、空間 boost, Galilei 変換で、 q が n 次元なら、 $n(n-1)/2 + 2n$ 個のパラメータがある。時間変数については boost の他に dilatation と conformal 変換の 3 つがある。 $n=3$ では全体で 12 個となる。この内、時間の変換は

$$t \rightarrow \frac{\alpha t + \beta}{\gamma t + 1}$$

dilatation は $t \rightarrow \alpha t, q \rightarrow q/\alpha^{1/2}$, conformal は $1/t \rightarrow 1/t + \gamma$ である。conformal の対称性はあまり知られていないが、この変換で Lagrangian は全微分だけ変化することが簡単に示せる。

これらの変換のいくつかに対しては $V \neq 0$ でも、対称性がある。この発想を次のように定義した Schrodinger 方程式の“対称性”で考えてみる¹²⁾。それは

$$t \rightarrow \int dt \frac{1}{d(t)^2}, \quad q \rightarrow \frac{R}{d(t)} \frac{q + y(t)}{d(t)}$$

なる変換 (R は回転 matrix) で波動関数が次のように factorize 出来る分だけ変化するのを同一視する対称性である。

$$\psi(t, q) \rightarrow f(t, q) \psi(t, q).$$

ポテンシャル V はこの変換で次のように変換されるから、変換が含む任意関数 $d(t), y(t), l(t)$ は新変数について同じ型のポテンシャルになるようにとればよい。

$$V'[t', q'] - d^2 V[t, q] = \\ \frac{m}{2} d \ddot{d} q^2 + m R q (d \ddot{y} - d^2 \ddot{y}) + \frac{m}{2} (d \ddot{d} y^2 - d^2 \ddot{y} y + d^2 \dot{y})$$

最もこれが可能なのは上の表式から分かるように、変数 q について一次、2 次のポテンシャルに限られる。

上の議論は、観点を变えて、変換が含む関数を勝手にとった場合にポテンシャルの違う運動への map を行う変換ともみなせる。この発想は時間変数の変換で古典運動の種類がいかようにでも見れると先に述べたことと共通性がある。実際変数について一次（外力）、2 次の運動（調和振動）はすべて自由運動に map 出来る¹³⁾。またその逆もできる。この知見がどれだけ有効かはもっと考えてみる価値があるように思える。

References

- 1) W. ハイゼンベルグ「部分と全体」(山崎訳) みすず書房、1974 年。
- 2) F.Hoyle, W.A.Fowler, G.Burbidge and M.Burbidge, *Astrophys.J.*139(1964),909.
- 3) 佐藤文隆「素粒子論研究」36(1967), 385.
- 4) 佐藤文隆編「宇宙論と統一理論の展開」岩波書店、1987.
- 5) 例えば、W.H.Zurek, *Prog.Theor.Phys.*(1993),89(1993),no 2,280.
- 6) C.Jungnickel and R.McCormmach,
Intellectual Master of Nature : Theoretical Physics from Ohm to Einstein,
The University of Chicago Press,1986.
- 7) R.A.Matzner and L.C.Shepley, *Classical Mechanics*, Prentice-Hall International, Inc., 1991.
- 8) C.F.Yastremiz, "Galilean Extended Objects", DAMTP R-1991/11.
- 9) T.Padmanabhan, *Int.J.Modern Phys.*4(1989),4735.
- 10) C.Lanczos, *The Variational Principles of Mechanics*, Dover, 1st ed. 1949.
- 11) 例えば、A.Vilenkin, *Phys.Rev.*D39(1989),1116.
- 12) U.Niederer, *Helvetica Physica Acta*, 47(1974),167.
- 13) 高木伸氏は別の観点からこの種の問題を論じた。
S.Takagi, *Prog.Theor.Phys.*84(1990),1019;85(1991),463,723;86(1991),783.